Biofilm Dynamics and Role of Electricigens under Stressful Conditions for Wastewater Treatment, Bio-electricity Generation and Bio-monitoring

By

Iqra Sharafat

Department of Microbiology

Faculty of Biological Sciences

Quaid-i-Azam University

Islamabad

2022

Biofilm Dynamics and Role of Electricigens under Stressful Conditions for Wastewater Treatment, Bio-electricity Generation and Bio-monitoring

A thesis submitted to Department of Microbiology, Quaid-I-Azam University, Islamabad, Pakistan in the partial fulfillment of the requirements for the degree of

Doctor of Philosophy in Microbiology

By

Iqra Sharafat

Department of Microbiology

Faculty of Biological Sciences

Quaid-i-Azam University

Islamabad

2022

Dedicated to

ABBA, AMMI & SIBLINGS

For their unprecedented love and support

Author's Declaration

I, Iqra Sharafat, hereby state that my Ph.D. thesis titled **"Biofilm Dynamics and Role of Electricigens under Stressful Conditions for Wastewater Treatment, Bio-electricity Generation and Bio-monitoring"** is my own work and has not been submitted previously by me for taking any degree from Quaid-I-Azam University, Islamabad, Pakistan.

At any time if my statement is found to be incorrect even after my Graduate, the university has the right to withdraw my Ph.D. degree.

Iqra Sharafat
Date: 31-03-2022

iv

Plagiarism Undertaking

I solemnly declare that **"Biofilm Dynamics and Role of Electricigens under Stressful Conditions for Wastewater Treatment, Bio-electricity Generation and Bio-monitoring"** is solely my research work with no significant contribution from any other person. Small contribution/help wherever taken has been duly acknowledged and that complete thesis has been written by me.

I understand the zero-tolerance policy of the HEC and Quaid-I-Azam University towards plagiarism. Therefore, I as an Author of the above titled thesis declare that no portion of my thesis has been plagiarized and any material used as reference is properly referred/cited.

I undertake that if I am found guilty of any formal plagiarism in the above titled thesis even after award of Ph.D. degree and that HEC and the University has the right to publish my name on the HEC/University Website on which names of students are placed who submitted plagiarized thesis.

Student / Author Signature: _____

Name: Ms. Iqra Sharafat

Certificate of Approval

This is to certify that the research work presented in this thesis, entitled titled **"Biofilm Dynamics and Role of Electricigens under Stressful Conditions for Wastewater Treatment, Bio-electricity Generation and Bio-monitoring"** was conducted by **Ms. Iqra Sharafat** under the supervision of **Prof. Dr. Naeem Ali.** No part of this thesis has been submitted anywhere else for any other degree. This thesis is submitted to the Department of Microbiology, Quaid-i-Azam University, Islamabad in partial fulfillment of the requirements for the degree of Doctor of Philosophy in field of **Microbiology.**

Student Name: **Ms. Iqra Sharafat**   Signature:_____

Examination Committee:

a) External Examiner 1:   Signature:_____

Prof. Dr. Syed Habib Ali Bokhari
Vice-Chancellor, Kohsar University
Murree

b) External Examiner 2:   Signature:_____

Prof. Dr. Nisar Ahmed Kanhar
Department of Microbiology
Faculty of Natural Sciences
Shah Abdul Latif University
Khairpur, Sindh

Supervisor Name: **Prof. Dr. Naeem Ali**   Signature:_____

Name of HOD: **Prof. Dr. Aamer Ali Shah**   Signature:_____

CONTENTS

LIST OF FIGURES

LIST OF TABLES

LIST OF ABBREVIATIONS

WWT	Wastewater treatment
EPS	Extracellular polymeric substances
TVI	Trivalent iron
WTR	Waste tire rubber
TDR	Tire derived rubber
AGBR	Attached growth batch reactors
FISH	*Fluorescent in situ hybridization*
6-FAM	6-Carboxyfluorescein
CLSM	Confocal laser scanning microscopy
DIA	Digital image analysis
SEM	Scanning electron microscope
DO	Dissolved oxygen
VFA	Volatile fatty acids
AOB	Ammonium oxidizing bacteria
NOB	Nitrite oxidizing bacteria
FTIR	Fourier transform infrared spectroscopy
MFC	Microbial fuel cell
SCMFC	Single chamber microbial fuel cell
DCMFC	Double chamber microbial fuel cell
FPMFC	Flat plate microbial fuel cell
EAB	Electrochemically active bacteria
EAM	Electrochemically active microbes
PEM	Proton exchange membrane
OTUs	Operational taxonomic units
PANI	Polyaniline
CNTs	Carbon nanotubes
LB	Luria Bertani

COD	Chemical oxygen demand
BOD	Biological oxygen demand
MCL	Maximum Composite Likelihood
DLVO	*Derjaguin Landai Verwey Overbeek*
XDLVO	*Extended DLVO theory*
MRD	modified Robbins device
MTP	Microtiter plate
CRA	Congo red agar
TCP	Tissue culture plate
EET	Extracellular electron transfer
GGA	Glucose and glutamic acid
Lm	*Listeria monocytogenes*
LSM	*Listeria* synthetic medium
BHI	Brain heart infusion
WT	Wild type
CV	Cyclic voltammetry
DMK	Demethylmenaquinone kinase
SHE	Standard hydrogen electrode
WE	Working electrode
TSG	Template stripped gold
SAM	Self-assembled monolayers
MOPS	3-morpholinopropane-1-sulfonic acid
PFA	Paraformaldehyde
ARM	Aerobic respiration media
PES	Polyether sulfone
SDG	Sustainable development goal

Acknowledgements

Abstract

The growing concern in the environmental perspective demands cost-effective treatment systems for wastewater and monitoring before it is discharged into the environment. Biofilms have successfully been used in water and wastewater treatment processes for well over a century. Biological wastewater treatment in suspended or attached growth reactors is an energy intensive process and there is need for improving the nutrient removal efficiency. Bioelectricity production through bioremediation of liquid and solid waste is one of the thrust areas of research in the environmental circles. Among different treatment technologies currently under investigation or being practically used, Microbial fuel cell (MFC) has been proposed quite effective. This technique uses electrochemically active microbes (EAM) for electricity generation using organic and inorganic waste in liquid or solid state. Electrochemically active microbial strains are cost effective biological catalysts in wastewater treatment and bioelectricity (energy) production in MFC. Microbial fuel cell technology also has scope for biomonitoring of different pollutants in the wastewater. In MFC based biosensor, the strength of current corresponds to the amounts of pollutants.

The first phase of the study employed a multifaceted strategy, whereby, the microbial consortia of municipal sewage/wastewater was employed in attached growth batch reactors (AGBR) for investigating the treatment efficiency and microbial diversity under the effect of different metals such as ferric iron (Fe^{3+}) and aluminum (Al^{3+}). The results of the studies revealed 38% improved COD removal in the AGBR with 8.5mg/L iron and its supplementation supported more biofilm biomass. Fluorescent in situ hybridization (FISH) with phylogenetic oligonucleotide probes coupled with confocal laser scanning microscopy (CLSM) and digital image analysis showed an increase in the density of eubacteria and beta proteobacteria whereas gamma proteobacteria decreased with an increasing concentration of Fe^{3+}. Likewise, the COD (mg/l) of the sludge was reduced (28.68%) with Al^{3+} (2.5 mg/l) but the sludge digestibility decreased at higher concentrations (4.5 mg/l-6.5 mg/l) of Al^{3+} compared to the control. Conventional (culture based heterotrophic plate count) and molecular based studies (FISH-CLSM, and 16S rDNA sequencing) indicated limiting effect of increasing concentrations of Al^{3+} (0mg/l-6.5 mg/l), though non-significant, on the bacterial density and diversity. The bacterial density decreased (7.33%) with an increase in Al^{3+} concentration (0 mg/l-6.5 mg/l).

Extracellular polymeric substances (EPS) are biopolymers self-produced by microorganisms, widely studied for their economic importance as the biocoagulants to replace chemical-based coagulants in the sludge flocculation and for applications in food industries.EPS producing bacteria were isolated from biofilms developed on support material such as waste tire rubber in the attached growth batch reactors with and without the incorporation of different concentrations of iron and aluminum. The bacteria were screened, identified and characterized for their EPS production potentials using different assays. An about 66% of the bacterial isolates were capsule forming (Anthony's capsule staining) whereas 30% of

them strong biofilm formers. Dry weight and viscosity measurement revealed higher slime EPS (two-fold) and viscosity production in pure cultures of bacteria rather than in consortium. Nevertheless, higher carbohydrates production was higher in consortia compared to pure culture of bacteria. Scanning electron microscopy (SEM) and Fourier transform infrared (FTIR) spectra further confirmed variations in EPS production and its components. Highest EPS production was noticed in *Enterobacter* sp., *Citrobacter* sp., *Clostridium* sp. and *Candidimonas* sp. through 16SrRNA gene sequencing.

In the second phase of the study, the conventional approach of treating wastewater in the attached growth reactors was studied in microbial fuel cells (MFCs) where this biocatalysis was basically integrated with the energy production and biomonitoring. MFCs, operated in a fed batch mode with microbial communities from cropland soil and lake sediment showed an about 87.7% and 45% improved voltage output, respectively when supplemented with iron compared to control. Illumina *MiSeq* sequencing showed predominant enrichment of genera; *Pseudomonas*, *Sedimentibacter, Aminobacterium*, *Clostridium and Flavobacterium.* Alpha rarefaction curves and Shannon index revealed higher enrichment of diverse bacterial community on anodic biofilm from soil than the sediment treated with Fe^{3+}.MFC inoculated with the sediment sample supported enrichment of delta-proteobacteria (included *Shewanella* sp. and *Geobacter* sp.) with iron. The isolated electrochemically active bacteria (EAB) were identified as *Staphylococcus* sp., *Bacillus* sp., *Streptomyces* sp. and *Gordonia* sp. based on 16SrRNA sequencing.

Mediator-less dual chamber microbial fuel cells (MFC) were fabricated and operated to evaluate their role as biosensing devices for BOD measurements using natural (activated sludge) and artificial formulated bacterial (*Pseudomonas aeruginosa, Staphylococcus aureus* and *Bacillus circulans*) consortia. The study validated a considerable application of MFC as a biosensor device for effective and continuous monitoring of BOD in water. The MFC biosensors were optimized and calibrated at pH 7, temperature 37 ^{o}C using 100 mM phosphate buffer with 100 mM NaCl solution as a catholyte at 10 kΩ external resistance. The power density (14.2 mWcm^{-2}) achieved with MFC-I with the sludge consortium was 5 folds higher than MFC-II with artificial consortium. The relative performance of MFC-I, in terms of stability (55-60 days) and reproducibility (±15.4%), was double than MFC-II biosensor. The co-existence of different electron acceptors such as phosphate, nitrate and nitrite at low concentration in the anolyte had an insignificant effect on the biosensor performance. Molecular based phylogeny revealed the bacterial community structure in the sludge was considerably altered during enrichment in MFC.

Gram positive bacteria are generally considered weak electricigens due to the presence of thick non-conductive cell wall. An eight genes-based locus, responsible for extracellular electron transfer (EET), has recently been reported in *Listeria monocytogenes,* a Gram-positive food borne pathogen. So, the role of Ndh1/NDH-2a and Ndh2/NDH-2b in respiration and EET was investigated using electrochemical techniques and by growing wild type (WT), mutant and complementary strains of *L. monocytogenes*

EGDe in single chamber bioelectrochemical cells with ultra-smooth template stripped gold (TSG) electrodes modified with self-assembled monolayers (SAMs) of carboxylic acid terminated thiols. The results of the study revealed that Ndh2/NDH-2b is involved in EET and *L. monocytogenes* was able to respire in the absence of Ndh1/NDH-2a.

Overall, the findings of the studies indicate that supplementation of Fe^{3+} enhanced the sludge digestibility, microbial fuel cell (MFC) performance and significantly impacted the bacteria density and diversity. Natural activated sludge-based consortium in MFC biosensor proved to be more stable for continuous monitoring of BOD. The identified bacteria have high potential to be used for different applications such as wastewater treatment, biopolymer and electricity production and can be considered as the potential candidates for further studies.

CHAPTER 1:   INTRODUCTION

1.1.   Background

Currently, the population of the world is about 7.3 billion and it is anticipated to rise to 10 billion, with global energy demands expected to grow to 160 % from 60% by the year 2050 (Y. Zhou et al., 2019, Nations, 2019). Concerns regarding clean water supply and provision of adequate energy have been raised in the energy and water sectors worldwide (Bahar et al., 2020). This leads to search for sustainable methods for treatment of wastewater for reuse and supply of renewable energy (Dhanya et al., 2020). Besides, the growing trends of intensive industrialization and the use of chemicals in agriculture have contributed to accumulation of several toxic persistent compounds in aquatic and terrestrial environments viz. heavy metals and organic compounds (Messina et al., 2019). More than 2 billion tons per annum of waste is produced globally. About 42 million tons of this waste is comprised of electronic waste heavily contaminated with toxic substances (Walters & Fuentes Loureiro, 2020). While the presence of these pollutants poses an ecological risk, and a threat to the natural environment and public health, bioremediation processes can degrade or remove such pollutants (H. Zhang et al., 2020). Effective remediation of contaminants inevitably depends on real-time monitoring of contaminants such as organic pollutants and heavy metals in the environments (Parra-Arroyo et al., 2020). Hence, monitoring hazardous compounds in the environments is of paramount significance in order to comply with the environmental legislations and guidelines.

Pakistan has almost exhausted its available freshwater resources (Talpur et al., 2020).The situation is aggravated by the direct and indirect input of contaminated effluents from municipal [2000 million gallons (7.5708×10^9 L) of sewage/day] and industrial sources into the water bodies ("Pakistan Strateg. Ctry. Environ. Assess.," 2006). The country is largely devoid of any wastewater and solid waste management systems. In addition, the available conventional treatment systems are either ineffective or they are not sustainable due to high input of energy in them. Discharge of wastewater with high chemical oxygen demand (COD) and biological oxygen demand (BOD) into water bodies creates huge ecological deterioration (Murtaza & Zia, 2012). According to available data, more than 26% of the domestic vegetables in Pakistan are cultivated with wastewater which creates huge human health concerns (Ensink et al., 2004). Bacteriological contamination of drinking water has been regarded as a major contributor to water-borne diseases (Nabi et al., 2019,Daud et al., 2017). Besides freshwater crises, Pakistan is also facing a huge power shortage of almost 7.075 MW leading to closure of 30-40% industrial plants. Electricity consumption per capita has increased from 500 kWh to more than 960 kWh during 2012–2019 (Irfan et al., 2020). The massive gap between the demand and supply of energy has brought economic progress (shaving off about 2% of the annual GDG) of country at stake (Abdullah et al., 2020).

Biofilm based system is a well-developed technology for wastewater treatment and offers several advantages such as operational flexibility, higher active biomass concentration and reduced hydraulic retention time.

Microbial communities in the biofilms break down nutrients and remove different pathogens from wastewater. Biofilm formation is a complex process that can be broadly explained under the following steps; preconditioning of substrate surface, reversible attachment, irreversible attachment, EPS production, development and maturation (Collins et al., 2020). Studies have reported the bacterial population dynamics and the context of the relationship governing microorganism co-existence within biofilm matrices (Garrett et al., 2008, Fish et al., 2016,Paula et al., 2020,Costerton et al., 1994,Driscoll et al., 2007). All in all, these studies have consolidated the existence of biofilms as a dominant mode of growth that is exhibited by microorganisms in nutrient-sufficient hydrated environments irrespective of the type of ecosystem. Microbial consortia within biofilms respond to environmental and internal conditions. Specific factors that influence biofilms structure include; temperature, nutrients, pH, shear force and support surface properties (Ponomareva et al., 2018). Biofilms have been used for the treatment of wastewater having varying and complex composition of compounds using different reactors such as moving membrane biofilm reactors and attached growth biofilm bioreactors (Ozturk et al., 2019,Sharafat et al., 2018). Aggregation within wastewater treatment processes such as activated sludge flocs and granules are commonly used to increase the separation and process efficiency of wastewater treatment (Zeng et al., 2016). Coagulants are used for eliminating soluble organic and colloidal matter from the aqueous phase during the process (Hansen et al., 2018). The mode of action of coagulants is through transitional changes in particle charge density; thereby decreasing the concentration of biodegradable organic matter (Tetteh & Rathilal, 2019). Increasing the dose of certain coagulants has been reported to remove proteins and other polysaccharides (Amuda & Amoo, 2007).

Wastewater treatment consumes huge amounts of energy and is an energy intensive process (Mani, 2020, Tang et al., 2020). Nonetheless, wastewater itself contains abundant organic nutrients that can be exploited to generate energy and convert the wastewater treatment into energy gaining process rather than energy consuming (Thulasinathan et al., 2020, Bader et al., 2021, Yildiz, 2012). Among different growing technologies for this, bioelectrochemical treatment of wastewater is a promising biotechnological approach with simultaneous renewable energy generation. In this context, Microbial fuel cell (MFC) technology represents a new way for generation of renewable energy (electricity) from what would otherwise be considered 'waste'. It is a cost-effective electricity production using exoelectrogenic bacteria that convert chemical energy to the electrical energy using redox mediators, nanowires and membrane-bound electron carriers during respiration and extracellular electron transfer (EET). It can produce power in a wide range of conditions and is capable for detection and monitoring of pollutants in diverse environmental samples.

Microorganisms that possess extracellular electron transfer (EET) capability have gained considerable attention due to their impending ability to generate electricity by metabolizing organic waste besides other biotechnological applications e.g. bioremediation, biosensing and microbial electrosynthesis (Shi et al., 2016,Zou et al., 2019). Typically, MFC is comprised of an anaerobic chamber separated from aerobic abiotic

chamber by proton exchange material (salt bridge or proton exchange membrane). Microorganisms colonize the anode and degrade organic substrates into protons (H^+), electrons and carbon dioxide (Slate et al., 2019). Carbon dioxide is released into anolyte solution as a byproduct where protons and electrons travel towards cathode. The streaming of electrons through external circuit generates electric current, whereas, proton (H^+) progresses internally towards cathode where it is either oxidized to form water or reduced to liberate hydrogen gas. The potential difference between an electro-oxidation reaction of a fuel (anodic reaction) and an electro-reduction reaction of an oxidant (cathodic reaction) drive the current through the external circuit of the system in the MFC (Modestra et al., 2020).

Numerous factors affect the activity of biofilms and performance of biofilm reactors and MFCs; reactor configuration, microorganisms (biocatalyst), operational conditions, mediators and type of substrate(s) (Angelaalincy et al., 2018). Iron (Fe) is one of the vital nutritional elements for bacteriological growth. It acts as an electron acceptor coupling oxidation of organic matter with iron reduction during microbial respiration. It is a part of all heme enzymes including hydro-peroxidases and cytochromes. The presence of Fe^{3+} promotes or controls biofilms at its narrowly defined range of concentrations. Lack of iron limits microbial growth where bacteria display iron scavenging mechanisms such as siderophores (iron chelators) production for its acquisition (Connor et al., 2016). Salts of iron are used for flocculation in the wastewater treatment processes. Similarly, aluminum ($AlCl_3$) is a commonly used flocculent with excellent coagulation properties (Rong et al., 2013). Aluminum based coagulants have been reported to effectively enhance membrane filterability and act as a biofoulant in membrane reactors by impeding the development of gel layer on surface of membrane, retarding biofilm development, and removing fouling agents from the surroundings (Wu et al., 2006). It is also known to affect biological life and is a non-essential metal (Klotz et al., 2017). Due to the positive charge, these ions deferentially react with anionic ligands such as citrate, carboxylate, phosphate groups, and nucleotides in the EPS and negatively charged surfaces of bacteria (Zhang et al., 2011). The interactions between metals and microorganisms enhance or inhibit the biofilm activity and coagulation process at their particular concentration(s) (Rasamiravaka et al., 2015,Al-Saati et al., 2016). The precise determination of these concentrations can lead to a better understanding for improved industrial and wastewater treatment processes (Brennan, 2012).

The studies have reported that iron, in its ferric and ferrous forms, affects the bioelectrochemical processes biotically and abiotically. Biotically, intrinsic participation of ferric ions as a cofactor can alter the levels and activity of proteins for energy metabolism and distinct metabolic pathways (Ruiz-Urigüen et al., 2018). Abiotically, these are involved in redox reactions, electron shuttling and catalysis (Lu et al., 2015). Ferric iron has been identified as an important factor affecting the biofilm formation on the electrodes and anodic oxidation subsequently, the performance of MFCs (Banin et al., 2005, Wu et al., 2013). However, the effect in its readily available forms such as ferric iron in waste streams, soils and sediments on energy metabolism

and mixed culture exoelectrogens' ecology in the electrode biofilms is still less clear and needs to be investigated (Wei et al., 2013, Jiang et al., 2016).

Electroactive bacteria use different mechanisms to transfer electrons to the surfaces of anodes. Gram negative model bacteria such as *Geobacter* sp. produce conductive pili (nanowires) (Lovley & Walker, 2019) while *Shewanella oneidensis* uses MtrCAB (outer membrane cytochromes) (Yingxiu Cao et al., 2019) for transfer of electrons to the anode or minerals. Bacteria achieve direct electron transfer via cytochromes and nanowires or synthesize and release reduced shuttling compounds that are oxidized at the surfaces of anodes in turn accomplishing the electron conductance. Electricigens produce self-mediating metabolites such as, *Shewanella oneidensis* (riboflavins) (Kees et al., 2019)*), Klebsiella* (quinones) (Guo et al., 2020) and *Pseudomonas* (phenazines) (Guan et al., 2019)*.* An extensive research on extracellular electron transfer (EET) mechanisms has been carried out in Gram negative bacteria. Gram positive bacteria have generally been considered as weak electricigens, mainly due to the presence of thick non-conducting cell wall and are, therefore, less understood (Pankratova et al., 2019). Recently, number of Gram-positive bacteria including food borne pathogen *Listeria monocytogenes* has been reported for the EET potential through flavin based pathways. An eight genes based uncharacterized locus has been reported for its role in EET (Light et al., 2018).   Further understanding the role of these genes and the respective proteins would be contributory to improving the bioelectrochemical processes using Gram positive bacteria.

Microbial fuel cell based biosensors have been known as an outstanding potential substitute for an instant and convenient monitoring of diverse pollutants in various environments (Zhou et al., 2017). Currently, the detection of pollutants such as biological oxygen demand (BOD) and metals is carried out by time consuming chemical methods in laboratories or by expensive kits. The recognition elements within the traditional biosensors are fluorescent reporter proteins, enzymes, or antibodies which require laborious implementation procedures and are expensive (Pankratova et al., 2019). Anodic biofilms act as bioreceptors to the presence of toxicants in feeding streams and the subsequent response in the form of quantifiable current change is directly associated to the metabolic activities of biofilms at anodes without the need for an external transducers (Do et al., 2020). Still, there are some critical challenges linked with performance of MFC based biosensors that limit their practical application such as relatively expensive PEM, a lack of repeatability due to variation in EAMs in the samples from diverse areas, and need to improve selectivity and specificity in mixed environments (Cui et al., 2019,Sun et al., 2015). Further studies are required to tackle the aforementioned challenges and further improve the applicability of MFC biosensors. While considering mixed cultures as bioreceptors, the perceived risk could be reduced by understanding the microbial community compositions and dynamics under a range of substrate utilities for adoption of MFC biosensor technology.

1.2. Aims and Objectives of the Research Work

The specific aim of the study was to develop integrated devices/processes for wastewater treatment, bio-electricity generation and biomonitoring with an improved performance and explore the electron transfer mechanisms used by electrochemically active bacteria (EAB).

The following objectives were achieved by conducting the outlined study;

1. To investigate the effects of different concentrations of metals/cations such as; ferric iron (Fe^{3+}) and aluminum (Al^{3+}) on the sludge digestibility, microbial community structure and metabolism within biofilms developed in the attached growth batch reactors using different conventional and molecular techniques (chapter 3).

2. Screening, identification and characterization of extracellular polymeric substances (EPS) biopolymer producing bacteria with high potential for the EPS production and biofilm formation capabilities (chapter 4).

3. Characterize the electrochemical performance of microbial fuel cells (MFCs) and microbial community dynamics within anodic biofilms under the influence of trivalent iron [Fe(III)] using soil, sediment and/or wastewater as the inocula (chapter 5).

4. Evaluate the potential of microbial fuel cell (MFC) based electrochemical biosensors for the detection and continuous monitoring of organic pollutants i.e. biological oxygen demand (BOD) in wastewater and compare the efficiency of activated sludge and artificially designed consortia of different electrogenic bacteria for biosensing (chapter 6).

5. Investigate the role of Ndh1/NDH-2a and Ndh2/NDH-2b in respiration and extracellular electron transfer (EET) in *Listeria monocytogenes* using electrochemical techniques and bespoke glass single chamber bioelectrochemical reactors with template stripped gold (TSG) electrodes modified with self-assembled monolayers (SAM) of carboxylic acid terminated thiols (chapter 7).

CHAPTER 2:   **REVIEW OF LITERATURE**

2.1. Need for Water and Energy

Water and energy are among those key universal components that are essentially required for sustaining the modern civilization. Fossil fuels have supported the economies of all the countries in the world and industrialization over the past century (Zhang et al., 2020). Increasing global warming, depletion of natural sources and water and energy scarcities has led to mounting international tensions. Available data suggest that an about 20% countries and 2.7 billion population in the world would suffer from severe water shortage and safe drinking water by the year 2025 (UNESCO Publishing and Earthscan Publications, 2009). Also, according to the projected estimations, the respective depletion times for the gas, coal, and oil reservoirs are approximately 52, 114, and 50 years only (BP, 2017). Global energy demands will become more extensive in coming decades; therefore, current infrastructure requires changes accordingly to meet energy demand.

At present, environmental pollution is also one of the major problems we are encountering. It is gradually increasing and causing a severe damage to the ecosystem (Sinha et al., 2020). In recent past soil and water have been adversely affected due to uncontrolled industrialization and urbanization. Declining productivity and increasing pollution could spell disaster on residents of earth. The water and soil are significantly polluted by hazardous agricultural and industrial wastes, including pesticides, heavy metals, herbicides, and other toxic substances (Brena et al., 2013). Most of contaminants accumulate and persist for a long time in the environment due to their recalcitrant nature, where they can enter into the food chain (Nigam & Shukla, 2015). This has an adverse effect on quality of life and its longevity. Therefore, detection and monitoring of such environmental pollutants are very important for the health and sustainability of environmental and biological systems.

In Pakistan, rapid urban growth, industrialization, unsustainable water consumption and poor sanitation have created huge water and energy crises. A more recent study has indicated an available water supply of less than 1,000 m³ per capita, which has put Pakistan in the list of water stressed countries. This situation may result in creating huge ecological stress, biodiversity loss, increase in infectious diseases and decrease in agricultural productivity. Apart from water crises, Pakistan is facing a huge shortfall in energy in the last few years. These two issues are costing huge economic deficits to the country. Till now, Pakistan is largely devoid of any proper wastewater management systems, besides, hydroelectricity and fossil fuel have been the major source of energy. The available conventional wastewater treatment and energy producing systems are either too expensive or they are contributing significant environmental issues (Thurston, et al., 1985, Das, 2017) . Considering the dwindling situation of both water and energy, it is high time to expand innovative cost effective, sustainable alternative energy sources along with water treatment systems. This alarming condition has catalyzed the research on finding alternate energy sources and sustainable

technologies for wastewater treatment, power generation and detection/monitoring of environmental pollutants.

2.2. Biofilms are a Solution to solve these Problems

It is a well-known fact that wastewater treatment processes consume substantial amounts of energy. Wastewater contains abundant amounts of organic sources that can be exploited to turn these energy intensive process into energy generating processes using different technologies (Yildiz, 2012). Currently, waste to fuel has been the most effective contemporary approach in managing these two major problem areas of the world. Anaerobic digestion in biological reactors such as attached growth, suspended growth and bioelectrochemical reactors (microbial fuel cells) is applied to use the catalytic activity of microorganisms to recover energy from wastewater and generate water for reuse. Microbial biofilms are employed in these reactors to achieve enhanced efficiency of the processes (Yang et al., 2019,Angelaalincy et al., 2018, Qureshi et al., 2005). Therefore, developing these sustainable technologies for effective wastewater management and energy generation from waste is of paramount importance to address the issues of water scarcity and environmental conservation in our country. Still, a lot more has to be done at scientific as well as practical level and Pakistan needs to catch up these technologies to meet the current challenges.

2.3. Microbial Biofilms and Wastewater Treatment

Biofilms are unanimously agreed to be aggregates of single or multiple types of cells that are embedded and encompassed in a self-produced hydrated complex matrix and irreversibly attached to the supporting substrate ((Davey & O'toole, 2000, Kolenbrander et al., 2010, Sutherland, 2001). The concept of microorganisms existing as multicellular communities was introduced quite late in the time line of microbiology-almost three centuries after *Antoni van Leeuwenhoek* (Martinko, 2003) observed the 'animalcules' under his microscope i.e. the first reported work describing the growth of bacteria in attached slime layers in the 1940's. The term biofilm appeared in the scientific lexicon after further three decades/1984 to describe these microbial slimes (Bryers, 2000)

In 1940s the increased adherence of marine microbiota to surfaces that were introduced into the abiotic environment was termed "bottle effect" (Heukelekian & Heller, 1940). This finding was later supported by the observation made by Zobell, (1943) in his study that reported a significantly higher number of microorganisms attached to surfaces as compared to the surrounding sea water. However, it was with the advent of the electron microscope that an in-depth and finer exploration of biofilms was enabled as the higher magnification and resolution was provided as compared to the light microscope. Transmission electron microscope (TEM) and scanning electron microscope (SEM) allowed an even more detailed investigation of biofilms in trickling filters to be carried out and revealed the microbial diversity existing within biofilms (Jones et al., 1969). Furthermore, in this research study with the use of Ruthenium Red; a polysaccharide targeting stain, along with the use of fixative osmium tetraoxide, it was also shown that biofilm matrix is in fact polysaccharide in nature (Heukelekian & Heller, 1940). In 1973, microbial biofilms

in industrial water systems were reported to be persistent in these systems and were also chlorine resistant (Characklis, 1973). In 1978,the mechanism by which microbial life attached to both biotic and abiotic surfaces and the advantages that were gained by such an attached growth was explained on the basis of their existence in river streams and dental plaques (Costerton et al., 1978). Following this work, research on biofilms has been carried out in the medical, environment and industrial settings.

In the 90s, majority of the work on biofilms relied on the use of techniques such as SEM and culture-based work for characterization of biofilms. However, in the last decade, two important thrusts dramatically improved our capacity to understanding biofilms; utilizing confocal laser scanning microscope (CLSM) and studying genes in biofilm forming bacteria for their biofilm forming capabilities (Doiron et al., 2012). The biofilm formation process can be broadly divided sequentially into 9 steps that collectively contribute and facilitate the process by which microorganisms are enabled to come in close proximity to a surface, firmly attach to it, stimulate quorum sensing and evolve into intricate structures (Chmielewski & Frank, 2003). These steps include; adsorption or coating of ambient macromolecules present in the immediate liquid environment on to the attachment surface by natural contact or intentional pre-coating, deposition of the planktonic cells, their subsequent adsorption; the de-attachment of reversibly bound cells, initiation of cell-cell signalling molecules that results in the stimulation of exopolysaccharide production, nutrient and metabolic by-products transfer across the biofilm, and the shedding and removal of biofilms from the surface (Bryers & Ratner, 2004).

Various factors influence microbial attachment to surfaces and the initiating process of biofilm formation. With respect to the substratum's adhesion surface properties generally texture, charge, polarity and presence of film influence the biofilm formation. Generally, a surface that is hydrophobic, carries a charge, has a rough texture, and a conditioned film developed over it positively favours biofilm development (Min et al., 2006). While in the surrounding bulk liquid the pH, flow velocity, nature of cations, temperature, nutrient availability and presence of antimicrobial compounds also affect biofilm development (Simões et al., 2011). A positive correlation is seen between the nutrient flow, sheer stress and flow velocity and biofilm development, when the aforementioned parameters are below their respective critical values (Stoodley et al., 1999). Similarly, cell surface properties such as extracellular appendages, cell surface hydrophobicity, participation in quorum sensing and exopolysaccharide molecules are also important determinants that positively contribute to the biofilm phenomenon (Stoodley et al., 1999, Allison, 2003). The former two play a pivotal role in cell adherence to each other as well as to the supporting surface. Extracellular surface appendages such as pili, fimbriae, prothecae, and stalks have a lower surface interaction with the substrate but nevertheless have been documented to play a significant role in biofilm formation (Min et al., 2006). Flagella primary function is to transport and overcome the repulsive forces at the surface through its propulsive movements (Sutherland, 2001, Zobell, 1943, Simões et al., 2011, Min et al., 2006, Donlan, 2002a). Similarly pili are believed to enhance adherence by surmounting the electrostatic repulsion barrier

between cells and the surface by making the cells more adhesive (Harbron & Kent, 1988) although they may not necessarily play a part in biofilm formation (Chmielewski & Frank, 2003, Stoodley et al., 1999).

Surfaces that provide bacteria with a moist environment, in addition to nutrient exchange and most importantly a surface anchorage will support biofilm growth and development (Harbron & Kent, 1988). The substrates supporting biofilms range from biotic surfaces like soil, aquatic interfaces and biological matrices to abiotic surfaces that include prosthetic devices, urinary catheters, implants, water and waste water pipelines to name a few (Allison, 2003). In view of this ubiquity of biofilms, 99% of microorganisms live in biofilms mode (Vu et al., 2009), and their impact in various disciplines ranging from medical to biotechnology has resulted in a paradigm shift in the subject of biofilms from a specific-field based approach to a more holistic approach that is multi-disciplinary (Czaczyk & Myszka, 2007).

2.3.1. Extracellular Polymeric Substance (EPS) Matrix

The extracellular polymeric slime is a major constituent of the biofilm architecture-a fact that is supported by two empirical findings; it constitutes 50%-90% of total organic content of biofilms and makes up about 90% of the total dry matter of biofilms as opposed to the embedded microbial cells that comprise only 10% of the dry weight fraction of biofilms (Flemming & Wingender, 2010). Because of the role it serves as the scaffold of biofilms, the extent to which bacteria will adhere to surfaces as well as co-aggregate is influenced to a great extent by the exopolysaccharide production (Frank & Belfort, 2003). The EPS role in adherence is attributed to its preconditioning of the substrate surfaces via the development of a film around the cells and the facilitation of interaction between the cells with each other and the constituents by virtue of its complex chemical nature (Olofsson et al., 2003, Walker, 2005Donlan & Costerton, 2002). The integral role played by EPS is not only limited to adherence and co-aggregation but extends to encompass cohesion, retention, protection, sorption of organic and inorganic ions, spatial environment for catalytic activity and stabilization of enzymes, quorum sensing, export of cell components (Flemming & Wingender, 2010, Donlan & Costerton, 2002, Gilbert et al., 1997, Nichols et al., 1989, Gacesa, 1998, Schink, 1997).

The variations observed in the rheological and adhesive properties of the EPS are due to the variations that occur in its physical and chemical properties (Frank & Belfort, 2003), in response to the fluxes in the shear forces, availability of nutrients and the temperature in the external environment (Flemming & Wingender, 2010). Dubbed as the "dark matter of biofilms" due to the diversity of biopolymers present in its matrix and the challenges faced in their identification (Flemming etal., 2007), EPS are primarily composed of polysaccharides (Garrett et al., 2008) but also contain other constituents e.g. proteins, lipids, nucleic acid and humic substances (Branda et al., 2005). In addition the biofilm matrix is largely composed of water that confers a buffering capacity on the biofilm microbiota against changes in the water potential of the surrounding external environment (Flemming & Wingender, 2010).

The polysaccharides that are commonly found in EPS, vary in different bacteria, for instance in case of Gram negative bacteria, they are either polyanionic or neutral (Sutherland, 2001) whereas the EPS of the former usually has a positive charge (Hussain et al., 1993). The negative charge that is observed is due the presence of ketal-linked pyruvates and uronic acids (Sutherland, 2001) and confers the biofilms with the ability to associate with divalent cations such as magnesium, calcium and iron; thereby increasing the tensile strength of the biofilm due to cross-linking between the polymer strands (Flemming et al., 2000). The EPS secreted by coagulase negative *Staphylococcus* sp. was determined by Hussain et al. to be a mixture of techoic acids with a small quantity of proteins. Furthermore, the EPS of a biofilm maybe hydrophobic, hydrophilic or display both properties (Hussain et al., 1993). Moreover, the solubility of EPS depends on the structure and composition of the constituent polysaccharides of the EPS. For instance, 1-3 and 1-4 linked hexoses confer a larger rigidity and insolubility to EPS (Sutherland, 2001). Apart from this contrary, to previous held belief, EPS show heterogeneity in their structure-with micro colonies representing the basic aggregating units that are separated from each other by interstitial voids (Flemming & Wingender, 2010, Kaplan, 2010, Donlan, 2002b). Bacterial biofilm development by different organisms was studied by determining the specific binding value of lectins to simple sugars. It was demonstrated that the amount of EPS produced by different organisms is different, with the amount increasing with the age of the biofilm (Leriche et al., 2000).

Methods used for extracting EPS are classified into the following categories; physical, chemical and combination of physical-chemical methods (Stoodley et al., 1997). Physical methods involve using physical force to separate EPS from cells and include the following techniques; sonication, sonication followed by centrifugation, ultra-centrifugation, dialysis (Sheng et al., 2010), cation exchange (Comte et al., 2006) and heating (King & Forster, 1990). Chemical methods encompass those techniques in which a chemical reagent is used as an extractive agent to loosen the EPS from the cells (Frølund et al., 1996). Chemical reagents used in chemical methods include EDTA, CER, NaCl, acidic treatment, $NH_4OH/EDTA$, sulfide, NaOH, glutaraldehyde, crown ether and enzymes (Karapanagiotis et al., 1989). The advantage of physical methods is that while the EPS extracted is less, there is also a less chance of contamination from cell lysis. Whereas in the case of chemical methods, the yield of EPS is greater but the probability of cell lysis occurring is also more (Stoodley et al., 1997). The combination of both physical and chemical methods provides an edge over relying on just physical or chemical methods as it gives a higher yield while ensuring reproducibility of the method(Liu&Fang,2002).

Different physical along with chemical methods were compared for EPS extraction of *Salmonella* SA1685 cells and noted that EPS yield is dependent on the methodology used. The highest yield was from the ethanol method, followed then by lypholization method. Whereas the sonication method had the lowest but quickest yield amongst all three methods studied. In addition, all methods were dependent on the experimental conditions, which in this case were ionic strength and exposure (Wingender et al., 1999).

The EPS extracted can be analyzed for the constituents using various methods that include the conventional colorimetric method that is used for the identification of carbohydrates and proteins (Gong et al., 2009), FTIR (Lowry et al., 1951), IR (Wingender et al., 1999), HPSEC (Omoike & Chorover, 2004), GC-MS (Garrote et al., 1992) to name a few sophisticated techniques. In addition the shift to innovative techniques such as ESEM, AFSM, CLSM has enabled the analysis of an undisturbed hydrated biofilm environment that in turn has allowed a more holistic understanding of the three dimensional structure of the EPS (Tolker-Nielsen & Molin, 2000).

2.3.2. Bacterial Diversity

The bacterial population in biofilm can be identified using either culture dependant techniques, or molecular based approaches (Deng et al., 2012). Though the traditional culture dependant techniques enable the identification of bacteria based on biochemical characteristics and the morphology of the isolated colonies, these techniques are limited by the inherent biasness introduced by the culture media. Furthermore, non-culturable bacteria cannot be identified nor is the dynamics of the microbial communities reflected (Belila et al., 2012).

On the other hand molecular based techniques, such as 16 S rRNA identification followed by quantitative FISH provide a more definite characterization of microbial communities residing within the biofilms; therefore this combined approach drawing the use of these two aforementioned molecular techniques has been termed 'full-cycle rRNA study' (Snaidr et al., 1999, Layton et al., 2000, Juretschko et al., 2002). Moreover, FISH-MAR has also been applied to carry out an accurate study of the growth of filamentous organisms in activated sludge (Gieseke et al., 2001). Nitrifying bacteria that have been extensively cited in literature include *Nitrosomonas europaea* and *Nitrobacter* (Douterelo et al., 2014). Studies have shown that prevalence of *Nitrobacter* is much higher than *Nitrosomonas europaea* (Fu et al., 2010, Dionisi et al., 2002, Daims et al., 2001). Diversity of nitrifying bacteria studied in two lab scale reactors using fluorescently labelled rRNA targeting oligonucleotides, operating at different retention times. The results of this study concluded that majority of the ammonium oxidizing bacteria (AOB) were from subclass of β-proteobacteria, with one population having a close affinity with *Nitrosomonas europaea,* while other population had no close relationship with the characterized AOBs at that time. Dominant species carrying out denitrification were mainly the *Nitrospira* species. In addition, an interesting finding was that diversity of nitrifiers was independent of the retention time of the reactors(Nogueira et al., 2002). Quantitative FISH was used to reveal that the dominating species in the biofilm detected by the probes were members of β-*proteobacteria*. The other significant genera belonged to α-Proteobacteria, *Planctomycetes, Chloroflexi* and the phylum *Nitrospira.* Within the *β-proteobacteria*, 34% and 36% of

the microbial population comprised of *Azoarcus sensu* and *Zoogloea ramigera*, respectively, were the members of this class *in situ* (Juretschko et al., 2002). Amongst the ammonia oxidizing bacteria, an abundance of *Alcaligenes latus, Brachymonas denitrificans* and *Nitrosococcus mobilis* has been reported. A PCR-DGGE based study carried out to analyse the microbial population present within the biofilm of an anaerobic reactor that used wastewater as a substrate showed the dominance of bacteria in the following order; *Clostridia, Bacteroides, Delta-proteobacteria* and *Flavobacterium* (Mohan et al., 2010).

Gomez-Alvarez et al., (2012) characterized microbial diversity in biofilms on wastewater pipelines using molecular studies based on metagenomics studies. Two sections of a severely corroded pipe were used, the top section of the pipe and the bottom surface of the pipe. The authors concluded that aerobic and facultative anaerobes were supported in the top section of the pipe and the bottom of the pipe supported anaerobes belonging to delta-proteobacteria e.g., *Bacteroides* and *Clostridium*.In addition, their findings concluded that bacterial genomic sequences that comprised 90% of the sequences were predominant in the community genome. These bacteria belonged to the Bacteroidetes, Actinobacteria, Firmicutes and Proteobacteria class (Gomez-Alvarez et al., 2012).

2.3.3. Significance of the Surfaces

Biofilm attachment to surfaces has been extensively studied with respect to microbiologically induced corrosion (MIC) or biofouling of piping surfaces employed in water, waste water, oil and gas distribution networks, bioreactor membranes or propagating surfaces (Schwermer et al., 2008, Nguyen et al., 2012). The preference of bacteria to grow on surfaces rather than in the aqueous phase (Kim et al., 2012) is contributed by a complex interaction between the bacterial and substrate surface's chemistries and the aqueous phase. Initially, the adherence to surfaces is due to an initial attraction between surfaces and cells (Rijnaarts et al., 1995). Both physical and chemical forces influence attachment. Several theories exist that aim to explain these physicochemical interactions.

The well-known *Derjaguin-Landai-Verwey-Overbeek (DLVO)*theory explains the interactions between the microorganisms and surfaces as arising from the equilibrium between the attractive Vander Waals forces and repulsive forces arising from the charge interactions between the substrate surface and the cell's surface (Loosdrecht et al., 1990, Rutter & Vincent, 1984). However, the DLVO theory is considered flawed and is greatly limited by several considerations that it does not account for (i) the molecular interactions between the cell and the surface (ii) molecular appendages that are contributing to the surface interactions and substratum roughness (iii) a simplified assumption that a direct relationship exists between the charges on a cell surface and the substratum's surface (Walker et al., 2004). The thermodynamic theory takes into consideration various factors such as the Gibbs free energy of the interacting surfaces and the aqueous phase as well as various interacting forces (Busscher & van der Mei, 1997). Bacterial attachment is explained through three theories; Neumman's theory, Electron-electron donor approach and Polar dispersion approach (Busscher et al., 1984). The limitations of this theory are many such as interpretations are not based on the kinetic model, attachment is considered to be a

reversible process although in reality it is the opposite and the difficulty in finding out the free energy of interacting surfaces (Morra & Cassinelli, 1997).

The *extended DLVO theory (*XDLVO) theory tries to explain bacterial attachment in physicochemical terms by filling in some of the gaps in the previous two theories (Oss et al., 1986). Firstly in addition to the distant dependent forces it also takes in to account acid-base interactions and hydration energy (Meinders et al., 1995). Secondly, forces are accounted for in a time dependent manner, that is, an exponential decrease in acid-base interactions is measured (Katsikogianni et al., 2004).

Although these physicochemical theories have helped explain some of the attachment processes involved in biofilm they have not been able to explain the whole process due to time dependent variations that are introduced in a system when bacterial aggregation on surfaces begins and post conditioning is initiated due to various metabolite production and degradation (Mack, 1999). Furthermore, bacterial surfaces are complex and biological factors such as gene expression are not accounted for (Heilmann et al., 1996). However, through these theories one can set up a framework for predicting the phenomenon of bacterial adhesion to different substratum (Katsikogianni et al., 2004).

2.3.4. Significance of Ions in Wastewater Treatment

After the adherence of bacterial cells to the surfaces, the EPS matrix of biofilms is influenced by the characteristics of the support materials. The existence of cations on the surface of materials act as lipopolysaccharide cross linkers and promote the integrity of the cell membranes (Garny et al., 2008).

The physicochemical theories discussed above take into great consideration the role of cations, as these positively charged species play an integral role on cross linking the EPS matrix and in stabilizing the integrity of the outer cell membrane surface (Song & Leff, 2006, Wilén et al., 2008, Kara et al., 2008). Moreover, wastewater treatment technologies that manipulate biofilms for treatment purposes, such as the moving-bed biofilm reactor, have directed research to focus on the effect of wastewater composition on biofilm activity and stability (Ødegaard, 2006). In particular studies focused on calcium, one of the commonly found divalent cations, have shown that it effects the attachment and de-attachment of biofilms (Ahimou et al., 2007, Huang & Pinder, 1995, Körstgens et al., 2001) due to the ability of divalent cations to intercalate the negatively charged chemical constituents of the EPS matrix; thus increasing the mechanical stability of biofilms. Furthermore, the findings of Sobek and Higgins (Sobek & Higgins 2002) led them to conclude that the biofilm EPS layer acts an ion exchange resin, where the divalent inter-linkages are in a dynamic state due to the constant competition between monovalent and divalent/trivalent cations.

In industrial wastewater treatment the application of divalent cations to increase activated sludge stability, flocculation and dewaterability has been studied (Flemming & Wingender, 2001). Moreover, the role of trivalent cations, particularly Fe^{3+} and Al^{3+} has also been studied with regards to stabilizing the EPS of activated sludge flocs, with a positive correlation described between the trivalent ion concentration and flocculation (Li et al., 2014, Park et al., 2006). However, the role of these flocculating agents has not been extensively studied (Park et al., 2006, C. Park et al., 2010). Fang et al., (2002) studied the effects of toxic

metals, commonly present in wastewater discharged by heavy industries, on the sulfate reducing bacteria (SRB) biofilms that are commonly found on steel pipelines. Metals studied included Cu, Zn, Pb, Cr and Al and were taken at a concentrations range between 20mgl⁻-50mgl⁻. The biofilm structure was examined using atomic force microscope (AFM), scanning electron microscope (SEM), and EPS analysis. SRB were reduced the most in case of Cu^{2+} followed by Cd^{2+} with aluminum affecting the least i.e., 77% of sulfate was reduced in the reactor. It was also observed that cluster formation and EPS secretion is enhanced when toxic metals were present and that microbial induced corrosion (MIC) was caused as a result of the acidic nature of EPS (Lewandowski et al., 1994) and its inherent iron chelating property (Beech et al., 1998). In another study the influence exerted by aluminum and copper on the bacterial biofilms was studied in different growth media. It was found that media composition and buffering capacity both influence metal effect on the growth of biofilm. *P. aeruginosa,* a biofilm former, possesses the mechanism to resist heavy metals from the environment by absorption of toxic ions in the EPS (Booth et al., 2013).

2.3.5. Biofilm Reactors

Biofilm reactors used in in vitro studies are based on the following two basic types of systems; batch reactor systems, and open systems. The most widely used model is the microtiter plate model (Cerca et al., 2005, Peeters et al., 2008, Shakeri et al., 2007), that falls in the closed batch reactor design (Vandecandelaere et al., 2016). In the MTP, biofilm being studied is grown on the polystyrene surfaces of the microtiter wells or on coupons placed within these wells (Coenye & Nelis, 2010). The popularity of this model arises from the ease in handling it and simultaneously carrying out a multitude of batches or experiments under the same conditions or varying conditions of substrate concentration, nutrient composition, and inhibitory substances (Niu & Gilbert, 2004). In addition, the effect of varying different parameters that influence biofilm development such as oxygen and carbon dioxide concentrations, nutrient concentration, hydrodynamic shear stress and temperature, can be monitored easily (Stepanović et al., 2000, Krom et al., 2007). It is also used widely for distinguishing non-biofilm formers from biofilm forming isolates and strains (Wang et al., 2020, Jiménez-Fernández et al., 2016). Moreover, MTP is popularly applied for thorough studying of how conditioning materials affect the biofilm development (Prijck et al., 2010). As the method is a closed batch reactor it is limited by its inherent design such that with the passage of time the environmental conditions change and constitute a dynamic variable (Coenye & Nelis, 2010).

Converse to the design of closed systems, open biofilm systems involve a continuous and semi-continuous addition of nutrients into and removal of waste out of the biofilm reactors (Busscher & Van Der Mei, 2006). Subsequently, based on their operation they are sub-categorized as; plug flow reactors and continuous flow stirred tank reactors. The operation system in the latter works at a steady state i.e., concentration does not vary as the effluent rate is equal to the dilution rate. Furthermore, it is comprised of homogenous mixing with the dilution rate kept greater than the doubling time of microorganisms so the growth of only fixed bacterial cells occurs within the reactor. In former case, mixing occurs through

diffusion where the flow of influents is axial, with conditions progressively changing through the reactor (Coenye & Nelis, 2010).

One of the flow systems commonly used for studying biofilm formation under fluid flow conditions and in a reproducible manner is the modified Robbins device (MRD) (Jass et al., 1995). The MRD has a stainless steel or plastic body with an internal construction consisting of vertically arranged rectangular cross sections that contain numerous linearly arranged ports and each port holds a pressed-fit plug with a disc inserted in it. The discs serve as surfaces on which the biofilm is developed (Honraet & Nelis, 2006, Krom et al., 2009). A flow cell is a derivative of the MRD. It enables real time study of biofilms by using non-destructive techniques such as microscopic analysis (Sternberg & Tolker-Nielsen, 2006). They were initially used for studying the efficacy of biofilms for the biodegradation of different recalcitrant compounds (Møller et al., 1997, Lappann et al., 2006). However, the applicability of flow cells has extended to studying biofilm formation by clinically relevant strains like *L. pneumophila,Neisseria meningitidis*, (Mampel et al., 2006), *P. aeruginosa* (Haagensen et al., 2007), and *Staphylococcus epidermidis* (Qin et al., 2007) for studies on oral biofilms (Foster & Kolenbrander, 2004).The formation of biofilms on surfaces in the food industry, water and waste water distribution system has been extensively studied using flow cell models. In a study employing the flow cells, *L.monocytogenes* biofilms were developed on FC 81 Model flow cell that was connected to TLSCM to study the real time non-destructive genotype and structural variations in the biofilm in a time dependent manner. The study included biofilm studies under both batch and dynamic conditions. It was observed that morphology of cells changed from both short rods to mesh-network when the operation of the cell was switched from static to continuous flow (Habimana et al., 2009, Liu & Tay, 2002).

2.4. Microbial Potential for Bio-electricity Production and Microbial Fuel Cell Technology

In 1911 M.C. Potter first suggested the concept of electric current generation from bacterium *Escherichia coli*. A microbial fuel cell (MFC) uses bacterial catalytic reactions to convert the chemical energy of organic substrates into electrical energy. The performance of an MFC depends on the exoelectrogenic microorganisms and mechanism involved in extracellular electron transfer (EET). Therefore, understanding the microbial community composition and dynamics of biofilms on the surface of the electrodes is important besides studying their electron transfer pathways (Cao et al., 2019). A number of ecological conditions, such as type of inoculums and nutrients, temperature, pH, presence of exogenous mediators and light affect the structure of microbial communities of biofilms in the MFCs (Angelaalincy et al., 2018, Jones & Buie, 2019). Therefore, optimizing these conditions for improved enrichment of exoelectrogens and current generation is essential. Typically, MFC is comprised of an anaerobic biotic chamber separated from aerobic abiotic chamber by proton exchange material (salt bridge or proton exchange membrane) (Palanisamy et al., 2019). Microbial fuel cell (MFC) is expected to be the next generation fuel technology that exploits oxidizing potential of microorganisms for treatment of wastewater as well as production of electric energy. It is principally based on enzymatic reactions of electricity producing microorganisms to convert the chemical energy of bioconvertible organic

compounds into electrical power (Rahimnejad et al., 2015). Bacterial biofilm on anode metabolizes organic matters and produces protons and electrons. Proton exchange membrane (PEM) allows the diffusion of protons across the chamber where electrons from anodic biofilm are transported to cathode via external circuit where electrochemical reduction of oxygen occurs to complete the cathodic reaction (Sivasankar et al., 2018). High redox potential and unlimited availability in air makes oxygen preferable electron acceptor in MFC operation. At cathode surface, different metallic and non-metallic catalysts are used to reduce the cathodic activation over-potential and improve system performance. The transfer of electron from cells to anode can occur either directly by nanowires and outer surface proteins or indirectly by using natural and synthetic mediators (Zhang et al., 2019,Yang et al., 2020).

NASA conducted advance research for application of MFC in space missions (Collins, 1986). Later Allen and Bennetto studies in early 80s started a very active and new research period of MFC work and brought new insight of mediators role in electron transfer to anode surface from microorganism but MFC receives interdisciplinary interest of electrochemistry, engineering and microbiology with the discovery of particular bacterial genera *Geobacter* and *Shewanella* sp. have ability to directly transfer electron from their cellular metabolic pathway to anode (Allen & Bennetto, 1993). The significance of MFC technology was increased later, when it was found that bacterial community present on anode are not only responsible for electricity generation, but they can also bring about organic matters or wastes biodegradation (Rabaey et al., 2005, Logan, 2007). MFC has been primarily centered for the treatment of domestic wastewater and production of renewable energy (hydrogen) and electricity (Munoz-Cupa et al., 2021). Remarkable improvements have been done so far in MFC technology for the purpose to enhance power output which includes introduction of novel electrode material, replacement of membrane with separator, use of artificial electron shuttles and transition from dual chamber to single chamber scheme (Franks & Nevin, 2010).

MFC has been examined for various other applications including: the unique concept of power generation by using sediment's organic matter makes sediment microbial fuel cell (SMFC) a reliable energy source in remote areas (Algar et al., 2020). MFC technology gained significance when it was recognized as an opportunity to treat wastewater by metabolizing organic matter. A double chamber cell with carbon felt electrode was designed by Zekker et al., (2020) to study exoelectrogenic role of anammox biomass as an inoculum and comparing it with usually used inoculum i.e., mixed-anaerobic sludge. They analyzed nitrogen removal, electricity generation, waste-water treatment and found improved results with ANAMMOX biomass. Nguyen et al. (2020) found significant role of Chlorophyta, Proteobacteria, Bacteroidetes, and Cyanobacteria for nutrient removal and electricity generation in MFCs(Nguyen & Min, 2020). A limitation to their system was lack of current production at HRT lower than 10h and higher than 60h. Khajeh et al., (2020) made a successful attempt to decolorize wastewater along with electricity generation using dairy products. Similarly, Long et al., (2019)treated azo-dye wastewater with MFC in continuous flow. During a span of 400 days, the power output declined with time as microbes responsible for electricity production decreased. Zhang et al., (2020) concluded that electricity generation, COD and

nitrogen removal are in positive correlation with cathode's DO concentrations. Their designed MFC was independent of external electricity source, pH solution and AEM circulation device. Further, exoelectrogens showed involvement besides ammonia and nitrite oxidizing bacteria. About 36.90% of fermentative or hydrolytic bacteria were utilized by Zhang et al., (2019) as the electrode microbiome for stable and long-term electricity generation alongside waste water treatment. The variations in the different aspects of MFC design and electron transport mechanism formulate different types of MFCs which differ in their electrogenic potential such as electricity generation capabilities.

2.4.1. Architecture and Performance of Microbial Fuel Cell

The power of microbial fuel cell (MFC) is dependent on the several factors (Fig.2.1) such as, MFC design (double chamber or single chamber), MFC architecture (membrane or membraneless), mode of operation (batch or continuous), nature of cathode (biotic or abiotic), type of MFC (mediated MFC or mediator less MFC) and fuel type (bio-electricity or bio-hydrogen). Various obligate and facultative anaerobes are capable to produce hydrogen gas by metabolizing organic waste.
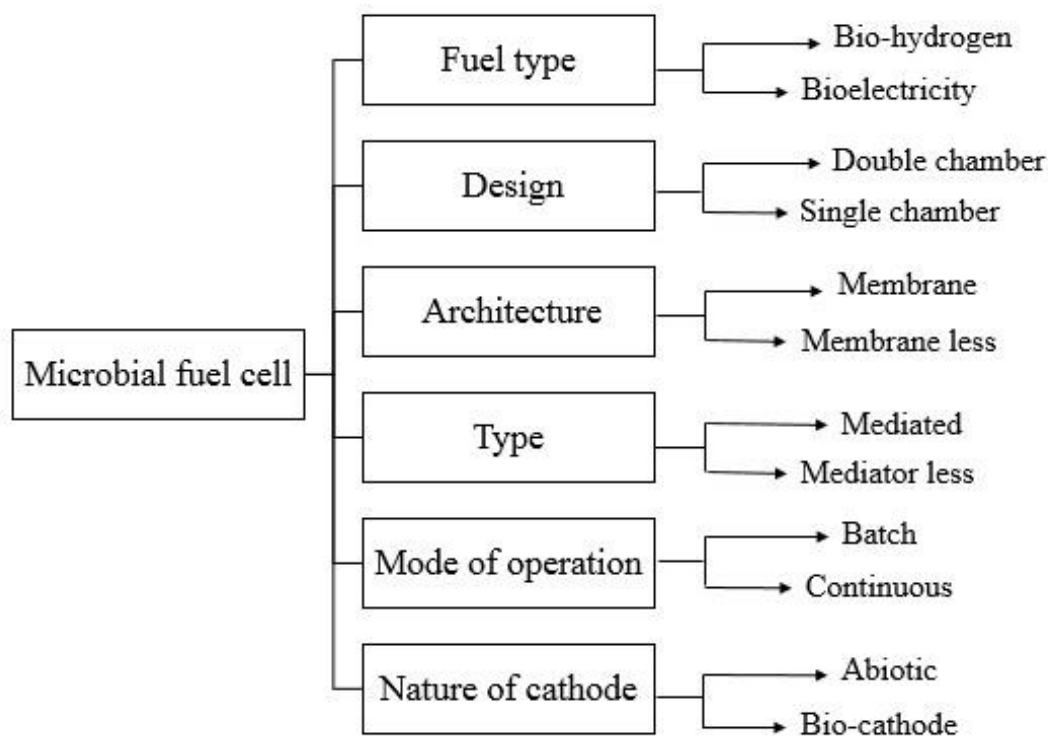
Figure 2. 1 Various operational settings employed in MFC technology.

Double chamber MFCs are commonly used for wastewater treatment with simultaneous current production but the use of single chamber system is also increasing.

2.4.1.1. Double Chamber MFC

Microbial fuel cell technology offers a striking means to categorize wastewater as an eco-friendly renewable source of energy. The usual design of double chamber has two characteristic compartments separated by partition. One chamber is operated under aerobic conditions (cathode) and other operates in oxygen limited conditions (anode). On the basis of partition system employed double chamber

arrangement of MFC can be further classified into salt bridge MFC or membrane MFC. Partition serves as proton exchange system between both compartments. Moreover, it tends blocks oxygen diffusion into anode from cathode. Protons are conducted internally across the bridge in salt bridge MFC and via proton exchange membrane (PEM) in membrane MFC. Double chamber design is generally suitable for treatment of wastewater. Maximum current of 0.84 mA has been indicated to produce in double chamber MFC using domestic wastewater of 75% strength (Liu et al., 2013). Internal resistance of salt bridge is comparatively higher than proton exchange membranes which lead to ohmic losses and reduction in COD removal efficiency. Due to these limitations single chamber MFC is considered more efficient for wastewater treatment and concurrent energy generation. The typical double chamber MFC is H-shaped where half section is anaerobic and other half is aerobic. In anode chamber anaerobic conditions are established, microorganisms oxidize organic substrates of wastewater under oxygen deficient conditions. In the absence of conventional terminal electron acceptor (oxygen), electron is consistently delivered to the anode. The potential difference between the electrodes derives electrons travel towards cathode. This movement of electrons generates electric current. The succeeding reaction is completed when subsequent electron combines with protons at anode to form water. The rate of reduction reaction at cathode signifies the performance of system (Hamed et al., 2020).

Electron transfer to anode is facilitated either directly or indirectly. Direct electron transfer occurs either via c-type cytochromes or bacterial nanowires (pili and flagella) (Santoro et al., 2012). An economical MFC design replaces PEM with salt bridge. Salt bridge consists of agar as solidifying agent and conducting salts e.g. KCL or NaCl to carry protons through the junction. A glass rod packed with saline agar is fixed between anode and cathode chambers. Due to considerable high internal resistance of salt bridge MFC power generation is inadequate which is limited to 3 mWm^{-2}. However cost-effective structure of salt bridge MFC sorts it an attractive option for wastewater treatment (Liu & Logan, 2004). Membrane MFCs use polymers of Nafion or Ultrex affixed between compartments (Koók et al., 2020).The main functions achieved by PEM involve separation of chambers, oxygen blockade into cathode as well as wastewater confinement into anode. The power density is influenced by rate of proton transfer via PEM. Insufficient conduction of protons through PEM makes the process relatively slow (Watanabe, 2008,Osman et al., 2010).The leakage of oxygen into anode caused by fouled PEM affects the performance of cell. Fouling is predominantly due to presence of suspended solids and contaminants present in wastewater. Rigorous aeration is desired to maintain high level of dissolved oxygen in anode which makes the double chamber design costly for practical applications. Moreover, PEM increases the overall cost of construction, and offers high resistance. In addition, PEM employed in double chamber MFC are expensive, offers considerable resistance in operation. Thus, power density of double chamber design is low as compared to single chamber system. In SCMFC highest current density of 0.25mA/cm² was examined when using paper industry wastewater. However current density of 0.005 $mAcm^{-2}$ was reported when double chamber system was used with same substrate (Logan & Regan, 2006b,Choudhury et al., 2017).

2.4.1.2. Single Chamber MFC

In contrast to dual chamber organization single chamber design encompasses both electrodes i.e. anode and cathode positioned in one compartment. The electrodes may be retained either distant or adjacent separated via PEM. Increased power output of SCMFC is influenced by decreased space between anode and cathode as it tends to reduce internal distance of system. Moreover SCMFC scheme excludes the usage of catholyte with oxygen in air (Cheng et al., 2011). In contrast to double chamber assembly of SCMFC is more economical and produce relatively higher power (Du et al., 2007). High molecular oxygen concentration in air and absence of need to employ vigorous aeration reasonably improved cathodic performance is achieved. In SCMFC lesser cell volume is able to supply higher power. Highest current density of 71 mA/m^2 was produced from SCMFC with working volume of 220ml. SCMFC can also be operated in membrane-less air cathode assembly to obtain even greater energy output (Zhang et al., 2011). Nevertheless, absence of membrane reduces the overall resistance, on other hand CE and bacterial catalytic activity is compromised due to increased diffusion of oxygen into anode.

In SCMFC anode comprised of characteristic carbon based material while cathode is either made of permeable carbon or PEM bounded carbon (Zhao et al., 2006). Predominantly in this arrangement carbon anode is associated with air-cathode. Gas diffusion layer marks a boundary between anode and cathode to block oxygen intrusion into anode. The cathodic reactions occur at adjoining line of anode and cathode electrodes. Electrons and protons released from bacterial metabolism combine with oxygen in air on inner side of cathode to form water (Choudhury et al., 2017). The reduced cost, lack of aeration and no use of oxidizing agent makes SCMFC more pliable to employ for wastewater treatment (Liu & Logan, 2004) SCMFC is more simple and easy to scale up in comparison to double chamber MFC. However main issue of cathode flooding and drying needed to be managed during operation. Various designs of SCMFC have been proposed so far at laboratory scale. Increasing the cathodic surface area enhance cell performance by 62% whereas increasing the anodic surface area improve energy efficiency by 12%. Cylindrical air-cathode surrounded by eight graphite anode design was proposed by university of Pennsylvania. Highest power density of 26mW/m^2 was generated with COD removal efficiency of 80% with this system using domestic wastewater (Liu et al., 2004). Air-cathode assembly is most commonly used cathode SCMFC operation (Bond & Lovley, 2003). The air-cathode is in connection with atmospheric air on one side (outer) and to wastewater on other side (inside). Anode is kept airtight to prevent oxygen diffusion. However in MEC that produce hydrogen gas both chambers are anaerobic at and PEM is wrapped around cathode to preclude oxygen reaction at cathode (Liu & Logan, 2004). Similarly following this principle multilayered air-cathode can be fabricated in SCMFC where gas- diffusion layer separates anode and cathode as well as prevents oxygen from atmosphere to enter anode. In addition, GLD layer offers protection from corrosion and water leakage. Passive diffusion of oxygen to cathode decreases energy demands. Carbon cloth and carbon paper are used to assemble GDL layer in air-cathode (Lovley, 2006). Energy generation in terms of greater current density and power density is achieved in SCMFC using air-cathode (Liu et al., 2005). Due to high oxygen flux in air cathodic reaction is significantly enhanced (Cheng et al., 2006). The abundant availability of conventional electron acceptor is main reason for

higher power generation. COD removal efficiency is more or less alike in both designs such as double chamber MFC and SCMFC. However SCMFC exhibits relatively stable COD removal efficiency than double chamber MFC (Logan et al., 2007). Membrane-less scheme is more economically approachable in SCMFC as it produces relatively greater power due to reduced resistance (Liu et al., 2004). However columbic efficiency is lower in membrane-less air-cathode (Liu & Logan, 2004). Oxygen contents are increased in anode due to permeability of membrane that reduces the catalytic activity of bacteria (Logan, 2010,Wen et al., 2010). Moreover, membrane-less air- cathode system is more likely to suffer from microbial contamination due to biofilm development on anode side of air-cathode (Kim et al., 2011). In 2005 Min *et al* studied that SCMFC with air-cathode operated with animal wastewater produced 79% greater power density i.e., 261 mW/m² than domestic wastewater (14678 mWm⁻²). In SCMFC power density is improved e.g. increased to 371710 mW⁻² (Min et al., 2005). The single chamber MFC with air-cathode is more reliable to use and practical to apply in real world because it offers higher electricity generation, reduces the construction cost and requires low maintenance as compared to double chamber MFC.
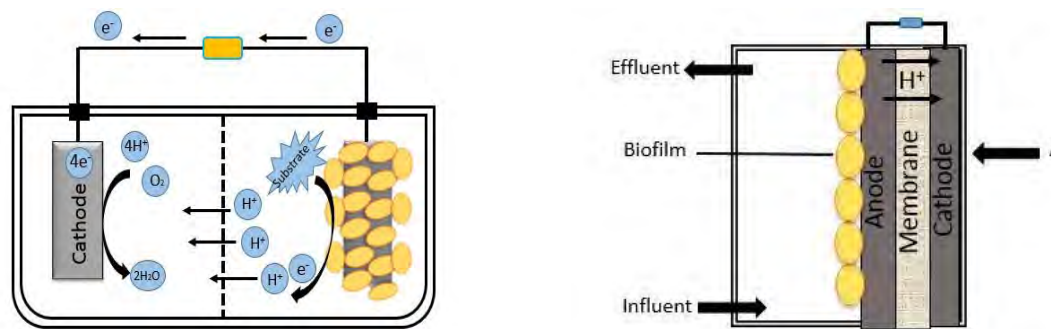
Figure 2. 2 Double chamber (left) and single chamber (right) MFC.

2.4.1.3. Mechanism of Electron Transfer

A wide range of electroactive bacteria interact at the anode (electro-reduction) and cathode (electro-oxidation) of MFCs for current generation. The need for wastewater treatment due to scarcity of water resources and environmental concerns encourage for the use of wastewater and other cost-effective sources as a fuel for MFC. However, the term electricigens, electrode reducers or electrobacteria is predominantly assigned exclusively to those microorganisms that tend to completely oxidize the organic matter into carbon dioxide. These microorganisms are essentially metal reducing in nature. Microorganisms capable to donate electrons to the anode(s) to prime power production are specifically referred as electrode reducers or electrode reducing bacteria (Lovley & Nevin, 2014). Most prominent electricigens belong to the family of *Geobacteraceae* that can proficiently create power under the conditions of inadequate electron acceptors (Leang et al., 2013). Electricigens has made possible to construct microbial fuel cell that can offer potential advantage over hydrogen fuel cell.

2.4.1.3.1. Direct Electron Transfer via *c*-type cytochromes

In 1990s B-H. Kim, identified the mechanism of direct electron transfer to anode without employing mediating molecules. Direct electron transfer demands that either bacterial cell membrane or membrane

bound organelles essentially have a physical connection with the anode electrode surface. Metal reducing microorganisms that inhabit the sediments such as *Geobacter* sp., *Rhodoferax* sp., *Aeromonas hydrophila,* and *Shewanella* sp. have ability to directly transfer the electrons to anode without assistance of soluble shuttles (Cheng et al., 2010). These species harbour the cell surface redox active proteins i.e. c-type cytochromes (OmcS), OmcE, multi heme proteins in their outer membrane and inner membrane governing the straight transfer of the electron to the insoluble mineral surface, such as oxide minerals or MFC anode (Malvankar et al., 2012). *Geobacter sulfurreducens* localize most of their membrane-bound respiratory enzymes on the outer membrane to ensure the direct contact with extracellular electron acceptor such as ferric ion. However, these respiratory enzymes behave in the same manner at anode of MFC. The efficiency of this mechanism is often hindered by dense cell population at anode. It is assumed that 100% columbic efficiency is plausible by direct electron transfer through cytochromes (Nevin et al., 2008). Current generation through metal reducing bacteria depends on proficiency of direct electron transfer and electrochemical activity of bacteria which in turn relies on bacterial concentration and physical contact with anode (Zhu et al., 2011). MFC inoculated with bacterial consortia generated maximum power of 120 mWm^{-2} whereas power density of 270 mWm^{-2} was achieved when pure culture of *Bacillus Subtilis* was employed. Electrochemically active consortia can be developed by enrichment culture techniques. The inocula in mediator-less MFC encompasses both pure and mixed culture of microorganisms (Park & Zeikus, 2000). Mixed culture inoculum is considered cost-effective for practical MFC operations such as, treatment of industrial and domestic influent (Gil et al., 2003).

2.4.1.3.2. Bacterial Nanowires

The long-range electron transfer to the anode is brought about through specialized cell surface conductive pili known as microbial nanowires. The pilin proteins of molecular pili connect to the outer membrane bound *c*-type cytochromes that marks pilin conductivity and conduits the electrons to the exterior of the cell creating probable chance to transfer the electrons even at considerable distance from anode (Gorby et al., 2006). *Geobacter* species are prominent for producing conductive pili or flagella during their growth on Fe^{2+} oxides. Pili and flagella tend to organize an electrical link among cell and Fe^{2+} oxides. Besides *Geobacter* spp. many other dissimilatory metal reducing bacteria also produce pili such as *Shewanella oneidensis* MR-1and non-metal reducing bacteria *Synechocystis* PCC 6803. The development of conductive nanowires lead to the formation of dense electroactive biofilm on anode , thus increasing anode efficiency and ultimately MFC performance up to 10 folds (Strycharz-Glaven et al., 2011). Pili may form an entangled conductive network of nanowires to facilitate electron transfer to the anode. Moreover, pili may also connect cells interior to the conductive biofilm that mediate electron transfer towards anode. Anodic biofilm itself as a whole can act as a conductive matrix and pili represent one of its component (Strycharz-Glaven et al., 2011). Further exploration is required regarding the mechanism of electron transfer through the pili. It has yet to be determined that either conductive nanowires have direct contact to anode surface or bacteria in biofilm have a definite cell-to-cell interaction.

2.4.1.3.3. Conductive Biofilm

Geobacter sulfurreducens is capable of forming electrically conductive biofilm at anode where cytochromes and electron shuttles can readily be withdrawn out of the cell into biofilm matrix to feasibly subsidize electron transfer towards anode (Malvankar et al., 2012). The biofilm is moderately thick (50µm) to facilitate electron transfer from cells that are at substantial distance from anode (Fig.13). The conductive biofilm fashioned at anode has preeminent characteristic to acts as a solid conductor that tends to adjust the electrical potential in the interior of matrix in response to current to mark feasible electron acceptance from bacteria and its conductance to anode (Marcus et al., 2007).
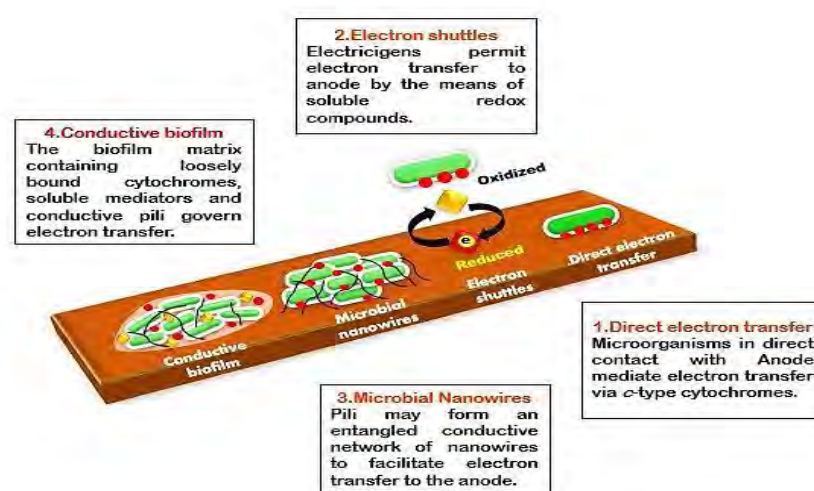
Figure 2. 3 Different mechanisms of extracellular electron transfer (EET) to anode.

Red dots denote c-type cytochromes whereas blocks represent mediator. Thin black lines illustrate conductive pili and cloudy base represents biofilm matrix.

2.4.1.3.4. Electron Shuttles (Mediated MFC)

Allen and Bennetto (1980)**,** established the basic design of MFC that is currently employed in this technology. Moreover, the use of artificial mediators in MFC was also considered to improve current density. Electron transfer to anode is accomplished either indirectly (electron shuttles) or directly (c-type cytochromes, nanowires, conductive biofilm) (Fig.13). In some instances, electricigens permit electron transfer to anode by the means of soluble redox components recognized as electron shuttles which allow long range connection to anode. Mediator compounds are very well stable in both reduced also oxidized state and may be natural or artificial in nature (Harwani, 2013).

Electron transfer through mediators is most commonly applied mechanism in MFC that can be categorized into sub-types, Diffusive electron transfer, which employs freely diffusible mediators that penetrate the microbial cell to deliver electrons from intracellular metabolites to extracellular anode material. Non-diffusive electron transfer, in which mediator molecules are assimilated either on microbial cell surface or anode of MFC (Fig.13) and receive electrons from cell surface without invading into the cell (Logan &Rabaey, 2012). On the basis of the nature of mediators and their linking tactics, electron

transfer mechanism by way of diffusible mediators is further classified as, Electron transfer via artificial mediators, exogenously added artificial mediators such as potassium ferricyanide and benzoquinone are adept to move inside the microbial cell, accept the electron from intracellular carriers and diffuse out of the cell in reduced form to reoxidize at anode by delivering the electron to the anode. Many exogenous mediators are toxic in nature and have short term stability that discourages their use in MFC (Schröder, 2007). Electron transfer via primary metabolite, includes the products primarily related to metabolism, such as, substrate degradation metabolites or reduced electron acceptors and are similar within all the groups of microorganisms e.g. H_2 and H_2S (Schröder, 2007). Electron transfer via secondary metabolite, species specific low molecular weight reversible reduced compounds such as melanin, menaquinone, and reduced riboflavins that are formed by microorganisms such as *Shewanella sp.* to shuttle electrons from respiratory enzymes to the anode under the conditions of low redox potential when electron acceptors are limited (Gorby et al., 2006). Members of genus *Pseudomonas* are well known for producing secondary metabolites that function as redox molecules. Phenazine based compounds produced under anaerobic conditions directly enhance current density (Pham et al., 2008). More recently attention has been drawn to iron (ferrous and ferric iron) in bioelectrochemical systems for electron shuttling and redox reactions (Mancílio et al., 2020).

In spite of enhanced electron transfer, mediators are not generally encouraged for usage in MFC due to some downsides effects (Gil et al., 2003). Neutral red has been reported as an effective electron mediator but needs to be replaced frequently to commence the transfer of electrons and is not self-sustaining (Park & Zeikus, 2000). Therefore, mediated MFC cannot be engaged for operation of extended duration (Read et al., 2010). Even though mediators have been demonstrated to enhance the rate of electron transfer but mediators are expensive, unsustainable and toxic. Further research is required for exploring low-cost quality and non-toxic mediators.

2.4.1.4. Exoelectrogens

Earth atmosphere was devoid of oxygen in early years but still life evolved million years ago by utilizing different mechanisms to reduce compounds for their survival. Metabolism of anaerobes is adapted to drive respiration in the absence of gaseous oxygen. A wide range of electron acceptors including nitrate, sulphate and carbon dioxide can be used by these bacteria. Most anaerobic bacteria prefer soluble electron acceptors (nitrate or sulfate) that diffuse back into cell via cell membrane where bacteria (in MFC) known as exoelectrogens or electrochemically active bacteria (EAB) have ability to directly transfer electrons in outer environment of cell. The direct electrons transfer to a conductive materials or chemicals that are non-immediate electron acceptor distinguish electrochemically active bacteria from anaerobes (Logan & Regan, 2006b). Recently, the studies on exoelectrogens have provided remarkable information about *Shewanella* and *Geobacter species,* two dissimilatory metal reducing model organisms (Chae et al., 2008). Electrochemically active biofilms plays a great role of sustainable bioenergy production but apart from MFC these bacteria are also involve in oxidation and reduction of metals, heavy metals sorption and complex formation and the phosphorus and carbon cycle (Babauta et al., 2012). *Geobacter sulfurreducens*

efficiently produces current in the fuel cells with the electrode as the only source of electron acceptor. The gene encoding OmcF a mono-heme c-type cytochrome present in the outer membrane is essential for optimal Fe^{3+} reduction and electricity generation in MFCs. *Geobacter sulfurreducens* properly localize most of their membrane bound respiratory enzymes on the outer membrane to ensure the direct contact with extracellular electron acceptor such as ferric ion, and cytochromes perform in the exact way with electrode in a MFC (Okada et al., 1999, Fornero et al., 2010). Extensive research has been conducted on electrochemically active Gram-negative bacteria. Gram positive bacteria are generally considered as weak electricigens due to their thick cell wall architecture and presence of peptidoglycan. However, recent studies have described Gram positive electrobacteria. Light et al., (2019)have reported the presence of flavin mediated extracellular electron transfer (EET) pathway in the foodborne pathogen *Listeria monocytogenes*. Similarly, *Thermincola potens* strain JR employs contact dependent mechanism for the EET from cell membrane to the cell surface using c-type cytochromes (Wrighton et al., 2011). Gram positive lactic acid bacteria *Enterococcus faecalis* uses demethyl menaquinone in the respiratory chain for EET without heam proteins (Pankratova et al., 2018).

2.4.1.5. Electrode Material

The electrode material employed in MFCs greatly affects the performance. Several materials have been examined as potential candidates for electrodes to improve the system performance. Selection of electrodes depends upon the properties such as conductivity, surface area, cost, electrochemical stability, surface properties and resistant to microbial degradation. Graphite (rods or plates), carbon mesh, carbon cloth, carbon felt and graphite fibre brush are commonly used as anode due to their electrochemical stability, large surface area and high electric conductivity (Logan & Rabaey, 2012,Logan & Regan, 2006a). Both abiotic and biotic cathodes can be used in double chamber system. Most frequently used cathodes are platinum, activated carbon, different graphite based cathode material and stain less steel mesh (You et al., 2007,Chen et al., 2008).

Conductive carbons allotropes such as graphite rod, glassy and amorphous carbon are resistant to microbial degradation and are effectively used as electrodes in MFCs. Because of low cost, inertness and easy availability graphite is most commonly used as electrode. Glassy and amorphous carbon including carbon fibre, carbon cloth and carbon sponge has been investigated as anodes in many studies where graphite cloth has been tested as a cathode. Graphite rod offers limited surface area. On the contrary, the large surface area is provided by graphite plates. However, the limiting factor in the performance of graphite as both cathode and anode is mass transport (Yaqoob et al., 2020). Thus, slow down electron transport from cathode, transport of fuel to anode and by-products transport away from anode. Graphite brush and fibre electrode provides the maximum porosities and surface areas for anodes which positively influence biofilm development. Conventional industrial machines for brush making are used to create graphite brushes from carbon fibres. Graphite or carbon fibre provides relatively small diameter. Therefore, immensely great surface area can be attained. The non-corrosive metal wire can be used to made core wire of graphite brush (Hutchinson et al., 2011, Liu et al., 2017).

Sseveral types of carbon-based electrodes such as carbon paper, brushes, foam and cloth are commonly used as electrode in MFC due to high conductivity and appropriate for bacterial growth. Carbon paper is slightly stiff and hard but still easily connected to wire by using epoxy. Carbon cloth has better porosity and is more flexible than carbon paper. In comparison to carbon cloth and paper, carbon foams have not been widely used in research but provide more space for biofilm development and are much thicker (Li et al., 2017, Wang et al., 2007). Carbon nanotubes/polyaniline (PANI) carbon paper based electrodes in the fuel cells also has showed improved power performance and low ohmic resistance (Wang et al., 2013).

2.4.1.6. Proton Exchange Membrane (PEM)

To improve power generation and to lessen internal resistivity of system salt bridge is substituted with PEM. The use of PEM amends efficacy and portability but at the same time increases the cost of cell. The principal purpose of PEM is to perform proton transfer. This prohibits anode from contact to oxygen in addition to other oxidizing agents (H_2O_2, K_2MnO_4) to facilitate reaction completion at cathode. The rate of transfer of protons through PEM from anode to cathode defines the power generation capability of system. However, proton conduction through PEM is relatively a time consuming process thereby producing high ohmic resistance (Watanabe, 2008,Osman et al., 2010). Therefore, transfer of proton across the membrane is a rate limiting factor in MFC operation. The poor cathodic reaction is mainly due to efficiency of PEM to transfer protons across the barrier. Nafion and Ultrex are commonly employed polymers as PEM (Ghassemi & Slaughter, 2017). Glass wools and other porous polymers have also been considered in lab. None of them turned out to be as competent as Nafion. Thus are not frequently used in this technology (Grzebyk & Poźniak, 2005). Amongst all of membranes used Nafion 117 has shown tremendous H^+ transfer proficiency. However Nafion application in fuel cell technology undergo numerous complications such as, oxygen diffusion towards cathode, substrate limitations, transference of other cation than protons and biofouling resulted from Nafion permeability to oxygen (Chae et al., 2008).

PEM is an important component of fuel cell assembly. Appropriate fitting techniques are required due to desiccating and blockage risks. The PEM assembly is robust and important process to sort it operational for practical applications (Rozendal et al., 2006). The ratio of PEM projected area to system operational volume is essential in describing MFC performance (Logan, 2010, Wen et al., 2010). PEM and platinum employed as catalyst at cathode are somewhat costly. These limitations discourage the use of membrane MFC for large scale wastewater treatment. Furthermore, dissolved contaminants and suspended solids deposition onto membrane pollute the Nafion polymer causing fouling problems. PEM is therefore essential for efficient MFC performance but to make this technology practical for upscale purposes it is necessary to reduce manufacturing cost. Elimination of PEM from cell construction will permit integration of MFC for wastewater treatment (Jang et al., 2004). PEM fouling usually happen in the course of long term operation of microbial fuel cell (MFC) since biofilm develops manifestly on PEM surface that results in deterioration of MFC competence (Chae et al., 2008). Fouling adversely affect several function executed by PEM for instance ion exchange capability, diffusion coefficient and membrane conductivity PEM (Okada et al., 1999). Fouling is predominantly the result of biofilm

development which implicates precipitation of various inorganic salts which weakens MFC performance consequently decreasing current production (Tran et al., 2009). The fouling raises PEM resistance up to 20 % that subsidizes internal resistance of scheme (Choi et al., 2011).

To ensure viable current production the fouled PEM needs to be replaced with new one. However, this increases cost of operation thus, complicating MFC practical application. In order to evade these issues of membrane fouling there is a necessity to develop membrane that exhibits longer stability, lower resistance and higher coefficient of cations diffusion (Rozendal et al., 2006, Fornero et al., 2010, Zhang et al., 2009).

2.4.1.7. Cathode

The cathode material and designs are one of the greatest challenges in MFC architecture. The cathodic reaction is quiet challenging to engineer because protons, electrons and oxygen all must meet at cathode.

2.4.1.7.1. Platinum Catalysts Coating

Platinum (Pt) catalytic activity with oxygen is more efficient than other electrodes. Therefore offer less resistant to electron flow and provides high power density but the use of platinum is confined to research lab because they are not cost effective (Mateo et al., 2017). Platinum is an excellent cathode for reduction of electron acceptor because of low resistivity which makes it catalytic activity more appealing. Pure platinum is only used in lab for research purpose because of its high cost. Power production with platinum as cathode and anode might suffer from various limitations such as mass transport limitation which result in decrease of current generation (Song et al., 2019, Sealy, 2008). In addition, during wide scale application of MFC such as waste water treatment platinum cathode suffer from sulphide poisoning which limit platinum used in sulphur abundant system (Feng et al., 2012). Although graphite doped with platinum is quite an efficient cathode that only costs a small fraction of platinum and suitable for long-term use.

2.4.1.7.2. Non-Pt Catalysts Coating

Several investigations are conducted to replace platinum in MFC with other metals and their complexes to reduce microbial fuel cell cost and make it more sustainable. Ferric oxides, manganese oxides, iron and cobalt complexes are alternate catalysts used to replace platinum but their excessive use is responsible for secondary poisoning. Several cathodic catalysts such as iron oxide, manganese complex and cobalt oxide are used to increase the oxidation reduction but these catalysts are often unsustainable and cause secondary pollution which limit their use in large scale waste water treatment plant (Ucar et al., 2017). Abiotic chemical cathodes are expensive, requires mediator and might be subjected to poisoning which is a main hindrance to apply MFC in real world (He & Angenent, 2006).

2.4.1.7.3. Air- cathode

The single chamber MFC with air cathode are more reliable to use and practical to apply in real world because it offers higher electricity generation, reduces the construction cost and requires low maintenance as compared to double chambered MFC (Fig: 3.4). Air cathode used in single chamber MFC provide

great advantage over double chamber MFC with cathode suspended in water because O_2 does not need to be dissolved in water and direct oxygen transfer occur from air to cathode (Liu & Logan, 2004). The current and power density is much higher in single chamber MFC due to high oxygen flux when compared with double chambered MFC. The oxygen availability in air is higher than the water. The abundant terminal electron acceptors are responsible for the higher electricity production. The single and double chambered MFC efficiency in COD removal is almost similar but single chamber MFC displayed more stable COD removal when compared with double chamber MFC (Logan, 2009). The placement of cathode in water is not necessary in all MFC design. In hydrogen fuel cells the PEM is wrapped around cathode so that at the electrode oxygen from the air can react directly. This technique of using air diffusion cathode is successfully employed to generate energy from wastewater in the single chamber fuel cell (Liu & Logan, 2004).
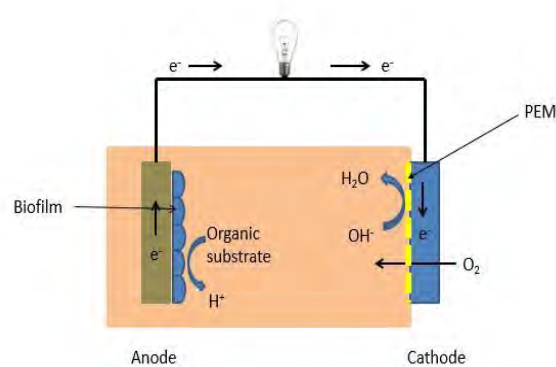
Figure 2. 4 Amicrobial fuel cell with air cathode.

2.4.2. Challenges and Applications

So far, the primary focus of MFC has been electricity production from waste but MFC technology has also been examined for wastewater treatment, hydrogen production, bioremediation, sediment microbial fuel cell and biosensor. In order to challenge other renewable energy generating technology, MFC cost and material must be reasonably economical as compare to fossil fuel. The building cost of electricity plant is 1,000 $ per kW (Brown & D, 1981) where the construction cost of an MFC system is not known because commercially MFC reactor are not yet built. But still microbial fuel cells (MFCs) provide an attractive method to add wastewater among the list of environment friendly, renewable energy sources. In addition to wastewater treatment and generation of renewable energy MFC ensure other applications such as electricity generation using sediment organic matter by placing the anaerobic electrode in marine sediments. Electricity generated by MFC might not be sufficient to act as reliable source of renewable energy but it is economically feasible to support devices in distant marine sites.

2.4.2.1. Wastewater Treatment

Electricity production from domestic wastewater along with waste water treatment is studied more than any other area of MFC applications (Liu & Logan, 2004). A wide range of complex mixture including domestic wastewater (Min & Logan, 2004), marine sediments (Hong et al., 2009) and non-toxic wastewater can be used as fuel to operate MFC without mediator addition. These materials are very

complex in nature and may contain substances like humic and fulvic acid, redox active compounds (riboflavin, flavin) and sulphur residues (Abrevaya et al., 2015). These substances present in sample can perform as natural mediators in system and facilitate electrons transfer by mixed mechanism (non-mediated along with mediated). One of the great advantages of MFC is organic matter direct utilization by bacterial biofilm on anode as carbon source but its application in real world as energy source is limited due to low power density. Except some recalcitrant molecules and xenobiotics majority of wastewater organic matter is converted by bacterial metabolic pathways into energy (Kim et al., 2004).

2.4.2.2. Hydrogen Production

Bio-hydrogen has been produced using suitable microorganisms either readily disseminated in medium or immobilized on anode of modified MFC regarded as microbial electrolysis cell (MEC) (Call & Logan, 2008) by electrohydrogenesis with higher efficiency than water electrolysis. By degrading organic matterbacteria release electrons that combine with proton at cathode to form hydrogen gas. In order to produce hydrogen gas, oxygen must be removed at cathode otherwise oxygen presence could lead to water production. Hydrogen gas is an alternative; zero emission fuel can be used to power motors, cars and airplanes. Similar to MFC, Hydrogen fuel cells used hydrogen gas as fuel are comparatively more mature and developed system (Wieckowski & Nørskov, 2010). Hydrogen production from MEC is better than other bio-hydrogen production processes by two ways, first, by using mixed microbial consortia consisting of anode respiring bacteria (ARB) as well as fermenting bacteria numerous organic substrates become utilizable. Electrochemically active ARB in MEC are proficient to consume quite composite substrates whereas hydrogen production via fermentation is often confined to fairly pure substrates such as, acids, sugars and alcohols (Mohan et al., 2008). Second, higher yields up to 67% to 91% can be obtained by complete oxidation of non-fermentable substrates to CO_2. The advantage of hydrogen producing MEC above electricity generating MFC is low energy consumption by MEC and hydrogen gas can be stored for future use in transportation and electricity generation.

2.4.2.3. Bioremediation

In an MFC, bacterial catalytic activity converts organic matter to electrons that are donated to anode through mediators or nanowires which combines with oxygen and proton to form water at cathode, but it seems that electron transfer process at cathode can be reverse for the reduction of soluble ions. Uranium and nitrate can be reduced to insoluble form by bacteria present on cathode can accept electron from cathode to reduce uranium and nitrate to their insoluble form (Wang et al., 2020). The removal of various undesirable compounds including perchlorate and nitrate can be achieved in biocathode (Rozendal et al., 2008, Córdova-Bautista et al., 2020).

2.4.2.4. Biosensing

Among all the applications of aforementioned bioelectrochemical system, electricity production is most essential and obvious one. The current produced in these systems is directly linked to the concentration and activity of limiting reactant. This phenomenon has provided a great opportunity to researchers for the development of another important area of fuel cells application and research i.e., biosensor. A typical

biosensor is an arrangement comprising of two transducer elements such as physical and biochemical which convert concentration of analytes into detectable electrical signal. It is essential to have both transducers be in close vicinity to analytes for their determination (Verrastro et al., 2016). The magnitude of signal is directly related to the concentration of compound. The diversity and possibilities to design biosensors with a wide range of transducers and biological material have been recently reviewed by some authors in studies including acetate, lactate and BOD biosensor (Turner&Karube, 1987). On the basis of transducer type, biosensor can be classified into thermal, optical, piezoelectric and electrochemical sensor. Electrochemical biosensors are further categorized based on their function into conductometric, amperometric and potentiometric sensors (Luo & Davis, 2013). Green fluorescence protein-based biosensor (Cieri et al., 2018), ion-selective electrode (Radić et al., 2020), BTEX sensor (Yurko et al., 2019), Clark oxygen electrode for BOD measurement (Ejeian et al., 2018) and O_2-sensitive fluorescent material-based biosensor (Chu & Syu, 2017, Dmitriev, 2018) are few examples of biosensor commercially available in market.

A microbial fuel cell (MFC) based biosensor is an analytical device that produces an electrical signal proportional to the concentration of target analyte by integrating bacteria as biological sensing components (Zhou et al., 2017). MFC have great potential as convenient biosensor because of system sensitivity to many components and simplicity in term electronics, mechanics and signal acquisition. It can monitor continuously, quite simple in operation and comparatively low cost. In MFC biosensor, electrogenic bacteria attach on the anode and produce an electrical signal which is detected by multimeter. Therefore, no transducer is required to convert the signal into a readable signal because MFC itself can be used as transducer or detector (Stein, 2011). The enrichment of electricigens in the anode chamber of a MFC biosensor as biological sensing element is achieved via two strategies. In one case, the bacterial consortium is developed using anaerobic sludge, soil, or domestic wastewater as a source of inoculum (Deng et al., 2015, Zeng et al., 2017). In other case, pure cultures of bacteria have been used as the inoculum in different studies (Wang et al., 2013, Wang et al., 2016).

2.5. MFC as a Biosensor for Detection of BOD

Biochemical oxygen demand (BOD) is the quantity of dissolved oxygen (DO) required by microorganisms for oxidation of substances in the water and other environments and is a critical parameter generally used in water quality monitoring (Jouanneau et al., 2014). Various principles have been proposed in past to design systems for rapid oxygen measurement including amperometric Clark's oxygen electrode (Lei et al., 2006) and electrochemical devices using redox mediators such as ferricyanide which is reduced by cellular enzymatic activity into ferricyanide (Bonetto et al., 2011). Similarly, various microorganisms including yeast (Chen et al., 2002), *Bacillus subtilis* (Tan & Qian, 1997) *and Serratia marcescens* (Kim & Kwon, 1999) were immobilized and consumption of dissolve oxygen by these organisms was measured using DO electrode to develop BOD sensor. The first MFC biosensor for BOD could not provide a definite BOD value for the wastewater of industrial origin (Karube et al., 1977). But, the MFC showed a stable performance for continuous monitoring of BOD in a

subsequent study carried out for a period of over 5 years with a limit of detection (LOD) of 2.58 mg l^{-1}(Kim et al., 2003). The use of MFC as a biosensor was first time suggested using membrane double chamber MFC with carbon as a cathode (Karube et al., 1977). *Clostridiumbutyricum* biofilm was grown on Pt anode. Formic acid and hydrogen production by the immobilized *C. butyricum* biofilm increased with strength of BOD standard solution and the amount of current measured was directly proportional to strength of BOD solution. After the initial work, Kim et al., (2003) further studied and recognized MFC utilization as BOD biosensor. Wastewater from starch processing plant was used as a source to colonize electrogenic bacteria on anode and after biofilm formation the system was run for a period of 5 years. A good correlation was observed among measured current and BOD values using MFC based biosensor. Moreover, comparisons with standard method of BOD5 and system reproducibility have shown remarkably positive results. For real-time on-site monitoring of wastewater, a system working on similar principle was proposed later. The system was verified using synthetic wastewater and samples were filtered once measured to prevent clogging. Likewise, a single chamber MFC biosensor was developed to detect the concentration of organic content (BOD sensor) using glucose and real wastewater with a response time of about 3-5 minutes and a reproducibility of 7 months. The coulombic efficiency of biosensor in small volume (12.5ml) was relatively higher than in larger volume (25ml) (Kumlanghan et al., 2007).

For the analysis of low BOD concentration wastewater, mediator less MFC with anode enriched with oligotrophs was operated for 8 weeks with uncontaminated fresh water lakes and rivers sediment as inoculum. To monitor wastewater with low BOD, this system is optimized to low microbial activity by limiting cathode oxygen concentration and reducing surface area of proton exchange membrane. Long term operational stability, high repeatability and reproducibility were observed with this oligotrophic MFC. For real-time monitoring of wastewater similar two chamber system with graphite felt was proposed later by same authors. A flow rate (0.35 ml min^{-1}) was applied at anode to assay this MFC as continuous senor (Chang et al., 2004). Flow rate and inoculation at anode governs the time required for current stabilization in MFC based BOD sensor. Current reached to a new steady state within 1 hour once MFC was fed with artificial wastewaters of different strength; contrary to these 30 days were required for stabilization when MFC was inoculated by activated sludge. Later that year same group studied MFC dynamic response to optimize system hydraulic retention time and successfully achieved the response time of 5 min. by reducing the working volume of anode up to 5 ml (Moon et al., 2004).

In 2004 Ming and Logan studied relation of power density with chemical oxygen demand by using numerous organic matters including glucose, sucrose, starch, acetate and butyrate in flat plate microbial fuel cell (FPMFC) design. Their work demonstrated the use of MFC transducer principle to measure polymeric hydrocarbon of complex nature. They showed that the presence of oxygen and nitrate in analytical system assay medium will interferes with MFC signal, sharp decline in current output was observed in MFC fed with sample having terminal electron acceptors having redox potential higher than anode (Chang et al., 2004). Therefore, inhibitory effect of potential electron acceptors (oxygen and

nitrate) present in environmental sample is eliminated by the addition of respiratory inhibitors such as cyanide derivatives for accurate BOD monitoring. The setup of single chamber MFC was suggested to achieve structure simplification by replacing cathode compartment with air cathode. Higher operational stability of 7 months and reproducibility over 1% CE were observed (Di Lorenzo et al., 2009).

A sensor takes longer time to measure the BOD concentration with higher strength of the sample. Therefore, to analyse high strength samples in reasonable amount of time high strength samples were diluted. The BOD values can also be measured by microbial fuel cell either by calculating the coulomb or monitoring maximum current. For a system measuring the BOD, a standard deviation (SD) of 30.5 mg/l is acceptable which corresponds to a ±15.4% variation in the repeatability. In previous studies, the BOD values monitored by the MFCs carried out for a period of 1 year presented a standard deviation between ±3% - ±12% (Kim et al., 2003, Kharkwal et al., 2017). The reproducibility of single strain biofilm type MFC sensors showed a variation from ±2.4% to ±10% (Liu et al., 2000). Moreover, BOD biosensor values were compared with values of BOD_5 standard method, all the measured sample result lie within American Public Health Association (APHA) with a standard deviation (SD) of 30.5 mg/L. In biosensors, operational stability of the systems is an essential aspect to be considered. In order to develop a reliable biosensor, system must have a stable performance over a desired operational time period. The nature of a DO probe limits the stability of conventional BOD sensor based on DO monitoring. Typical, Clark-type DO probe system consists of a platinum cathode and a silver anode, anode metal of Clark's oxygen electrode can be easily oxidized. Consequently, it is essential to regularly clean the anode surface and fresh the electrolyte solution of DO probe where microbial fuel cell-type BOD sensor can be operated for 7 to 140 d and over 5 years without any services (Liu et al., 2000). Optimization studies have suggested a fuel feeding rate of MFC ~ 0.53mL min⁻ to shorten the response time of the MFC sensor (Moon et al., 2004).

Lithotrophic bacteria have been utilized for detection of different compounds including iron (Pham, 2018, Wang et al., 2013). A protocol for online monitoring of different compounds in microbial fuel cell was describes(Stein et al., 2012). Dávila et al., (2011) developed a novel silicon based microfabricated MFC biosensor for the detection of toxic compounds in the water whereby a fall in power output was recorded when the sample was administered in the MFC (Dávila et al., 2011). A linear relationship has been demonstrated between voltage and concentration of para-nitrophenol in MFC (Chen et al., 2016). These observations reveal the opportunity for the advancement of MFC as BOD biosensor.

2.5.1. Microbial Fuel Cell Biosensors versus Microbial and Enzyme based Biosensors

MFC biosensors are stable devices to monitor the toxic substances; however, the performance and characteristics of these biosensors rely on the architecture of the MFC, microorganisms employed (as a catalyst), substrates and ecological conditions. Each biosensor may show a different limit of detection (LOD) under different environments due to such elements and are less specific (Labro et al., 2017, Moon et al., 2005). Enzyme biosensors, on the other contrary, show a higher specificity compared to the MFC biosensors for their substrates and inhibitors with a detection limit of up to 0.003mgl⁻¹ (Chatterjee &

Chen, 2012). Nonetheless, application of enzyme biosensors has limitations due to laborious and time-consuming enzyme purification and immobilization procedures associated with them. Furthermore, toxic compounds such as heavy metals are may alter the structure of proteins as a result of which enzymes are denatured. In microbial biosensors, microbes are immobilized on the surface of the support media using complex protocols for the output. MFC biosensors have been proposed as portable and cost-effective devices for measurement of different contaminants as the sensors are capable to directly reflect the concentration of pollutants by producing an electrochemical signal that can be directly monitors without the need for integration of additional transducers. In MFCs, bacteria encode multiple enzymes for a wide range of toxicants and are able to avoid the deficiency of enzyme biosensors. MFC biosensors have provided new opportunities for fast and cost-effective monitoring of pollutants in different environments and foods; however, there are certain limitations that need to be addressed. Presence of complex compounds and co-existence of ions in the wastewater and effluents may affect both the stability and sensitivity of MFC biosensors. Furthermore, as the conventional parameters such as external resistance and anode potential affect the performance of MFCs so optimization of these parameters is important. More research is needed to improve the efficiency and address the limitations in MFC biosensors in order to achieve trace and high throughput detections (Stein et al., 2012a, Stein et al., 2012b, Sun et al., 2015).

2.6. Conclusion

Microbial fuel cell (MFC) has potential for wastewater treatment and electricity production, and application of this technology for monitoring of toxic substances in the environment as an efficient biosensing system will promote safe environmental, agriculture, industrial activity leading to improved public health and security. Biomonitoring will lead to controlled and responsible consumption of agrochemicals which will lead to viable fertility of soil, better food and water quality and availability. Eco-friendly biological environment fingerprinting will attempt to address global issues like climate change and land/water conservation due to impeded forces of artificial chemicals in environmental sustainability (SDG # 14-17). Besides, these efforts will ensure sustainable consumption and production practices in developing countries like Pakistan to meet international commercial practices for increasing exports leading to economic development. Ultimately, this will help in reducing poverty specifically arising due to economic issue.

CHAPTER 3 (A)

Effects of Metals on Biofilm Development and Microbial Community in Attached Growth Bioreactors

Study 3A

Title: Interactive Effect of Trivalent Iron on Activated Sludge Digestion and Biofilm Structure in Attached Growth Reactor of Waste Tire Rubber

CHAPTER 3 (A): Interactive Effect of Trivalent Iron on Activated Sludge Digestion and Biofilm Structure in Attached Growth Reactor of Waste Tire Rubber

Abstract

Waste tire rubber (WTR) has been introduced as an alternative, novel media for biofilm development in several experimental systems including attached growth bioreactors. In this context, four laboratory-scale static batch bioreactors containing WTR as a support material for biofilm development were run under anoxic condition for 90 days using waste activated sludge as an inoculum under the influence of different concentrations (2.5, 6.5, 8.5 mg/l) of trivalent ferric iron (Fe^{3+}). The data revealed that activated sludge with a Fe^{3+} concentration of 8.5 mg/l treatment supported the maximum bacterial biomass [4.73E + 10 CFU/ml cm^2]; besides, it removed 38% more chemical oxygen demand compared to Fe^{3+} free condition from the reactor. Biochemical testing and 16S rDNA phylogenetic analysis of WTR-derived biofilm communities further suggested the role of varying concentrations of Fe^{3+} on the density and diversity of members of Enterobacteria(ceae), ammonium (AOB) and nitrite oxidizing bacteria. Furthermore, Fluorescent in situ hybridization with phylogenetic oligonucleotide probes and confocal laser scanning microscopy of WTR biofilms indicated a significant increase in density of eubacteria (3.00E + 01 to.05E + 02 cells/cm^2) and beta proteobacteria (8.10E + 01 to 1.42E + 02 cells/cm^2), respectively, with an increase in Fe^{3+} concentration in the reactors, whereas, the cell density of gamma proteobacteria in biofilms decreased. Tissue culture plate (TCP) assay showed 96% of isolated bacteria as strong biofilm formers. Congo red agar (CRA) and tube method showed 34% and 67% as strong biofilm formers, respectively.

Keywords: Biofilm, waste tire rubber (WTR), waste water treatment (WWT), trivalent iron (Fe^{3+}), community composition, Fluorescence in situ hybridization (FISH), Confocal laser scanning microscopy (CLSM), Scanning electron microscopy (SEM), Fourier transform infrared (FTIR) spectroscopy.

Highlights

- Waste tire is applied as a cost-effective support material for biofilm development.

- Addition of Fe^{3+} to activated sludge improved the bioflocculation and COD removal.

- Higher Fe^{3+} concentration supported higher bacterial density and affected diversity of bacteria.

3.1 Introduction

The global demand for tires is estimated to rise 4.1% per year to 3.0 billion units by 2019 which corresponds to approximately 34 million tons of waste tires production annually(Fridonia,2019.) .The increasing number of waste tires poses a serious environmental threat due to their complex and resistant chemical nature in natural environment (Shu & Huang, 2014, Chyan et al., 2013, Sienkiewicz et al., 2012) .The extent to which these discarded tires pose an environmental and public health concerns generally increases when they are buried as evidenced by the approximately 4 billion used tires in landfills and stockpiles worldwide (Managing End-of-Life Tires - World Business Council for Sustainable Development (WBCSD), 2019, Review of Management of Used Tyres at Landfill Sites, 2006.) Waste tire stockpiles provide habitats for disease spreading mosquitoes, snakes, rodents (Environment Protection Authority Waste Guidelines Waste Tyres, 2010, Tang et al., 2006, Barbooti et al., 2004) and those sites may not be utilized in future.

Majority of industrialized countries have banned scrap tires from landfills and legislations have been enacted for end of life tires management (Serumgard, 2014) in order to prevent the spread of diseases and environmental pollution. Some alternate options include pyrolysis, energy recovery, retreading, product and material recycling (Nkosi & Muzenda, 2014, ETRMA Annual Report 2014, End-of-Life Tires - World Business Council for Sustainable Development (WBCSD),2019). Mainly scrap tires are treated for material recovery (39%) and energy (37%) (ETRMA Annual Report 2014). Conversion of waste tires into alternative fuels in different industrial units like cement and lime kilns, paper and thermal power stations, environmental and engineering projects needs complying with various environmental and financial constraints and is not a satisfactory solution to the waste problem (Chyan et al., 2013, Holst et al., 1998) . Nevertheless, there is a need for devising more feasible means of treating waste tires with lower financial and technical requirements.

Environmentalists have focused on reducing the treatment costs of wastewater treatment and solid waste disposal. Biofilm-based attached growth reactors using support material like waste tire rubber (WTR) have been viewed as a cost-effective and highly efficient solution in order to meet the environmental conservation and disposal regulations (Addison et al., 2011, Calderón et al., 2012). Rubber has been proposed as one of the most suitable support materials for biofilm development as it holds low density and large surface area (Andersson et al., 2008). WTR was applied as a biofilm carrier in constructed wetland for the removal of nitrogen, chemical oxygen demand (COD) and BOD of wastewater (Chyan et

al.,2013. Tang et al.(2006) suggested the potential use of rubber as a primary treatment technology that could increase the efficiency of a secondary wastewater treatment process. Similarly, when used tires were applied in anaerobic fixed bed reactors, a 60% reduction in BOD was achieved(Reyes et al., 1999).

Iron (Fe) and iron salts have been reported as important environmental signaling entities in biofilm development (Banin et al., 2005, Monds & O'Toole, 2009). Iron is essentially important for the growth of bacteria like several other nutritional elements such as carbon, nitrogen and phosphorus. For instance, it is a component of heme enzymes, for example, hydroperoxidases and cytochromes. It is an electron acceptor that chains dissimilatory ferric iron (Fe^{3+}) reduction with oxidation of organic matter during the course of anaerobic respiration (Appenzeller et al., 2005). During dissimilatory Fe^{3+} reduction, extra electrons released from energy production are transported to solid Fe^{3+}-bearing minerals outside of bacterial cells. As a result, the Fe^{3+} minerals are converted either to Fe^{2+} minerals or to soluble Fe^{2+} which can be leached out from the sediment system or soil. This increased iron solubility may cause the release of inorganic compounds bound to Fe^{3+} oxides such as various toxic metals and iron cyclin (Zhang et al., 2009, Scala et al., 2006).

Cation ions have been shown to exert a significant impact on properties of activated sludge(Nguyen et al., 2008) . Monovalent to divalent ratio of cations in influent is an indicator of sludge physiognomies according to postulates of divalent cation bridging theory (Peeters et al., 2011, Higgins & Novak, 1997b) . Flocculation and treatment efficiency of waste water treatment plants (WWTP) also rely on the type of the cation coming with the influent, that is, Na^+, Ca^{2+}, Mg^{2+}, Al^{3+}, Fe^{2+}, Fe^{3+}(Park 2006,Zhou et al., 2015,Nielsen & Keiding, 1998,Watanabe et al., 1999). Divalent cations foster bio-flocculation compared to monovalent cations(Novak, 2001) Fe^{2+} has more pronounced role in granules stability and is more important than Ca^{2+} and Mg^{2+}(Park & Helm, 2008). Due to their higher charge valence and outstanding affinity with multidentate negatively charged ligands in EPS, trivalent (TVI) Fe and Al contribute to extra stability of granules in sludge and are of great significance in this regard(Park et al., 2006, Park & Helm, 2008.,Beech & Sunner, 2004) . Appenzeller et al., (2005) also reported superior flocculation capability of Fe^{3+} compared to Fe^{2+} (Appenzeller et al., 2005). Along with proper choice of coagulant as an important consideration, its proper dosage also plays a significant role (Kawamura, 1976). Although multivalent cations such as trivalent iron salts are widely employed as coagulants in WWTP, little is known about their impacts on wastewater biomass and coagulation.

To our knowledge, this is the first direct demonstration of the impacts of trivalent ferric iron concentrations on the WTR biofilm community structures and performance of batch biofilm reactors under anoxic conditions. The specific hypothesis of the present study was that Fe^{3+} affects positively the floc formation and associated biofilm structure which then subsequently helps activated sludge process performance. The study evaluated the feasibility of applying WTR as an alternative, cost-effective and sustainable support material and investigated the interactive effects of trivalent iron (Fe^{3+}), serving as a nutrient, electron acceptor and a bioflocculant on sludge digestion performance and associated biofilms in attached growth batch reactors (AGBR) under anoxic conditions. Specific emphasis was given to

ammonium oxidizing bacteria (AOB) and nitrite oxidizing bacteria (NOB). Besides, spatial organization and population dynamics of eubacteria, beta and gamma proteobacteria were determined using FISH (*fluorescent in situ hybridization*) coupled with CLSM (confocal laser scanning microscopy) and digital image analysis.

3.2 Methodology

3.2.1. Experimental Set-up and Operation

Experiments were conducted with four laboratory-scale rectangular AGBR, 4 liter each, run under anoxic condition for a period of 90 days for the treatment of municipal sewage. The support material used in the reactors to develop biofilms was passenger car WTR strips (length; 11 cm, width; 4.065 cm, thickness; 0.13 cm, surface area; 93.48 cm^2) suspended vertically in the reactors with iron wire such that their three fourth part was covered with WAS. WTR contained crumb rubber (70%), steel (17%), fiber and scrap (13%) (Evans, 2006) . The reactors consisted of plastic material, with a flat bottom (length: 9 inches, width: 6.2 inches, height: 5.5 inches). Each reactor was filled with 2 l activated sludge obtained from municipal WWTP in Islamabad, Pakistan, 1l minimal salt medium, 5 g starch and 5 g technical agar (Oxoid). The characteristics of wastewater from that treatment facility, according to European standards, were as follows: hydraulic retention time: 7 days, mixed liquor suspended solids: 3000– 3500 mg/l, total suspended solids (TSS) (influent): 230–235 mg/l, TSS (effluent): (35 mg/l), COD (influent): 400–440 mg/l, COD (effluent): 150 mg/l. The activated sludge was transported to the laboratory at 4 °C within one hour after collection. The reactors were covered with black paper to prevent algal growth and left initially for 2 days at 30 ± 2 °C temperature in an incubator to help growth of biofilm on the support media. Fe(OH)$_3$ was added in varying concentrations (2.5 mg/l, 6.5 mg/l and 8.5 mg/l) in three experimental reactors and mixed with stirrers, whereas one reactor served as a control with no supplementation of Fe^{3+}. Mechanical stirring was performed periodically with stainless steel stirrers to ensure adequate oxygen diffusion and the homogeneity of the mixed liquor in the bioreactors.

3.2.2. Physico-Chemical Analysis of Activated Sludge in AGBR

The pH of the samples was determined in the laboratory by using 'Digital Sartorius (pp 15) pH meter'. Before each measurement, the pH meter was calibrated using distilled water. Dissolved oxygen (DO) mg/l was measured by using 'Crison OXI 45+ DO meter' with 5120 electrodes. The electrode of the instrument was washed with distilled water before and after analysis of each sample. COD of samples was determined using commercial kits (CSB/COD, Merck, Germany) with measuring capacity within a range of 25 mg/l–2500 mg/l. COD values were recorded using spectroquant Pharo 300 (Merck) after cooling of vials. APHA standard method 3500 was used to measure nitrite nitrogen (NO$_2^-$–N), whereas EPA standard method 4500 for nitrate nitrogen (NO$_3^-$–N) measurement in the samples (Standard Methods, 2005). Alkalinity (mEq/l) and VFA (mg/l) were determined by using the titration-based method (Buchauer, 1998, Moosebrugger et al., 1993).

3.2.3. Bacterial Characterization of WTR-derived Biofilms

Total viable cell counts of WTR-derived biofilms developed under the influence of different Fe^{3+} concentrations were estimated using standard spread plate method on nutrient agar plates. 1 cm^2 sections of WTR with attached biofilms were washed with sterile distilled water three times to remove loosely attached planktonic bacteria followed by scrapping the biofilms off using a sterile scalpel blade along with brief sonication (Vukanti et al., 2009) of materials in water bath (Yamato 934) to remove biofilm bacteria and dislodge the clumps in capped sterile tubes with 10 ml sterile distilled water. For bacterial enumeration, the biomass suspensions underwent 10-fold standard serial dilutions before being plate counted on nutrient agar plates incubated at 37 °C for 24 h before colony enumeration. Three replicas were used for each sample analyzed. The strength of bacterial populations in each biofilm was determined in terms of CFU/ml cm^{-2} of WTR and analyzed statistically with t-test using Microsoft excel 2016. Representative bacteria were selected and identified according to Bergey's manual of bacteriology (Bergey, 1994) based on their morphology, colony color, motility, Gram's stain and biochemical tests. Morphological study of bacterial isolates involved considering the following physical characteristics (Table 3.1).

Table 3. 1Selection criteria for bacteria based on colony morphology, color and motility.

No.	Feature	Description
1	Size of colony	Small, moderate or large, pinpoint
2	Form	Irregular/regular, circular, rhizoidal, filamentous
3	Pigmentation	Color of colony or medium
4	Elevation	Flat, convex, raised
5	Opacity	Opaque translucent, transparent

3.2.4. Molecular Identification of AOB and NOB

3.2.4.1. DNA Extraction, PCR and Sequencing

To evaluate the impact of Fe^{3+} on species of AOB and NOB, that is, Nitrobacter, total genomic DNA of each biofilm sample was extracted using commercial kit (Norgen Biotech Corp. Soil DNA Isolation kit, Catalog. 26500) following manufacturer's recommendations. Partial 16S rDNA gene of AOB was amplified by using primer Nso190F (5ʹGGAGCAAAGCAGGGGATCG-3ʹ) and Nso 1255R (5ʹCGCCATTGTATTACGTGTGA-3ʹ) as described previously (Purkhold et al., 2000). To detect Nitrobacter species Nitro-1198F (5ʹACCCCTAGCAAATCGCTGACC-3ʹ) and Nitro-1423R (5ʹCTTCACCCCAGTCGCTGACC-3ʹ) primer pair was employed to amplify the target gene fragments (Table 3.2). All primers were synthesized by Invitrogen (Shanghai, China), whereas, PCR and sequencing of the produced amplicons was carried out by Macrogen (Korea).

3.2.4.2. Phylogenetic Analysis

The obtained nucleotide sequences of all samples in this study have been submitted to NCBI GenBank database under accession numbers KU705711- KU705712 (385 bp) and KU710442 (328 bp) (Table 3.1).

Ambiguities in the sequences were removed before further analysis. Homologs of each gene sequence were retrieved using Blastn from the nucleotide database (http://www.ncbi. nlm.nih.gov/BLAST/). Only sequences with greater than 90% homology were selected. The collected data were used to construct Neighbor-Joining trees using MEGA 6.0 software with 1000 bootstrap replicates to obtain confidence in the branching points.

Table 3. 2 Primers used for the amplification of target genes from whole genomes of biofilm samples.

No.	Sample	Primer	Target region	Reference	Specificity	Accession no.
1	Control-WTR	Nitro-1198f	1198[a]	(Langone et al., 2014)	16S, *Nitrobacter* spp.	KU705712
		Nitro-1423r	1423[a]	(Langone et al., 2014)	16S, *Nitrobacter* spp.	
2	Fe^{3+}-6.5 (mg/l)-WTR	Nso190f		(Purkhold et al., 2000)	AOB, 16S rDNA	KU710442
		Nso 1225	1224–1243	(Purkhold et al., 2000)		
3	Fe^{3+}-8.5 (mg/l)-WTR	Nitro-1198F		(Langone et al., 2014)	*Nitrobacter* spp.	KU705711
		Nitro-1423r		(Langone et al., 2014)		

a*E. coli* numbering.

3.2.5. Characterization of Biofilm forming Ability of Bacteria using Biofilm Assays

3.2.5.1. Test Tube Method

Tube test method describes the biofilm forming capability of bacterial isolates qualitatively as stated by Christensen and his colleagues previously (Tang et al.,2006, Barbooti et al., 2004, Serumgard, 2014, Nkosi and Muzenda, 2014., ETRMA Annual Report 2014). All bacterial isolates were inoculated into glass test tubes containing 10ml of tryptic soy broth with 2 % dextrose in it and incubated overnight at a temperature of 37 ^{o}C ±2 ^{o}C. The test tubes were gently emptied then and washed three times with PBS (pH, 7.3) carefully. Tubes were air dried in an inverted form and stained with 0.1 % crystal violet while gently rotating the tubes. Again, washed the tubes with distilled water and dried upside down in air at room temperature. An isolate was recorded as a strong biofilm former when there was a strong violet film at the bottom and wall of tube and scored as 2. Similarly, moderate film forming isolates were scored 1 and no/weak film formers as 0.

3.2.5.2. Congo Red Agar Method

As described by Freeman, 1989, CRA is also a qualitative test for the estimation of bacterial film formation (Nkosiand Muzenda, 2014, Managing End-of-Life Tires - World Business Council for Sustainable Development (WBCSD), Holst et al., 1998, Serumgard, 2014). CRA culturing medium contained tryptic soy agar (Oxoid) with 2% agar. Concentrated solution of CR indicator was prepared and autoclaved, separately at 121°C temperature for 15 min. and then mixed with autoclaved TSA when it had reached 55°C. All bacterial isolates were inoculated on CRA plates for 24 to 48 hours at 37 ^{o}C ±2 ^{o}C to detect EPS production. Black, crystal like, dry colonies indicated positive results whereas pink color specified weak sliming.

3.2.5.3. Tissue Culture Plate (TCP) Method

Micro titer 96 well plate test method generally known as TCP method designed by Christensen (ETRMA Annual Report, 2014) is the gold standard test for detection of biofilm forming ability of bacteria (Holst et al., 1998). In the present work, the same method was applied with some modifications with respect to incubation period and fixation method.

All bacterial isolates were incubated in sterile test tubes containing 10 ml of trypticase soy broth with 2% dextrose as carbon source and incubated for 24 hours at 37 ^{o}C of temperature. Cultures from the tubes were then diluted in the ratio of 1:100 (volume 200 µl) with sterile fresh TSB into the wells of 96 well sterile polystyrene tissue culture plates with flat bottoms. Sterile TSB was inoculated as negative control. After incubation of tissue culture plates for 24 hours at 37 ^{o}C, wells were decanted, washed with 200 µl of PBS (pH, 7.2) three times to exclude planktonic bacteria and plates were then placed in an oven set at 50°C for the purpose of heat fixation.

The films were then stained with 0.1% crystal violet, washed with distilled water to remove the excessive crystal violet and air dried. OD of wells was quantified by using ELISA autoreader (Biorad) at 590 nm. Experiment was replicated three times and standard deviation of average values of data was obtained. OD values were used as an index of biofilm formation of bacterial isolates (Table 3.3).

Table 3. 3 Scale for measurement of biofilm formation ability of bacterial strains.

No.	Average OD	Biofilm Formation
1	≤ ODc / ODc < ~ ≤ 2x ODc	Non/weak
2	2x ODc < ~ ≤ 4x ODc	Moderate
3	> 4x ODc	Strong

(Cut-off value of optical density (OD$_c$): OD$_{ave}$. of negative control + 3(standard deviation of negative control).

3.2.6. Nitrification Rate of Biofilms under Varying Concentrations of Fe^{3+}

Nitrogen removal rate in microorganisms depends not only on substrate conversion during respiration but also on interactions among microorganisms within biofilms. Therefore, for the quantification of nitrification activity of biofilms *in situ*, enriched cultivation technique was applied. Protocol of Ma et al., 2014 and Anderson et al., 2008 was followed with some modifications as described by (Addison et al.,2011, Calderón et al., 2012).

Composition of enrichment media used to investigate the activity of nitrifiers was NaHCO$_3$, 13.8 g/l, NH$_4$Cl, 70.18 mg/l, K$_2$HPO$_4$, 0.236 g/l and 0.25 ml of trace elements. Biofilm was scraped off from 1cm^2 area of each biofilm carrier and collected in sterile capped glass tubes having 1 ml PBS, sonicated for 2-3

minutes to dissolve microorganism from the carriers thoroughly and finally, added into presterilized 250 ml flasks containing 100 ml of enrichment medium each under sterile conditions. Fe(OH)$_3$ was added in its pre-specified concentrations in flasks as in the case of reactors described above, to check the nitrification potential under the influence of iron. Flasks were covered with black paper to inhibit light and growth of algae. The cultivation conditions were: temperature, 30℃; shaker speed, 140 rpm and experiment period, 30 days. The concentrations of nitrite and nitrate were detected in each flask at day 0, 15th and 30th day of experiment using method 4500 (APHA, 2005).

3.2.7. FISH and CLSM of WTR biofilms

3.2.5.1. Use of Reference Cells and FISH Optimization

In order to carry out optimization of hybridization conditions, specificity of the probes was evaluated by applying pure cultures of bacteria. Bacillus subtilis (accession number: KJ600795) and Pseudomonas aeruginosa (ATCC ® 9027™) strains were deposited as positive reference controls for beta (β) and gamma (ϒ) populations of proteobacteria, respectively, on the initial wells of Teflon-coated 10 well glass slides to obtain FISH results accordingly. Both reference strains were hybridized individually with eubacterial mixture of probes (EUB-338, EUB338-II, EUB338-III), β, ϒ as well as mixtures of EUB probes + β, EUB mixture + ϒ and EUB mixture + β + ϒ probes. Moreover, Bacillus (a reference strain for β proteobacteria) was hybridized with ϒ probe and similarly P. aeruginosa (a reference strain for ϒ proteobacteria) was hybridized with β probe in order to check their specificity using different channels of CLSM. CLSM observations showed that all probes fluoresced accordingly and there was no cross-hybridization observed (Fig A3).

3.2.5.2. Preparation of Cell Smears and Biofilm Fixation

Protocol as described previously by Amann et al. (1990), Manz et al. (1993) and Wijeyekoon et al. (2004) was followed for non-disruptive fixation and analysis of sessile bacteria with some modifications for optimization purposes(Amann et al., 1990, Manz et al., 1993, Wijeyekoon et al., 2004). Biofilms on WTR were washed with sterile distilled water three times to remove loosely bound planktonic bacteria. Biofilms were removed carefully from 1 cm^2 area of WTR support material and transferred to Teflon-coated wells of 10 well glass slides. A positive as well as a negative control were incorporated into two of the 10 wells on each slide to avoid ambiguous interpretation of results. Samples were then washed with PBS (pH, 7.2), fixed with 4% paraformaldehyde (PFA) solution (2 hours at -20 °C) and again washed with PBS (pH, 7.2) to remove the fixative. Slides were then successively dehydrated with 50%, 80% and 100% ethanol for three minutes each, conserved at room temperature until further processing.

3.2.5.3. Hybridization with Fluorescently Labeled Oligonucleotide Probes

Protocol described by Manz et al., (1999) , Amann et al. (1990) and Nielsen et al.(FISH Handbook for Biological Wastewater Treatment | IWA Publishing,2009.) was followed with incorporation of some modifications for hybridization of fluorescently labeled probes. Each well of slide was covered with 18 μl of hybridization buffer [0.9 M NaCl, 20 mM Tris/HCl (pH 7.2), 0.01% SDS, 35% deionized formamide] and 2 μl of 5′ end 5, 6- FAM (derivative of FLUOS, that is, amine reactive succinimidyl esters of

carboxyfluorescein) labeled oligonucleotide probe(s). Eubacterial probes EUB-338, EUB-II and EUB-III (Manz et al 1993,Schmid et al., 2003, Xu et al., 2014, Daims et al., 2006) detect majority of the domain bacteria, including Verrucomicrobiales and Planctomicetales (Bertaux et al., 2007, Pavlekovic et al., 2009). The probes β42a (Manz et al 1999, Xu et al.,2014) and γ42a (Amann et al., 1990, Manz et al 1993, Nielsen, 2009, Lin et al., 2009) are specific for the members of beta (β) and gamma (γ) subdivisions of proteobacteria (Table 3.4). The 23S rRNA targeted probe BET42a and GAM42a unlabeled competitor oligonucleotides (GAM42a and BET42a, respectively) were incorporated into the hybridization mixture to ensure hybridization specificity. All fluorescent and unlabeled competitor probes were ordered from α-oligos (Montrial, Canada). The slides were kept in hybridization chamber and incubated for 90 min. at 46°C. Hybridization buffer was drawn off with tissue paper placed at the edges of the slides. Subsequently, the slides were transferred to 50 ml pre-warmed washing buffer (20 mM Tris/HCl, 0.01% SDS, 5M NaCl) and incubated at 48°C for 20 min. The slides were then briefly rinsed with distilled water, allowed to air dry and mounted in Citifluor prior to microscopy.

3.2.5.4. Image Collection

A Fluo View^{TM} (Fv1000) CSLM, equipped with high-resolution multi-Argon-ion Lasers (405 nm–559 nm) was used for image acquisition of probe(s) hybridized biofilm samples. The images were collected, using UPLSAPO X102, 0.6 to 1.3 numerical apertures oil immersion lenses. Multiple fields of view were selected at random containing maximum information (cells) and later their average was used to calculate total cells per cm^2. Optical sections were collected at a distance of 1.14 µm from upper surface of biofilms in Kalman filtration mode for noise reduction and stored in TIFF format for subsequent processing. Total population of eubacteria, β and γ proteobacteria was quantified in sequential mode. Nonspecific fluorescence of polymeric substances was manually eliminated. Only those results were considered positive that provided good signals with target cells.

3.2.5.5. Digital Image Analysis

The cell counts of three or more images were calculated by *daime* (digital image analysis in microbial ecology) software (Daimset al., 2006) and their average was determined. Image analysis resulted in information on such parameters as cell area (biomass), cell number and proportion of cells hybridizing with any of the nucleotide probe(s). In cases where biofilm samples were partly damaged or lost, the affected images were excluded from further analysis. Upper and lower size cut-offs were applied to eliminate objects too small or large to be bacteria during image processing (Manz et al., 1999).

Table 3. 4 end 5,6-FAM labeled 16S rRNA oligonucleotide probes used in this study, their target organisms and stringencies.

No.	Probe (Full name)[b]	Specificity	Binding Position[c] (bp)	Sequence (5'-3')	FA[d] (%)	NaCl (M)	Reference
1	EUB338 (S-D-Bact-0338-a-A-18)	Domain bacteria	338–355	GCT GCC TCC CGT AGG AGT	35	5	(Manz et al., 1993,Schmid et al., 2003)
2	EUB338- II (S-*-BactP-0338-a-A-18)	Bacterial lineages not targeted by EUB338 and EUBIII, *Planctomycetales*	338–355	GCA GCC ACC CGT AGG TGT	35	5	(Manz et al., 1993,Schmid et al., 2003,Pavlekov ic et al., 2009)
3	EUB338- III (S-*-BactV-0338-a-A-18)	Bacterial lineages not covered by EUB338 and EUB338 and EUB338II, *Verrucomicrobiales*	338–355	GCT GCC ACC CGT AGG TGT	35	5	(Manz et al., 1993,Schmid et al., 2003,Pavlekov ic et al., 2009)
4	Bet42a[e] (L-C-bProt-1027-a-A-17)	class *Betaproteobacteria*	1027 – 1043	GCCTTCCCACTTCGTTT	35	5	(Manz et al., 1999,Xu et al., 2014)
5	Gam42a[e] (L-C-gProt-1027-a-A-17)	class *Gammaproteobacteria*	1027 – 1043	GCCTTCCCACATCGTTT	35	5	(Amann et al., 1990,Manz et al., 1993,*FISH Handbook for Biological Wastewater Treatment | IWA Publishing*,200 9,Lin et al., 2009)

b; Full name of 16S rRNA gene-targeted oligonucleotide probe(s) is based on the nomenclature of Alm et al.(Alm et al., 1996).

c; Probe binding positions according to *E. coli* 16S rRNA gene numbering (Brosius et al., 1981).

d; FA = Percent Formamide in hybridization buffer.

e; Competitor probes of Bet42a and Gam42a were added to the hybridization buffer as unlabeled oligonucleotide probes in equimolar amounts as the labeled probes to enhance the hybridization specificity (Manz et al., 1993).

3.2.8. Scanning Electron Microscopy of Biofilms on WTR

To characterize the surface morphology of biofilms on WTR, scanning electron microscopy (SEM) of the biofilms developed on waste tire rubber in attached growth batch reactors under the effect of Fe^{3+} (0mg/l-8.5mg/l) was carried out. The biofilms on sections of WTR were washed with phosphate buffer and fixed with glutaraldehyde (2%) followed by osmium tetroxide (1%). The biofilm cells were dehydrated in increasing concentrations (40%-100%) of ethanol. The prepared specimens were mounted on copper stubs and gold coated through sputter coater (JFC-1500, auto coater, JEOL, Tokyo, Japan) by generating vacuum using high voltage. An about 25 mA current (50 s) was used for plasma generation and subsequent gold coating on the samples. Gold coated samples were then placed under the column in chamber and finally the micrographs were recorded under SEM (JSM-6490A, JEOL) at different magnification intensities starting from X100 to X20,000 and recorded.

3.2.9. Characterization of Extracellular Polymeric Substance (EPS) of Biofilms by Fourier Transform Infrared Spectroscopy (FTIR)

For the characterization of exopolymeric substances, FTIR spectroscopy is a non-destructive technique for observing time resolved accumulation of EPS in biofilms and presence of functional groups in EPS along with conformational alterations on the materials of interest (Andersson et al., 2008). In the present study, method described by Coates (2000) was used for sample treatment before performing FTIR (Reyes et al., 1999). In the first step, EPS was precipitated by taking threefold volume of cold absolute ethanol with one volume of biofilm from 1 cm^2 of WTR in sterile Eppendorf tubes. The Eppendorf tubes were incubated for about two hours on ice and subsequently, centrifuged at 10,000 rpm and 4℃ temperature for 20 minutes. Ethanol was evaporated by placing Eppendorf tubes at 45℃-50℃ in drying oven and FTIR was performed using *TENSOR 27* FTIR apparatus.

3.3. Results

3.3.1. Physico-chemical Profile of Activated Sludge in AGBR

Physico-chemical profile of the activated sludge varied significantly and improved under the influence of different concentrations of Fe^{3+} in different AGBR containing WTR (Table 3.3). About 25–38% more COD removal efficiency was achieved in the AGBR under the influence of different concentrations of Fe^{3+} compared to the control reactor. It was the maximum when 8.5 mg/l Fe^{3+} was used in the reactor (Table 3.3). Alkalinity values declined from 9.5 mEq/l initially in activated sludge to 7.5 mEq/l at 0 and 2.5 mg/l Fe^{3+}, whereas, 5 mEq/l at 6.5 and 8.5 mg/l of Fe^{3+} in reactors after 90 days of treatment. Volatile fatty acids (VFA) (mg/l) increased from 147.5 mg/l under control condition to 475 at 8.5 mg/l of Fe^{3+} after the treatment period (Table 3.3). DO (mg/l) varied in the range of 0.25–2.12 mg/l during incubation. Though a minor variation in the pH was observed, it remained in the range of 7.19–7.36 (Table 3.5). Concentration of both NO^-_2−N and NO^-_3−N was monitored for four weeks in the WAS of the reactors.

Nitrite produced by AOB was consumed by NOB and further oxidized to nitrate. There was higher removal of NO^-_2-N from 59.34% to 77.05% at week 2 followed by a decline in its removal rate from 75.82% to 31.15% at week 4 at 0 to 6.5 mg/l of Fe^{3+}, respectively. Fe^{3+} favored NO^-_3-N removal initially at week 2 at its 2.5 and 6.5 mg /l concentrations, that is, 5.41% and 35.65%, respectively, but affected it adversely at the corresponding concentrations when measured at week 4 (Table 3. 6).

3.3.2. Dynamics of WTR-derived biofilm bacterial communities under varying Fe^{3+} regimens

The impact of Fe^{3+} concentrations on the WTR-derived biofilm microbial communities was examined using culture-dependent and -independent (molecular) techniques. Overall, significant differences in the microbial community structure emerged between the experimental test and control biofilms. A linear positive correlation was observed ($p < .05$) between bacterial densities and increasing concentrations of Fe^{3+}. Biofilms grown in reactors with no (control) or very low (2.5 mg/l) concentration of Fe^{3+} supported bacterial density in terms of CFU/ml cm^2 of WTR as 2.96E + 09 and 3.65E + 09, respectively, that further increased to 4.19E + 10 at 6.5 mg/l. Maximum bacterial count was observed at 8.5 mg/l of Fe^{3+}, that is, 4.73E + 10 CFU/ml cm^2 (Fig A1, Table A1). Biochemical characterization of culturable bacteria isolated from these biofilms revealed that majority of them were gram-negative related to *Klebseilla* sp., *Vibrio* sp., *E. coli* sp., predominantly *Pseudomonas* sp. and Gram-positive bacteria; *Bacillus* sp. and *Staphylococcus* sp. (Table A7).

16S rDNA phylogenetic inference analysis indicated the presence of several species of AOB and genus Nitrobacter and relationships among them in biofilms established on WTR with and without addition of Fe^{3+}. BLAST search using sequence (385 bp) amplified with Nitro1198f/ Nitro-1423r primers from biofilm of control reactor indicated closely related organisms within the database and the presence of *Nitrobacter winogradskyi* Nb-255, *N. winogradskyi* ATCC 14123, *N. winogradskyi* ATCC 25381, N. sp. TH21, N. sp. BS5/19, N. sp. PBAB17, N. sp. PBAB10, N. sp. NBW1, N. vulgaris NBW3, *N. vulgaris* strain K48, N. sp. 311, N. sp. LIP, some uncultured Nitrobacter sp. clones (Nit, 1-G, NCAAH, K-OTU6493) and nitrite oxidizing bacterium MPN2 (Fig. 3.3). WTR at the highest concentration (8.5 mg/l) of Fe^{3+} applied supported growth of some additional species of genus *Nitrobacter*, that is, N. sp. 219 strain 219, *N. winogradskyi* strain Engel and uncultured bacterium clone IIEAI-rp13Nit along with those that appeared in control (Fig. 3.4). Similarly, there were four Nitrobacter species (accession No.: AM286374.1-AM286376.1, AM286391.1) present in the biofilm of control reactor but absent at 8.5 m/l. Blast similarity results of 328 bp sequence amplified using primers Nso190f/Nso1225r from WTR biofilm sample grown at 6.5 mg/l Fe^{3+} indicated the presence of several species of genus *Nitrosomonas,* some uncultured ammonium oxidizing and other bacterial clones (Fig. 3.5). The percentage homologies and E (expect) values of the organisms along with their accession numbers are enlisted (Table A2).

Table 3. 5 Physicochemical profile of activated sludge under the influence of different Fe^{3+} concentrations in AGBRs.

Parameter	AGBR-I-(control) (w)	AGBR-II (2.5 mg/l) (x)	% removal (w−x) at Fe^{3+}-2.5mg/l	AGBR-III (6.5 mg/l) (y)	% removal (x−y) at Fe^{3+}-6.5mg/l	AGBR-IV (y−z) (8.5 mg/l) (z)	% removal at Fe^{3+}-

										8.5mg/l
pH	7.32	7.19			7.24			7.36		0.55
COD (mg/l)	509	383	−24.75	126	344	−32.42	39	316	28	−37.92
Average DO (mg/l)	2	0.25			0.9			2.12		6.00
Alkalinity (mEq/l)	7.5	7.5		0.00	5		2.50	5	2.50	−33.33
VFA (mg/l)	147.5	260	43.27	−127.5	250	41.00	−102.5	475	−327.5	68.95

Table 3.6 Nitrate and nitrate nitrogen concentrations (mg/l) and their percent variations in activated sludge of batch reactors at different Fe^{3+} dosages during four weeks of operation.

Fe^{3+} (mg/l)	Week 1	Week 2	Week 4	Week 1	Week 2	Week 4	Week 2	Week 4	Week 2	Week 4
0	182	74	44	168.3	206.6	163.7	−59.34	−75.82	18.54	2.73
2.5	75	17	27	273.7	258.9	132.6	−77.33	−64	−5.41	51.5
6.5	61	14	42	220.5	141.9	128.1	−77.05	−31.15	−35.65	41.9
8.5	17	12	61	150.6	182	183	−29.41	72.13	17.25	−17.7

3.3.3. Biofilm Forming Potential of bacteria

Bacteria isolated from all biofilms developed under the effect of range of Fe^{3+} concentrations in AGBRs were quantified for their biofilm formation abilities by biofilm assays such as Congo red agar (CRA) assay, tube method (TM) and tissue culture plate (TCP) assay, the gold standard method for this purpose, and the data was compared. Results revealed that all the bacterial strains seem to have dissimilar biofilm formation tendencies (Fig. 3.1, Table 3.5).

The tube method (TM) showed 67.08 % of total 79 bacterial isolates were strong biofilm formers, 26.58 % moderate and only 5.0% weak or non-biofilm formers. Results of 1.26% bacteria remained indeterminate by TM. The Congo red agar method detected 34.18% isolates as strong, 8.87% intermediate and 40% weak/none biofilm formers. TCP assay indicated 96.20% isolates were strong biofilm formers and only 3.79% as moderate biofilm formers (Fig. 3.1, Table 3.7).

Statistically, the non-biofilm formers by all methods were considered as true negatives, whereas, non-biofilm forming by CRA and TM but not by TCP was taken as false negatives. Similarly, biofilm producers by all three assays were true positives yet biofilm formers by CRA and TM but nor by micro titer method were recorded as false positives.
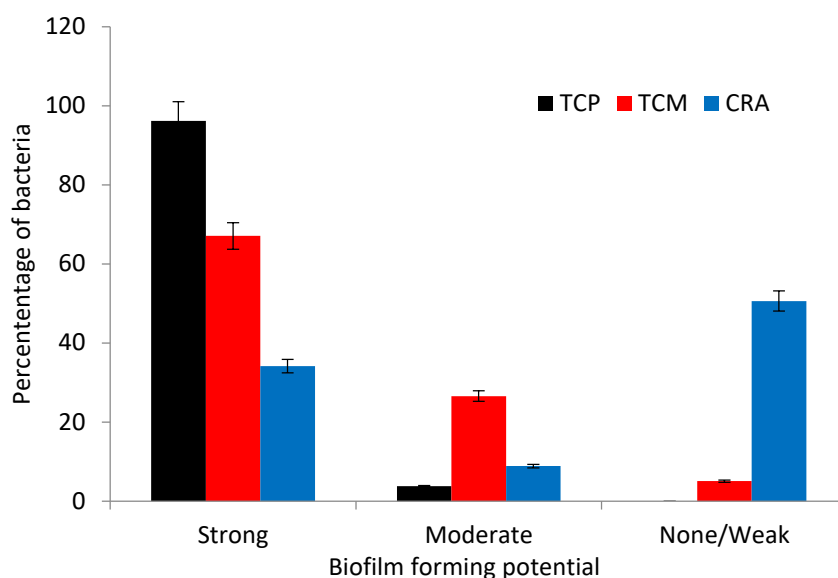
Figure 3. 1 Biofilm forming potential of bacteria (weak, moderate, strong).
The bacteria were isolated from the biofilms developed under the effect of varying concentrations of Fe^{3+} using; tissue culture plate (TCP), tube method (TM) and Congo red agar (CRA) method.

Table 3. 7 Biofilm formation ability of isolated bacteria assessed by TCP, TM and CRA methods.

Biofilm formation	TCPn(%)	TMn(%)	CRAn(%)
Strong	76(96.20)	53(67.08)	27(34.18)
Moderate	3(3.79)	21(26.58)	7(8.87)
None/Weak	0(0)	4(5.06)	40(50.63)

(Total bacterial isolates evaluated: 79, Indeterminate results in CRA: 5, Indeterminate results in tube method: 1)

3.3.4. Nitrification Rate of Biofilms

Previously, nitrogen removal efficiencies of several systems and planktonic cultures have been investigated, however, very little is known about nitrogen removal performance of their biofilms. In order to investigate the nitrification and denitrification potential of nitrifying and denitrifying bacteria in multispecies biofilms under the effect of varying Fe^{3+} concentrations, biofilms on WTR (cm^{-2}) were fed with ammonium enriched medium and $Fe(OH)_3$ (0 mg/l, 2.5 mg/l, 6.5 mg/l, 8.5 mg/l) and incubated in dark on shaker under agitated conditions (140rpm). Relative effects of the support material with respect to Fe^{3+} concentrations on nitrification rate were monitored for a period of 30 days at different intervals and data was compared.

In the biofilms, maximum accumulation of NO_2^- -N occurred at Fe-6.5 mg/l concentration with a value of 3.19 mg/l after 30th days that declined at Fe-8.5 mg/l indicating that this concentration of iron was inhibitory to the AOB activity. There was an increase in NO_3^- -N from undetectable range - 2.6 mg/l, undetectable - 3.62 mg/l, undetectable - 2.789 mg/l and undetectable - 2.788 mg/l at 2.5, 6.5, 8.5 mg/l concentrations of ferric iron and control, respectively (Figure 3.2).
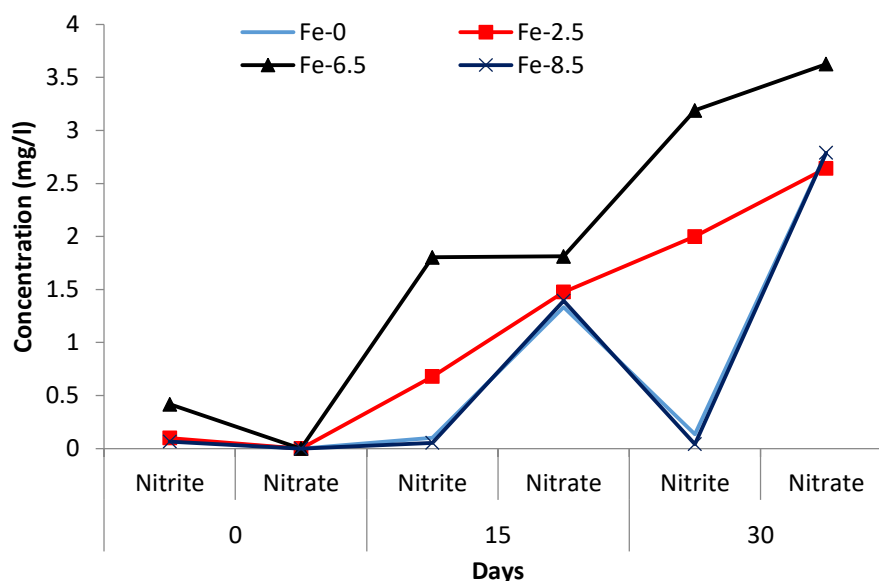
Figure 3. 2 Nitrite-nitrogen and nitrate-nitrogen accumulation and transformation rate (mg/l) in biofilm developed on tire rubber (TR) at different concentrations of Fe^{3+}.

3.3.5. Characterization of WTR biofilms by FISH

The impact of different dosages of Fe^{3+} on the coaggregation patterns and quantitative distribution of populations of eubacteria, beta and gamma proteobacteria on WTR biofilms was studied by FISH followed by scanning with CLSM. The structure and porosity of experimental biofilm samples at varying Fe^{3+} concentrations differed considerably than the biofilm developed under controlled conditions (with no Fe^{3+}) (Fig. 7) on WTR in AGBR. Visual observations and scanning electron micrographs (SEM) also depicted that mature biofilms at higher Fe^{3+} concentrations contained massive extracellular polymeric substances (EPS) and detritus and showed a distinct orientation to flow (Fig. 3. 6).

Deposited cells could not be distinguished easily from the growing cells in CLSM images of hybridized biofilms on WTR. Optical sections of biofilm from control reactor showed higher cell counts in the sections from the upper portion of biofilm, yet comparatively lesser than in experimental biofilm sections. Images from lower parts of biofilms showed more porosity. There were more surface irregularities in biofilms of reactors supplemented with Fe^{3+} compared to the reactor operated without exogenous supplementation of Fe^{3+}, indicating their structural heterogeneity. Hybridization experiments with 5′ end 5, 6-FAM labeled fluorescent phylogenetic probes showed the presence of small and large bacterial rods and cocci in isolated form as well as in aggregates and microcolonies. Compact and less porous portions of biofilms contained bacteria restricted to the surface areas of biofilms. In contrast, when the microstructure of biofilm was loose, they were also located in the interior of biofilms.

Nitrobacter sp. LIP|AM286385.1|
Nitrobacter sp. PBAB17|AY508476.1|
Uncultured *Nitrobacter* sp. clone K-OTU6493|KM580410.1|
Uncultured *Nitrobacter* sp. clone 1-G|EU305569.1|
Nitrobacter sp. TH21|AF080257.1|
Nitrobacter winogradskyi strain Nb-255|NR 074324.1|
Nitrobacter sp. BS5/19|AM286387.1|
Nitrobacter vulgaris strain K48|AM286381.1|
Nitrobacter sp. NBW1|KF618620.1|
Nitrobacter sp. 311|AM286397.1|
Nitrobacter sp. 219|AM286375.1|
Nitrobacter winogradskyi Nb-255|CP000115.1|
Nitrobacter winogradskyi strain ATCC 14123|AM114521.1|
Biofilm-Ctrl|KU705712|
Nitrobacter winogradskyi ATCC 25381|L35506.1|
Uncultured *Nitrobacter* sp. clone Nit4|HM061139.1|
Nitrobacter sp. Nato strain Nato |AM286376.1|
Nitrobacter winogradskyi strain Engel|AM286374.1|
Nitrobacter sp. PBAB10 |AY508475.1|
Nitrite-oxidizing bacterium MPN2|AY135357.1|
Uncultured *Nitrobacter* sp. clone NCAAH 30N18|KR537220.1|
Nitrobacter sp. Termite2|AM286391.1|
E.coli ATCC 11775T|X80725.1|

0.02

Figure 3. 3 Evolutionary relationships of taxa found in WTR-derived biofilm from AGBR run under control condition.
The primer pair used was Nitro-1198F and Nitro-1423R specific for all *Nitrobacter* species. The evolutionary history was inferred using the 1000 replicates of Neighbor-Joining method. The optimal tree with the sum of branch length = 0.23256771 is shown. The evolutionary distances were computed using the maximum composite likelihood method. All positions containing gaps and missing data were eliminated. Evolutionary analyses were conducted in Mega6.

3.3.5.1. In situ Detection of eubacteria: Digital analysis of FISH-CLSM images with *daime* indicated a positive linear correlation between eubacterial cells per cm^2 of WTR biofilm surface area and increasing concentration of Fe^{3+} (Figure A4). There was observed a difference of $7.5E + 02$ cells cm^{-2} (71.43% more cells) as the concentration increased from 2.5 to 8.5 mg/l of Fe^{3+} with $3.00E + 01$, $4.40E + 01$ and $1.05E + 02$ cells cm^{-2} at 2.5, 6.5 and 8.5 mg/l, respectively (Table A3).

3.3.5.2. In situ Detection of beta proteobacteria: Representative photomicrographs showed the presence of β proteobacteria within the bacterial community of WTR-derived biofilm. The proportion of β proteobacteria contained 42.96% more cells at 8.5 mg/l compared to control, with a difference of $6.10E + 01$ cells between the two extreme concentrations, that is, $1.42E + 02$ cells cm^{2-}at 8.5 mg/l and $8.10E + 01$ cells cm^{-2} in the absence of Fe^{3+} (Table A3).

3.3.5.3. In situ Detection of gamma proteobacteria: Contrary to the eubacteria and β proteobacteria populations, Υ population cell count followed an inverse relationship with increasing Fe^{3+} concentrations.

There was 53.42% abundance of ϒ cells when enumerated in biofilm incubated with 2.5 than at 6.5 mg/l Fe^{3+} with a significant difference of 3.90E + 01 cells cm^{2-} of WTR biofilm. The cell count was 7.30E + 01, 5.50E + 01 and 3.40E + 01 cells cm^{2-} at 2.5, 6.5 and 8.5 mg/l of Fe^{3+}, respectively (Table A3).

3.3.5.4. Biovolume Fraction

Biovolume fraction, calculated by *daime* for each sampling point in this study, was found to be 100% in virtually all cases except in case of biofilm from control reactor for β population where it was observed to be 101.7%. It was recorded 0% in case of negative control.

Figure 3. 4 Evolutionary relationships of taxa found in WTR-derived biofilm from AGBR run at 8.5 mg/l Fe^{3+}.

 The primer pair used was Nitro-1198F and Nitro-1423R specific for all *Nitrobacter* species. The evolutionary history was inferred using the 1000 replicates of Neighbor-Joining method. The optimal tree with the sum of branch length = 0.25955927 is shown. The evolutionary distances were computed using the maximum composite likelihood method. All positions containing gaps and missing data were eliminated. Evolutionary analyses were conducted in MEGA6.
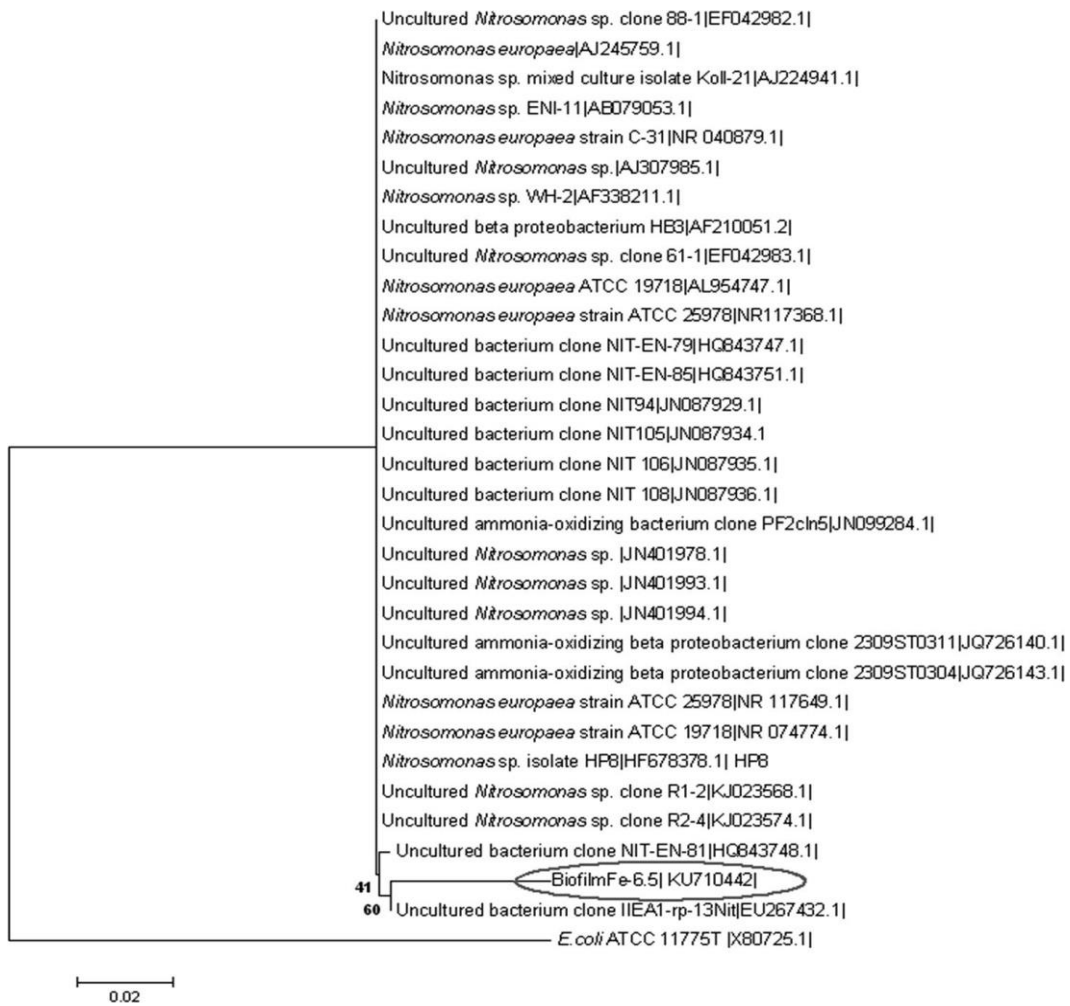
Figure 3. 5 Evolutionary relationships of taxa found in WTR-derived biofilm from AGBR run at 8.5 mg/l Fe^{3+}.

The primer pair used was Nitro-1198F and Nitro-1423R specific for all *Nitrobacter* species. The evolutionary history was inferred using the 1000 replicates of Neighbor-Joining method. The optimal tree with the sum of branch length = 0.25955927 is shown. The evolutionary distances were computed using the maximum composite likelihood method. All positions containing gaps and missing data were eliminated. Evolutionary analyses were conducted in MEGA6.
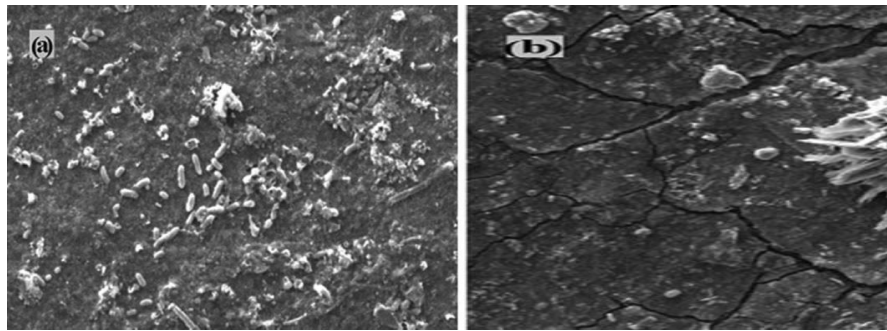
Figure 3. 6 Scanning electron microscopy (SEM) of biofilms on WTR developed under different concentrations of Fe^{3+}.

(a) Bacilli and coccid-shaped bacterial cells of biofilm embedded within thick mat of EPS on the surface of WTR after 90 days of exposure to 8.5 m/l Fe^{3+} (b) comparatively a smaller number of bacterial cells and thin EPS mat along with crevices in biofilm developed on the surface of WTR after 90 days without addition of Fe^{3+}.
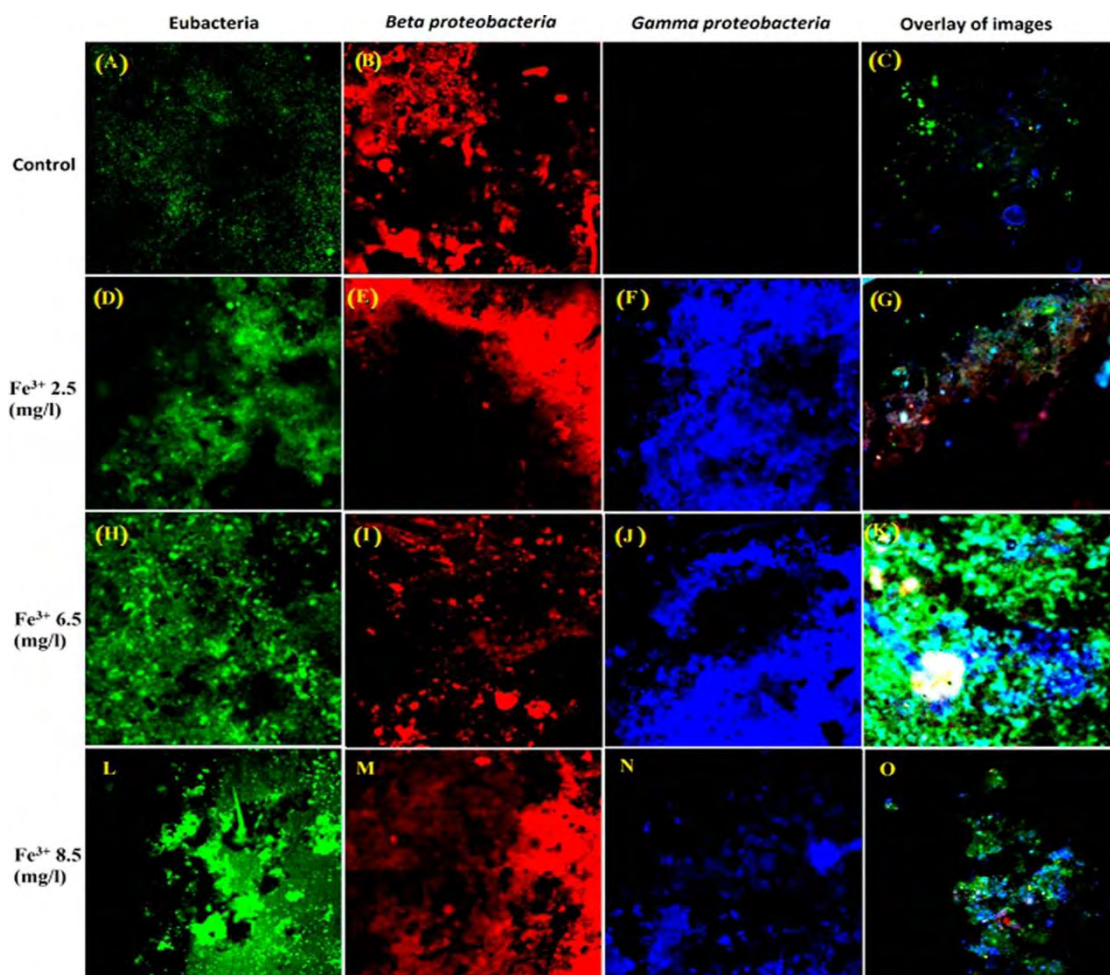
Figure 3. 7 CLSM images of biofilms on WTR in (AGBR developed under varying concentrations of Fe^{3+}.

First row represents biofilm of control reactor (A) Eubacteria, (B) beta proteobacteria, (C) overlay of both images. Second, third and fourth rows show biofilms of AGBR inoculated with 2.5, 6.5 and 8.5 mg/l of Fe^{3+}, respectively, where images in green color (D, H, L) depict eubacteria, red (E, I, M) show β proteobacteria, blue (F, J, N) indicate Υ proteobacteria, (G, K, O) overlay of respective eubacteria, β and Υ proteobacteria images produced using mixed channels. Yellow and pink signals do not yield from

binding of probes but are the result of overlaying of images, that is, red and green give yellow, red and white give pink. Background fluorescence was reduced by CLSM technique.

3.3.6. Characterization of Extracellular Polymeric Substance (EPS) of Biofilms by Fourier Transform Infrared Spectroscopy (FTIR)

The biofilms developed on waste tire rubber under varying Fe^{3+} concentrations were characterized by Fourier Transform Infrared spectroscopy (FTIR) to determine the presence or absence of specific molecular fragments (functional groups) in the EPS and the spectra were compared as shown below.

The IR spectrum of WTR biofilm with Fe-2.5 mg/l generated a stretch for carboxylic acids with a spike at 3271.94 cm$^-$ with 97% transmittance. It also exhibited bends of alkenes and C-H bonding at 1629 cm$^-$ and 1531.03 cm$^-$ and medium to small scissoring bends of NH_2 bonding with corresponding percentage transmittance in the range of 94% to 100%. The biofilm demonstrated more production of proteinaceous components in its spectrum.

The spectrum of biofilm with Fe-6.5 mg/l test was observed with thin pointed bend in the left of spectrum region with 90% transmittance indicating carboxylic acid production at 3237.38 cm$^-$. Narrowly pointed transmittance bends at 1644.38 cm$^-$ and 1636.49 cm$^-$referred to –NH_2 group whereas 1452.19 was indicator of alkane (C-H) bonding along with increasing transmittance from 87% to 93%. The weakest transmittance less than 80% was observed at 1113.73 cm$^-$ linked to C-N, C-C and C-O types of bonding. As compared to the former biofilm, there was predominance of acids, amines and alcoholic functional groups. At Fe-8.5 mg/l, a wide sharply pointed band at 3272.61 cm$^-$ and a deepest strong, peaked band at 1035.03 cm$^-$ (81% transmittance) were attributed to carboxylic acid and C-O-C bonding of ethers and esters.

In comparison to Fe^{3+} supplemented biofilms, very different IR spectra patterns were recorded biofilm grown without supplementation of Fe^{3+}. The peaks appeared at 3276.45 cm$^-$, 1452.90 cm$^-$ and 1049.94 cm$^-$ that were attributed to C=O-OH, (sp^3) C-H bonding of alkanes and C-O-C groups of ethers and esters. The upshots were an indicative of great variation in biofilm structural components on WTR material under varying Fe^{3+} concentrations (Fig. 3.8).

Figure 3. 8 FTIR of biofilms on WTR in (AGBR developed under varying concentrations of Fe^{3+} (Red: Control, Black: Fe-2.5 mg/l, Yellow: Fe-6.5 mg/l, Blue: Fe-8.5 mg/l).

3.4. Discussion

Studies have indicated the role of physical, chemical and biological parameters, namely, substratum characteristics, hydrodynamic shear, types and concentrations of nutrients (Wijeyekoon et al., 2004,Liu et al., 2012) and bio-flocculants (Parket al., 2006) in the natural selection of certain types of microbes in biofilms in attached growth reactors. In this perspective, ferric iron ($Fe^{3+)}$ has been reported to be playing an important role in the growth of bacteria (Appenzeller et al., 2005) and in the bio-flocculation of activated sludge due to its higher charge valency compared to monovalent and divalent bio-flocculants (Murthyand Novak, Wilén et al., 2003) . Bacteria in biofilms have been reported to respond in a narrow iron concentration range (Massonet et al., 2006). Keeping in view this study has focused on investigating the impacts of different concentrations of Fe^{3+} on biofilm structure of WTR and associated activated sludge digestion in AGBR. The findings in the research work validated the critical limits of Fe^{3+} that could help establish a controlled bioreactor where specific bacterial population(s) could be promoted or controlled in order to achieve optimum efficiency. Moreover, it has highlighted the utility of WTR as an efficient support material in attached growth reactors as a cost-effective solution.

COD generally reflects total oxygen consumed by organic and inorganic compounds when oxidized in water (Yang et al., 2009). Greater COD should result with lower amounts of cationic biocolloids, higher anionic contents and poorer floc structure. Aerobic treatment is recommended for COD concentration of less than 1500 mg/l and anaerobic treatment for higher COD values of up to 50,000 mg/l (Mutombo, 2014). In this present study, the COD of sludge was reduced significantly from 24.75% to 38% when concentration of Fe^{3+} was increased from 2.5 mg/l–8.5 mg/l in AGBR under anoxic conditions (Table 3). Gradual increase in COD removal might be attributed to the presence of iron and its increasing concentration in retaining bio-polymers (cations bind with proteins, polysaccharides, DNA, RNA and

lipids) within the sludge flocs. Adsorptive interactions between the floc bio-polymer constituents and iron hydroxyl minerals have been reported playing a specific role in stabilizing the sludge floc structure (Murthy and Novak, 2001). Enhanced oxidation of organic and inorganic compounds is also due to higher activities of both autotrophic and heterotrophic bacteria in the presence of Fe^{3+} as terminal electron acceptor (Scala et al., 2006, Park et al ., 2006, Muller, 2001).

Greater degree of apparent flocculation, sludge settleability and dewatering concentration has been linked with cations (Higgins & Novak, 1997a) . Solubility and toxicity effects of some metals as well as buffering capacity of some media have been determined by levels of acidity or alkalinity (Barbooti et al., 2004). Hence, about 69% increase in VFA content (Table 3.3) of sludge slurry under treated condition (Fe^{3+} = 8.5 mg/l) is therefore complimentary to previous sludge digestion. Furthermore, the reduction of iron under anaerobic condition has been linked with deflocculation and reduction of volatile acid residues pH within the reactors varied within a narrow range of 7.1–7.32. Addition of Fe^{3+} and ammonium metabolism is supposed to be involved in lowering media pH (Woznica et al., 2010). But variation of both pH and alkalinity within a narrow range might be due to the buffering effect of K_2HPO_4 and KH_2PO_4 in the AGBRs (Woznica et al., 2010, Merrylin et al., 2013).

Microbial density and diversity of WTR biofilms were affected by the application of different Fe^{3+} concentrations, as revealed by viable count plate (CFU $ml^{-1}cm^2$) (Figure A1), 16S rDNA sequencing (Figures 3-5) and imaging techniques such as FISH– CLSM and SEM. The changing concentrations of nitrite (NO_2^--N) and nitrate nitrogen (NO_3^--N) in sludge slurry further confirmed that the metabolic activities of the bacteria in biofilms were also affected. Nitrification and associated nitrifying bacteria are ubiquitous in water distribution systems (Lipponen et al., 2002). Varying NO_2^--N and NO_3^--N concentrations with time indicate the presence of both AOB and NOB in WAS. Low DO has always an adverse impact on nitrification and favors denitrification (Breisha & Winter, 2010, Rajesh Banu et al., 2009). Denitrifying bacteria prefer nitrogen oxides under oxygen-limiting condition as terminal electron acceptors (Woznica et al., 2010). Wastewater treatment under low DO is a possible means to control the inhibitory effect of oxygen on denitrification (Tan & Ng, 2008). Studies have mentioned different removal rates of nitrogen compounds due to coagulants and other operational conditions (Do et al., 2013, Banu et al., 2011). The presence of Fe^{3+} increased the NO_3^- removal rate from 13.1% to 62.2% in a subsurface flow constructed wetland that used WTR chips as bio carriers (Chyan et al., 2013). Likewise, 87.30% NO_2^- removal and 45% increase in NO_3^- concentration were observed when activated sludge was incubated with tire-derived rubber under anoxic conditions (Naz et al., 2014). In this study, decreasing order of values of NO_2^--N with increasing concentrations of Fe^{3+} at first week of incubation exhibited the inhibitory effect of Fe^{3+} and low DO on ammonium metabolism of AOB.

This might also be due to inhibition in AOB activity resulting from spatial competition between AOB and heterotrophs (Breisha and Winter , 2010,Lo et al., 2010). Heterotrophs such as Pseudomonas and *E.coli* sp. have been reported for their nitrification ability in organic wastewater (Handbook of Water and Wastewater Microbiology - 1st Edition, 2003) . Increase in NO_2^--N stimulated the activity of NOB.

Maximum removal rate of $NO_2^- -N$ and $NO_3^- -N$ in activated sludge occurred in reactors fed with 0 and 8.5 mg/l Fe^{3+} after three weeks, that is, 75.82% and 17.7%, respectively (Table 3.4). The decline in $NO_2^- -N$ and buildup of $NO_3^- -N$ concentration might be due to the activities of NOB as reported earlier (Sakuma et al., 2008).

The most prominent genera of bacteria responsible for the removal of contaminants in wastewater are α-Proteobacteria, β-Proteobacteria, γ-Proteobacteria, ε-Proteobacteria and Bacteroidetes (Linet al., 2009, Low et al., 2000). The heterogeneous nature of bacteria in these genera and symbiotic and competitive interactions among them helps decomposition of organic and inorganic compounds in sludge. Biochemical testing of bacteria isolated from WTR biofilms indicated mainly the presence of *Klebseilla* sp., *Vibrio* sp., *Bacillus* sp. and *Staphylococcus* sp. with predominance of Pseudomonas sp. Similar microbiology of wastewater biofilms has been reported in the past (Naz et al., 2014, Wojnowska-Baryła et al., 2010) where *P. aeruginosa* sp. have been indicated to grow and form biofilms under any condition that allows them to grow (Toole & Kolter, 1998). Nevertheless, Naz et al. (2014) reported inability of *P. aeruginosa* to form biofilm on tire-derived rubber (Nazet al., 2014). Yet, we observed that it grew on WTR at each Fe^{3+} concentration applied. Molecular phylogenetic analysis revealed the presence of a diverse species of both AOB and NOB, suggesting their significant role in Fe^{3+} treated biofilm reactors. Variation in the presence of *Nitrobacter* species on WTR at different concentrations (0 and 8.5 mg/l Fe^{3+}) further suggested the dosage response. of Fe^{3+}, that is, N. sp. 219 strain 219, *N. winogradskyi* strain Engel and uncultured bacterium clone IIEAI-rp-13Nit were found in biofilm treated with 8.5 mg/l Fe^{3+} (Figure 3.4), whereas *Nitrobacter winogradskyi* strain Engel, *Nitrobacter* sp. 219, *Nitrobacter* sp. *Nato* strain Nato, *Nitrobacter* sp. Termite2 appeared only at 0 mg/l of Fe^{3+} (Fig. 3.3).

WTR-derived biofilms supported higher bacterial density at higher levels of Fe^{3+}. An increase of about 4.44E + 10 CFU/ml cm^2 in bacterial count was observed when Fe^{3+} concentration increased from 0 to 8.5 mg/l with a difference of 4.44E + 10 CFU/ml cm^2 (Fig. A1). Previously, Park (Parkand Helm, 2008) and Novak (Novak, 1998) have also reported improved bio-flocculation and associated biofilm development in the presence of Fe^{3+}. Similarly, Yang et al. mentioned that *P. aeruginosa* biofilm formation was favored at 5 μM of Fe^{3+} along with expression of *pqs* quorum sensing operon and release of extracellular DNA that acted as intercellular connectors (Yang et al., 2007).

Hybridization with fluorescently labeled probes (EUB338 mixture, β42a, γ42a) coupled with CLSM of Fe^{3+} treated WTR biofilms revealed that higher Fe^{3+} concentration influenced the growth of selective bacterial groups creating an intricate landscape of microhabitats that subsequently lead to a stru0ctured localization of bacterial communities. The darker areas in CLSM images presented voids and grooves with rough surfaces in biofilm textures filled with deposited cells (Fig. 3.7). Wijeyekon et al. (2004) have also given evidence of such base layer, suggesting that biofilms' growth extended laterally. CLSM images cytometry indicated that the eubacteria and ratios of proteobacteria classes varied considerably under varying Fe^{3+} treatments (Table A3). About 71.43% eubacteria and 42.96% higher cell counts of β proteobacteria were calculated at 8.5 mg/l of Fe^{3+} than in control condition. Contrarily, the dominance of

ϒ proteobacteria was 53.42% less under the said treatment. Bacteria belonging to different taxonomic groups grew intermingled. Higher β to ϒ ratio of Proteobacteria in biofilms was also reported previously in conventional activated sludge system, membrane bioreactors and water drainage systems (Manz et al., 1993, Lin et al., 2009, Sofia et al., 2004,Snaidr et al., 1997).

3.5. Conclusion

The study established a vital role of WTR in attached growth batch reactors (AGBRs). Besides, it critically revealed a positive impact of trivalent iron (TVI) in establishing biofilms in reactors and associated digestion and flocculation of activated sludge. Overall, bacterial community fluctuated greatly under varying regimens of Fe^{3+} treatment. Nevertheless, the count and types of specific bacterial community, namely, Enterobacteriaceae, AOB, NOB and higher β/γ ratio in WTR biofilm positively correlated with the ongoing metabolism (nitrification) and digestion rate of organic contaminants in sludge. Most of isolated bacteria ($\approx$ 96%) were strong biofilm formers using tissue culture plate assay.

CHAPTER 3 (B)

Effects of Metals on Biofilm Development and Microbial Community in Attached Growth Bioreactors

Study 3B

Title: Effects of Aluminum (Al^{3+}) on Sludge Digestion and Biofilm Development in Attached Growth Batch Reactors using Tire-derived Rubber as a Media

CHAPTER 3 (B): Effects of Aluminum (Al^{3+}) on Sludge Digestion and Biofilm Development in Attached Growth Batch Reactors using Tire-derived Rubber as a Media

Abstract

Effects of varying concentrations of aluminum (Al^{3+}) on sludge digestion and biofilm development on waste tire rubber were determined in attached growth batch reactors (AGBR) for 30 d under anoxic conditions. The strategy was bi-pronged where performance of the reactors was measured through activated sludge liquor digestibility and nitrogen removal viz. chemical oxygen demand (COD), NO_2^--N/NO_3^--N, respectively. Overall, increase in Al^{3+} concentration (0 mg/l–6.5 mg/l) resulted a decrease (7.33%) in bacterial density. Biochemical characterization of the bacterial isolates confirmed that most of them were gram negative. Moreover, fluorescence in situ hybridization (FISH) coupled with confocal laser scanning microscopy (CLSM) and spatial distribution analysis of the biofilms indicated presence of beta and gamma proteobacteria. Bacterial population densities decreased with increasing levels of Al^{3+}. Tissue culture plate (TCP) assay revealed 93.4% of isolated bacterial proportion was strong biofilm formers. Test tube method and Congo red agar assays showed ˜67% and 63% bacteria were strong biofilm formers. Additionally, sludge digestibility decreased in the reactors as high levels of COD (438 mg/l) and volatile fatty acids (VFA; 350 mg/l) were recorded at 6.5 mg/l of Al^{3+}. Ammonium nitrogen (NH_4^+-N) transformation measured as NO_3^--N and NO_2^--N indicated an overall decrease in both the inorganic forms of nitrogen with highest elimination rate of NO_2^- at 4.5 mg/l Al^{3+}, whereas, lowest was recorded at 2.5 mg/l Al^{3+}. Generally, the study revealed a limiting effect of Al^{3+} concentration at specific levels on sludge digestibility, bacterial density, diversity and metabolism in the AGBR.

Keywords: Aluminum (Al^{3+}); Biofilms; Wastewater treatment; Community composition; Tire-derived rubber; Fluorescence in situ hybridization (FISH); Confocal laser scanning microscopy (CLSM), Scanning electron microscopy (SEM), Fourier transform infrared spectroscopy (FTIR).

3.1. Introduction

Ubiquity of biofilms as recalcitrant three-dimensional matrices on biotic and abiotic surfaces translates into a unique conundrum. The inherent bio-catalysis of complex compounds and production of secondary metabolites by biofilms has been exploited to develop environmentally sustainable and novel technologies for waste water treatment and energy production (Todhanakasem, 2017, Yoshizawa et al., 2014). Great economic losses have been incurred due to the unmitigated growth of biofilms on surfaces and membrane filters presenting a com-pounding challenge that needs to be circumvented. The preference of bacteria to grow on attached rather than in the suspended phase (Katsikogianni et al., 2004) is contributed by a complex interaction between the bacteria and surface chemistry of support material (Tuson & Weibel, 2013). The tendency of bacteria to attach to surfaces has been extensively studied with respect to microbiologically induced corrosion or biofouling of piping surfaces employed in water, waste water, oil and gas distribution networks, bioreactor membranes or other propagating surfaces (Yikmis & Steinbüchel, 2012) . In order to promote environmentally sustainable technologies, it is imperative to

address the issue of low cost of treatment options by focusing on usage of cheap biofilm support materials. Billions of used tires are stockpiled annually owing to unavailability of their alternate applications. In this context, waste tire-derived rubber has been viewed as an alternative to different costly materials in attached growth biofilm reactors due to its good surface area, less toxicity to microorganisms and size distribution. Previously, a number of bioreactors, such as trickling filters and hybrid sludge biofilm bed reactor using tire-derived rubber as support, have been run with considerable treatment efficiencies (Tang et al., 2006, Park et al., 2014, Park, 2008, Naz et al., 2014). Still, detailed understanding of the factors influencing biofilm structure and growth is imperative to harness the potential of the said bioreactors.

Typically, aluminum ions and poly-alum compounds have been recommended as effective coagulants for removal of chemical oxygen demand (COD) and bio-logical oxygen demand (BOD) in wastewater treatment (González et al., 2007). Iron and aluminum hydroxide coatings on filtering materials such as sand have also been reported to effectively remove fecal coliforms from water(Park, 2008) and achieved a reduction of 4 log in the bacterial count after passing waste water through sand columns coated with iron and aluminum hydroxide. Similarly, Zhu et al. (2012) indicated that aluminum sulfate removed color and COD by 72% and 90%, respectively (Zhu et al., 2012).

In vitro studies to evaluate the effect of different parameters such as oxygen, carbon dioxide, nutrients on biofilm formation rely on the use of biofilm reactors that can be either batch reactor or open systems (Vu et al., 2009, Samanovic et al., 2012, Nan et al., 2015). The advent of scanning and transmission electron microscopy enabled an in-depth exploration and higher resolution of biofilms to be studied (Teitzel & Parsek, 2003) . Bacterial density and biochemical identification have been conducted using conventional culture-based methods. However, these methods have their limitations such as inability to identify non-culturable bacteria. Two major thrusts in the previous two decades have impacted our understanding of biofilms including molecular methods such as fluorescence in situ hybridization (FISH) and confocal laser scanning microscopy (CLSM) (Douterelo et al., 2014, Neu & Lawrence, 2014). Herten et al.(Herten et al., 2017) quantified *Staphylococcus aureus* biofilm formation on vascular graft surfaces by using conventional culture based techniques to determine colony forming units and validated their findings qualitatively using scanning electron microscopy (SEM). Fish et al. (2015) characterized the physical composition and microbial community composition of biofilms of their full scale model water distribution system using fluorescent CLSM and digital image analysis (DIA) (Fish et al., 2015). Similarly, Sharafat et al. (2018) quantified microbial density in biofilms developed on waste tire rubber with FISH and CLSM (Sharafat et al., 2018).

Despite established role of aluminum as a coagulant, the role of these flocculating agents on biofilm development dynamics and floc stability has not been extensively studied specifically with regards to Al^{3+} (Park et al., 2010, Park, Muller, 2006, Murthy et al., 1998) . A gap exists in our understanding of aluminum's role in terms of overall microbial diversity in biological wastewater treatment and water sanitation systems. Thus, this study evaluated the effects of varying concentrations of aluminum on

biofilm development and associated bacterial densities on tire-derived rubber as a cheap support material through conventional and molecular based techniques such as FISH and CLSM. Besides, the effect of varying concentrations of aluminum on reactors performance was monitored in terms of waste water's sludge digestibility along with nitrification rates.

3.2. Materials and Methods

3.2.1. Development of Biofilms on Tire-derived Rubber Support

3.2.1.1. Sampling

Activated sludge was collected from municipal waste water treatment plant located in Islamabad, Pakistan, in sterilized plastic containers. Sample was transported within an hour to laboratory in cold sampling box and stored at 4°C prior to inoculation into the reactors on the same day.

3.2.1.2. Set up and Operation of Attached Growth Batch Bioreactors

Strips of waste tire-derived rubber (TDR) (surface area: 93.48 cm^3) were cut and vertically aligned in four attached growth batch reactors (AGBR) in duplicate, with a total capacity of 4 l each and working volume of 3 l. The TDR strips incorporated in the reactors were of a passenger car and they were suspended inside the reactors with an iron wire such that three fourth was covered with waste activated sludge. The composition of the TDR included crumb rubber (70%), fibers and scrap (13%) and steel (17%) (The Composition of a Tyre: Typical Components, 2006.). Composition of the medium used within each reactor was as follows: 2 L activated sludge, 1 l minimal salt media (64g Na_2HPO_4, 15g KH_2PO_4, 2.5 g NaCl, 5.0 g NH_4Cl, 1 M Mg_2SO_4, 20% glucose and 1 M $CaCl_2$), 5 mL trace elements (10mg $ZnSO_4.7H_2O$, 3mg $MnSO_4$, 1mg $CoCl_2.6H_2O$, 20mg $NiCl_2.6H_2O$, 30mg $Na_2Mo.2H_2O$, 30 mg H_3BO_3, 1mg $CuCl_2.2H_2O$, 1mg $CuSO_4$), 5g starch and 5g technical agar (Oxoid). The characterization of the wastewater from this facility, according to European Standards was as follows: HRT: 7 d, MLSS: 3,000–3,500 mg/l, TSS: influents; 230–235 mg/l, effluents: 35 mg/l, BOD: 190–200 mg/l, COD (Influent): ≈700 mg/l, COD (effluent): 150 mg/l. The batch reactors were covered with black paper to prevent any algal growth and incubated at 30°C ± 2°C. After incubation of 2 d as an acclimatization period, three reactors were dosed with three different concentrations of $AlCl_3$ (2.5, 4.5 and 6.5 mg/l) and homogenized with stirrers, whereas, control reactor received no aluminum. The reactors were incubated under anoxic condition at 30°C for a period of 30 d. Mechanical stirring was carried out with sterile stainless stirrers periodically to ensure appropriate oxygen diffusion and homogeneity of the contents in the reactors.

3.2.2. Physico-Chemical Characterization of Activated Sludge Liquor in Reactors

Sludge digestion in the reactors was measured in terms of different physicochemical parameters. COD (mg/l), VFA (mg/l) and alkalinity (mEq/l) of sludge were measured initially and at final stage (after 30 d of treatment), using COD commercial kits (Merck, Germany, detection range; 25–2,500 mg/l) and three point titration method (Buchauer, 1998) , respectively. In addition, NO_3-N and NO_2-N of the activated sludge were measured, using APHA 4500 NO_3-N and APHA 4500 NO_2–N methods respectively. (Arnold E. Greenberg, Lenore S. Clesceri, 1992)The pH of the samples was determined periodically using

"Digital Sartorius (pp 15) pH meter". Dissolved oxygen (DO) was monitored with "Crison OXI45+ DO meter" that contained 5120 electrodes. The electrode of the meter was washed three times with distilled water before analyzing each sample.

3.2.3. Evaluation of Bacterial Density in Biofilms of Tire-derived Rubber

Biofilms developed on TDR, under the influence of different aluminum concentrations after enrichment culture technique, were gently washed with PBS to remove any planktonic microorganism. The biofilms were scraped off from 1 cm^2 sections of the support using sterile surgical blade. The cuttings were then sonicated at 1–2 kHz for 3 min. Bacterial biofilm density on the tire-derived support surface was determined on the basis of CFU/mL cm^2 using heterotrophic plate count method on nutrient agar plates in triplicate and analyzed statistically with t-test using Microsoft excel 2015. Pure cultures of bacteria obtained on nutrient agar plates were biochemically characterized and identified using standard procedures and following Bergey's Manual of Determinative Bacteriology (Bergey, 1994).

3.2.4. Biofilm Forming Potential of Isolated Bacteria

Bacteria isolated from each biofilm on TDR developed under the effect of different concentrations of aluminumwere evaluated for their biofilm formation ability using biofilm formation assays such as congo red agar (CRA) assay, tube method (TM) and tissue culture plate or microtiter plate (MTP) assay as described in study 3A.

3.2.5. Molecular Characterization of Autotrophic Nitrifying Population in Activated Sludge and Biofilms Developed on Tire Rubber under Varying Concentration of Al^{3+}

Autotrophic nitrifying populations (ammonium oxidizing bacteria and nitrite oxidizing bacteria) were identified from the biofilm developed on tire derived rubber at Al^{3+} (4.5 mg/l), using 16SrRNA sequencing. The DNA from the biofilms was extracted using Norgen Biotech. Soil DNA Isolation Kit (Cat. 26500), as per the manufacturer's instructions. Primers used for amplification and sequencing are described in study 3A.

3.2.6. Nitrifying Activity of Bacterial Community in the Biofilms Treated with Varying Concentrations of Al^{3+} under Shake Flask Conditions

The aim of this experiment was to determine the effect of Al^{3+} on predominant autotrophic nitrifying and heterotrophic nitrifying population residing within the biofilms. One cm^2 cuttings of the biofilm containing TDR was taken from each batch reactors and added into 100 ml of autoclaved sterile N-enrichment media. The composition of the media (mg/l) was $NaHCO_3$ (13.8 mg), NH_4Cl (70.18 mg), K_2HPO_4 (0.236 g) and trace elements (0.25 ml). Specified concentrations of Al^{3+} were added to each flask and the flasks were covered with black paper to prevent any photoinhibition of the nitrifiers. The flasks were placed in shaker-incubators at 32°C and sampling was carried out aseptically each week. The samples were then analyzed for NO_3 and NO_2 by using APHA 4500 standard protocol and using Merck Pharo Spectroquant.

3.2.7. Scanning Electron Microscopy of Biofilms on TDR

To visualize the surface morphology of biofilms on TDR, SEM of the biofilms on TDR from attached growth batch reactors was carried out. Small sections of fixed biofilm samples on TDR were mounted on copper stubs and sputter coated with gold layer. Then vacuum was generated by applying high voltage in ion sputtering device (JFC-1500, auto coater, JEOL, Tokyo, Japan) for gold deposition on biofilms. 25 mA current for approximately 50 s was used for plasma generation and subsequent gold coating on the samples. Gold coated samples were then placed under the column in chamber and finally the micrographs were observed under SEM (JSM-6490A, JEOL) at different magnification intensities starting from X100 to X20,000 and recorded.

3.2.8. Microbial Community Analysis of Biofilms by FISH and Confocal Laser Scanning Microscope

To check the specificity of fluorescent probes and for hybridization optimization, bacterial strains, that is, *Bacillussubtilis*; accession no. KJ600795 and *Pseudomonas aeruginosa* ATCC ® 9027TM) were applied as positive reference cells for β and ϒ communities of proteobacteria in the upper wells of the slides (Figs.S1 and S2). Biofilms on TDR were washed with sterile distilled water to remove planktonic microorganisms. The biofilms were transferred from 1 cm2 surface area of the support media to 10 well Teflon coated glass slides followed by fixation with 4% paraformaldehyde (PFA) for 2 h (–20°C) according to protocols described by Manz et al. (Manz et al., 1999), with slight modifications for non-disruptive fixation of bacteria. After washing samples with PBS (pH 7.2), the samples were successively dehydrated using 50%, 80% and 100% ethanol and stored at room temperature before further processing. 18 µl of hybridization buffer (20mM Tris HCl (pH 7.2), NaCl0.9 M), 0.01% sodium dodecyl sulfide (SDS), 35% formamide (deionized) and 2 µL of 5′ end fluorescently labeled 5, 6 FAM (FLUOS derivatives; amine reactive succinimidyl esters of carboxyfluorescein) oligonucleotide probes were pipetted out into each well. 2 µL of corresponding unlabeled competitor probes were also added to ensure specific binding. Fluorescent labeled probes and their corresponding unlabeled competitors, used in this study, were obtained from α-oligos (Montreal, Canada). Details of fluorescent probes (Gam42a and Beta-42a) are mentioned in Table 1. After incubating slides for 90 min in hybridization chamber at 46°C, the slides were washed with prewarmed washing buffer (Tris/HCl20 mM, 0.01% SDS, 5 M NaCl), rinsed with distilled water, dried and mounted in Citifluor. Prepared hybridized slides were viewed under FluoViewTM (Fv1000) confocal laser scanning microscope equipped with multi argon ion lasers (409–552 nm) and optical sections were collected under Kalman filtration mode. Multiple fields of views (FOV) were selected containing maximum cells for image acquisition.

Table 3 . 1 Sequences and specificity of 5′ end 5,6-FAM labeled 16S rRNA oligonucleotide probes.

No.	Probe (Full name)[a]	Specificity	Binding positionb (bp)	5′-End labeled (5,6-FAM) probe sequence	References
1	EUB338- I (S-D-Bact-0338-a-A-18)	16S rRNA, majority of bacteria	338–355	GCTGCCTCCCGTAGGAGT	(Amann et al., 1990)
2	EUB338- II (S-*-BactP-0338-a-A-18)	16S rRNA, bacteria not targeted by EUB338-I	338–355	GCAGCCACCCGTAGG TGT	(Daims et al., 2006)
3	EUB338- III (S-*-BactV-0338-a-A-18)	16S rRNA, bacteria not covered by EUB338-I and EUB338-II, *Verrucomicrobiales*	338–355	GCTGCCACCCGTAGGTGT	
4	Bet42ac (L-C-bProt-1027-a-A-17)	β-Proteobacteria	1,027–1,043	GCCTTCCCACTTCGTTT	(Manz et al., 1999)
5	Gam42ac (L-C-gProt-1027-a-A-17)	γ-Proteobacteria	1,027–1,043	GCCTTCCCACATCGTTT	(Manz et al., 1999)

[a]Full name of 16S rRNA gene-targeted oligonucleotide probe(s) is based on the nomenclature of Alm et al. .(Alm et al., 1996)

[b]Probe binding positions according to *E. coli* 16S rRNA gene numbering .(Brosius et al., 1981)

cCompetitor probes of Bet42a and Gam42a were also added to the hybridization buffer as unlabeled oligonucleotide probes in equimolar amounts as the labeled probes to enhance the hybridization specificity (Manz W et al., 1999).

The images were reserved in TIFF format for further processing. Quantification of the microbial populations (average of three images) was carried out using *daime* (DIA in microbial ecology) software (Daims et al., 2006). Only those results were included in analysis that showed significant intensity of signals with the target cells. The image analysis provided us information on parameters, that is, cell numbers, bio-volume fraction and biomass (area of cells). Upper and lower cut offs were chosen to avoid objects to avoid objects (too small or large) to be bacteria during image processing.

3.2.9.FTIR of EPS of Biofilms Developed on Different Materials under Varying Conditions of AlCl₃

EPS of the biofilms formed was analysed using the method described by Jiao et. al. (Jiao et al., 2010) The biofilm sample was scraped off from the TDR using a sterilized surgical blade carefully. Approximately 0.5 ml of sample was scraped into sterile Eppendorf tubes. Precipitation of EPS from biofilms was carried out using ethanol. A 3:1 ratio of 100% cold ethanol was added gradually along the walls of the Eppendorf was used for precipitation. The Eppendorf tubes were then incubated on ice for 2 hours, and immediately afterwards centrifuged at 17500Xg for 20 minutes at 4 °C. The pellet was then dried overnight at 50 °C in an oven incubator. This procedure was applied to all the materials in the three reactors.

3.3. Results

The study presented herein evaluated the effects of $AlCl_3$, a commonly used coagulant in wastewater treatment, on biofilm development as well as the effect exerted by material surface (tire rubber) on biofilm development. For this purpose, attached growth biofilm batch reactors (AGBR) were set up to which a particular concentration of $AlCl_3$ was added. Microbial profiling of the biofilms was carried out by a tri-pronged strategy. Firstly, conventional bacterial enumeration based on heterotrophic plate count of the biofilms from a cm^2 area of each of the surfaces under study and developed under varying $AlCl_3$ concentrations (mg/l) was carried out. Microbiological structure of the biofilms was determined by isolating and then following the conventional scheme of identification of the isolates based on microscopy, differential media growth and biochemical tests as per the *Bergey's* Manual of Descriptive Bacteriology. The second strategy to study microbial community structure of autotrophic bacteria was based on molecular characterization of the nitrifying population in the biofilm of tire rubber at a particular concentration of Al^{3+} (4.5 mg/l), untreated biofilm and raw activated sludge. Thirdly, biofilm micro-profiling was conducted through image analysis techniques comprising of scanning electron microscopy (SEM) and confocal laser scanning microscopy (CLSM). SEM of biofilms on tire rubber was carried out at a particular concentration of Al^{3+} (4.5 mg/l). CLSM-FISH was carried out to study the bacterial spatial distribution as well as to enumerate the total bacteria present within the biofilms as well as different bacteria on the basis of whether they belonged to Phyla *B-proteobacteria* or *Gamma proteobacteria.* In addition to the microbiological structural profiling, biochemical nature of EPS from the biofilms was analyzed using FTIR analysis.

3.3.1. Physicochemical Profile of Activated Sludge in AGBR under Varying Concentrations of Al^{3+}

Varying concentrations of Al^{3+} proved to have a significant effect on the overall digestion of sludge in the AGBR in 30 days. COD (mg/l) of raw sludge was reduced when treated with different concentrations of Al^{3+} compared with untreated sample. Maximum removal of COD was 28.68% at 2.5 mg/l of Al^{3+} followed by 27.11% and 13.95% at 4.5 and 6.5 mg/l Al^{3+}, respectively (Fig. 3.1).
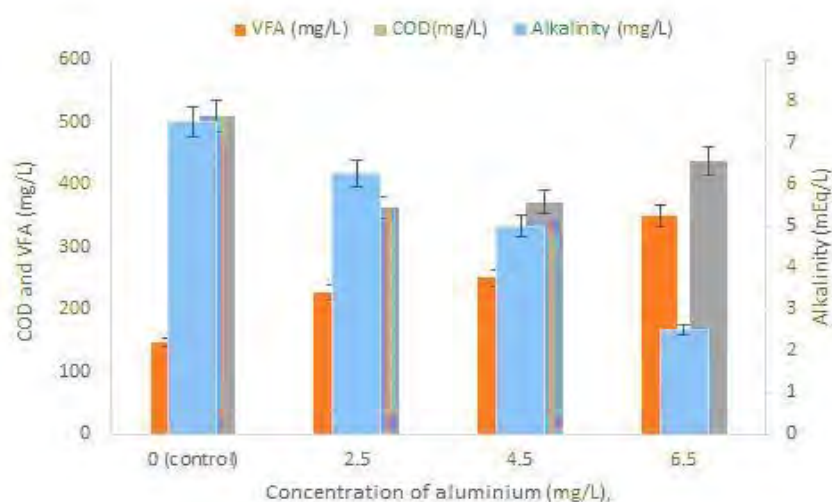
Figure 3 . 1 Variation in concentration of COD, volatile fatty acid (VFA) and alkalinity of sludge in attached growth batch reactors after 30 d of treatment.
Raw sludge characteristics were; COD; 700 mg/l, VFA; 27.5 mg/l, alkalinity; 9.5 mg/l).

VFA and alkalinity of the activated sludge seed were determined to be around 9.5 mg/l and 27.5 mEq/l, respectively. After incubation in AGBR, alkalinity of activated sludge decreased with increase in Al^{3+} concentration in the reactors. Under control condition (Al^{3+} = 0 mg/l) it remained 7.5 mEq/l whereas, minimum alkalinity of 2.5 mEq/l was observed at 6.5 mg/l of Al^{3+} (Fig. 3.1). Contrarily, minimum level (147.5 mg/l) of VFA was observed under control condition that increased with increasing concentration in the following order: 227.5, 250 and 350 mg/l for 2.5, 4.5 and 6.5 mg/l of Al^{3+}, respectively (Fig. 3.1, Table 3.1).

Table 3 . 2 Characteristics of treated activated sludge as COD, volatile fatty acid and alkalinity in AGBR after 30 d of treatment.

Concentration (mg/L)	VFA (mg/L)	Alkalinity	COD (mg/L)
Control (0)	147.6	7.54	509
2.5	227.67	6.25	363
4.5	250.03	4.9	371
6.5	350	2.5	438

Note: Characteristics of raw sludge before treatment: COD, 700 mg/l, VFA, 27.5 mg/l, Alkalinity, 9.5.

Nitrate and nitrite concentration were monitored as indicators of sludge digestion and performance efficacy of the attached growth batch biofilm reactors (AGBRs), by sampling and then carrying out analysis of the activated sludge liquor, from the AGBRs at weekly intervals, over a period of four weeks. The concentration (mg/l) of nitrite nitrogen in the reactor serving as control (0 mg/l Al^{3+}) and those dosed with a range of Al^{3+} concentrations, that is, 2.5, 4.5 and 6.5 mg/l were as follows: 182.0mg/l, 39.0mg/l, 47.0mg/l and 59.0 mg/L, respectively, at the first week of operation. Percentage change for NO_2^- was highest, that is, 77% (96 mg/l) at 2.5 mg/l followed by control, 4.5mg/l and then 6.5 mg/l of Al^{3+} (Fig. 3.2). Trend for NO_2^--N (mg/l) followed a linear decrease in the first 3 weeks of incubation for untreated

sludge (0 mg/l Al^{3+}). Whereas, under treated conditions an increase in NO_2^--N (mg/l) till midweek with a linear decrease in the proceeding next was observed. Difference in the rate of percentage change of nitrite concentration between consecutive weeks for treated reactors followed a decreasing trend with increasing concentration of Al^{3+}. The final concentrations of nitrite in the reactors on 30th day were 28.05%, 21.13% and 14.91%, for 2.5, 4.5 and 6.5 mg/l of Al^{3+}, respectively.

Nitrates concentration decreased with time specifically under experimental (treated) conditions. Initial reading for nitrate concentration in treated and control sludge samples (2.5mg/l, 4.5mg/l and 6.5 mg/l of Al^{3+}) were 168.8mg/l, 219.7mg/l, 249.2mg/l and 216.1 mg/l, which decreased to 163.7, 148.4, 114.2 and 115.8 mg/l, respectively, in the third week. The decreasing trends in nitrates reduction rates were 54.17%, 46.41%, 32.40% and 30.2% at 4.5mg/l, 6.5mg/l, 2.5mg/l and 0 mg/l of Al^{3+}, respectively (Fig 3.2; Table3. 2). Under control condition, there was 22.39% increase in nitrate concentration by the second week, followed with a decline in the third week from 206.6mg/l to 163.7 mg/l, that is, a percentage decrease of 20.76%.
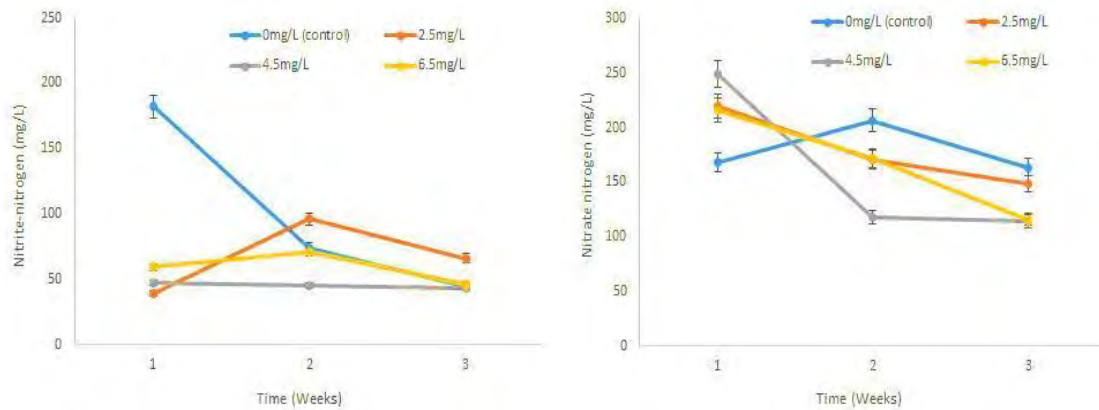
Figure 3 . 2 Transformation rate of nitrogen.
Transformation rate of nitrogen was measured in terms of NO_2^- (mg/l) and NO_3^- (mg/l) in the attached growth batch reactors treated at different concentrations of Al^{3+} (2.5 mg/l, 4.5 mg/l and 6.5 mg/l) over a period of 4 weeks. Time points: 1 = 7th day, 2 = 15th day, 3 = 30th day.

Table 3 . 3 Transformation rate of nitrogen in terms of NO_2^- (mg/l) and NO_3^- (mg/l) in the attached growth batch reactors treated at different concentrations of Al^{3+} (0mg/l *l*, 2.5mg/l, 4.5mg/l and 6.5 mg/l) over a period of 4 weeks. Time points; 1= 7th day, 2=15th day, 3= 30th day.

Sample	Week	Week	Week	A	B	% A	% B
	1	2	3	0	0	Decrease	Decrease
Concentration of nitrites (mg/l)							
Control	182	74	44	10.8	13.8	59.34	73.4
Al - 2.5	39	96	66	2.7	3	59.3	76.92
Al - 4.5	47	45	43	2	4	40	8.5
Al - 6.5	59	71	46	12a	13	20.33a	22.03%
Concentration of nitrates (mg/l)							
Control	168.8	206.6	163.7	37.8	18.35	22.39a	30.2
Al - 2.5	219.7	170.5	148.4	49.2	7.13	22.39	32.45
Al - 4.5	249.2	118.1	114.2	13.11	52.6	52.6	54.17
Al - 6.5	216.1	172.6	115.8	4.34	10.03	20.09	46.41

a%increase

The pH of Attached Growth Biofilm Batch Reactors was maintained at around 6-8 due to the buffering effect of K_2HPO_4 and KH_2PO_4, present in the MSM media. The pH of control ranged from 7.47-7.06, whereas in the case of attached growth biofilm reactor (AGBR) with varying concentrations of Al^{3+} (2.5 mg/l, 4.5 mg/l and 6.5 mg/l) the pH was in the following range: 6.59-7.88, 6.54-7.45 and 6.1-7.73, respectively (Fig.3.3).
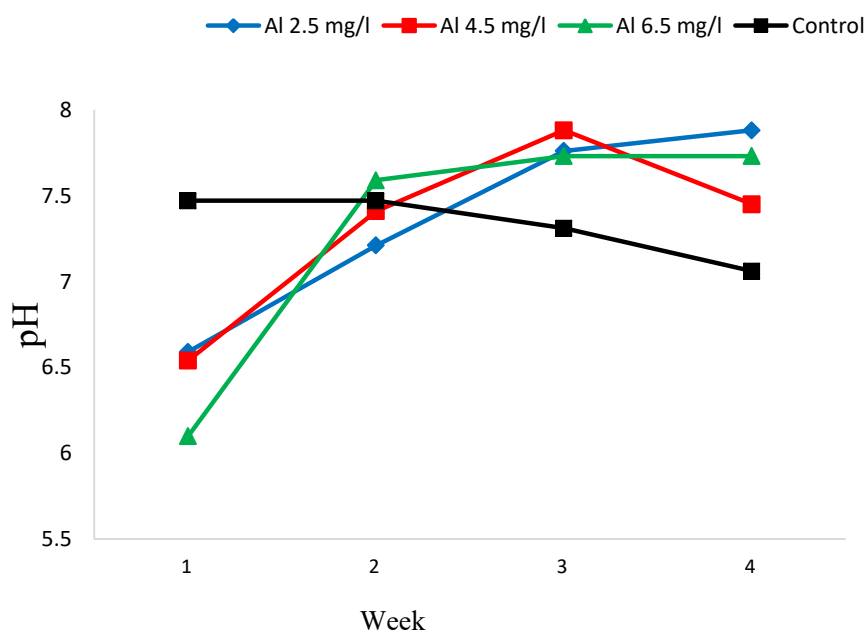
Figure 3 . 3 pH monitored over four weeks for the attached growth batch reactors (AGBRs).

3.3.2. Effect of Aluminum (mg/l) on Bacterial Density (CFU/mL cm^2) in Biofilms

Different concentrations of Al^{3+} (mg/l) proved to have insignificant ($p > 0.05$) limiting effect on bacterial growth in biofilm developed on TDR after a period of 30 days (A.1, A.2). Under control condition, bacterial count was 9.05E+09 CFU/ml cm2. However, it reduced by 91.25% when 2.5 mg/l of Al^{3+} was used in the reactor. Further increase in Al^{3+} (mg/l) proved to be more limiting and bacterial count reduced to 98.65% and 98.58% at 4.5mg/l and 6.5 mg/l of Al^{3+}, respectively (Fig. 3.4, Table S3). Scanning electron micrographs also demonstrated similar results (Figs. 3.10-3.11). However, the colony morphologies on the sample that had gone through treatment analysis were more diverse. Isolation of bacteria was done from dilution plates on nutrient agar plates. 28 cultures were isolated. Gram staining was done that showed the presence of 11 Gram positive bacteria in which there were only one-Gram positive cocci and 17 Gram negative bacteria (Table A9-B).

A total of 13 different bacterial genera were identified on the basis of morphology and biochemical assays (Table S4). Majority of the isolates were gram negative, a typical representation of sludge microflora. Potential bacterial isolates included species of genera: *Pseudomonas*, *Bacillus*, *Enterobacter*, *Serratia*, *Proteus*, *Citrobacter*, *Klebsiella pneumoniae*, *Salmonella*, *Staphylococcus*, *Streptococcus* and *Shigella*.
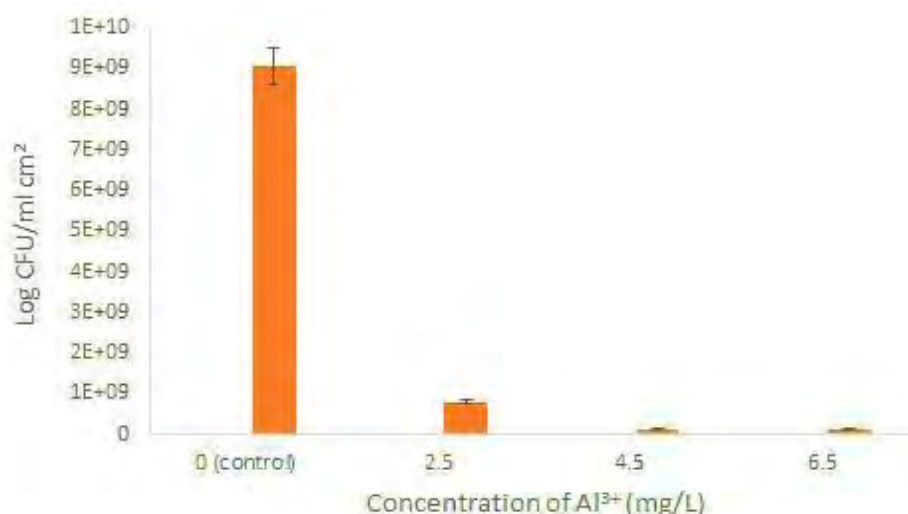
Figure 3 . 4 Culture and physiological based bacterial density (CFU/ml cm^2) in biofilms developed on TDR under the influence of different aluminum concentrations (mg/l).

3.3.3. Biofilm Forming Ability of the Bacterial Isolates

The distinct colony morphologies on nutrient agar were used to select the isolates from the biofilms, which were then streaked on plates to establish their purity. A total of 77 isolates were then tested for their biofilm forming ability using the three assays; CRA, Tube method and microtiter plate assay. It was found that CRA gave the lowest positives at a total of 48 whereas the number of non- biofilm formers was 28 (Table A5-B, Table 4.10). On the other hand, tube method gave around 4 weak or non-biofilm formers while there were 21 moderate and 51 strong biofilm formers (Table A6-B). Tissue culture plate method gave 5 weak and 71 strong biofilm formers. For the microtiter plate there were 71 strong biofilm formers determined and the rest were moderate biofilm formers (Table A7-B).
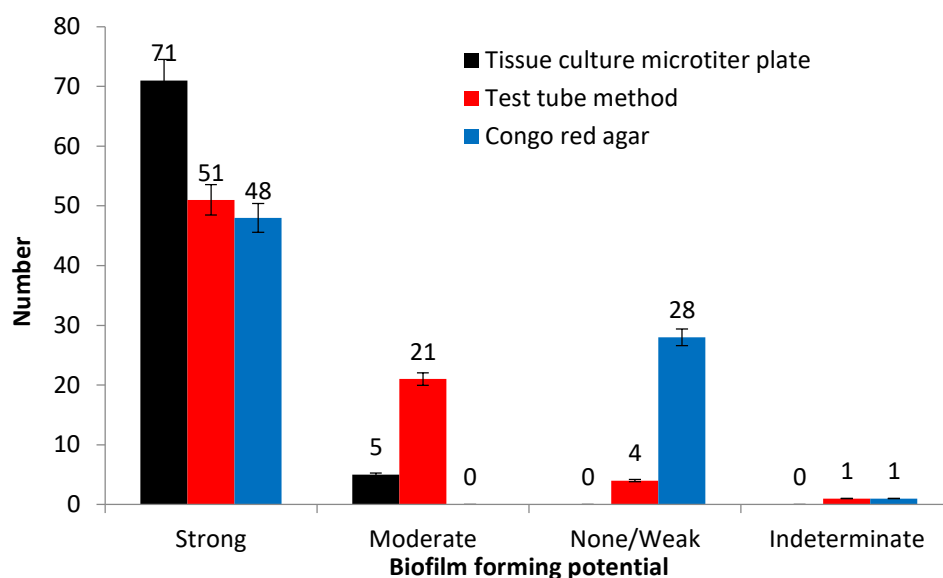
Figure 3 . 5 Comparative distribution of biofilm formers (weak, moderate and strong) in different assays; Tissue culture plate, Test tube method and Congo red agar assay (n=76).
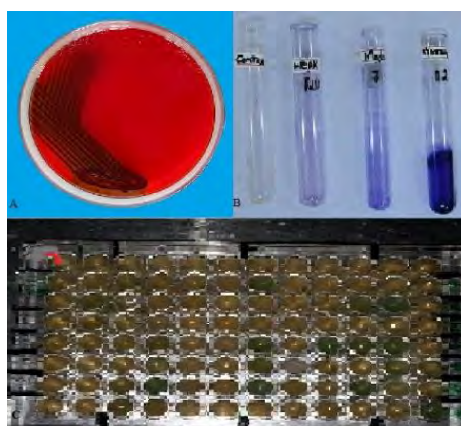
Figure 3.6 Assays for determination of Biofilm forming ability of bacteria.
A. Positive congo red agar plate test. The black crystalline colonies formed by the isolate A indicate the presence of EPS proteins. **B.** Test-tube Method (24-hour incubation); starting from left, control i.e., TSI broth with no culture inoculated, isolate 9-weak biofilm former, isolate 7 showing moderate biofilm forming ability, isolate 3 showing strong biofilm forming ability with the highest intensity of crystal violet stain. **C.** Microtiter plate test; top view of the microtiter plate. Culture broth of isolated strains were dispensed in the polystyrene well of the flat bottom microtiter plate. The green colour indicates the presence of pigment production by the isolated strain.

3.3.4. Biochemical Identification of the Selected Bacterial Isolates from Biofilm

On the basis of their morphologies, on Nutrient agar (Table A), a total of 28 isolates were selected and streaked on MacConkey and EMB differential media. Comparison of the morphologies on nutrient agar plates and differential media is given in Table 4.8. The isolates were also stained by Gram staining. Gram staining of isolates gave 20% of gram positives and 80% of Gram-negative bacteria. (Table A). They were then biochemically analysed according to the Bergey's Manual of Systematic Bacteriology. Isolates from the biofilm were identified as *Enterobacter, Pseudomonas, Serratia, Klebsiella, Salmonella, Proteus, Bacillus, Staphylococcus, Shigella and Citrobacter and E.coli*.

Table 3 . 4 Colony morphology of isolates on different media, MacConkey, nutrient agar and EMB.

ISOLATE	EMB	MacConkey Agar	Nutrient Agar
46	colourless	No growth	tiny, translucent, yellow, uneven, flat and shiny
47	No growth	No significant growth, transparent, NLF	medium,creamy,shiny,wavy margins, flat
E- 8	light pink, slimy, swarming	Greenish tinge, NLF	Medium, white, smooth, even margins and spreading growth.
65	Pink	L.F, light pink	small, transparent, even margins, flat and dull
101	No growth	NLF, transparent	String forming, opaque and translucent.
50	Transparent	NLF, transparent	Large, creamy, wavy margins, flat, dull
F	Dark purple, mucoid, shiny	No growth	Small, white, smooth, shiny, circular, even margins, flat.
98	pink, swarming, mucoid, shiny	Greenish, NLF	round, swarming, greenish, pseudo like smell, medium sized.
121	Light pink, slimy, swarming	Pink, L. F	small pin head sized, clear transparent, round, raised.
D	pink, mucoid, shiny, swarming	NLF, white	Tiny, colourless, uneven, flat, dull.

120	mucoid, pink, shiny	No growth	round, moist, off-white.
121	purple, shiny	L.F, pink	small pin head sized, clear transparent, round, raised.
32	Shiny, purple	NLF, transparent	flat, dry colonies, medium, pale and regular margins.
A-1	Purple, mucoid	NLF, white	Large, circular, white, mucoid, smooth, even margins, slightly raised.
A-8	Colourless, appears crystalline	NLF, white	White, convex, entire and circular
99	off-white, creamy	Pale yellow, NLF	Small, round, transparent.
H	light purple, shiny	NLF, transparent	Small, circular, off-white, smooth colonies
102	swarming, pink colour	NLF, blackish grey	White, thick, moist, irregular margins.
M	White, dry	No growth	Small, pale orange, raised, smooth, even margins
D- 10	purple, slimy, mucoid	LF, Pink	round, opaque, mucoid, bulging
64	Dark purple	No growth	medium, creamy, even margins, circular shape, sticky and mucoid
G	Pink	NLF, white	Tiny, circular, smooth, even margins, sticky

E-5	Pink	No growth	Small, pale, shiny, round, even, flat.
D-3	Purple	NLF, dull pink	Off-white, irregular margins, thick and mucoid
E-6	Purple	NLF, off-white	Large, rhizoidal, creamy, raised and shiny
D- 14	pink (baby)	NLF, transparent	Large, creamy, wavy margins, thick, spreading, raised and shiny
J	Pink	No growth	Tiny, light yellow, smooth, thick margins, raised, mucoid.
A-4	pale pink, mucoid	NLF, light yellowish, transparent	Pale, mucoid, thick margins and regular, raised
P	purple - pink, mucoid, swarming	NLF, greenish	Small, Shiny, off-white, mucoid, irregular margins, smooth colonies
L	purple, swarming	NLF, dull pink	Small, white, smooth, raised, convex, even margins
38	No growth	NLF, off white	Small, creamy, raised, smooth, mucoid, convex.
B	No growth	No growth	Small, yellowish, round, flat and shiny

Table 3 . 5 Identification of selected bacterial isolates on the basis of biochemical tests. TSI= Triple Sugar Iron, MR=Methyl Red, VP=Vogues Proskauer. ± indicates variable result for Urease test.

Isolate code name	TSI			MR	VP	SIM			UREASE	CATALASE	oxidase	Nitrite Rd	SIMMON CITRATE	Identified Bacteria
	SLANT/BUTT	H2S	GAS			MOTILITY	KOVAC'S	BUBBLES						
J	K/K	−	−	−	−	+	−	−	−	+	+	+	+	*Corynebacterium*
M	K/NC	−	−	+	+	−	−	−	−	+	+	+	−	*Micrococcus*
D-3	A/A	−	+	+	−	+	−	−	+	+	+	+	−	*Serratia*
64	K/A	−	−	−	+	−	−	−	−	+	+	+	+	*Enterobacter*
65	K/K	−	−	−	−	+	−	−	±	−	+	+	−	*Acinetobacter*
D-14	K/A	−	−	+	−	+	−	+	−	+	+	+	+	*Pseudomonas*
E-6	K/K	−	−	−	−	−	−	−	±	+	−	+	+	*Proteus*
46	A/K	−	−	−	−	+	−	−	±	+	−	+	+	*Clostridium /Bacillus*
	TSI			MR	VP	SIM			Urease	Catalase	oxidase	Nitrite Rd	Simmons citrate	Identified Bacteria
	Slant/Butt	H2S	GAS			Motility	KOVAC'S	BUBBLES						

47	A/A	+	–	–	+	+	–	+	–	+	+	+	–	*Corynebacterium/ Mycobacterium*
L	A/K	–	–	–	–	+	+	–	±	+	+	+	+	*Citrobacterer*
D	K/A	–	–	–	–	+	–	–	±	+	+	+	+	*Aerogenes*
D-11	K/A	-	–			+	–	-	–	+	+	+	+	*Bacillus*
D-10	K/A	–	–	–	–	+	–	–	–	+	–	+	–	*K.pneumoniae*
F	K/A	–	–	–	+	+	–	+	–	+	+	+	+	*Klebsiella,*
H	K/K	–	–	–	–	+	–	+	±	+	+	+	–	*Enterobacter*
E-8	K/K	–	–	–	–	+	–	–	±	+	+	+	+	*Pseudomonas*
P	K/K	–	–	–	–	+	–	–	–	+	+	+	+	*Salmonella*
38	K/K	–	–	+	–	+	–	–	+	+	+	+	–	*Proteus*
A1	A/A	–	+	–	+	+	–	–	–	+	+	+	+	*Enterobacter*
E-5	A/K	–	–	–	–	+	–	–	±	+	–	+	–	*Serratia*
121	NC/NC	-	-	-	-	+	+	-	-	+	+	+	-	*E. coli*

43	K/A	-	-			-	-		+	+	+	-	*Staphylococcus*
50	K/NC	-	-	-	-	-	-	-	+	+	+	-	Indeterminate
A8	K/K	-	-	-	-	+	-	-	±	-	-	+	+	*Serratia*
A4	A/K	-	+	-	-	+	-	-	-	+	+	+	-	*Shigella*
G	K/K	-	-	-	-	+	-	-	+	+	+	+	+	*Burkholderia*
101	K/A	-	-	+	-	+	-	-	-	+	+	+	+	*Staphylococcus*
54	A/A	-	-	-	+	+	-	-	-	+	+	+	-	*Enterobacter*
32	A/K	-	-	-	+	+	-	-	±	-	+	+	-	*Bacillus megaterium*

3.3.5. Molecular Characterization of Nitrifying Bacteria in Activated Sludge and Biofilms Developed on Tire Rubber under Varying Concentration of Al^{3+}

Molecular characterization of biofilms was carried out as it is a more holistic approach to studying the consortia present in environmental samples and compensates for the draw backs associated with conventional culture techniques. It is especially significant as a tool when the microbial groups of interest are autotrophic nitrifiers, which are not only difficult to culture but are also most likely to be suppressed and dominated by the growth of heterotrophs. The DNA from the biofilms was extracted using DNA Soil kit (Norgen, Korea), whereas for activated sludge phenol-chloroform method was used. The primers (as described above) were used for biofilm samples and activated sludge, respectively. The results from sequencing were blasted using NCBI BLAST short nucleotide sequences. The E- value and the sequences derived from BLAST, as a probable indication of the presence of these organisms in the respective samples. Phylogenetic diversity of ammonia oxidizing and nitrite oxidizing bacteria in the biofilm sample from tire rubber exposed to Al^{3+} treatment at 4.5 mg/l, in the attached growth batch reactors (AGBR)

conditions, is depicted in phylogenetic tree shown in Fig. 3.7. Results show that nitrifying population from the tire rubber developed under the elemental influence ofAl^{3+}4.5 mg/l had a higher diversity of bacteria in terms of greater number of *Bradyrhizobium* species that included *Bradyrhizobium japonicum* USDA 110, E109, SEMIA strains. In addition, *Nitrosococcus watsoni*, *Nitrosococcus halophilus*, *Rhodopseudomonas palustris*, *Nitrobacter winogradski* were also most likely present. Similarly, Fig. 3.8 shows the microbial diversity of the AOB s and NOB s for biofilm sample from tire rubber developed in the control AGABR. The diversity of nitrifiers is most likely comprising of *Bradyrhizobium japonicum*, *Rhodopseudomonas, B. oligotrophum*, *Nitrobacter hamburgensis*, *Bradyrhizobium* species BTAA1. Whereas in the case of activated sludge (Fig.3.9) Bradyrhizobium japonicum, *B. diazoefficiens*, *Nitrosomonas europea, Nitrospira multiformis*, and *Oligotropha carboxidovarans* are identified as the autotrophic nitrifiers.

Bradyrhizobium japonicum strain E109 |CP010313.1|(2)
Bradyrhizobium japonicum coproporphyrinogen III|AF276709.1|
Bradyrhizobium japonicum USDA 6 DNA |AP012206.1|(3)
Bradyrhizobium japonicum strain E109 |CP010313.1|
Bradyrhizobium japonicum USDA 6 DNA |AP012206.1|(2)
Nitrosococcus oceani ATCC 19707 |CP000127.1|(4)
Nitrobacter winogradskyi Nb-255 |CP000115.1|
Nitrosococcus oceani ATCC 19707 |CP000127.1|(2)
Nitrosococcus watsoni |CP002086.1|
Rhodopseudomonas palustris |CP000283.1|
Bradyrhizobium japonicum USDA 110 DNA |BA000040.2|(5)
Bradyrhizobium japonicum SEMIA 5079 |CP007569.1|(2)
Bradyrhizobium japonicum |AF322013.1|
Rhodopseudomonas palustris DX-1 |CP002418.1|
Nitrosococcus oceani ATCC 19707 |CP000127.1|(3)
Bradyrhizobium oligotrophicum |AP012603.1|
Nitrosococcus oceani ATCC 19707 |CP000127.1|
Bradyrhizobium japonicum USDA 110 DNA |BA000040.2|
Bradyrhizobium japonicum USDA 110 DNA |BA000040.2|(2)
Bradyrhizobium japonicum USDA 110 DNA |BA000040.2|(3)
Bradyrhizobium japonicum |JX135475.1|
Nitrosococcus halophilus Nc4 |CP001798.1|(3)
Nitrosococcus oceani ATCC 19707 |CP000127.1|:
150223-31 Dk-bf4 190F.ab1317
Nitrosospira multiformis |CP000103.1|
Nitrosococcus halophilus Nc4 |CP001798.1|
Bradyrhizobium japonicum USDA 110 DNA |BA000040.2|(6)
Nitrosococcus watsoni |CP002086.1|(2)
Bradyrhizobium sp. |AP012279.1|(2)
Nitrosococcus halophilus Nc4 |CP001798.1|(2)
Bradyrhizobium japonicum USDA 110 DNA |BA000040.2|(4)
Rhodopseudomonas palustris DX-1 |CP002418.1|(2)
Rhodopseudomonas palustris |CP000283.1|(2)
Bradyrhizobium japonicum |CP010313.1|
Bradyrhizobium japonicum SEMIA 5079 |CP007569.1|
Bradyrhizobium japonicum USDA 6 DNA |AP012206.1|
Bradyrhizobium oligotrophicum |AP012603.1|(2)
Nitrosococcus halophilus Nc4 |CP001798.1|(4)
Rhodopseudomonas palustris |CP001096.1|
Rhodopseudomonas palustris |BX572597.1|
B.japonicum |X99588.1|
Bradyrhizobium japonicum SEMIA 5079 |CP007569.1|(3)
Bradyrhizobium japonicum SEMIA 5079 |CP007569.1|(4)
Bradyrhizobium sp. |AP012279.1|
Nitrobacter winogradskyi Nb-255 |CP000115.1|(2)
Nitrosococcus watsoni C-113 |CP002086.1|

Figure 3.6 Computation of Molecular Phylogenetic tree using the Maximum Likelihood method.

Molecular Phylogenetic analysis of the bacterial diversity derived from biofilm developed under treatment with Al^{3+} 4.5 mg/l on tire rubber. The evolutionary history was inferred by using the Maximum Likelihood method based on the Tamura-Nei model (Tamura & Nei, 1993). The bootstrap consensus tree inferred from 500 replicates(Felsenstein, 1985) is taken to represent the evolutionary history of the taxa analyzed (Felsenstein, 1985). Initial tree(s) for the heuristic search were obtained automatically by applying Neighbor-Join and BioNJ algorithms to a matrix of pairwise distances estimated using the Maximum Composite Likelihood (MCL) approach, and then selecting the topology with superior log likelihood value. The analysis involved 46 nucleotide sequences. Codon positions included were 1st+2nd+3rd+Noncoding. All positions containing gaps and missing data were eliminated. There were a total of 15 positions in the final dataset. Evolutionary analyses were conducted in MEGA6 (Tamura et al., 2013).
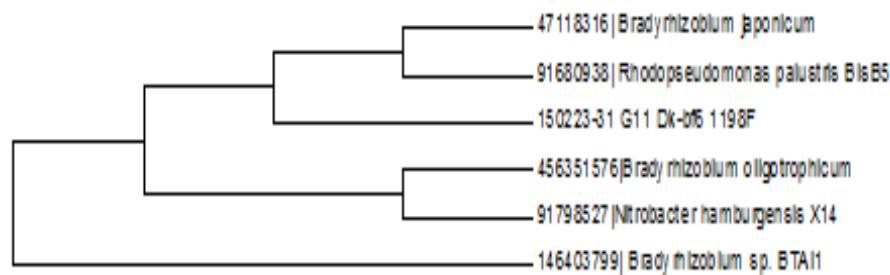
Figure 3.7 Molecular Phylogenetic analysis of the bacterial diversity derived from biofilm developed on tire rubber, in control membrane biofilm reactor.

Computation of Molecular Phylogenetic tree using the Maximum Likelihood method based on the Tamura-Nei model (Tamura & Nei, 1993). The bootstrap consensus tree inferred from 500 replicates (Felsenstein, 1985) is taken to represent the evolutionary history of the taxa analysed(Felsenstein, 1985) . Branches corresponding to partitions reproduced in less than 50% bootstrap replicates are collapsed. Initial tree(s) for the heuristic search were obtained automatically by applying Neighbor-Join and BioNJ algorithms to a matrix of pairwise distances estimated using the Maximum Composite Likelihood (MCL) approach, and then selecting the topology with superior log likelihood value. The analysis involved 46 nucleotide sequences. Codon positions included were 1st+2nd+3rd+Noncoding. All positions containing gaps and missing data were eliminated. There were a total of 24 positions in the final dataset. Evolutionary analyses were conducted in MEGA6 (Tamura et al., 2013).

Figure 3 . 8 Molecular Phylogenetic analysis of the bacterial diversity of activated sludge.

Computation of Molecular Phylogenetic tree using the Maximum Likelihood method. The evolutionary history was inferred by using the Maximum Likelihood method based on the Tamura-Nei model. The bootstrap consensus tree inferred from 500 replicates (Yoshizawa et al., 2014) is taken to represent the evolutionary history of the taxa analysed (Felsenstein, 1985). Branches corresponding to partitions reproduced in less than 50% bootstrap replicates are collapsed. Initial tree(s) for the heuristic search were obtained automatically by applying Neighbor-Join and BioNJ algorithms to a matrix of pairwise distances estimated using the Maximum Composite Likelihood (MCL) approach, and then selecting the topology with superior log likelihood value. The analysis involved 46 nucleotide sequences. Codon positions included were 1st+2nd+3rd+Noncoding. All positions containing gaps and missing data were eliminated. There were a total of 24 positions in the final dataset. Evolutionary analyses were conducted in MEGA6 (Tamura et al., 2013).

3.3.6. Nitrification Activity of Bacterial Communities in the Biofilms Developed on Tire Derived Rubber, Treated with Varying Concentrations of Al^{3+} under Shake Flask Conditions

Four coupons of 1 cm^2 from each support surface, in the attached growth biofilm reactors, were cut and each was placed in four separate foiled flasks (in duplicate), containing N-media. To each flask, different concentrations of $AlCl_3$ were added whereas the fourth flask served as a control. The flasks were incubated in a shaker incubator. The purpose of the experiment was to evaluate the trends in NO_3^- and NO_2^- concentration with time, under the influence of varying concentrations of Al^{3+} as an evaluation of the nitrifying activity of the biofilms developed on the surfaces.

Increase in the NO_2^- concentration indicates the oxidation of NH_3 present in the N-enrichment media, and that NH_4^+ had not been depleted from the media when the batch study was completed. The varying effect of Al^{3+} concentrations on nitrification showed differences in the readings between the different concentrations of $AlCl_3$, on the support surface. An overall increase in NO_2^- was observed; however, there was no particular consistent pattern being followed for nitrite concentration trend at different concentrations.

At Al 2.5 mg/l, tire rubber, NO_2^- concentration increased progressively from 0.0667 mg/l to 0.1668 mg/l and then to 0.2670 mg/l in the final recorded reading, with the rate of increase from day one of sampling (X_1) to the 30th day (X_3) being 75.02%. However, the increase in NO_2 production with time de-accelerated from X3-X2 as percentage change was 37.53% whereas for X2-X1 it was 60.1%. Again, at Al 4.5 mg/l, the nitrite concentration decreased over time. At Al 6.5 mg/l the concentration of NO_2^- was observed to be increasing. With the concentration being the highest, it showed an overall percentage change in NO_2^- with the rate of increase being 6.369%. The aluminum concentration increased NO_2^- overall concentrations but decreased at Al 4.5 mg/l. It is to be noted that percentage change between the first two consecutive weeks is high for concentrations at Al 2.5 mg/l and Al 4.5 mg/l but there is a decrease in the rate of increase of concentration of NO_2^- at Al 6.5 mg/l.

NO_2^- concentration in the shake flasks control experiment showed an increasing trend in overall percentage of NO_2^- concentration giving a 60% change. The rate of change of percentage in NO_2^- concentration with time by comparing the difference between X_1-X_2 and X_3-X_2 reveals that for tire rubber the NO_2^- is increasing at a near constant rate as X_1-X_2= 60.01% and X_3-X_2= 62.5%.

For tire rubber, the rate of percentage change in NO_2^- concentration is decreasing as X_2-X_1 is 86% that then decreases to 56.83% for X_3-X_2. For Al^{3+} 6.5 mg/l, the nitrite concentration with there is decreasing concentration of NO_2^- with time with the overall percentage change in concentration (X1-X3) up to 36.6%. The rate of percentage change in NO_2^- concentration with time by comparing the difference between X_1-X_2 and X_3-X_2 reveals that for tire rubber the NO_2^- is decreasing at a near constant rate as X_1-X_2= 21.36% and X_3-X_2= 23.05%.

Table 3 . 9 Nitrification activity of bacterial community in the biofilm developed on tire derived rubber, treated with varying concentrations of Al^{3+} under shake flask conditions.

Al^{3+} (mg/l)	Concentration of nitrite nitrogen (mg/l)				
	X1(1)	X2 (15)	X3 (30)	A= (X1-X2)%	B= (X3-X2)%
0 (control)	0.0835	0.109	0.1336	30.54	60.00
2.5	0.067	0.167	0.267	60.01	75.02
4.5	0.0317	0.234	0.3670	86.00	91.36
6.5	0.0500	0.0412	0.0317	21.359	36.60

3.3.7. Scanning Electron Microscopy (SEM) analysis of Biofilms

SEM is used in biofilm studies for a conclusive understanding of development, distribution along with the elucidation of the relationship between biofilms and the surfaces on which they are grown. SEM was carried out to study the biofilm development with respect to the surface topography and varying elemental concentrations on tire rubber at Al^{3+} 4.5 mg/l and compared with results from SEM images from control (Fig. 3.10-3.11). EPS and bacteria could be easily identified embedded within the matrix, which could be seen clearly seen as a complex structure that was housing the microorganisms.
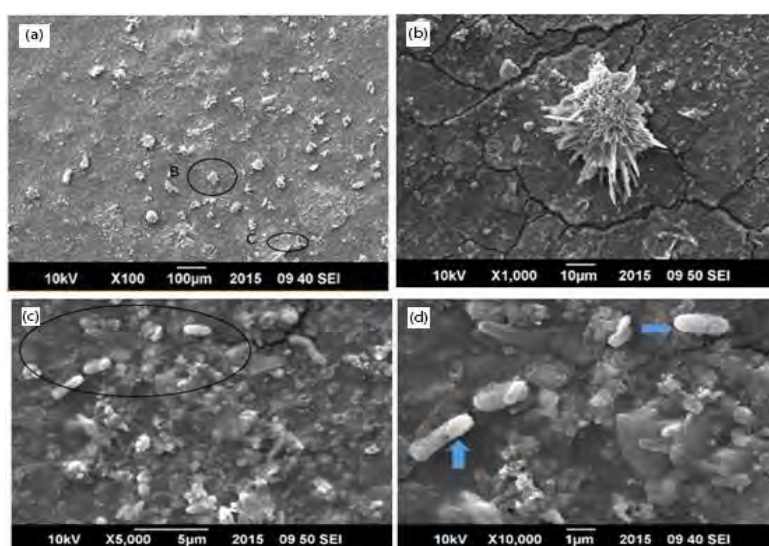
Table 3 . 10 SEM images showing the formation of biofilms on untreated tire rubber (0 mg/l Al^{3+}).
(a) Deposition can be seen at lower magnification of X100. Areas encircled "B" and "C" are further magnified at a resolution of X1,000 and X5,000, respectively. (b) At X1,000, calcite or mineral deposition having astral radiating arms is observed. (c) At X5,000, EPS matrix covering the tire rubber surface is clearly observed. Thick and long elongated rods are observed. The encircled area was magnified to a higher resolution of X10,000 to observe the microbial morphologies clearly. (d) At X10,000 magnification, elongated rods are prominent, there is a thick EPS matrix within which microorganisms are embedded.
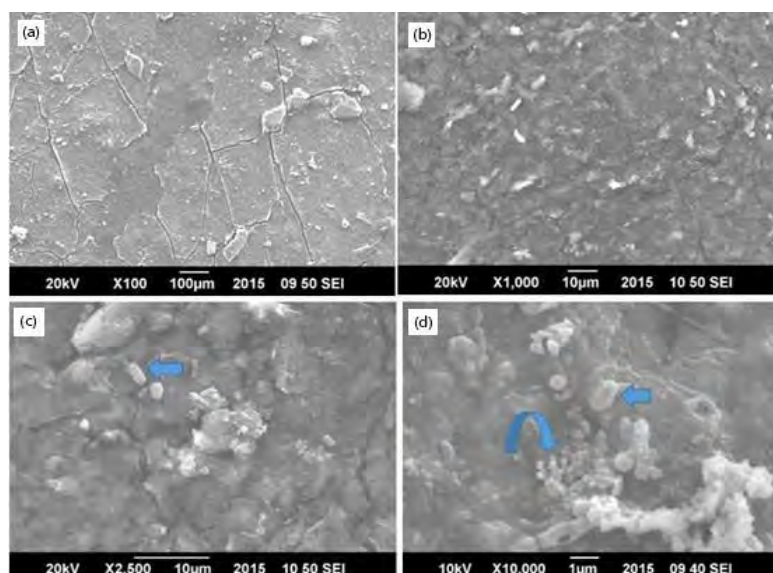
Table 3 . 11 SEM images of biofilms on tire-derived rubber at 4.5 mg/l Al^{3+}.
(a) Cracks and crevices are present as part of the surface topology of the rubber tire. (b) Deposition of minerals can also be seen as dense white structures. (c) and (d) Arrows indicate that cocci and rods are present. Microbial density is less as compared with biofilm from control reactor.

3.3.8. *FISH-CLSM of Biofilms on TDR under the Influence of Aluminum*

CLSM was carried out to enumerate the total bacterial population count as well as to study the relative distribution of the Phyla *β -proteobacteria* and *G-Proteobacteria* bacteria present within the biofilm developed on tire rubber support surface as well as to enumerate them. The overall population was studied using EUB probe set; EUB I, II and II. In addition, two phyla were targeted *β-proteobacteria* and *ϒ-proteobacteria* using the probes ϒ-42 and β-42. The specificity and working of the probes were firstly checked using pure cultures of *Psuedomonas ATCC 9027* and *Bacillus subtilis KJ600795* as representatives for *ϒ-* and *β-proteobacteria*, respectively (Fig. 3.12). The images shown (Fig. 3.12), show the hybridization of the EUB mix probe set; EUB I, II and III to pure culture of *Pseudomonas*. Fluorescing images due to hybridization of the ϒ-42 probes to the pure culture and the absence of any fluorescence when hybridization reaction was carried out with β-42 probes shows the cross validation of the β-42 probes. The blank image indicated an absence of any hybridization reaction with fixed smear of *Pseudomonas* due to the specificity of the β-42 probes that only hybridized with the pure culture of rod-shaped bacilli.

Images of biofilms on TDR obtained from FISH and CLSM are given in Fig. 3.14. EUB probes that targeted the whole eubacterial population showed green fluorescence, whereas beta-proteobacteria and gamma-proteobacteria labeled in separate wells gave red and blue fluorescence, respectively. Moreover, the images depicted aggregating cells and flocs within which overlapping colors, that is, yellow, pink and purple were observed due to the co-aggregation of different bacterial species.

Figure 3. 2 depicts targeted bacterial population enumerated using *daime* image analysis software. Eubacterial population exhibited an increasing trend with increasing concentration of Al^{3+} (mg/l) that showed an appreciable decrease when the concentration further increased to 6.5 mg/l. At 100x

magnification, the highest average object counts in one FOV, that is, 8.02E+02 count of Eubacterial population was recorded in control biofilm, followed by 2.08E+02, 9.20E+01 and 9.00E+01 at 4.5, 6.5 and 2.5 mg/l of Al3+, respectively. Conversely, the population of gamma and beta-Proteobacteria decreased with increasing concentration of Al^{3+} (mg/l).
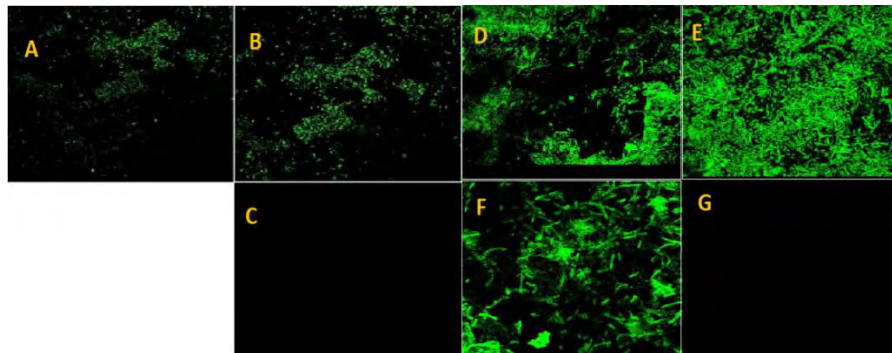
Table 3 . 12 Pure culture of Pseudomonas fixed on 3 wells of Teflon coated slide.
Starting from left in clockwise direction images depict: **A**. Fluorescens due to hybridization with EUB-mix probe set (EUB I, II and III) probes **B.** Hybridization with ϒ-42 probes also produces fluorescence. **C.** no fluorescence produced with β-42 probes establishing specificity of the probes with only the G-proteobacterial population. Pure culture of Bacillus fixed on 4 wells of the slide. Images depict: **D**. Fluorescens due to hybridization with EUB-mix probe set (EUB I, II and III) probes **E.** Hybridization with Beta probes also produces fluorescence. **F.** fluorescing green rods depicting bacilli when mixture of probes; EUB probe set+ Beta probes along with the Beta probe competitors were used. **G.** no fluorescence produced with Gamma probes establishing specificity of the probes with only the β-population.
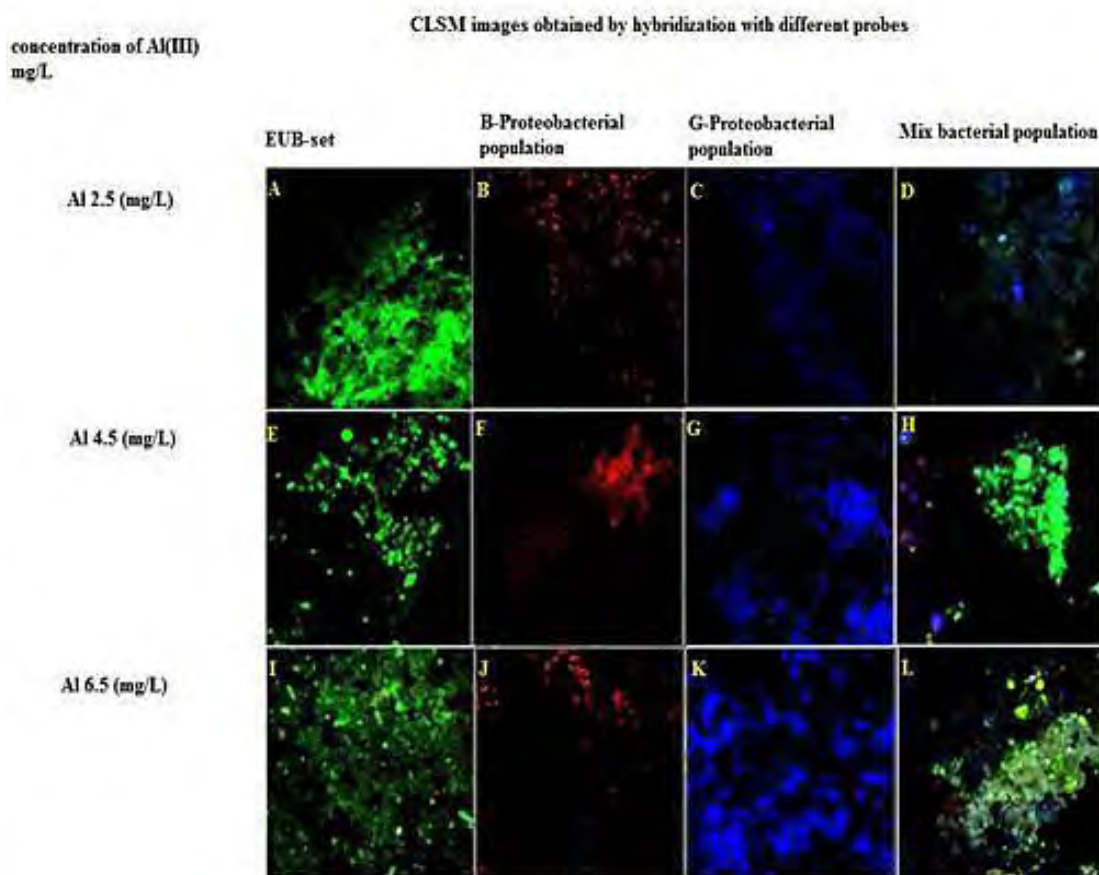
Table 3 . 13 CLSM of biofilm, at 10x, developed on tire rubber surface taken from AGBR dosed with Al3+ (2.5, 4.5, 6.5 mg/l, respectively).

(A) EUB mixture of probes depicting the population of eubacteria. (B) β-42+unlabeled competitor probe depicting β-proteobacterial population. (C) γ-42 probe + competitive inhibitor depicting the γ-proteobacteria as blue fluorescing cells. (D) Mixed probes hybridized simultaneously. CLSM of biofilms at Al^{3+} (4.5 mg/l). (E) EUB mixture of probes depicting the general population. (F) β-42 + unlabeled competitor probe depicting β-proteobacterial population. (G) γ-42 probe + competitive inhibitor depicting the γ-proteobacteria as blue fluorescing cells. (H) Mixed probes hybridized simultaneously. CLSM of biofilm, at Al^{3+} (6.5 mg/l). (I) EUB mixture of probes depicting the general population. (J) β-42+unlabeled competitor probe. (K) γ-42 probe + competitive inhibitor. (L) Mixed probes hybridized simultaneously, overlap of probes produces secondary color fluorescence. In figure: ϒ, gamma, β, beta.
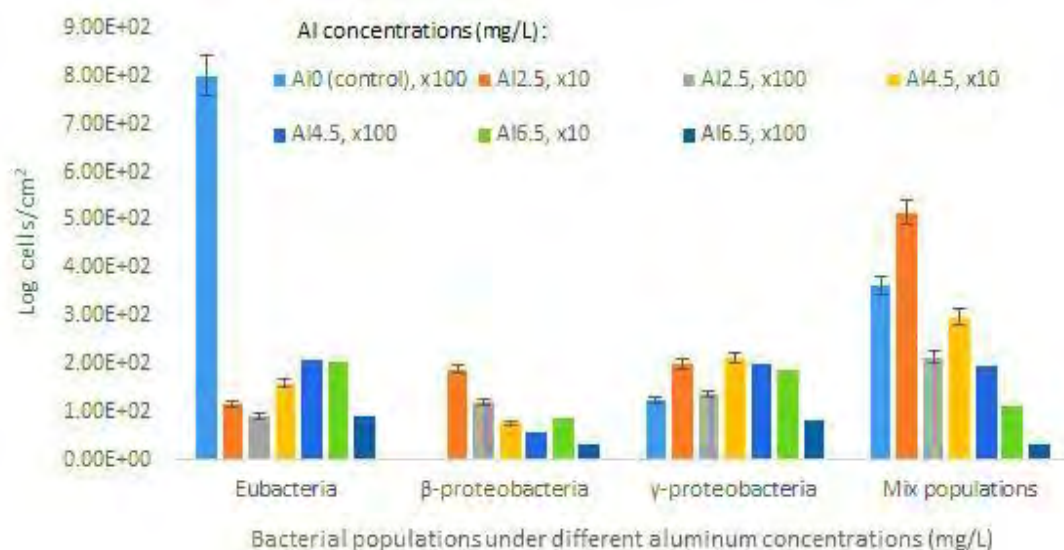
Table 3 . 14 Bacterial population count, quantified using DAIME software, for the biofilms developed under varying concentrations of Al^{3+} (0mg/l, 4.5mg/l, 6.5 mg/l).
Carboxyfluorescein (FAM)-labeled probes targeting Eubacterial, β-proteobacterial and γ-proteobacterial population were used for individual sections of the biofilm from tire-derived rubber support and viewed under confocal laser scanning microscopy.

At 100x, the population of γ-proteobacteria (object count 1.35 E+02) was greater than β-proteobacteria (object count 1.19E+02). Similarly, for the biofilm developed on tire-derived rubber at 4.5 mg/l Al^{3+} (mg/l) the approximate object counts of β- and γ-proteobacteria were 7.60E+01 and 2.12E+02, respectively. The same trend, that is, the dominance of γ-proteobacteria over β-proteobacteria was observed in the FOV taken at 100x magnification, with an average count of 5.60E+01 and 2.01E+02, respectively. Biofilm sample taken from tire rubber treated with 6.5 mg/l Al^{3+} gave higher object count (8.00E+01) for γ-proteobacteria than β-proteobacteria (3.00E+01) at 100x magnification.

3.3.9. Fourier Transform Infrared Spectroscopy (FTIR) of EPS of Biofilms developed on TDR

FTIR was carried out on the EPS extracted from the biofilms developed on the materials i.e., tire rubber under different concentrations of Al^{3+}. The spectra were compared to observe changes in the EPS biochemical profile at different concentrations. To simplify the spectra analysis, the peaks obtained for all the samples were divided to fall into three wavelengths (cm^{-1}) ranging from 3500-3000 cm^{-1}, 2000-1500 cm^{-1} and 1300-600 cm^{-1}.

Overall, FTIR spectra for tire rubber followed a decreasing transmittance percentage with decreasing concentration of Al^{3+}, with control giving the lowest percentage transmittance. Control TDR showed two peaks in the range 3000 cm^{-1}-3500 cm^{-1} with a lower percentage absorbance compared to the biofilms formed at the three concentrations of Al^{3+}. The presence of two peaks in this region indicated the presence of primary and secondary amines are for Al^{3+} 4.5 mg/l, Al^{3+} 6.5 mg/l and control whereas a single peak in Al^{3+} 2.5 mg/l indicates the presence of a secondary amine. The presence of peaks in the 3300 cm^{-1}-2500 cm^{-1} range specifies the presence of carboxylic acid for all the samples. With higher transmittance percentage being given by control and decreasing percentage transmittance observed with decreasing

Al^{3+}concentration. While both Al 4.5 mg/l and Al 2.5 mg/l show the same functional group i.e. -OH and phenols and C-H stretch of alkenes with peak values at 3273.77 and 2925.08 cm^{-1} shown in Al 4.5 mg/l spectra and peak values at 3271.28cm^{-1} and 2967.42 cm^{-1}for Al 2.5 mg/l. Same functional groups were observed for Al 6.5 mg/l. Peaks at 2922.52cm^{-1} and 3276.85 cm^{-1} in the spectra of control tire rubber indicates the presence of –OH stretch and terminal alkynes. Thereby, indicating that macromolecular diversity is more complex due the addition of Al^{3+} compared to control even though quantity of sugar residues, proteins and lipids as markers of microbiology and structural components of the biofilms is greater for control compared to biofilm developed under the influence of Al^{3+} (2.5 mg/l, 4.5 mg/l and 6.5 mg/l). In addition, the quantity of proteins, lipids and carbohydrates decreased with increasing concentrations of Al^{3+} (Fig. 3.15).
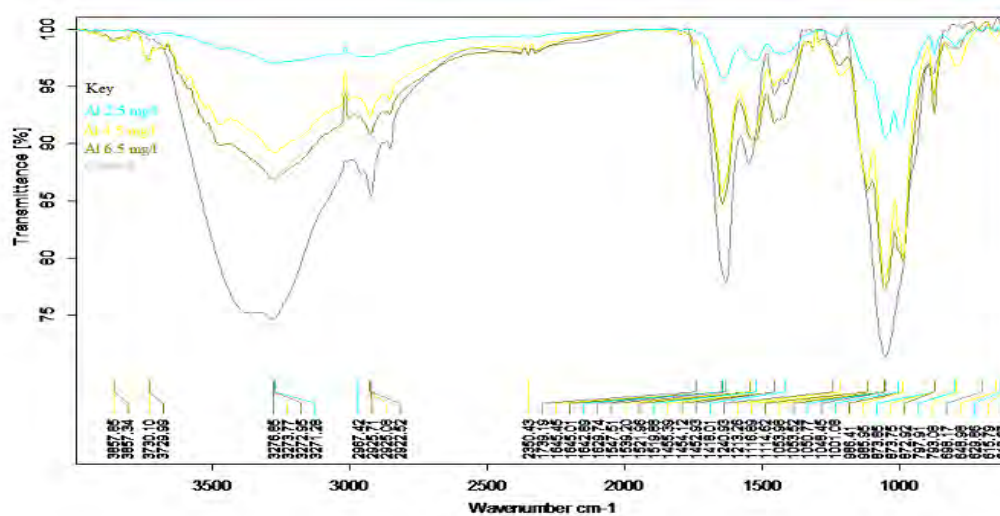
Table 3 . 15 FTIR transmittance spectra of EPS developed on tire rubber at varying concentrations of AlCl₃.

3.4. Discussion

The unmitigated growth of biofilms over surfaces in potable water and sanitary systems has been presented as a nuisance factor leading toward microbially induced corrosion(Beech et al., 2006, Mansouri et al., 2010) , contamination of eatables and associated problems ("WHO Assessing Microbial Safety of Drinking Water: Improving Approaches and Methods," 2016, Borella et al., 2005, Brooks & Flint, 2008, Shi & Zhu, 2009) . Simultaneously, biofilms functioning as catalytic matrices on attached growth reactors have been viewed as being vital for possible biodegradation and biotransformation of water contaminants specifically of soluble nature (Domaradzka et al., 2015, Saratale et al., 2010) . Biofilms matrix in wastewater treatment systems and their interaction with heavy metals have been reported previously (Koechler et al., 2015, Teitzel and Parsek , 2003) . The role of Al^{3+} in ground water has been established as an important coagulant for removal of organic and inorganic matter (Shon et al., 2004, Park et al,2003). However, its role in biofilm development particularly on diversity of potential bacteria with regards to waste water technology has not been studied extensively compared with other metal elements. The study comprehensively established the limiting effects of narrow range (2.5mg/l–6.5 mg/l) of aluminum concentrations on the density and diversity of bacteria on TDR biofilms in AGBR. Gamma proteobacteria compared with beta-proteobacteria dominated the overall proteobacterial population. Additionally, the residual amount of aluminum proved to be affecting the sludge digestibility and related performance of the reactor.

The presence of Al^{3+} (mg/l) in the aqueous environment has been associated with mitigation of biofilm development on support surfaces and bacterial physiological processes such as porphyrin metabolism (Domaradzka et al,2015, Scharf et al., 1994), DNA chelation, (Guida et al., 1991, Guzzo et al., 1992) and intracellular accumulation due to siderophores production (De Carvalho et al., 1982, Silver & Walderhaug, 1992). Transmission electron microscopy (TEM) and SYTOX staining conducted by Yaganza et al. (Yaganza et al., 2004) revealed that $AlCl_3$ loosened the cell wall, subsequently causing leakage and rupturing of bacterial cells, and nucleic acid complexation when exposure time was lengthened. Though these transformations were marked at higher concentration (0.2 M) of Al^{3+}, they were also reported at lower concentrations (0.05 M and 0.1 M). Besides, it was also established that toxicity was not influenced by pH but was primarily due to Al^{3+}. Therefore, considering the occurrence of an almost neutral pH in the AGBR it can be clearly deduced that increasing Al^{3+} concentration (mg/l) only placed a metabolic stress on microbial population. The mechanism of toxicity of aluminum ions has been attributed to the nature of Al^{3+} ions as low charged complex acid $[Al(H_2O)_6]_3$ ion, in aqueous environment. As indicated by cytoplasmic accretion these acidic complexes reported to be diffusing in to the cell by disrupting the cell wall and forming complexes with catalytic subunits and nucleic acids (Johnson & Wood, 1990, Wood, 1995, Ma, 2007) . In addition, Gossett et al. (1997) in their study on the negative effects of metal coagulants revealed that there was a substantial decrease in volatile solids destruction, methane production, COD removal, organic nitrogen catabolism and alkalinity production (Ghyoot & Verstraete, 1997). The underlying mechanisms causing the aforementioned problems was

attributed to the phenomenon of coagulants "locking up" substrates such as proteins(Stevenson, 1933) or phosphate limitation caused by aluminum and iron precipitation of phosphorus.

Bacterial densities on TDR biofilm revealed by FISH-CLSM (Fig.3.7) were complimentary to ones obtained through conventional culture based bacterial counting (CFU/ml cm2) method. Moving across the concentration gradients, inhibitory effect of increasing Al^{3+} concentration (mg/l) were reflected in the spatial distribution of gamma-and beta-proteobacteria. The increase in Al^{3+} concentration (mg/l) led to an overall decrease in the gamma and beta-proteobacterial populations. Furthermore, the ratio of gamma-proteobacteria on tire rubber for all concentrations was greater than β-proteobacterial population (Fig. 3. 5), with highest number of bacteria from both phyla in 2.5 mg/l, followed by 4.5 mg/l and then 6.5 mg/l of Al^{3+}. Similarly, bacterial profiling based on CLSM and molecular characterization conducted by Lin (1993), on different piping surfaces coupons indicated that for stainless steel, PVC, and cast iron the ratio of gamma-proteobacteria was significantly greater than β-proteobacteria (Lin, 1993). Similarly,predominance of gamma-proteobacteria has been reported over beta-proteobacteria on highly contaminated chromium soil (Desai et al., 2009). Furthermore, predominance of gamma-proteobacteria was reported by Sun et al. (Sun et al., 2010) in the two 16S rDNA clone libraries they had constructed of the endophytic bacterial community isolated from copper resistant plants grown on copper contaminated soil.

Previously different fixed film reactors demonstrated establishment of bacterial biofilms. Although various physical and chemical factors proved to be effecting bacterial growth (Berekaa et al., 2000, Sheehan et al., 2006).Vukanti et al., (2009) in their study on tire rubber crumb in landfills isolated culturable aerobic and anaerobic bacteria that included *Bacillus megaterium*, *Bacillus pumilus*, *Bacillus cereus*, *Arthrobacter globiformis*, *Flavobacterium* sp., *Clostridium* sp., *Enterobacter aerogenes,* *Enterococcus faecium* and *Cellulosimicrobium cellulans.* Nevertheless, microbicidal products such as accelerators, antioxidants and vulcanizing agents proved to be inhibitory for certain bacteria while other constituents of tire rubber exerted positive influence on biofilm formation (Holst et al., 1998). In this context, Zn^{2+}in tire rubber has been reported specifically for development of biofilm by *Salmonella enterica* subsp. *Enterica* serovar *Typhimurium* (Crampton et al., 2014) .

Since, activated sludge was used as a seed, biochemical characterization of bacterial isolates demonstrated presence of species of *Enterobacter*, *Pseudomonas*, *Serratia*, *Klebsiella*, *Salmonella*, *Proteus*, *Bacillus*, *Staphylococcus*, *Shigella*, *Citrobacter* and *E. coli* (Table S4). Likewise, members of *Enterobacteriaceae* including *Aeromonas*, *Campylobacter*, *Pseudomonas*, *Salmonella*, and *Helicobacter* have been reported in biofilms developed on plastic and metallic piping materials (Dufour 2013, Szewzyk et al., 2000, Hunter et al., 2001, Lee & Kim, 2003). September and coworkers (September et al., 2007) in their study reported the incidence of *Pseudomonas*, *Shigella*, *E. coli*, *Salmonella* and *Vibrio* spp. withinbiofilm samples that were isolated from drinking water supply pipelines in South Africa.

Biological reactors containing tire-derived rubber as support materials have also been found considerably effective in treatment of wastewater. Barros et al., (2010) compared the efficacy of two anaerobic

fluidized bioreactors (AFBR) that used different support materials including polyethylene and tire rubber. According to their findings, tire rubber AFBR showed better performance possibly due to better biofilm development on it. Besides, physical features of tire rubber might have provided crevices; shielding biofilms colonization (Barroset al., 2010). Minor amount of aluminum, that is, 2.5 mg/l proved to be important regarding percentage change of NO_2^- in the sludge whereas, further decrease or increase in aluminum proved to be considerably limiting (Fig. 3.3). Decrease in NO_3-N, in aerobic trickling filters, has been previously associated with presence of anammox bacteria in the reactor (Wilsenach et al., 2014) as these facilitate complete ammonia removal and denitrification of nitrite with ammonia as the electron donor (Loosdrecht & Jetten, 2002) via autotrophic pathways without the requirement for organic carbon. The highest removal of COD at lower concentration (2.5 mg/l) Al^{3+} might be due to higher contribution of heterotrophic bacteria in denitrification of nitrogenous compounds (Hochmair et al., 2020) . VFA and alkalinity of the AGBR showed an inverse relationship with each other in sludge digestion. Increase in aluminum resulted in a decrease in alkalinity with a simultaneous increase in case of VFA (Fig.3.2). The effect of heavy metals such as Cd, Cu, Zn, Pb and Cr on the VFA production in an anaerobic digester showed that higher concentrations of Pb, Zn and Cd increased the production of VFA by 160%–700%. Further, reports have mentioned stimulating effect on VFAs production by the addition of Ni and Zn. Nevertheless, limiting effect on VFAs production was observed with Cu and Pb. The rational for the increase in VFA concentration with increasing concentration for certain metal ions has not been well elucidated. However, it is imperative to recall that VFA production is due to acidogenic bacteria converting organic acid into short chain fatty acids, making them more resistant to environmental stresses. So, it can be hypothesized that these organic acids bind to Al^{3+} and inhibit its toxic effect (Jones et al., 1996). The activity differences with increasing Al^{3+} concentrations might be due to the stress exerted by Al^{3+} mg/l on the metabolic pathway of heterotrophic bacteria (Johnson & Wood, 1990).

3.5 Conclusion

Tire-derived rubber supported a high diversity of bacteria and proved to be a suitable support material for developing biofilms in attached growth bioreactors. Simultaneous use of aluminum as a coagulant proved to be limiting sludge digestibility and AGBR performance. Conventional and molecular studies consolidated the fact that increasing aluminum concentrations under batch conditions have a limiting effect, though non-significant, on bacterial density as well as diversity. Therefore, a wider range of Al^{3+} (mg/l) concentration must be studied in order to find out the positive impacts on sludge stability and associated digestion with effective indigenous microbial consortium.

3.6 Future Prospects

There is need for studying the interactions occurring withing bacteria under the stress conditions i.e., antagonistic and mutualistic interactions governing the microbial interactions. Quorum sensing and fluctuations in the metabolites production could be used to evaluate the biofilm-based reactors performance or to inhibit the membrane biofouling. Also, biofilm modeling studies would help to

determine the complex interplay of different parameters influencing the biofilm formation and their activities.

CHAPTER 4

Characterization of Extracellular Polymeric Substances (EPS) Producing Bacterial Strains Isolated from Attached Growth Reactor Biofilms

Study Title: Extracellular Polymeric Substances (EPS) Producing Bacterial Strains Isolated from Attached Growth Reactor Biofilms of Municipal Wastewater: Identification and EPS Production Potential

CHAPTER 4: Extracellular Polymeric Substances (EPS) Producing Bacterial Strains Isolated from Attached Growth Reactor Biofilms of Municipal Wastewater: Identification and EPS Production Potential

Abstract

The sludge settling and dewatering is a major problem in the wastewater treatment plants (WWTP). To overcome this problem synthetic polymers and coagulants, hazardous to the public health and environment, are used to facilitate the coagulation. Environment friendly biocoagulants, the extracellular polymeric substances (EPS), produced by bacteria have been reported as an alternative to this approach. In this context, 50 extracellular polymeric substances (EPS) producing bacteria, isolated from biofilms developed on support material such as waste tire rubber in the attached growth batch reactors with and without the incorporation of different concentrations of iron and aluminum were screened, identified and characterized for their EPS forming potential. Congo red agar assay indicated 15 strong slime producers, 24 intermediate slime producers and 11 non-slime formers. The tube method indicated 15 strong, 15 moderate, 12 weak slime and 8 non-slime producers. Microtiter plate assay also revealed 15 strong while 35 moderate biofilm formers. Dry weight analyses showed the greater concentration of broth (5.33 g/l–24.7 g/l) and slime EPS (1.33–13.33 g/l) produced by individual bacteria as compared to consortia broth (5.66–8.86 g/l) and slime EPS (3.22–6.57 g/l). Similarly, the viscosity measurements showed EPS production of individual bacteria was greater and it ranged between 16,950 mPas–43,450 mPas. Overall, carbohydrate content was higher in consortia EPS (1.233 mg/ml–1.887 mg/ml) than EPS of individual bacteria (0.504–0.610 mg/ml). Protein content varied in individual bacteria (0.227–0.52 mg/ml) as well as in consortia (0.178–0.974 mg/ml). Fourier transform infrared (FTIR) spectra of the EPS extract (bacteria and consortia) revealed the presence of varied concentrations of functional groups of carbohydrates, proteins, lipids and nucleic acids. A great deal of EPS production was observed by consortia of six bacteria through scanning electron microscopy (SEM). The bacteria associated with highest EPS production were identified as *Enterobacter* sp., *Citrobacter* sp., *Clostridium* sp. and *Candidimonas* sp. through 16SrRNA gene sequencing.

Keywords: Biofilm, Extracellular polymeric substances (EPS), bacteria, consortia, 16S rRNA sequencing, Fourier transform infrared spectroscopy (FTIR), Scanning electron microscopy (SEM).

4.1. Introduction

The large quantities of sludge generation and its efficient removal during treatment wastewater has been quite challenging to manage (Tripathy & De, 2006, Zhou et al., 2014). The sludge dewatering and settling are major problems in wastewater treatment plants (WWTP) mainly due to the bulking of sludge caused by filamentous and non-filamentous organisms in the wastewater. Settling of sludge and dewatering are usually carried out through conventional physicochemical methods. Cationic or anionic synthetic polymers such as polyethylene imine/polyacrylamide derivatives combined with cations (Fe^{3+}, Al^{3+}) facilitate flocculation and settling of sludge by neutralizing the negative charge of sludge (Vijayaraghavan et al., 2011). Nonetheless, the use of chemical coagulants is expensive and affects soil

microorganisms when the sludge is applied to agricultural land. Also, chemically dewatered sludge harms the microbial community of the environments such as composting in the receiving soil environments during agricultural spreading (Subramanian et al., 2010). Furthermore, these cause unstable shear stress, altered pH of the treated water and decreased operational efficiency at low temperature (Tripathy & De, 2006, Vijayaraghavan,Sivakumar, Kumar, 2011, Wiśniewska et al., 2016). To overcome these challenges, use of ecofriendly and less expensive biocoagulants/biopolymers produced by microorganisms has been proposed as an alternative to the physicochemical approaches. The microorganisms produce extracellular polymeric substances (EPS) which help in the sludge flocculation (Govoreanu et al., 2004, Klemeš et al., 2010).

EPS are three-dimensional, secondary metabolites, highly hydrated and gel-like, sticky or mucoid materials. They are composed of 50 to 90% of the total organic carbon viz. carbohydrates, proteins, lipids, nucleic acids, uronic acids and other cellular constituents (Brostow et al., 2009). Viscoelastic properties of EPS provide mechanical stability to the biomass or biofilm matrix as micro colonies divided by interstitial spaces and networks comprising a viscous and watery part called liquid phase (Subramanian et al., 2010, Rosenberg et al., 2013). Bacteria release two types of EPS outside their cells; slime and capsular EPS that play an important function in the sludge settling process. The slime type of EPS is generally loosely bound to the cell walls of bacteria and is washed out during harvesting procedures. Capsular EPS remain attached to the cell walls of microorganisms during these procedures due to their higher stability. The EPS help in the formation of bioflocs in collaboration with inorganic/organic elements, filamentous microbial cells and aggregates (Tripathy & De, 2006). Furthermore, these facilitate in bioaggregation, sludge biomass retention and solid-liquid separation due to syntrophic association by the juxtaposition of microorganisms (Patil et al., 2011,Sun et al., 2015). The dominant EPS producing bacteria in the sludge include *Enterobacter* spp., *Serratia* spp., *Pseudomonas* spp.*, Bacillus* spp.*, Microbacterium* spp., *Aureobasidium* spp.*, Escherichia* spp., *Achromobacter* spp.*, Saccharomycete, Proteus mirabilis including* lactic acid bacteria (LAB) and others (Subramanian et al., 2007, 2010, Guo et al., 2013, Kurane et al., 1994, Subudhi et al., 2014,Jiao et al., 2010, Singha, 2012).

Both attached and suspended growth bioreactors work on the biocatalytic characteristics of bacteria to form bioaggregates that hold and slowly remove complex contaminants in the simpler forms (Azizi et al., 2013, Ruiz-Marin et al., 2010, Sombatsompop et al., 2006). Previous studies on models of multispecies biofilms have demonstrated biofilm development was highly influenced by bacterial interactions within consortia which is considered as real "heart" of the sludge system (Achilli et al., 2011, Donlan, 2002, Yang et al., 2011). The antagonism and collaborative interactions provide them competitive advantage of energy requiring EPS synthesis over higher cellular growth which provides them protective shield against external hostile conditions such as change in pH, temperature, biocides, dehydration, ultraviolet radiation (distort DNA), host immune defenses and protozoan grazers (Burmlle et al., 2006; Ruiz-Marin et al., 2010). It also plays an important role in adsorption of dissolved xenobiotics organic composites, pollutants and metals (Hg, Zn, Ar, Cd, Pb and Cu) and good emulsification activity. Bioflocculation is

dependent on the growth conditions of the biofilms and is typically affected by the type, amount and physicochemical characteristics of the EPS (Comte et al., 2008, Pal & Paul, 2008, Sheng et al., 2010, Tourney & Ngwenya, 2014). Increase in carbohydrate and protein content of EPS has direct effect on flocculating activity (Li & Yang, 2007, Liu & Fang, 2003).

We isolated bacteria from the biofilms developed on the support materials such as waste tire rubber (data for biofilms on support materials other than waste tire rubber is not shown in these studies) in attached growth batch reactors (AGBRs) operated with and without incorporation of metals (aluminum and iron) (chapter 3, study A and B). The present study was planned to screen, identify and characterize the isolated bacteria in order to evaluate their potential for EPS production using different qualitative and quantitative techniques. The bacteria were identified using biochemical and 16SrRNA sequencing.

4.2. Material and Methods

4.2.1. Selection of Extracellular Polymeric Substances (EPS) Producing Bacteria

A total of fifty (50) bacterial strains out of 210 were selected, isolated from biofilms developed in attached growth batch reactors under the influence of different concentrations of Fe^{3+} (0 mg/l-8.5 mg/l) and Al^{3+} (0-6.5 mg/l) as described in chapter 3 (study 1 and 2). Heterotrophic plate count was used for the growth assessment of isolated EPS producing bacteria and incubated at 35 °C ± 2 °C for 48–72 hours. The bacteria were selected on the basis of their morphology, Gram's staining and biofilm formation capabilities. The slime EPS was identified by Maneval's capsule staining whereas Anthony's capsule staining was used to identify the bacterial surface capsular EPS.

4.2.2. Slime/biofilm Formation Assays

4.2.2.1. Congo Red Agar

Bacterial isolates were qualitatively evaluated for slime production by Congo Red Agar (CRA) assay, a method. The composition of EPS producing media was (g/l): Brain heart infusion broth 37.0 g (Difco); Sucrose 50.0 g; Congo red dye 0.8 g; and agar 10.0 g, autoclaved at 121 °C for 15 minutes. Concentrated solution of Congo red dye was prepared and sterilized discretely and added to the autoclaved BHI and sucrose at 55 °C. The plates were streaked and inoculated with bacteria, incubated at 37 °C for 24-hours followed by overnight incubation at ambient temperature (Nyenje et al., 2013, Taj et al., 2012).

4.2.2.2. Tube Method

Slime production of isolated bacterial strains was tested by Christensen et al. method. A loopful of colonies from 24 hours culture plates were inoculated in tryptic soy broth (TSB) test tubes, kept at 37 °C for overnight incubation. Bacterial broth was decanted before staining with safranin (1%) for 5 minutes. The tubes were positioned upside down and left to dry at ambient temperature. After that results were recorded and graded as strong (+++), moderate (++), weak (+) and non-slime formers (Christensen et al., 1985, Taj et al., 2012).

4.2.2.3. Microtiter Plate Assay (MTP)

The calorimetric and quantitative assay for biofilm detection has been reported as a gold- standard process. Luria-Bertani (LB) broth was used for the bacterial growth at 37 °C for 24 hours. The bacterial cultures were diluted (1:100) with fresh medium and 200μl of diluted culture was aliquoted per well of microtiter plate (MTP). The medium was moderately removed; after 24 hour and about 200 μl of phosphate buffer saline (PBS) solution (0.1 M, pH 7.4) was used to wash three times the microtiter plate wells, then air dried for 15 minutes. After that 200μl of crystal violet (1%) was used to stain the MTP wells for 15 minutes at room temperature. PBS buffer (200 μl) was used to wash the unbound crystal violet stain and air-dried for 15 minutes. About 200μl of 33% glacial acetic acid was used to solubilize the unbound crystal violet. Microtiter plate count reader (BioTek™800TS absorbance reader, Catalog: BT800TS) was used to measure the OD_{630} of samples (Christensen et al., 1985, Nyenje et al., 2013).

4.2.3. Quantitative Production and Characterization of EPS

EPS producing bacterial strains were grown individually as well as in consortium on mineral salt medium. For quantitative production of EPS, the composition of mineral medium was as follows (g/l): KH_2PO_4 1.0; K_2HPO_4 2.0; NH_4Cl 1.0; Yeast extract 0.01; $MgSO_4.7H_2O$ 0.2; glucose 25.0. The medium's initial pH was set at 7.0 ± 0.2. $MgSO_4$ and glucose was syringe filtered separately and mixed aseptically with the aforementioned ingredients before inoculation. From the PCA (plate count agar) plates, bacterial strains were inoculated in the mineral medium, and kept at 32 °C for incubation in an orbital shaker at 150 rpm for 72 hours (Liu et al., 2015).

After growing bacterial cultures individually and as consortium for 72 hours, the medium was centrifuged at 7500 rpm for 20 minutes at 4 °C. The supernatant contained the slime EPS while pellet contained the microorganisms and capsular EPS. The bacterial broth containing both capsular and slime EPS was used for further analyses. The EPS were stored at 4°C (APHA, 2012).

4.2.3.1. Measurement of Dry Weight of EPS

The quantitative estimation of EPS (slime/capsular) and bacterial broth was carried out. After 72 hours of incubation, the consortia and bacterial broth were taken into vials and centrifuged for 15 minutes at 7500 rpm (4 °C) to obtain EPS from cell mass. The one volume of absolute ethanol was added to one volume of collected supernatant (1:1) in new vials for precipitation and incubated for 24 hours at 4 °C. To collect the precipitated EPS, the mixture was centrifuged for 15 minutes at 7500 rpm after incubation. The supernatant was decanted and the pellet (EPS) was dried at room temperature (APHA, 2012, Zhang et al., 1999).

4.2.3.2. Analysis of EPS Production

After 72 hours of incubation, the culture broth became viscous due to production of EPS. EPS production was measured in terms of viscosity of culture broth by using VP 1060 spindle R7, at 60 rpm and ambient temperature.

4.2.3.3. Screening of Consortia for Biofilm Development Potential

For consortia development, the six best EPS producing bacterial strains were selected for development of biofilm on small sized pebbles. A total of 4 combinations were prepared from six bacteria for biofilm development. The bacterial strains were refreshed and a loop full of bacterial cultures was inoculated in the vials containing mineral broth (as above) and incubated at 32 °C±2 °C for 72 hours. 1 ml aliquot of each bacterial broth was inoculated into sterilized tubes containing 9 ml mineral medium containing small sized pebbles as a support material for biofilm development and incubated at 37 °C for 10 days. After 10 days, the samples were fixed and stored for scanning electron microscopy (SEM) (Weiss & Cargill, 1992, Zuroff & Curtis, 2012).

4.2.3.4. Characterization of Slime EPS

Extracted slime EPS was characterized in terms of carbohydrate and protein content of selected six bacteria as well as four consortia. UV-sulfuric acid method was used to determine the total carbohydrates (TC) content of extracted EPS using glucose as a standard (Albalasmeh et al., 2013). Lowry method was used to determine the total protein (TP) content of the extracted EPS where bovine serum albumin was used as a standard (Pihlasalo et al., 2012, Walker, 2002).

4.2.3.5. Scanning Electron Microscopy (SEM) of EPS

The fixed biofilm samples on the surface of pebbles were fitted on the stubs by using carbon tape and to cover the edges of sample. To ensure the conduction of electron beam, silver paste conduction (SPI-CHEM) was done. A high voltage and vacuum of 102 atm. was created in the sputtering chamber for gold coating on the samples by using SPI-MODULE (sputter coater). A current of 25 mA for 50 sec was used to create plasma and gold was deposited on the samples. Finally, the sample was loaded on the holder and placed in chamber under the column. The EPS of biofilms was observed under *4000X, 6000X, 8,500X, 10,000X* magnification powers under scanning electron microscope (JSM 5910, JEOL, Japan).

4.2.3.6. Fourier Transformed-Infrared Spectroscopy (FTIR) of EPS

After 72 hours of incubation or fermentation, the bacterial broth and consortia were taken into Eppendorf tubes and centrifuged for 15 minutes at 7500 rpm (4 °C) to obtain EPS. Firstly, EPS was precipitated by adding 2 volumes of 100% cold ethanol to the collected supernatant and incubated on ice overnight. The precipitates were then centrifuged at 10,000 rpm for 20 min at 4°C and dried in an oven at 50 °C overnight (Jiao et al., 2010). FTIR (Bruker tensor 2500) was used to detect chemical composition the EPS in different bacteria and consortia.

4.2.4. Identification of Bacteria

Isolated bacterial were identified on the basis of Gram's staining, colony appearance and standard biochemical tests (Breakwell et al., 2009, Neu, 2000, Owen et al., 2013). Based on EPS production capability, 4 isolates were selected for molecular identification on the basis of 16S rRNA gene sequencing. The DNA was extracted from pure bacterial cultures using Biofilm DNA Isolation Kit 62300 (Norgen Biotek Corp.) following manufacturers recommendations. The samples were shipped and 16SrRNA sequencing was performed by Macrogen, Korea. 16S rRNA gene sequences were PCR

amplified using universal primers 27F (5'-AGAGTTTGATCMTGGCTCAG-3') and 1492R (5'-TACGGYTACCTTGTTACGACTT-3'). The retrieved sequences were subjected to taxonomic assignments using BlastX (https://blast.ncbi.nlm.nih.gov/Blast.cgi) tool and phylogenetic trees were constructed through MegaX. The sequences were submitted to GenBank to obtain accession numbers.

4.3. Results

A total of fifty (50) bacterial strains were isolated from biofilms developed on different support materials. Biofilm and slime EPS production ability of the isolated bacteria was evaluated using qualitative and quantitative assays. Selected bacterial isolates were then typically examined for EPS production and its characterization.

4.3.1. Morphological Characteristics of Bacterial Strains on Nutrient Agar and Plate Count Agar

Bacterial strains (n=50) were selected on the basis of mucoid or string forming ability and subsequently screened for their ability to produce EPS. Then bacterial isolates were characterized on morphological (pigmentation, shape, size, margins, elevation, opacity and texture) (Fig. 4.1) and biochemical (oxidase, catalase, sulfide indole motility, KOVAC's and Simmons citrate Tests) basis (Table 4.1).
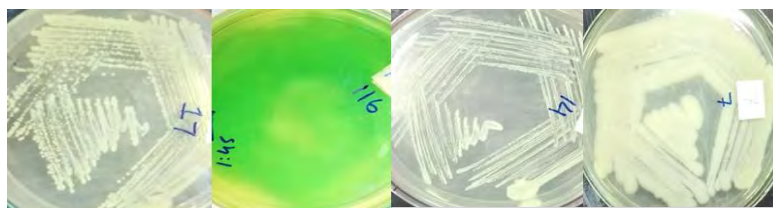
Figure 4. 1 Growth of representative isolated bacteria on plate count agar (PCA).

Table 4. 1 Morphology, Gram's staining and biochemical tests of the bacterial (n=50) isolates.

s.	Morphology	Metal concentrations (mg/ L) in the attached growth reactor	Gram's staining	O	C	SIM Motility	S Indole	TSI	MacConkey agar	Lactose fermentation	Potential bacterial sp.
1	White, pinpointed, entire, circular, raised, opaque, shiny	Fe 8.5,	-, bacilli	-	+	+	+	+	A/A, gas	LF	*Escherichia coli*
2	White, medium, undulate, irregular, raised, opaque, shiny	Fe 8.5	-, bacilli	-	+	+	-	+	A/K	LF	*Citrobacter spp.*
3	Colorless, smooth, pinpointed, entire, circular, transparent	Fe 8.5	-, bacilli	-	+	+	-	+	K/A, gas	NLF	*Salmonella spp.*
4	Slightly pale, pinpointed, entire, flat, circular, shiny, translucent	Fe 8.5	-, bacilli	-	+	+	-	+	K/A, H2S production	NLF	*Salmonella spp.*
5	White, small, undulate, raised, rhizoidal, opaque, shiny	Fe 8.5	-, bacilli	-	+	+	-	-	A/K, H2S production	LF	*Citrobacter spp.*
6	White, small, entire, circular, raised, shiny translucent	Fe 8.5	-, coccobacilli	-	+	+	+	+	A/A, gas	LF	*Escherichia coli*
7	Creamy, large, erose, irregular, raised, shiny, opaque	Fe 8.5	-, bacilli	-	+	+	-	+	A/A	NLF	*Serratia spp.*
8	Colorless, pinpointed, entire, circular, flat, shiny, transparent	Fe 2.5	-, cocci	+	+	-	-	+	K/K, H2S production	NLF	*Neisseria spp.*
9	White, pinpointed, entire, circular, flat, shiny,	Fe 2.5	-, bacilli	-	+	+	-	+	A/A, H2S	LF	*Citrobacter spp.*

No	Colony morphology										
	translucent									production		
10	Slight pale, pinpointed, entire, circular, flat, shiny, opaque	Fe 2.5	-, bacilli	-	+	+	-	+	A/K, H2S production	LF	*Citrobacter spp.*
11	Creamy, medium, undulate, rhizoidal, raised, shiny, translucent	Fe 2.5	-, cocci	+	+	-	-	-	K/A, gas	NLF	*Neisseria spp.*
12	White, medium, entire, circular, raised, shiny, opaque	Fe 2.5	-, bacilli	-	+	+	-	+	K/A	LF	*Citrobacter spp.*
13	White, pinpointed, entire, punctiform, flat, shiny, translucent	Al 6.5	-, bacilli	-	+	+	-	-	A/A, gas	LF	*Enterobacter spp.*
14	White, small, entire, circular, raised, shiny, translucent	Al 6.5	+, cocci	+	+	+	-	-	K/A	no growth	*Staphylococci spp.*
15	White, small, entire, circular, flat, shiny, opaque	Al 6.	-, Bacilli	-	+	+	-	+	A/A	LF	*Enterobacter spp.*
16	Yellow, pinpointed, entire, circular, flat, shiny, opaque	Al 6.5	+, cocci	+	+	+	-	-	K/K, H2S production	no growth	*Micrococcus spp.*
17	White, small, entire, circular, flat, shiny, opaque	Al 6.5	+, Cocci	+	+	+	-	-	K/A	no growth	*Staphylococci spp.*
18	Yellow, pinpointed, entire, circular, flat, shiny, opaque	Al 6.5	+, cocci	+	+	-	-	-	A/A	no growth	*Micrococcus spp.*
19	Colorless, pinpointed, entire, punctiform, flat, shiny, transparent	Al 6.5	-, cocci	+	+	-	-	-	K/K	NLF	*Neisseria spp.*
20	Creamy, pinpointed, undulate, rhizoidal, raised, shiny, translucent	Al 6.5	-, Cocci	+	+	-	-	-	K/A	NLF	*Neisseria spp.*
21	Slight pale, medium, entire, circular, flat, shiny, opaque	Fe 2.5	+, bacilli	+	+	-	-	+	K/A, H2S production	no growth	*Corynebacterium spp.*
22	White, small, entire, circular, flat, shiny, opaque	Fe 2.5	+, bacilli	-	+	+	+	-	K/A	no growth	*Bacillus spp.*
23	White, pinpointed, entire, punctiform, raised, shiny, opaque	Fe 2.5	-, bacilli	-	+	-	+	-	A/A, gas	LF	*Klebsiella spp.*
24	White, pinpointed, entire, circular, flat, shiny, translucent	Al 6.5	+, cocci	+	+	+	-	-	A/A	no growth	*Staphylococci spp.*
25	White, medium, entire, punctiform, flat, shiny, translucent	Al 6.5	-, Bacilli	-	+	+	+	+	K/A, H2S production	LF	*Erwinia spp.*
26	Yellow, pinpointed, entire, circular, flat, shiny, translucent	Al 6.5	+, cocci	+	+	+	-	-	K/K	no growth	*Staphylococci spp.*
27	White, medium, entire, circular, flat, shiny, opaque	Al 6.5	-, bacilli	-	+	+	-	-	A/A	LF	*Serratia spp.*
28	Creamy, medium, entire, circular, flat, shiny, opaque	Fe 6.5	-, bacilli	-	+	+	+	-	A/A, gas	LF	*Escherichia coli*
29	White, pinpointed, entire, punctiform, flat, shiny, opaque	C	-, cocci	+	+	+	-	-	A/A	NLF	*Neisseria spp.*
30	Colorless, medium, undulate, irregular, flat, shiny, translucent	C	-, bacilli	+	+	+	-	+	A/K	NLF	*Ewingella spp.*
31	White, small, filamentous, circular, raised, shiny, opaque	C	-, bacilli	+	+	+	-	-	K/K	NLF	*Pseudomonas spp.*
32	White, small, entire, circular, flat, shiny, opaque	Fe8.5	-, bacilli	-	+	+	-	-	K/A	LF	*Serratia spp.*
33	Yellowish, small, entire, circular, raised, shiny, translucent	Fe 8.5	-, Bacilli	+	+	+	-	+	K/K	NLF	*Pseudomonas spp.*
34	Green, large, entire, punctiform, raised, shiny, translucent	Fe 8.5	-, Bacilli	+	+	+	-	+	K/K	NLF	*Pseudomonas spp.*
3	Yellow, pinpointed, entire, circular, raised, shiny,	C	-, bacilli	+	+	+	-	+	K/A	NLF	*Pseudomonas spp.*

No.	Colony morphology		Gram, shape						TSI	LF	Organism
5	translucent, spreading growth										
36	Colorless, large, entire, circular, Clear transparent, mucoid, string forming, spreading growth	C	-, bacilli	+	+	-	-	-	K/K	NLF	*Pseudomonas spp.*
37	Colorless, small, undulate, punctiform, flat, shiny, transparent	Fe 8.5	-, bacilli	-	+	-	+	-	K/K	LF	*Klebsiella spp.*
38	White, large, enire, irregular, raised, shiny, opaque	Fe 8.5	+, bacilli	-	+	+	+	-	K/K	no growth	*Bacillus spp.*
39	White, pinpointed, entire, punctiform, flat, shiny, opaque	Fe 8.5	-, bacilli	- \	+	-	+	+	A/A	LF	*Klebsiella spp.*
40	White, small, undulate, irregular, flat, shiny, translucent	Al 4.5	+, bacilli	+	+	+	-	+	K/A, gas	no growth	*Bacillus spp.*
41	Colorless, small, entire, punctiform, raised, shiny, transparent	Al 2.5	-, bacilli	-	+	+	+	+	A/A, gas	LF	*Citrobacter spp.*
42	Colorless, pinpointed, entire, circular, flat, dull, translucent	Al 2.5	-, bacilli	-	+	+	-	+	K/A, gas	NLF	*Shigella spp.*
43	White, pinpointed, entire, punctiform, raised, shiny, opaque	Al 6.5	-, Bacilli	-	+	+	-	+	A/A	LF	*Enterobacter spp.*
44	Creamy, pinpointed, entire, circular, raised, shiny, opaque	Al 6.5	-, bacilli	-	+	+	+	+	K/K, H2S production	LF	*Erwinia spp.*
45	Medium, white, smooth, even margins and spready growth	Al 6.5	+, Cocci	+	+	+	+	+	A/A, gas	no growth	*Staphylococcus spp.*
46	Yellow, small, entire, punctiform, raised, shiny, translucent	Al 6.5	+, cocci	+	+	+	-	-	K/ A, gas	no growth	*Micrococcus spp.*
47	Slight pale, large, undulate, circular, umbonate, shiny, opaque	Al 6.5	-, bacilli	-	+	+	-	-	A/K	LF	*Serratia spp.*
48	Creamy, large, erose, irregular, umbonate, shiny, rough, opaque	Al 4.5	-, bacilli	-	+	+	+	-	A/A	LF	*Escherichia coli*
49	White, large, lobate, irregular, flat, shiny, opaque	Al 4.5	-, Bacilli	-	-	-	-	+	A/K	NLF	*Shigella spp.*
50	Creamy, small, filamentous, irregular, raised, shiny, opaque	C	-, bacilli	+	-	+	-	+	K/A	LF	*Serratia spp.*

C; control, SIM; Sulfide indole motility test, TSI; Triple sugar iron test, A; Acidic, K; Alkaline, LF; Lactose fermenter, NLF; Non-lactose fermenter, O= oxidase, C; Catalase. S; Simmons citrate.

Table 4. 2 Microbiological characteristics of EPS producing bacterial strains (n=50).

Bacterial strains	Maneval's capsule stain	Anthony's capsule stain	Microtiter plate assay	Viscosity (mPas)	Dry weight	
					Bacterial broth (g/L)	Slime EPS (g/L)
1	+	+	1.117	38,100	11.27	6.00
2	+	+	0.883	31,300	13.33	4.67
3	+	-	0.871	16,950	8.00	1.33
4	+	+	1.011	38,300	9.34	2.67

5	+	+	0.991	18,350	8.67	2.00
6	+	+	0.793	41,100	9.33	3.33
7	+	-	0.910	31,700	8.00	2.67
8	+	-	1.124	24,300	6.00	2.00
9	+	+	0.912	23,600	10.67	2.67
10	+	+	0.938	29,450	9.33	3.33
11	+	-	0.956	33,200	6.67	2.67
12	+	-	2.158	33,600	23.33	9.33
13	+	+	1.028	43,450	6.67	4.00
14	+	-	0.870	21,150	16.66	3.33
15	+	-	0.974	27,300	6.66	1.33
16	+	-	1.020	42,950	8.00	2.00
17	+	-	0.910	33,250	13.00	4.67
18	+	-	0.927	30,750	17.33	12.00
19	+	+	0.987	30,300	9.33	2.00
20	+	+	1.064	18,500	5.33	1.33
21	+	+	0.845	34,850	8.00	3.33
22	+	+	0.962	34,000	10.00	2.00
23	+	-	0.791	18,900	8.67	4.00
24	+	+	0.883	21,450	12.00	2.00
25	+	+	1.013	42,500	11.34	6.67
26	+	-	1.060	27,200	8.66	3.33

27	+	+	0.921	29,550	13.33	8.00
28	+	+	1.010	40,950	19.33	5.33
29	+	+	0.871	24,250	24.66	13.33
30	+	+	1.012	38,000	16.66	3.33
31	+	-	0.994	32,600	8.66	3.33
32	+	+	1.312	18,450	13.33	5.33
33	+	+	1.221	36,900	10.66	3.33
34	+	-	0.868	40,200	12.67	4.00
35	+	+	0.793	33,150	8.00	2.00
36	+	-	0.766	36,800	13.33	3.33
37	+	+	0.933	37,650	10.33	4.00
38	+	-	0.876	22,350	12.67	5.33
39	+	+	1.301	37,000	10.67	2.67
40	+	+	1.025	27,550	18.00	4.67
41	+	+	0.915	37,550	9.33	3.33
42	+	+	0.877	18,200	10.67	3.33
43	+	+	0.996	31,200	12.00	4.00
44	+	+	0.836	32,750	9.33	5.33
45	+	-	0.667	36,850	8.67	2.67
46	+	+	0.939	18,500	12.00	5.33
47	+	+	0.827	35,350	8.00	1.33
48	+	+	1.029	37,550	5.33	1.33

49	+	+	0.892	40,200	20.00	2.67
50	+	+	1.149	38,800	10.00	3.33
C1	–	–	–	29,050	5.66	3.22
C2	–	–	–	29,850	7.124	5.71
C3	–	–	–	28,800	8.864	5.85
C4	–	–	–	30,150	7.18	6.57

4.3.2. Characterization of EPS Producing Bacteria

4.3.2.1. Identification of Bacteria Based on Gram's Staining and Biochemical Tests

Bacterial isolates isolated form biofilms were characterized based on morphological (pigmentation, shape, size, margins, elevation, opacity and texture) and biochemical tests. An about 50 bacterial strains were selected on the basis of mucoid or string forming ability and subsequently screened for their ability to produce EPS. Gram's staining and the biochemical results indicated most of these bacteria were Gram and facultative anaerobes. The abundant phyla included Proteobacteria, Firmicutes and Actinobacteria. The bacterial isolates included species of genera Citrobacter (6), *Serratia* (5), Enterobacter (2), *Klebsiella* (2), Salmonella (1), *Shigella* (2), *Erwinia* (2), *Ewingella (1)* from the family Enterobacteriaceae. The species of the genera *Neisseria* (5), *Pseudomonas (6), Bacillus* (3), *Micrococcus* (3) and *Corynebacterium* (3) were also identified.

4.3.3. EPS Staining

4.3.3.1. Maneval's Capsule Stain

The cells stained pink or red color and the background was stained dark while the capsule remained transparent. The selected all fifty (50) strains had the capsule around their cells under the light microscope at *100X* magnification, which showed the presence of slime EPS (Table 4.2, Fig 4.2). All the selected strains isolated from biofilms were loosely bound or slime EPS formers.

4.3.3.2. Anthony's Capsule Stain

Crystal violet stained both the background and cells while capsule remain unstained. The selected 33 out of 50 bacterial strains were found to have capsule around the cells which showed the presence of strongly bound capsule with cell wall (Table 4.2, Fig 4.2). The other 17 bacterial strains revealed absence of capsule around cells, considered as a negative result.
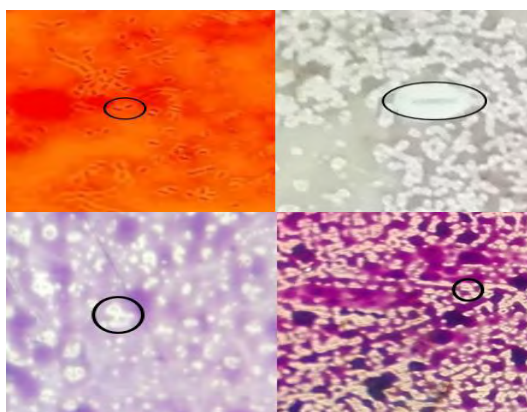
Figure 4. 2 EPS staining of biofilm forming bacteria.
Images of (upper) Maneval's capsule staining; capsule layer surrounding the bacteria (n=50) observed at *100X* magnification. Circles indicating the transparent area (capsule) around cells. (lower) Anthony's capsule staining; capsule layer surrounding the bacteria (n=50) at *100X* magnificationunder light microscope. Circles indicating the transparent area (capsule) around cells.

4.3.4. Slime/Biofilm Formation Assays

4.3.4.1. Congo Red Agar (CRA)

In qualitative CRA assay, 30% bacterial isolates (15 of 50) with black colonies indicated strong slime/biofilm production ability. A total of 48% (24 of 50) bacterial isolates with dark red colonies and 12% (6 of 50) with light red colonies indicated the moderate and weak slime/biofilm production respectively. Remaining bacterial isolates with pink colonies 10% (5 of 50) indicated non-slime producers (Fig. 4.2, Table 4.3, Fig. 4.3-4.4).

Table 4. 3 Slime production assay of bacterial strains (n=50) by qualitative Congo red agar test.

Slime production	Colour and morphology of bacterial colonies	No. of isolates	Percentage (%)	Total %
Positive	Black colonies (dry crystalline consistency)	15	30	
Intermediate	Black smooth colonies	7	14	
Week	Red colonies (dry crystalline consistency)	17	34	
Negative (Non-adherent)	Red smooth colonies	6	12	22
	Pink colonies	5	10	
Total		50	100	
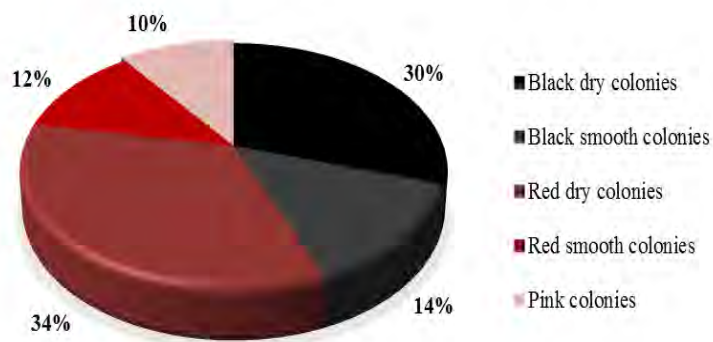
Figure 4. 3   Percentage distribution of slime EPS producing bacteria (n=50) using qualitative screening assay (CRA).
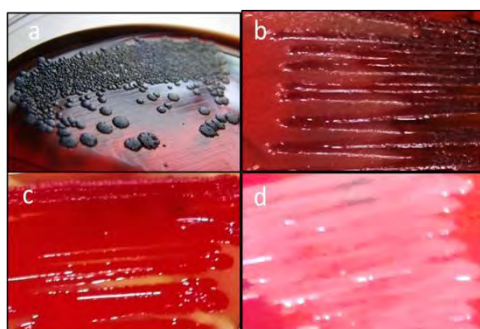
Figure 4. 4 Growth of bacteria on Congo red agar showing (a) black colonies (positive); (b) dark red colonies with dry consistency (moderate); (c, d) red/pink (negative) non-slime producers.

4.3.4.2. Tube Method (TM)

The adherence of safranin stain on the inner side of glass tubes indicated the slime production. Out of 50 bacterial strains, number of strong (+++) and moderate (++) slime producers was same i.e., 15 (30%). Whereas, 12 (24%) showed weak slime production or adherence (+) and remaining 8 (16%) bacterial strains were then non-slime producers (Fig. 4.2, Table 4.4, Fig. 4.5, 4.6).

Table 4. 4 Slime production by test tube qualitative method.

Slime production	No of isolates	Percentage (%)
Strong	15	30
Moderate	15	30
Weak	12	24
Negative	8	16
Total	50	100
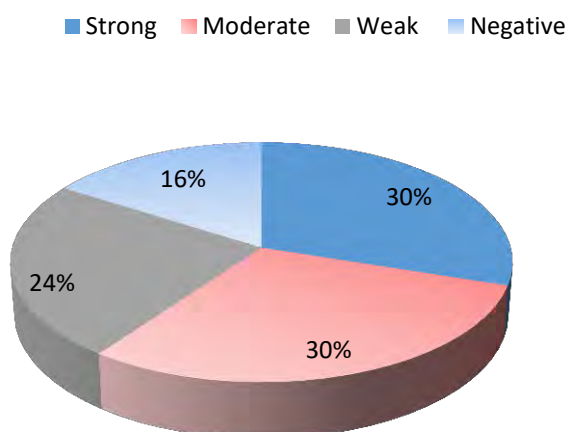
Figure 4. 5 %age distribution of slime producing bacteria (n=50) using qualitative test tube method.
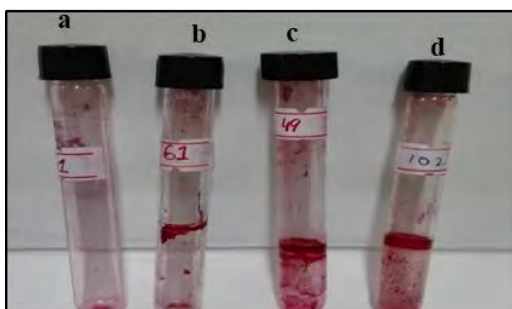
Figure 4. 6 Glass test tubes stained with safranin (1%) showing different degrees of slime production
(a) non-slime production; (b) week slime production; (c) moderate slime production; (d) strong slime production (qualitative test tube method).

4.3.4.3. Microtiter Plate (MTP) Assay

Microtiter plate assay indicated 15 (30%) bacterial strains as strong slime/biofilm formers and 35 (70%) as moderate slime/biofilm formers. All bacterial strains were biofilm formers and none of the bacteria was detected as non-adherent (Table 4.5, Fig 4.7-4.8). The comparative analysis showed that 30% bacterial strains (different in each assay) were strong slime/biofilm formers. The bacterial strains as 4, 12, 13, 16, 25, 34, 39, 44, 46, 48 and 50 were strong to moderate in each assay. The other bacterial results varied in each assay.

Table 4. 5 Microtiter plate (MTP) assay for biofilm production.

Biofilm production	No of isolates	Percent age (%)
Strong	15	30
Moderate	35	70
Week	0	0
Non adherent	0	0
Total	50	100
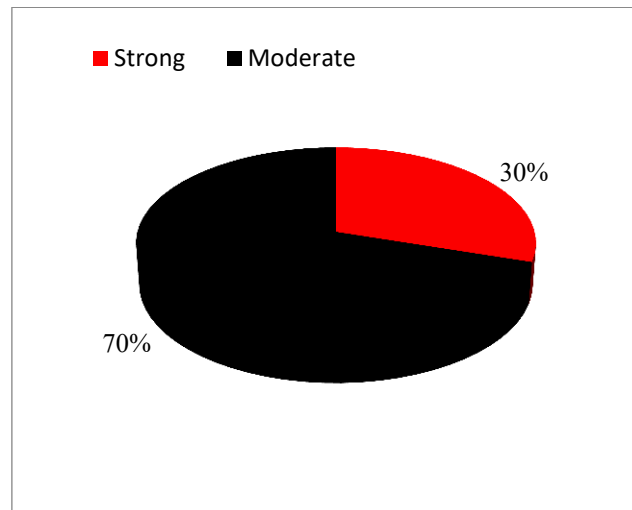
Figure 4. 7 Percentage distribution of biofilm forming bacteria (n=50) using quantitative assay (microtiter plate assay).
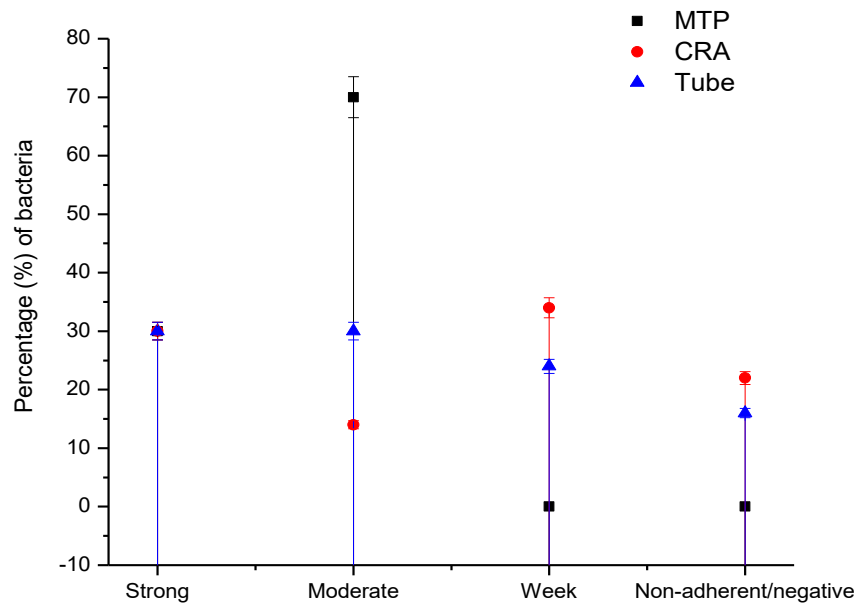
Figure 4. 8 Comparative analysis of slime/biofilm formation by Congo red Agar, tube method and microtiter plate assays.

4.3.5. Quantitative Production of EPS

4.3.5.1. Dry Weight

The slime EPS concentration varied and in the range of 1.33−13.33 g/l, produced by bacterial isolates as well as consortia. In bacterial broth, total EPS (slime, capsular and bacterial cells) was in the range of 5.33–24.7 g/l. However, the quantity of slime EPS (3.22–6.57 g/l) and total EPS (5.66–8.86 g/l) produced by four consortia was considerably less than that produced by individual bacteria (Fig. 4.9). The slime EPS produced by bacteria (1.33−13.33 g/l) varied with consortia (3.22−6.57 g/l).
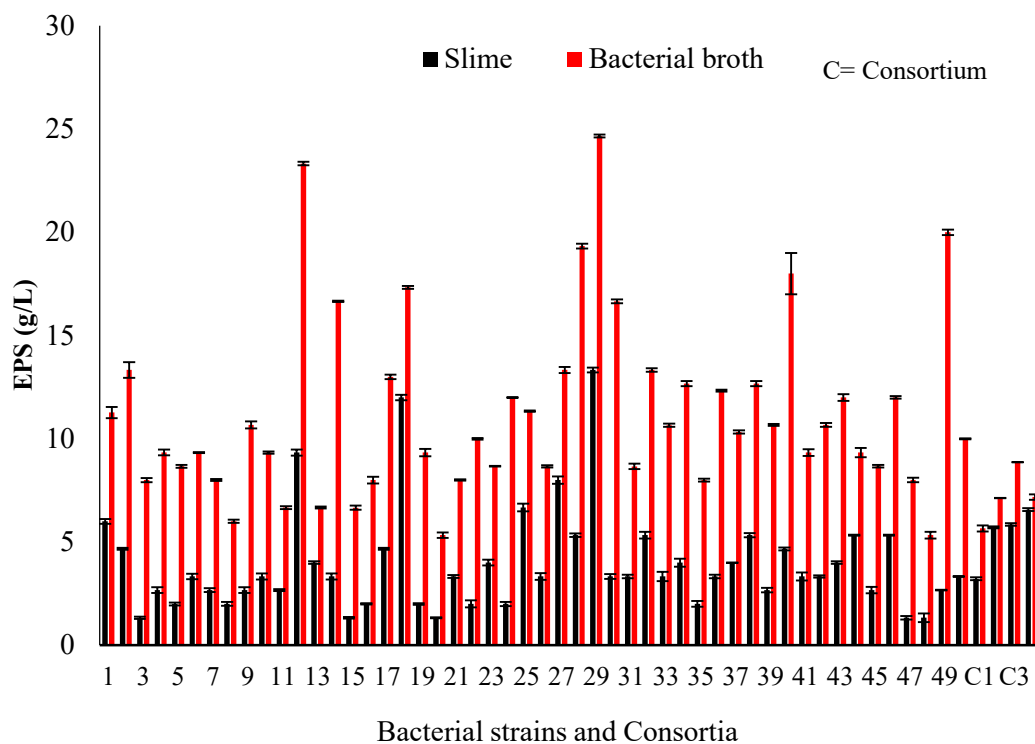
Figure 4. 9 EPS or biopolymer concentrations produced by bacterial isolates (n=50) and 4 consortia (72 hours of incubation at initial pH 7).

4.3.5.2. Viscosity

After 72 hours of fermentation, viscosity of individual bacterial as well as consortia broth was measured by VP 1060 viscometer. The measured viscosity of culture broths was in the range of 16,950–43,450 mPas and of 4 consortia was 28,800–30,150 mPas. Viscosity in some specific bacteria (4, 6, 13, 16, 25, 28, 34, 39, 48, 49 and 50) was higher as compared to other bacteria and 4 consortia due to EPS production (Fig. 4.10).
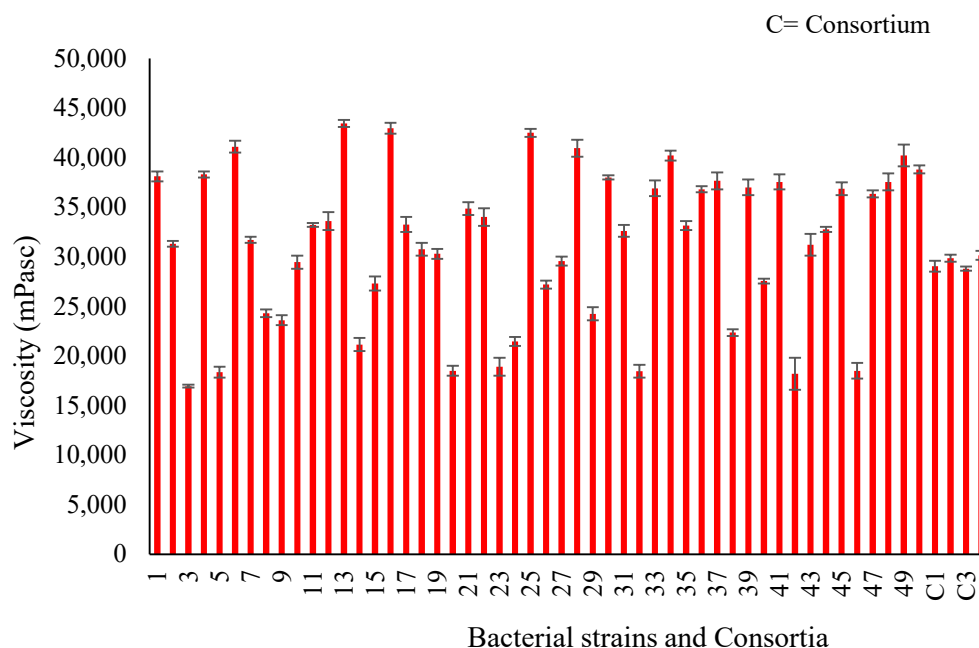
C= Consortium

Figure 4. 10 Viscosity of culture media by bacteria (n=50) and 4 consortia (after 3 days of fermentation at initial pH 7.0).

4.3.6. Selection of Six Best EPS Producing Bacterial Strains and Consortia Development

On the basis of assays (Maneval's and Anthony's capsule stain, CRA, TM, MTP, dry weight and viscosity) six best EPS producing bacterial strains were selected for consortia/biofilm development. Four combinations as consortium 1 (25, 4, 13, 39), consortium 2 (4, 25, 34, 39), consortium 3 (4, 13, 25, 48, 39) and consortium 4 (4, 13, 25, 48, 39, 48) were prepared. Further, analyses of bacterial strains and consortia were done on the basis of biochemical characterization (carbohydrate and protein), FTIR spectra and SEM (Table 4. 6).

Table 4. 6 Selection of six best EPS producing different bacteria on the basis of qualitative and quantitative assays and their Biochemical characterizations (TC and TP).

No	Bacterial strains	Dry weight				Chemical characterization	
		Bacterial broth (g/L)±1	Bacterial broth-duplicate	Slime EPS (g/L) ±1	Slime EPS-duplicate	TC (%)±5	TP (%)±5
1	4	9.34	9.35	2.25	3.11	72.8	27.2
2	13	6.67	6.68	3.81	4.23	67.11	32.9
3	25	11.32	11.36	7.44	5.90	73.7	26.3
4	34	12.69	12.64	4.22	3.81	68.3	31.7
5	39	10.72	10.61	2.65	2.69	68.78	31.22
6	48	5.35	5.31	1.67	1.00	54.6	45.4
7	consortium 1	5.69	5.63	3.00	3.43	89.7	10.3
8	consortium 2	7.14	7.111	5.73	5.69	81.19	18.81
9	consortium 3	8.537	9.2	5.91	5.80	73.18	26.82
10	consortium 4	6.91	7.44	6.59	6.54	65.95	34.05

4.3.7. Polysaccharide and Protein estimation of EPS

Total carbohydrate concentration in EPS produced by individual bacterial strains was in the range 0.504−0.91 mg/ml and of 4 consortia was in the range of 1.283−1.887 mg/ml. Maximum quantity of carbohydrate was 0.91 mg/ml produced by bacteria '34' and 1.887 mg/ml produced by consortium 4 (combination of 6 bacteria). Carbohydrate concentration produced by consortia was more than by individual bacteria (Table 4.6, Fig 4.11A).

Total protein concentration in EPS produced by individual bacterial strains was in the range 0.2278 −0.5214 mg/ml and by consortia (1, 2, 3, 4), was in the range of 0.1784−0.9742 mg/ml. Maximum quantity of protein was 0.5214 mg ml^{-1} produced by bacteria '39' and 0.9742 mgml^{-1} was produced by consortium 4 (combination of 6 bacteria). Protein concentration was varied among individual bacteria and consortia. The total protein content was less than total polysaccharides in bacteria as well as in consortia (Table 4.6, Fig. 4.11B).

The percentage of carbohydrate content was found to be higher than protein content of EPS produced by individual bacterial strains and consortium. The maximum carbohydrate content was 73.7%, produced by individual bacteria '25' and 89.7% was produced by the consortium 1. The maximum protein quantity produced was 45.4% by individual bacteria 48' and 34.04% by consortium 4 (Table 4.6).
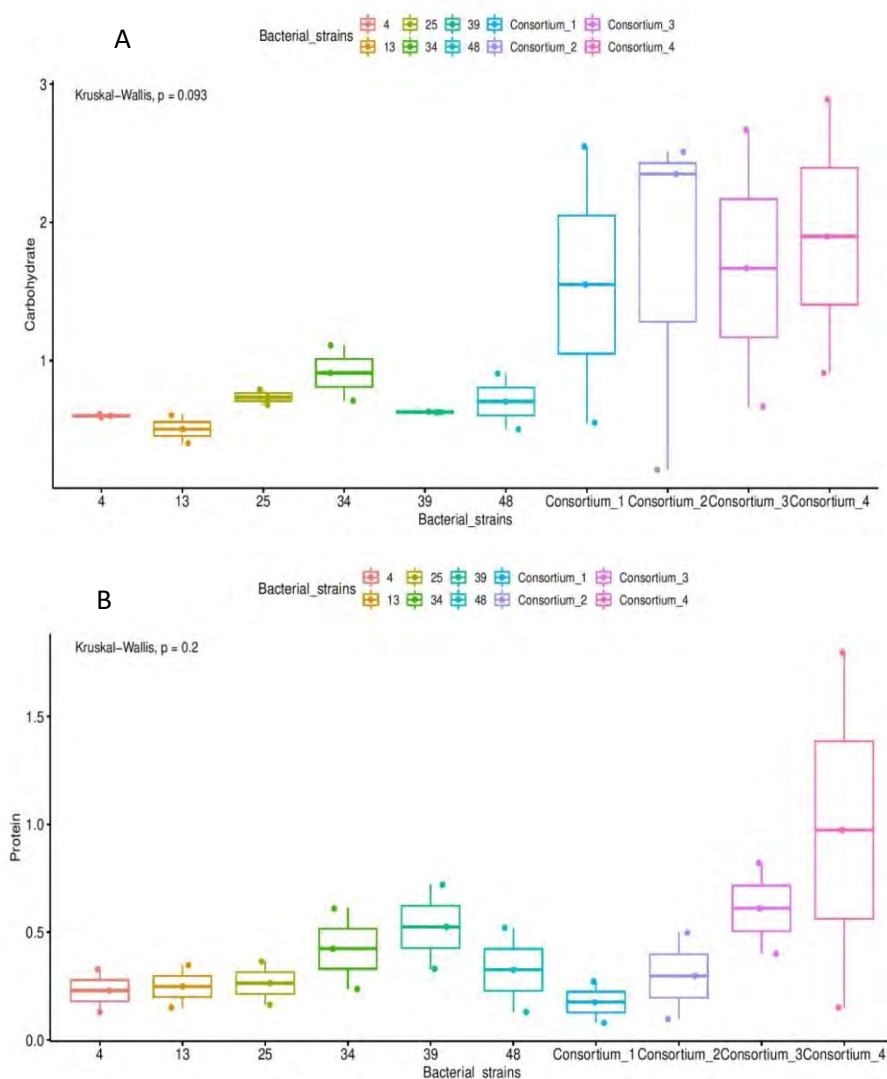
Figure 4. 11(A) Total carbohydrates (TC) and (B) total protein (TP) content of partially purified EPS from six selected pure bacteria and 4 consortia.

4.3.8. Fourier Transformed-Infrared Spectroscopy

FTIR spectra specified the presence of carbohydrates (800−1200 cm^{-1}), proteins (1,500−1,700 cm^{-1}), lipids (2,860−2,930 cm^{-1}) and nucleic acids (900−1,300 cm^{-1}) of EPS (Alvarez-Ordóñez et al., 2011; Faghihzadeh et al., 2016). No significant difference was observed in EPS peaks of bacteria and consortia (Fig.4.12 – 4.14) which depicted that chemical composition of EPS was the same. Peaks of carbohydrates and proteins were dominant in EPS of bacteria and consortia as compared to other organic materials. The FTIR spectrum of the purified EPS samples of six bacterial strains exposed characteristic functional groups such as peak 3358.17 cm^{-1} represented the O–H bond. The absorption bands at 2970cm^{-1} −2980cm^{-1} represented =C–H stretchand functional group alkenes. The absorption bands at 2880−2890 cm^{-1} represented theC–H stretch and functional group alkanes. Peaks near 2830cm^{-1} –2835 cm^{-1} represented −CHO stretch and functional group aldehydes. The absorption bands at 2125 cm^{-1} −2135 cm^{-1} represented –C≡C– stretch and functional group alkynes (Faghihzadeh et al., 2016). Enol and amide groups were represented by the 1650cm^{-1} –1540 cm^{-1} range. Peaks near 1649 cm^{-1} and 1650 cm^{-1} represented the amide and C-N bending of protein and peptide amines. Peaks 1421.72 cm^{-1} and 1483 cm^{-1}

represented C–C stretch (in–ring) and functional group aromatics and 1331.26 cm^{-1} represented N–O symmetric stretch and functional group nitro compounds (Cao et al., 2011). Presence of monomers (galactose, glucose and mannose) was observed between 900cm^{-1}−1200 cm^{-1} peaks. The absorption bands at 1086.15 cm^{-1} represented C–N stretch and functional groups alcohol, carboxylic acid, esters and ethers. Peak 1044.91 cm^{-1} represented C–N stretch and functional group aliphatic amines. The absorption bands at 878.38 cm^{-1} represented the glycosidic bond and 758.91 cm^{-1} represented C–H rock. Peak 1770 cm^{-1} represented the C=O stretch and functional group COOH. The absorption band at 841 cm^{-1} represented the asymmetric ester O−P−O stretch (nucleic acids) (Fig. 4.14) (Cao et al., 2011, Omoike & Chorover, 2004). Carboxyl groups function as binding sites for divalent cations, showed by FTIR spectra. The EPS was more complex due to presence of different functional groups.
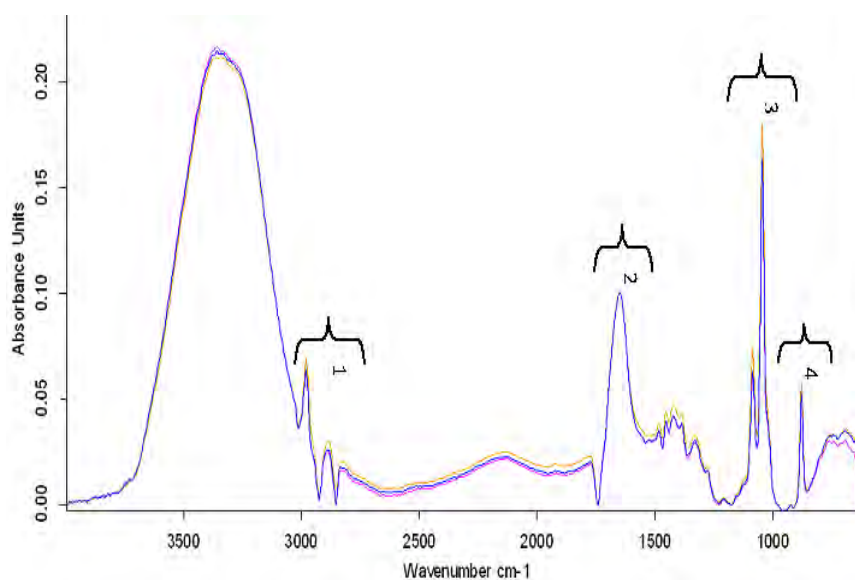
Figure 4. 12 (A) FTIR spectra of EPS of bacterial strains.
4 (pink), 25 (blue) and 48 (yellow). Peaks (1), =C–H (alkenes), C–H (alkanes) and −CHO vibrations in lipids; peak (2), enol and amides I/II in proteins; peaks (3), functional group −OH, −COOH, esters, ethers and aliphatic amines vibrations in carbohydrates; peak (4), glycosidic bond in carbohydrates.
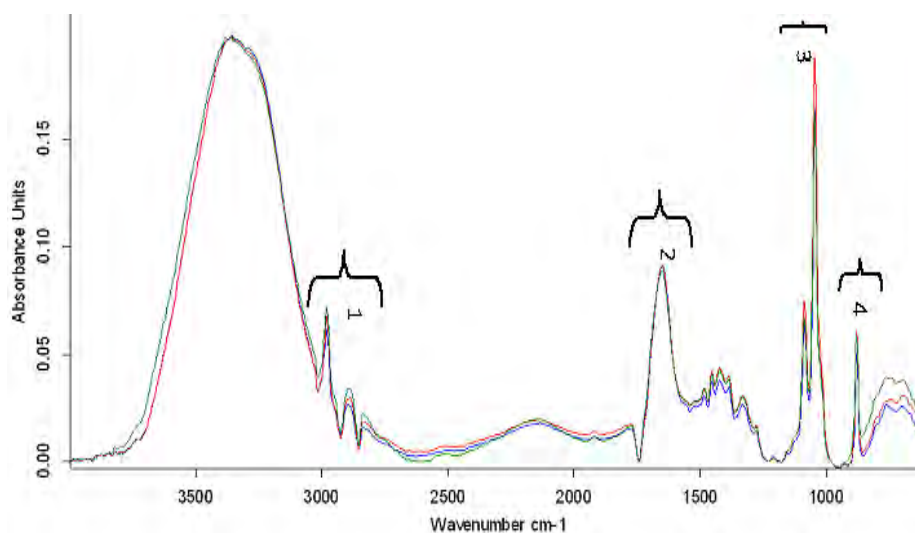
Figure 4. 13 (B) FTIR spectra of EPS of bacterial strains

13 (green), 34 (red) and 39 (blue). peak (1), =C–H (alkenes), C–H (alkanes) and −CHO vibrations in lipids; peak (2), enol and amides I/II in proteins; peaks (3), functional group −OH, −COOH, esters, ethersand aliphatic amines vibrations in carbohydrates; peak (4), glycosidic bond in carbohydrates.
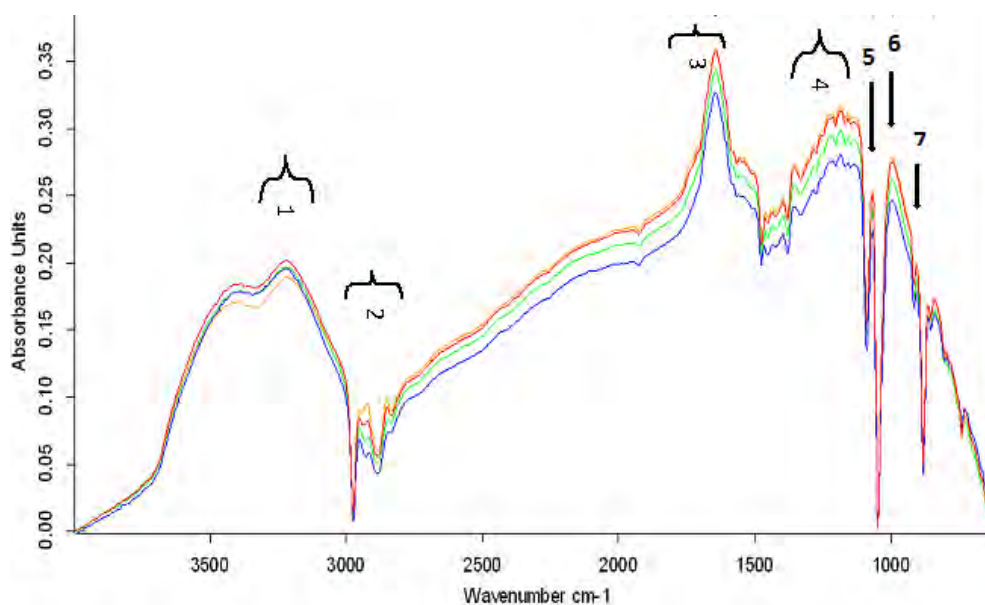
Figure 4. 14 (C) FTIR spectra of EPS of consortia.

1 (yellow), 2 (green), 3 (red) and 4 (blue). peak 1; −OH group, peak (2); CH stretch (CH_2/ CH_3 groups), peak 3; C=O stretch (amide I), peak 4; −CH_2 stretch, peak 5; C-O-C/ C-O-P stretch in carbohydrates, peak 6; asymmetric ester O-P-O stretch (nucleic acids), peak 7; –NH vibrations.

4.3.9. Scanning Electron Microscopy (SEM)

Scanning electron microscopy showed the images of EPS of biofilms developed on pebbles, of 4 different consortia at different magnifications. Thick EPS matrix covered the bacterial cells and transport channels were seen in the images (Fig. 4.15).EPS surface microstructure showed that the produced EPS exhibited compact like and porous structure which indicated the potential of EPS as a thickener, viscosifying or as stabilizing agent for novel products. The microorganisms were not prominent due to viscous EPS production.
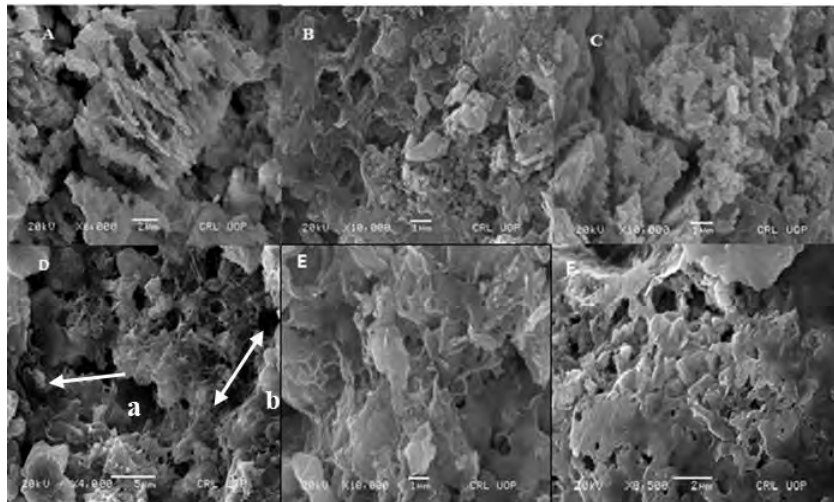
Figure 4. 15 Scanning electron micrographs of biofilms of different consortia.
(A, B) Scanning electron micrographs showing thick EPS matrix and channels for the transport of nutrients in EPS of consortia 1 (25, 4, 13, 39) at X6,000 and X10,000 (C) Exopolymer matrix covering the bacterial cells of consortia 2 (4, 25, 34, 39) at X10,000.(D); Scanning electron micrographs of EPS at *4,000*X and 10,000X resolution power of consortia 3 (4, 13, 25, 48, 39) (D) *a*; exopolymer matrix covering the cell mass *b*; EPS fibers for attachment of bacterial cells and transport channels. (E); Cells covered by thick, mucoid EPS. (F); Extracellular polymeric substances (EPS) produced by consortia 4 (4, 13, 25, 48, 39, 48) covering the bacterial cells.

4.3.10. Identification of Bacteria based on 16SrRNA Sequencing
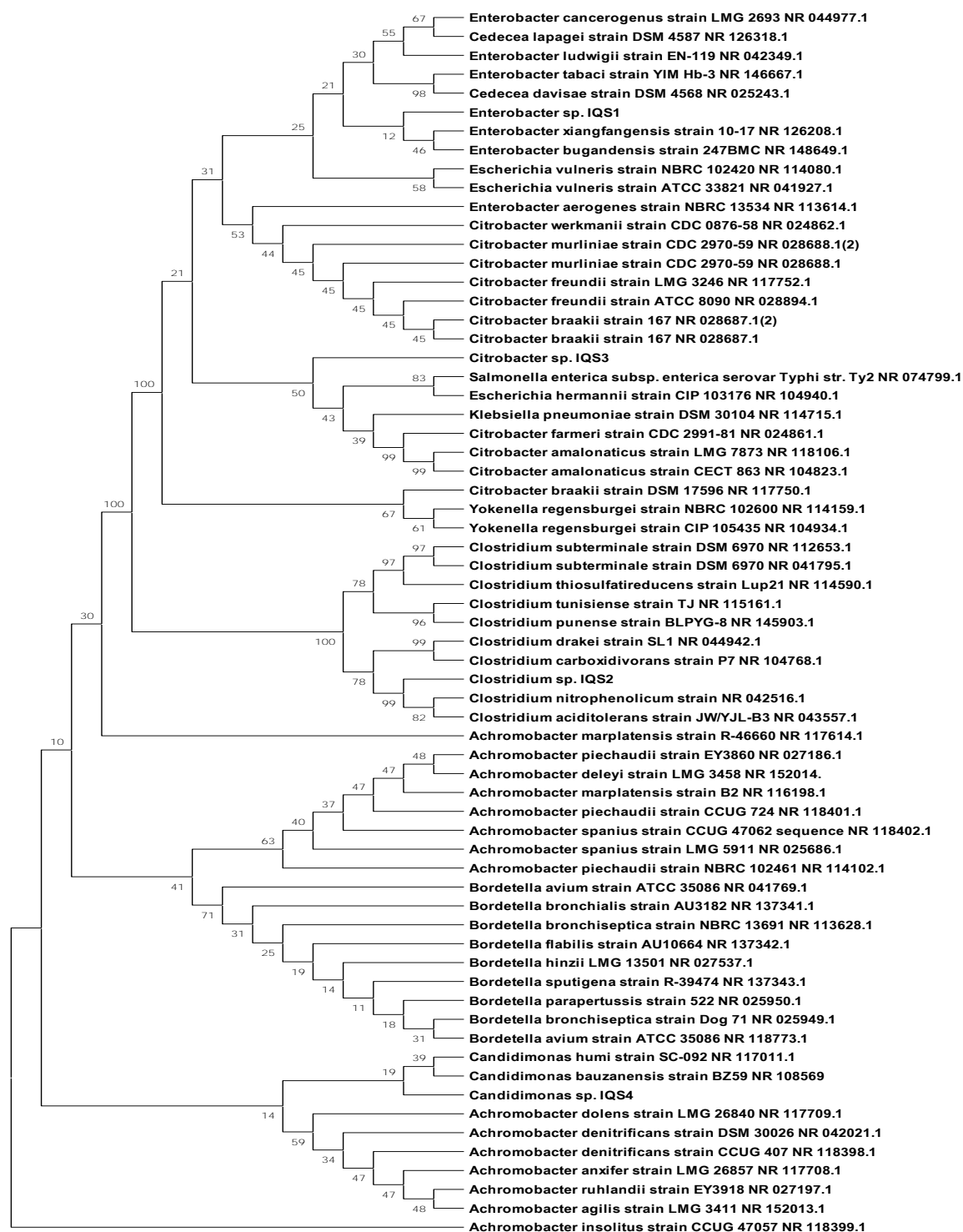
Figure 4. 16 Phylogenetic tree and evolutionary relationships between the isolated bacteria and related bacteria.

Neighbor-Joining method was used to infer the evolutionary history of the bacterial isolates (Zhou et al., 2014). Bootstap consensus tree of 500 replicates was taken for representation of evolutionary history of the analyzed taxa (Tripathy & De, 2006). The Maximum Composite Likelihood (MCL) method was used to compute the evolutionary distances as number of base substitutions per site (Vijayaraghavan, G.; Sivakumar, T.; Vimal Kumar, 2011). The analysis involved 65 nucleotides and 514 positions in final dataset. Any position that had <95 % site coverage was removed. The analyses were performed in MEGAX (Sbramanian et al., 2010).

4.4. Discussion

Extracellular polymeric substances (EPS) substantially affect the characteristics of sludge and wastewater treatment efficiency; however, the specific mechanisms and the pertinence to their compositional properties still need to be studied. Filling this knowledge gap would lead an increase in our capability in optimizing the wastewater treatment process (Yu, 2020,Sheng et al., 2010). EPS production depends on different factors such as metabolic routes, variation in properties and chemical composition of EPS of bacterial strains (Mikkelsen & Keiding, 2002). In this study, EPS producing bacteria were isolated from sludge and different biofilms of attached growth developed in the presence and absence of different metals. The bacteria were evaluated for their EPS production potentials both qualitatively and quantitatively on individual basis and in artificially formulated consortia form using different EPS production assays. Three types of EPS such as slime EPS, capsular EPS and broth (mixture of both slime and capsular EPS) were harvested and partially characterized. The bacterial isolates were identified using standard biochemical tests and 16SrRNS sequencing.

The results (biochemical tests) of the study indicated majority of the bacteria were facultative anaerobes and were identified by 16SrRNA sequencing as *Enterobacter* sp., *Citrobacter* sp., *Clostridium* sp. and *Candidimonas* sp. EPS staining (Anthony's capsule staining) results revealed that 66% (33) bacterial strains had a strong capsule whereas all (50) bacteria contained loosely bound slime EPS in their cell walls. Microtiter plate assay (Devaraj, 2015, Hassan et al., 2011, College, 2014) showed 15 (30%) bacteria were strong biofilm formers. Slime EPS producing bacteria were able to form a relatively longer mucoid string than the capsule containing bacteria. Subramanian et al. (2010) isolated exopolymeric substances producing bacteria from municipal wastewater sludge that belonged to the genera *Bacillus, Enterobacter, Pseudomonas, Yersinia, Microbacterium, Pantoea, and Pectobacterium*. The slime EPS producing bacteria could form mucoid strings of greater 2cm contrary to the bacteria with capsular EPS (Subramanian et al., 2010). The concentration of slime EPS produced by the bacteria lied in the range 1.33g/l−13.33 g/l, almost twice than the slime EPS by the bacteria in consortia form that varied in the range (3.22g/l−6.57 g/l). Subramanian et al. (2010) also observed less slime EPS production by the consortium of different bacteria in the minimal media Subramanian et al., 2010). This reduction in the concentration of slime EPS is due to the presence of competitive interactions among bacteria in consortium form.

Higher concentration of carbohydrates was produced by consortia (1.283 mgml^{-1} −1.887 mgml^{-1}) compared to the individual bacteria (0.504 mgml^{-1}−0.91 mgml^{-1}). Varying protein concentrations were produced by individual bacteria (0.2278 mgml^{-1} l−0.5214 mgml^{-1}) and the consortia (0.1784 mgml^{-1}−0.9742 mgml^{-1}). The concentration of carbohydrate content was more in EPS biochemical characterization than the protein content by individual bacterial strains as well as consortia. The maximum carbohydrate content was 73.7% and 89.7% produced by individual bacteria '25' and consortium 1. The maximum protein quantity produced was 45.4% by the bacteria 'B-26' and 34.04% by consortium 4. TC/TP ratio depicted that carbohydrate possessed major role in bioflocculation process, sludge settling and dewatering due to the interaction between cations (in sludge) and anions (bacteria).

Higher carbohydrates/protein ratios play significant role in enhanced settling of sludge and sludge dewatering. Higher concentration of carbohydrates has also been reported by individual bacteria in study by Subramanian et al. (2010). Polysaccharides are important for establishing bridges between their negatively charged components and cations in the sludge subsequently leading to sludge flocculation. However, some studies have reported significant role of proteins in making bridges with multivalent cations through hydrophobic interactions contributing to the sludge flocs (Higgins & Novak, 1997b, Higgins & Novak, 1997a, Jorand et al., 1998). Moreover, growth under different ecological conditions such as on rough surfaces and substrates contributes to variations in the composition of EPS (Garnier et al., 2005,Houghton & Stephenson, 2002, Urbain et al., 1993,O'Toole, 2003, Wsche et al., 2002).. Viscosity measurements indicated that EPS production by consortia was lower than by some individual bacteria. Variation in final cell concentration had a lesser impact than diverse quantity of EPS produced by the bacterial strains, a major reason of variation in viscosity concentration (Subramanian et al., 2007, 2010).

FTIR spectra indicated the presence of different content of carboxylic acids, amines and amide groups, glycosidic linkages, double and triple bonds of carbon corresponding to the presence of proteins, carbohydrates, lipids and nucleic acids, respectively (Jiao et al., 2010). Higher peaks of proteins in EPS of consortia displayed an anomalous behavior contrary to biochemical results. This again could be attributed to the competitive inhibitive interactions among bacteria in consortia. No significant difference was observed in EPS microstructure of different consortia by Scanning electron micrographs. The biofilm appeared compact, rough and porous due to presence of channels and grooves for transportation of nutrients and thick EPS matrix was covering the bacterial cells at different resolutions. Microorganisms were embedded in thick and viscous layers of EPS.

4.5. Conclusion

Out of the total screened bacteria isolated from activated sludge and biofilms developed on waste tire rubber in attached growth reactors, 15 (30%) bacteria were strong biofilm formers according to microtiter plate method and 33 (66%) bacteria contained capsular EPS. Almost all bacteria showed the potential for slime EPS production. The consortia associated EPS contained a higher proportion of polysaccharides (1.233 mgml^{-1} –1.887 mgml^{-1}) than the EPS produced by individual bacteria (0.504mg/ml –0.610 mg/ml). Protein concentration varied from 0.227 mgml^{-1} –0.52 mgml^{-1} by individual bacteria and 0.178mg/ml – 0.974 mgml^{-1} by the consortia. Highest carbohydrate was produced by bacteria '25' (73.7%), and consortium 1 (89.7%) whereas maximum protein was produced by bacteria 'B-26' (45.4%) and consortium 4 (34.04%). The bacterial that demonstrated highest EPS production potential were identified as *Enterobacter* sp., *Citrobacter* sp, *Clostridium* sp. and *Candidimonas* sp.

4.6. Future Prospects

Bioflocculation capability of each bacterial strain and consortia should be studied using kaolin clay assay. The extracted slimes should be studied in terms of their sludge volume index, settleability, flocculation and capillary suction time such as dewatering of sludge besides EPS mediated heavy metals removal. The biopolymers may be characterized further using different molecular and physicochemical methods. The

isolated bacteria need to be characterized for the *eps* producing genes using molecular techniques such as molecular probes and primers. The *eps* genes can be cloned for enhanced EPS production. Furthermore, the behavior of EPS should be investigated with supplementation of divalent and polyvalent cations viz. calcium, and iron for sludge the settleability.

CHAPTER 5

Effect of Metals on Electroactive Biofilms and Performance of Microbial Fuel Cells

Study Title: Trivalent Iron Shaped the Microbial Community Structure to Enhance the Electrochemical Performance of Microbial Fuel Cells Inoculated with Soil and Sediment

Chapter 5: Trivalent Iron Shaped the Microbial Community Structure to Enhance the Electrochemical Performance of Microbial Fuel Cells Inoculated with Soil and

Abstract

Bioelectrochemical performance of bacterial communities of cropland soil and lake sediment was evaluated in double chamber microbial fuel cells (MFCs) under the effect of trivalent iron [Fe(III)]. The MFCs were operated in a fed batch mode and their voltage output was measured for a period of 40 days. The highest outputs recorded under untreated conditions using cropland soil and lake sediment were 154 mV (current density= 0.06 mAcm^{-2}, power density = 9.5 mWcm^{-2}) and 137 mV (current density; 0.06 mAcm^{-2}, power density; 7.5 mWcm^{-2}), respectively. An about 87.7% (voltage; 289 mV, power density; 33.4 mWcm^{-2}) and 45% (voltage: 160 mV, current density; 0.06 mAcm^{-2}, power density; 10.24 mWcm^{-2}) increase in voltage output was measured in the respective soil and sediment inoculated MFCs under iron treatment. The COD removal rate increased from 40% and 35% to 69% and 65% under the treated conditions. Alpha rarefaction curves and Shannon index revealed soil derived biofilms contained the most diverse bacterial communities and diversity significantly reduced in sediment biofilm treated with Fe^{3+}. Illumina *MiSeq* sequencing and scanning electron microscopy indicated the presence of a diverse microbial diversity where the Proteobacteria, Bacteriodetes and Firmicutes were the most abundant phyla. Predominant genera included *Pseudomonas*, *Sedimentibacter, Aminobacterium*, *Clostridium and Flavobacterium sp*. The MFCs with sediment supported the delta-proteobacteria; the class that includes *Shewanella* sp. and *Geobacter* sp., higher in the presence of Fe^{3+} than soil-MFCs. Based on the 16SrRNA sequencing, isolated bacteria were identified as *Staphylococcus* sp., *Bacillus* sp., *Streptomyces* sp. and *Gordonia* sp., already reported for their electricity generation potential.

Key Words: Microbial fuel cell Microbial fuel cell; Ferric iron [Fe(III)]; Cropland soil; Lake sediment; Exoelectrogens; Illumina *Miseq* sequencing, 16S rRNA sequencing.

Highlights

- Electrochemical performance and microbial community dynamics within anodic biofilms were evaluated in dual chamber microbial fuel cells under the influence of trivalent iron.

- Ferric iron enhanced the power generation potential of microbial fuel cells.

- Microbial fuel cell inoculated with soil and dosed with iron generated the highest voltage.

- Illumina Miseq revealed ferric iron shaped the microbial community of anodic biofilms.

- Soil derived biofilms contained the most diverse bacterial communities.

- Proteobacteria, Bacteriodetes and Firmicutes were the most abundant phyla.

5.1 Introduction

Over exploitation of the fossil fuels, resulting in a continuous environmental damage has driven the search for alternate sustainable sources and technologies for renewable energy generation essential to tackle the environmental challenges (Chatterjee & Huang, 2020). Bioelectrochemical systems (BES) have emerged as an opportunity to address both issues; dwindling supply of fossil fuels and increasing demand for better waste management technologies by eco-electrogenic treatment of complex substances (Obileke *et al.*, 2021, Afsharian and Rahimnejad, 2022). Microbial fuel cell (MFC) technology exploits the potential of electroactive bacteria to oxidize the organic wastes and produce electricity. The electrons released through microbial catalysis are transferred to the anode which serves as an intermediate electron sink, either via direct electron transfer or through mediators, and then transferred from anode through external resistance and subsequently consumed at the cathode (Scott et al., 2016, Logan et al., 2006a, Pasupuleti *et al.*, 2016).

Numerous studies have reported the use of MFCs using water, wastewater and marine environments for power generation and identification of exoelectrogens than soil. Soil has potential to be used for electricity generation, using MFCs, whereby, soil source exoelectrogenic microorganisms carry out catalysis for conversion of chemical energy of soil organic compounds into electricity. Recently, soil MFCs are being employed for simultaneous pollutant mitigation and biosensing from soils and sediments (Simeon *et al.*, 2022, Jiang et al., 2015, Nandy *et al.*, 2015, Wang et al., 2012, Arends et al., 2014, Huang et al., 2011, Kondaveeti *et al.*, 2019). Similarly, sediment MFC has great remediation potential for soil pollutants where sediment serves as a sink for various contaminants (Abbas et al., 2019b, Wu *et al.*, 2017). Sediment MFC has been demonstrated as a means of energy source for low power oceanographic sensors in remote settings (Algar *et al.*, 2020). Liang *et al.* (2020) reported improved power potential and removal of polycyclic aromatic hydrocarbons (phenanthrene; 78.1% $_{max.}$ with carbon nanotubes, pyrene; 69.6% $_{max.}$ with graphene oxide) in sediment MFCs (Liang *et al.*, 2020). Mohanakrishna et al. (2020) applied MFCs for remediation of petroleum hydrocarbons in petroleum refinery effluent and achieved a highest substrate degradation efficiency of 0.42 Kg COD /m^{3}day and COD removal 63.10 % with 80:20 feed (Mohanakrishna, Abu-Reesh and Pant, 2020). The performance of microbial fuel cells depends on the type and activity of electrobacteria in the soils. However, no significant knowledge is available about the microbial diversity in different soils and their extracellular electricity generation characteristics (Jiang et al., 2016).

A number of factors such as reactor configuration, electrode materials, microorganism serving as biocatalysts, and operational conditions affect the performance of MFC. Biofilm on the electrode(s) is a key element affecting the power generation (Islam et al., 2019, Janicek et al., 2014, Chen et al., 2019). MFCs have successfully been inoculated using pure cultures mainly the *Geobacter* and *Shewanella* sp. (Yates et al., 2013, Shi et al., 2019). Natural environmental systems such as soils and sediments are comprised of a myriad of lithotrophs associated with removal of nutrients and compounds otherwise hard to be disposed through different anthropic waste streams (Mancílio *et al.*, 2020). Based on ecological impacts of these compounds on the microbial energy metabolisms, application strategies are devised for

treatment of such waste compounds i.e., heavy metals, and facilitating the electron transfer independently from the supply of organic carbon. Elaborating such processes within MFCs would make it possible to identify new electrogenic bacterial strains and understand the metabolic complexity of mixed cultures. Various uncontrolled oxidation processes inside the MFCs for energy metabolism and understanding how these compounds affect the ecological relationships among different microbial communities remains an unexplored opportunity.

Iron is regularly found in different waste streams including textile, detergent manufacturing industries, mineral processing wastewater, soils and sediments (Miran et al., 2017, Baek et al., 2019). The studies have reported that iron, in its ferric and ferrous forms, affects the bioelectrochemical processes biotically and abiotically. Metal reducing bacteria are capable to consume extracellular insoluble metals for respiration. Ferric ions as protein cofactors may alter the expression and activity of proteins for energy metabolism (Ruiz-Urigüen et al., 2018). Iron is a critical factor affecting the formation of biofilms on the electrodes and flavin secretion in electroactive bacteria (Liu *et al.*, 2018, Liu et al., 2017a, Hunter et al., 2013, Wu et al., 2013, Banin et al., 2005). Exogenous Fe (III) into MFCs boosts anaerobic digestion and anodic oxidation which results in improved mineralization of volatile fatty acids (VFA) (Zhang et al., 2013, Peng et al., 2012, Ji et al., 2011). Abiotically, it has role in redox reactions, electron shuttling and catalysis contributing to accelerated enrichments of iron reducing consortia in MFCs (Ferreira & Salgueiro, 2018, Lu et al., 2015, Wang *et al.*, 2010). Kim and coworkers (2005) reported the application of electrode coated with iron oxide and Fe^{3+} (100 mM) supplementation enhanced the power generation and coulombic efficiencies of the reactors up to 80% (Kim et al., 2005). Kato et al. (2012) evidenced the involvement of electrically conductive ferric iron derived magnetite mineral particles in interspecies electron transfer and to the anodes (Kato, Hashimoto and Watanabe, 2012). The electrogenic bacteria can grow under Fe^{3+} in a range of 5 μM–50 μM in non-contaminated soils (Nevin and Lovley, 2010) (Lovley, Holmes and Nevin, 2004) and up to 5 g/l–24 g/l iron in contaminated soils (Martins *et al.*, 2009). Wu et al. (2013) used 6 mM ferric iron in MFC and reported an increase (53.3%) in current density with *Shewanella* spp. (Wu *et al.*, 2013). Supplementation of Fe^{3+} in the range 16 mM to 55 mM has been used for enrichment of iron reducing electricigens in MFCs using different soils (Jiang *et al.*, 2016, Becerril-Varela *et al.*, 2021). To optimize the ecological conditions for enrichment of exoelectrogens, investigating the effects of ferric ions and their synthetic salts, in bioelectrochemical processes has sparked interest for better engineering approaches (Liu et al., 2018). Abiotic role of Fe^{3+} in MFCs for enhanced current density and remediation of recalcitrant compounds has been studied primarily considering reduction and reoxidation of Fe^{2+} in the cathode (Ren *et al.*, 2012). But the effect of Fe^{3+} supplementation on the microbial community of electrodes is not fully explored. Nevertheless, the effect, in its readily available states such as ferric iron in the waste streams, soils and sediments on energy metabolism and mixed cultures exoelectrogens' ecology in the electrode biofilms, is still elusive and needs to be investigated (Wei et al., 2013).

Available studies on iron in MFCs focus mainly on the abiotic impact of iron supplementation. Considering the above critical reviews and to filld the scientific gaps, the present study aimed to evaluate both abiotic as well as biotic effects of incorporation of Fe^{3+} on the electrochemical performance of dual chamber microbial fuel cells and dynamics of microbial communities in the anodic biofilms. Microbial community structure of the cropland soil and lake sediment from Pakistan and the associated anodic biofilms in MFCs was analyzed for the first-time using Illumina *Miseq* sequencing of 16S rRNA gene amplicons and related to the monitoring of nutritional availability. Exoelectrogenic bacteria were isolated and identified using standard microbiological tests and 16S rRNA sequencing. The obtained enrichments may further be applied for remediation in different environments such as those contaminated with heavy metals.

5.2 Material and Methods

5.2.1 Sampling

Soil and sediment samples were collected from cropland located at Botanical Research Garden (33.738049° N, 73.160775° E) Quaid-i-Azam University, Islamabad Pakistan and Rawal Lake (Lake View) (33.7155° N, 73.1305° E), Islamabad Pakistan. For soil, surface litter was removed and dug up to 1 foot down the earth at three different randomly selected sites (0.5 m × 0.5 m) and, mixed to represent a site. The sediment was dug with the help of sterile spatula at three different sites up to half foot down the sediment sites, mixed and collected into a new sterile polyethylene bag. The sample bags were sealed airtight and brought into the laboratory within 20 minutes after collection. The samples were sieved through 2 mm diameter mesh, flushed with nitrogen gas to create anaerobic conditions and stored into refrigerator at 4°C for less than 1 week before series of experiments such as soil property characterization, MFCs operation and enrichment of iron reducing bacteria.
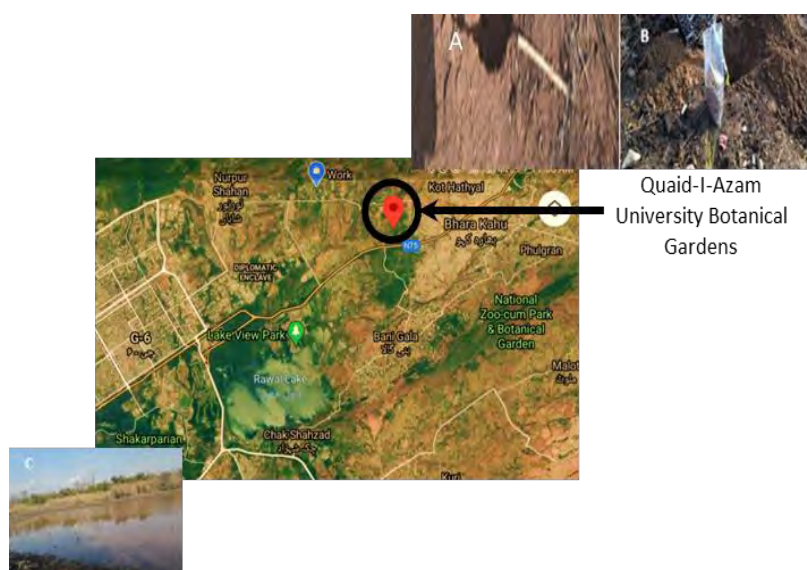
Figure 5. 1 Sampling sites
 (A and B) cultivated land/cropland soil collected from Quaid-i-Azam University Botanical Gardens, Islamabad, Pakistan (C) Rawal Lake; the sediment was collected from Rawal Lake, Islamabad, Pakistan.

5.2.2 Soil and Sediment Characterization

Each sample was divided in aliquots to determine theirphysiochemical properties before performing experiments. The analyses were carried out at the National Agricultural Research Centre, Islamabad, Pakistan following standard protocols. Texture of soil was determined using the sieve and pipette method. Soil organic carbon (OC) content was calculated by K_2CrO_4 oxidation. Soil pH was measured at 1:2.5 (soil: water) ratio while the electrical conductivity (EC) at 1:5 (soil: water). Total/extractable phosphorus was measured by colorimetry following NaOH digestion. Kjeldahl digestion was used to measure total nitrogen (TN), and organic matter, nitrate nitrogen, potassium (NPK), total organic carbon, oxidizable carbon, calcium and magnesium were determined by methods as described (Black et al., 1965).

5.2.3 Microbial Fuel Cell Construction and Operation

H-shaped microbial fuel cells (MFCs) with proton exchange membrane were constructed using polyacrylic bottles (total volume; 400ml) for anode and cathode chambers. Both anode and cathode chambers were separated with a proton exchange membrane (DuPont™ Nafion ® 115, 5cm^2) fixed within two plexiglass slabs. Holes of 3cm diameter were drilled in plexi glass slabs and membrane was sandwiched between the two slabs. The slabs were fixed with the help of screws and attached with chamber bottles. The joints were sealed with silicone sealant or epoxy glue to avoid any potential leakage. Carbon cloth [(EC-CC1-060), 5 cm^2] and graphite paper sheets (7.0 cmx3.0 cm) served as the anode and cathode, respectively. Both chambers contained inlets and outlets for adding substrate and collection of samples when required. The electrodes were autoclaved at 121 ^{o}C for 20 min. before processing further and assembled using copper wire (diameter: 0.8 mm).
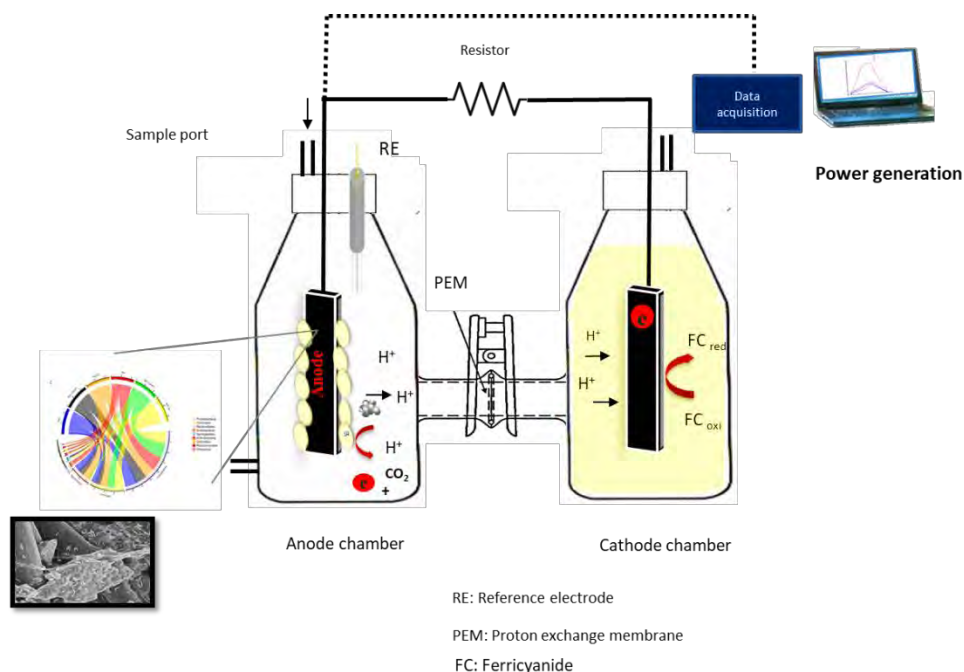
Figure 5. 2 Schematic diagram of double chamber microbial fuel cell (DCMFC) with proton exchange membrane (PEM).

5.2.3.1 Composition of Anolyte and Catholyte

The microbial growth medium (anolyte) contained basal medium (BM) along with mineral and vitamin solutions. The composition of basal media (per liter) was: peptone 8 g, yeast extract 1 g, NH_4Cl 0.12 g, sodium acetate 16 g, NaCl 5 g, K_2HPO_4 1.2 g, cysteine hydrochloride 1 g, resazurin (redox indicator) 1mg, Wolfe's mineral solution 5 ml, and Wolfe's vitamin solutions (Sigma-Aldrich ,Co., St. Louis, MO, USA) 5 ml (Lovley et al., 1987, Lovley & Phillips, 1986). Wolfe's mineral solution/L contained nitrilotriacetic acid 1.5 g, $MgSO_4.7H_2O$ 3.0 g, $MnSO_4.H_2O$ 0.5 g, NaCl 1.0g, $FeSO_4.7H_2O$ 0.1 g, $CoCl_2.6H_2O$ 0.1 g, $CaCl_2$ 0.1 g, $ZnSO_4.7H_2O$ 0.1 g, $CuSO_4.5H_2O$ 0.01 g, $AlK(SO_4)_2.12H_2O$ 0.01 g, H_3BO_3 0.01 g, $Na_2MoO_4.2H_2O$ 0.01 g and distilled water 1.0 liter. Iron resource was provided in the form of 25 mM Fe_2O_3 (Sigma-Aldrich). The medium was boiled with N_2 gas for 20 min.-30 min. and then was autoclaved in bottles. The pH of the medium was maintained at 6.7. Potassium ferricyanide 50 mM [$K_3Fe(CN)_6$] in equimolar phosphate buffer (pH 7) was used as a catholyte. The PBS (phosphate buffer saline) contained NaH_2PO_4 4.904 g/l, Na_2HPO_4 9.125 g/l, NH_4Cl 0.62 g/l and KCl 0.26 g/l in distilled water (1 liter).

5.2.3.2 Microbial Fuel Cell Operation

Anaerobic basal media (300 ml) with 5 ml/l Wolfe's vitamin and Wolfe's mineral solution each was injected in anodic chambers of microbial fuel cells. The inoculum (2 g per 100 ml) from both soil and sediment samples was incorporated in each MFC anode. Colony forming units (CFU) of each sample per gram were calculated before inoculating in the cells to know the estimated number of microorganisms (inoculum size) added in each experiment by serial dilution technique. The cells were dosed with anhydrous 25 mM Fe_2O_3 whereas the cells without iron served as control. The anaerobic conditions were maintained in the anodic chambers with sterile N_2 gas for ≈20 mins before they were placed into anaerobic incubator at 37 ^{o}C in dark under agitated conditions (100 rpm) for a period of 40 days for biofilm development and power generation. One control cell received no iron dose and another control was run under the same conditions with chloroform sterilized soil or sediment to confirm the voltage was generated from microbial electron transfer processes. MFCs inoculated with soil and Fe (0 mM), soil and Fe (25 mM), sediment and Fe (0 mM) and sediment and Fe (25 mM) were designated as MFC-soil-control, MFC-soil-Fe, MFC-sediment-control and MFC-sediment-Fe, respectively.

Open circuit voltage was recorded using a precision multimeter (UT33C, UNI-T) till voltage became steady state. Both electrodes were connected to an external circuit with a resistance of 100Ω using copper wire and voltage was monitored on daily basis with the help of multimeter for a period of 40 days. For polarization studies, resistors of load ranging from 100 Ω-15000 Ω were applied. MFCs were operated in fed batch mode and anode solution was refreshed every week followed by purging with oxygen free sterile nitrogen gas for 20 min to maintain anaerobic conditions in the reactors. Samples were collected periodically from each anode chamber through outlet for various analyses. COD (mg/L) was measured using commercial kits (Spectroquant® test kits, Merckmillipor, Catalog No. 1170590001). The pH was monitored every week using Sartorius pH meter PP15. MQuant® 110004 (Merck) test kits were used for

measurement of Fe^{2+} ions formed through ferric reduction following the manufacturer's recommendations.

5.2.3.3 Electrochemical Measurements

The voltage across various external resistors (100Ω-15000Ω) and open circuit voltage (OCV) was measured by precision multimeter regularly. The current (mA) was measured from voltage using Ohm's law

I=Vcell/Rcell   (1)

Current density (mA/cm^2) was determined by equation 2,

$J = V_{Cell}/R_{ext} A$ (2)

Power (mW) was calculated from voltage (V) and current (I) by using the formula:

P=Icell xVcell   (3)

Whereas, Power density (mW/cm^2) was calculated by the equation 4

$P = V^2_{Cell}/R_{ext} A$ (4)

Where, 'V' is the measured voltage of cell, 'R' is external resistor and 'A' is projected surface area of electrode.

The Coulombic efficiency in similar systems has been well reported (~20% for an external resistance of 1000 Ω) and was not measured in these experiments (Zhang et al., 2009, Yates et al., 2013).

Cyclic voltammetry (CV) is used to study the oxidation and reduction processes of molecular species and extracellular electron transfer (EET) interactions between exoelectogenic bacteria and electrodes in MFCs. CV was performed using a three-electrode configuration to measure the variations in redox potential over a potential range of −1V to +1V (scan rate = 100 mV s^{-1}) using a potentiostat (WMPG1000) at turnover conditions. Electrochemical measurements were carried out using anode as working electrode (WE), cathode the as counter electrode (CE) and Ag/AgCl vs SHE as a reference electrode (RE).

5.2.4 Ultrastructure of Anodic Biofilms

Scanning electron microscope has been used successfully to characterize surface morphology and ultrastructure of microbial biofilms. To visualize the surface morphology of biofilms developed on carbon cloth in anodic chambers of MFCs under treated (with anhydrous ferric oxide) and control conditions, scanning electron microscopy was carried out. Biofilms on electrode surface were washed with PBS to remove planktonic microorganisms. A small piece ($\approx$ 1 cm^2) of carbon cloth with biofilm was excised with sterile scissors and placed in sterile PBS buffer solution. Each sample were fixed in 2% glutaraldehyde (v/v) for 2h and washed three times (20 min per wash) with sodium cacodylate (0.1M). The fixed biofilm samples were continually dehydrated with different concentrations of ethanol and stored in absolute ethanol at 4°C. The samples were dried by critical point drying and small sections of fixed biofilm samples on carbon cloth were mounted on the copper stubs and sputter coated with gold layer. Then vacuum was generated by applying high voltage (20 kV) in ion sputtering JFC-1500, auto coater (JEOL, Tokyo, Japan) for gold deposition on biofilms. An about 25 mA current for approximately

50s was used for generation of plasma and subsequent gold coating on the samples. Gold coated samples were then placed under the column in chamber and finally the micrographs were observed under SEM (JSM-6490A, JEOL) at different magnification intensities starting from X 100 to X 20,000 and recorded.

5.2.5 Illumina *MiSeq* Sequencing for Characterization of Microbial Diversity

After MFCs were operated for 40 days, the anode biofilms of MFCs (control, treated with 25 mM Fe^{3+}) were sampled for genomic DNA extraction by using PowerSoil® DNA Isolation Kit 12888-50 (MoBio Laboratories, Inc.) according the manufacturer's instructions. Prior to DNA extraction, small pieces (≈1cm2) of biofilm laden carbon cloth were cut down and added into few ml of phosphate buffer solution (PBS). Each sample was sonicated for 5min. using a sonicator to detach all the cells from the anode surfaces. Concentration and purity were determined by Nano drop (NP-50, Implen DNA GmbH).

5.2.5.1 Methods of *MiSeq*

The PCR primers 515/806 containing a barcode on forward primer and specific for the V4 variable region of 16SrRNA gene were used in a 28-cycle polymerase chain reaction (PCR) using HotStarTaq Plus Master Mix Kit (Qiagen, USA). The conditions applied were: 94 °C temperature for 3 minutes followed by 28 cycles of 94 °C for 30 seconds, a temperature of 53 °C and 72 °C for 40 seconds and 1 minute, respectively. Finally, an elongation step was performed at 72 °C for 5 minutes. The PCR amplified products were checked on 2% agarose gel to determine the intensity of the bands. Multiple samples were pooled together in equivalent proportions on the basis of DNA concentration and their molecular weights. The samples were subsequently purified with calibrated Ampure XP beads and the purified products were used for preparation of Illumina DNA libraries. The sequencing was carried out at MRDNA (www.mrdnalab.com, Shallowater, TX, USA) on *MiSeq* platform following the guidelines by the manufacturer.

5.2.5.2 Data Processing

The sequences data (Q25) obtained from the sequencing process was processed using the MRDNA ribosomal and functional genes analysis pipelines (www.mrdnalab.com, MRDNA, Texas, USA). The sequences were joined, depleted of primers and barcodes. Short sequences, less than 150 bp, with ambiguous base calls and homopolymer runs (PGM/S5) were also removed. Operational taxonomic units (OTUs) were finally generated after the sequences were denoised, and singleton and chimeras were removed. The OTUs were defined by the clustering at a 97% similarity (3% divergence). The final OTUs obtained were taxonomically classified with BLASTn against the database from NCBI and RDPII (www.ncbi.nlm.nih.gov, http://rdp.cme.msu.edu). The counts and percentage files were generated which contained actual number of sequences and relative proportion of sequences of each sample in accordance to the taxonomic classification.

5.2.6 Evaluation of Bacterial Density and Taxonomic Analysis of Bacteria

Biofilms developed on carbon cloth in the anode chambers with and without Fe^{3+} were gently washed-off with PBS to remove the planktonic microorganisms. The biofilms on carbon material (≈1 cm^2 sections) were scrapped off using sterile blades followed by sonication at 1–2 kHz for 3 min in PBS solution.

Bacterial density was determined on the basis of CFU mL^{-1}cm^{-2} using heterotrophic plate count method on *Luria Bertani* (LB) agar plates in triplicate and analyzed statistically with t-test using Origin 8.5. The plates were incubated at 37 ^{o}C in an anaerobic incubator for a period of 24 hours. Pure cultures of bacteria obtained on LB agar plates were distinguished from each other on the basis of their morphology, biochemically characterized and identified using standard procedures of *Bergey's*manual of systematic bacteriology (D Bergey; Whitman; Goodfellow; K.m pfer; Hans-Jürgen, 2005).

For identification of bacterial isolates on the basis of 16S rDNA sequencing, DNA was extracted from pure overnight fresh bacterial cultures using Biofilm DNA Isolation Kit 62300 (Norgen Biotek Corp.) following manufacturers recommendations and shipped to Macrogen, Korea for PCR and subsequent 16SrDNA sequencing. PCR amplification was carried out using universal primers 27F (5'-AGAGTTTGATCMTGGCTCAG-3') and 1492R (5'-TACGGYTACCTTGTTACGACTT-3'). The sequences were subjected to taxonomic classification using BlastX, phylogenetic analysis was performed using Mega 7. The sequences were submitted to the NCBI GenBank and accession numbers were retrieved.

5.2.7 Characterization of Extracellular Polymeric Substance (EPS) by Fourier Transform Infrared (FTIR) Spectroscopy

Fourier transform infrared spectroscopy (FTIR) is a non-destructive technique for characterization of composition of EPS besides conformational alterations in biofilms if any. Method described by Coates (2000) was used for sample pretreatment before performing FTIR (Lu et al., 2015) . Briefly, EPS was precipitated by taking threefold volume of cold absolute ethanol with one volume of biofilm from 1 cm^{2} of each sample in sterile microcentrifuge tubes. The tubes were incubated for about two hours on ice and centrifuged (10,000 rpm) at 4℃ for 20 minutes. Ethanol was evaporated at 45℃ – 50℃ in drying oven and FTIR was performed using *TENSOR 27* FTIR apparatus.

5.3 Results

In this study, electrochemically active microorganisms present in cropland soil and the lake sediment from Pakistan were enriched with ferric iron Fe^{3+} (25 mM) to grow electrogenic biofilms on the surfaces of anodes in microbial fuel cells (MFCs). The characteristics of power generation in MFCs were investigated and findings of the study revealed that the sample origin, physiognomies and incorporation of iron Fe^{3+} are important drivers affecting MFCs performance and shaping associated microbial ecology.

5.3.1 Physiochemical Analysis of Soil and Sediment

Physicochemical properties of soil and sediment have been summarized in the table 5.1. Texture of soil collected from cropland was silt loam (silt + clay; 45.2%, clay; 21.2%, sand; 24%), whereas, lake sediment was clay loam (silt + clay; 57.2%, clay; 33.2%, sand; 24%).

Table 5. 1 Physiochemical properties of soil and sediment.

	pH	Electrical conductivity (µS/cm)	% oxidizable carbon	% Total Organic carbon	% Organic matter	% Total Nitrogen	Nitrate nitrogen mg/kg	Extractable Phosphorus mg/kg	Soil texture
Cropland soil	8.263	271	0.5	0.7203	1.254	0.06	8.059955	8.09856	Silt loam
Lake sediment	8.008	683	0.634	0.846	1.473	0.07	5.71622	8.3762	Clay loam

5.3.2 Electricity Generation

Open circuit voltage (OCV) was measured for 7 to 10 days till the voltage (mV) became steady state. In the beginning, the OCV was 604 mV, 806 mV, 885 mV and 1060 mV obtained from MFC-soil-control (Fe: 0 mM), MFC-soil-Fe (Fe: 25 mM), MFC-sediment-control (Fe: 0 mM), and MFC-sediment-Fe (Fe: 25 mM), respectively. After the voltage reached to a steady state, circuit was closed with 100 ohm resistance and closed circuit voltage was measured.

For polarization studies, a range of resistances (100-15000 ohm) were applied. Voltage tracking on daily basis indicated adding Fe^{3+} in MFCs positively affected the electrochemical activity of microorganisms in both soil and sediment MFCs compared to the MFCs without Fe^{3+}. Initially, the voltage output in the MFC soil-control was 90 mV (current density; 0.036 $mAcm^{-2}$, power density; 3.24 $mWcm^{-2}$) and 140 mV (current density; 0.056 $mAcm^{-2}$, power density; 7.84 $mWcm^{-2}$) with Fe^{3+} treated soil, $\approx$55.5% higher than the voltage recorded from MFC control. The voltage increased continuously till it reached to 154 mV (current density= 0.0616 $mAcm^{-2}$, power density = 9.5 $mWcm^{-2}$) and 289 mv (current density; 0.1156 $mAcm^{-2}$, power density; 33.41 $mWcm^{-2}$) (87.7% more under treated condition) on 10th day of operation, respectively followed by a drop in voltage to 89 mV and 120 mV on 22nd and 18th day with control and treated soil, respectively. Later, MFC soil-control showed fluctuations in voltage generation with maximum voltage 186 mV at 32nd day with a corresponding power density 13.84 $mWcm^{-2}$ which continuously dropped to 81 mV at day 40. The potential of MFC with soil-Fe sample again shifted to rise and showed two considerable peaks at 220 mV (power density; 19.36 $mWcm^{-2}$) and 175mV (power density; 5.29 $mWcm^{-2}$) with further decline to 111 mV (power density; 4.9 $mWcm^{-2}$) on 40th day (Fig. 5.3).

Similar initial voltage output of 92 mV (current density; 0.0368 $mAcm^{-2}$, power density; 3.3856 $mWcm^{-2}$) and 118 mV (current density; 0.0472 $mAcm^{-2}$, power density; 5.5696 $mWcm^{-2}$) was recorded with untreated and treated sediment in the MFCs. In the untreated cells, the voltage increased up to 117 mV on 4th day and then declined till 11th day (27 mV at day 15). The highest value of voltage was achieved on the 18th day such as 137 mV (current density; 0.0546 $mAcm^{-2}$, power density; 7.4529 $mWcm^{-2}$). An about 28% increase in voltage output was observed with Fe^{3+} augmented sediment MFC. An increase in voltage up to 160 mV (current density; 0.064 $mAcm^{-2}$, power density; 10.24 $mWcm^{-2}$) was recorded for the first 5 days (36.8% increase in the presence of Fe^{3+}) with a subsequent decline for the next 10 days (43 mV at

day 15). Again, there was a rise in voltage for the next 7 days reaching a maximum value of 115 mV (current density; 0.046 mAcm^{-2}, power density; 5.29 mWcm^{-2}) on 22nd day. Nevertheless, higher voltage output was achieved on 18th and 27th day from sediment MFC without adding Fe^{3+} compared to Fe^{3+}-treated sediment MFC. After 27th day, voltage output of sediment-Fe MFC dominated (an increase in voltage at day 34 as generated at day 5 (160 mV)) with a variation of 45.5% improved output as compared to control (Fig.5.3). Variations in voltage output and power density during experiments have been shown in Fig. 5.3 and 5.4 (a).

Overall, the highest voltage (289 mV) was achieved from soil MFC in the presence of ferric iron with a corresponding power density 33.4 mWcm^{-2}. The next highest voltage was generated by soil MFC control (186 mV, 13.8 m Wcm^{-2}) followed by sediment–MFC with iron (160 mV, 10.24 mWcm^{-2}), respectively (Figure 1). Similarly, soil-MFC with and without iron, presented relatively improved operational stability by showing a gradual increase in voltage for initial 10 days of operation compared to sediment MFCs.
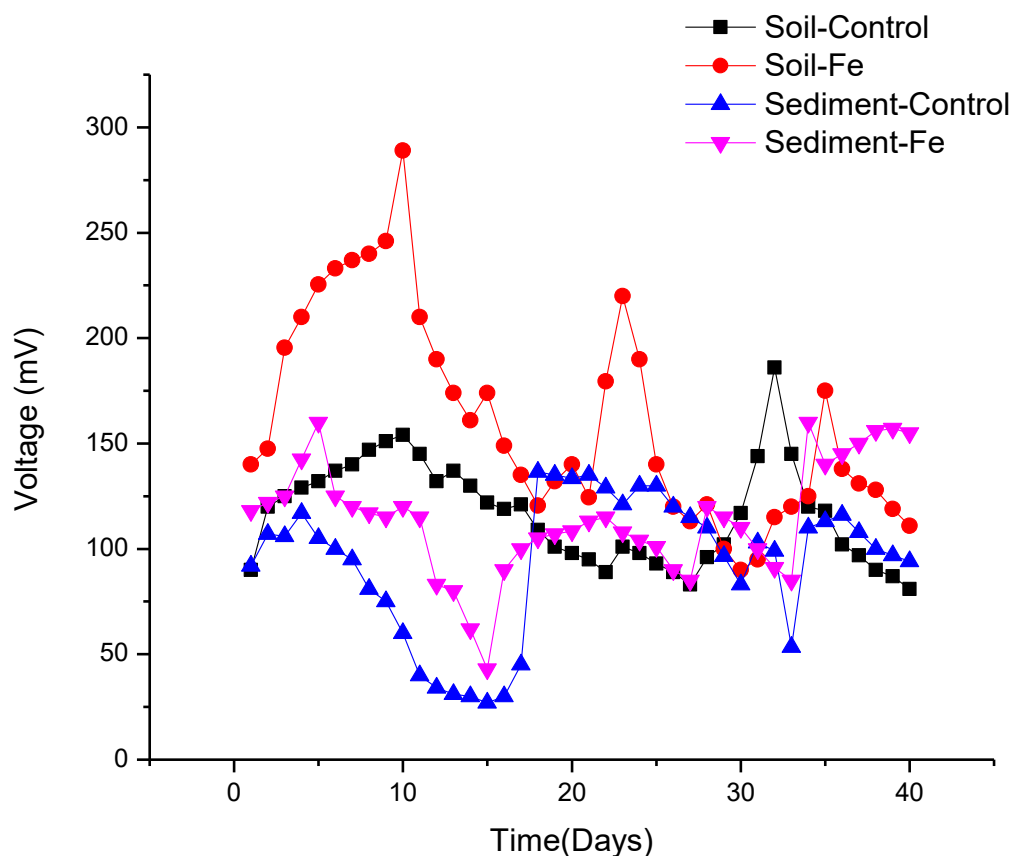
Figure 5. 3 MFC voltage (closed circuit) and power density (mWcm^{-2}) as a function of time monitored for a period of 40 days using cropland soil and lake sediment samples under control (Fe^{3+}; 0 mM) and treated conditions (Fe^{3+}; 25 mM).

5.3.2.1 Polarization Studies

A range of external resistances (100 Ω-15000 Ω) were used for polarization curves to quantify electricity generating capability of each MFC. Fe^{3+} improved the power density in MFCs with cropland soil and lake

sediment. Power density tripled in MFC (33.3 mWcm^{-2} vs. 11.2 mWcm^{-2} from MFC control) with soil augmented with Fe^{3+} and 1.4 times (13 mWcm^{-2} vs. 9.45 mWcm^{-2} from control) in Fe^{3+} supplemented sediment MFC compared to the controls (Fig. 5.5 a-b).
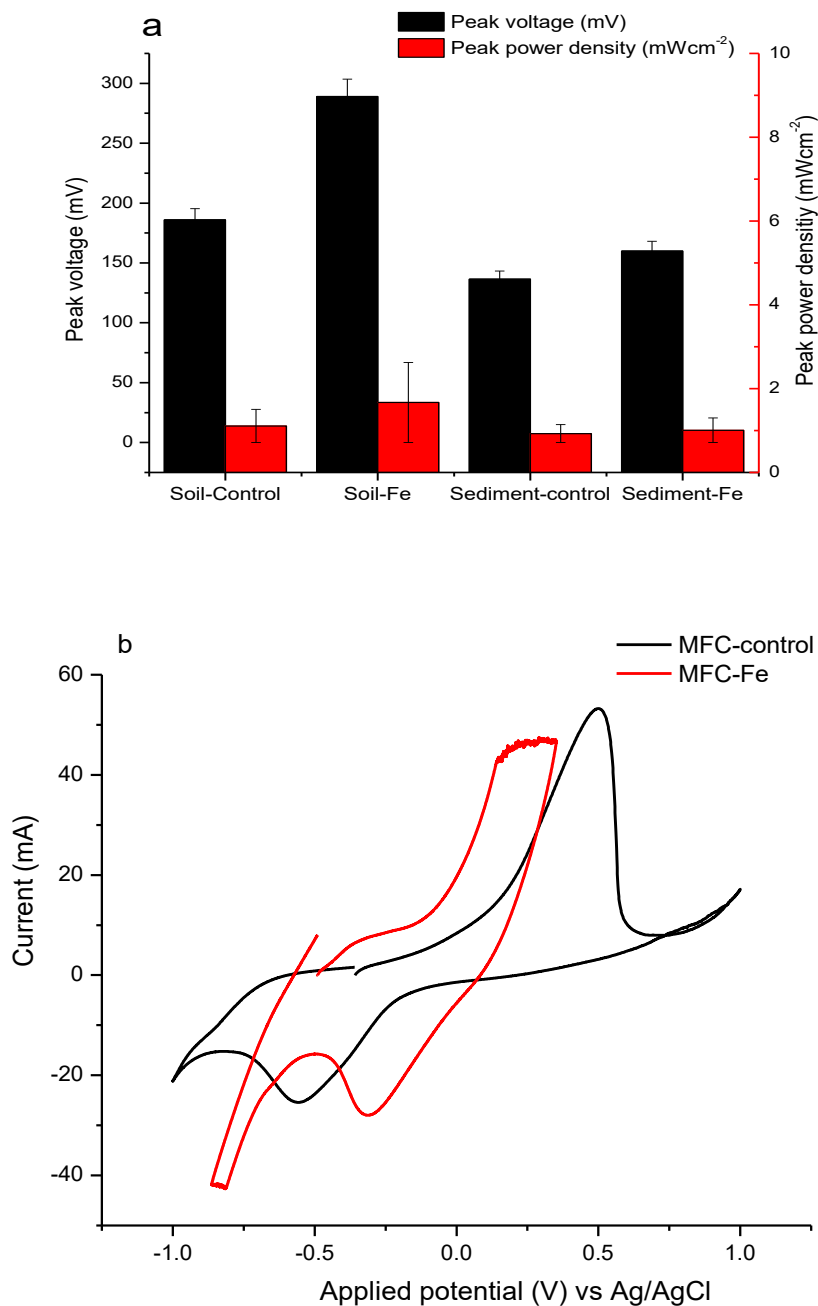
Figure 5. 4 Peak voltage, power density and cyclic voltammetry (CV) of electrogenic biofilms
(a) Peak voltage (mV) and peak power density of MFCs operated using cropland soil and lake sediment samples under control (Fe^{3+}; 0 mM) and treated conditions (Fe^{3+}; 25 mM). Data are represented as means (error bars: percentage error) where, F value: 26.8211, P < 0.05. (b) Cyclic voltammograms of soil inoculated MFC in the presence and absence of Fe^{3+}.
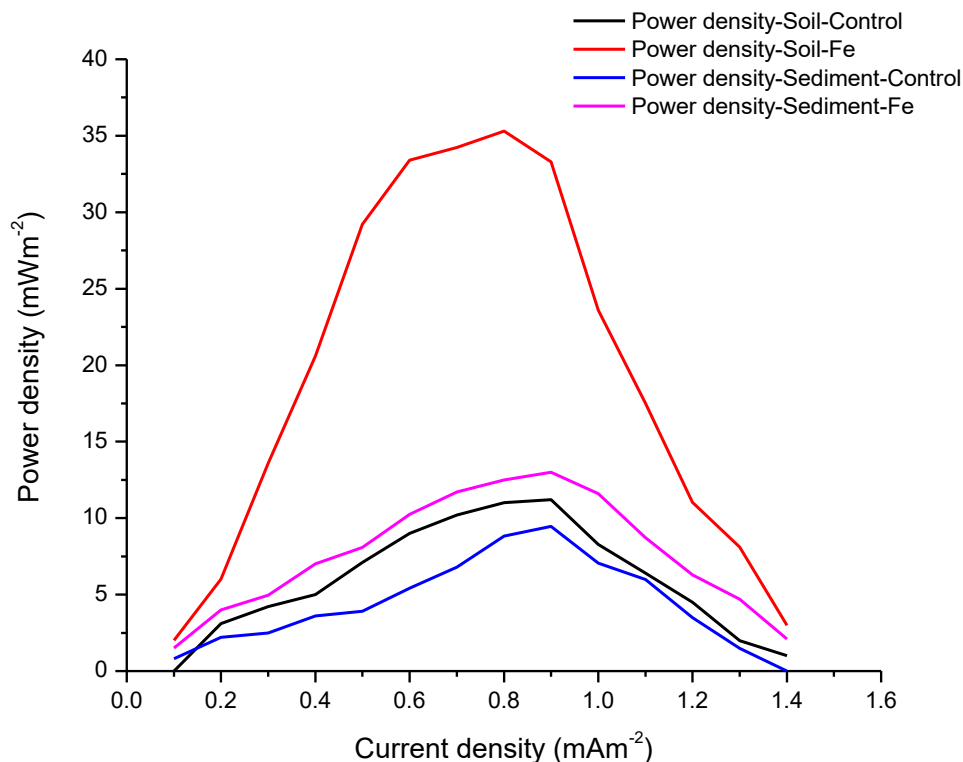
Figure 5. 5 Polarization curves of MFCs inoculated with soil and sediment.
Polarization curves of soil and sediment MFCs under control (Fe^{3+}; 0 mM) and treated conditions (Fe^{3+}; 25 mM).

5.3.2.2 Cyclic Voltammetry

Electrochemical activity of electroactive biofilms in MFCs was measured with cyclic voltammetry (Figure 5.4(b)). Both Soil and sediment MFCs amended with Fe^{3+} showed significantly higher electrochemical activity such as 52.06 mA and 53.04 mA than the MFCs without Fe^{3+} i.e. 2.23 mA and 47 mA, respectively.

5.3.3 Substrate Oxidation Rate and Removal of COD

Generation of electrical energy directly correlated with the substrate utilization rate such as acetate and depicted through COD removal rates. The current generation evidenced a direct relation with COD removal rates. COD removal rates of 43% and 49.7% were recorded at the completion of experiment in the unironed MFCs containing soil and sediment samples. Supplementation of Fe^{3+} enhanced the degradation of substrate which resulted out in higher COD mg/l removal rate (74.2% and 68.91%) in MFCs with soil and sediment, respectively. Higher COD removal rate corresponds well to the MFCs with improved electrochemical activity such as MFC-soil-Fe and MFC-sediment-Fe exhibited ~87.7% (voltage$_{max}$; 289 mv, power density$_{max}$; 33.41 mWcm^{-2}) and 36.8% (voltage$_{max}$; 160 mV, power density$_{max}$; 10.24 mWcm^{-2}) improved power generation under treated conditions with higher COD removal rate (Fig. 5.6A).

In the MFC with untreated soil, initial COD (5820 mg/l) was reduced to 5460 mg/l and 4800 mg/l after 1st week and 2nd week, respectively which declined to 3310 mg/l (%-removal efficiency; 43.13%) after 4th week. With MFC-soil-Fe, the initial COD such as 6200 mg/l in the anolyte declined to 5560 mg/l and 4620 at 1st and 2nd week and subsequently 1900 mg/l after 4th week of operation (%-removal efficiency; 74.2%) (Fig. 5.6B-C). MFC-sediment-control with a COD of 5800 mg/l in the beginning reduced to 5250 mg/l and 4750 mg/l after a period of 1st and 2nd week in order and 2920 mg/l after 4th week (removal efficiency; 49.7%). Likewise, MFC-sediment with Fe with an initial COD of 6272 mg/l showed a COD of 5547 mg/l and 4523 mg/l at 1st and 2nd week of operation followed by a further decline upto 1950 mg/l (% removal efficiency; 68.91%) (Fig. 5.6B-C).

The anolytes from MFCs inoculated with soil and sediment (with and without Fe) were also collected on weekly basis to monitor microbial activity and degradation of substrate (acetate) by measuring variations in OD_{254} values. Gradual decrease in values of OD_{254} indicated microbial oxidative activities. Soil MFC with Fe^{3+} indicated an about 80.05% (OD_{254} decreased from 1.2 at week 1 to 0.2 at week 4) increase in degradation of organic matter compared to 69.6% (OD_{254} decreased from 1.3 at week 1 to 0.39 at week 4) increase in sediment MFC in the presence of Fe^{3+} (Fig. 5.7). Microbially mediated oxidative activity broke down complex organic molecules into simpler organics which might be further oxidized into water and carbon dioxide.

Initial pH value of each anodic suspension was adjusted to 7.0 and was monitored throughout the experimental period at an interval of 7days. The pH of MFCs fed with iron, showed a decrease in pH from first week and ranged between 6.5-6.7 throughout the operation whereas in MFCs without iron, pH persisted close to pH 7.0 (Fig. 5.6D).

Table 5. 2 COD (mg/l) of MFCs inoculated with cropland soil and lake sediment samples measured periodically in the presence and absence of Fe^{3+}.

Week	MFC-Soil-control	MFC-Soil-Fe	MFC-Sediment-control	MFC-Sediment-Fe
1	6.2	10.32	9.5	11.56
2	17.53	25.5	18.1	27.89
3	30.33	40.16	36.03	44.02
4	43.13	74.2	49.66	68.91
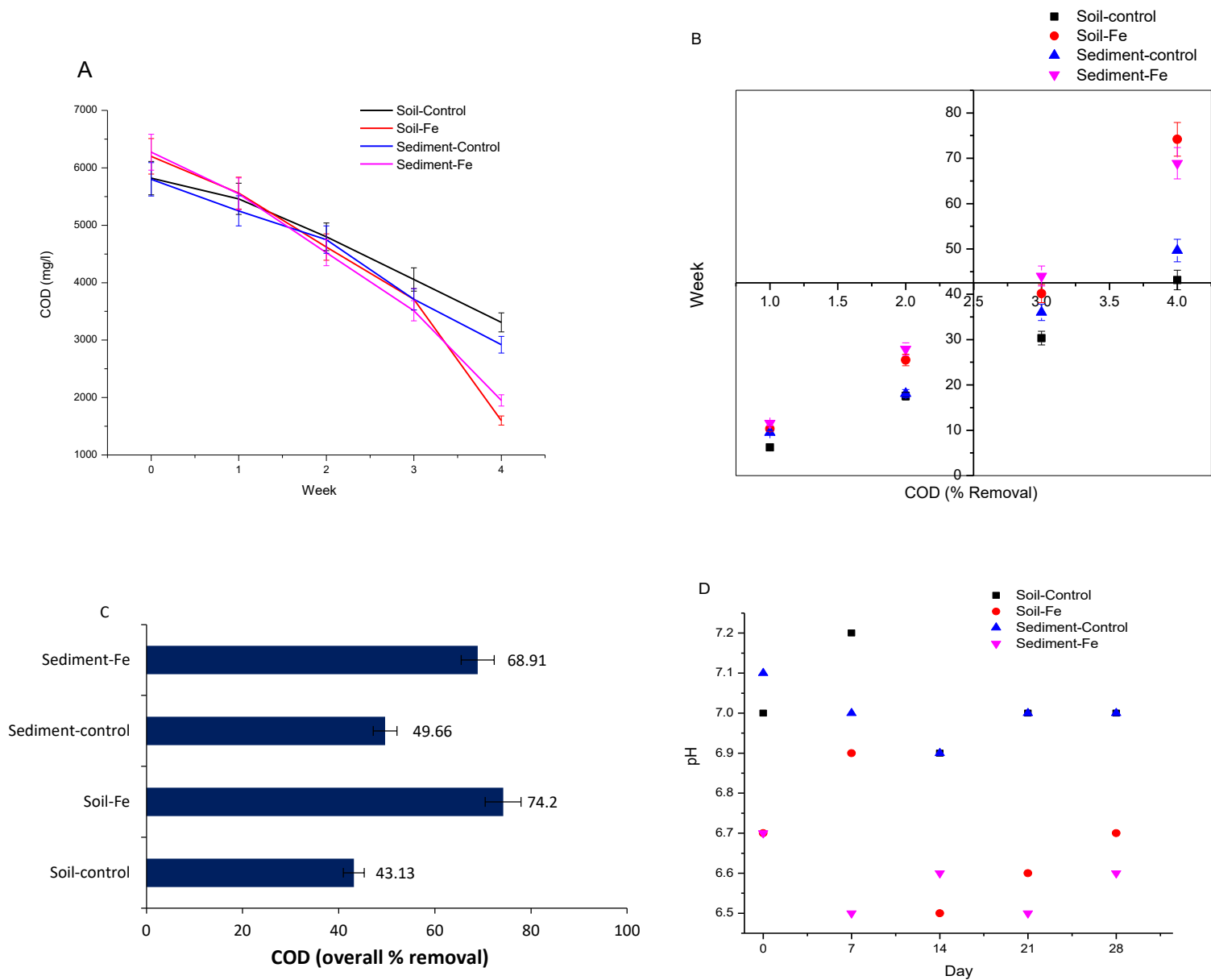
Figure 5. 6 COD and pH assessment of MFCs.

(A) COD removal of MFCs inoculated with cropland soil and lake sediment samples supplemented with $0mM/L$ and $25mM$ Fe^{3+} for a period of 30 days (B) COD removal efficiencies (percent removal) for a period of 30 days and (C) overall percent removal of COD after 30 days in MFCs (D) pH variation in the anodic suspension measured at different times.
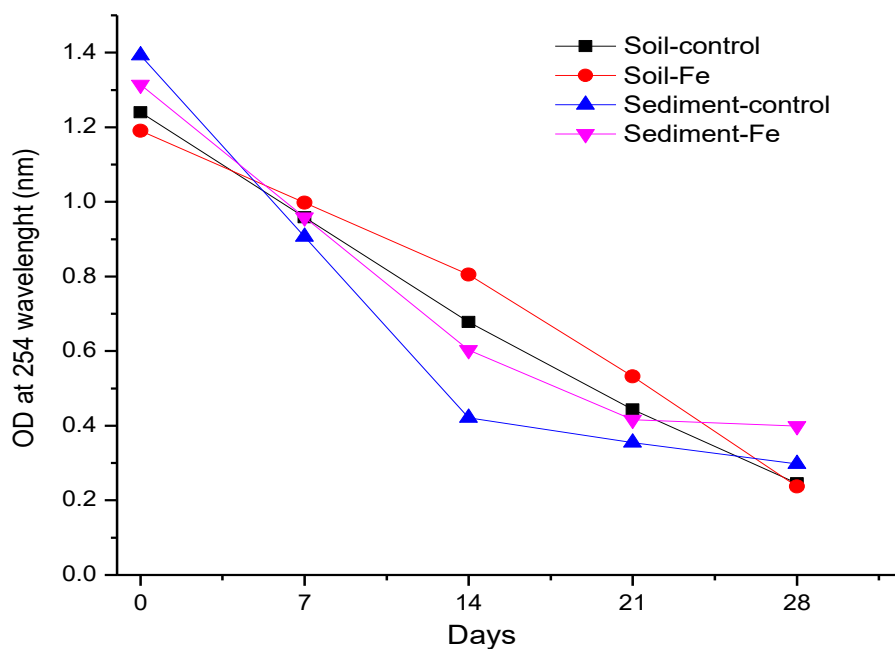
Figure 5. 7 Variations in UV-254 values of anodic suspension during MFCs operation.

5.3.4 Reduction of Fe (III) into Fe (II)

The ferrous iron concentration in soil and sediment samples was 12.0 mgl^{-1} and 4.5 mgl^{-1} at the start of experiment. After Fe^{3+} supplementation and with time, Fe^{2+} ions, produced by ferric reduction, started accumulating for transporting electrons to the electrode. Fe^{2+} concentration showed a continuous increase to 50 mgl^{-1} and 25 mgl^{-1} at 14th day, 250 mgl^{-1} and 100 mgl^{-1} at 21st day and 500 mgl^{-1} and 250 mgl^{-1} after 4 weeks of operation in soil and sediment MFCs respectively, with iron (Fig. 5.8).
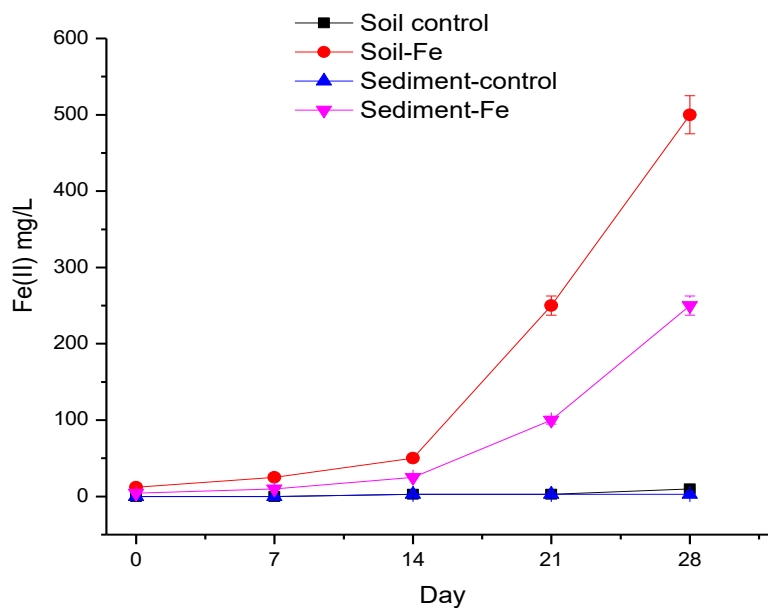
Figure 5. 8 Reduction of ferric iron (Fe^{3+}) into ferrous iron (Fe^{2+}) measured at different times during MFCs operation inoculated with soil and sediment samples.

5.3.5 Biofilm Mass and Cell Density

The performance of MFCs and power generation has been linked to the enriched biofilms on the surface of anode (carbon cloth) in the MFCs. Under control conditions, the dry anodic biomass (40 days) was 0.6 $mgcm^{-2}$ and 0.5$mgcm^{-2}$ in soil and sediment MFC without Fe^{3+}, greater than in Fe treated anodes. Under Fe (III) supplementation, the biomass of anode was 0.2 $mgcm^{-2}$ and 0.1 $mgcm^{-2}$ of the soil and sediment fuel cells, respectively. The CFU/ml cm^{-2} obtained was higher from soil (4.E+00) than sediment (2.E+00) in MFCs treated with $Fe^{3+.}$ In MFCs without Fe^{3+}, CFU obtained using soil (9.E+00) sample again superseded the sediment (7.E+00) sample (Fig. 5.9).
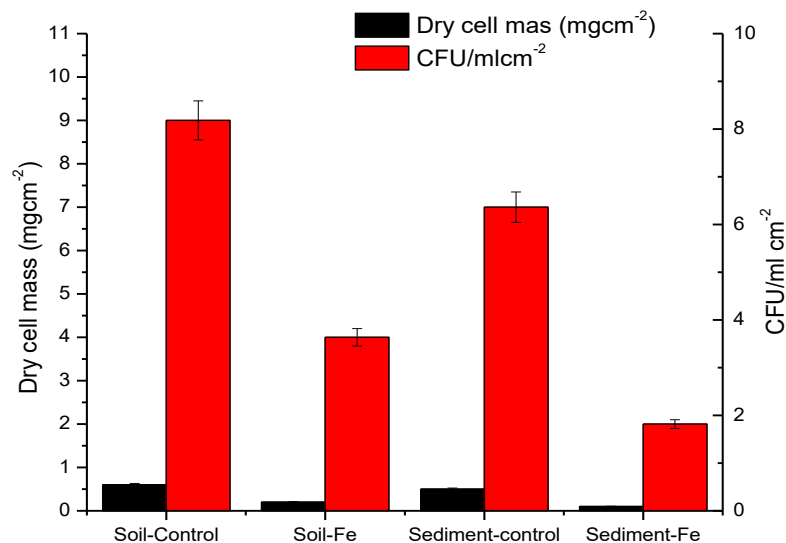
Figure 5. 9 Dry mass and cell density of biofilm attached to the electrode surface.

SEM micrographs of biofilms in MFCs inoculated with soil in the presence of Fe^{3+} at different resolutions showed comparatively more microbial abundance (mixed culture biofilms) and compactness (Fig. 5.10) than biofilms grown in the absence of Fe^{3+} (images not shown here). There was more abundance of mix species microbial consortia in the biofilms enriched in the presence of Fe^{3+}. Besides the presence of microorganisms in the biofilms, presence of mineral deposits was also recorded.
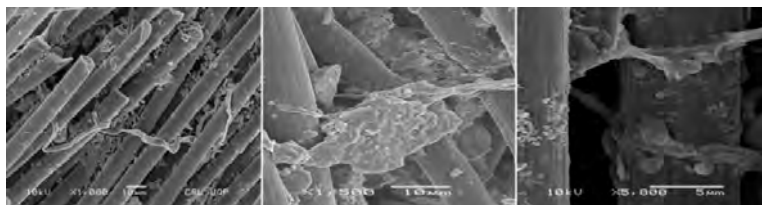
Figure 5. 10 Scanning electron microscopy (SEM) micrographs of biofilms developed on the surface of carbon cloth in anodic chamber of MFCs inoculated with cropland soil at x1000, x15,00 and x5,000 in the presence of Fe^{3+}.

5.3.6 Taxonomic Analysis of Bacterial Isolates

Initially the bacterial isolates from andic biofilms of MFC reactors were biochemically characterized. Later they were identified on molecular basis using 16S rDNA sequencing as *Pseudomonas aeruginosa*, *E. coli*, *Staphylococcus* sp., *Bacillus* sp., *Streptomyces* sp., *Salmonella* sp. and *Gordonia* sp. (Fig. 5.11).
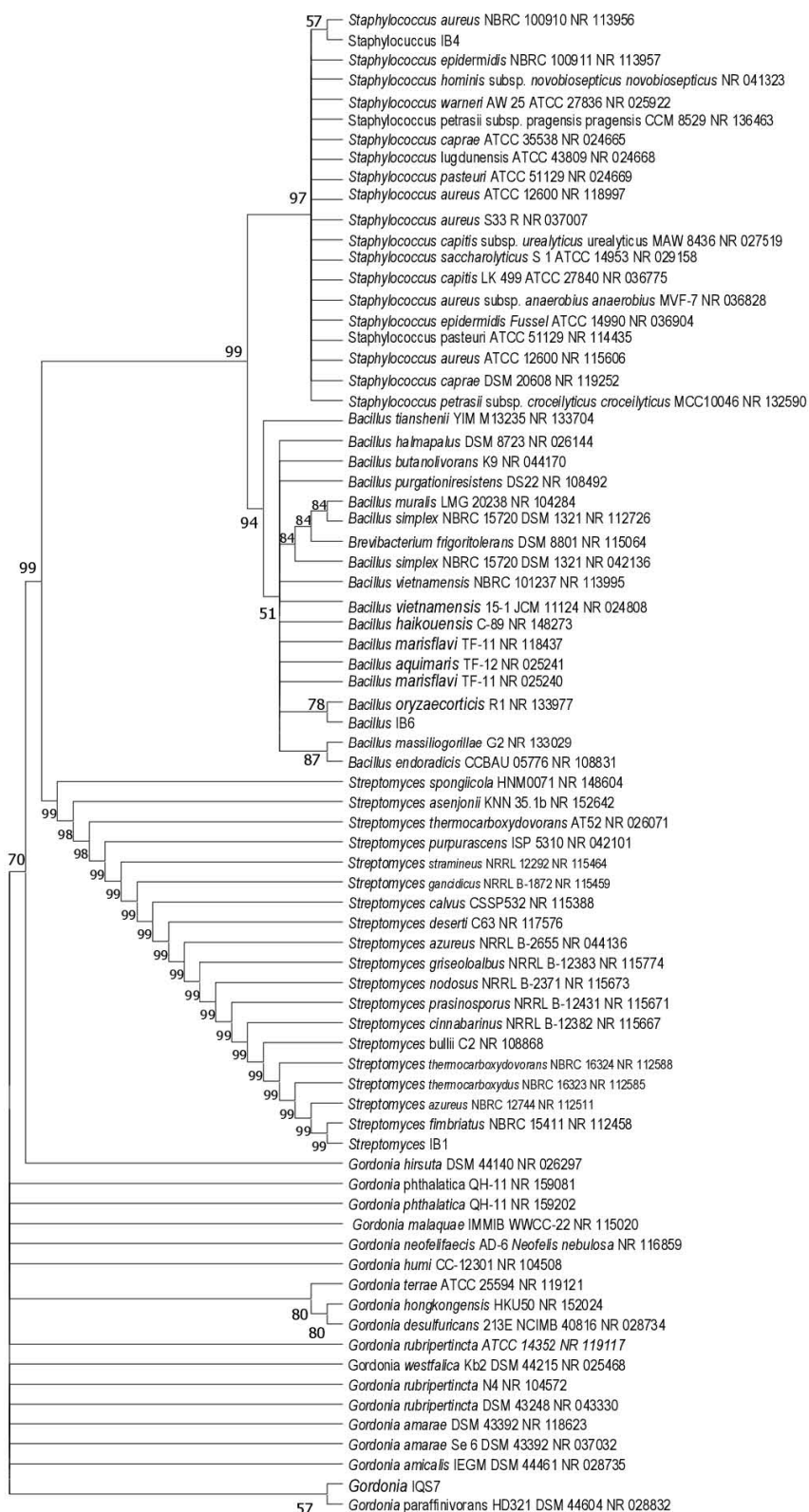
Figure 5. 11 The phylogenetic tree representing the evolutionary relationships of isolated bacteria. Based on their relationships, bacteria have been identified as *Staphylococcus* sp., *Bacillus* sp., *Streptomyces* sp. and *Gordonia* sp. and assigned names as *Staphylococcus* IB4, *Bacillus* IB6, *Streptomyces* IB1 and *Gordonia* IQS7. The tree was constructed using the Neighbor-Joining method (Saitou, 1987). The Maximum Composite Likelihood (MCL) method was used to calculate the evolutionary distances and the analysis contained 75 nucleotide sequences (Tamura et al., 2004). The proportion of replicate trees is shown in terms of percentage next to the branches in bootstrap test (all

linked taxa cluster together in the bootstrap test with 500 replicates (Felsenstein, 1985). Partial deletion method was used to remove all the positions with less than 95% site coverage. The final dataset possessed 278 positions. The evolutionary analysis was performed and tree was constructed with MEGA X (Kumar et al., 2018).

5.3.7 Molecular Taxonomy of Anodic Biofilm Bacteria

The bacterial community of anodic biofilms from soil and sediment MFCs was characterized using Illumina *Miseq* sequencing where V4 hypervariable regions were targeted within the bacterial 16S rRNA genes. After the trimming, number of observed operational taxonomic units (OTU) 10651, 11604, 9290, 37037, 11379 and 9342 for raw sediment, MFC-sediment-control, MFC sediment-Fe, raw soil, MFC soil-control and MFC soil-Fe, respectively. Alpha diversity rarefaction curves based on the number of observed OTUs and sequencing depth indicated that the analysis obtained enough readings to be representative of the sample's actual biodiversity (Fig. 5.12(A)). However, the curves using data sets approached but did not achieve a plateau suggesting the diversity of the bacterial communities was not fully captured.

The highest biodiversity was found in cropland soil sample (Shannon index: 4.08) while biofilm of MFC sediment-Fe contained the lowest biodiversity (Shannon index: 2.44) (Table 5.3). A higher Shannon index of soil (4.08) compared to the sediment sample (3.18) correlated it to be more diverse, later being less diverse. Similar results were observed when the Simpson index was calculated, which serves as an indicator of species evenness whose values were inversely related to biodiversity (Table 5.3), (Fig. 5.13). Numbers of observed OTUs represent the richness of microorganisms. Thereby, abundance-based coverage estimator (ACE) and Chao1 (richness estimator based on singletons and doubletons) was measured to estimate the richness of different bacterial communities. Non-metric multidimensional scaling (NMDS) and weighted unifrac principal component plot indicated the microbial communities of sediment and biofilms of MFCs sediment-control and sediment-Fe grouped together. Microbial communities of soil and biofilms developed from soil in MFCs with and with iron supplementation presented huge microbial diversity (Fig. 5.12 (B)).
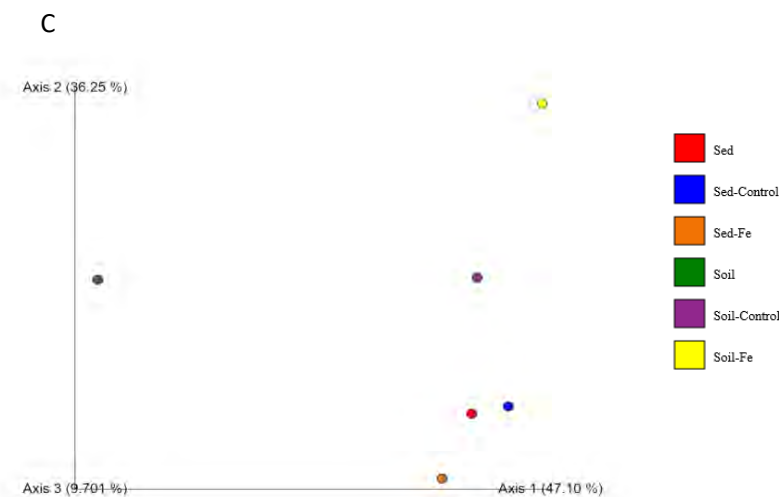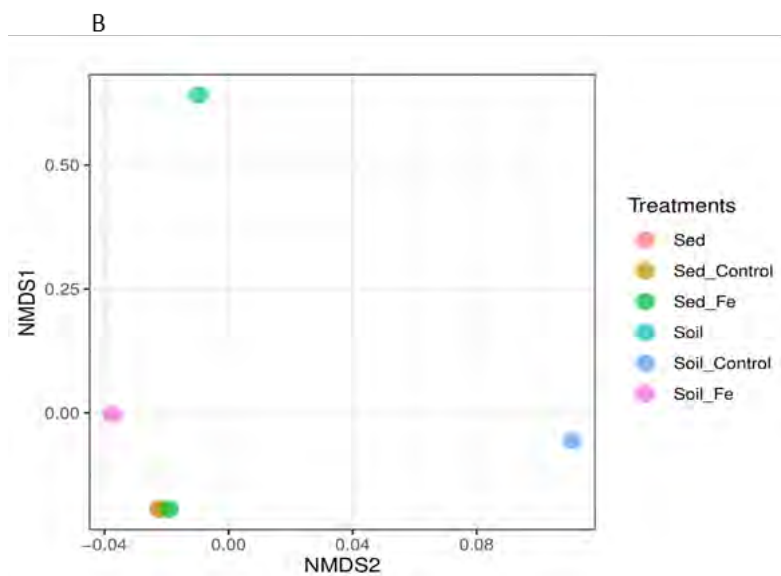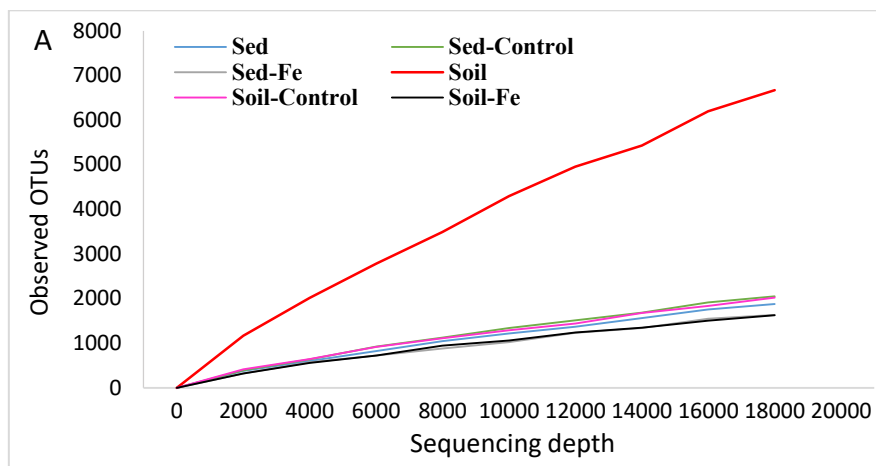
Figure 5. 12 Bacterial diversity of raw samples and enriched biofilm samples analyzed by alpha rarefa curves, NMDS plot and weighted unifrac principal component.

(A) Alpha diversity rarefaction curves based on the number of observed OTUs and sequencing depth indicated the analysis obtained enough readings to be representative of real microbial diversity (B) NMDS (upper)/weighted unifrac principal component (lower) plot presenting microbial communities of sediment and biofilms derived from sediment based MFCs grouped together whereas microbial communities of soil and soil based MFCs showed great diversity.

Table 5. 3 Analysis of microbial diversity in cropland soil, lake sediment and MFCs biofilms using Illumina *MiSeq* sequencing.

Treatment	ACE *	Chao1	Good's Coverage	Pielou	Shannon Weiner index	Simpson index
Soil	939.2001	953.1266	0.998229	0.6092	4.0753	0.9156
MFC Soil-control	499.6739	487.2632	0.998257	0.4775	2.8135	0.9029
MFC soil-Fe	337.327	412.8667	0.99623	0.5591	2.9221	0.9157
Sediment	522.4171	564.5	0.9984487	0.5354	3.3000	0.9136
MFC sediment-control	533.6397	526.0233	0.997948	0.5514	3.1849	0.9251
MFC sediment-Fe	499.6714	536.0732	0.998469	0.4354	2.4431	0.8625

Abundance based coverage estimator*
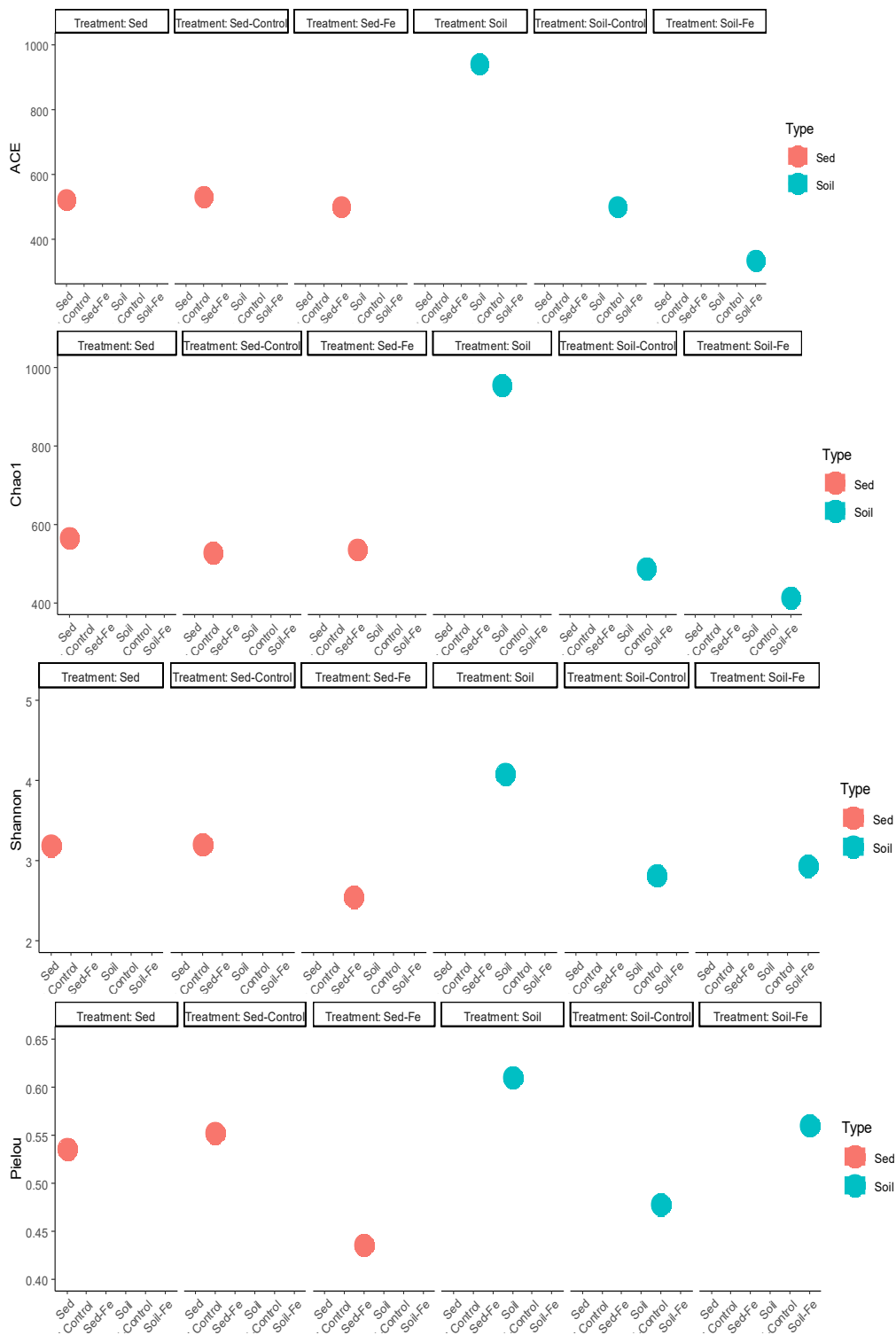
Figure 5. 13 Alpha diversity calculated using ACE, Chao1, Shannon and Pielou indexes of cropland soil, lake sediment and biofilms developed in MFCs under treated (Fe3^{+}; 25mM) and control (Fe^{3+}; 0 mM) conditions.

5.3.8 Structure of the Microbial Community in the Anodic Biofilms

5.3.8.1 Relative Abundance at Phylum Level

Our results demonstrated that presence of ferric iron (25 mM) shaped the microbial community and Proteobacteria, Firmicutes and Bacteroidetes dominated the phylum level of Fe^{3+}-reducing bacteria in MFCs biofilms (Fig. 5.14A). The representative phyla such as Proteobacteria, Firmicutes and Bacteroidetes, frequently reported in bioelectrochemical systems, were dominant in all biofilm communities. Phylum Proteobacteria, which includes exoelectrogenic bacteria such as delta proteobacteria (genus *Geobacter)*, were most abundant in all biofilm communities. The presence of Proteobacteria was highest in the soil inoculated MFC biofilm (61.3%) and soil (60%). Lake sediment and MFC sediment-control biofilm comprised of Proteobacteria in equal abundance i.e., 49% whereas biofilm of MFC sediment with iron contained the least (41.8%). Phylum Firmicutes was most abundant in the biofilm communities of MFC soil-Fe (37.6%) followed by soil-control (34%), sediment-Fe (28.5%) sediment-control (21.6%) and raw sediment (19.6%). Raw soil contained the lowest Firmicutes such as 1.14%. Members of Proteobacteria and Firmicutes are well known fermenters and exist as syntrophic partners behaving as anode respiring bacteria (ARBs) and fermenters, respectively.

Phylum Bacteroidetes was dominant (24.17%–27.0%) in the MFCs sediment-Fe (27.0%), sediment-control (25.4%), anodic biofilms and sediment (24.17%), respectively. There was significant difference in the abundance of Bacteroidetes in the sediment and soil based MFCs. Its abundance was low (1.9%–3.3%) in the communities of soil and MFCs inoculated with soil in the presence and absence of Fe^{3+}. Phylum Chloroflexi, nitrifying bacteria, were detected in all communities in relatively low (0.1%-5.1%) fractions. It was most abundant in soil (5.1%) and MFC soil-Fe (0.4%) communities and least abundant in sediment (0.10%). Phylum Planctomycetes was only observed in soil communities (4.9%) that disappeared in MFCs communities. The figure 5.14B presents the hierarchical cluster analysis of major phyla.
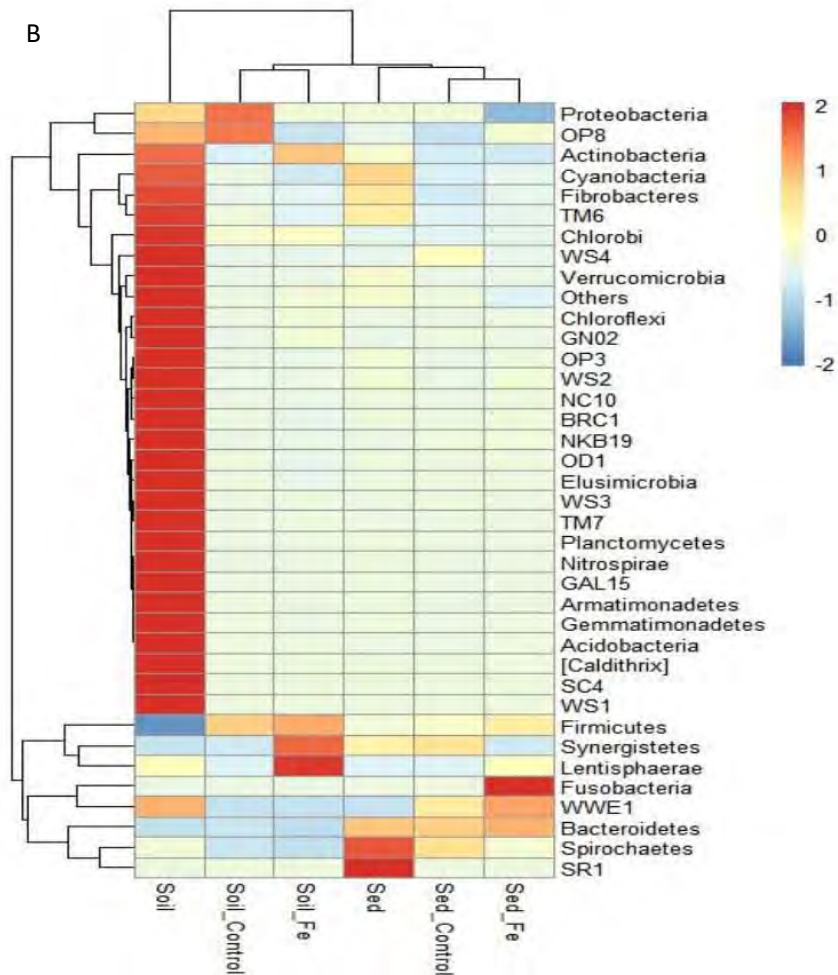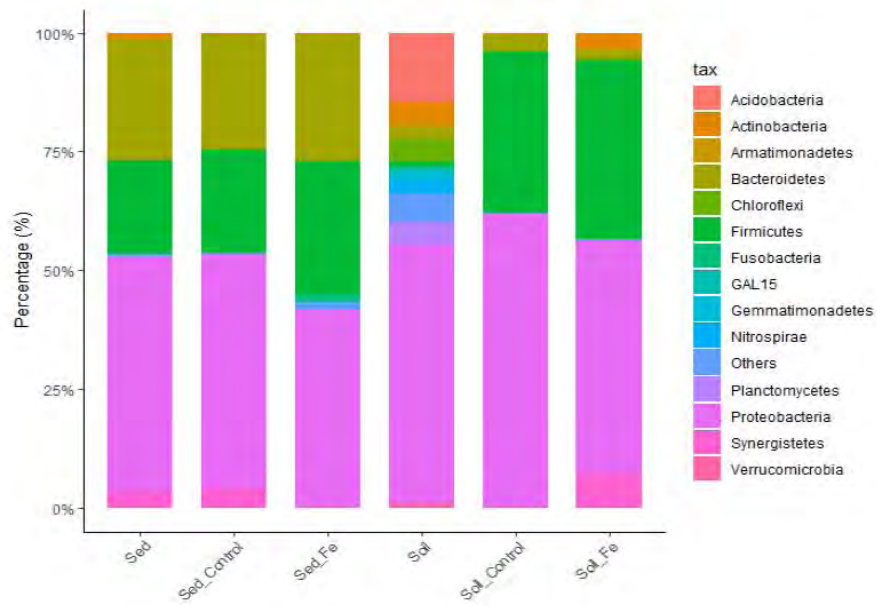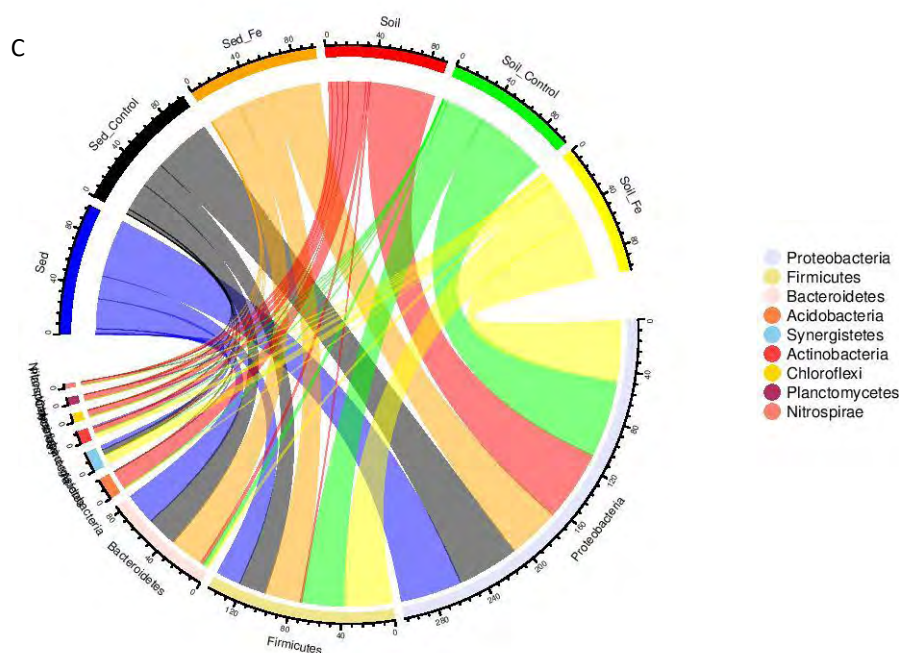
Figure 5. 14 Predominant phyla in the raw soil and sediment samples and enriched biofilms.
(A) Relative (percent) abundance of top phyla obtained through Illumina *MiSeq* sequencing (B) Hierarchical cluster analysis of predominant phyla (C) Rosette form of predominant phyla in the cropland soil, lake sediment raw samples and biofilms in the MFCs under treated (Fe^{3+}; 25 mM) and control (Fe^{3+}; 0 mM) conditions.

5.3.8.2 Relative Abundance at Class Level

The figure 5.15 depicts the microbial community composition of soil, sediment and MFCs anodic biofilms at class level (top 15). Species of α-proteobacteria were found most dominant in soil (13.7%) that dropped to 0.25% in MFC soil-control and negligible in MFC soil containing iron. Similarly, alpha-proteobacteria reduced from 0.35% in sediment to 0.14% in MFC in the presence of sediment and iron. Betaproteobacteria showed increase in their density (5.38% in soil to 12.2% in MFC soil-Fe biofilm) in biofilm of soil in MFC with iron while a decrease in case of sediment (4.52% in sediment to 0.74% in MFC sediment-Fe). γ-proteobacteria comprised a considerably significant proportion of microbial communities in all biofilms among proteobacteria. Its proportion increased from 32.1% in soil to 36.5% and 55.1% in MFCs with soil in the presence and absence of iron whereas altered slightly (41%-44%) in sediment and sediment associated biofilms in MFCs. Delta-proteobacteria reduced from 4.20% in soil to 0.31% in MFCs biofilms. In sediment, its percentage was 0.24% that increased to 0.5% in MFC sediment-Fe. Class clostridia also comprised a major fraction of microbial community in each sample. It showed enrichment from 4.21% and 12.4% in soil and sediment to 36.5% and 24.7% in MFC with soil and sediment in the presence of iron, respectively.
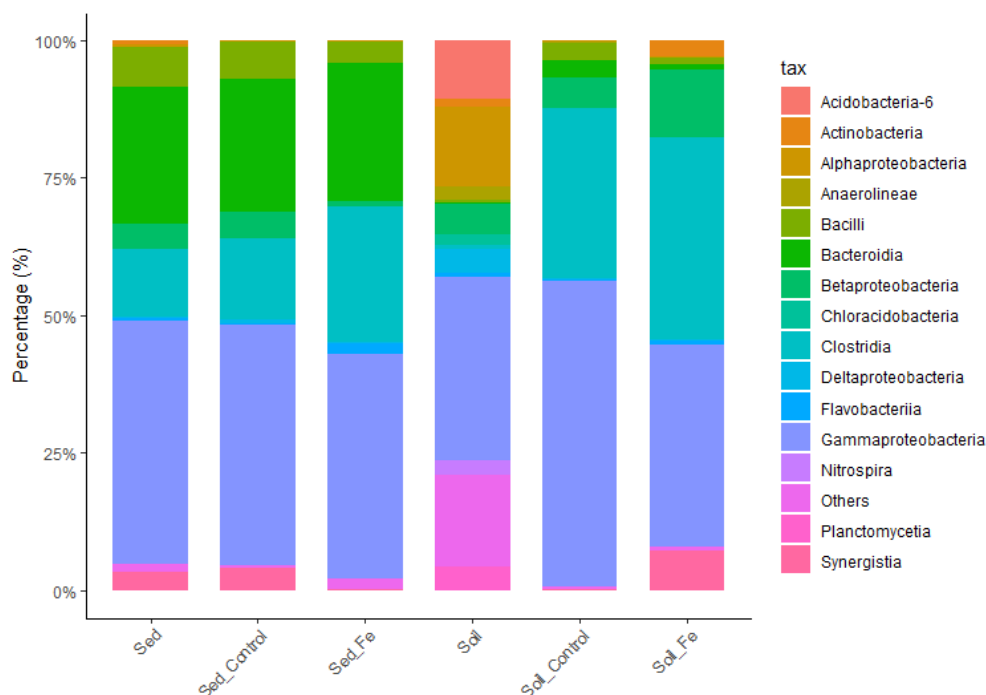
Figure 5. 15 Relative (percent) abundance of predominant microbial communities at the class level in the cropland soil, lake sediment and biofilms in the MFCs under treated (Fe^{3+}; 25 mM) and control (Fe^{3+}; 0 mM) conditions.

5.3.8.3 Relative Abundance at Genus Level

Genus level characterization further illustrates the functional roles of microorganisms in the MFCs biofilm communities. It is evident from the fig. 5.16A, the genus *Pseudomonas* predominates in all biofilms with the least proportion in biofilm of MFC-soil without iron (6%) and the most in raw soil sample (26.5%). Among the treated samples with iron, the greater fraction was recorded in biofilm of MFC with sediment (16.35%) than with soil (7.5%). Genus *Sedimentibacter* increased from 5.4% to 16.6% in MFC containing soil and iron. *Aminobacterium* enriched from 0.3% in soil and 2.7% in sediment to 4.8% and 3.2% in their respective MFC biofilms (with iron). Other important genera whose growth was supported on MFC anodes include *Providencia* (0.06%-8.2%), *Proteus* (0.2%-11.2%), *Clostridium* (0.31%-6.2%), *Flavobacterium* (0.2%-1.83%) and *Bacteroides* (0.2%-1.22%) besides many other.

Figure 5.16B illustrates the heat map analysis of microbial communities in all samples. The heatmap package of R language calculates the Euclidean distance between samples by using the quantitative information and clusters samples using the Euclidean distance. After normalizing, the microorganisms with related properties cluster together whereas microorganisms with distinct properties are located far from each other. The genera such as *Enterobacter*, *Shewanella, Flavobacterium*, *SMB*53, *Bacillus* and *Cetobacterium* clustered together and were dominant in MFCs with sediment in the presence of Fe^{3+}. *Geobacter*, *Legionella*, *Sediminibacterium*, *Planctomycetes*, *Pseudomonas* and *Anaeromyxobacter* clustered together besides *Thermomonas*. Proportion of main exoelectrogenic genera *Geobacter, Shewanella, Flavobacterium* and *Thiobacillus* is shown in figure 5.17A-B.
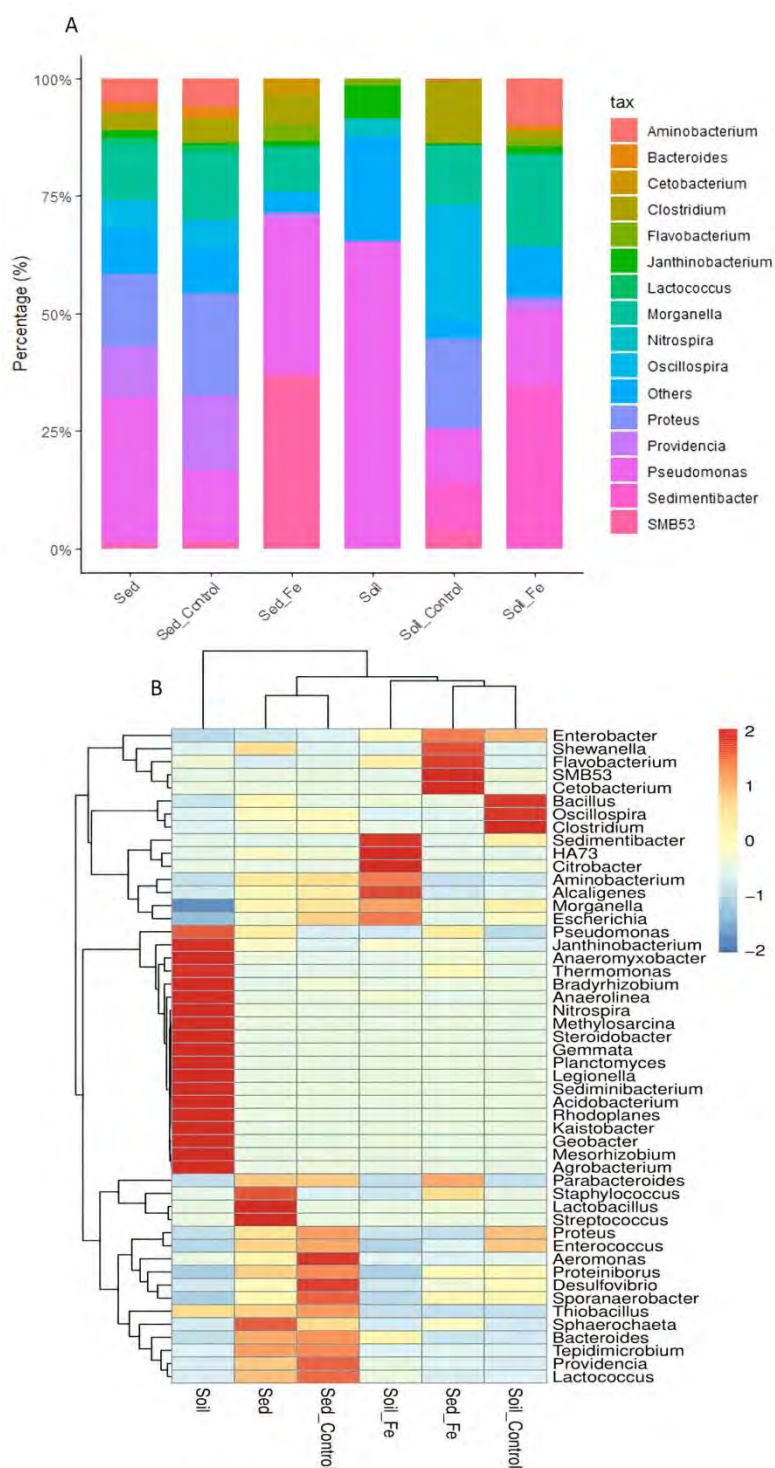
Figure 5. 16 Relative abundance of top genera obtained through Illumina *MiSeq* sequencing
(A) Relative abundance (percentage) (B) Heatmap and hierarchical cluster analysis of predominantly abundant genera in each sample (cropland soil, lake sediment and biofilms in the MFCs) under treated (Fe^{3+}; 25 mM) and control (Fe^{3+}; 0 mM) conditions. Hierarchical tree was constructed by Ward Clustering (WC) algorithm and Euclidean Distance measurement. The colour bars specify the relative abundance of the genera.

A

B
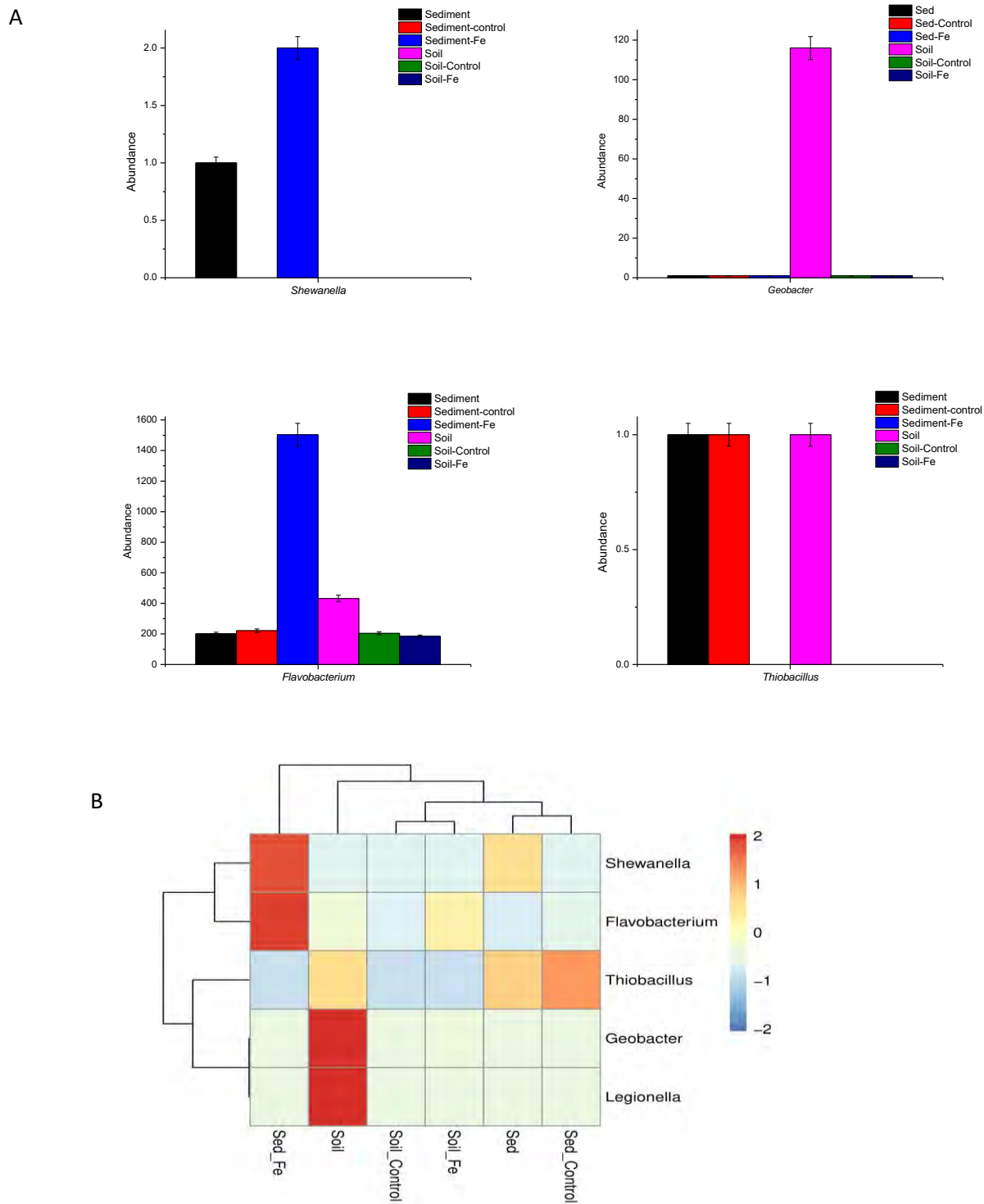
Figure 5. 17   (A) Proportion of important genera *Shewanella*, *Geobacter*, *Flavobacterium* and *Thiobacillus* involved in electron transfer (B) Hierarchical cluster analysis and heat map of genera.

5.4 Discussion

In the present study, we investigated the characteristics of power generation in microbial fuel cells (MFCs) using cropland soil and lake sediment of Pakistani origin for a period of 40 days. The findings of the study revealed that the sample origin, physiognomies and incorporation of iron Fe^{3+} are important drivers for the power generation and shaping associated microbial ecology. We isolated 10 bacterial strains from the raw samples and enriched biofilms, and grew them on metal containing media. 4 bacterial isolates were selected based on their metal reduction potential. The 16SrRNA sequencing and phylogenetic analysis revealed they belong to *Staphylococcus* sp., *Streptomyces* sp., *Bacillus* sp., and *Gordonia* sp. Such bacteria have also been previously reported as potential exoelectrogens , for their catalytic properties and application in Microbial Fuel Cell reactors (Flimban et al., 2019, Anam et al., 2017, Chaturvedi & Verma, 2016, Zhao et al., 2019).

The time of voltage stabilization varies in every microbial fuel cell and depends upon the nature of sample and biofilm development on the anode surface. In our study, the voltage took 7 days to become stable for soil inoculated MFCs and 10 days for the sediment based MFCs. This variation in time for voltage stabilization shows time required to exoelectrogens for adjustment in the MFCs environment for their activities. Comparable stabilization time periods have been published in several reports such as Lucca et al. (2020) reported a period of 5 days by sediment MFCs for voltage stabilization (Mancílio et al., 2020). Abbas et al. (2019) stated voltage stabilization needed 14 and 20 days in open and closed sediment MFCs, respectively (Abbas et al., 2019a). Similarly, An et al. (2010) observed a period of 13 days was required for steady state voltage in the MFC (An et al., 2010).

Addition of iron (25 mM) boosted the electrochemical activity of microorganisms in the MFCs. The next highest voltage was generated by soil MFC control (186 mV, 13.8 m Wcm^{-2}) followed by sediment MFC with iron (160 mV, 10.24 $mWcm^{-2}$), respectively (Figure 1). Similarly, soil-MFC with and without iron, presented relatively improved operational stability by showing a gradual increase in voltage for initial 10 days of operation compared to sediment MFCs. The results of power generation in this study are comparable to those reported in earlier studies. Jiang *et al.*, (2016) recorded a maximum of 148 mV voltage using 7 different soils in MFCs and power density ranged between 16.4 mWm^{-2} to 28.6 mWm^{-2} produced by bacterial isolates enriched by dosing 25 mM Fe^{3+} in soils (Jiang *et al.*, 2016). The maximum power densities obtained in the present study ranged between 7.45 mWm^{-2} to 33.4 mWm^{-2} are similar to the findings of this study. The differences could be due to internal and externals resistances and other MFC parameters used in both studies besides ecology of samples. Mancílio *et al.*, (2020) used dual chamber MFCs (250 ml) inoculated with Brazilian marine sediment and wastewaters contaminated with ferric iron (100 mM) in the anodes to investigate the microbial ecology and associated metabolism. The authors reported 0.39 V achieved and a stable electrochemical performance under iron augmentation in the anode and platinum cathode (20%). The results of present study also signify the role of Fe^{3+} in establishing the electrochemical stability of MFCs (Fig. 1) (Mancílio *et al.*, 2020). Ferric iron (200 uM) enhanced the current generation of MFC to 0.95 Wm^{-3} than that of control (0.75 Wm^{-3}) (Liu *et al.*, 2018).

Becerril-Varela *et al.*, (2021) applied 3 different Fe^{3+} concentrations (16 mM - 55 mM) in varying molar ratios with acetate and a highest current density of 11.37 mAm^{-2} using 16 mM Fe^{3+} concentration in anodes (Becerril-Varela *et al.*, 2021).

The concentration for Fe^{3+} was chosen based on the studies and recommendations on electrogenic bacteria tolerance in the presence of iron various environments (Jiang *et al.*, 2016, Wu *et al.*, 2013, Nevin and Lovley, 2010, Martins *et al.*, 2009, Lovley, Holmes and Nevin, 2004). Iron, through reversible electron transfer reaction, provides several advantages such as fast reaction, high standard potentials and biological degradability (Heijne et al., 2006). Studies have assessed ferric iron and other metals as an electron acceptor in the cathodic chambers of MFCs (Ferreira & Salgueiro, 2018, Mashkour *et al.*, 2017, Lu et al., 2015, Zhang et al., 2013). Studies have investigated the abiotic role of Fe^{3+} in the anodes in redox processes to some extent but how Fe^{3+} affects the ecology, extracellular electron transfer and metabolism of microorganisms largely remain unexplored (Ferreira and Salgueiro, 2018, Ucar, Zhang and Angelidaki, 2017, Ren *et al.*, 2012). Iron (Fe^{3+}) might form magnetite in the microbial fuel cells (Kato et al., 2012). Being part of ferredoxin, it also been reported for activating the enzymes in bacteria to help in growth of biofilms (Liu et al., 2018, Ruiz-Urigüen et al., Liu et al., 2017a, Hunter et al., 2013, 2018, Ucar et al., 2017). Power generation reported at concentrations of Fe^{3+} used indicates need for further exploring a broader range of concentrations in the anodes of soil and sediment MFCs.

Iron (Fe^{3+}) might form magnetite in the bioelectrochemical systems and performs the function of an electron mediator for extracellular electron transfer (Kato et al., 2012). Being part of ferredoxin, it also has been reported for activating the enzymes in bacteria to help in growth of biofilms (Liu et al., 2018, Ucar et al., 2017). Jiang et al. (2016) evaluated the effect of soil characteristics on power generation and to enrich iron reducing bacteria with supplementation of 25 mM Fe^{3+} using carbon-based electrodes in MFCs. The authors reported generation of different peak voltages (102.6 mV- 148.1 mV) using three different soils and exoelectrogens achieved at different times (Jiang et al., 2016). Qian et al. (2017) reported a voltage of about 0.55 V in MFCs provided with 100 mM iron. Presence of oxidation and reduction peaks in this study showed that the process was reversible. The CV obtained from anodic biofilm of sediment MFC control showed an oxidation peak close to + 0.25 V and a corresponding reduction peak close to - 0.25 V vs. Ag/AgCl. With Fe^{3+}, the CV of sediment-MFC exhibited two oxidation peaks at - 0.6 V and 0.5 V vs. Ag/AgCl (with a corresponding current 7.13 mA and 35.8 mA, respectively) and two reduction peaks; close to – 0.6 V and + 0.5 V in order vs. Ag/AgCl RE suggesting the activation of two redox systems. The voltammograms are typical of bacteria whose outer membrane proteins are involved in electrochemical activities and electron transfer (Becerril-Varela *et al.*, 2021). Absence of redox peaks in sterile media and biofilm less anode presented the involvement of bioelectrochemical activities of bacteria in MFCs.

Generation of electrical energy directly correlated with the substrate utilization rate such as acetate and depicted through COD removal rates. COD (mg/l) is measured to determine the conversion of fuel in MFCs into electricity, growth of biomass or through competitive reactions with other electron acceptors

i.e. oxygen, sulfate and nitrate (Logan et al., 2006). The maximum removal of COD such as $\approx$ 74.2% and 49.2% in MFCs with soil and sediment in the presence of iron positively correlated with maximum voltage and power generation indicating the exhaustion of organic components. An about 80.05% increase in degradation of organic matter by soil inoculated MFC than only 69.6% sediment inoculated MFC in the presence of Fe^{3+} monitored through variations in the OD_{254} values also depicted the microbial activities (Fig.5.5). These findings are comparable to the previous studies (Xu et al., 2017, González-Gamboa et al., 2017) where decrease in UV-254 values with the passage of time indicated organic matter was being decomposed by microbial activities in the cells.

Polarization studies also established the role of ferric iron by showing 3 times (33.3 mWcm^{-2} vs.11.2mWcm^{-2} from control) and 1.4 times (13 mWcm^{-2} vs.9.45 mWcm^{-2} from control) more power density in the presence of Fe^{3+} than control experiments using soil and sediment, respectively (Fig. 5.5). MFCs with neutral pH favor exoelectrogenic microorganisms for electricity generation. A higher pH also increases the electrochemical activity of riboflavin, a metabolite responsible for extracellular electron transfer in some species (Yong et al., 2013). MFCs have been operated at a pH less than 4.0 and produced high densities of current by acidophilic bacterium (Liu et al., 2017b, Sasaki et al., 2016). Slight proclivity of pH towards acidic side did not negatively affect the power generation instead organic content and electron acceptor (Fe^{3+}) have been the most important factors for power generation. A decrease in pH can be attributed to increased metabolic activities of microorganisms in the presence of Fe with increased formation of protons.

Our results demonstrated iron (25 mM) supplementation shaped the microbial community and Proteobacteria, Firmicutes and Bacteroidetes dominated the phylum level of Fe^{3+}-reducing bacteria in MFCs biofilms. These phyla have been reported as representative phyla in bioelectrochemical systems (BESs) (Eyiuche et al., 2017, Yamashita et al., 2016, Liang et al., 2019). Most exoelectrogens are Gram negative and belong to the phylum Proteobacteria (Deng et al., 2017). Among Proteobacteria, class delta proteobacteria and its representative genus *Geobacter* are highly important exoelectrogens such as *Geobacter sulfurreducens* and *Shewanella oneidensis* (Ishii et al., 2017). The enrichment of delta-proteobacteria was supported more by biofilms of sediment based MFCs (0.5%) with Fe^{3+} than soil based MFCs (0.31%). The presence of *Geobacter* species indicated that electricigens equivalent to *Geobacter sulfurreducens* and *Shewanella oneidensis* were present in soil and lake sediment and contributed to power generation. Members of phylum Firmicutes appeared most abundant in the biofilm communities of MFC soil-Fe (37.6%) and sediment-Fe (28.5%) compared to the untreated and raw samples indicating enrichment of Firmicutes members under the effect of iron. There are no significant studies on the role of Gram positive bacteria for electricity generation but Firmicutes, have often been described for their electrogenic potential (Wrighton et al., 2008). Similarly, Bacterioidetes, predominantly observed in sediment inoculated MFC under the effect of iron (27.0%) in the present study, are usually found in fermentative bioelectrochemical systems and carry out biodegradation of polymeric substances such as proteins and carbohydrates (Chen et al., 2019). The significant difference in the abundance of

Bacteroidetes in the sediment and soil based MFCs is an indication of the effect of nature of soil, organic contents and iron incorporation. Phylum Planctomycetes, observed only in soil communities (4.9%), includes aerobic heterotrophic and anaerobic ammonium oxidation bacteria (anammox). Their absence in MFCs represented acetate as a major source of substrate and no or insignificant utilization of nitrate to nitrite oxidation for power generation coupled with iron reduction. The phyla disappeared in MFCs communities as there are no reports on the presence of exoelectrogenic microorganisms in this phylum (Mancílio et al., 2020). Actinobacteria, supported by MFC soil-Fe biofilm only include versatile hydrogen degrading microbes assisting in organics degradation. Both Actinobacteria and Acidobacteria are underrepresented phyla and their role in electricity generation has not been explored much. Iron has been reported widely to promote the growth of *Pseudomonas sp.* The predominance of *Pseudomonas* sp. in biofilms of sediment-Fe and soil-Fe shows iron associated respiration and interfacial iron redox reactions for the electron transfer (Nelson et al., 2019, Minandri et al., 2016). *Pseudomonas* sp., *E. coli* and *Klebsiella* sp. have been reported for removal of metals by adsorption mechanism (Becerril-Varela *et al.*, 2021, Macrae and Edwards, 1972). Therefore, there is possibility that part of precipitates in anode chambers were due to bacterial adsorption of iron. Genus *Sedimentibacter* increased from 5.4% to 16.6% in soil MFC in the presence of iron. *Sedimentibacter* species have been reported for their heavy metal removal and as a part of bioelectroremediation communities but their precise role in MFC biofilms is still unknown (Abbas *et al.*, 2019). *Aminobacterium* enriched from 0.3% in soil and 2.7% in sediment to 4.8% and 3.2% in their respective MFC biofilms with iron. Other important genera enriched in the anodes included *Providencia* (0.06%-8.2%), *Proteus* (0.2%-11.2%), *Clostridium* (0.31%-6.2%), *Flavobacterium* (0.2%-1.83%) and *Bacteroides* (0.2%-1.22%) besides many other. Numerous *Clostridium* species have been isolated from different soil MFCs spiked with ferric iron and shown for their electrogenic capabilities. *Clostridium butyricum* species were the first Gram positive bacteria demonstrated for their exoelectrogenic capability (Jiang *et al.*, 2016, Park *et al.*, 2001). Similarly, *Providencia sp.* are fermenting bacteria which have been identified applied for electricity generation. *Providencia rettgeri* fed MFC with agarose embedded paper proton exchange membrane generated a current density of 11.26 Am^{-3}(Nara *et al.*, 2020). *Aminobacterium*, from family Synergistaceae, are fermentative bacteria. Aminobacteria, detected in the present study, are weakly correlated with electricity generation. Theses bacteria have been reported in anaerobic bioreactors and bioelectrochemical systems and grow with solid materials (Li *et al.*, 2013). *Shewanella* species such as *S. oneidensis* MR-1 are facultative anaerobic bacterial and well known model bacteria for EET. Related studies have shown the presence and isolation of Shewanella species in sediment and soil MFCs such as Inohana *et al.*, (2020) isolated S*hewanella algae* from sediment MFC using electrode plate culture devices which is capable to generate electricity from fermentation products (Inohana *et al.*, 2020). Combined with the results of voltage, power density and microbial community analysis, it can be concluded that the anode enriched with better electrogenic biofilms showed higher electric performance.

Combined with the results of voltage, power density and microbial community analyzed using high throughput sequencing, it can be concluded that the carbon cloth (anode) enriched with more biofilms showed better electric performance.

5.5 Conclusion

The findings of the study revealed the supplementation of ferric iron (25mM) positively affected the power generation potential of MFCs. The soil inoculated MFC with iron augmentation generated the highest voltage (289 mV, 33.4 mWcm^{-2}). Ferric iron also shaped the microbial community of MFCs inoculated with both soil and sediment and resulted in decrease of bacterial diversity. Proteobacteria, Firmicutes and Bacteroidetes were the predominant phyla. *Pseudomonas* sp., *Sedimentibacter sp., Aminobacterium* sp., *Clostridium* sp. *and Flavobacterium sp.* were the abundant genera besides others. The results also indicated the presence of *Geobacter* and *Shewanella* species in both samples. The isolated bacteria were identified as *Staphylococcus* sp., *Bacillus* sp., *Streptomyces* sp. and *Gordonia* sp. based on 16SrRNA sequencing already reported for their electricity generation potential. This is the first comprehensive study characterizing the potential of electrochemically active bacteria using cropland and lake sediment from Pakistan. Overall, the results of the study demonstrated enrichment of electrogenic consortia in microbial fuel cells capable of deriving energy by iron reducing bacteria from soil and sediment.

5.6 Future Prospects

The study explored the impact of exogenous supplementation of Fe^{3+} on the electron transfer rate and focused on monitoring the bacterial dynamics in the associated anode biofilms. However, in order to further establish the role of iron in bioelectrochemical processes, more studies need to be carried out. An extended range of concentrations of metals must be applied to determine their optimal concentrations and their impacts on the microbial communities. In addition, synergistic effect of metals, pH, nutrients, temperature and correlation analysis of these factors also needs to be further investigated. The isolated bacteria need to be characterized for their exoelectrogenic potential and their elaborate extracellular electron transfer mechanisms be identified. Furthermore, their optimum operational parameters also need to be defined using appropriate models.

CHAPTER 6

Microbial Fuel Cell based Biosensors for Detection and Monitoring Biological Oxygen Demand (BOD)

Study Title: Comparing Natural and Artificially Designed Bacterial Consortia as Biosensing Elements for Rapid Non- Specific Detection of Organic Pollutant through Microbial Fuel Cell

Chpater 6: Comparing Natural and Artificially Designed Bacterial Consortia as Biosensing Elements for Rapid Non- Specific Detection of Organic Pollutant through Microbial Fuel Cell

Abstract

The standard 5-days biochemical oxygen demand (BOD) method used for determination of biologically oxidizable organic material in wastewater considered to be laborious, time consuming and costly. Mediator-less microbial fuel cell (MFC) based biosensor offers an efficient alternative approach for real time monitoring of biodegradable organic matter in wastewater. Here we constructed an H- shaped MFC biosensor for comparing the efficiency of a complex natural (activated sludge) and artificially designed bacterial (*Pseudomonas aeruginosa, Staphylococcus aureus* and *Bacillus circulans*) consortia as biological sensing elements for BOD measurements. Initially, the MFC biosensor was optimized and calibrated at pH 7 and temperature 37°C using 100 mM phosphate buffer with 100 mM NaCl solution as catholyte at 10 kΩ external resistance. Maximum power density of 14.2 mW/cm^2 was generated by MFC-I with sludge consortium and it was 5 folds higher than MFC-II with artificial consortium. Standard glucose and glutamic acid (GGA) solutions were used for establishing the calibration curves between different BOD concentrations (50-250 mg/l) and voltage (mV) outputs in MFC. The regression equations for MFC-I and MFC-II biosensors were recorded as y_1= 0.7834x- 11.638 and y_2 = 0.1667x + 0.8476 respectively. Linear regression analysis revealed that 1 unit (mg/l) increase in organic load caused a voltage increase of 0.78 mV and 0.16 mV in the MFCs (I and II) reactors respectively. The relative performance in terms of stability (55-60 days) and reproducibility (within ±15.4%) of MFC-I BOD biosensor was almost double than MFC-II. The varying low concentrations of different electron acceptors (phosphate, nitrate and nitrite) in anodic compartments did not affect the performance of MFC biosensors.

Keywords: MFC biosensor, Biochemical oxygen demand (BOD), Natural consortia, Artificial consortia, Pyrosequencing.

6.1. Introduction

Biochemical oxygen demand (BOD) is commonly used as international index by environment protection agencies for assessment of organic matter load (pollutants) in wastewater. Many industries regularly monitor their effluents to comply with the requirements of regulatory agencies (Parkash, 2016). Generally, the conventional BOD method used to analyze wastewater is not only time consuming (almost 5 days) but it also demands nitrification inhibitors (such as allyl-thiourea) and extensive training of the technicians to achieve reproducible results. Therefore, BOD$_5$ method is not considered suitable for dynamic intervention and real time monitoring in aquatic environments (such as ponds, lakes, rivers and ground water and wastewater). Several BOD biosensors based on bioluminescent, UV absorbance, enzymatic reactions and oxygen consumption by immobilized bacterial cells have been designed to overcome the aforementioned drawbacks. However, these methods demonstrated relatively unstable performance due to membrane fouling, volatile operation and limited utilization of substrate by reference bacteria (Yamashita et al., 2016). A microbial fuel cell (MFC) based non-specific biosensor has been

considered as a feasible alternative to the aforesaid methods for in-situ and ex-situ BOD monitoring of water bodies (Chouler & Di Lorenzo, 2015).

Microbial fuel cell (MFC) is an electrochemical device that converts chemical energy of wastewater into electric energy by using bacterial catalytic reaction (Anam et al., 2017). Therefore, it is an environment friendly approach for wastewater treatment and renewable energy generation (in the form of electric current or bio-hydrogen. Recently, MFC has been viewed as a potential biosensing device for organic load measurement in aqueous environment. Redox electrochemical mediators that are phenolic toxic compounds (such as phenazine derivatives and flavins) have been usually employed to facilitate electrons transfer from bacterial cells to electrode (Yousaf et al., 2017) . Exoelectrogenic metal reducing bacteria such as *Shewanella putrefaciens, Rhodoferax ferrireducen* and *Geobacter sulfureducen* have also been reported in direct shuttling of electrons attached to anode (Su et al., 2011).Considering the operational suitability, lower electronic requisites, mechanical simplicity, good signal acquisition, sensitivity to change in organic load, high reproducibility and cost effectiveness, mediator-less MFC is considered more promising approach for developing an organic matter biosensor (Hsieh & Chung, 2014).

Previously, various MFC biosensors have been fabricated by immobilizing biological recognition element (bacterial cells) on physical transducer or in close proximity with transducer to convert biochemical changes into readable signals (Du et al., 2008) . These biosensors have been successfully tested for monitoring COD, BOD, volatile fatty acid, anaerobic digestion and toxic components (cadmium, sodium acetate, chromium, and nitrate) in analyte. Pure culture biofilms of *Bacillus subtilis, Serratia marcescens* and *Photobacterium phosphoreum* have been designed for assessment of assimilable organic contamination in wastewater (Verma & Singh, 2013). The use of single bacterial species in MFC biosensor has challenges of substrates selection and toxicity due to hazardous compounds that ultimately limit the electrode sensitivity. The major drawback of pure culture biosensor is inaccurate measurement of BOD concentration as only limited range of sample contaminants are metabolized (Aracic et al., 2015). Therefore, some studies have used complex bacterial community in MFC based BOD biosensors to estimate the total biodegradable organic matter of wastewater. Although the diverse nature of unknown bacterial community in sludge has been recognized as a limiting factor in terms of repeatability and stability of biosensing system (Liu & Mattiasson, 2002) . Micro-aerophilic, anoxic and anaerobic bacteria produce different electric outputs utilizing organic matter through various metabolic pathways following Monod growth kinetics. Hence, it is essential to consider the effects of bacterial substrate consumption rate on MFC performance and BOD measurements of wastewater (Z et al.,2008, Sharpe, 2003). The concept of MFC based biosensor has been known for decades but uncertainty in architecture, instability, unavailability of standardized bacterial consortium and continuous maintenance limit its commercial applications (Abrevaya et al., 2015, Sumaraj and Ghangrekar, 2014).

Bio-electrochemical system generates a specific measurable current signal that depends on organic analyte concentration. Theoretically, a high signal output results from high BOD concentration but in MFC infrastructure various operating parameters such as fuel (substrate) type, nature of biological

recognition element, substrate utilization rate, electron acceptors, co-existing ions and liquid retention time in anode greatly affect its biosensing ability (Abrevaya et al., 2015, Zheng et al., 2015) . Various positively and negatively charged ions (such as nitrate, nitrite, ferric, phosphate and sulfate) are potential redox electron acceptors and commonly found in wastewater at concentration much higher than H^+ ions. Therefore, the function of traditional cation exchange membranes in MFC significantly reduce the signal production by MFC biosensor (Tran et al., 2016). To accurately measure the BOD in wastewater, electron acceptors must be removed or anode must be essentially supplemented with respiratory inhibitors (azide and cynaide) to reduce the interference from co-existing electron acceptors (Bonetto et al., 2011).

This study highlighted the comparative efficiency of an artificially designed bacterial consortium with sludge biofilm in analogous setup of MFC based biosensor to analyze the BOD concentrations of wastewater through voltage generation performance. The operational properties of MFC biosensors including start up time, inoculation, immobilization, stability, response time, repeatability and linearity were established and validated. The structure of bacterial community developed on anode from activated sludge was characterized in detail through next generation pyrosequencing sequencing using 16S rRNA gene. The relative abundance of different ions (phosphate, ammonium, nitrate and nitrite) in the anolytes affecting the signal transduction and performance of MFC were continuouslymonitored.

6.2. Materials andMethods

6.2.1.   Microbial Fuel CellSetup

A dual chamber MFC was built with 120 ml polyacrylic plastic bottles joined together by two tubes (length 2.5 cm and diameter 25 cm²) holding a piece of proton exchange membrane (5.0 cm×5.0 cm, Nafion 115, Gas Hub Pte Ltd, Du Pont, USA). The proton exchange membrane was pre-treated by immersing in 0.1 M HCl for 3-4 hours at room temperature to remove any possible contamination. Holes of 26 cm² diameter were drilled in the two prosaic plastic slabs (5 cm x 5 cm) to insert the tubes. Screws (2 inches) were used to join the mouth of tubes holding membrane (Fig. 6.1). The internal volume of 100mL was used for anolyte and catholyte. Polished graphite rods (2 mm×22 mm) were suspended via copper wire (diameter = 0.8 mm) in both chambers to complete the external circuit. Black Ice T 401 Waterproof Sheets (9" x 11") were used to polish graphite rods in order to enhance the microbial adsorption on the surface of rod during biofilm formation. Inlet and outlet ports (4 mm diameter) with plastic stoppers were installed at the top of anode chamber for inoculation, replacement of medium and sampling through syringe. Reactors were operated in fed-batch mode at 37 °C in an incubator. Air saturated sterile buffer and salt solution (100 mM phosphate buffer saline + 100 mM NaCl solution) were fed into cathode chamber of reactors. The potential difference between anode and cathode was measured continuously via digital multimeter (model: UT33B; UNI-T) by varying the resistance from 50 Ω to 20,000 Ω. All experiments were performed in triplicate and the mean values were recorded.
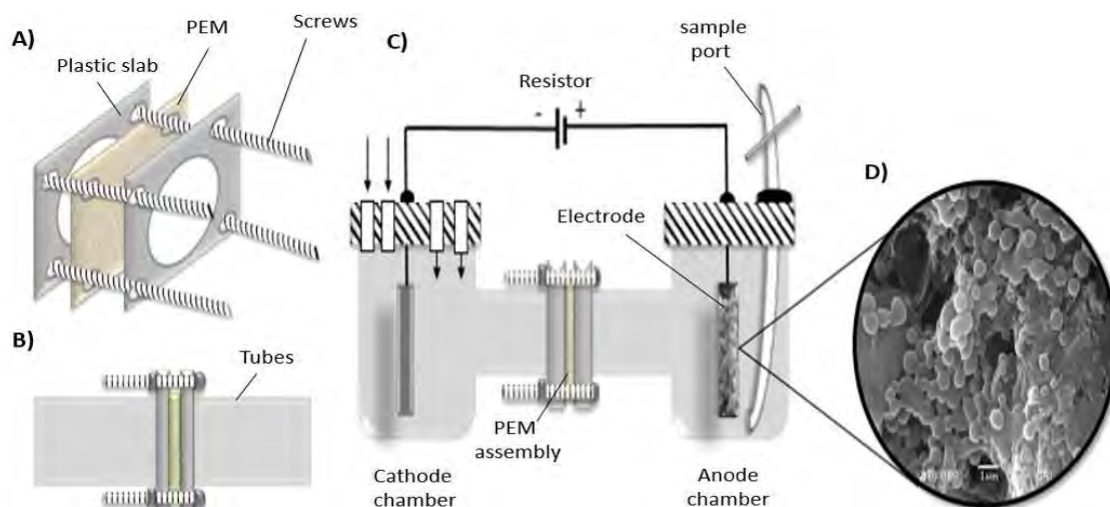
Figure 6. 1 Double chamber H-shaped mediator less MFC biosensor A) Proton exchange membrane (Nafion) assembly B) Plastics holding a piece of PEM through slabs and screws C) Schematic diagram of MFC setup D) Biofilm on anode.

6.2.2. Enrichment of Electrochemical Active Bacteria

MFC-I was operated by feeding domestic wastewater (Table: 6.1) inoculated with activated sludge in anodic compartment with retention period of 10 days. For MFC-I, an aliquot of 4 ml activated sludge was mixed with 96 ml domestic wastewater (inoculum/anolyte ratio: 1/24 [v/v]) in serum bottle and introduced in anode chamber under anaerobic conditions to initiate the experiment. After approximately 5 weeks of continuous operation under optimum conditions (temp.: 37 °C and pH:7) the cell potential reached a steady state indicating the development of mature biofilm. An artificial consortium of *Pseudomonas aeruginosa, Staphylococcus aureus* and *Bacillus circulans* was developed on anode surface of MFC-II by inoculating the full loop colony of each bacterial species in 100 ml sterilized nutrient broth. These bacterial cultures were isolated on nutrient medium from 1% inoculum of domestic wastewater used in MFC-I by means of standard microbiological cultural techniques. Sub- culturing of *Pseudomonas aeruginosa, Staphylococcus aureus* and *Bacillus circulans* at 37 °C for 24 hours was repeatedly done in nutrient agar for 4-5 days before using as inoculum. MFC-II was incubated at 37 °C for 4 weeks after inoculation and nutrient broth was refreshed after every 72 hours to avoid the organic matter exhaustion. Anode solution was purged with oxygen free nitrogen gas for 10-15 min after every 24 hours to maintain anoxic conditions. Both reactors were operated in fed batch mode and operational conditions were kept constant.

Table 6. 1 Physico-chemical characteristics of domestic wastewater (I-9, Islamabad, Pk) used in double chamber MFC.

Parameter	Concentration range	Mean value
pH	5.9-7.3	6.6±0.7
COD (mg/L)	497-780	638±141
BOD$_5$ (mg/L)	169.8-485.2	327.5±157
Conductivity (S/m)	0.01-0.13	0.07±0.06
TS (mg/L)	870-10500	9600±1500

6.2.3. Operation of MFCBiosensors

Once biofilms were matured, anode chambers were fed with fresh mineral medium (MM) containing 50 mg l^{-1} glucose at 24 hours retention period until new steady state of cell potentials were reached (approximately 3-4 days). Activated sludge and artificially designed bacterial consortia were then used in MFCs as biological sensing elements. The operating properties of MFC biosensors were evaluated by feeding the five different concentrations (50, 100, 150, 200 and 250 mgl^{-1}) of glucose and glutamic acid (GGA) standard solution to validate the relationship between different BOD concentrations and system respective voltage response. The basic mineral composition of GGA medium was: NaHCO$_3$ 2.5gl^{-1}, KCl 0.1gl^{-1}, CaCl$_2$·2H2O 0.1gl^{-1}, NH$_4$Cl 1.5gl^{-1}, MgSO$_4$·7H$_2$O0.1gl^{-1}, MgCl$_2$·6H$_2$O0.1gl^{-1}, NaCl0.1gl^{-1}, MnCl$_2$·4H$_2$O0.005gl^{-1}, NaH$_2$PO$_4$0.6gl^{-1} and NaMoO$_4$·2H$_2$O 0.001 gl^{-1}. Each concentration was introduced at least three times to get the average results.

6.2.4.   Analysis and Calculations

6.2.4.1. Physicochemical Analysis

Standard methods from American Public Health Association (APHA, 20th Edition, 1995) were used to analyze the quality of domestic wastewater immediately after collection. All samples were filtered prior to analysis through 11 μm size filter paper. Soluble chemical oxygen demand (COD) and pH of wastewater were estimated using HACH 5220 COD method and bench top pH meter respectively. The COD removal of natural and artificial consortia was determined between 10 and 40 days. The COD removal efficiency (%) was calculated according to: CODr = COD$_{in}$– COD$_{out}$/ CODin where COD$_{in}$ is the COD (mgl^{-1}) concentration measured in the influent of anode compartment and COD$_{out}$ is the COD (mgl^{-1}) concentration measured in the effluent of anode compartment. The BOD of wastewater samples was determined via Standard 5-Days respirometric Method (5210B) by using DO meter. After 5 days of incubation, BOD was calculated as: BOD mg/l = (Initial DO - DO$_5$) x Dilution Factor. Where Dilution Factor = Bottle Volume (300 ml)/Sample Volume, DO= initial DO of diluted sample and DO$_5$ = DO of diluted sample after 5 days incubation at 20 °C under darkness in order to avoid algal respiration. Measurements of inorganic compounds: ammonium (Nessler reagent method), nitrate (Phenol di-sulphonic acid colorimetric method) and nitrite (Sulfanilamide colorimetric method) along with phosphate (Stannous chloride method) were made in duplicate. The dry masses of biofilms were

determined by drying the electrodes at 105 °C and heating it at high 550 °C before and after the formation of biofilms. The weights of the electrodes were determined in order to calculate the volatile suspended solid per cm^2 of electrode surface area.

6.2.4.2. Electrochemical Analysis

MFCs were initially operated at open circuit voltage (OCV) without any external circuit resistance for several hours. Once voltage became stable the system circuit was closed with 10kΩ resistor. The voltage between anode and cathode was measured by using a digital multimeter (model: UT33B; UNI-T). For the applied resistance methods, cell current (I) was calculated from Ohm's law: I=U/R. Where, U is the recorded potential and R is the external resistance. Polarization studies were conducted using single cycle method by varying external resistor load from 50 Ω to 20 KΩ in decreasing order and each resistance was connected for 20 min. These polarization curves were used to evaluate the internal resistance and maximum power. The current and power densities were normalized by the projected electrode surface area (1.45 cm^2). The power density (mW/cm^2) was calculated by using the formula P.D = IU/A and current density (mA/cm^2) as C.D = U/A; where A (cm^2) is the projected surface area of electrode.

6.2.4.3. Microbiological Analysis

At the experiment end, anode bacterial community was analysed by transferring biofilm attached on anode surface to a saline phosphate buffer solution (1.3 mM KCl, 0.5 mM KH_2PO_4, 135 mM NaCl, 3.2 mM Na_2HPO_4 pH: 7.4). Shaking was followed by 4-5 episodes of sonication (30sec) to suspend biofilm in the buffer from anode. This biomass suspension from MFC anode was used for the molecular analysis of bacterial community composition while the remaining sub-sample of biofilm suspension was used as inoculum for identification and isolation of different bacterial species through culture dependent techniques. The combination of culturing and molecular methods was used for the detail examination of bacterial diversity on MFC biofilm.

6.2.4.3.1. Cultural Independent Characterization of Bacterial Communities

(i) Dry Weight

The dry mass of biofilm was determined by calculating volatile suspended solid per cm^2 of electrode surface area. The weight of electrodes with similar surface area one with biofilm and one without biofilm was compare to quantify biofilm mass per surface area. Anode with electricgenic biofilm was dried at 105 °C followed by weighed, it was later burned at high temperature (550 °C) and weighed again. The gain in electrode weight (expressed in mg/cm^2) was a measure of biofilm biomass developed on electrode surface during MFC operation.

(ii) EPS Characterization

The extracellular polymeric substances (EPS) of biofilm developed on MFC anode was characterized to gain further insight of biofilm structural integrity. Biofilm covered anode was transferred from MFC setup to 50ml of TE buffer pH 7.5 containing 10 mM EDTA, 10 mM Trizma base and 2.5% NaCl. Biofilm was removed from anode through sonication followed by centrifugation for 20 min. at 3500 rpm. For further extraction this concentrated biomass suspension was suspended in 10ml of a 0.85% sodium chloride solution containing 0.22% formaldehyde for 30 min at 80 °C and centrifuge for 30 min at 3500

rpm. Finally, the protein (EPSp) and carbohydrate (EPSc) content of biofilm EPS in extraction solution was measured through Lowry and phenol/sulfuric acid method. Total EPS of biofilm was calculated by adding carbohydrate (EPSc) and protein (EPSp) content:

EPS= EPS carbohydrate content + EPS protein content

Phenol - Sulfuric Acid method was used for the quantification of EPS total carbohydrate content in MFC biofilm sample. This colorimetric method of carbohydrate analysis was the modification of himedia carbohydrates estimation kit.

Procedure

- Glucose Standard stock solution (1mg/ml) was prepared.
- Different dilutions (20mg/ml, 40mg/ml, 60mg/ml, 80mg/ml and 100 mg/ml) were prepared from the standard glucose solution (1mg/ml), the absorbance of all dilution was measured by a spectrophotometer at 490nm to construct a standard curve of concentration versus absorbance.
- 1 ml of 5 % phenol solution was added to 1ml of the anodic biomass suspension.
- Then 5 ml concentrated Sulfuric acid we added to the tube.
- After 9-10 minutes, the contents of the tubes were mixed well and placed in a water bath set at 25-30 °C for 20 minutes.
- The carbohydrate content of the unknown sample was measured from curve value corresponding to the absorbance of the sample.

Lowry's Method was used for the analysis of EPS protein content in MFC biofilm sample. Following reagents were required to estimate the protein amount in given biofilm sample by Lowry's method:

- 2% Na_2CO_3 in 0.1 N NaOH
- 1% Sodium potassium tartrate in water.
- 0.5% $CuSO_4.5 H_2O$ in water.
- Reagent I: Mix 48 ml of 2% Na_2CO_3, 1 ml of 1% NaK and 1 ml 0.5% $CuSO_4.5 H_2O$.
- Reagent II- 1 part Folin-Phenol [2 N]: 1 part water

Procedure

- Bovine serum albumin (BSA) standard solution (1 mg/ ml) was prepared.
- Different dilutions (30-150mg/ml) of BSA working standard solution were made by adding 0.2 ml of BSA in 5 test tubes and make up to 1ml using distilled water and the test tube with 1ml distilled water serves as blank.
- Add 4.5 ml of Reagent I to each dilution and incubate for 10 minutes.
- After incubation cool at room temperature, add 0.5 ml of reagent II and incubate for 30 minutes.
- Measure the absorbance at 660 nm through spectrophotometer and plot the standard curve.
- Estimate the amount of protein in unknown sample from the standard curve.

(iii) DNA Extraction

Graphite rod along with biofilm was transferred to 4-5 ml of PBS and sonicated for 20 min. to detach bacterial cell from anode surface. This biomass suspension was used for the DNA extraction to analyse microbial community harbouring on anode through pyrosequencing. DNA was extracted from anode biofilm following DNA isolation Kit (Cat: 24700, Norgen Biotek Corp.) protocol. Purified genomic DNA was stored at 4°C till further processing.

(iv) Pyrosequencing

The quantity and quality of purified genomic DNA was confirmed prior to pyrosequencing by using NanoDrop 2000 UV-Vis Spectrophotometer. DNA samples were sent to Molecular Research (MRDNA) 503 Clovis Road Shallowater Texas for 545 pyrosequencing analysis. Amplicon libraries were constructed for 454 pyrosequencing using different sets of primers: 104F and 530R targeting the 16S rRNA genes of bacterial domain. At MR DNA, targeted genes were sequenced on *MiSeq* according to manufacturer's recommendations. Pipeline sequence data was further processed by joining sequences; the sequences lacking the barcodes <150bp and the sequences having ambiguous bases were removed. Sequences were denoised, operational taxonomic units (OTUs) were generated and illusions removed. Operational taxonomic units (OTUs) allow the comparison of community structures without assigning sequences into taxonomic ranks. Operational taxonomic units (OTUs) were defined by collecting at 3% divergence (97% similarity). Final OTUs were taxonomically classified using BLAST against a curated database derived from GreenGenes, RDPII and NCBI.

6.2.4.3.2. Culture-dependent Characterization of Bacterial Community

Biomass suspension of MFC anode was subjected to bacteriological characterization by conventional serial dilution method. Anodic biofilm was dissolved in saline solution with help of sonication as mentioned above. Then the biofilm samples were serially diluted in to 9ml of distilled water up to 10^{-5}. Each dilution (10^{-1}, 10^{-3} and 10^{-5}) was spread on Nutrient Agar (NA) plates and incubated for 24 hrs at 37 °C. After incubation different bacterial colonies on media were identified and classified on the basis of their morphology and biochemical test.

(i) Colony Forming Unit (CFU)

The colonies appeared on nutrient agar plates from serial dilution after 24-48 hours of incubation at 37 °C were counted through digital colony counter (EKDS, DC-3, Kayagaki) to determine the viable cell load in biofilm and the CFU/ml of biofilm suspension was calculated with the formula:

CFU / ml = colonies x dilution factor/ Volume plated (ml)

(ii) Isolation and Identification of Bacterial Isolates

Different bacterial colonies on basic nutrient media were further cultivated on various selective and differential media to isolate or identify specific bacteria and distinguish bacterial growth characteristics. Eosin methylene blue (EMB) agar, *blood agar, Staphylococcus* and MacConkey's agar (MaC) media were used for this purpose. Bacterial isolates were further identified through characterization of distinguishing morphological properties, classification on the basis of cell wall constituents through Gram

staining and biochemical tests:

(iii) Scanning Electron Microscopy of Biofilm

Scanning electron microscopy (SEM) of MFC biofilm on anode was performed at the centralized resource laboratory, Department of Physics, UOP, Pakistan (Pk). The primary objective of high-resolution microscopic examination was to monitor morphology of predominant bacteria on anode. The graphite rods were removed from MFC anode chambers and after washing with distilled water immersed overnight in formaldehyde (2-5%) for the sample fixation.

The graphite rod was dried for 50 min by using the drier KADA$^®$ 85 U/SMD having heat gun at 200˚C and dried samples were fixed on copper stub by using electrically-conductive carbon tape on both sides. The edges of sample were covered with electrically conductive material (silver paste conduction, SPI-CHEM) to guarantee the conduction of electron beam. Vacuum (10^2 atm) and high voltage was created in chamber to deposit gold on target sample by using sputter coater. The sample was prepared and mounted on the sample holder; it was loaded in chamber under the column. Several minutes was required by pump to create vacuum. Once sufficient vacuum level (below 7.5x10-5 Torr) was achieved, column valve was open and high voltage beam run up the anode surface. Finally, the surface morphology of biofilm was observed on the monitor screen.

(iv) Gram Staining and Biochemical Characterization

Use a sterile loop to prepare smear of the isolated bacterial culture on glass slide and heat fixed it. Add few drops of crystal violet (primary stain) on heat fixed smear for one minute, briefly rinsed with tap water and drain. Gram's Iodine was applied for 1 minute as mordant to fix the dye and then it was rinsed with tap water. After that, decolorizing agent (95% ethyl alcohol) was poured on slide for no more than 15 second and wash-off the smear on slide with tap water. Finally, flood the slide with safranin (counter strain) and rinsed through water after 30 second. All the slides were dried and observed with light microscope under oil emulsion lens (100X). Gram staining was performed to observe various characters (Gram reaction: pink or purple colour, shape and arrangement) of available organism.

Morphological characteristics of isolated bacterial colonies on basic nutrient agar media were examined in detail for identification. Following morphological characteristics of bacterial culture were studied for identification of bacteria (Table: 6.2).

Table 6. 2 Gram staining and colony characteristics.

Characteristics	Observations
Gram reaction	Gram positive, Gram negative
Shape	Cocci, Bacilli, Spiral
Arrangement	Single, Pair, Chain, Cluster, Irregular
Size	Pin-point, Small, Moderate, Large
Color	White, Grey, Yellow, etc.
Form	Punctiform, Circular, Irregular, Rhizoid
Opacity	Opaque, Transparent, Translucent
Margin	Entire, Lobate, Undulate, Serrate, Filamentous
Elevation	Flat, Raised, Convex
Consistency	Buttery, Viscid, Brittle, Mucoid
Surface	Smooth, Glistening, Rough, Dull
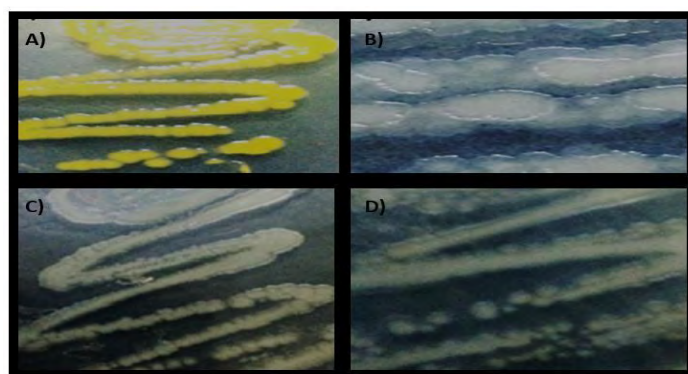
Figure 6. 2 Colony morphology of different isolated bacterial strains

A) Yellow, round, entire and opaque. B) Irregular, undulant and opaque. C) Small, round and opaque. D) Irregular, opaque and small colonies.

The isolated bacterial strains were subjected to various biochemical tests to identify the bacterial such as catalase, oxidase, urease, citrate, MR-VP test, triple sugar iron test, and SIM test.

(v) Microtiter Dish Biofilm Formation Assay

Screening of isolated bacterial culture for biofilm formation was done with microtiter dish biofilm formation assay. This simple assay allows the quantitative assessment of biofilm development on the wall and bottom of a microtiter dish well through absorbance in plate reader at 550 nm.

Procedure

Isolated cultures were grown overnight in mineral medium (NaCl, 4.0g/l; NH₄Cl, 1.0g/l; KCl, 0.1g/l; KH₂PO₄, 0.1 g/l; MgSO₄.7H₂O, 0.2 g/l; CaCl₂.2H₂O, 0.04 g/l) supplemented with 5g of glucose. For biofilm assays overnight culture were diluted (1:100) into fresh medium, 100µl of each dilution was added in 4-8 replicate wells. The microtiter plate was incubated for 4-24 hrs at 37 °C. After incubation, the wells contents were dumped out by turning the plate over and shaking out the liquid. The plate was gently rinsed with water to remove remaining media components and unattached cell to avoid background staining. 125 µL of crystal violet solution (0.1%) was added to each well of the microtiter plate and incubated for 10-15 min at room temperature. The plate was washed with water for 3-4 times by sinking in a water tub to significantly remove the excessive dye and cell. The microtiter plate was dried for few hours or overnight by turning it upside down. To solubilize the CV, 125 µl of 30% acetic acid solution was added to each well of the microtiter plate. The microtiter plate was incubated for 10-15 min at room temperature. 125µl of the solubilized CV was transferred to a new microtiter plate; the absorbance was measured at 550 nm in a plate reader where 30% acetic acid in water was used as the blank.

(vi) MTT 3-(4,5-dimethylthiazol-2-yl)-2,5-diphenyltetrazolium bromide Reduction Assay:

Metabolic assay was used for the further screening of cultures viability in biofilm. Cell survival and metabolic activity of isolated bacterial culture was assessed by the reduction of tetrazolium salt MTT (*Thiazolyl Blue* Tetrazolium Bromide) into formazan through a mitochondrial enzyme (succinate-dehydrogenase). The metabolic rate of isolates is proportional to the amount of formazan produced.

Procedure

The isolated cultures were grown overnight at 37°C in mineral medium (g/litre) (NaCl, 4.0; NH₄Cl, 1.0; KCl, 0.1; KH₂PO₄, 0.1; MgSO₄.7H₂O, 0.2; CaCl₂.2H₂O, 0.04) supplemented with 5 g of glucose. The cells were seeded in 4-8 replicate wells of 96-well microtiter plate and incubated at 37°C for 24 hours. 20 µL of MTT (5mg/ml) was added to each well and incubated at 37 °C for 4hours. The medium was removed from each well by inverting the microtiter plate and shaking it. 200 µl of DMSO was added to each well and absorbance was recorded at 595 nm. The wells with no cells and DMSO served as the blank
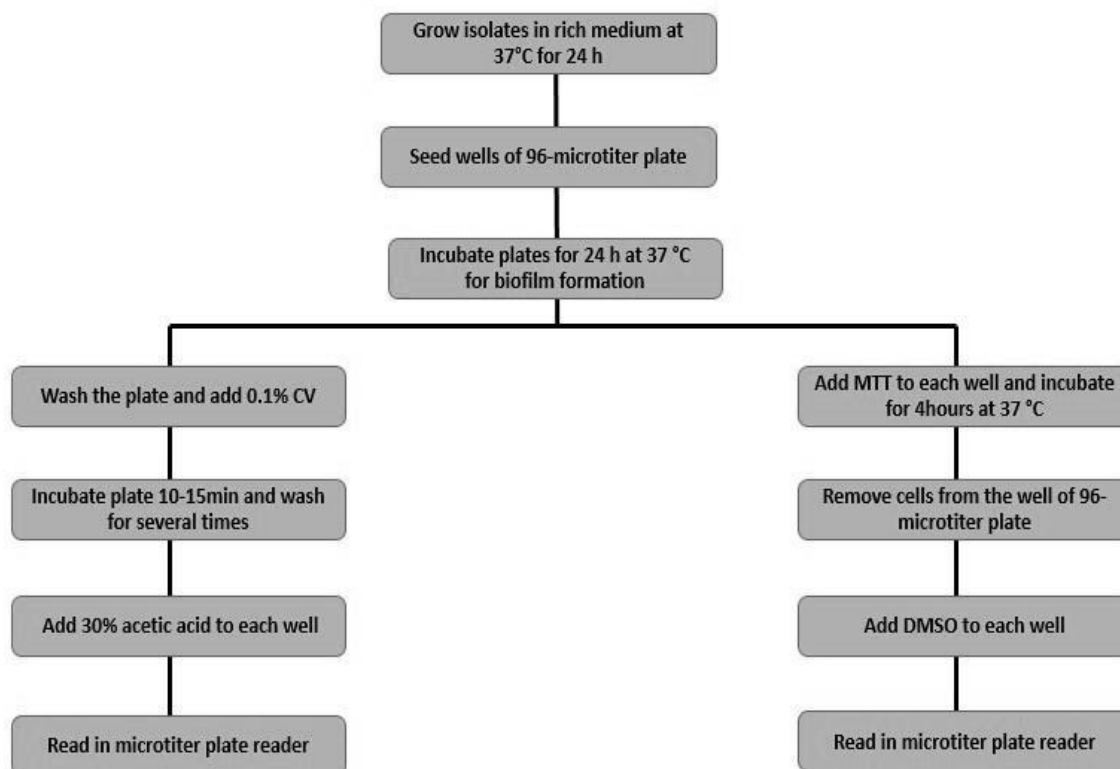
Figure 6. 3 A flow chart diagram summarizing the different steps of the microtiter plate biofilm formation assay and MTT reduction assay procedure.
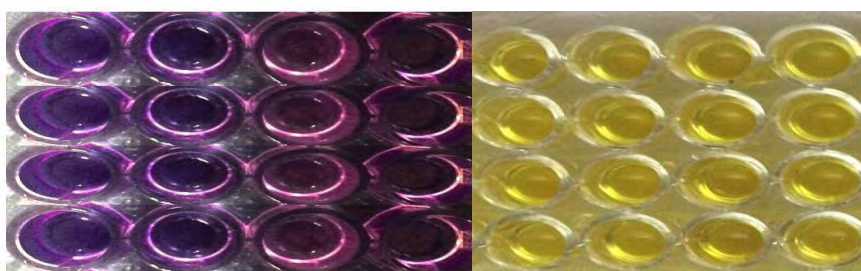
Figure 6. 4 (Left) Biofilm formation assay of bacterial isolates in 96 well microtiter plate (Right) MTT assay of bacterial isolates in 96 well microtiter plate.

6.3. Results

The effects of different operational factors including; temperature, pH, cathode electrolyte and external resistance were evaluated for the optimum fed-batch performance of dual chamber Nafion membrane containing MFC as an electric current generation tool and BOD biosensor using mixed (sludge) and separate bacterial isolates. The detailed results are as under:

6.3.1.   Electrochemical Characterization of MFC Biosensor

MFC reactors exhibited consistent reproducible cycles of voltage generation after two successive weeks of inoculation, indicating successful acclimation of bacteria on anodes. Mineral medium containing 50 mgL^{-1} of glucose was fed into the reactors for 3-4 days prior conducting biosensing operation in order to ensure the stability of the reactors. A pre-developed activated sludge biofilm was used in anodic chamber of MFC-I biosensor. The corresponding open circuit voltage (OCV) of 0.68±0.1V was recorded

immediately after MFC was fed with sewage sludge and wastewater. Initially, the potential remained below 250mV then the voltage gradually increased to 453±5 mV on 18th day. During first 35 days of operation MFC-I generated maximum power of 14.2±1 mWcm^2, afterwards, a decline in system performance was observed. Whereas, MFC-II operated with artificial consortium produced a maximum voltage of 198.9±2 mV on 13th day. A stable voltage with average current of 0.031 ± < 0.01 mA and 0.019 ± < 0.005 mA was recorded in MFC-I and MFC-II respectively during the last 2 weeks of operation. The maximum current density of MFC-I with sludge was 66% higher than that of MFC-II with artificial consortium (*Staphylococcus aureus*, *Pseudomonas aeruginosa* and *Bacillus circulans*). During single cycle polarization studies voltage output was observed with each resistance loads (from 50 Ω to 20 KΩ) after 20 min interval. Voltage exhibited a sharp decline at higher current densities resulting in occurrence of power overshoot but then power decreased rapidly. While, current density increased continuously (Fig. 6.2). The COD removal was monitored during the start and stable phase of MFCI operation between days 10-40. The current density of MFC-I was around 0.02±< 0.005 mAcm^2 during day 10th to 15th, thereafter, it exponentially increased up to 0.041±0.005 mA on 30th day. The COD removal efficiency of MFC-I was increased from 58% to 74% as current density increased between 10th to 20th days and ultimately it reached up to 95.7% on 40[th]day.
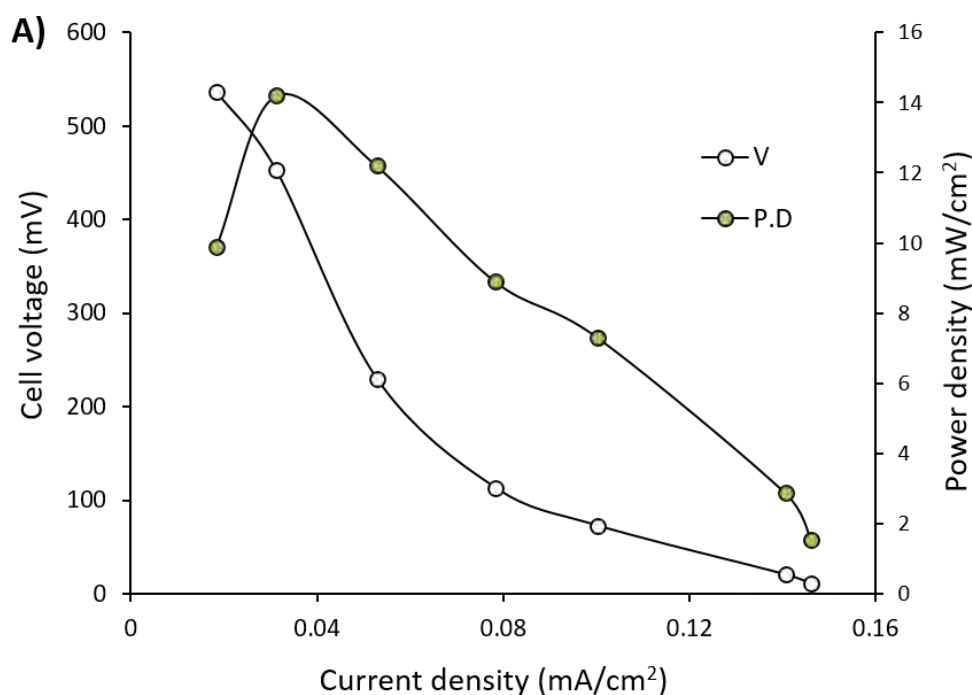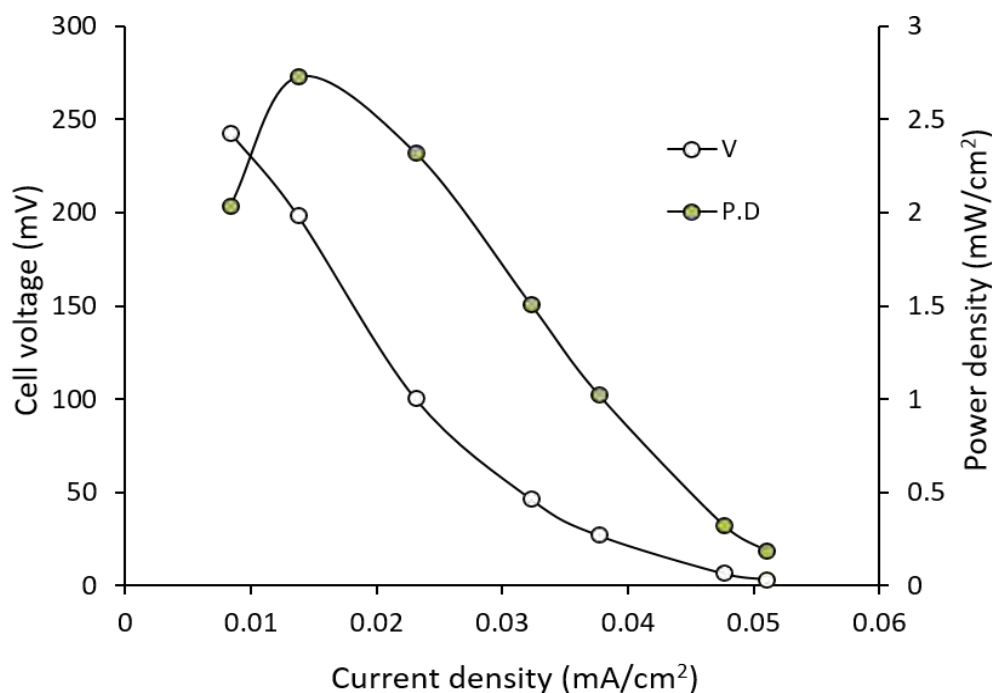
Figure 6. 5 Polarization and Power density curves of; A) MFC-I and B) MFC-II.
This indicated that electrochemically active bacteria turned highly metabolically active during the last two weeks. Whereas, the COD removal efficiency of MFC-II with artificial consortium remained lower and it was 72% during the final week of experiment.

6.3.2. Calibration of MFCBiosensor

MFC-I and MFC-II were supplied with different concentrations (50mg/l-250mg/l) of standard solution of glucose and glutamic acid (GGA) under optimal working conditions to establish a relation between BOD and respective voltage outputs. The steady state response times of BOD biosensors were monitored following replacement of anodic GGA standard solution with its new successive concentration (Fig. 3). An acceptable positive correlation (> 90%, r^2 = 0.9) was achieved between different concentrations of standard solutions and voltage outputs validating MFC as a BOD biosensor. The regression equations for MFC-I and MFC-II biosensor were established to be y_1= 0.7834x-11.638 (r^2 = 0.9804 or 98%) and y_2= 0.1667x + 0.8476 (r^2= 0.9891 or 98.9%) respectively. Where, 0.7834 and 0.1667 were slopes of regression lines (b), x represented the predictor variable (organic load of wastewater) and y was the response variable (voltage output of system). The Y-intercept (a) was the point where line cut the y-axis and can be intercepted as the value predicted for voltage only if x = 0. Thus, it was inferred from the regression equations that with each 1 mg/l increase in organic load the voltage responses were increased by 0.7 mV for MFC-I and 0.1 mV for MFC-II biosensor (Fig. 6.3). Furthermore, in extrapolating the BOD (mg/l) samples from different waterbodies (stream, wetland and domestic treatment plants), same regression equations were applied. To interpret the biodegradable organic load of sample through biosensor a variation in voltage was recorded after introducing the wastewater in anode chamber and voltage response was used for calculating the BOD (mg/l) through these equations.
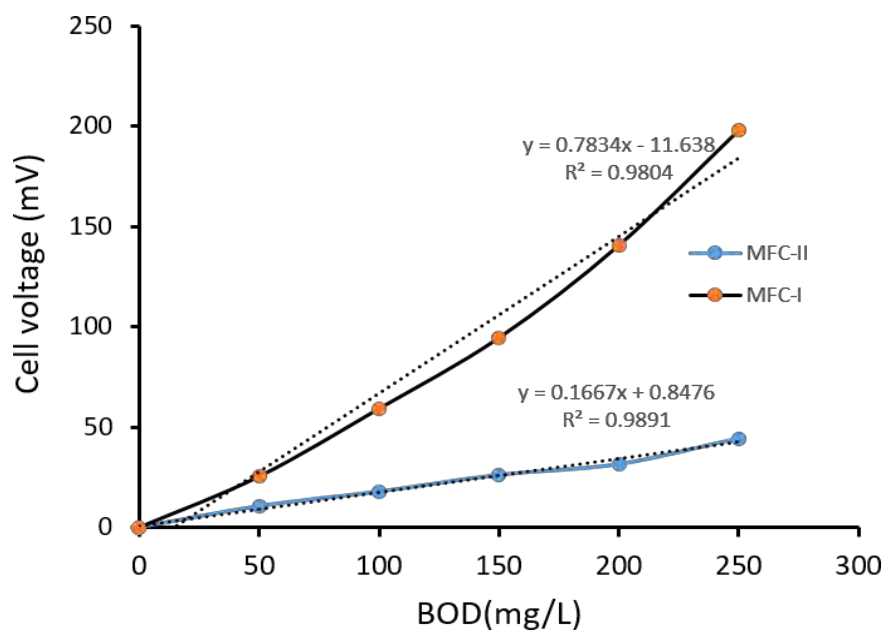
Figure 6. 6 Relationship between different BOD concentration and voltage outputs of MFC-I and MFC- II biosensors.

6.3.3. Performance Characteristics of MFC Biosensor

Different performance parameters of MFC biosensors including stability, response time and reproducibility were analysed during operation and the detailed are as follows:

6.3.3.1. ResponseTime

The time period required to achieve a stable operating voltage (OV) following the addition of organic matter in anode compartment was recorded as the response time. Response time of MFC biosensor depends upon BOD concentration, type of MFC and operational conditions. Higher the sample strength longer the time required to measure the BOD in MFC biosensor. MFC-I required approximately 60 min to detect a BOD concentration of 13.6 mg/l, whereas, it took about 21 h for BOD concentration of 989.4 mg/l. Therefore, samples with high COD were diluted before subjecting to bio-sensing test (Table: 6.2). Dilution technique was also used to avoid extrapolation outside the range of collected data points because relationship may not be linear beyond that point. In terms of voltage output, the response of MFC-II was much quicker than MFC-I but has shown a percentage error of about 25%.

Table 6. 3 BOD of different water samples (stream, wetland and domestic treatment plants) measured by MFC biosensors and standard 5-days method.

No	Wastewater Type	MFC BOD Biosensor			BOD$_5$
		Type	(mg/L)	Response Time(min)	(mg/L)
1	Stream	MFC-I	16±0.9	60±1	13.6±0.2
2	Domestic wastewater	MFC-I	980±15	1260±3	989.4±1.2
3	Stream	MFC-I	40±0.2	180±1	29.9±0.5
4	Wetland	MFC-I	30±0.5	255±0.9	42.1±0.3
5	Domestic wastewater	MFC-I	60±0.7	210±2	36.04±0.2
6	Wetland	MFC-II	100±1.4	120±2	102±1
7	Domestic wastewater	MFC-II	57±3.5	160±1	273±0.3
8	Stream	MFC-II	60±0.2	70±3	67±2
9	Wetland	MFC-II	90±0.8	100±2	88±0.9

6.1.1.1. Repeatability and Comparison of MFC BOD Biosensor with Standard BOD$_5$Method
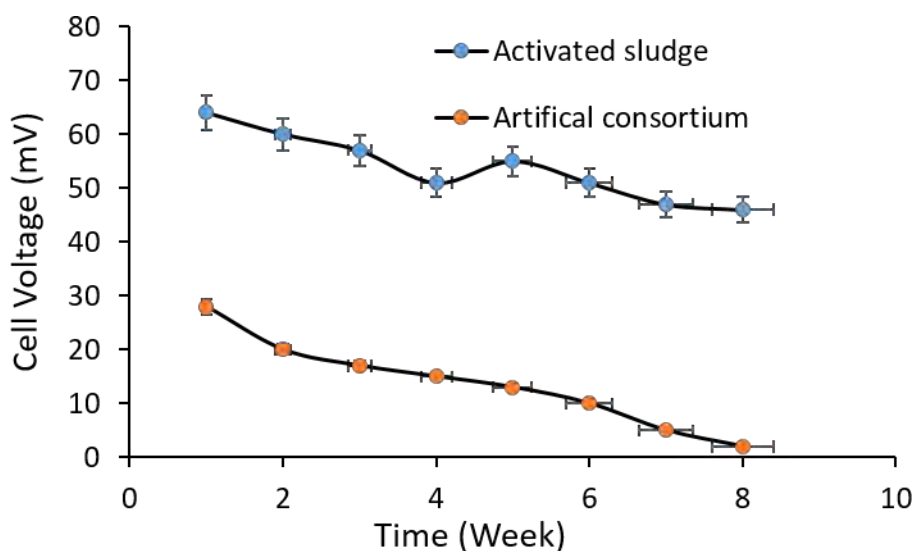
Figure 6. 7 Repeatability and comparison of MFC BOD biosensor with standard BOD5 method in successive 7-8 cycles using regular intake of mineral medium (COD100mg/l) after every 24 hours.

According to the APHA BOD$_5$ method, a standard deviation of ±30.5 mg/L is acceptable that is equivalent to ±15.4% variation in precision (Liu and Mattiasson, 2002). To determine the repeatability of biosensing system anodic chamber was operated with mineral medium (COD = 100 mg/l) for 24 hours in

repeated 7-8 cycles and the voltage responses were recorded. The variation in repeatability was ±5 mV in MFC-I biosensor qualifying acceptable limit. However, a considerable variation in MFC-II biosensor signals was observed after 3 weeks (Fig. 6.4). Furthermore, the values from BOD biosensors were comparable to BOD_5 standard method and measured results remained within APHA acceptable limits (Table: 6.2).

6.1.1.2. Operational Stability

The stability of MFC biosensors in terms of voltage outputs was monitored regularly throughout the operation. During the entire period voltage output remained considerably stable. A voltage fluctuation of about 65.8±0.3 to 45.7±1 mV was recorded in 2 months for MFC-I and 25.8±1 to 11.2±1.1 mV in 1.5 months for MFC-II when fed with BOD standard solution (100 mg/l) of GGA. Overall, the stability of bacterial consortium of activated sludge was 55% higher than artificially developed consortium.

6.1.1.3. Effect of Co-existing Ions on MFC-I Biosensor
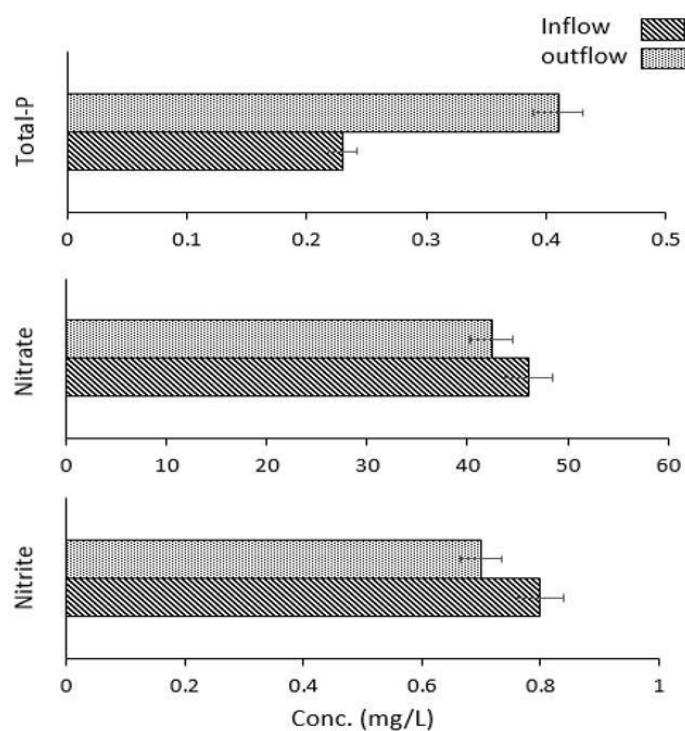
Figure 6. 8 Variation in electron acceptors (concentration) during development of biofilm in MFC-I.

Domesticandindustrialwastewatergenerallycontainhighconcentrationsofoxygengas(O_2), charged ions and inorganic compounds such as phosphate (PO_4^{3-}), ammonium (NH_4^+), nitrate (NO_3^-), nitrite (NO_2^-) and sulfate (SO_4^{2-}) that can greatly influence the signal output. Therefore, domestic wastewater sample was purged with oxygen free nitrogen gas to create the anaerobic conditions before introducing into MFC. Phosphate (PO_4^{3-}), ammonium (NH_4^+), nitrate (NO_3^-) and nitrite (NO_2^-) concentrations were continually measured in wastewater samples during immobilization process through standard methods. The average amount of different electrons acceptors was; Total-P 0.23±0.1 mg/l, NO $^-$ 46.1±3 mg/l, and NO $^-$ 0.8±0.1

mg/l. Under optimum conditions ammonium was removed by 37%, whereas, nitrite (NO_2^--N) and nitrate (NO_3^--N) by 5-10% in 10 days. A slight increase ($0.23\pm0.1-0.41\pm0.13$ mg/l) in orthophosphate (PO_4^{3-}) was occurred during MFC operation (Fig. 6.5).

Table 6. 4 Change in COD and inorganic compound concentration of domestic wastewater at different operating conditions fed batch MFC reactor.

Factor		Change in concentration (%)				
		COD	**Ammonia**	**Nitrate**	**Nitrite**	**Phosphate**
Temperature(^{o}C)	15	-67	-17	-6	-67	+98
	25	-29	-35	-8	-15	+21
	37	-95.7	-60	-7.5	-9.8	+72
	45	-96.4	-75	-6	-9	+67
pH	5	-27.1	-17	-6	-25	+17
	7	-87	-56	-7	-10	+72
	9	-15.9	-44	-1	-12.5	+79
Catholyte	NaCl+ PBS	-95.7	-77	-8	-5	+78
	HCl+PBS	-58.4	-45	-6	-15	+47

6.1.1. Ultrastructure and Quantitative Analysis of Bacteria in AnodicBiofilms
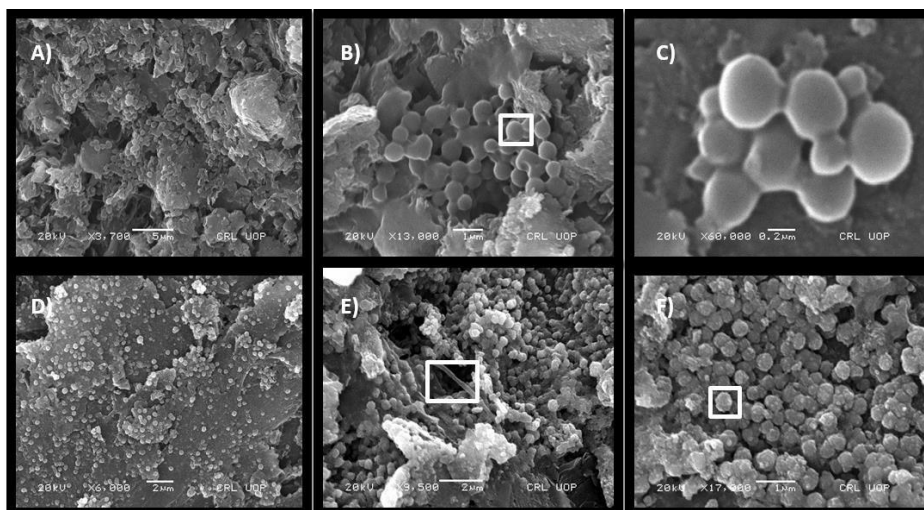
Figure 6. 9 Scanning electron microscopic (SEM) A) of biofilms
A) broad overview of the MFC-I biofilm at 3700X B) Multiple layers of cells extending from the anode of the MFC-I and white square indicate round shaped cell C) Aggregate of round cells D) A broad overview of MFC-II anode biofilm at 6000X E) Multiple layers of cell extending from anode surface and white square indicate filament shaped structure extending between cells F) Round shaped cells held by extracellular polymeric substances (EPS).

The structure and morphology of biofilms formed on anode surfaces were analysed by scanning electron microscopy (SEM) (3400N, HITACHI instrument). A thick smooth coverage of biofilm biomass was observed on anodes of MFC-I and MFC-II (Fig. 6.6). Figure 6A highlights the anode surface of MFC-I with appreciable amount of biofilm attached and majority of individual bacterial cells were uniform spherical shaped cocci. Under higher magnification (60, 000 X), a compact biofilm structure was evident where clumps of heterogeneous shaped cells were tightly interconnected by polymeric viscous materials (Fig. 6C). SEM of artificial consortium in MFC-II illustrated less biofilm density than MFC-I. The extracellular polymeric matrix was holding ovoid shape bacterial cells on anode with interconnecting filaments (Fig. 6D). The high density of bacterial cells on MFC-I anode surface was further confirmed by the biofilm dry mass analysis. The dry weight of mature (5 weeks) sludge biofilm was 3.31 mgcm^{-2}, whereas, it was 0.81 mgcm^{-2} for artificial consortium. An about 75% less biofilm biomass was found on anodic surface of MFC-I compared to MFC-II.

6.1.2. Molecular Phylogeny of Bacteria (454-Pyrosequencing)
454-Pyrosequencing was used to reveal the diversity of bacterial community present in activated sludge inoculum and biofilm enriched on MFC-I anode (Fig. 6.7). The resultant sequences were grouped into 24 different phyla in sludge and 12 phyla in anodic biofilm. *Gemmatimonada* (12.6%), *Comamonadaceae* (9.5%), *Rhodocyclaceae (5.4%), Syntrophaceae* (3.8%), *Xanthomonadaceae* (3.2%), *Spirochaetaceae (2.7%), Nitrospiraceae* (2.5%), *Erysipelotrichaceae* (2.5%), *Thiotrichaceae* (2.4%), *Corynebacteriaceae (2.2%), Ectothiorhodospiraceae* (2.0%), *Fibrobacteraceae* (1.7%), *Saprospiraceae (1.7%), Acetobacteraceae* (1.6%), *Helicobacteraceae (1.6%), Acidobacteriaceae* (1.4%), *Beijerinckiaceae* (1.3%), *Thermoanaerobacteraceae* (1.3%), *Pseudomonadaceae* (1.3%), *Rhodospirillaceae* (1.1%),

Sinobacteraceae (1.1%), *Burkholderiaceae* (1.0%), *Hyphomicrobiaceae* (1.0%), *Verrucomicrobiaceae* (1.0%) were the dominant families in activated sludge. Pyrosequencing of microbial communities associated with anode revealed that *Caulobacteraceae* (26.6%), *Oxalobacteraceae* (13.6%) and *Pseudomonadaceae* (8.3%) were the three top most abundant families in anodic community while rest of the includes *Rhodobacteraceae* (6.7%), *Xanthomonadaceae* (6.2%), *Bradyrhizobiaceae* (4.1%), *Sphingomonadaceae* (3.1%), *Burkholderiaceae* (3.2%), *Alcaligenaceae* (5.9%), *Rhodocyclaceae* (2.1%), *Nitrosomonadaceae* (3.3%), *Comamonadaceae* (2.5%) and others (<2%).

The most active genera in sludge inoculum were *Gemmatimonas* (12.6%), *Schlegelella* (9.1%), *Syntrophus* (3.5%), *Nitrospira* (2.5%), *Beggiatoa* (2.4%), *Bulleidia* (2.4%), *Nitrospira* (2.4%), *Denitratisoma* (1.9%) andothers (<1.7%). However, *Brevundimonas* (26.2%), *Massilia* (9.9%), *Pseudomonas* (8.3%), and *Paracoccus* (6.7%) were the most active genera comprising 51% of the total anode bacterial community in MFC (Fig. 6). *Caulobacteraceae* (26.6%), *Oxalobacteraceae* (13.6%) and *Pseudomonadaceae* (8.3%) were the most dominant families in anodic biofilm.
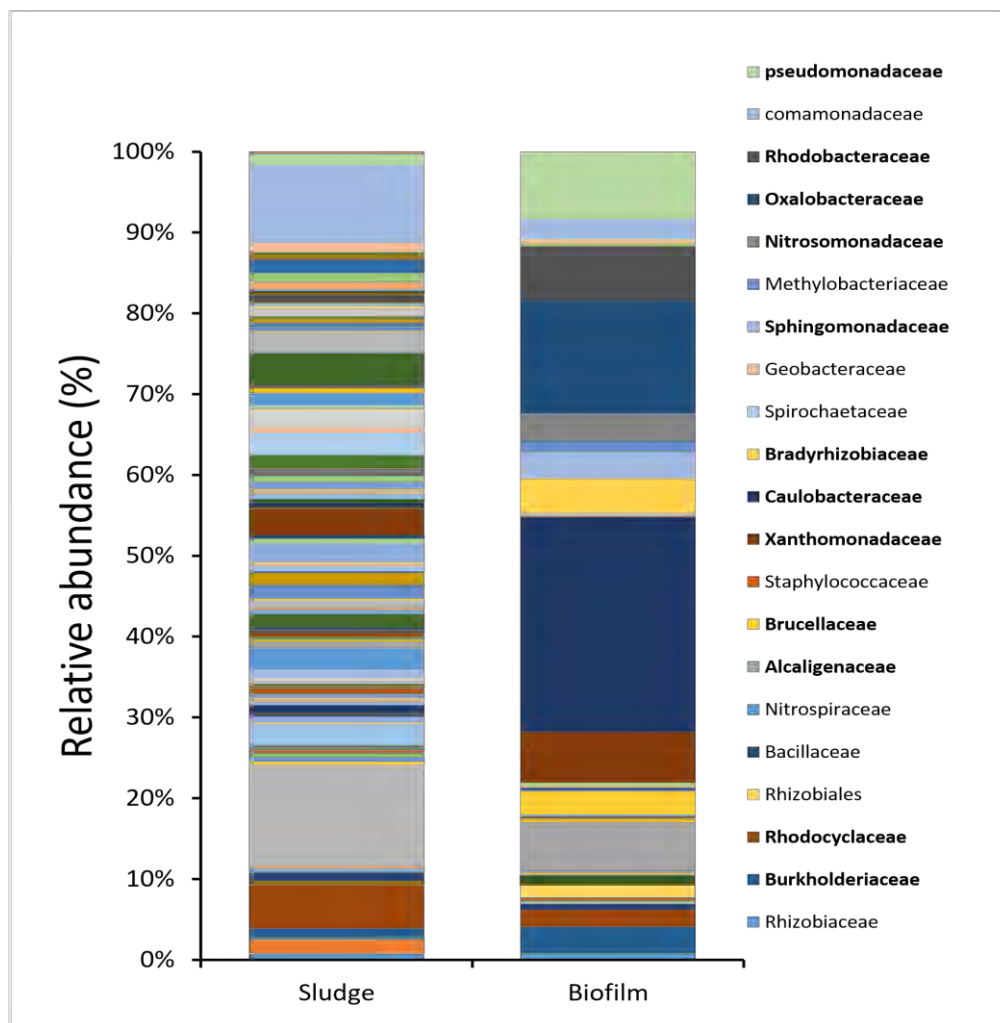
Figure 6. 10 Relative abundances of dominant bacterial family in activated sludge inoculum and anodic microbial community.
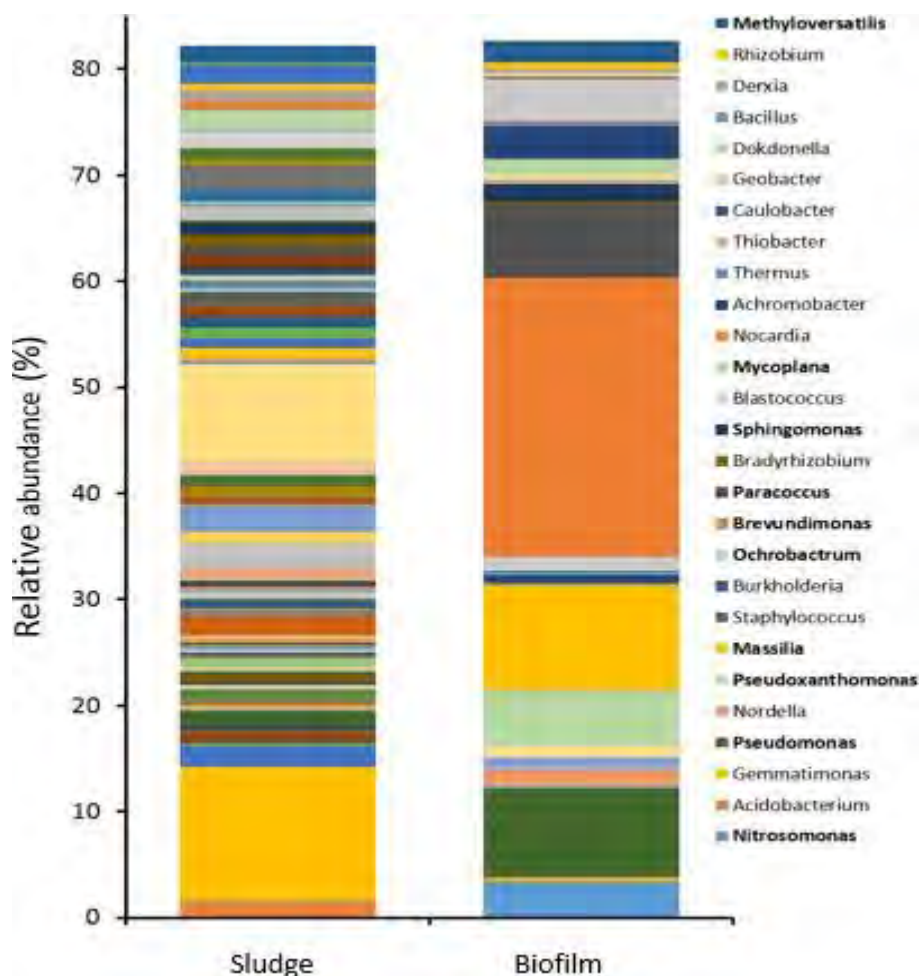
Figure 6. 11   Relative abundances of dominant bacterial genera in activated sludge inoculum and anodic biofilm.

6.3.6. Dry Mass and EPS Characterization

The dry mass of 60 and 21 days anodic biofilm was determined by calculating volatile suspended solid per cm^2 of electrode surface area to estimate the biofilm mass. The amount of biofilm formed with activated sludge and artificial consortia was 3.31 ± 1.8 mg/cm^2 and 0.82 ± 0.1 mg/cm^2, expressed as mass of VSS per surface area of the anode. EPS carbohydrate content was determined by using the phenol/sulfuric acid method and protein content using Lowry method. The glucose and BSA calibration curve are shown in figure: 5.20.The protein (EPSp) and carbohydrate (EPSc) content of activated sludge biofilm EPS in 1ml of extraction solution was 0.54 mgl^{-1} and 5400 mg^{-1}. Total EPS of activated sludge and artificial biofilm was 5400.54 mg^{-1} and 1350.13 mg^{-1} calculated by adding EPSc and EPSp.

A)

$y = 2.2786x - 0.0643$
$R^2 = 0.9879$

B)

$y = 0.001x + 0.0387$
$R^2 = 0.9988$
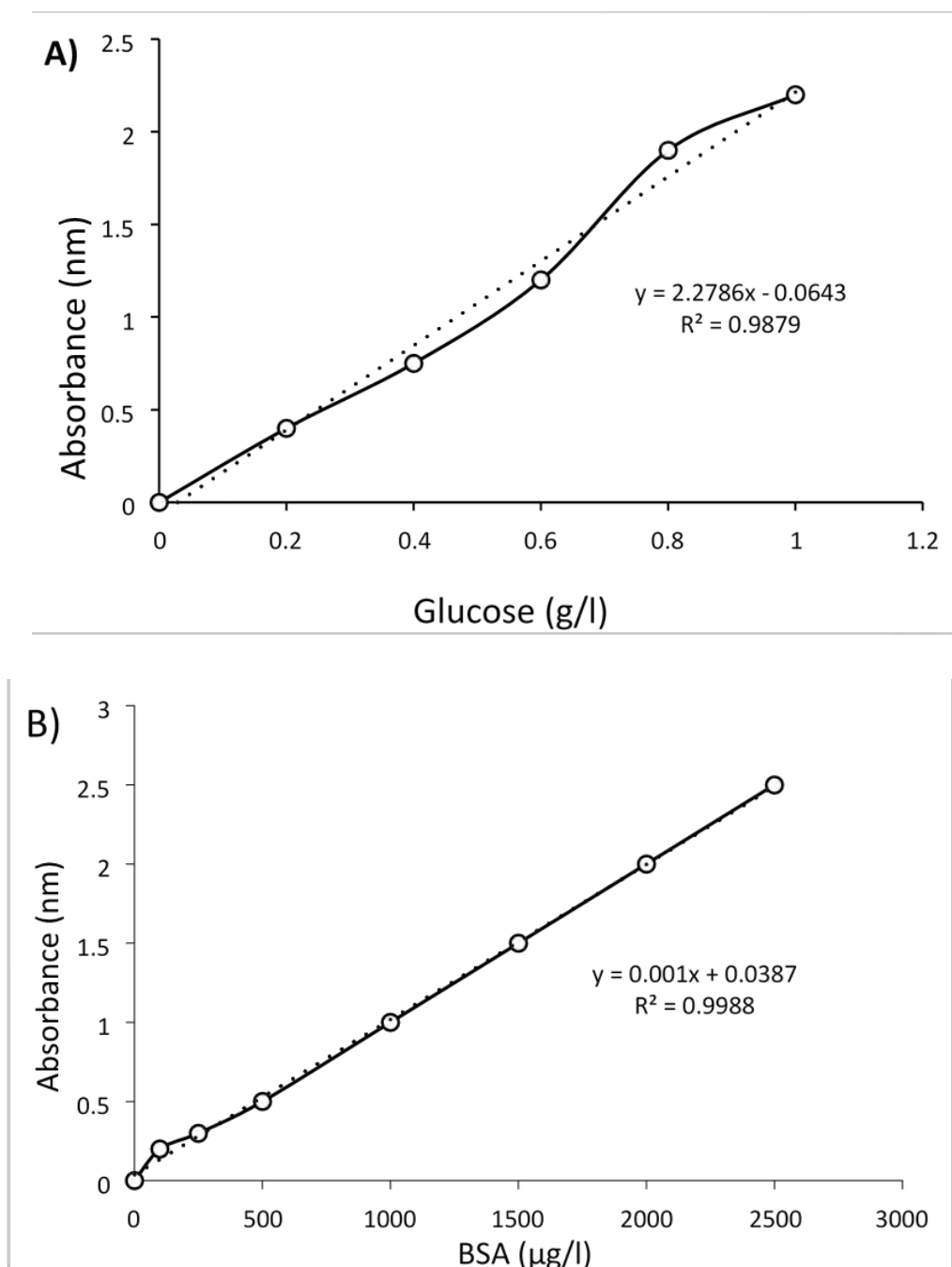
Figure 6. 12 Calibration curve for determination of EPS carbohydrate content using the phenol/sulfuric acid method and protein content using Lowry method A) Glucose calibration curve B) Bovine serum albumin calibration curve.

6.3.7. Culturing of MFC Biofilm

In the biofilm Gram positive bacteria were dominant and Gram-negative bacteria were also observed. Total microbial count in 1 ml of sample was 3.0×10^5. Isolated bacterial strains were identified as *Staphylococcus, Pseudomonas* and various *Bacillus* species, detail biochemical characterization of isolated bacterial strains is shown in below table:

Table 6. 5 Identification of isolated bacterial strain through biochemical tests.

	Colony morphology	Gram staining	MA	EMB	Blood agar	SM	SIM	TSI	MR-VP	TGB	Oxidase and catalase	Urease test	SCT	Possible identify
1	Size: small Margin: undulate Form: circular Elevation: flat Color: white Opacity: opaque Surface: rough, slightly glistening Consistency: viscid	Reaction: G+ Shape: bacilli Arrangement: long chain	-	-	α-hemolysis	-	Su: - I: - M: +	G: + S: + L: + H$_2$S: Gas:+	+	- FA	+	-	-	-	*Paenibacillus* sp.
2	Size: irregular Margin: filament Form: irregularly spread Elevation: flat Color: white Opacity: opaque Surface: dull Consistency: butyrous	Reaction: G+ Shape: bacilli Arrangement: Extensively branched chain	-	-	B-hemolysis	-	Su: - I: - M: +	G: + S: + L: + H$_2$S: Gas: -	+	- FA	+	-	-	-	*Bacillus* sp.
3	Size: punctiform Margin: entire Form: circular Elevation: raised Color: white Opacity: opaque Surface: glistening Consistency: butyrous	Reaction: G+ Shape: bacilli Arrangement: small chain	-	-	α-hemolysis	-	Su: - I: - M: +	G: + S: + L: + H$_2$S: - Gas: -	+	+ FA	+	-	-	-	*Bacillus siamensis*
4	Size: punctiform Margin: entire Form: circular Elevation: raised Color: grey Opacity: opaque Surface: glistening Consistency: viscid	Reaction: G+ Shape: bacilli Arrangement: chain	-	-	β hemolysis	-	Su: - I: - M: -	G: + S: + L: + H$_2$S: ---Gas: -	+	- FA	+	-	-	-	*Bacillus* sp.

No	Colony morphology	Gram reaction			Hemolysis		SIM	Biochemical			TGB					Organism
5	Size: very small Margin: undulant Form: punctiform Elevation: flat Color: white Opacity: opaque Surface: glistening Consistency: buttery	Reaction: G+ Shape: bacilli Arrangement: chain	-	-	β hemolysis	+	Su: - I: - M: +	G: + S: + L: + H2S: - Gas: -	+	-	FA	+	-	-	-	*Bacillus circulans*
6	Size: small Margin: entire Form: circular Elevation: convex Color: yellow Opacity: opaque Surface: smooth Consistency: viscid	Reaction: G+ Shape: bacilli Arrangement: chain	-	-	β hemolysis	+	Su: - I: - M: - Gas: -	G: + S: + L: + H2S: -	+	-	FA	+	-	-	-	*Staphylococcus areus*
7	Size: small Margin: undulant Form: irregular Elevation: flat Color: white Opacity: opaque Surface: dull Consistency: viscid	Reaction: G+ Shape: bacilli Arrangement: chain	-	-	α-hemolysis	-	Su: - I: - M: +	G: + S: + L: + H2S: -	+	+	FA	+	-	-	-	*Bacillus acidiproducens*
8	Size: small Margin: entire Form: circular Elevation: convex Color: green blue Opacity: opaque Surface: smooth Consistency	Reaction: G- Shape: bacilli Arrangement: single	+	+	β-hemolysis	-	Su: - I: - M: + Gas: -	G: - S: - L: - H2S: -	-	-	A	+	-	-	-	*Pseudomonas aeruginosa*

MA= MacConkey agar, **EMB**= Eosin methylene blue, **TSI**= Triple sugar iron, **SIM**= Sulphide indole motility, **SM**= *Staphylococcus* medium, **SCT**= Simmon citrate test, **TGB**= Thioglycolate broth, **MR-VP**= Methyl red and Voges proskauer, **G**= Glucose, **S**= Sucrose, **L**= Lactose, **M**= Motility, **I**= Indole, **Su**= Sulphide, **(+)** = Growth, **(-)** = No growth.

6.1.3.   1. Biofilm formation and MTT reduction assay

The biofilm formation and metabolic activity of bacterial species isolated from MFC anode inoculated with activated sludge were further understand for the development of new MFC biosensor having specific bacterial culture as bio-sensing element at anode. 8 bacterial isolates were compared for their biofilm formation and metabolic ability result illustrated (Fig. 6.12) that out of 8 bacterial isolates 7 adhered to the walls of the microtiter plate but still variation was observed in biofilm formation. The measurement of optical density divided the bacterial isolates as weak or moderate biofilm formers. The majority of the

bacterial isolates demonstrated weak adherence (75%) while rest showed moderate (12.5%) adherence and non-adherent (12.5%), no strong adherent isolates were found (Fig. 6.13). The optical density of non-adherent and strong adherent isolates was 0.15 and 0.6 nm, respectively (Table 6.6).

To determine and compare the viability of 8 different bacterial isolates MTT formazan assay was conducted. 96-well microtiter plates determined the amount formazan production through absorbance. After 24 h of incubation, the absorbance was determined through plate reader at absorbance range of 540 nm-600 nm. High optical density correlates with high formazan production and low optical density correlates with low formazan production, optical density of most of isolates lies in the range of 0.15-0.19 nm.
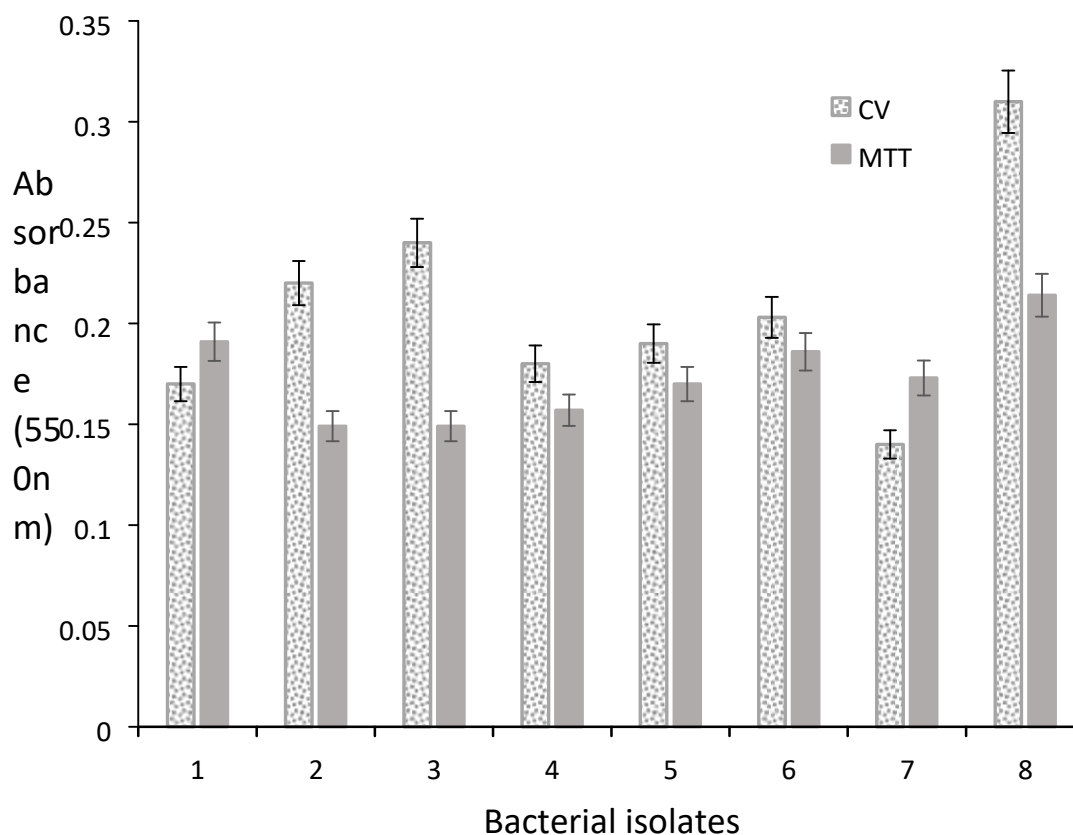
Figure 6. 13 Biofilm formation and metabolic activity of bacteria isolated from MFC anode were quantified by crystal violet and MTT reduction assay.

The biofilm formation strength was calculated by following formula to classify isolates on the basis of adherence:

Table 6. 6 Classification of bacterial isolates.

Average OD value	Biofilm production
OD ≤ ODc	Non-adherent
ODc<OD ≤ 2 × ODc	Weakly adherent
2×ODc <OD ≤ 4 × ODc	Moderately adherent
4 × ODc < OD	Strongly adherent

Optical density cut-off value (ODc) = average OD of negative control + 3x standard deviation (SD) of negative control.
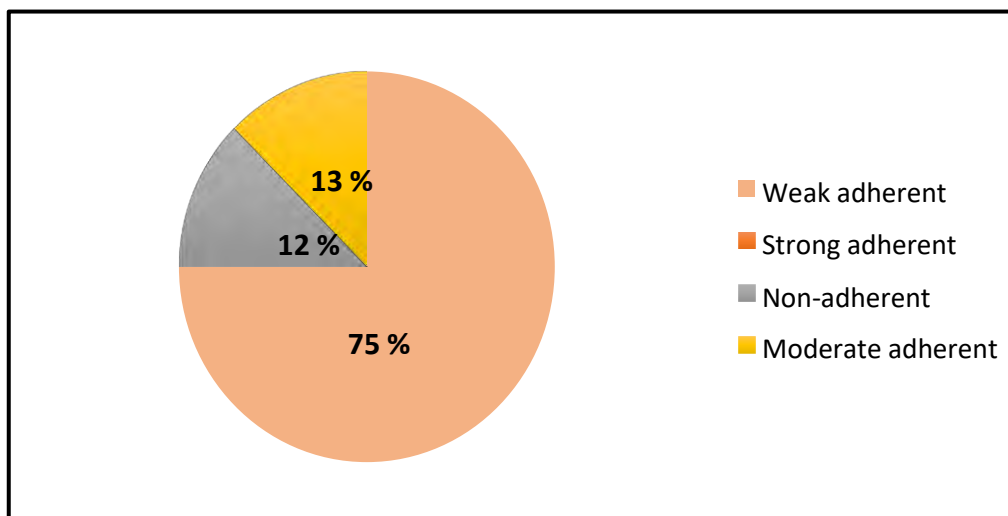
Figure 6. 14 Classification of bacterial isolates in to strong, moderate, weak and non-adherent on the basis of their biofilm forming ability.

6.2.Discussion

Microbial fuel cells (MFC) is a growing alternative green energy technology that also offers a wide range of other applications (Feng et al., 2015). Previous research has been mainly focused on the use of MFC as electric energy generation device. Recently, MFC has gained much attention in environmental sector to use it as a potential biosensing element in monitoring of wastewater treatment. MFC biosensor is emerging as a promising option for BOD measurements considering its high operational stability, reproducibility and broad substrate versatility (Liu et al., 2000). In this study, the maximum power density achieved by artificially developed consortia was 2.7 mWcm^{-2}. This was lower than power density

achieved with natural consortia on MFC-I electrode i.e., up to 14.2 mWcm^{-2} at 10 KΩ circuit load. Similar properties of MFC biosensor were evident in the current study, however, current density versus BOD sensing were comparatively higher with natural bacterial consortium than artificial consortium used. Enhanced performance of MFC reactors in terms of current generation has been previously linked with highly active electrogenic biofilms (Rabaey et al., 2005) encompassing greater diversity of anodophillic bacteria(Sumaraj and Ghangrekar, 2014) with pili network of appendages (Malvankar et al., 2012) .

An equitable analyte detection can be achieved with the microbial electrochemical system(Sazykin et al., 2016) . This could offer an economically attractive, environment friendly and rapid alternative for measuring the organic load in water as BOD because it minimizes the input and later exhaustion of expensive reagents that are used in standard BOD protocols (Moon et al., 2004). A good linear relationship was observed between MFC voltage responses and organic loading rates (Figure: 6.3). A similar linear relationship between electrical signals and different BOD concentrations ranging from 20– 100 mg/l and 1–25 g/l was reported by Gil (Gil et al., 2003) and Kumlanghan (Kumlanghan et al., 2007), respectively. Both MFC types showed good performance in terms of BOD sensing when GGA solution was used as a standard(Liu et al., 2011) . However, while sensing organic pollutant load in domestic wastewater sample (Hsieh and Chung, 2014), MFC-II showed 25% error that was far out of acceptable range of ±15 mg/l. This might have happened due to limited substrate utilization spectrum of artificially developed bacterial consortium. Presence of toxic compounds and heavy metal ions in wastewater have also been associated towards creating erratic electronic response by MFC reactors (Wu et al., 2017).

Higher the organic strength of water the longer the time MFC biosensor took for measuring the BOD (Table: 2). Thus, dilution techniques were employed to analyze the high strength organic wastewater in terms of BOD (Carpenter et al., 2011) . Overall, the electrical response time (min) increased with greater bacterial diversity on anode. Slow electrogenic response of natural consortium than artificial consortium might be due to excessive accumulation of extra polymeric substance (EPS) on anode. Besides, development of thick biofilm on anode surface has been reported to suppress the mass transfer rate of nutrients between bacteria and the outside environment resulting in a rapid decline of catabolic reactions of bacteria (Verma and Singh, 2013). Both MFC configurations used in this study remained stable for 30 days following the biofilm immobilization, however, stability and biosensing response output decreased afterwards. MFC-I proved to be 57% more stable in operation as a biosensing device than MFC-II. Greater bacterial diversity and associated environmental compatibilities in sludge consortium with broad substrate specificity and resistance to adverse environmental conditions might have offered better stability and reproducibility to MFC-I biosensor (Liuet al., 2000, Tront et al., 2008) . Nevertheless, MFC-I with sludge bacterial consortium needed continuous maintenance after construction (Bee et al., 2015).

Despite successful operation of MFC biosensor, challenges of varying bacterial diversity and density in natural consortium always vary with time, source and environmental conditions (Sumaraj and Ghangrekar, 2014) . 454 pyrosequencing successfully revealed the molecular phylogeny of bacterial community composition in MFC-I anode developed from sludge. *Proteobacteria, Chlorflexi,*

Bacteroidetes, Actinobacteria and *Cyanobacteria* were the most dominant phyla in biofilms. However, chances of duplicating the same bacterial community in other MFC biosensors would always be a great challenge. Such limitations always create drawbacks in marketing the MFC reactors as biosensors. Though laboratory defined consortia have limited substrate utilization spectrum and issues in dealing with diverse wastewater samples (Peixoto et al., 2011), still they should be developed more comprehensively taking some vital environmental bacterial isolates with greater physiological capability. In this context, new combinations of ATCC bacterial species should be tested to develop universal bacterial consortia for optimum and sustainable commercial use in MFC biosensor (Yamashita et al., 2016, Sazykin et al., 2016).

Generally, increase in nitrites and nitrates are inversely related with the decreasing levels of ammonium in any organic wastewater system. However, in this case slight decrease (5-10%) in nitrogenous electron acceptors after 10-days retention time of MFC was observed indicated low density and related functionality of denitrifies in bacterial community. Therefore, signal output of the reactor remained high and stable during operation. Though, higher concentration of different inorganic compounds could be negatively effecting performance of MFC (He et al., 2009). A slight increase (0.23-0.41mg/l) in orthophosphate (PO_4 3-) during MFC operation might has been occurred from degradation of organic matter at low redox potential in the reactor. Overall, low concentrations of different inorganic electron acceptors did not pose any major limitation in the biosensing step as was reported previously (Logroño et al., 2016).

6.3. Conclusion

The study validated the importance of microbial fuel cell (MFC) as a biosensor device for efficient and continuous monitoring of BOD in water. Comparatively, MFC based mediator-less biosensor operated with mixed biofilm (60 days) presented good performance regarding all electrochemical characteristics including: long-term stability, good reproducibility and linearity for BOD measurement. Optimum MFC biosensor performance was achieved at temperature: 37°C and pH: 7. 100mM PBS+100mM NaCl proved to be more efficient cathode solution as compare to 100mM PBS+100mM HCl creating a voltage of 443 ± 10mV or power density of 6188.8 ± 0.89mWm^{-2}. Bacterial communities of anode were found to be capable of considerably high COD removal efficiency (95.7%). Molecular based phylogeny revealed the microbial community structure was considerably changed during enrichment in MFC. *Staphylococcus areus, Pseudomonas aeruginosa* and *Bacillus circulans* were selected from CV and MTT assay for the development of new MFC biosensor inoculated mixture of bacteria isolated from previously operated biosensor as bio-sensing element. MFC biosensor developed in this study with mixed biofilm system showed better electrochemical performance than mixture of pure culture biofilm. The co-existence of different electron acceptors (phosphate, nitrate and nitrite) at low concentration in the anolyte demonstrated an insignificant effect on MFC performance.

6.4. Future Prospects

The analytical characteristics (selectivity, stability, reproducibility and sensitivity) of MFC biosensor must be improve so that system can be self-sustainable in comparison to other traditional analytical methods and gain acceptance as a standard method. The approach of screening new electrogenic bacteria or consortia that are capable to metabolize a broad range of organic matter including complex polymers relatively fast could be applied to improve MFC biosensor applicability. Directed evolution of mediators involve in extracellular electron transfer and construction of genetic recombinant bacteria could be applied but perhaps the technique of MFC biosensor is not mature enough to pursue gene manipulation methods. The range of response time, detection limit, stability and repeatability differ for each research work, the outcomes of study encourage doing more research.

CHAPTER 7

Extracellular Electron Transfer in Gram Positive *Listeria monocytogenes*

Study Title: Investigating the Role of Ndh1and Ndh2 proteins in Extracellular Electron Transfer in *Listeria monocytogenes*

CHAPTER 7

Investigating the Role of Ndh1and Ndh2 proteins in Extracellular Electron Transfer in *Listeria monocytogenes*

Abstract

Electrobacteriapossess the extracellular electrons transfer (EET) ability to respire on different solid phase electrodes or minerals through different physiological mechanisms. Gram negative model exoelectrogens such as*Geobacter sulfurreducens and* Shewanella *oneidensis* MR-1 have extensively been studied for their EET capabilities. Gram positive bacteria are generally believed to possess weak extracellular electron shuttling activity due to the presence of thick non-conductive cell wall and are, therefore, less understood. *Listeria monocytogenes*, a food-borne pathogen and facultative anaerobe, has recently been reported to possess a novel electron transport chain and can transfer electrons to electrode or iron through a distinctive non-haem flavin based EET. An eight genes-based locus has been identified responsible for the EET in *L. monocytogenes*. Among these genes, Ndh1/NDH-2a and Ndh2/NDH-2b have been proposed to function in respiration and EET using a menaquinone and demethylmenaquinone derivative and need to be characterized further. The present study used chronoamperometry and cyclic voltammetry (CV) to investigate the role of Ndh1/NDH-2a and Ndh2/NDH-2b in EET by growing wild type (WT) and mutant strains (*Δndh1/Δndh-2a, Δndh2 /Δndh-2b,* and *Δndh1/Δndh-2a complementary)* of *Listeria monocytogenes* EGDe in single chamber bioelectrochemical cells with template stripped ultra-smooth gold electrodes modified with self-assembled monolayers (SAMs) of carboxylic acid terminated thiols. The cyclic voltammograms of *L. monocytogenes* showed a catalytic wave at an onset potential of -0.2V and +0.1V which recognized as due to flavin and reduction of iron, respectively. The mutant strain *Δndh1/Δndh-2a* grew on aerobic respiration medium and demonstrated electrochemical activity in the electrochemical cell using TSG electrode and glucose as a source of carbon whereas *Δndh2 /Δndh-2b* failed to show any electrochemical activity in the electrochemical cell. The chronoamperometry and CV results of the study revealed Ndh2/NDH-2b is involved in EET and *L. monocytogenes* was able to respire in the absence of Ndh1/NDH-2a.

Key words: Extracellular electron transfer (EET), Gram positive electrogens, *Listeria monocytogenes* (*Lm*), Ndh1/NDH-2a/complex I, Ndh2/NDH-2b, Cyclic voltammetry, Chronoamperometry.Template stripped gold electrodes, Surface assembled monolayers (SAMs).

7.1 Introduction

Strategies of microbial energy metabolism are variable across the microbial world and it fundamentally reflects the distinct physiochemical features of their environment. Microorganisms residing in anoxic environments respire a range of compounds such as redox-active minerals that contain Fe^{2+}, Fe^{3+} or manganese Mn^{4+} (Kracke et al., 2015). Mineral respiring microorganisms transfer electrons to polyvalent metal ions associated with these minerals and vice versa through haem-based electron transfer process (Pankratova et al., 2019). Bacteria that possess extracellular electron transfer (EET) capability have gained significant attention due to numerous biotechnological applications such as bioremediation,

recovery of metals, microbial fuel cells, biosensing and microbial electrosynthesis(Hederstedt et al., 2020,Pankratova et al., 2019). Bioelectrochemical techniques are governed by the effective microbe-electrode interactions which, in turn, are defined by the characteristics of EET of exoelectrogens(Zheng et al., 2020).

The research on extracellular electron transfer has mainly been carried out in Gram negative bacteria using *Shewanella oneidensis* MR-1 and *Geobacter sulfurreducents*. *Shewanella oneidensis* transfers electrons using outer membrane cytochromes such as MtrCAB. *S. oneidensis* also releases flavins extracellularly that facilitate electron transfer to the electrodes and minerals (Cisternas et al., 2018, Kees et al., 2019). *Geobacter* species use pili and nanowires to transfer electrons between cells and minerals. Gram positive bacteria are generally considered weak exoelectrogens due to their cell wall architectures. A number of Gram positive electrogenic bacteria have been isolated from different microbial fuel cells (MFC) of different configurations and ecological conditions. *Clostridium butyricum* is one of the iron reducing elctrogeinc bacteria isolated initially from a mediator-less MFC. Different electrochemical techniques have been used to study the electroactivity of *C. butyricum* but the mechanisms employed by this bacterium for the transfer of electrons are still unknown (Park et al., 2001). Nonetheless, role of riboflavins has been reported as mediators in extracellular metal reduction process in the *Clostridium* community (Fuller et al., 2014). Recently, Gram positive members of phylum Firmicutes have been reported for their extracellular electron transfer abilities (Pankratova, Hederstedt, et al., 2019). Gorton et al. (2009) reported first the electric communication from *Bacillus subtilis* to the gold and graphite electrodes (Coman et al., 2009). The quinone containing polymer when combined with the respiratory chain of Gram positive *Enterococcus faecalis* in bioelectrochemical cells, enhanced the electron transfer to the electrode (Pankratova, Pankratov, et al., 2019). Again, the transfer of electrons from reduced demethylmenaquinone (DMK) in the outer membrane of *E. faecalis* to the conductive surfaces is not fully known. Gram positive solventogenic *Clostridium acetobutylicum* showed increased flavin secretion under low iron availability in the bioelectrochemical system (Engel et al., 2019). Gram positive *Listeria monocytogenes* is a food borne pathogen associated with decomposing plant matter in the environment and transforms into an intracellular pathogen when enters a mammalian host. It has recently been reported to possess ferric reductase activity and a distinct flavin based EET mechanism for transfer of electrons outside the cells using forward genetics screen. An eight genes based uncharacterized locus has been identified with role in electron transfer (Fig. 7.1). Genes in the locus encode a type II NADH dehydrogenase, a flavoprotein (PplA), two small proteins *EetA* and *EetB*, and enzymes for quinone synthesis. A similar gene cluster is present in many other Gram-positive bacteria, including *Enterococcus faecalis* (Hederstedt et al., 2020). Type II NADH dehydrogenase, Ndh1/complex 1/NDH-2a (lmo2389) is known to catalyze the transfer of electrons from NADH in the respiration (Kerscher et al., 2007). One of the genes in the locus encodes for a protein Ndh2/NDH-2b (lmo2638), 40-70 kDa type II NADH quinone oxidoreductase, has been proposed for its role in ferric reduction and EET using microbial fuel cell and graphite felt anode. Ndh2/NDH-2b contains an N-terminal type II NADH dehydrogenase domain and a C-terminal domain absent from functionally characterized enzymes (Light et al., 2018). Similarly, the role

of Ndh1/NDH-2a in respiration and/or electron transfer activity needs to be further investigated. The studies prompted us to determine the involvement and extent to which Ndh1/NDH-2a and Ndh2/NDH-2b are involved in extracellular electron transfer in *Listeria monocytogenes* EGDe. The wild type (WT), mutant strains *Δndh1/Δndh-2a, Δndh2 /Δndh-2b,* and Δndh1/*Δndh-2a complementary strains* were grown on template stripped gold (TSG) electrodes modified with self-assembled monolayer (SAM) of carboxylic acid terminated thiols in bespoke glass bioelectrochemical cells and characterized using cyclic voltammetry and chronoamperometry.
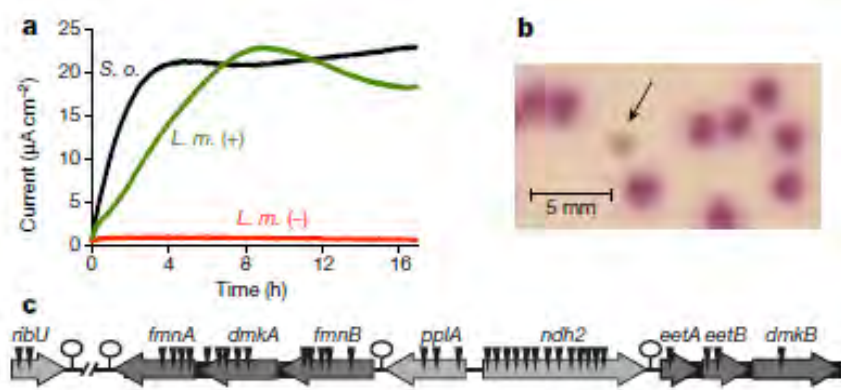
Figure 7. 1 An eight genes based uncharacterized locus associated with extracellular electron transfer (EET) activity in Listeria monocytogenes
(a) Current generation from *L. monocytogenes* (*L. m.*) and *Shewanella oneidensis* (*S. o*) inoculated into MFCs. For the *L. m*, glucose was present (+) as an electron donor or (−) absent in the medium. For *S. o.*, lactate was used as an electron donor (b) One of the thirty-six mutant strains identified from ferric iron reduction screening after the ferrozine agar overlay (c) uncharacterized genes on the locus. Names have been given based on the putative functions of the proteins that they encode (Light et al., 2018).

7.2 Materials and Methods

7.2.1 Growth of *Shewanella oneidensis*-MR1

The chemicals and materials used in this study were obtained from Sigma-Aldrich unless otherwise stated. The *Shewanella oneidensis* MR-1 culture was grown aerobically in 50 ml LB broth (30 $^{\circ}$C, 200 rpm, 16 h) in a flask to an OD_{600}nm > 1. 1 ml of this grown culture was used to inoculate 50 ml of LB supplemented with 50mM lactate and 25mM fumarate using 12.5M stock in a 50ml falcon tube. The top of the tube was fastened shut and the culture was grown overnight at 0 rpm and 30 $^{\circ}$C. The bacteria reached a maximum OD_{600}nm of ~0.7 and pH of 6.25-6.50 before growth ceased. The cells were pelleted via centrifugation (3220 g, 15 min) and washed twice with sterilized 10 ml MOPS buffer (20 mM MOPS, 30mM Na_2SO_4, pH 7.4) before resuspension in 5 ml MOPS buffer. The washed MR-1 suspension was stored at 4 $^{\circ}$C and used within 1-2 h for the electrochemical experiments.

Defined media (DM) contained the following ingredients (per litre): 1.5 g of NH_4Cl (Melford), 0.1g of KCl (BDH laboratory supplies), 0.625 g of Na_2HPO_4 (Melford), 0.213 g of Na_2SO_4, 0.103g of $CaCl_2.2H_2O$ (Fisher Scientific), 0.095g of $MgCl_2$ (ACROS organics), 1.51g of PIPES, 2 ml of trace minerals solution and 10 ml of vitamin solution. In addition to this, lactate was added to a concentration of 10mM. The pH of DM was ~7.4. The defined media was sterilized by filter sterilization (0.22 μm).

The trace mineral solution contained (per litre) 1 g $FeCl_2.4H_2O$, 0.3 g $CoCl_2.6H_2O$, 0.5g of $MnCl_2.4H_2O$, 0.2 g $ZnCl_2$, 0.02 g H_3BO_3, 0.05 g $Na_2MoO_4 \cdot 2H_2O$ (ACROS organics), 0.1 g $NiSO_4 \cdot 6H_2O$, 0.008 g $Na_2WO_4.2H_2O$ (ACROS organics), 0.002 g $CuCl_2 \cdot 2H_2O$ (ACROS organics), 0.006 g $Na_2SeO_3.5H_2O$. The vitamin solution contained (per litre) 0.002 g folic acid, 0.002 g biotin, 0.001 g B6 (pyridoxine) HCl, 0.005 g B2 (riboflavin), 0.005 g B1 (thiamine) HCl, 0.005 g pantothenic acid (Santa Cruz Biotechnology), 0.005 g nicotinic acid, 0.005 g *p*-aminobenzoic acid, 0.005 g lipoic acid, 0.2 g choline chloride, and 0.001 g B12 (cobalamin) crystalline.

7.2.1.1 Supernatant Analysis

MR-1 (OD_{600}nm = 0.25) was incubated for ~22 hours in 2 ml MOPS buffer with 10 mM sodium lactate on a TSG electrode modified with 8OH:8COOH (57:43) mixed SAM and poised at +0.25 V (SHE). To separate the cells from supernatant, the suspension collected from the EC cell was centrifuged at 4500 g and filtered through a 0.22 µm polyethersulfone (PES) filter. The filtered supernatant was analyzed by voltammetry, using fresh TSG electrodes that were prepared as described above.

7.2.2 Growth of Listeria monocytogenes Strains

Listeria monocytogenes wild type, mutant and complementary strains were grown from the frozen stock cultures maintained at -80 ºC on brain heart infusion (Bacto) plates at 37 °C. The deletion mutant and complementary strains were constructed by site specific chromosomal mutagenesis and d IPTG-inducible gene expression after electroporation of *L. monocytogenes* (Monk et al., 2008) and generously provided by the laboratory of Yoshio Nakatani, University of Otago, New Zealand. The strains were derived from the *L. monocytogenes* EGDe. Growth was taken from the BHI plates to inoculate 50 ml *Listeria* synthetic medium (LSM) (Whiteley et al., 2015) containing 50mM glycerol (aerobic respiration medium) and incubated in a flask to an OD_{600} nm = 0.1. 2 ml (OD 0.1) of culture was inoculated in the electrochemical cell (EC) with 55.5 mM glucose using 1M stock and poised at +0.25 V (SHE) for ˜21h with continuous argon gas supply. To confirm that the electron transfer is due to the electrochemical activity of the cells, the *L. monocytogenes* cells were filtered out from the suspension and the remaining filtrate was analysed again by CV in the EC applying fresh electrode. To find the presence of biofilm on the surface of electrode in the EC after 20 hours, the *Lm* suspension with cells was removed and replaced with fresh LSM and glucose. The electrode was poised again at 0.05 V for 15-20 hours and CV was recorded.

7.2.3 Self-assembled Monolayer (SAM) Modified Template Stripped Gold Electrodes

The template-stripped gold (TSG) electrodes were prepared following the protocol as described previously (Stamou et al., 1997). For self-assembled monolayers (SAMs) on the surfaces of electrodes, the TSG glass slides were incubated in 1 ml H_2O (Milli-Q) with 1 mM of thiol, 8-mercapto-1-octanol (8-OH) to form a neutral surface electrode or a 57:43 mixture of 8-OH and 8-mercaptooctanoic acid (8-COOH) for a negatively charged surface electrode. The slides were incubated in the thiol solution at 4 ºC for at least 16 h. Before use, the electrodes were washed with isopropanol and dried under a stream of N_2 gas.

7.2.4 Electrochemical Analysis

For the electrochemical experiments, a bespoke glass single chamber electrochemical cell (EC) held in a Faraday cage, was used in a standard three-electrode set-up (Figure 7.2). TSG electrode (surface area = 0.24 cm^2) modified with a neutral or negative SAM served as a working electrode and was embedded in a polytetrafluoroethylene (PTFE) holder with a rubber O-ring seal. The electrochemical cell was assembled with working electrode (modified TSG) placed with a copper wire in the holder along with a platinum wire counter electrode and a mercury/mercury sulphate (Hg/Hg$_2$SO$_4$) or a saturated Ag/AgCl reference electrode (Radiometer analytical, France). The potentials applied were converted with respect to a standard hydrogen electrode (SHE) such as +651 mV vs SHE for the Hg/Hg$_2$SO4 and 0.2V vs SHE for Ag/AgCl reference electrode. MOPS buffer (20 mM MOPS, 30 mM Na$_2$SO$_4$, pH 7.4) or a defined media (composition described under section 7.2.1) was used as a basal electrolyte solution for all experiments, continuously purged with Argon, unless stated otherwise.

Before the start of each experiment, the SAM condition was qualitatively examined using electrochemical impedance spectroscopy (EIS) for the presence of pin hole defects in the SAM films (Boubour & Bruce Lennox, 2000, Sharma et al., 2016). Presence of defects in the SAMs contributes to the impedance of films which affects the permeability and leakiness of the SAMs. Excessive permeability is detected in the form of significant decrease in phase angle in the Bode phase plot from 90° under low frequency (< ~50 Hz). An angle below 85° indicated the SAM was of poor quality and was not applied in the experiment. Multiple electrodes were prepared for each experiment to replace the electrode with poor SAM and for repeated testing.

For a typical experiment, 2ml (OD$_{600}$ = 0.1) of the *Listeria* cultures in aerobic respiration medium was added in the electrochemical cell (EC) and then 50mM glucose (source of carbon for the respiration) using 1M stock solution. The electrode was poised at + 0.25 V vs SHE (0.05 V vs Ag/AgCl) for 21h with continuous supply of Ar to promote the e EET to the working electrode. For the experiments with *S. oneidensis* MR-1 (the reference strain), the washed MR-1 was added to the electrochemical cell to an OD$_{600}$ nm=0.45. Sodium lactate (10 mM) was added from a 200 mM stock solution and the electrode was poised at +0.25 V vs SHE. Cyclic voltammetry was used to assess the interaction of bacteria on the modified electrodes at different times. In some experiments, where needed, defined media (DM) replaced the MOPS buffer as the basal electrolyte solution.

The electrochemical measurements were carried out using an Autolab electrochemical analyser (Ecochemie, Utrecht, Netherlands) equipped with a PGSTAT 128N potentiostat, SCANGEN and ADC750 modules, and a FRA2 frequency analyser (Ecochemie). CV measurements were regularly recorded by holding the potential at 0 V for 5 s before cycling the potential between +0.4 V to −0.4 V vs. SHE at a scan rate of 0.01 V/s. The electrochemical experiments reported in this study were carried out at 20 °C. The experiments were also performed in dual chamber microbial fuel cells using graphite felt anode and platinum as a cathode following the methods of Light et al., (2018) (data not shown here).
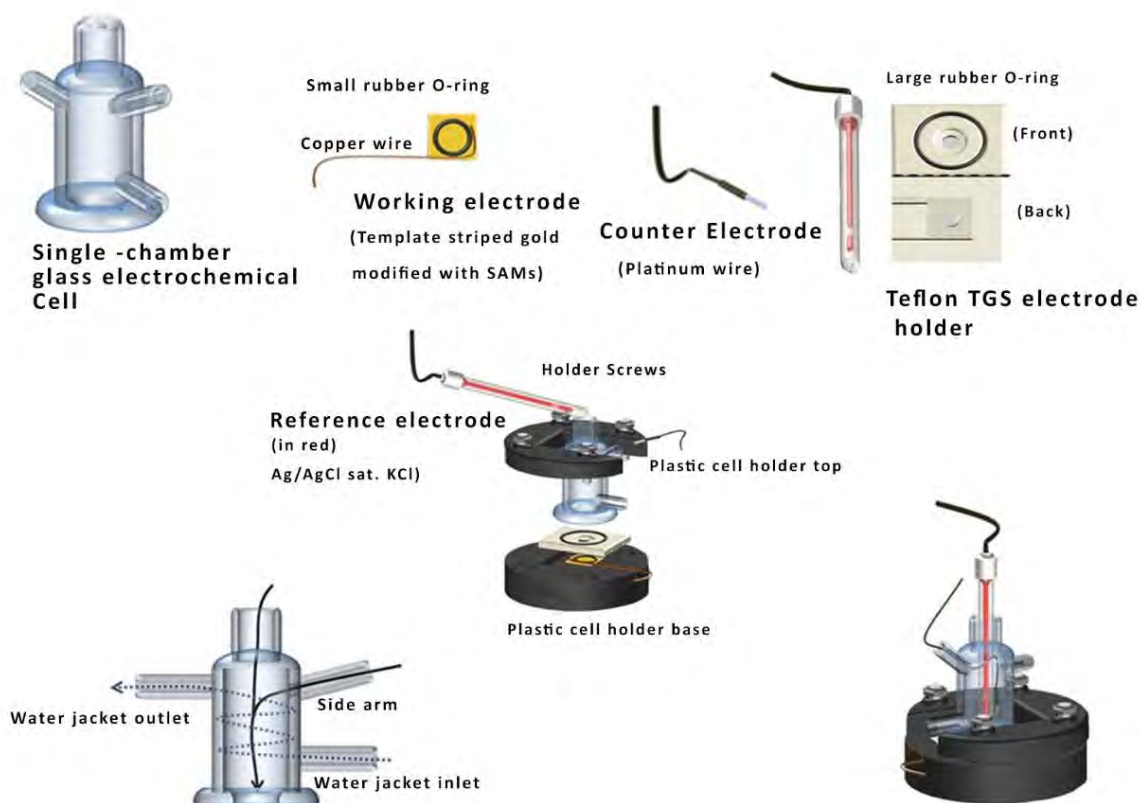
Figure 7. 2 Diagram of the bespoke glass electrochemical cell set up that was employed in the electrochemical experiments for this study.

7.3 Results

Generally, the carbon-based electrodes with higher surface to volume ratio are preferred to apply in bioelectrochemical systems (BES) for growth of bacteria/biofilms to study electrochemical activities. This study used ultra-smooth template stripped gold electrodes with self-assembled monolayers (SAM) in single chamber electrochemical cells for reproducible surface properties in low capacitances and precision voltammetry for understanding extracellular electron transfer (EET) mechanisms in *Listeria monocytogenes*. MOPS buffer (pH 7.4) was used in the electrochemical cell as a basal electrolyte to avoid complications in analysis due to the presence of redox molecules and trace elements.

7.3.1. Extracellular Electron Transfer in *Shewanella oneidensis* MR-1

Shewanella oneidensis was grown in LB broth at $30^{\circ}C$ and 200 rpm aerobically to an OD_{600} (nm)> 1, was used to inoculate 50ml LB broth containing lactate (50 mM) and fumarate (25 mM) and grown anaerobically. When the bacteria reached an $OD_{600} \approx 0.7$, the MR-1 cells were pelleted by centrifugation (3230 g for 15 min.), washed twice with filter sterilized MOPS buffer (20 mM MOPS, 30 mM Na_2SO_4, pH 7.4) and resuspended in 5ml MOPS buffer. The washed MR-1 suspension was added in the electrochemical cell (EC) fitted with the gold electrodes containing SAMs of either neutral (8-mercapto-

1-octanol (8-OH)) or negative (8-OH and 8-mercaptooctanoic acid (8-COOH)) surface. For respiration activity, lactate was added as a source of carbon and the electrodes were poised at +0.25 V versus, SHE. The catalytic waves started to appear after ≈ 3 hours with different onset potentials in case of both surfaces at -0.2V for the neutral surface (Figure 7.3-7.4), and +0.1 V for the negative surface (Figure 7.5). The different onset potentials on both surfaces indicated different surface chemistry affects the mechanism used by the bacteria to transfer electrons to the electrodes. The catalytic current at -0.2V is generally accepted to be due to the electron transfer mechanism via flavin (Carmona-Martinez et al., 2011) whereas the onset at +0.1V is due to EET mechanism that involved iron for electron transfer to the electrode.
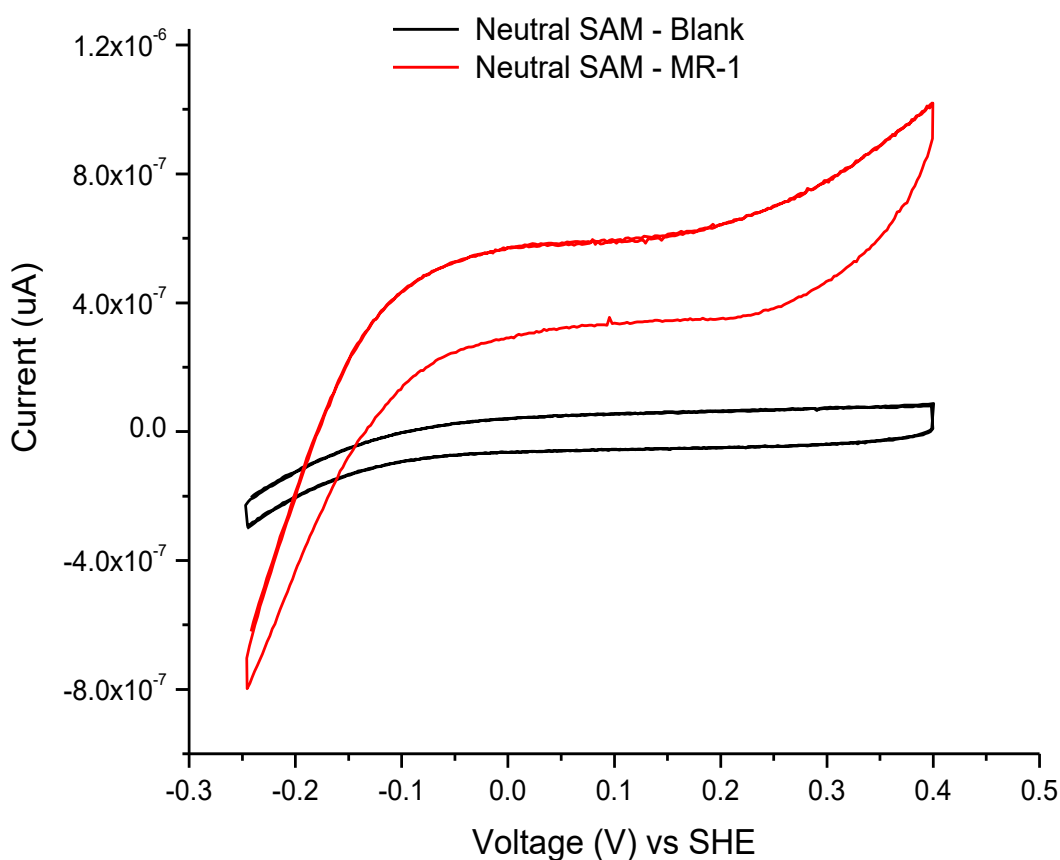
Figure 7. 3 Cyclic voltammograms (CV) of *Shewanella oneidensis*-MR1

CV *of S oneidensis*-MR1 on template stripped gold (TSG) electrode modified with surface assembled monolayer (SAM) of 8-OH (neutral surface), after incubation of MR1 in 10mM lactate (DL), 20mM MOPS buffer (20mM MOPS, 30mM Na_2SO_4, pH 7.4) at +0.25V for 24 hours at 20°C in electrochemical cell. **Black** line; baseline measured before incubation with MR-1 for TSG electrode modified with SAM of 8-OH.Red line; CV obtained after 24 hours of incubation of MR-1 into the electrochemical cell at 20°C. Reference electrode; Ag/AgCl. Scan rate 0.01V/s.
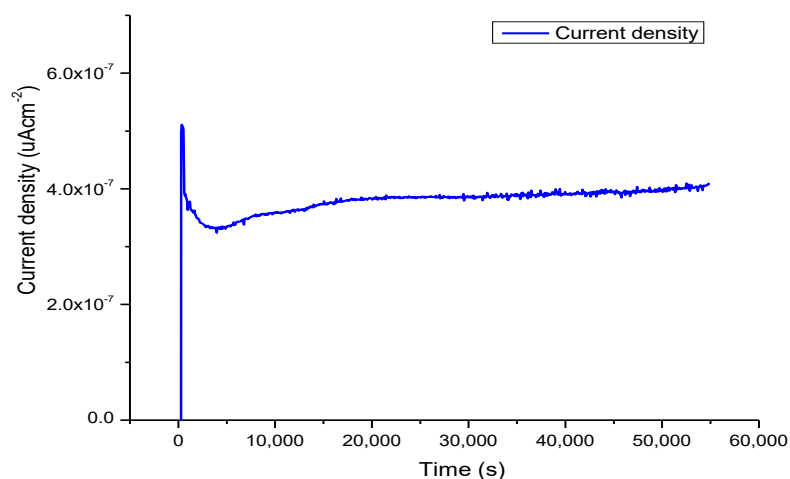
Figure 7. 4 Chronoamperometry of *S. oneidensis* MR-1 on TSG electrode modified with surface assembled monolayer (SAM) of 8-OH (neutral surface), after incubation of MR-1 in 10mM lactate, 20 mM MOPS poised at +0.25 V for 21 hours at 20 °C in the electrochemical cell.
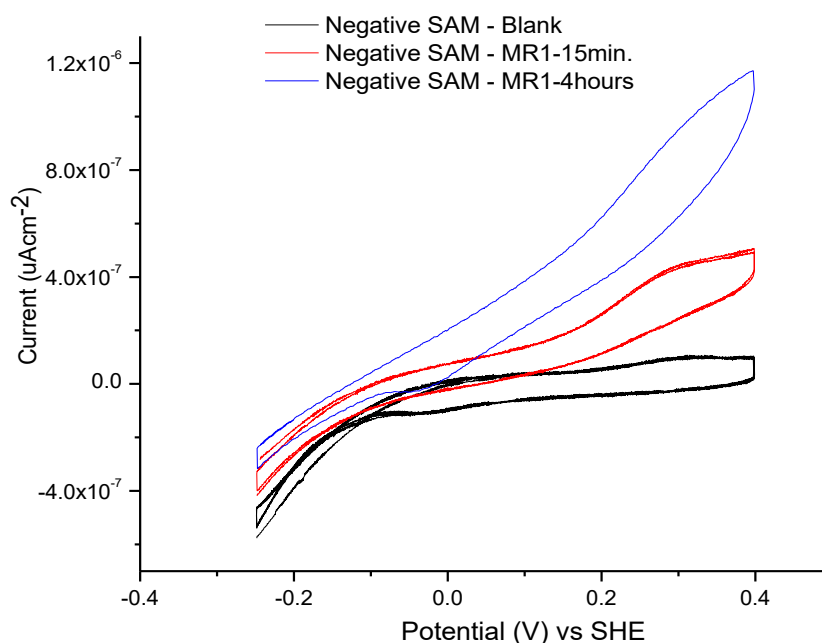
Figure 7. 5 Cyclic voltammograms (CV) of S. oneidensis MR-1

CV of *S. oneidensis* MR-1 on template stripped gold (TSG) electrode modified with surface assembled monolayer (SAM) of mixed 8-OH:8-COOH (negative surface), after incubation of MR-1 (OD_{600} = 0.3) in

10mM lactate (DL), 20mM MOPS buffer (20 mM MOPS, 30 mM Na_2SO_4, pH 7.4) at +0.25V for 4 hours at 20 $^\circ$C. **Black**; Baseline measured before incubation with MR-1 for TSG electrode modified with SAM of mixed 8-OH:8-COOH. Red; CV obtained after 15 minutes of incubation of MR- into the electrochemical cell. Blue; CV after ≈ 3.5 hours of MR1 incubation into the electrochemical cell at 20 $^\circ$C. Reference electrode; Ag/AgCl, Scan rate; 0.01V/s.

7.3.2. Extracellular Electron Transfer in *Listeria monocytogenes (Lm)*

The wild type, mutant and complementary strains of *Listeria monocytogenes* were grown on brain heart infusion (Bacto) at 37 $^\circ$C (Figure 7.6). Filter sterilized brain heart infusion (Bacto) medium or modified chemically defined modified Listeria synthetic medium (LSM) (Whiteley et al., 2015) containing 0.8 µM FMN as the sole flavin was used in all studies. For aerobic respiration medium (ARM), the 55.5 mM glucose in the LSM was replaced with glycerol (50mM). *L. monocytogenes* growth was taken from the plates to inoculate 50 ml LSM with 50mM glycerol (aerobic respiration medium). A small proportion (2 ml) of the culture grown in the ARM (OD_{600} = 0.1) was added into the electrochemical cell along with 55 mM glucose and poised at +0.25 V (SHE) with continuous argon purging.
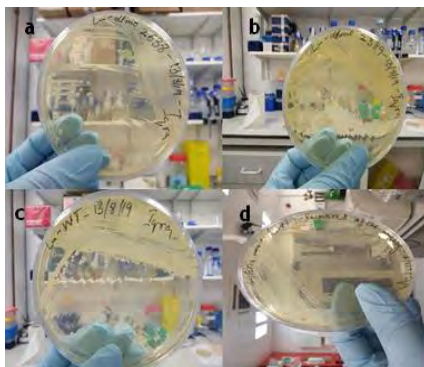
Figure 7. 6 Growth of *Listeria monocytogenes* strains
(a) *Listeria monocytogenes* EGDe wild type growth on brain heart infusion (BHI) agar plate after 24 hours (b) *L. monocytogenes* EGDe *dlmo* 2389 (*Δndh1/ndh-2a*) growth on brain heart infusion (BHI) agar plate after 24 hours (c) *L. monocytogenes* EGDe *dlmo* 2638 (*Δndh2/Δndh-2b*) growth on brain heart infusion (BHI) agar plate after 24 hours. (d) *L. monocytogenes* EGDe wild type growth recovered on brain heart infusion agar plate after washing (with MOPS buffer; pH 7.4) and overnight incubation anaerobically at 37 $^\circ$C.

Table 7. 1 Growth (OD$_{600}$) measurements of *S. oneidensis* and *L. monocytogenes* in different growth media.

No.	Bacteria/media	OD$_{600}$
1	*S. oneidensis* MR-1 in defined media at t0	0.05
2	*S. oneidensis* MR-1 grown aerobically in defined medium	0.159
3	MR1 grown anaerobically (overnight) in defined medium using 1ml suspension of MR-1 in LB broth (grown aerobically).	0.154 (0.209 after 48hours of incubation)
4	OD$_{600}$ of media recovered after centrifugation and removal of MR-1 cells (incubated anaerobically in defined medium)	0.07
5	Brain heart infusion broth	0.1
6	*Listeria monocytogenes* (wild type) after overnight incubation in brain heart infusion broth	0.171 1.4
7	*L. monocytogenes* dlmo2389-(*Δndh1*/*Δndh-2a*) (aerobic growth in BHI after 24hours)	2.6
8	*L. monocytogenes* dlmo2389 (anaerobic growth after 24 hours in falcon tube)	0.184
9	Listeria synthetic medium (LSM)	0.048
10	*L. monocytogenes* wild type + LSM (incubated overnight aerobically)	0.193
11	*L. monocytogenes* wild type + LSM (incubated overnight anaerobically in 50 ml falcon tube)	0.111
	L. monocytogenes wild type (pellet from 2 ml aerobic growth) + LSM(incubated overnight	0.36

	(17h) anaerobically in 50 ml falcon tube)	
12	*L. monocytogenesdlmo*2389 -(*Δndh1*/*Δndh-2a*) + LSM (anaerobic growth after ≈20 hours in falcon tube)	0.092

For the extracellular electron transfer activity, the electrodes were poised at +0.25V with the *L. monocytogenes* WT strain up to an OD_{600} of 0.1 in the electrochemical cell and glucose as a source of carbon. A weak catalytic wave appeared with an onset potential at -0.2V and a second wave at an onset potential of +0.1 V, after ˜3 hours the electrodes were poised (Fig. 7.7). To validate that the catalytic waves are due to the activity of *L. monocytogenes* biofilm on the surface of electrode, the contents of electrochemical cell were removed and replaced with fresh LSM and glucose. The catalytic waves were not observed in the CV scanned immediately after the electrode was poised but the wave appeared at an onset potential of +0.1 V after 15h (Fig. 7.8). To further ensure that the catalytic current and waves are due to the electrochemical activity of the bacteria, the contents of the electrochemical cell were removed, the medium separated from the bacterial cell using centrifugation and filtration (0.22 um). The electrolyte/medium without bacteria was again incorporated into the electrochemical cell using a fresh electrode and the CV was recorded. The CV obtained from the filtered supernatant demonstrated the catalytic waves were due to electrochemical activity of the bacteria (Fig. 7.9).

To determine the presence of onset potential at -0.2 V, the *L. monocytogenes* WT strain culture in the aerobic respiration medium was grown on the TSG electrode in the MOPS buffer as a basal electrolyte with the addition of 10uM riboflavin. The CV after 21h of poising the electrode showed the presence of electro catalytic wave at an onset potential -0.2 V (Fig. 7.10).

Figure 7. 7 Cyclic voltammograms of *Listeria monocytogenes* wild type (WT) strain (OD600; 0.1)

L. monocytogenes wild type (WT) wasgrown on TSG electrodes modified with SAMs of pure 8- OH (neutral surface) after incubation of 0h, 3.5h and 17h in the modified LSM and glucose in the electrochemical cell poised at +0.25 V. **Black** line; The baseline measured with MOPS buffer before incubation with *L. monocytogenes* for TSG electrodes modified with SAMs of 8- OH. Red; CV obtained after adding *L. monocytogenes* (OD_{600}; 0.1) at t = 0. Blue; CV obtained after adding *L. monocytogenes* (OD_{600}; 0.1) at t = 3.5h. Magenta; CV obtained after adding *L. monocytogenes* (OD_{600}; 0.1) at t = 17h. Reference electrode: Ag/AgCl, Scan rate: 0.01 V/s.

*The growth was taken from BHI plate for inoculation into LSM + 50 mM glycerol (aerobic respiration media).
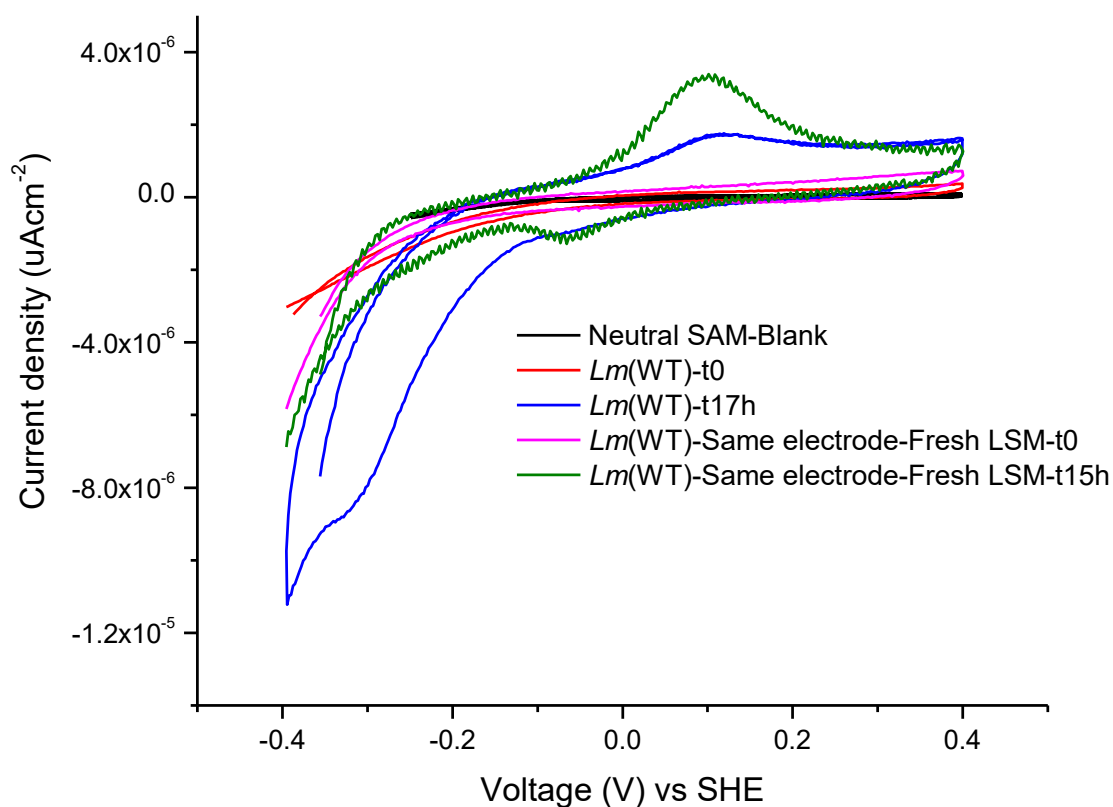
Figure 7. 8 Cyclic voltammograms of *L. monocytogenes* wild type (WT) strain (OD600; 0.1)
L. monocytogenes wild type (WT) strain**was** grown on TSG electrodes modified with SAMs of pure 8-OH (neutral surface) after incubation of 0h (red line), and 17h (blue line) in the modified LSM and glucose in the electrochemical cell poised at +0.25 V. **Black** line; The baseline measured with MOPS buffer before incubation with *L. monocytogenes* for TSG electrodes modified with SAMs of 8- OH. Magenta line; CV obtained using the same electrode (containing bacterial growth) with fresh LSM at t = 0h. Green line; CV obtained using the same electrode (containing bacterial growth) with fresh LSM at t = 015. Reference electrode: Ag/AgCl, Scan rate: 0.01V/s.
*The growth was taken from BHI plate for inoculation into LSM + 50 mM glycerol (Aerobic respiration media).

Figure 7. 9 Cyclic voltammograms of *L. monocytogenes* **wild type (WT) strain (OD600; 0.1).**
L. monocytogenes wild type (WT) strain**was** grown on TSG electrodes modified with SAMs of pure 8-OH (neutral surface) after incubation of 0h (red line), and 17h (blue line) in the modified LSM and glucose in the electrochemical cell poised at +0.25 V. Black line; The baseline measured with MOPS buffer before incubation with *L. monocytogenes* for TSG electrodes modified with SAMs of 8- OH. Magenta line; CV obtained using the fresh TSG electrode and filtered supernatant (growth medium used to grow *L. monocytogenes* for ~20 hours in the electrochemical cell after removing the *L. monocytogenes* cells by centrifugation and filtration (0.22 um filter). Reference electrode: Ag/AgCl, Scan rate: 0.01 V/s.
*The growth was taken from BHI plate for inoculation into LSM + 50 mM glycerol (aerobic respiration media).
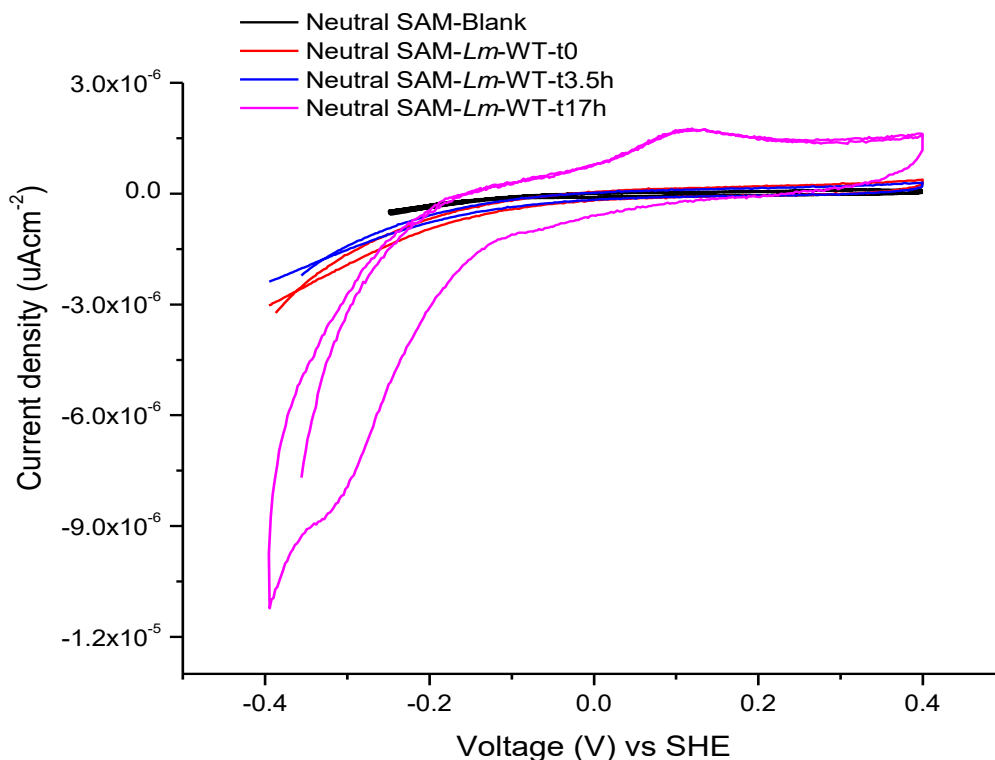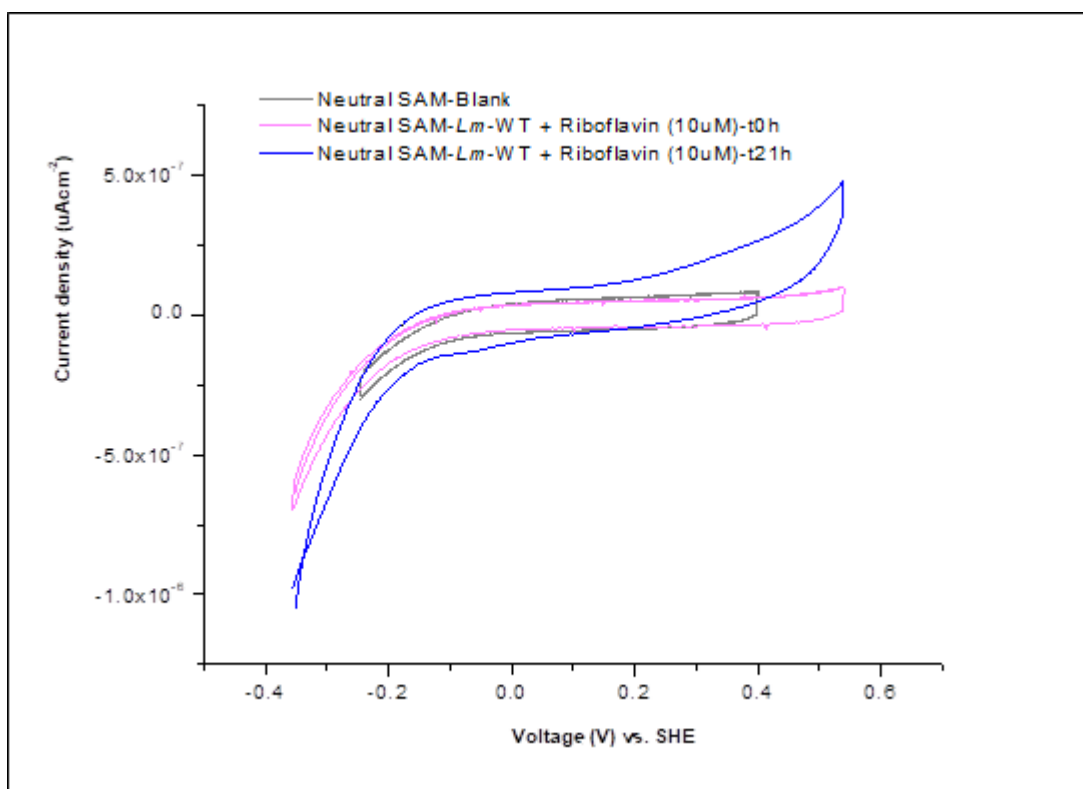
Figure 7. 10 Cyclic voltammograms of *L monocytogenes* wild type (WT) strain (OD600; 0.1).
L. monocytogenes wild type (WT) strain was grown on TSG electrodes modified with SAMs of pure 8-OH (neutral surface) poised at +0.25 V after incubation of 0h and 21h in the MOPS buffer electrolyte (pH 7.4) in the presence of 10uM riboflavin. **Grey** line; the baseline measured with MOPS buffer before incubation with *L. monocytogenes* using TSG electrodes modified with SAMs of 8- OH. **Magenta;** CV obtained after adding *L. monocytogenes* (OD$_{600}$; 0.1) and riboflavin (10 uM) at t = 0h. **Blue**; CV obtained after adding *L. monocytogenes* (OD$_{600}$; 0.1) and riboflavin (10 uM) at t = 21h. Reference electrode: Ag/AgCl, Scan rate: 0.01 V/s.
*The growth was taken from BHI plate for inoculation into LSM + 50mM glycerol (Aerobic respiration media).

The *Listeria monocytogenesdlmo*2389 (*Δndh1/ndh-2a*) strain (OD$_{600}$; 0.1) in the aerobic respiration medium was added into the electrochemical cell with TSG electrodes and glucose was added as a source of carbon. The catalytic waves again appeared at an onset potential of -0.2 V and +0.1 V after the electrodes were poised at +0.25 V (SHE). The *Δndh1/ndh-2a* strain, in contrast to the wild type strain, showed more catalytic current (Figure 7.12). Then the contents of the electrochemical cell were removed and replaced with fresh LSM. The same electrode containing the bacterial cells was poised at +0.25 V for another period of 16.5h and CV was recorded. The voltammograms obtained (Fig. 7.12) showed the catalytic waves at the same onset potentials as in figure 7.11.
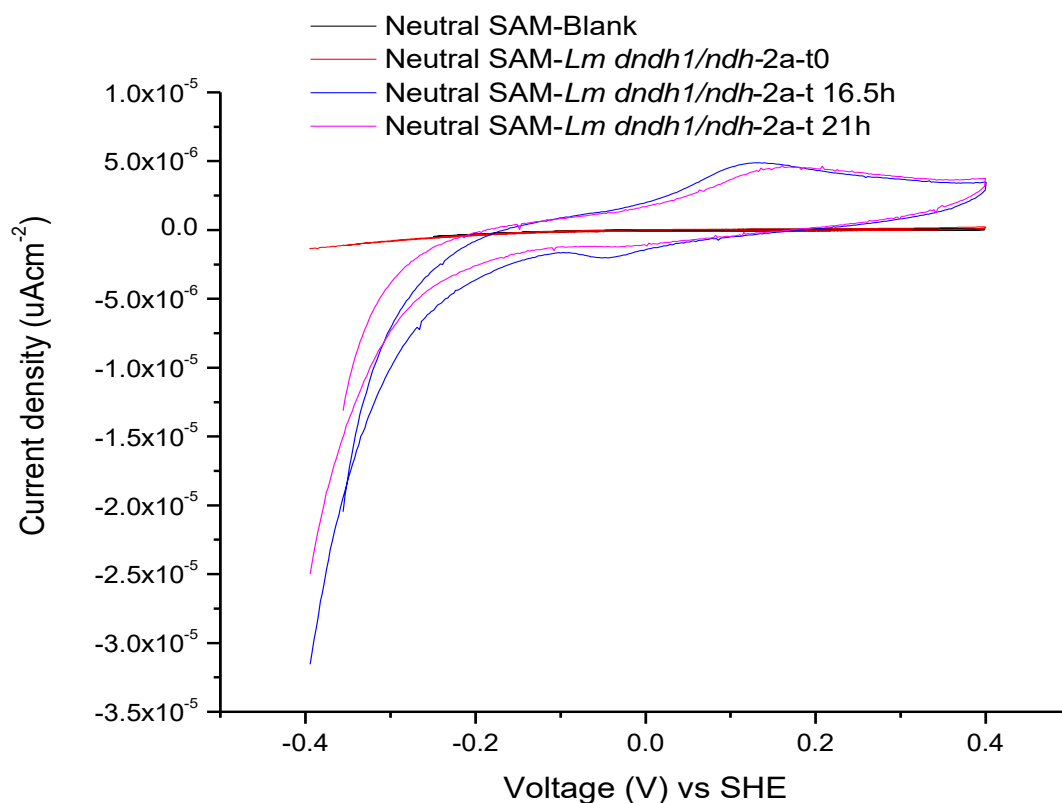
Figure 7. 11 Cyclic voltammograms of *L. monocytogenes* dlmo2389 (Δndh1/ndh-2a) strain (OD600; 0.1).

*L. monocytogenesdlmo*2389 (*Δndh1/ndh-2a*) strain was grown on TSG electrodes modified with SAMs of pure 8- OH (neutral surface) after incubation of 0h, 16.5h and 21h in the modified LSM and glucose in the electrochemical cell poised at +0.25 V (SHE). **Black** line; The baseline measured with MOPS buffer before incubation with *L. monocytogenes dlmo*2389 using TSG electrodes modified with SAMs of 8- OH. Red; CV obtained after adding *dlmo*2389 (OD$_{600}$; 0.1) at t = 0. Blue; CV obtained after adding *L. monocytogenes* (OD$_{600}$; 0.1) at t = 16.5h. Magenta; CV obtained after adding *L. monocytogenes* (OD$_{600}$; 0.1) at t = 21h.   Reference electrode: Ag/AgCl, Scan rate: 0.01 V/s. *Growth was taken from BHI plate for inoculation into LSM + 50 mM glycerol (Aerobic respiration media; OD600: 0.1).
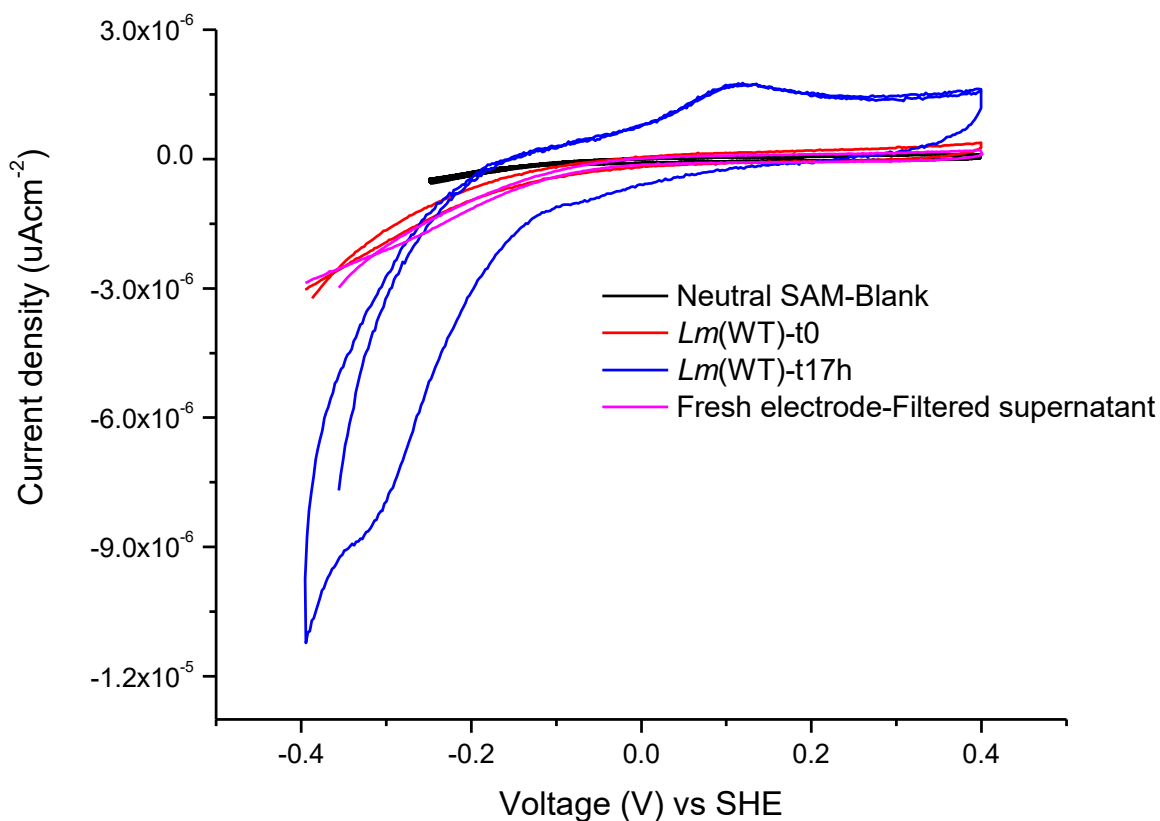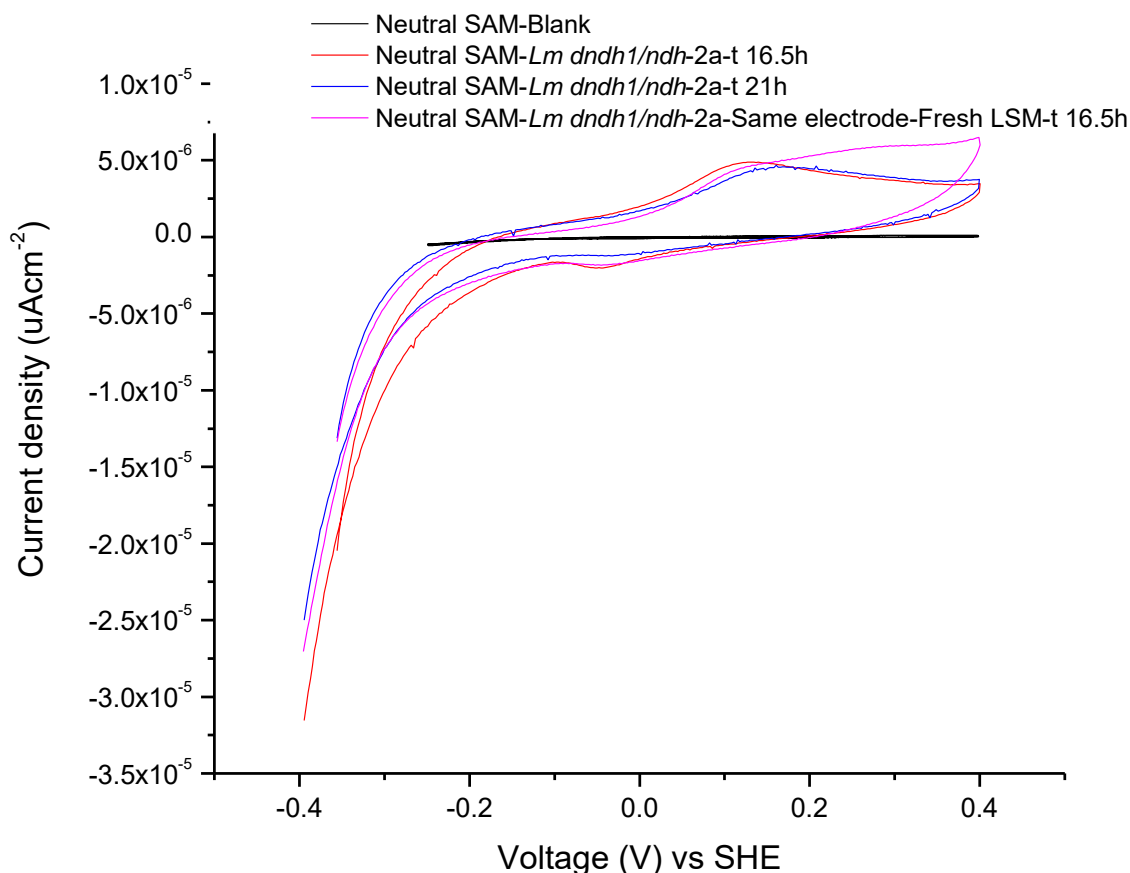
Figure 7. 12 Cyclic voltammograms of *L. monocytogenes* dlmo2389 (Δndh1/ndh-2a) strain

*L. monocytogenesdlmo*2389 (*Δndh1/ndh-2a*) strain wasgrown on TSG electrodes modified with SAMs of pure 8- OH (neutral surface) after incubation of 16.5h (red line), and 21h (blue line) in the modified LSM and glucose in the electrochemical cell poised at +0.25 V (SHE). **Black** line; the baseline measured with MOPS buffer before incubation with *L. monocytogenesdlmo*2389 for TSG electrodes modified with SAMs of 8- OH. Magenta line; CV obtained using the same electrode (containing bacterial growth/biofilm) with fresh LSM and glucose at t = 16.5h. Reference electrode: Ag/AgCl, Scan rate: 0.01 V/s (the growth was taken from BHI plate for inoculation into LSM + 50 mM glycerol (aerobic respiration medium; OD_{600}; 0.1)).

The *Listeria monocytogenesdlmo*2638 (*Δndh2/ndh-2b*) failed to show any significant electrochemical activity when the electrode was poised at +0.25 V for ˜20-21 hours (Fig. 7.13-7.15). The chronoamperometry figure (Fig. 7.18) shows the absence of electron transfer to the electrode. The *L. monocytogenesdlmo*2389 (*Δndh1/ndh-2a*) complementary strain showed catalytic waves at an onset potential of ˜-0.2 V and +0.1 V as shown by the *L. monocytogenesdlmo*2389 (*Δndh1/ndh-2a*) (Fig. 7.16).
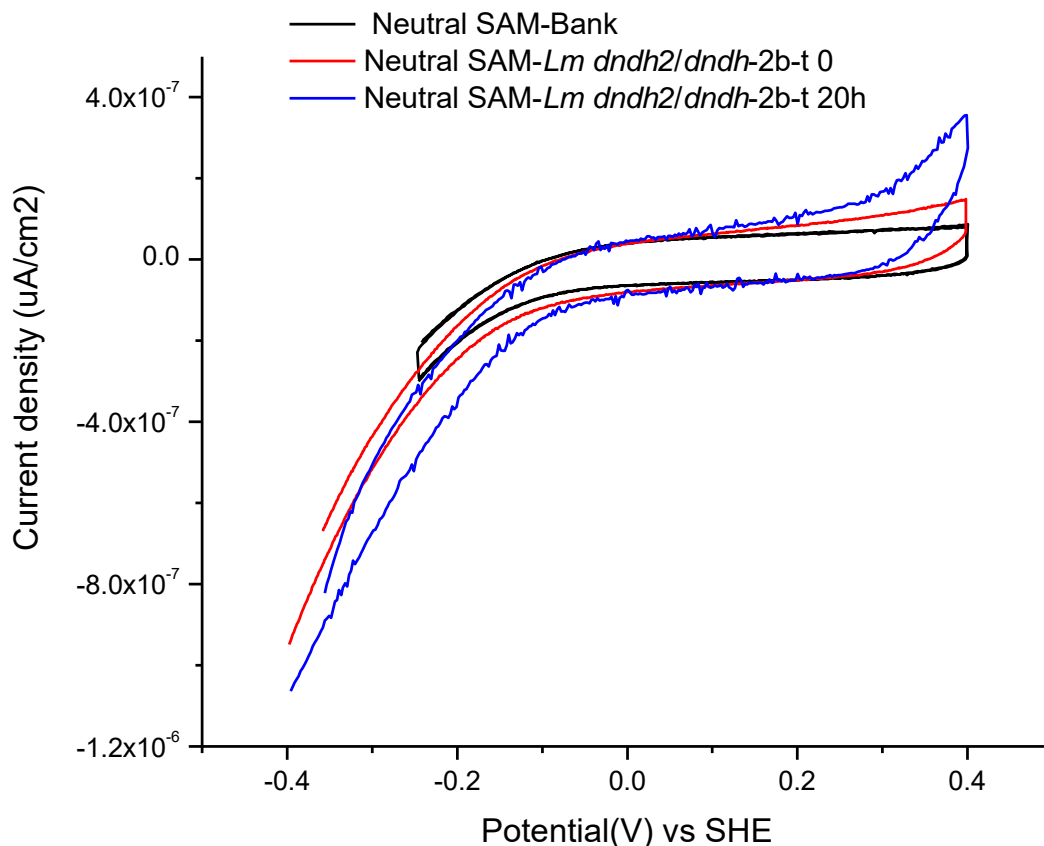
Figure 7. 13 Cyclic voltammograms of *L. monocytogenes* dlmo2638 (Δndh2/ndh-2b)

L. monocytogenes dlmo2638 (Δndh2/ndh-2b) strain wasgrown on TSG electrodes modified with SAMs of pure 8- OH (neutral surface) after incubation of 0h and 20h in the modified LSM and glucose in the electrochemical cell poised at +0.25 V (SHE). **Black** line; the baseline measured with MOPS buffer before incubation with *L. monocytogenes* dlmo2638 using the electrodes modified with SAMs of 8- OH. Red; CV obtained after adding dlmo2638 (OD_{600}; 0.1) at t = 0. Blue; CV obtained after adding *L. monocytogenes* (OD_{600}; 0.1) at t = 20h.   Reference electrode: Ag/AgCl, Scan rate: 0.01 V/s.

*Growth was taken from BHI plate for inoculation into LSM + 50 mM glycerol (aerobic respiration media; OD_{600}: 0.1).
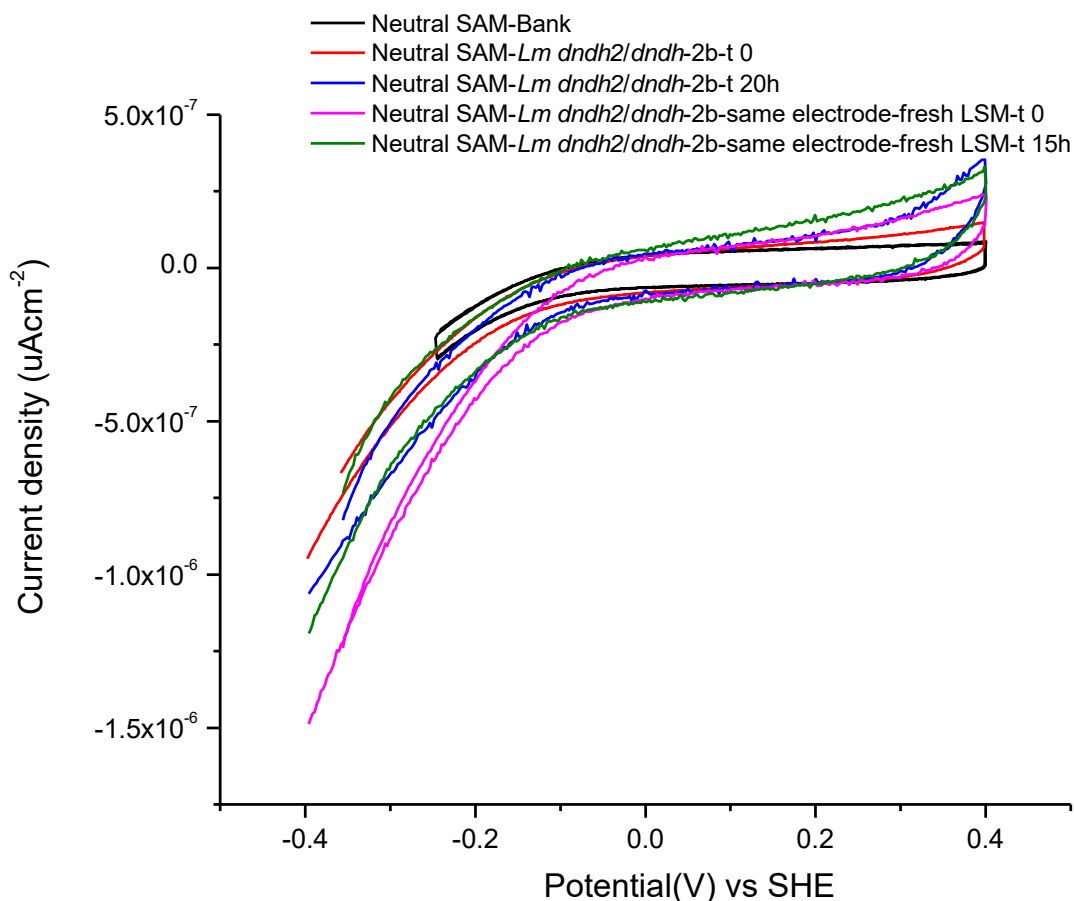
Figure 7. 14 Cyclic voltammograms of *L. monocytogenes* dlmo2638 (Δndh2/ndh-2b).
*Listeria monocytogenesdlmo*2638 (*Δndh2/ndh-2b*) strain was grown on TSG electrodes modified with SAMs of pure 8- OH (neutral surface) after incubation of 0h (red line), and 20h (blue line) in the modified LSM and glucose in the electrochemical cell poised at +0.25 V (SHE). **Black** line; the baseline measured with MOPS buffer before incubation with *L. monocytogenesdlmo*2638 using TSG electrodes modified with SAMs of 8- OH. Magenta line; CV obtained using the same electrode (containing bacterial growth/biofilm) with fresh LSM and glucose (55 mM) at t = 0h. Green line; CV obtained using the same electrode (containing bacterial growth/biofilm) with fresh LSM and glucose at t = 15h. Reference electrode: Ag/AgCl, Scan rate: 0.01 V/s.

*Growth was taken from BHI plate for inoculation into LSM + 50 mM glycerol (Aerobic respiration medium; OD_{600}; 0.1).
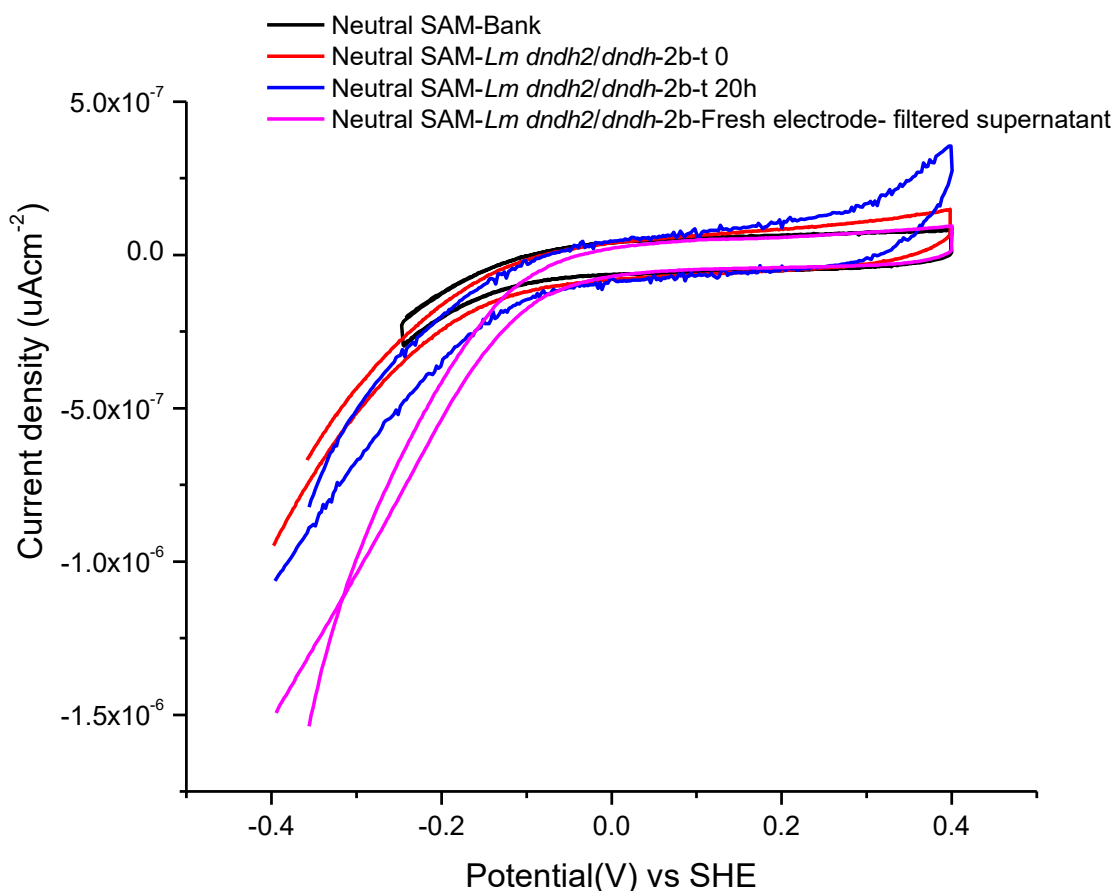
Figure 7. 15 Cyclic voltammograms of _L. monocytogenes_ dlmo2638 (Δndh2/ndh-2b).
_L monocytogenesdlmo_2638 (_Δndh2/ndh-2b_) strain was grown on TSG electrodes modified with SAMs of pure 8- OH (neutral surface) after incubation of 0h (red line), and 20h (blue line) in the modified LSM and glucose in the electrochemical cell poised at +0.25 V (SHE). **Black** line; the baseline measured with MOPS buffer before incubation with _L. monocytogenes Δlmo_2638 using the electrodes modified with SAMs of 8- OH. Magenta line; CV obtained using the fresh TSG electrode and filtered supernatant (growth medium used to grow _L. monocytogenes Δlmo_2638 for ~20 hours in the electrochemical cell after removing the _L. monocytogenes Δlmo_2638 cells by centrifugation and filtration (0.22 um filter). Reference electrode: Ag/AgCl, Scan rate: 0.01 V/s.
*Growth was taken from BHI plate for inoculation into LSM + 50 mM glycerol (aerobic respiration media; OD_{600}; 0.1).
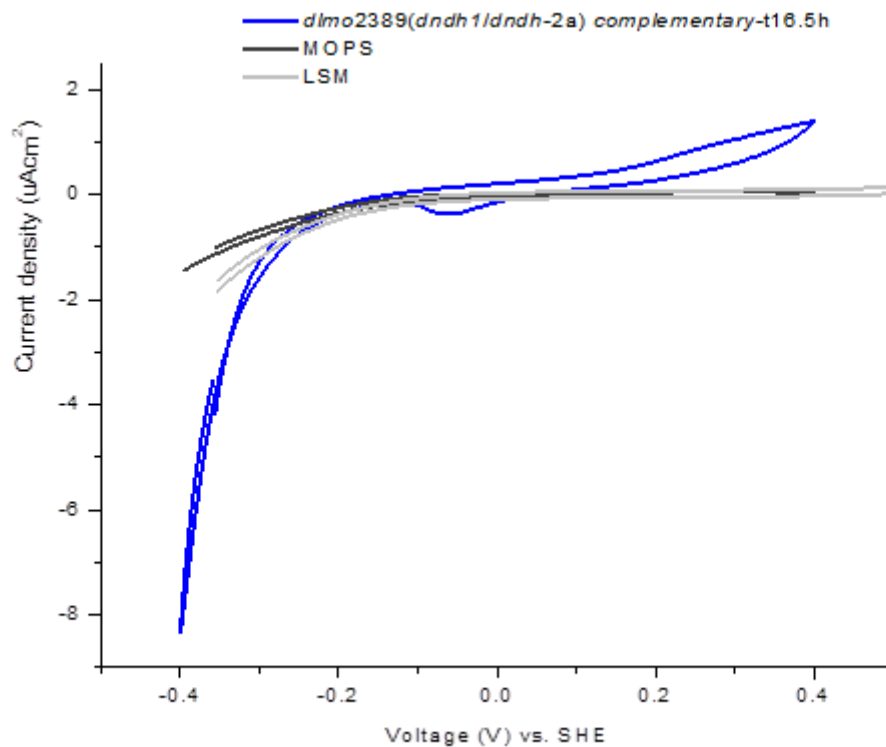
Figure 7. 16 Cyclic voltammograms of *L. monocytogenes* **dlmo2389 (Δndh1/Δndh -2a) complementary strain.**

*L. monocytogenesdlmo*2389 (*Δndh1/Δndh* -2a) complementary strainwas grown on TSG electrodes modified with SAMs of pure 8- OH (neutral surface) (blue line) after incubation of 16.5h in the modified LSM and glucose in the electrochemical cell poised at +0.25 V. **Black** and grey lines; The baselines measured with MOPS buffer and LSM before incubation with *L. monocytogenes dlmo*2389 complementary strain using TSG electrodes modified with SAMs of 8- OH.   Reference electrode: Ag/AgCl, Scan rate: 0.01 V/s, d=Δ, Voltage applied: +0.4 V - 0.4 V/s.

*Growth was taken from BHI plate for inoculation into LSM + 50 mM glycerol (Aerobic respiration media; OD_{600}; 0.1).

Chronoamperometry Results of *Listeria monocytogenes*strains (WT, *Δnhd1/Δndh-2a*, Δndh2-ndh-2b, *Δnhd1/Δndh-2a* complementary)

Figure 7. 17 Chronoamperometry of different *L. monocytogenes* strains.
*L. monocytogenes*strainsWT, dlmo2389 (*Δnhd1/Δndh-2a*), dlmo2639 (Δndh2-ndh-2b) and dlmo2389 (*Δnhd1/Δndh-2a)* complementary strains were poised at + 0.25 V (SHE) for approximately 21 hours using modified LSM with 55mM glucose. The strains were initially grown in aerobic respiration medium (LSM with glycerol) up to an OD_{600} of 0.1 and added into the electrochemical cells fitted with TSG electrodes with neutral surface. Reference electrode: Ag/AgCl, the graphs were drawn as an average of three independent experiments.

7.4. Discussion

Gram negative bacteria such as *Shewanella oneidensis* MR-1 are able to secrete redox active flavins to transfer electrons from the surface of the bacterial cell to the electron acceptors in a process known as 'electron shuttling'. *Listeria monocytogenes*, as an auxotroph utilizes flavin molecules from its environments. Still, when riboflavin was introduced into the anodic chamber of microbial fuel cell there was observed an increase in current generation (data not shown). This clearly suggests that *L. monocytogenes* could use environmental flavin as mediators in electrons transfer electrons to respective electron acceptors. Light et al. (2018) reported similar role of environmental flavin in case of *L. monocytogenes*. According to the proposed molecular model, in *L. monocytogenes,* electrons travel from NADH to membrane confined quinone to the flavoprotein (PplA) or flavin shuttles and subsequently to the terminal electron acceptor (Light et al., 2018). Here, the template stripped gold electrodes supported the growth of *L. monocytogenes* on TSG electrodes with neutral surface. The catalytic currents spikes at

an onset potential of ≈ -0.2 V are generally recognized to originate from an EET mechanism via flavins either as freely diffusing electron mediators or bound as co-factors to outer membrane cytochromes (Marsili et al., 2008). To establish that onset potential -0.2 V is due to flavin, the *L. monocytogenes* was grown using MOPS buffer (pH 7.4) as a basal electrolyte. The appearance of catalytic wave at -0.2V validated that the wave was due to flavin.

In our study, *Listeria monocytogenes* (wild type strain) was grown on ultra-smooth gold electrodes in the presence of glucose substrate. However, Ndh2 (NDH-2b) mutant strain *Δndh2 (Δndh-2b)* failed to grow under the same conditions. Light et al. (2018) performed a similar study on *L. monocytogenes* whereby, the authors investigated the role of Ndh2/NDH-2b in extracellular electron transfer (EET) using DmkA, DmkB and Ndh2/NDH-2 mutant strains. Mutants were grown on an aerobic respiration medium (ARM) using glycerol as a non-fermentative sole carbon source and found that the mutant strains grew similar to the wild type strains. The NAD$^+$/NADH ratio in the presence of ferric iron was found negligible compared to the wild type strain. 1,4-dihydroxy-2-naphthoyl-CoA (DHNA) and isopentenyl pyrophosphate (IPP) utilize DmkA, DmkB (the analogue proteins of highly conserved enzymes MenA, MenG and HepT) and MenA, MenG and HepT to generate DMK and MK, respectively. The experiments conducted by our group showed no electrochemical activity using Ndh2/NDH-2b in vitro with DMK and ubiquinone. The involvement of Ndh2/NDH-2b in the electrochemical activity using *Listeria* WT and *Δndh/ndh-2a* strains led us to the idea that Ndh2/NDH-2b might be able to transfer electrons to the eetA directly without the involvement of DMK derivative.

To further clarify the relationship between EET and respiration, the deficient strains *ΔcydABΔqoxA* (a positive control that lacks terminal cytochrome oxidase for aerobic respiration), *ΔmenA, hepT*:tn and *Δndh/Δndh-2a* were inoculated on aerobic respiration medium with glycerol by the authors (Light et. al. 2018). The mutant strains maintained the ferric iron reductase activity of wild type level but showed no growth on the media. The result supported the idea that menaquinone derivative MK and demethylmenaquinone derivative DMK are used by Ndh1/NDH-2a and Ndh2/NDH-2b for aerobic respiration and EET, respectively (Fig. 7.17). Here, the mutant strain *Δndh1/Δndh-2a* grew on aerobic respiration medium and demonstrated electrochemical activity in the electrochemical cell using TSG electrode and glucose as a source of carbon (Fig. 7.11). The growth and electron transfer activity of mutant *Δndh1/Δndh-2a* confirmed that EET also has an integral role in respiration. Previously, Ferric iron reduction in *Enterococcus faecalis* has been associated with membrane associated proteins; Ndh2/NDH-2b and EetA. Moreover, these enzymes in *E. faecalis* and *L. monocytogenes* are considered to be homologous (Pankratova et al., 2018). Therefore, there is possibility that *L. monocytogenes* constitutes Ndh2/NDH-2b and EetA/EetB based pathway to transfer electrons to the extracellular reductases in the absence of Ndh1/NDH-2a. *L.* monocytogenes is a facultative anaerobe and the EET pathway has been reported obligatory for its survival in the intestinal lumen, whereas, in the internalized cells, the electron transport chain using cytochrome bd and aa$_3$ is adopted for the survival (Corbett et al., 2017). More recently, an extracellular subfamily of reductases has been reported for transfer of electrons to the

extracellular reductases (Light et al., 2019). One of these enzymes has been identified as fumarate reductase. *L. monocytogenes* has shown its ability to respire on fumarate, therefore, from these insights we can speculate the general role of EET in respiration.
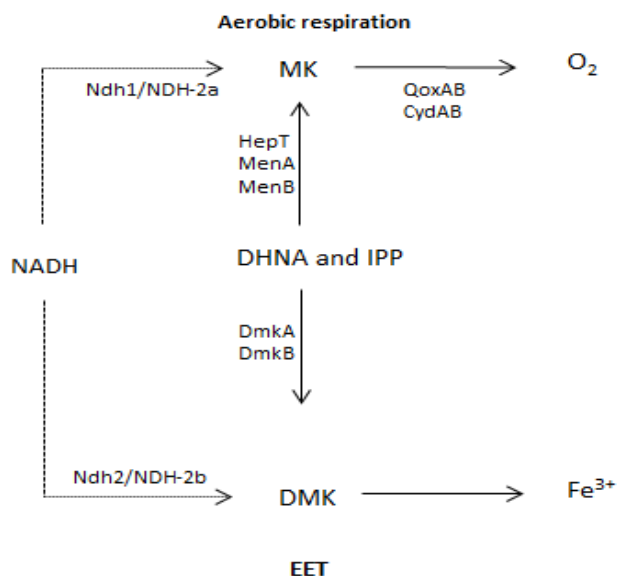
Figure 7. 18 Possible electron pathways for aerobic respiration and extracellular electron transfer (EET) in *L. monocytogenes*; Ndh1/NDH-2a and Ndh2/NDH-2b use MK and DMK derivatives for respiration and EET, respectively (Light et al., 2018).

7.5. Conclusion

In this study, we investigated the role of Ndh1/NDH-2a/complex I and Ndh2/NDH-2b in the respiration and extracellular electron transfer (EET) in Gram positive food-borne pathogen *Listeria monocytogenes* by determining the electron transfer capabilities of wild type (WT), mutant and complementary strains (*Δndh1/Δndh-2a, Δndh2 /Δndh-2b,* and *Δndh1/Δndh-2a complementary)* of *L. monocytogenes* in the bioelectrochemical cell with ultra-flat gold electrodes containing neutral SAM. The Ndh2/NDH-2b has role in extracellular electron transfer with or without the use of DMK to the subsequent components of electron transfer pathway. *L. monocytogenes* showed the ability to respirein the absence of Ndh1/NDH-2a indicating the role of EET in respiration. The characterization of EET pathways in Gram positive bacteria such as *L. monocytogenes* established their applications in bioelectrochemical processes and bioenergetics and needs to be explored further.

7.6. Future Prospects

Self-assembled monolayer (SAM) modified gold electrodes are not commonly used in the microbial electrochemical cells with MOPS buffer as a growth medium. For this reason, the experiments should be carried out using the more typical electrode materials such as carbon-based electrodes along with other substrates as growth medium. The experiments were performed using negative surface gold electrodes in the bespoke electrochemical cells and graphite felt anodes (with platinum cathode) in the microbial fuel

cells (MFCs). The experiments using graphite felt or other carbon based electrodes are incomplete (data not shown here) and   need to be carried out. The effect of different surfaces on the EET mechanisms used by *L. monocytogenes* should be investigated. Furthermore, the role of genes such as *eetA* and *eetB* needs to be explored in flavin mediated EET pathways in *L. monocytogenes*. Given the role of Ndh2/Ndh-2b in EET has been investigated; there is need to explore the presence of more NDH proteins besides investigating the association of Ndh2 with EET in *L. Monocytogenes.*

Chapter 8: References

Chapter 1 and 2

Abdullah, F. Bin, Iqbal, R., Hyder, S. I., & Jawaid, M. (2020). Energy security indicators for Pakistan: An integrated approach. Renewable and Sustainable Energy Reviews. (133) 110-122. https://doi.org/10.1016/j.rser.2020.110122

Abrevaya, X. C., Sacco, N. J., Bonetto, M. C., Hilding-Ohlsson, A., & Cortón, E. (2015). Analytical applications of microbial fuel cells. Part I: Biochemical oxygen demand. Biosensors and Bioelectronics. https://doi.org/10.1016/j.bios.

Ahimou, F., Semmens, M. J., Novak, P. J., & Haugstad, G. (2007). Biofilm cohesiveness measurement using a novel atomic force microscopy methodology. Applied and Environmental Microbiology. https://doi.org/10.1128/AEM.02388-06

Al-Saati, N. H. A., Hwaidi, E. H., & Jassam, S. H. (2016). Comparing cactus (Opuntia spp.) and alum as coagulants for water treatment at Al-Mashroo Canal: a case study. International Journal of Environmental Science and Technology, 13(12), 2875–2882. https://doi.org/10.1007/s13762-016-1114-0

Algar, C. K., Howard, A., Ward, C., & Wanger, G. (2020). Sediment microbial fuel cells as a barrier to sulfide accumulation and their potential for sediment remediation beneath aquaculture pens. Scientific Reports. https://doi.org/10.1038/s41598-020-70002-4

Allen, R. M., & Bennetto, H. P. (1993). Microbial fuel-cells - Electricity production from carbohydrates. Applied Biochemistry and Biotechnology, 39–40(1), 27–40. https://doi.org/10.1007/BF02918975

Allison, D. G. (2003). The biofilm matrix. Biofouling. https://doi.org/10.1080/0892701031000072190

Amuda, O. S., & Amoo, I. A. (2007). Coagulation/flocculation process and sludge conditioning in beverage industrial wastewater treatment. Journal of Hazardous Materials, 141(3), 778–783. https://doi.org/10.1016/j.jhazmat.2006.07.044

Angelaalincy, M. J., Navanietha Krishnaraj, R., Shakambari, G., Ashokkumar, B., Kathiresan, S., & Varalakshmi, P. (2018). Biofilm Engineering Approaches for Improving the Performance of Microbial Fuel Cells and Bioelectrochemical Systems. Frontiers in Energy Research. https://doi.org/10.3389/fenrg.2018.00063

Babauta, J., Renslow, R., Lewandowski, Z., & Beyenal, H. (2012). Electrochemically active biofilms: Facts and fiction. A review. In Biofouling. https://doi.org/10.1080/08927014.2012.710324

Bader, N. Ben, Germec, M., & Turhan, I. (2021). Ethanol production from different medium compositions of rice husk hydrolysate by using Scheffersomyces stipitis in a repeated-batch biofilm reactor and its modeling. Process Biochemistry, 100, 26–38. https://doi.org/10.1016/j.procbio.2020.09.018

Bahar, N. H. A., Lo, M., Sanjaya, M., Van Vianen, J., Alexander, P., Ickowitz, A., & Sunderland, T. (2020). Meeting the food security challenge for nine billion people in 2050: What impact on forests? https://doi.org/10.1016/j.gloenvcha.2020.102056

Banin, E., Vasil, M. L., & Greenberg, E. P. (2005). Iron and *Pseudomonas aeruginosa* biofilm formation. Proceedings of the National Academy of Sciences of the United States of America. https://doi.org/10.1073/pnas.0504266102

Beech, I. B., Zinkevich, V., Tapper, R., & Gubner, R. (1998). Direct involvement of an extracellular complex produced by a marine sulfate-reducing bacterium in deterioration of steel. Geomicrobiology Journal. https://doi.org/10.1080/01490459809378069

Belila, A., Snoussi, M., & Hassan, A. (2012). Rapid qualitative characterization of bacterial community in eutrophicated wastewater stabilization plant by T-RFLP method based on 16S rRNA genes. World Journal of Microbiology and Biotechnology. https://doi.org/10.1007/s11274-011-0802-7

Bryers & D. James, Biofilms II: Process Analysis and Applications | Wiley. (2000). https://www.wiley.com/en-us/Biofilms+II%3A+Process+Analysis+and+Applications-p-

9780471296560

Bond, D. R., & Lovley, D. R. (2003). Electricity production by Geobacter sulfurreducens attached to electrodes. Applied and Environmental Microbiology. https://doi.org/10.1128/AEM.69.3.1548-1555.2003

Bonetto, M. C., Sacco, N. J., Ohlsson, A. H., & Cortón, E. (2011). Assessing the effect of oxygen and microbial inhibitors to optimize ferricyanide-mediated BOD assay. Talanta, 85(1), 455–462. https://doi.org/10.1016/j.talanta.2011.04.007

Booth, S. C., George, I. F. S., Zannoni, D., Cappelletti, M., Duggan, G. E., Ceri, H., & Turner, R. J. (2013). Effect of aluminium and copper on biofilm development of Pseudomonas pseudoalcaligenes KF707 and P. fluorescens as a function of different media compositions. Metallomics. https://doi.org/10.1039/c3mt20240b

BP. (2017). BP Statistical Review of World Energy 2017.

Branda, S. S., Vik, Å., Friedman, L., & Kolter, R. (2005). Biofilms: The matrix revisited. In Trends in Microbiology. https://doi.org/10.1016/j.tim.2004.11.006

Brena, B., González-Pombo, P., & Batista-Viera, F. (2013). Immobilization of enzymes: A literature survey. In Methods in Molecular Biology. https://doi.org/10.1007/978-1-62703-550-7_2

Brennan, A. (2012). Investigating Pilot Scale Performance on an Activated Sludge Wastewater Treatment System With A High Rate Anaerobic Side Stream Reactor. Civil and Environmental Engineering, 1–63. https://doi.org/10.7275/PCDX-WV39

Brown, & D, T. (1981). Coal gasification - combined cycles for electricity production.

Bryers, J. D., & Ratner, B. D. (2004). Bioinspired implant materials befuddle bacteria. In ASM News.

Busscher, H. J., & van der Mei, H. C. (1997). Physico-chemical interactions in initial microbial adhesion and relevance for biofilm formation. In Advances in dental research. https://doi.org/10.1177/08959374970110011301

Busscher, H. J., Weerkamp, A. H., van Der Mei, H. C., van Pelt, A. W., de Jong, H. P., & Arends, J. (1984). Measurement of the surface free energy of bacterial cell surfaces and its relevance for adhesion. Applied and Environmental Microbiology. https://doi.org/10.1128/aem.48.5.980-983.1984

Busscher, Henk J., & Van Der Mei, H. C. (2006). Microbial adhesion in flow displacement systems. In Clinical Microbiology Reviews. https://doi.org/10.1128/CMR.19.1.127-141.2006

C. F. Thurston,'* H. P. Bennett0, G. M. D., & J. R. Mason, S. D. R. A. J. L. S. (1985). Glucose Metabolism in a Microbial Fuel Cell. Stoichiometry of Product Formation in a Thionine-mediated Proteus vulgaris Fuel Cell and its Relation to Coulombic Yields. Journd Qf' General Microbiulugj~, 131(6), 393–140.

Call, D., & Logan, B. E. (2008). Hydrogen production in a single chamber microbial electrolysis cell lacking a membrane. Environmental Science and Technology. https://doi.org/10.1021/es8001822

Cao, Yingxiu, Song, M., Li, F., Li, C., Lin, X., Chen, Y., Chen, Y., Xu, J., Ding, Q., & Song, H. (2019). A synthetic plasmid toolkit for shewanella oneidensis MR-1. Frontiers in Microbiology. https://doi.org/10.3389/fmicb.2019.00410

Cao, Yujin, Mu, H., Liu, W., Zhang, R., Guo, J., Xian, M., & Liu, H. (2019). Electricigens in the anode of microbial fuel cells: Pure cultures versus mixed communities. In Microbial Cell Factories. https://doi.org/10.1186/s12934-019-1087-z

Cerca, N., Martins, S., Cerca, F., Jefferson, K. K., Pier, G. B., Oliveira, R., & Azeredo, J. (2005). Comparative assessment of antibiotic susceptibility of coagulase-negative staphylococci in biofilm versus planktonic culture as assessed by bacterial enumeration or rapid XTT colorimetry. Journal of Antimicrobial Chemotherapy. https://doi.org/10.1093/jac/dki217

Chae, K. J., Choi, M., Ajayi, F. F., Park, W., Chang, I. S., & Kim, I. S. (2008). Mass transport through a proton exchange membrane (Nafion) in microbial fuel cells. Energy and Fuels. https://doi.org/10.1021/ef700308u

Chang, I. S., Jang, J. K., Gil, G. C., Kim, M., Kim, H. J., Cho, B. W., & Kim, B. H. (2004). Continuous determination of biochemical oxygen demand using microbial fuel cell type biosensor. Biosensors and Bioelectronics. https://doi.org/10.1016/S0956-5663(03)00272-0

Characklis, W. G. (1973). Attached microbial growths-II. Frictional resistance due to microbial slimes. In Water Research. https://doi.org/10.1016/0043-1354(73)90002-X

Chatterjee, S., & Chen, A. (2012). Functionalization of carbon buckypaper for the sensitive determination of hydrogen peroxide in human urine. Biosensors and Bioelectronics. https://doi.org/10.1016/j.bios.2012.03.005

Chen, D., Cao, Y., Liu, B., & Kong, J. (2002). A BOD biosensor based on a microorganism immobilized on an Al_2O_3 sol-gel matrix. Analytical and Bioanalytical Chemistry. https://doi.org/10.1007/s00216-001-1214-6

Chen, G. W., Choi, S. J., Lee, T. H., Lee, G. Y., Cha, J. H., & Kim, C. W. (2008). Application of biocathode in microbial fuel cells: Cell performance and microbial community. Applied Microbiology and Biotechnology. https://doi.org/10.1007/s00253-008-1451-0

Chen, Z., Niu, Y., Zhao, S., Khan, A., Ling, Z., Chen, Y., Liu, P., & Li, X. (2016). A novel biosensor for p-nitrophenol based on an aerobic anode microbial fuel cell. Biosensors and Bioelectronics. https://doi.org/10.1016/j.bios.2016.06.007

Cheng, K. Y., Ho, G., & Cord-Ruwisch, R. (2010). Anodophilic Biofilm Catalyzes Cathodic Oxygen Reduction. Environmental Science & Technology. https://doi.org/10.1021/es9023833

Cheng, S., Liu, H., & Logan, B. E. (2006). Power densities using different cathode catalysts (Pt and CoTMPP) and polymer binders (Nafion and PTFE) in single chamber microbial fuel cells. Environmental Science and Technology. https://doi.org/10.1021/es0512071

Cheng, S., Xing, D., & Logan, B. E. (2011). Electricity generation of single-chamber microbial fuel cells at low temperatures. Biosensors and Bioelectronics. https://doi.org/10.1016/j.bios.2010.05.016

Chmielewski, R. A. N., & Frank, J. F. (2003). Biofilm formation and control in food processing facilities. Comprehensive Reviews in Food Science and Food Safety. https://doi.org/10.1111/j.1541-4337.2003.tb00012.x

Choi, M. J., Chae, K. J., Ajayi, F. F., Kim, K. Y., Yu, H. W., Kim, C. won, & Kim, I. S. (2011). Effects of biofouling on ion transport through cation exchange membranes and microbial fuel cell performance. Bioresource Technology. https://doi.org/10.1016/j.biortech.2010.06.129

Choudhury, P., Uday, U. S. P., Mahata, N., Nath Tiwari, O., Narayan Ray, R., Kanti Bandyopadhyay, T., & Bhunia, B. (2017). Performance improvement of microbial fuel cells for waste water treatment along with value addition: A review on past achievements and recent perspectives. In Renewable and Sustainable Energy Reviews. https://doi.org/10.1016/j.rser.2017.05.098

Chu, C.-S., & Syu, J.-J. (2017). Optical sensor for dual sensing of oxygen and carbon dioxide based on sensing films coated on filter paper. Applied Optics. https://doi.org/10.1364/ao.56.001225

Cieri, D., Vicario, M., Giacomello, M., Vallese, F., Filadi, R., Wagner, T., Pozzan, T., Pizzo, P., Scorrano, L., Brini, M., & Calì, T. (2018). SPLICS: A split green fluorescent protein-based contact site sensor for narrow and wide heterotypic organelle juxtaposition. Cell Death and Differentiation. https://doi.org/10.1038/s41418-017-0033-z

Coenye, T., & Nelis, H. J. (2010). In vitro and in vivo model systems to study microbial biofilm formation. In Journal of Microbiological Methods. https://doi.org/10.1016/j.mimet.2010.08.018

Collins, A. J., Jarrod Smith, T., Sondermann, H., & O'Toole, G. A. (2020). From Input to Output: The Lap/c-di-GMP Biofilm Regulatory Circuit. In Annual Review of Microbiology (Vol. 74, pp. 607–631). Annual Reviews Inc. https://doi.org/10.1146/annurev-micro-011520-094214

COLLINS, D. (1986). Handbook of batteries and fuel cells By David Linden, published by McGraw-Hill Book Company GmbH., Hamburg, F.R.G., 1984; 1024. Journal of Power Sources. https://doi.org/10.1016/0378-7753(86)80059-3

Comte, S., Guibaud, G., & Baudu, M. (2006). Relations between extraction protocols for activated sludge

extracellular polymeric substances (EPS) and EPS complexation properties: Part I. Comparison of the efficiency of eight EPS extraction methods. Enzyme and Microbial Technology. https://doi.org/10.1016/j.enzmictec.2005.06.016

Córdova-Bautista, Y., Ramírez-Morales, E., Pérez-Hernández, B., Ojeda-Morales, M. E., López-Lázaro, J. S., & Martínez-Pereyra, G. (2020). Electricity Production and Bioremediation from Synthetic Sugar Industry Wastewater by Using Microbial Isolate in Microbial Fuel Cell. Sugar Tech. https://doi.org/10.1007/s12355-020-00830-1

Costerton, J. W., Geesey, G. G., & Cheng, K. J. (1978). How bacteria stick. Scientific American. https://doi.org/10.1038/scientificamerican0178-86

Costerton, J. W., Lewandowski, Z., DeBeer, D., Caldwell, D., Korber, D., & James, G. (1994). Biofilms, the customized microniche. In Journal of Bacteriology. 176 (8), 2137–2142. American Society for Microbiology. https://doi.org/10.1128/jb.176.8.2137-2142.1994

Cui, Y., Lai, B., & Tang, X. (2019). Microbial fuel cell-based biosensors. Biosensors. https://doi.org/10.3390/bios9030092

Czaczyk, K., & Myszka, K. (2007). Biosynthesis of extracellular polymeric substances (EPS) and its role in microbial biofilm formation. In Polish Journal of Environmental Studies.

Daims, H., Nielsen, J. L., Nielsen, P. H., Schleifer, K. H., & Wagner, M. (2001). In Situ Characterization of Nitrospira-Like Nitrite-Oxidizing Bacteria Active in Wastewater Treatment Plants. Applied and Environmental Microbiology. https://doi.org/10.1128/aem.67.11.5273-5284.2001

Das, H. (2017). Citation: Das H. Water Pollution…! A Serious Civic Issue of Karachi. Journal of Environmental Studiestudies, 3(2), 1–3.

Daud, M. K., Nafees, M., Ali, S., Rizwan, M., Bajwa, R. A., Shakoor, M. B., Arshad, M. U., Chatha, S. A. S., Deeba, F., Murad, W., Malook, I., & Zhu, S. J. (2017). Drinking Water Quality Status and Contamination in Pakistan. BioMed Research International (Vol. 2017). Hindawi Limited. https://doi.org/10.1155/2017/7908183

Davey, M. E., & O'toole, G. A. (2000). Microbial Biofilms: from Ecology to Molecular Genetics. Microbiology and Molecular Biology Reviews, 64(4), 847–867. https://doi.org/10.1128/mmbr.64.4.847-867.2000

Dávila, D., Esquivel, J. P., Sabaté, N., & Mas, J. (2011). Silicon-based microfabricated microbial fuel cell toxicity sensor. Biosensors and Bioelectronics. https://doi.org/10.1016/j.bios.2010.10.025

De Prijck, K., De Smet, N., Rymarczyk-Machal, M., Van Driessche, G., Devreese, B., Coenye, T., Schacht, E., & Nelis, H. J. (2010). Candida albicans biofilm formation on peptide functionalized polydimethylsiloxane. Biofouling. https://doi.org/10.1080/08927010903501908

Deng, H., Jiang, Y. B., Zhou, Y. W., Shen, K., & Zhong, W. H. (2015). Using electrical signals of microbial fuel cells to detect copper stress on soil microorganisms. European Journal of Soil Science, 66(2), 369–377. https://doi.org/10.1111/ejss.12215

Deng, Y., Zhang, Y., Gao, Y., Li, D., Liu, R., Liu, M., Zhang, H., Hu, B., Yu, T., & Yang, M. (2012). Microbial community compositional analysis for series reactors treating high level antibiotic wastewater. Environmental Science and Technology. https://doi.org/10.1021/es2025998

Dhanya, B. S., Mishra, A., Chandel, A. K., & Verma, M. L. (2020). Development of sustainable approaches for converting the organic waste to bioenergy. Science of the Total Environment, 723, 138109. https://doi.org/10.1016/j.scitotenv.2020.138109

Di Lorenzo, M., Curtis, T. P., Head, I. M., & Scott, K. (2009). A single-chamber microbial fuel cell as a biosensor for wastewaters. Water Research. https://doi.org/10.1016/j.watres.2009.01.005

Dionisi, H. M., Layton, A. C., Harms, G., Gregory, I. R., Robinson, K. G., & Sayler, G. S. (2002). Quantification of Nitrosomonas oligotropha-like ammonia-oxidizing bacteria and nitrospira spp. from full-scale wastewater treatment plants by competitive PCR. Applied and Environmental Microbiology. https://doi.org/10.1128/AEM.68.1.245-253.2002

Do, M. H., Ngo, H. H., Guo, W., Chang, S. W., Nguyen, D. D., Liu, Y., Varjani, S., & Kumar, M. (2020).

Microbial fuel cell-based biosensor for online monitoring wastewater quality: A critical review. Science of the Total Environment. https://doi.org/10.1016/j.scitotenv.2019.135612

Doiron, K., Linossier, I., Fay, F., Yong, J., Abd Wahid, E., Hadjiev, D., & Bourgougnon, N. (2012). Dynamic approaches of mixed species biofilm formation using modern technologies. Marine Environmental Research. https://doi.org/10.1016/j.marenvres.2012.04.001

Donlan, R. M. (2002). Biofilms: Microbial life on surfaces. Emerging Infectious Diseases (Vol. 8, Issue 9, pp. 881–890). https://doi.org/10.3201/eid0809.020063

Donlan, R. M., & Costerton, J. W. (2002). Biofilms: Survival mechanisms of clinically relevant microorganisms. In Clinical Microbiology Reviews (Vol. 15, Issue 2, pp. 167–193). American Society for Microbiology (ASM). https://doi.org/10.1128/CMR.15.2.167-193.2002

Douterelo, I., Boxall, J. B., Deines, P., Sekar, R., Fish, K. E., & Biggs, C. A. (2014). Methodological approaches for studying the microbial ecology of drinking water distribution systems. In Water Research (Vol. 65, pp. 134–156). Elsevier Ltd. https://doi.org/10.1016/j.watres.2014.07.008

Driscoll, J. A., Brody, S. L., & Kollef, M. H. (2007). The epidemiology, pathogenesis and treatment of *Pseudomonas aeruginosa* infections. Drugs 67 (3), 351–368. https://doi.org/10.2165/00003495-200767030-00003

Du, Z., Li, H., & Gu, T. (2007). A state of the art review on microbial fuel cells: A promising technology for wastewater treatment and bioenergy. In Biotechnology Advances. https://doi.org/10.1016/j.biotechadv.2007.05.004

editors: Ruslan I Dmitriev, D. B. P. (2018). Quenched-phosphorescence Detection of Molecular Oxygen: Applications in Life ... - Google Books. The Royal Society of Chemistry.

Ejeian, F., Etedali, P., Mansouri-Tehrani, H. A., Soozanipour, A., Low, Z. X., Asadnia, M., Taheri-Kafrani, A., & Razmjou, A. (2018). Biosensors for wastewater monitoring: A review. In Biosensors and Bioelectronics. https://doi.org/10.1016/j.bios.2018.07.019

Elisabeth Stein, N. (2011). A microbial fuel cell-based biosensor for the detection of toxic components in water.

Ensink, J. H. J., Mahmood, T., Van Der Hoek, W., Raschid-Sally, L., & Amerasinghe, F. P. (2004). A nationwide assessment of wastewater use in Pakistan: An obscure activity or a vitally important one? Water Policy, 6(3), 197–206. https://doi.org/10.2166/wp.2004.0013

Fang, H. H. P., Xu, L. C., & Chan, K. Y. (2002). Effects of toxic metals and chemicals on biofilm and biocorrosion. Water Research. https://doi.org/10.1016/S0043-1354(02)00207-5

Feng, Y., Shi, X., Wang, X., Lee, H., Liu, J., Qu, Y., He, W., Kumar, S. M. S., Kim, B. H., & Ren, N. (2012). Effects of sulfide on microbial fuel cells with platinum and nitrogen-doped carbon powder cathodes. Biosensors and Bioelectronics. https://doi.org/10.1016/j.bios.2011.08.030

Fish, K. E., Osborn, A. M., & Boxall, J. (2016). Characterising and understanding the impact of microbial biofilms and the extracellular polymeric substance (EPS) matrix in drinking water distribution systems. In Environmental Science: Water Research and Technology 2, (4), 614–630. Royal Society of Chemistry. https://doi.org/10.1039/c6ew00039h

Flemming, H.-C., Wingender, J., Griebe, T., & Mayer, C. (2000). Physico-chemical properties of biofilms. Biofilms: Recent Advances in Their Study and Control.

Flemming, H. C., & Wingender, J. (2001). Relevance of microbial extracellular polymeric substances (EPSs) - Part II: Technical aspcets. Water Science and Technology, 43(6), 9–16. https://doi.org/10.2166/wst.2001.0328

Flemming, Hans Curt, Neu, T. R., & Wozniak, D. J. (2007). The EPS matrix: The "House of Biofilm Cells." In Journal of Bacteriology. https://doi.org/10.1128/JB.00858-07

Flemming, Hans Curt, & Wingender, J. (2010). The biofilm matrix. In Nature Reviews Microbiology. https://doi.org/10.1038/nrmicro2415

Fornero, J. J., Rosenbaum, M., Cotta, M. A., & Angenent, L. T. (2010). Carbon dioxide addition to microbial fuel cell cathodes maintains sustainable catholyte ph and improves anolyte ph, alkalinity,

and conductivity. Environmental Science and Technology. https://doi.org/10.1021/es9031985

Foster, J. S., & Kolenbrander, P. E. (2004). Development of a multispecies oral bacterial community in a saliva-conditioned flow cell. Applied and Environmental Microbiology. https://doi.org/10.1128/AEM.70.7.4340-4348.2004

Frank, B. P., & Belfort, G. (2003). Polysaccharides and sticky membrane surfaces: Critical ionic effects. Journal of Membrane Science. https://doi.org/10.1016/S0376-7388(02)00502-1

Franks, A. E., & Nevin, K. P. (2010). Microbial fuel cells, a current review. In Energies. https://doi.org/10.3390/en3050899

Frølund, B., Suci, P. A., Langille, S., Weiner, R. M., & Geesey, G. G. (1996). Influence of protein conditioning films on binding of a bacterial polysaccharide adhesin from Hyphomonas MHS-3. Biofouling. https://doi.org/10.1080/08927019609386268

Fu, B., Liao, X., Ding, L., & Ren, H. (2010). Characterization of microbial community in an aerobic moving bed biofilm reactor applied for simultaneous nitrification and denitrification. World Journal of Microbiology and Biotechnology. https://doi.org/10.1007/s11274-010-0382-y

Gacesa, P. (1998). Bacterial alginate biosynthesis - Recent progress and future prospects. Microbiology. https://doi.org/10.1099/00221287-144-5-1133

Garny, K., Horn, H., & Neu, T. R. (2008). Interaction between biofilm development, structure and detachment in rotating annular reactors. Bioprocess and Biosystems Engineering. https://doi.org/10.1007/s00449-008-0212-x

Garrett, T. R., Bhakoo, M., & Zhang, Z. (2008). Bacterial adhesion and biofilms on surfaces. In Progress in Natural Science (Vol. 18, Issue 9, pp. 1049–1056). Science Press. https://doi.org/10.1016/j.pnsc.2008.04.001

Garrote, A., Bonet, R., Merino, S., Simon-Pujol, M. D., & Congregado, F. (1992). Occurrence of a capsule in *Aeromonas salmonicida*. FEMS Microbiology Letters. https://doi.org/10.1016/0378-1097(92)90417-M

Ghassemi, Z., & Slaughter, G. (2017). Biological fuel cells and membranes. Membranes. https://doi.org/10.3390/membranes7010003

Gieseke, A., Purkhold, U., Wagner, M., Amann, R., & Schramm, A. (2001). Community Structure and Activity Dynamics of Nitrifying Bacteria in a Phosphate-Removing Biofilm. Applied and Environmental Microbiology. https://doi.org/10.1128/AEM.67.3.1351-1362.2001

Gil, G. C., Chang, I. S., Kim, B. H., Kim, M., Jang, J. K., Park, H. S., & Kim, H. J. (2003). Operational parameters affecting the performance of a mediator-less microbial fuel cell. Biosensors and Bioelectronics. https://doi.org/10.1016/S0956-5663(02)00110-0

Gilbert, P., Das, J., & Foley, I. (1997). Biofilm susceptibility to antimicrobials. Advances in dental research. https://doi.org/10.1177/08959374970110010701

Gomez-Alvarez, V., Revetta, R. P., & Domingo, J. W. S. (2012). Metagenome analyses of corroded concrete wastewater pipe biofilms reveal a complex microbial system. BMC Microbiology. https://doi.org/10.1186/1471-2180-12-122

Gong, A. S., Bolster, C. H., Benavides, M., & Walker, S. L. (2009). Extraction and analysis of extracellular polymeric substances: Comparison of methods and extracellular polymeric substance levels in *Salmonella pullorum* sa 1685. Environmental Engineering Science. https://doi.org/10.1089/ees.2008.0398

Gorby, Y. A., Yanina, S., McLean, J. S., Rosso, K. M., Moyles, D., Dohnalkova, A., Beveridge, T. J., Chang, I. S., Kim, B. H., Kim, K. S., Culley, D. E., Reed, S. B., Romine, M. F., Saffarini, D. A., Hill, E. A., Shi, L., Elias, D. A., Kennedy, D. W., Pinchuk, G., Fredrickson, J. K. (2006). Electrically conductive bacterial nanowires produced by *Shewanella oneidensis* strain MR-1 and other microorganisms. Proceedings of the National Academy of Sciences of the United States of America. https://doi.org/10.1073/pnas.0604517103

Grzebyk, M., & Poźniak, G. (2005). Microbial fuel cells (MFCs) with interpolymer cation exchange

membranes. Separation and Purification Technology. https://doi.org/10.1016/j.seppur.2004.04.009

Guan, F., Yuan, X., Duan, J., Zhai, X., & Hou, B. (2019). Phenazine enables the anaerobic respiration of Pseudomonas aeruginosa via electron transfer with a polarised graphite electrode. International Biodeterioration and Biodegradation, 137, 8–13. https://doi.org/10.1016/j.ibiod.2018.11.002

Guo, Y., Wang, G., Zhang, H., Wen, H., & Li, W. (2020). Effects of biofilm transfer and electron mediators transfer on Klebsiella quasipneumoniae sp. 203 electricity generation performance in MFCs. Biotechnology for Biofuels, 13(1), 1–11. https://doi.org/10.1186/s13068-020-01800-1

Haagensen, J. A. J., Klausen, M., Ernst, R. K., Miller, S. I., Folkesson, A., Tolker-Nielsen, T., & Molin, S. (2007). Differentiation and distribution of colistin- and sodium dodecyl sulfate-tolerant cells in Pseudomonas aeruginosa biofilms. Journal of Bacteriology. https://doi.org/10.1128/JB.00720-06

Habimana, O., Meyrand, M., Meylheuc, T., Kulakauskas, S., & Briandet, R. (2009). Genetic features of resident biofilms determine attachment of Listeria monocytogenes. Applied and Environmental Microbiology. https://doi.org/10.1128/AEM.01333-09

Hamed, M. S., Majdi, H. S., & Hasan, B. O. (2020). Effect of Electrode Material and Hydrodynamics on the Produced Current in Double Chamber Microbial Fuel Cells. ACS Omega. https://doi.org/10.1021/acsomega.9b04451

Hansen, A. M., Kraus, T. E. C., Bachand, S. M., Horwath, W. R., & Bachand, P. A. M. (2018). Wetlands receiving water treated with coagulants improve water quality by removing dissolved organic carbon and disinfection byproduct precursors. Science of the Total Environment, 622–623, 603–613. https://doi.org/10.1016/j.scitotenv.2017.11.205

Harbron, R. S., & Kent, C. A. (1988). Aspects of Cell Adhesion. In Fouling Science and Technology (pp. 125–140). Springer Netherlands. https://doi.org/10.1007/978-94-009-2813-8_9

Harwani, D. (2013). Bacteria eating pollution and generating electricity. In International Journal of Pharma and Bio Sciences.

He, Z., & Angenent, L. T. (2006). Application of bacterial biocathodes in microbial fuel cells. In Electroanalysis. https://doi.org/10.1002/elan.200603628

Heilmann, C., Schweitzer, O., Gerke, C., Vanittanakom, N., Mack, D., & Götz, F. (1996). Molecular basis of intercellular adhesion in the biofilm-forming Staphylococcus epidermidis. Molecular Microbiology. https://doi.org/10.1111/j.1365-2958.1996.tb02548.x

Heukelekian, H., & Heller, A. (1940). Relation between Food Concentration and Surface for Bacterial Growth1. Journal of Bacteriology. https://doi.org/10.1128/jb.40.4.547-558.1940

Hong, S. W., Chang, I. S., Choi, Y. S., & Chung, T. H. (2009). Experimental evaluation of influential factors for electricity harvesting from sediment using microbial fuel cell. Bioresource Technology. https://doi.org/10.1016/j.biortech.2009.01.030

Honraet, K., & Nelis, H. J. (2006). Use of the modified robbins device and fluorescent staining to screen plant extracts for the inhibition of S. mutans biofilm formation. Journal of Microbiological Methods. https://doi.org/10.1016/j.mimet.2005.05.005

Huang, J., & Pinder, K. L. (1995). Effects of calcium on development of anaerobic acidogenic biofilms. Biotechnology and Bioengineering. https://doi.org/10.1002/bit.260450305

Hussain, M., Wilcox, M. H., & White, P. J. (1993). The slime of coagulase-negative staphylococci: Biochemistry and relation to adherence. FEMS Microbiology Letters. https://doi.org/10.1016/0378-1097(93)90596-T

Hutchinson, A. J., Tokash, J. C., & Logan, B. E. (2011). Analysis of carbon fiber brush loading in anodes on startup and performance of microbial fuel cells. Journal of Power Sources. https://doi.org/10.1016/j.jpowsour.2011.07.040

Irfan, M., Zhao, Z. Y., Panjwani, M. K., Mangi, F. H., Li, H., Jan, A., Ahmad, M., & Rehman, A. (2020). Assessing the energy dynamics of Pakistan: Prospects of biomass energy. Energy Reports, 6, 80–93. https://doi.org/10.1016/j.egyr.2019.11.161

Jang, J. K., Pham, T. H., Chang, I. S., Kang, K. H., Moon, H., Cho, K. S., & Kim, B. H. (2004).

Construction and operation of a novel mediator- and membrane-less microbial fuel cell. Process Biochemistry. https://doi.org/10.1016/S0032-9592(03)00203-6

Jass, J., Costerton, J. W., & Lappin-Scott, H. M. (1995). Assessment of a chemostat-coupled modified Robbins device to study biofilms. Journal of Industrial Microbiology. https://doi.org/10.1007/BF01569981

Jiang, Y. Bin, Zhong, W. H., Han, C., & Deng, H. (2016). Characterization of electricity generated by soil in microbial fuel cells and the isolation of soil source exoelectrogenic bacteria. Frontiers in Microbiology, 7(NOV), 1–10. https://doi.org/10.3389/fmicb.2016.01776

Jiménez-Fernández, A., López-Sánchez, A., Jiménez-Díaz, L., Navarrete, B., Calero, P., Platero, A. I., & Govantes, F. (2016). Complex Interplay between FleQ, cyclic diguanylate and multiple σ factors coordinately regulates flagellar motility and biofilm development in pseudomonas putida. PLoS ONE. https://doi.org/10.1371/journal.pone.0163142

Jones, A. A. D., & Buie, C. R. (2019). Continuous shear stress alters metabolism, mass-transport, and growth in electroactive biofilms independent of surface substrate transport. Scientific Reports. https://doi.org/10.1038/s41598-019-39267-2

Jones, H. C., Roth, I. L., & Sanders, W. M. (1969). Electron microscopic study of a slime layer. Journal of Bacteriology. https://doi.org/10.1128/jb.99.1.316-325.1969

Jouanneau, S., Recoules, L., Durand, M. J., Boukabache, A., Picot, V., Primault, Y., Lakel, A., Sengelin, M., Barillon, B., & Thouand, G. (2014). Methods for assessing biochemical oxygen demand (BOD): A review. In Water Research. https://doi.org/10.1016/j.watres.2013.10.066

Juretschko, S., Loy, A., Lehner, A., & Wagner, M. (2002). The microbial community composition of a nitrifying-denitrifying activated sludge from an industrial sewage treatment plant analyzed by the full-cycle rRNA approach. Systematic and Applied Microbiology. https://doi.org/10.1078/0723-2020-00093

Kaplan, J. B. (2010). Biofilm Dispersal: Mechanisms, Clinical Implications, and Potential Therapeutic Uses. In Journal of Dental Research. https://doi.org/10.1177/0022034509359403

Kara, F., Gurakan, G. C., & Sanin, F. D. (2008). Monovalent cations and their influence on activated sludge floc chemistry, structure, and physical characteristics. Biotechnology and Bioengineering. https://doi.org/10.1002/bit.21755

Karapanagiotis, N. K., Rudd, T., Sterritt, R. M., & Lester, J. N. (1989). Extraction and characterisation of extracellular polymers in digested sewage sludge. Journal of Chemical Technology & Biotechnology. https://doi.org/10.1002/jctb.280440203

Karube, I., Matsunaga, T., Mitsuda, S., & Suzuki, S. (1977). Microbial electrode BOD sensors. Biotechnology and Bioengineering, 19(10), 1535–1547. https://doi.org/10.1002/bit.260191010

Katsikogianni, M., Missirlis, Y. F., Harris, L., & Douglas, J. (2004). Concise review of mechanisms of bacterial adhesion to biomaterials and of techniques used in estimating bacteria-material interactions. In European Cells and Materials (Vol. 8, pp. 37–57). AO Research Institute Davos. https://doi.org/10.22203/eCM.v008a05

Kees, E. D., Pendleton, A. R., Paquete, C. M., Arriola, M. B., Kane, A. L., Kotloski, N. J., Intile, P. J., & Gralnick, J. A. (2019). Secreted flavin cofactors for anaerobic respiration of fumarate and urocanate by Shewanella oneidensis: Cost and role. Applied and Environmental Microbiology. https://doi.org/10.1128/AEM.00852-19

Kharkwal, S., Tan, Y. C., Lu, M., & Ng, H. Y. (2017). Development and long-term stability of a novel microbial fuel cell BOD sensor with MNo2 catalyst. International Journal of Molecular Sciences. https://doi.org/10.3390/ijms18020276

Kim, B. H., Park, H. S., Kim, H. J., Kim, G. T., Chang, I. S., Lee, J., & Phung, N. T. (2004). Enrichment of microbial community generating electricity using a fuel-cell-type electrochemical cell. Applied Microbiology and Biotechnology. https://doi.org/10.1007/s00253-003-1412-6

Kim, Byung Hong, Chang, I. S., Gil, G. C., Park, H. S., & Kim, H. J. (2003). Novel BOD (biological

oxygen demand) sensor using mediator-less microbial fuel cell. Biotechnology Letters. https://doi.org/10.1023/A:1022891231369

Kim, J., Park, H. D., & Chung, S. (2012). Microfluidic approaches to bacterial biofilm formation. In Molecules. https://doi.org/10.3390/molecules17089818

Kim, M. N., & Kwon, H. S. (1999). Biochemical oxygen demand sensor using serratia marcescens LSY 4. Biosensors and Bioelectronics. https://doi.org/10.1016/S0956-5663(98)00107-9

Kim, S., Chae, K. J., Choi, M. J., & Verstraete, W. (2011). Microbial fuel cells: Recent advances, bacterial communities and application beyond electricity generation. Environmental Engineering Research. https://doi.org/10.4491/eer.2008.13.2.051

King, R. O., & Forster, C. F. (1990). Effects of sonication on activated sludge. Enzyme and Microbial Technology. https://doi.org/10.1016/0141-0229(90)90082-2

Klotz, K., Weistenhöfer, W., Neff, F., Hartwig, A., Van Thriel, C., & Drexler, H. (2017). The health effects of aluminum exposure. Deutsches Arzteblatt International, 114(39), 653–659. https://doi.org/10.3238/arztebl.2017.0653

Kolenbrander, P. E., Palmer, R. J., Periasamy, S., & Jakubovics, N. S. (2010). Oral multispecies biofilm development and the key role of cell-cell distance. In Nature Reviews Microbiology. https://doi.org/10.1038/nrmicro2381

Koók, L., Dörgő, G., Bakonyi, P., Rózsenberszki, T., Nemestóthy, N., Bélafi-Bakó, K., & Abonyi, J. (2020). Directions of membrane separator development for microbial fuel cells: A retrospective analysis using frequent itemset mining and descriptive statistical approach. Journal of Power Sources. https://doi.org/10.1016/j.jpowsour.2020.229014

Körstgens, V., Flemming, H. C., Wingender, J., & Borchard, W. (2001). Influence of calcium ions on the mechanical properties of a model biofilm of mucoid Pseudomonas aeruginosa. Water Science and Technology. https://doi.org/10.2166/wst.2001.0338

Krom, B. P., Buijssen, K., Busscher, H. J., & Van Der Mei, H. C. (2009). Candida biofilm analysis in the artificial throat using fisH. Methods in Molecular Biology. https://doi.org/10.1007/978-1-60327-151-6_6

Krom, B. P., Cohen, J. B., McElhaney Feser, G. E., & Cihlar, R. L. (2007). Optimized candidal biofilm microtiter assay. Journal of Microbiological Methods. https://doi.org/10.1016/j.mimet.2006.08.003

Kumlanghan, A., Liu, J., Thavarungkul, P., Kanatharana, P., & Mattiasson, B. (2007). Microbial fuel cell-based biosensor for fast analysis of biodegradable organic matter. Biosensors and Bioelectronics. https://doi.org/10.1016/j.bios.2006.12.014

Labro, J., Craig, T., Wood, S. A., & Packer, M. A. (2017). Demonstration of the use of a photosynthetic microbial fuel cell as an environmental biosensor. International Journal of Nanotechnology. https://doi.org/10.1504/IJNT.2017.082467

Lappann, M., Haagensen, J. A. J., Claus, H., Vogel, U., & Molin, S. (2006). Meningococcal biofilm formation: Structure, development and phenotypes in a standardized continuous flow system. Molecular Microbiology. https://doi.org/10.1111/j.1365-2958.2006.05448.x

Layton, A. C., Karanth, P. N., Lajoie, C. A., Meyers, A. J., Gregory, I. R., Stapleton, R. D., Taylor, D. E., & Sayler, G. S. (2000). Quantification of Hyphomicrobium populations in activated sludge from an industrial wastewater treatment system as determined by 16S rRNA analysis. Applied and Environmental Microbiology. https://doi.org/10.1128/AEM.66.3.1167-1174.2000

Leang, C., Malvankar, N. S., Franks, A. E., Nevin, K. P., & Lovley, D. R. (2013). Engineering Geobacter sulfurreducens to produce a highly cohesive conductive matrix with enhanced capacity for current production. Energy and Environmental Science. https://doi.org/10.1039/c3ee40441b

Lei, Y., Chen, W., & Mulchandani, A. (2006). Microbial biosensors. In Analytica Chimica Acta. 568, (1–2), 200–210. Elsevier. https://doi.org/10.1016/j.aca.2005.11.065

Leriche, V., Sibille, P., & Carpentier, B. (2000). Use of an enzyme-linked lectinsorbent assay to monitor the shift in polysaccharide composition in bacterial biofilms. Applied and Environmental

Microbiology. https://doi.org/10.1128/AEM.66.5.1851-1856.2000

Lewandowski, Z., Funk, T., Roe, F., & Little, B. J. (1994). Spatial distribution of pH at mild steel surface using an iridium oxide microelectrode. ASTM Special Technical Publication.

Li, H., Wen, Y., Cao, A., Huang, J., & Zhou, Q. (2014). The influence of multivalent cations on the flocculation of activated sludge with different sludge retention times. Water Research. https://doi.org/10.1016/j.watres.2014.02.014

Li, S., Cheng, C., & Thomas, A. (2017). Carbon-Based Microbial-Fuel-Cell Electrodes: From Conductive Supports to Active Catalysts. In Advanced Materials. https://doi.org/10.1002/adma.201602547

Light, S. H., Méheust, R., Ferrell, J. L., Cho, J., Deng, D., Agostoni, M., Iavarone, A. T., Banfield, J. F., D'Orazio, S. E. F., & Portnoy, D. A. (2019). Extracellular electron transfer powers flavinylated extracellular reductases in Gram-positive bacteria. Proceedings of the National Academy of Sciences of the United States of America. https://doi.org/10.1073/pnas.1915678116

Light, S. H., Su, L., Rivera-Lugo, R., Cornejo, J. A., Louie, A., Iavarone, A. T., Ajo-Franklin, C. M., & Portnoy, D. A. (2018). A flavin-based extracellular electron transfer mechanism in diverse Gram-positive bacteria. Nature. https://doi.org/10.1038/s41586-018-0498-z

Liu, H., Cheng, S., & Logan, B. E. (2005). Production of electricity from acetate or butyrate using a single-chamber microbial fuel cell. Environmental Science and Technology. https://doi.org/10.1021/es048927c

Liu, H., & Fang, H. H. P. (2002). Extraction of extracellular polymeric substances (EPS) of sludges. Journal of Biotechnology. https://doi.org/10.1016/S0168-1656(02)00025-1

Liu, H., & Logan, B. E. (2004). Electricity generation using an air-cathode single chamber microbial fuel cell in the presence and absence of a proton exchange membrane. Environmental Science and Technology. https://doi.org/10.1021/es0499344

Liu, H., Ramnarayanan, R., & Logan, B. E. (2004). Production of Electricity during Wastewater Treatment Using a Single Chamber Microbial Fuel Cell. Environmental Science and Technology. https://doi.org/10.1021/es034923g

Liu, Jianbo, Liu, Y., Feng, C., Wang, Z., Jia, T., Gong, L., & Xu, L. (2017). Enhanced performance of microbial fuel cell using carbon microspheres modified graphite anode. Energy Science and Engineering. https://doi.org/10.1002/ese3.164

Liu, Jing, Björnsson, L., & Mattiasson, B. (2000). Immobilised activated sludge based biosensor for biochemical oxygen demand measurement. Biosensors and Bioelectronics, 14(12), 883–893. https://doi.org/10.1016/S0956-5663(99)00064-0

Liu, L., Tsyganova, O., Lee, D. J., Chang, J. S., Wang, A., & Ren, N. (2013). Double-chamber microbial fuel cells started up under room and low temperatures. International Journal of Hydrogen Energy. https://doi.org/10.1016/j.ijhydene.2013.02.090

Liu, Y., & Tay, J. H. (2002). The essential role of hydrodynamic shear force in the formation of biofilm and granular sludge. In Water Research. https://doi.org/10.1016/S0043-1354(01)00379-7

Logan, B., Cheng, S., Watson, V., & Estadt, G. (2007). Graphite fiber brush anodes for increased power production in air-cathode microbial fuel cells. Environmental Science and Technology. https://doi.org/10.1021/es062644y

Logan, B. E. (2007). Microbial Fuel Cells. In Microbial Fuel Cells. John Wiley & Sons, Inc. https://doi.org/10.1002/9780470258590

Logan, B. E. (2009). Exoelectrogenic bacteria that power microbial fuel cells. Nature Reviews Microbiology. https://doi.org/10.1038/nrmicro2113

Logan, B. E. (2010). Scaling up microbial fuel cells and other bioelectrochemical systems. In Applied Microbiology and Biotechnology. https://doi.org/10.1007/s00253-009-2378-9

Logan, B. E., & Rabaey, K. (2012). Conversion of wastes into bioelectricity and chemicals by using microbial electrochemical technologies. In Science. https://doi.org/10.1126/science.1217412

Logan, B. E., & Regan, J. M. (2006a). Electricity-producing bacterial communities in microbial fuel cells.

In Trends in Microbiology. https://doi.org/10.1016/j.tim.2006.10.003

Logan, B. E., & Regan, J. M. (2006b). Microbial fuel cells - Challenges and applications. In Environmental Science and Technology. https://doi.org/10.1021/es0627592

Long, X., Cao, X., Song, H., Nishimura, O., & Li, X. (2019). Characterization of electricity generation and microbial community structure over long-term operation of a microbial fuel cell. Bioresource Technology, 285, 121395. https://doi.org/10.1016/j.biortech.2019.121395

Lovley, D. R. (2006). Bug juice: Harvesting electricity with microorganisms. Nature Reviews Microbiology. https://doi.org/10.1038/nrmicro1442

Lovley, D. R., & Nevin, K. P. (2014). Electricity Production with Electricigens. Bioenergy. https://doi.org/10.1128/9781555815547.ch23

Lovley, D. R., & Walker, D. J. F. (2019). Geobacter Protein Nanowires. Frontiers in Microbiology. https://doi.org/10.3389/fmicb.2019.02078

Lowry, O. H., Rosebrough, N. J., Farr, A. L., & Randall, R. J. (1951). Protein measurement with the Folin phenol reagent. The Journal of Biological Chemistry. https://doi.org/10.1016/0922-338X(96)89160-4

Lu, Z., Chang, D., Ma, J., Huang, G., Cai, L., & Zhang, L. (2015). Behavior of metal ions in bioelectrochemical systems: A review. Journal of Power Sources. https://doi.org/10.1016/j.jpowsour.2014.10.168

Luo, X., & Davis, J. J. (2013). Electrical biosensors and the label free detection of protein disease biomarkers. Chemical Society Reviews. https://doi.org/10.1039/c3cs60077g

Mack, D. (1999). Molecular mechanisms of Staphylococcus epidermidis biofilm formation. Journal of Hospital Infection. https://doi.org/10.1016/S0195-6701(99)90074-9

Madigan, Martinko & Parker, Brock Biology of Microorganisms | Pearson. (2003). https://www.pearson.com/us/higher-education/product/Madigan-Brock-Biology-of-Microorganisms-10th-Edition/9780130662712.html

Malvankar, N. S., Lau, J., Nevin, K. P., Franks, A. E., Tuominen, M. T., & Lovley, D. R. (2012). Electrical conductivity in a mixed-species biofilm. Applied and Environmental Microbiology. https://doi.org/10.1128/AEM.01803-12

Malvankar, N. S., Mester, T., Tuominen, M. T., & Lovley, D. R. (2012). Supercapacitors based on c-type cytochromes using conductive nanostructured networks of living bacteria. ChemPhysChem. https://doi.org/10.1002/cphc.201100865

Mampel, J., Spirig, T., Weber, S. S., Haagensen, J. A. J., Molin, S., & Hilbi, H. (2006). Planktonic replication is essential for biofilm formation by Legionella pneumophila in a complex medium under static and dynamic flow conditions. Applied and Environmental Microbiology. https://doi.org/10.1128/AEM.72.4.2885-2895.2006

Mancílio, L. B. K., Ribeiro, G. A., Lopes, E. M., Kishi, L. T., Martins-Santana, L., de Siqueira, G. M. V., Andrade, A. R., Guazzaroni, M.-E., & Reginatto, V. (2020). Unusual microbial community and impact of iron and sulfate on microbial fuel cell ecology and performance. Current Research in Biotechnology, 2, 64–73. https://doi.org/10.1016/j.crbiot.2020.04.001

Mani, I. (2020). Biofilm in bioremediation. In Bioremediation of Pollutants (pp. 375–385). Elsevier. https://doi.org/10.1016/b978-0-12-819025-8.00018-1

Marcus, A. K., Torres, C. I., & Rittmann, B. E. (2007). Conduction-based modeling of the biofilm anode of a microbial fuel cell. Biotechnology and Bioengineering. https://doi.org/10.1002/bit.21533

Mateo, S., Fernandez-Morales, F. J., Cañizares, P., & Rodrigo, M. A. (2017). Influence of the Cathode Platinum Loading and of the Implementation of Membranes on the Performance of Air-Breathing Microbial Fuel Cells. Electrocatalysis. https://doi.org/10.1007/s12678-017-0393-7

Meinders, J. M., van der Mei, H. C., & Busscher, H. J. (1995). Deposition Efficiency and Reversibility of Bacterial Adhesion under Flow. Journal of Colloid And Interface Science. https://doi.org/10.1006/jcis.1995.9960

Messina, G. A., Regiart, M., Pereira, S. V., Bertolino, F. A., Aranda, P. R., Raba, J., & Fernández-Baldo, M. A. (2019). Nanomaterials in the Development of Biosensor and Application in the Determination of Pollutants in Water (pp. 195–215). Springer, Cham. https://doi.org/10.1007/978-3-030-02381-2_9

Min, B., Kim, J. R., Oh, S. E., Regan, J. M., & Logan, B. E. (2005). Electricity generation from swine wastewater using microbial fuel cells. Water Research. https://doi.org/10.1016/j.watres.2005.09.039

Min, B., & Logan, B. E. (2004). Continuous electricity generation from domestic wastewater and organic substrates in a flat plate microbial fuel cell. Environmental Science and Technology. https://doi.org/10.1021/es0491026

Min, S. C., Schraft, H., Hansen, L. T., & Mackereth, R. (2006). Effects of physicochemical surface characteristics of Listeria monocytogenes strains on attachment to glass. Food Microbiology. https://doi.org/10.1016/j.fm.2005.04.004

Modestra, J. A., Reddy, C. N., Krishna, K. V., Min, B., & Mohan, S. V. (2020). Regulated surface potential impacts bioelectrogenic activity, interfacial electron transfer and microbial dynamics in microbial fuel cell. Renewable Energy, 149, 424–434. https://doi.org/10.1016/j.renene.2019.12.018

Møller, S., Korber, D. R., Wolfaardt, G. M., Molin, S., & Caldwell, D. E. (1997). Impact of nutrient composition on a degradative biofilm community. Applied and Environmental Microbiology. https://doi.org/10.1128/aem.63.6.2432-2438.1997

Moon, H., Chang, I. S., Jang, J. K., Kim, K. S., Lee, J., Lovitt, R. W., & Kim, B. H. (2005). On-line monitoring of low biochemical oxygen demand through continuous operation of a mediator-less microbial fuel cell. Journal of Microbiology and Biotechnology.

Moon, H., Chang, I. S., Kang, K. H., Jang, J. K., & Kim, B. H. (2004). Improving the dynamic response of a mediator-less microbial fuel cell as a biochemical oxygen demand (BOD) sensor. Biotechnology Letters, 26(22), 1717–1721. https://doi.org/10.1007/s10529-004-3743-5

Morra, M., & Cassinelli, C. (1997). Bacterial adhesion to polymer surfaces: A critical review of surface thermodynamic approaches. Journal of Biomaterials Science, Polymer Edition. https://doi.org/10.1163/156856297X00263

Munoz-Cupa, C., Hu, Y., Xu, C., & Bassi, A. (2021). An overview of microbial fuel cell usage in wastewater treatment, resource recovery and energy production. In Science of the Total Environment. https://doi.org/10.1016/j.scitotenv.2020.142429

Murtaza, G., & Zia, M. H. (2012). Title: Wastewater Production, Treatment and Use in Pakistan.

Nabi, G., Ali, M., Khan, S., & Kumar, S. (2019). The crisis of water shortage and pollution in Pakistan: risk to public health, biodiversity, and ecosystem. In Environmental Science and Pollution Research (Vol. 26, Issue 11, pp. 10443–10445). Springer Verlag. https://doi.org/10.1007/s11356-019-04483-w

Nations, U. (2019). Growing at a slower pace, world population is expected to reach 9.7 billion in 2050 and could peak at nearly 11 billion around 2100 | UN DESA | United Nations Department of Economic and Social Affairs. Department of Economics and Social Affairs.

Nevin, K. P., Richter, H., Covalla, S. F., Johnson, J. P., Woodard, T. L., Orloff, A. L., Jia, H., Zhang, M., & Lovley, D. R. (2008). Power output and columbic efficiencies from biofilms of Geobacter sulfurreducens comparable to mixed community microbial fuel cells. Environmental Microbiology. https://doi.org/10.1111/j.1462-2920.2008.01675.x

Nguyen, H. T. H., & Min, B. (2020). Leachate treatment and electricity generation using an algae-cathode microbial fuel cell with continuous flow through the chambers in series. Science of the Total Environment. https://doi.org/10.1016/j.scitotenv.2020.138054

Nguyen, T., Roddick, F. A., & Fan, L. (2012). Biofouling of water treatment membranes: A review of the underlying causes, monitoring techniques and control measures. Membranes. https://doi.org/10.3390/membranes2040804

Nichols, W. W., Evans, M. J., Slack, M. P. E., & Walmsley, H. L. (1989). The penetration of antibiotics into aggregates of mucoid and non-mucoid Pseudomonas aeruginosa. Journal of General

Microbiology. https://doi.org/10.1099/00221287-135-5-1291

Nigam, V. K., & Shukla, P. (2015). Enzyme based biosensors for detection of environmental pollutants-A review. In Journal of Microbiology and Biotechnology. https://doi.org/10.4014/jmb.1504.04010

Niu, C., & Gilbert, E. S. (2004). Colorimetric method for identifying plant essential oil components that affect biofilm formation and structure. Applied and Environmental Microbiology. https://doi.org/10.1128/AEM.70.12.6951-6956.2004

Nogueira, R., Melo, L. F., Purkhold, U., Wuertz, S., & Wagner, M. (2002). Nitrifying and heterotrophic population dynamics in biofilm reactors: Effects of hydraulic retention time and the presence of organic carbon. Water Research. https://doi.org/10.1016/S0043-1354(01)00229-9

O'Connor, T. J., Zheng, H., VanRheenen, S. M., Ghosh, S., Cianciotto, N. P., & Isberg, R. R. (2016). Iron limitation triggers early egress by the intracellular bacterial pathogen legionella pneumophila. Infection and Immunity, 84(8), 2185–2197. https://doi.org/10.1128/IAI.01306-15

Ødegaard, H. (2006). Innovations in wastewater treatment: The moving bed biofilm process. Water Science and Technology. https://doi.org/10.2166/wst.2006.284

Okada, T., Ayato, Y., Yuasa, M., & Sekine, I. (1999). The effect of impurity cations on the transport characteristics of perfluorosulfonated ionomer membranes. Journal of Physical Chemistry B. https://doi.org/10.1021/jp983762d

Olofsson, A. C., Hermansson, M., & Elwing, H. (2003). N-acetyl-L-cysteine affects growth, extracellular polysaccharide production, and bacterial biofilm formation on solid surfaces. Applied and Environmental Microbiology. https://doi.org/10.1128/AEM.69.8.4814-4822.2003

Omoike, A., & Chorover, J. (2004). Spectroscopic study of extracellular polymeric substances from Bacillus subtilis: Aqueous chemistry and adsorption effects. In Biomacromolecules 5 (4), 1219–1230. https://doi.org/10.1021/bm034461z

Osman, M. H., Shah, A. A., & Walsh, F. C. (2010). Recent progress and continuing challenges in bio-fuel cells. Part II: Microbial. In Biosensors and Bioelectronics. https://doi.org/10.1016/j.bios.2010.08.057

Ozturk, A., Aygun, A., & Nas, B. (2019). Application of sequencing batch biofilm reactor (SBBR) in dairy wastewater treatment. Korean Journal of Chemical Engineering, 36(2), 248–254. https://doi.org/10.1007/s11814-018-0198-2

Pakistan Strategic Country Environmental Assessment. (2006). In Pakistan Strategic Country Environmental Assessment. https://doi.org/10.1596/33928

Palanisamy, G., Jung, H. Y., Sadhasivam, T., Kurkuri, M. D., Kim, S. C., & Roh, S. H. (2019). A comprehensive review on microbial fuel cell technologies: Processes, utilization, and advanced developments in electrodes and membranes. Journal of Cleaner Production. https://doi.org/10.1016/j.jclepro.2019.02.172

Pankratova, G., Hederstedt, L., & Gorton, L. (2019). Extracellular electron transfer features of Gram-positive bacteria. Analytica Chimica Acta, 1076, 32–47. https://doi.org/10.1016/j.aca.2019.05.007

Pankratova, G., Leech, D., Gorton, L., & Hederstedt, L. (2018). Extracellular Electron Transfer by the Gram-Positive Bacterium Enterococcus faecalis. Biochemistry. https://doi.org/10.1021/acs.biochem.8b00600

Park, C., Fang, Y., Murthy, S. N., & Novak, J. T. (2010). Effects of floc aluminum on activated sludge characteristics and removal of 17-α-ethinylestradiol in wastewater systems. Water Research, 44(5), 1335–1340. https://doi.org/10.1016/j.watres.2009.11.002

Park, D. H., & Zeikus, J. G. (2000). Electricity generation in microbial fuel cells using neutral red as an electronophore. Applied and Environmental Microbiology. https://doi.org/10.1128/AEM.66.4.1292-1297.2000

Parra-Arroyo, L., Parra-Saldivar, R., Ramirez-Mendoza, R. A., Keshavarz, T., & Iqbal, H. M. N. (2020). Laccase-Assisted Cues: State-of-the-Art Analytical Modalities for Detection, Quantification, and Redefining "Removal" of Environmentally Related Contaminants of High Concern (pp. 173–190).

Springer, Cham. https://doi.org/10.1007/978-3-030-47906-0_7

Paula, A. J., Hwang, G., & Koo, H. (2020). Dynamics of bacterial population growth in biofilms resemble spatial and structural aspects of urbanization. Nature Communications, 11(1), 1–14. https://doi.org/10.1038/s41467-020-15165-4

Peeters, E., Nelis, H. J., & Coenye, T. (2008). Comparison of multiple methods for quantification of microbial biofilms grown in microtiter plates. Journal of Microbiological Methods. https://doi.org/10.1016/j.mimet.2007.11.010

Pham, T. H., Boon, N., De Maeyer, K., Höfte, M., Rabaey, K., & Verstraete, W. (2008). Use of Pseudomonas species producing phenazine-based metabolites in the anodes of microbial fuel cells to improve electricity generation. Applied Microbiology and Biotechnology. https://doi.org/10.1007/s00253-008-1619-7

Ponomareva, A. L., Buzoleva, L. S., & Bogatyrenko, E. A. (2018). Abiotic Environmental Factors Affecting the Formation of Microbial Biofilms. Biology Bulletin, 45(5), 490–496. https://doi.org/10.1134/S106235901805014X

Qin, Z., Yang, X., Yang, L., Jiang, J., Ou, Y., Molin, S., & Qu, D. (2007). Formation and properties of in vitro biofilms of ica-negative Staphylococcus epidermidis clinical isolates. Journal of Medical Microbiology. https://doi.org/10.1099/jmm.0.46799-0

Qureshi, N., Annous, B. A., Ezeji, T. C., Karcher, P., & Maddox, I. S. (2005). Biofilm reactors for industrial bioconversion process: Employing potential of enhanced reaction rates. Microbial Cell Factories. https://doi.org/10.1186/1475-2859-4-24

Rabaey, K., Boon, N., Höfte, M., & Verstraete, W. (2005). Microbial phenazine production enhances electron transfer in biofuel cells. Environmental Science and Technology, 39(9), 3401–3408. https://doi.org/10.1021/es048563o

Radić, J., Bralić, M., Kolar, M., Genorio, B., Prkić, A., & Mitar, I. (2020). Development of the New Fluoride Ion-Selective Electrode Modified with FexOy Nanoparticles. Molecules, 25(21), 5213. https://doi.org/10.3390/molecules25215213

Rahimnejad, M., Adhami, A., Darvari, S., Zirepour, A., & Oh, S. E. (2015). Microbial fuel cell as new technol ogy for bioelectricity generation: A review. In Alexandria Engineering Journal. https://doi.org/10.1016/j.aej.2015.03.031

Rasamiravaka, T., Labtani, Q., Duez, P., & El Jaziri, M. (2015). The formation of biofilms by pseudomonas aeruginosa: A review of the natural and synthetic compounds interfering with control mechanisms. In BioMed Research International. https://doi.org/10.1155/2015/759348

Read, S. T., Dutta, P., Bond, P. L., Keller, J., & Rabaey, K. (2010). Initial development and structure of biofilms on microbial fuel cell anodes. BMC Microbiology. https://doi.org/10.1186/1471-2180-10-98

Relevance of microbial extracellular polymeric substances (EPSs)--Part I: Structural and ecological aspects - PubMed. 2001

Rijnaarts, H. H. M., Norde, W., Bouwer, E. J., Lyklema, J., & Zehnder, A. J. B. (1995). Reversibility and mechanism of bacterial adhesion. Colloids and Surfaces B: Biointerfaces. https://doi.org/10.1016/0927-7765(94)01146-V

Rong, H., Gao, B., Dong, M., Zhao, Y., Sun, S., YanWang, Yue, Q., & Li, Q. (2013). Characterization of size, strength and structure of aluminum-polymer dual-coagulant flocs under different pH and hydraulic conditions. Journal of Hazardous Materials, 252–253, 330–337. https://doi.org/10.1016/j.jhazmat.2013.03.011

Rozendal, R. A., Hamelers, H. V. M., & Buisman, C. J. N. (2006). Effects of membrane cation transport on pH and microbial fuel cell performance. Environmental Science and Technology. https://doi.org/10.1021/es060387r

Rozendal, R. A., Jeremiasse, A. W., Hamelers, H. V. M., & Buisman, C. J. N. (2008). Hydrogen production with a microbial biocathode. Environmental Science and Technology.

https://doi.org/10.1021/es071720+

Ruiz-Urigüen, M., Shuai, W., & Jaffé, P. R. (2018). Electrode colonization by the Feammox bacterium Acidimicrobiaceae sp. strain A6. Applied and Environmental Microbiology. https://doi.org/10.1128/AEM.02029-18

Rutter, P. R., & Vincent, B. (1984). Physicochemical Interactions of the Substratum, Microorganisms, and the Fluid Phase. In Microbial Adhesion and Aggregation. https://doi.org/10.1007/978-3-642-70137-5_3

Santoro, C., Lei, Y., Li, B., & Cristiani, P. (2012). Power generation from wastewater using single chamber microbial fuel cells (MFCs) with platinum-free cathodes and pre-colonized anodes. Biochemical Engineering Journal. https://doi.org/10.1016/j.bej.2011.12.006

Schink, B. (1997). Energetics of syntrophic cooperation in methanogenic degradation. Microbiology and Molecular Biology Reviews : MMBR. https://doi.org/10.1128/.61.2.262-280.1997

Schröder, U. (2007). Anodic electron transfer mechanisms in microbial fuel cells and their energy efficiency. Physical Chemistry Chemical Physics. https://doi.org/10.1039/b703627m

Schwermer, C. U., Lavik, G., Abed, R. M. M., Dunsmore, B., Ferdelman, T. G., Stoodley, P., Gieseke, A., & De Beer, D. (2008). Impact of nitrate on the structure and function of bacterial biofilm communities in pipelines used for injection of seawater into oil fields. Applied and Environmental Microbiology. https://doi.org/10.1128/AEM.02027-07

Sealy, C. (2008). The problem with platinum. In Materials Today. https://doi.org/10.1016/S1369-7021(08)70254-2

Shakeri, S., Kermanshahi, R. K., Moghaddam, M. M., & Emtiazi, G. (2007). Assessment of biofilm cell removal and killing and biocide efficacy using the microtiter plate test. Biofouling. https://doi.org/10.1080/08927010701190011

Sharafat, I., Saeed, D. K., Yasmin, S., Imran, A., Zafar, Z., Hameed, A., & Ali, N. (2018). Interactive effect of trivalent iron on activated sludge digestion and biofilm structure in attached growth reactor of waste tire rubber. Environmental Technology (United Kingdom), 39(2), 130–143. https://doi.org/10.1080/09593330.2017.1296894

Sheng, G. P., Yu, H. Q., & Li, X. Y. (2010). Extracellular polymeric substances (EPS) of microbial aggregates in biological wastewater treatment systems: A review. In Biotechnology Advances. https://doi.org/10.1016/j.biotechadv.2010.08.001

Shi, L., Dong, H., Reguera, G., Beyenal, H., Lu, A., Liu, J., Yu, H. Q., & Fredrickson, J. K. (2016). Extracellular electron transfer mechanisms between microorganisms and minerals. In Nature Reviews Microbiology (Vol. 14, Issue 10, pp. 651–662). Nature Publishing Group. https://doi.org/10.1038/nrmicro.2016.93

Simões, L. C., Lemos, M., Pereira, A. M., Abreu, A. C., Saavedra, M. J., & Simões, M. (2011). Persister cells in a biofilm treated with a biocide. Biofouling. https://doi.org/10.1080/08927014.2011.579599

Sinha, A., Sengupta, T., & Saha, T. (2020). Technology policy and environmental quality at crossroads: Designing SDG policies for select Asia Pacific countries. Technological Forecasting and Social Change. https://doi.org/10.1016/j.techfore.2020.120317

Sivasankar, V., Mylsamy, P., & Omine, K. (2018). Microbial fuel cell technology for bioelectricity. In Microbial Fuel Cell Technology for Bioelectricity. https://doi.org/10.1007/978-3-319-92904-0

Slate, A. J., Whitehead, K. A., Brownson, D. A. C., & Banks, C. E. (2019). Microbial fuel cells: An overview of current technology. In Renewable and Sustainable Energy Reviews (Vol. 101, pp. 60–81). Elsevier Ltd. https://doi.org/10.1016/j.rser.2018.09.044

Snaidr, J., Fuchs, B., Wallner, G., Wagner, M., Schleifer, K. H., & Amann, R. (1999). Phylogeny and in situ identification of a morphologically conspicuous bacterium, Candidatus Magnospira bakii, present at very low frequency in activated sludge. Environmental Microbiology. https://doi.org/10.1046/j.1462-2920.1999.00012.x

Song, B., & Leff, L. G. (2006). Influence of magnesium ions on biofilm formation by Pseudomonas

fluorescens. Microbiological Research. https://doi.org/10.1016/j.micres.2006.01.004

Song, H. L., Zhu, Y., & Li, J. (2019). Electron transfer mechanisms, characteristics and applications of biological cathode microbial fuel cells – A mini review. In Arabian Journal of Chemistry. https://doi.org/10.1016/j.arabjc.2015.01.008

Stein, Nienke E., Hamelers, H. V. M., & Buisman, C. N. J. (2012a). Influence of membrane type, current and potential on the response to chemical toxicants of a microbial fuel cell based biosensor. Sensors and Actuators, B: Chemical. https://doi.org/10.1016/j.snb.2011.10.060

Stein, Nienke E., Hamelers, H. V. M., & Buisman, C. N. J. (2012b). The effect of different control mechanisms on the sensitivity and recovery time of a microbial fuel cell based biosensor. Sensors and Actuators, B: Chemical. https://doi.org/10.1016/j.snb.2012.05.076

Stein, Nienke Elisabeth, Hamelers, H. M. V., Van Straten, G., & Keesman, K. J. (2012). On-line detection of toxic components using a microbial fuel cell-based biosensor. Journal of Process Control. https://doi.org/10.1016/j.jprocont.2012.07.009

Stepanović, S., Vuković, D., Dakić, I., Savić, B., & Švabić-Vlahović, M. (2000). A modified microtiter-plate test for quantification of staphylococcal biofilm formation. Journal of Microbiological Methods. https://doi.org/10.1016/S0167-7012(00)00122-6

Sternberg, C., & Tolker-Nielsen, T. (2006). Growing and Analyzing Biofilms in Flow Cells. In Current Protocols in Microbiology. https://doi.org/10.1002/9780471729259.mc01b02s00

Stoodley, P., Dodds, I., Boyle, J. D., & Lappin-Scott, H. M. (1999). Influence of hydrodynamics and nutrients on biofilm structure. Journal of Applied Microbiology Symposium Supplement. https://doi.org/10.1111/j.1365-2672.1998.tb05279.x

Stoodley, Paul, Boyle, J. D., Dodds, I., & Lappin-scott, H. M. (1997). Consensus Model Of Biofilm Structure. Water.

Strycharz-Glaven, S. M., Snider, R. M., Guiseppi-Elie, A., & Tender, L. M. (2011). On the electrical conductivity of microbial nanowires and biofilms. In Energy and Environmental Science. https://doi.org/10.1039/c1ee01753e

Sun, J. Z., Kingori, G. P., Si, R. W., Zhai, D. D., Liao, Z. H., Sun, D. Z., Zheng, T., & Yong, Y. C. (2015). Microbial fuel cell-based biosensors for environmental monitoring: A review. Water Science and Technology, 71(6), 801–809. https://doi.org/10.2166/wst.2015.035

Sutherland, I. W. (2001). Biofilm exopolysaccharides: A strong and sticky framework. In Microbiology. https://doi.org/10.1099/00221287-147-1-3

Sutherland, Ian W. (2001). The biofilm matrix - An immobilized but dynamic microbial environment. In Trends in Microbiology. https://doi.org/10.1016/S0966-842X(01)02012-1

Tajdid Khajeh, R., Aber, S., Nofouzi, K., & Ebrahimi, S. (2020). Treatment of mixed dairy and dye wastewater in anode of microbial fuel cell with simultaneous electricity generation. Environmental Science and Pollution Research, 1–13. https://doi.org/10.1007/s11356-020-10232-1

Talpur, B. D., Ullah, A., & Ahmed, S. (2020). Water consumption pattern and conservation measures in academic building: a case study of Jamshoro Pakistan. SN Applied Sciences, 2(11), 1781. https://doi.org/10.1007/s42452-020-03588-z

Tan, T. C., & Qian, Z. (1997). Dead Bacillus subtilis cells for sensing biochemical oxygen demand of waters and wastewaters. Sensors and Actuators, B: Chemical. https://doi.org/10.1016/S0925-4005(97)00013-0

Tang, K., Ooi, G. T. H., Torresi, E., Kaarsholm, K. M. S., Hambly, A., Sundmark, K., Lindholst, S., Sund, C., Kragelund, C., Christensson, M., Bester, K., & Andersen, H. R. (2020). Municipal wastewater treatment targeting pharmaceuticals by a pilot-scale hybrid attached biofilm and activated sludge system (Hybas^{TM}). Chemosphere, 259, 127397. https://doi.org/10.1016/j.chemosphere.2020.127397

Tetteh, E. K., & Rathilal, S. (2019). Application of Organic Coagulants in Water and Wastewater Treatment.

The Effect of Wastewater Cations on Activated Sludge Characteristics: Effects of Aluminum and Iron in Floc on JSTOR. (2006.) https://www.jstor.org/stable/25045939?seq=1

The Pham, H. (2018). Biosensors based on lithotrophic microbial fuel cells in relation to heterotrophic counterparts: research progress, challenges, and opportunities. AIMS Microbiology. https://doi.org/10.3934/microbiol.2018.3.567

Thulasinathan, B., Ebenezer, J. O., Bora, A., Nagarajan, A., Pugazhendhi, A., Jayabalan, T., Nainamohamed, S., Doble, M., & Alagarsamy, A. (2020). Bioelectricity generation and analysis of anode biofilm metabolites from septic tank wastewater in microbial fuel cells. International Journal of Energy Research, er.5734. https://doi.org/10.1002/er.5734

Tolker-Nielsen, T., & Molin, S. (2000). Spatial organization of microbial biofilm communities. Microbial Ecology. https://doi.org/10.1007/s002480000057

Tran, H. T., Kim, D. H., Oh, S. J., Rasool, K., Park, D. H., Zhang, R. H., & Ahn, D. H. (2009). Nitrifying biocathode enables effective electricity generation and sustainable wastewater treatment with microbial fuel cell. Water Science and Technology. https://doi.org/10.2166/wst.2009.209

Turner, Anthony P.F., Isao Karube, G. S. W. (1987). Biosensors-Fundamentals and Applications. Oxford University Press.

Ucar, D., Zhang, Y., & Angelidaki, I. (2017). An overview of electron acceptors in microbial fuel cells. In Frontiers in Microbiology (Vol. 8, Issue APR). Frontiers Research Foundation. https://doi.org/10.3389/fmicb.2017.00643

UNESCO Publishing and Earthscan Publications, F. (2009). Water in a Changing World - World Water Assessment Programme (United Nations).

Van Loosdrecht, M. C.M., Lyklema, J., Norde, W., & Zehnder, A. J. B. (1990). Influence of interfaces on microbial activity. In Microbiological Reviews. https://doi.org/10.1128/mmbr.54.1.75-87.1990

van Loosdrecht, Mark C. M., Norde, W., Lyklema, J., & Zehnder, A. J. B. (1990). Hydrophobic and electrostatic parameters in bacterial adhesion. Aquatic Sciences. https://doi.org/10.1007/bf00878244

Van Oss, C. J., Good, R. J., & Chaudhury, M. K. (1986). The role of van der Waals forces and hydrogen bonds in "hydrophobic interactions" between biopolymers and low energy surfaces. Journal of Colloid And Interface Science. https://doi.org/10.1016/0021-9797(86)90041-X

Vandecandelaere, I., Van Acker, H., & Coenye, T. (2016). A microplate-based system as in vitro model of biofilm growth and quantification. Methods in Molecular Biology. https://doi.org/10.1007/978-1-4939-2854-5_5

Venkata Mohan, S., Mohanakrishna, G., Srikanth, S., & Sarma, P. N. (2008). Harnessing of bioelectricity in microbial fuel cell (MFC) employing aerated cathode through anaerobic treatment of chemical wastewater using selectively enriched hydrogen producing mixed consortia. Fuel. https://doi.org/10.1016/j.fuel.2008.03.002

Venkata Mohan, S., Raghavulu, S. V., Goud, R. K., Srikanth, S., Babu, V. L., & Sarma, P. N. (2010). Microbial diversity analysis of long term operated biofilm configured anaerobic reactor producing biohydrogen from wastewater under diverse conditions. International Journal of Hydrogen Energy. https://doi.org/10.1016/j.ijhydene.2010.08.008

Verrastro, M., Cicco, N., Crispo, F., Morone, A., Dinescu, M., Dumitru, M., Favati, F., & Centonze, D. (2016). Amperometric biosensor based on Laccase immobilized onto a screen-printed electrode by Matrix Assisted Pulsed Laser Evaporation. Talanta. https://doi.org/10.1016/j.talanta.2016.03.072

Vu, B., Chen, M., Crawford, R. J., & Ivanova, E. P. (2009). Bacterial extracellular polysaccharides involved in biofilm formation. Molecules (Vol. 14, Issue 7, pp. 2535–2554). Molecules. https://doi.org/10.3390/molecules14072535

Walker, S. L. (2005). The role of nutrient presence on the adhesion kinetics of Burkholderia cepacia G4g and ENV435g. Colloids and Surfaces B: Biointerfaces. https://doi.org/10.1016/j.colsurfb.2005.08.007

Walker, S. L., Redman, J. A., & Elimelech, M. (2004). Role of cell surface lipopolysaccharides in

escherichia coli K12 adhesion and transport. Langmuir. https://doi.org/10.1021/la049511f

Walters, R., & Fuentes Loureiro, M. A. (2020). Waste Crime and the Global Transference of Hazardous Substances: A Southern Green Perspective. Critical Criminology, 28(3), 463–480. https://doi.org/10.1007/s10612-020-09522-4

Wang, C.-T., Huang, R.-Y., Lee, Y.-C., & Zhang, C.-D. (2013). Electrode Material of Carbon Nanotube/Polyaniline Carbon Paper Applied in Microbial Fuel Cells. Journal of Clean Energy Technologies. https://doi.org/10.7763/jocet.2013.v1.47

Wang, F., Deng, L., Huang, F., Wang, Z., Lu, Q., & Xu, C. (2020). Flagellar Motility Is Critical for Salmonella enterica Serovar Typhimurium Biofilm Development. Frontiers in Microbiology, 11, 1695. https://doi.org/10.3389/fmicb.2020.01695

Wang, G. H., Cheng, C. Y., Liu, M. H., Chen, T. Y., Hsieh, M. C., & Chung, Y. C. (2016). Utility of ochrobactrum anthropi yc152 in a microbial fuel cell as an early warning device for hexavalent chromium determination. Sensors (Switzerland). https://doi.org/10.3390/s16081272

Wang, Xiaofei, Aulenta, F., Puig, S., Esteve-Núñez, A., He, Y., Mu, Y., & Rabaey, K. (2020). Microbial electrochemistry for bioremediation. Environmental Science and Ecotechnology. https://doi.org/10.1016/j.ese.2020.100013

Wang, Xin, Gao, N., & Zhou, Q. (2013). Concentration responses of toxicity sensor with Shewanella oneidensis MR-1 growing in bioelectrochemical systems. Biosensors and Bioelectronics. https://doi.org/10.1016/j.bios.2012.12.029

Wang, Y., Wang, C. Y., & Chen, K. S. (2007). Elucidating differences between carbon paper and carbon cloth in polymer electrolyte fuel cells. Electrochimica Acta. https://doi.org/10.1016/j.electacta.2006.11.012

Watanabe, K. (2008). Recent Developments in Microbial Fuel Cell Technologies for Sustainable Bioenergy. Journal of Bioscience and Bioengineering. https://doi.org/10.1263/jbb.106.528

Wei, L., Han, H., & Shen, J. (2013). Effects of temperature and ferrous sulfate concentrations on the performance of microbial fuel cell. International Journal of Hydrogen Energy. https://doi.org/10.1016/j.ijhydene.2013.01.019

Wen, Q., Wu, Y., Zhao, L. X., Sun, Q., & Kong, F. Y. (2010). Electricity generation and brewery wastewater treatment from sequential anode-cathode microbial fuel cell. Journal of Zhejiang University: Science B. https://doi.org/10.1631/jzus.B0900272

Wieckowski, A., & Nørskov, J. K. (2010). Fuel Cell Science: Theory, Fundamentals, and Biocatalysis. In Fuel Cell Science: Theory, Fundamentals, and Biocatalysis. https://doi.org/10.1002/9780470630693

Wilén, B. M., Lumley, D., Mattsson, A., & Mino, T. (2008). Relationship between floc composition and flocculation and settling properties studied at a full scale activated sludge plant. Water Research. https://doi.org/10.1016/j.watres.2008.07.033

Wingender, J., Neu, T. R., & Flemming, H.-C. (1999). Microbial extracellular polymeric substances: characterization, structure, and function. In Springer.

Wrighton, K. C., Thrash, J. C., Melnyk, R. A., Bigi, J. P., Byrne-Bailey, K. G., Remis, J. P., Schichnes, D., Auer, M., Chang, C. J., & Coates, J. D. (2011). Evidence for direct electron transfer by a Gram-positive bacterium isolated from a microbial fuel cell. Applied and Environmental Microbiology. https://doi.org/10.1128/AEM.05365-11

Wu, D., Xing, D., Lu, L., Wei, M., Liu, B., & Ren, N. (2013). Ferric iron enhances electricity generation by Shewanella oneidensis MR-1 in MFCs. Bioresource Technology, 135, 630–634. https://doi.org/10.1016/j.biortech.2012.09.106

Wu, J., Chen, F., Huang, X., Geng, W., & Wen, X. (2006). Using inorganic coagulants to control membrane fouling in a submerged membrane bioreactor. Desalination, 197(1–3), 124–136. https://doi.org/10.1016/j.desal.2005.11.026

Yang, E., Chae, K. J., Choi, M. J., He, Z., & Kim, I. S. (2019). Critical review of bioelectrochemical systems integrated with membrane-based technologies for desalination, energy self-sufficiency, and

high-efficiency water and wastewater treatment. Desalination, 452(2018), 40–67. https://doi.org/10.1016/j.desal.2018.11.007

Yang, Y., Zhao, Y., Tang, C., Xu, L., Morgan, D., & Liu, R. (2020). Role of macrophyte species in constructed wetland-microbial fuel cell for simultaneous wastewater treatment and bioenergy generation. Chemical Engineering Journal. https://doi.org/10.1016/j.cej.2019.123708

Yaqoob, A. A., Ibrahim, M. N. M., Rafatullah, M., Chua, Y. S., Ahmad, A., & Umar, K. (2020). Recent advances in anodes for microbial fuel cells: An overview. In Materials. https://doi.org/10.3390/ma13092078

Yildiz, B. S. (2012). Water and wastewater treatment: Biological processes. In Metropolitan Sustainability: Understanding and Improving the Urban Environment (Woodhead P, pp. 406–428). Elsevier Ltd. https://doi.org/10.1533/9780857096463.3.406

You, S., Zhao, Q., Zhang, J., Jiang, J., Wan, C., Du, M., & Zhao, S. (2007). A graphite-granule membrane-less tubular air-cathode microbial fuel cell for power generation under continuously operational conditions. Journal of Power Sources. https://doi.org/10.1016/j.jpowsour.2007.07.063

Yurko, G., Roostaei, J., Dittrich, T., Xu, L., Ewing, M., Zhang, Y., & Shreve, G. (2019). Real-Time Sensor Response Characteristics of 3 Commercial Metal Oxide Sensors for Detection of BTEX and Chlorinated Aliphatic Hydrocarbon Organic Vapors. Chemosensors. https://doi.org/10.3390/chemosensors7030040

Zekker, I., Bhowmick, G. D., Priks, H., Nath, D., Rikmann, E., Jaagura, M., Tenno, T., Tämm, K., & Ghangrekar, M. M. (2020). ANAMMOX-denitrification biomass in microbial fuel cell to enhance the electricity generation and nitrogen removal efficiency. Biodegradation, 1–16. https://doi.org/10.1007/s10532-020-09907-w

Zeng, J., Gao, J. M., Chen, Y. P., Yan, P., Dong, Y., Shen, Y., Guo, J. S., Zeng, N., & Zhang, P. (2016). Composition and aggregation of extracellular polymeric substances (EPS) in hyperhaline and municipal wastewater treatment plants. Scientific Reports, 6(1), 1–9. https://doi.org/10.1038/srep26721

Zeng, L., Li, X., Shi, Y., Qi, Y., Huang, D., Tadé, M., Wang, S., & Liu, S. (2017). FePO4 based single chamber air-cathode microbial fuel cell for online monitoring levofloxacin. Biosensors and Bioelectronics. https://doi.org/10.1016/j.bios.2016.12.021

Zhang, H., Yuan, X., Xiong, T., Wang, H., & Jiang, L. (2020). Bioremediation of co-contaminated soil with heavy metals and pesticides: Influence factors, mechanisms and evaluation methods. In Chemical Engineering Journal 398, p. 1256-57. https://doi.org/10.1016/j.cej.2020.125657

Zhang, L., Fu, G., & Zhang, Z. (2019). Electricity generation and microbial community in long-running microbial fuel cell for high-salinity mustard tuber wastewater treatment. Bioelectrochemistry. https://doi.org/10.1016/j.bioelechem.2018.11.002

Zhang, S., Yang, F., Liu, C., Chen, X., Tan, X., Zhou, Y., Guo, F., & Jiang, W. (2020). Study on global industrialization and industry emission to achieve the 2 ∘C goal based on message model and LMDI approach. Energies. https://doi.org/10.3390/en13040825

Zhang, T., Zhang, L., Su, W., Gao, P., Li, D., He, X., & Zhang, Y. (2011). The direct electrocatalysis of phenazine-1-carboxylic acid excreted by Pseudomonas alcaliphila under alkaline condition in microbial fuel cells. Bioresource Technology. https://doi.org/10.1016/j.biortech.2011.04.093

Zhang, W., Zhang, X., Wang, D., Koga, Y., Rouse, J. D., & Furukawa, K. (2011). Trace elements enhance biofilm formation in UASB reactor for solo simple molecule wastewater treatment. Bioresource Technology. https://doi.org/10.1016/j.biortech.2011.06.095

Zhang, X., Cheng, S., Wang, X., Huang, X., & Logan, B. E. (2009). Separator characteristics for increasing performance of microbial fuel cells. Environmental Science and Technology. https://doi.org/10.1021/es901631p

Zhang, Yichong, Xu, Q., Huang, G., Zhang, L., & Liu, Y. (2020). Effect of dissolved oxygen concentration on nitrogen removal and electricity generation in self pH-buffer microbial fuel cell.

International Journal of Hydrogen Energy. https://doi.org/10.1016/j.ijhydene.2020.09.110

Zhang, Ying, Liu, M., Zhou, M., Yang, H., Liang, L., & Gu, T. (2019). Microbial fuel cell hybrid systems for wastewater treatment and bioenergy production: Synergistic effects, mechanisms and challenges. In Renewable and Sustainable Energy Reviews. https://doi.org/10.1016/j.rser.2018.12.027

Zhao, F., Harnisch, F., Schröder, U., Scholz, F., Bogdanoff, P., & Herrmann, I. (2006). Challenges and constraints of using oxygen cathodes in microbial fuel cells. Environmental Science and Technology. https://doi.org/10.1021/es060332p

Zhou, T., Han, H., Liu, P., Xiong, J., Tian, F., & Li, X. (2017). Microbial fuels cell-based biosensor for toxicity detection: A review. Sensors. 17(10), 1–21. https://doi.org/10.3390/s17102230

Zhou, Y., Varquez, A. C. G., & Kanda, M. (2019). High-resolution global urban growth projection based on multiple applications of the SLEUTH urban growth model. Scientific Data, 6(1), 1–10. https://doi.org/10.1038/s41597-019-0048-z

Zhu, F., Wang, W., Zhang, X., & Tao, G. (2011). Electricity generation in a membrane-less microbial fuel cell with down-flow feeding onto the cathode. Bioresource Technology. https://doi.org/10.1016/j.biortech.2011.04.062

Zobell, C. E. (1943). The Effect of Solid Surfaces upon Bacterial Activity1. Journal of Bacteriology. https://doi.org/10.1128/jb.46.1.39-56.1943

Zou, L., Huang, Y. hong, Long, Z. er, & Qiao, Y. (2019). On-going applications of *Shewanella* species in microbial electrochemical system for bioenergy, bioremediation and biosensing. World Journal of Microbiology and Biotechnology 35(1), pp. 1–9 https://doi.org/10.1007/s11274-018-2576-7

Chapter 3 (A)

Addison, S., Slade, A., & Dennis, M. (2011). Effects of substrate composition on the structure of microbial communities in wastewater using fluorescence in situ hybridisation. Systematic and Applied Microbiology, 34(5), 337–343. https://doi.org/10.1016/j.syapm.2010.10.006

Alm, E. W., Oerther, D. B., Larsen, N., Stahl, D. A., & Raskin, L. (1996). The oligonucleotide probe database. Applied and Environmental Microbiology 62 (10), pp. 3557–3559). https://doi.org/10.1128/aem.62.10.3557-3559.1996

Amann, R. I., Krumholz, L., & Stahl, D. A. (1990). Fluorescent-oligonucleotide probing of whole cells for determinative, phylogenetic, and environmental studies in microbiology. Journal of Bacteriology, 172(2), 762–770. https://doi.org/10.1128/jb.172.2.762-770.1990

Appenzeller, B. M. R., Yañez, C., Jorand, F., & Block, J. C. (2005). Advantage provided by iron for Escherichia coli growth and cultivability in drinking water. Applied and Environmental Microbiology, 71(9), 5621–5623. https://doi.org/10.1128/AEM.71.9.5621-5623.2005

Anderson S. (2008) Assessment of carrier materials for biofilm formation and denitrification. 64, p. 201-207 http://kth.diva-portal.org/smash/record.jsf?pid=diva2%3A209555&dswid=1327

Banin, E., Vasil, M. L., & Greenberg, E. P. (2005). Iron and *Pseudomonas aeruginosa* biofilm formation. Proceedings of the National Academy of Sciences of the United States of America. https://doi.org/10.1073/pnas.0504266102

Barbooti, M. M., Mohamed, T. J., Hussain, A. A., & Abas, F. O. (2004). Optimization of pyrolysis conditions of scrap tires under inert gas atmosphere. Journal of Analytical and Applied Pyrolysis. https://doi.org/10.1016/j.jaap.2004.05.001

Beech, I. B., & Sunner, J. (2004). Biocorrosion: Towards understanding interactions between biofilms and metals. In Current Opinion in Biotechnology 15, (3), 181–186. Curr Opin Biotechnol. https://doi.org/10.1016/j.copbio.2004.05.001

Bergey, D. (1994). Bergey's manual of determinative bacteriology. (Ninth edition /).

Bertaux, J., Gloger, U., Schmid, M., Hartmann, A., & Scheu, S. (2007). Routine fluorescence in situ hybridization in soil. Journal of Microbiological Methods, 69(3), 451–460. https://doi.org/10.1016/j.mimet.2007.02.012

Breisha, G. Z., & Winter, J. (2010). Bio-removal of nitrogen from wastewaters-A review. Undefined.

Brosius, J., Dull, T. J., Sleeter, D. D., & Noller, H. F. (1981). Gene organization and primary structure of a ribosomal RNA operon from Escherichia coli. Journal of Molecular Biology, 148(2), 107–127. https://doi.org/10.1016/0022-2836(81)90508-8

Buchauer, K. (1998). A comparison of two simple titration procedures to determine volatile fatty acids in influents to waste-water and sludge treatment processes. Undefined.

Calderón, K., Martín-Pascual, J., Poyatos, J. M., Rodelas, B., González-Martínez, A., & González-López, J. (2012). Comparative analysis of the bacterial diversity in a lab-scale moving bed biofilm reactor (MBBR) applied to treat urban wastewater under different operational conditions. Bioresource Technology, 121, 119–126. https://doi.org/10.1016/j.biortech.2012.06.078

Chyan, J. M., Senoro, D. B., Lin, C. J., Chen, P. J., & Chen, I. M. (2013). A novel biofilm carrier for pollutant removal in a constructed wetland based on waste rubber tire chips. International Biodeterioration and Biodegradation. https://doi.org/10.1016/j.ibiod.2013.04.010

Daims, H., Lücker, S., & Wagner, M. (2006). daime, a novel image analysis program for microbial ecology and biofilm research. Environmental Microbiology, 8(2), 200–213. https://doi.org/10.1111/j.1462-2920.2005.00880.x

Do, K. U., Banu, J. R., Kaliappan, S., & Yeom, I. T. (2013). Influence of the thermochemical sludge pretreatment on the nitrification of A/O reactor with the removal of phosphorus by simultaneous precipitation. Biotechnology and Bioprocess Engineering, 18(2), 313–320. https://doi.org/10.1007/s12257-012-0492-5

End-of-Life Tires - World Business Council for Sustainable Development (WBCSD). (2019.). Retrieved August 12, 2020, from https://www.wbcsd.org/Sector-Projects/Tire-Industry-Project/News/End-of-Life-Tires

Environment Protection Authority Waste Guidelines Waste tyres. (2010). www.environment.gov.au/settlements/waste/tyres/index.html

ETRMA annual report 2014.. Retrieved August 12, 2020, from https://www.etrma.org/wp-content/uploads/2019/09/etrma-annual-report-2014_web_single_pages.pdf

FISH Handbook for Biological Wastewater Treatment | IWA Publishing. (2009). Retrieved November 20, 2020, from https://www.iwapublishing.com/books/9781843392316/fish-handbook-biological-wastewater-treatment

Fridonia. (2019.). World Tires - Market Size, Market Share, Market Leaders, Demand Forecast, Sales, Company Profiles, Market Research, Industry Trends and Companies - Bridgestone, Michelin, and Goodyear. Retrieved August 12, 2020, from https://www.freedoniagroup.com/industry-study/world-tires-3357.htm

Handbook of Water and Wastewater Microbiology - 1st Edition, 2003, D. Mara & N. Horan (editors), Academic press, https://www.elsevier.com/books/handbook-of-water-and-wastewater-microbiology/mara/978-0-12-470100-7

Higgins, M. J., & Novak, J. T. (1997a). Dewatering and Settling of Activated Sludges : The Case for Using Cation Analysis Dewatering The sludges : and case settling for using of activated analysis cation. Water Environment Research, 69(2), 225–232. https://doi.org/10.2175/106143097X125380

Higgins, M. J., & Novak, J. T. (1997b). Characterization of Exocellular Protein and Its Role in Bioflocculation. Journal of Environmental Engineering, 123(5), 479–485. https://doi.org/10.1061/(asce)0733-9372(1997)123:5(479)

Holst, O., Stenberg, B., & Christiansson, M. (1998). Biotechnological possibilities for waste tyre-rubber treatment. Biodegradation, 9(3–4), 301–310. https://doi.org/10.1023/a:1008337708006

In-situ characterization of microbial community in an A/O submerged membrane bioreactor with nitrogen removal - PubMed. (2004.)https://pubmed.ncbi.nlm.nih.gov/15566185/

Influence of Cations on Activated-Sludge Effluent Quality on JSTOR. (2001). Retrieved November 20, 2020, from https://www.jstor.org/stable/25045457?seq=1

Internal circulation reactor: pushing the limits of anaerobic-eWISA. (2014). https://www.yumpu.com/en/document/view/19613280/internal-circulation-reactor-pushing-the-limits-of-anaerobic-ewisa

Kawamura, S. (1976). Considerations on Improving Flocculation. Journal - American Water Works Association, 68(6), 328–336. https://doi.org/10.1002/j.1551-8833.1976.tb02421.x

Langone, M., Yan, J., Haaijer, S. C. M., Op den Camp, H. J. M., Jetten, M. S. M., & Andreottola, G. (2014). Coexistence of nitrifying, anammox and denitrifying bacteria in a sequencing batch reactor. Frontiers in Microbiology, 5(FEB). https://doi.org/10.3389/fmicb.2014.00028

Lin, S., Wang, Y., Lin, J., Wang, X., & Gong, H. (2009). Dominant bacteria correlated with elimination of sludge in an innovative reactor. Progress in Natural Science, 19(12), 1765–1771. https://doi.org/10.1016/j.pnsc.2009.07.008

Lipponen, M. T. T., Suutari, M. H., & Martikainen, P. J. (2002). Occurrence of nitrifying bacteria and nitrification in Finnish drinking water distribution systems. Water Research, 36(17), 4319–4329. https://doi.org/10.1016/S0043-1354(02)00169-0

Liu, J., Zhou, X. H., & Shi, H. C. (2012). Inhibitory effects of pentachlorophenol on wastewater biofilms as determined by phospholipid analysis and microelectrode. Biochemical Engineering Journal, 66, 8–13. https://doi.org/10.1016/j.bej.2012.04.002

Lo, I. W., Lo, K. V., Mavinic, D. S., Shiskowski, D., & Ramey, W. (2010). Contributions of biofilm and suspended sludge to nitrogen transformation and nitrous oxide emission in hybrid sequencing batch system. Journal of Environmental Sciences, 22(7), 953–960. https://doi.org/10.1016/S1001-0742(09)60204-7

Low, E. W., Chase, H. A., Milner, M. G., & Curtis, T. P. (2000). Uncoupling of metabolism to reduce biomass production in the activated sludge process. Water Research, 34(12), 3204–3212. https://doi.org/10.1016/S0043-1354(99)00364-4

Managing End-of-Life Tires - World Business Council for Sustainable Development (WBCSD). (2019.). Retrieved August 12, 2020, from https://www.wbcsd.org/Sector-Projects/Tire-Industry-Project/Resources/Managing-End-of-Life-Tires

Manz, W., Szewzyk, U., Ericsson, P., Amann, R., Schleifer, K. H., & Stenstrom, T. A. (1993). In situ identification of bacteria in drinking water and adjoining biofilms by hybridization with 16S and 23S rRNA-directed fluorescent oligonucleotide probes. Applied and Environmental Microbiology, 59(7), 2293–2298. https://doi.org/10.1128/aem.59.7.2293-2298.1993

Manz, W., Wendt-Potthoff, K., Neu, T. R., Szewzyk, U., & Lawrence, J. R. (1999). Phylogenetic composition, spatial structure, and dynamics of lotic bacterial biofilms investigated by fluorescent in situ hybridization and confocal laser scanning microscopy. Microbial Ecology, 37(4), 225–237. https://doi.org/10.1007/s002489900148

Massonet, C., Pintens, V., Merckx, R., Anné, J., Lammertyn, E., & Van Eldere, J. (2006). Effect of iron on the expression of sirR and sitABC in biofilm-associated Staphylococcus epidermidis. BMC Microbiology, 6(1), 103. https://doi.org/10.1186/1471-2180-6-103

Merrylin, J., Kumar, S. A., Kaliappan, S., Yeom, I. T., & Banu, J. R. (2013). Biological pretreatment of non-flocculated sludge augments the biogas production in the anaerobic digestion of the pretreated waste activated sludge. Environmental Technology, 34(13–14), 2113–2123. https://doi.org/10.1080/09593330.2013.810294

Monds, R. D., & O'Toole, G. A. (2009). The developmental model of microbial biofilms: ten years of a paradigm up for review. In Trends in Microbiology (Vol. 17, Issue 2, pp. 73–87). Trends Microbiol. https://doi.org/10.1016/j.tim.2008.11.001

Muller, C. D. (2001). High-Intensity Shear as a Wet Sludge Disintegration Technology and a Mechanism for Floc Structure Analysis. Virginia Tech. https://vtechworks.lib.vt.edu/handle/10919/33650

Naz, I., Khatoon, N., Ali, M. I., Saroj, D. P., Batool, S. A., Ali, N., & Ahmed, S. (2014). Appraisal of the tire derived rubber (TDR) medium for wastewater treatment under aerobic and anaerobic conditions.

Journal of Chemical Technology & Biotechnology, 89(4), 587–596. https://doi.org/10.1002/jctb.4161

Nguyen, T. P., Hilal, N., Hankins, N. P., & Novak, J. T. (2008). The relationship between cation ions and polysaccharide on the floc formation of synthetic and activated sludge. Desalination, 227(1–3), 94–102. https://doi.org/10.1016/j.desal.2007.05.038

Nielsen, P. H., & Keiding, K. (1998). Disintegration of activated sludge flocs in presence of sulfide. Water Research, 32(2), 313–320. https://vbn.aau.dk/en/publications/disintegration-of-activated-sludge-flocs-in-presence-of-sulfide

Nkosi, N., & Muzenda, E. (2014). A review and discussion of waste tyre pyrolysis and derived products. Undefined.

O'Toole, G. A., & Kolter, R. (1998). Flagellar and twitching motility are necessary for Pseudomonas aeruginosa biofilm development. Molecular Microbiology, 30(2), 295–304. https://doi.org/10.1046/j.1365-2958.1998.01062.x

Park, C., & Helm, R. F. (2008). Application of metaproteomic analysis for studying extracellular polymeric substances (EPS) in activated sludge flocs and their fate in sludge digestion. Water Science and Technology, 57(12), 2009–2015. https://doi.org/10.2166/wst.2008.620

Pavlekovic, M., Schmid, M. C., Schmider-Poignee, N., Spring, S., Pilhofer, M., Gaul, T., Fiandaca, M., Löffler, F. E., Jetten, M., Schleifer, K. H., & Lee, N. M. (2009). Optimization of three FISH procedures for in situ detection of anaerobic ammonium oxidizing bacteria in biological wastewater treatment. Journal of Microbiological Methods, 78(2), 119–126. https://doi.org/10.1016/j.mimet.2009.04.003

Peeters, B., Dewil, R., Lechat, D., & Smets, I. Y. (2011). Quantification of the exchangeable calcium in activated sludge flocs and its implication to sludge settleability. Separation and Purification Technology, 83(1), 1–8. https://doi.org/10.1016/j.seppur.2011.04.008

Purkhold, U., Pommerening-Röser, A., Juretschko, S., Schmid, M. C., Koops, H. P., & Wagner, M. (2000). Phylogeny of all recognized species of ammonia oxidizers based on comparative 16S rRNA and amoA sequence analysis: Implications for molecular diversity surveys. Applied and Environmental Microbiology, 66(12), 5368–5382. https://doi.org/10.1128/AEM.66.12.5368-5382.2000

Rajesh Banu, J., Uan, D. K., Kaliappan, S., & Yeom, I. T. (2011). Effect of sludge pretreatment on the performance of anaerobic/ anoxic/ oxic membrane bioreactor treating domestic wastewater. International Journal of Environmental Science and Technology, 8(2), 281–290. https://doi.org/10.1007/bf03326216

Rajesh Banu, J., Uan, D. K., & Yeom, I. T. (2009). Nutrient removal in an A2O-MBR reactor with sludge reduction. Bioresource Technology, 100(16), 3820–3824. https://doi.org/10.1016/j.biortech.2008.12.054

Review of Management of Used Tyres at Landfill Sites. (2006) https://docplayer.net/18211503-Review-of-management-of-used-tyres-at-landfill-sites.html

Reyes, O., Sánchez, E., Rovirosa, N., Borja, R., Cruz, M., Colmenarejo, M. F., Escobedo, R., Ruiz, M., Rodríguez, X., & Correa, O. (1999). Low-strength wastewater treatment by a multistage anaerobic filter packed with waste tyre rubber. Bioresource Technology, 70(1), 55–60. https://doi.org/10.1016/S0960-8524(99)00010-3

Sabinet | Alkalinity measurement: Part 3 - A 5 pH point titration method to determine the carbonate and SCFA weak acidlbases in aqueous solution containing also known concentrations of other weak acid/bases. (1993). https://journals.co.za/content/waters/19/1/AJA03784738_1822

Sakuma, T., Jinsiriwanit, S., Hattori, T., & Deshusses, M. A. (2008). Removal of ammonia from contaminated air in a biotrickling filter - Denitrifying bioreactor combination system. Water Research, 42(17), 4507–4513. https://doi.org/10.1016/j.watres.2008.07.036

Scala, D. J., Hacherl, E. L., Cowan, R., Young, L. Y., & Kosson, D. S. (2006). Characterization of

Fe(III)-reducing enrichment cultures and isolation of Fe(III)-reducing bacteria from the Savannah River site, South Carolina. Research in Microbiology, 157(8), 772–783. https://doi.org/10.1016/j.resmic.2006.04.001

Schmid, M., Thill, A., Purkhold, U., Walcher, M., Bottero, J. Y., Ginestet, P., Nielsen, P. H., Wuertz, S., & Wagner, M. (2003). Characterization of activated sludge flocs by confocal laser scanning microscopy and image analysis. Water Research, 37(9), 2043–2052. https://doi.org/10.1016/S0043-1354(02)00616-4

Serumgard, J. (2014). Internalization of Scrap Tire Management Costs: A Review of the North American Experience. Igarss 2014. https://doi.org/10.1007/s13398-014-0173-7.2

Shu, X., & Huang, B. (2014). Recycling of waste tire rubber in asphalt and portland cement concrete: An overview. Construction and Building Materials. https://doi.org/10.1016/j.conbuildmat.2013.11.027

Sienkiewicz, M., Kucinska-Lipka, J., Janik, H., & Balas, A. (2012). Progress in used tyres management in the European Union: A review. Waste Management. https://doi.org/10.1016/j.wasman.2012.05.010

Snaidr, J., Amann, R., Huber, I., Ludwig, W., & Schleifer, K. H. (1997). Phylogenetic analysis and in situ identification of bacteria in activated sludge. Applied and Environmental Microbiology. https://doi.org/10.1128/aem.63.7.2884-2896.1997

Tan, T. W., & Ng, H. Y. (2008). Influence of mixed liquor recycle ratio and dissolved oxygen on performance of pre-denitrification submerged membrane bioreactors. Water Research, 42(4–5), 1122–1132. https://doi.org/10.1016/j.watres.2007.08.028

Tang, Z., Butkus, M. A., & Xie, Y. F. (2006). Crumb rubber filtration: A potential technology for ballast water treatment. Marine Environmental Research. https://doi.org/10.1016/j.marenvres.2005.06.003

The Composition of a Tyre: Typical Components (2006). https://docplayer.net/20736072-The-composition-of-a-tyre-typical-components.html

The Effect of Cationic Salt Addition on the Settling and Dewatering Properties of an Industrial Activated Sludge on JSTOR. (1998). https://www.jstor.org/stable/25045109

The Effect of Wastewater Cations on Activated Sludge Characteristics: Effects of Aluminum and Iron in Floc on JSTOR. (2006). https://www.jstor.org/stable/25045939?seq=1

Vukanti, R., Crissman, M., Leff, L. G., & Leff, A. A. (2009). Bacterial communities of tyre monofill sites: growth on tyre shreds and leachate. Journal of Applied Microbiology, 106(6), 1957–1966. https://doi.org/10.1111/j.1365-2672.2009.04157.x

Watanabe, M., Suzuki, Y., Sasaki, K., Nakashimada, Y., & Nishio, N. (1999). Flocculating property of extracellular polymeric substance derived from a marine photosynthetic bacterium, Rhodovulum sp. Journal of Bioscience and Bioengineering, 87(5), 625–629. https://doi.org/10.1016/S1389-1723(99)80125-X

Wijeyekoon, S., Mino, T., Satoh, H., & Matsuo, T. (2004). Effects of substrate loading rate on biofilm structure. Water Research, 38(10), 2479–2488. https://doi.org/10.1016/j.watres.2004.03.005

Wilén, B. M., Jin, B., & Lant, P. (2003). The influence of key chemical constituents in activated sludge on surface and flocculating properties. Water Research, 37(9), 2127–2139. https://doi.org/10.1016/S0043-1354(02)00629-2

Wojnowska-Baryła, I., Cydzik-Kwiatkowska, A., & Zielińska, M. (2010). The application of molecular techniques to the study of wastewater treatment systems. In Methods in molecular biology. 599, 157–183. Methods Mol Biol. https://doi.org/10.1007/978-1-60761-439-5_11

Woznica, A., Nowak, A., Beimfohr, C., Karczewski, J., & Bernas, T. (2010). Monitoring structure and activity of nitrifying bacterial biofilm in an automatic biodetector of water toxicity. Chemosphere, 78(9), 1121–1128. https://doi.org/10.1016/j.chemosphere.2009.12.035

Xu, T., Xing, M., Yang, J., Lv, B., Duan, T., & Nie, J. (2014). Tracking the composition and dominant components of the microbial community via polymerase chain reaction-denaturing gradient gel electrophoresis and fluorescence in situ hybridization during vermiconversion for liquid-state excess sludge stabilization. Bioresource Technology, 167, 100–107.

https://doi.org/10.1016/j.biortech.2014.05.109

Yang, L., Barken, K. B., Skindersoe, M. E., Christensen, A. B., Givskov, M., & Tolker-Nielsen, T. (2007). Effects of iron on DNA release and biofilm development by Pseudomonas aeruginosa. Microbiology, 153(5), 1318–1328. https://doi.org/10.1099/mic.0.2006/004911-0

YANG, Q., LIU, Z., & YANG, J. (2009). Simultaneous determination of chemical oxygen demand (COD) and biological oxygen demand (BOD5) in wastewater by near-infrared spectrometry. Journal of Water Resource and Protection, 01(04), 286–289. https://doi.org/10.4236/jwarp.2009.14035

Zhang, G., Dong, H., Jiang, H., Kukkadapu, R. K., Kim, J., Eberl, D., & Xu, Z. (2009). Biomineralization associated with microbial reduction of Fe3+ and oxidation of Fe2+ in solid minerals. American Mineralogist, 94(7), 1049–1058. https://doi.org/10.2138/am.2009.3136

Zhou, X. hong, Huang, B. cheng, Zhou, T., Liu, Y. chen, & Shi, H. chang. (2015). Aggregation behavior of engineered nanoparticles and their impact on activated sludge in wastewater treatment. Chemosphere, 119, 568–576. https://doi.org/10.1016/j.chemosphere.2014.07.037

Chapter 3 (B)

Addison, S., Slade, A., & Dennis, M. (2011). Effects of substrate composition on the structure of microbial communities in wastewater using fluorescence in situ hybridisation. Systematic and Applied Microbiology, 34(5), 337–343. https://doi.org/10.1016/j.syapm.2010.10.006

Alm, E. W., Oerther, D. B., Larsen, N., Stahl, D. A., & Raskin, L. (1996). The oligonucleotide probe database. In Applied and Environmental Microbiology (Vol. 62, Issue 10, pp. 3557–3559). American Society for Microbiology. https://doi.org/10.1128/aem.62.10.3557-3559.1996

Amann, R. I., Krumholz, L., & Stahl, D. A. (1990). Fluorescent-oligonucleotide probing of whole cells for determinative, phylogenetic, and environmental studies in microbiology. Journal of Bacteriology, 172(2), 762–770. https://doi.org/10.1128/jb.172.2.762-770.1990

Appenzeller, B. M. R., Yañez, C., Jorand, F., & Block, J. C. (2005). Advantage provided by iron for Escherichia coli growth and cultivability in drinking water. Applied and Environmental Microbiology, 71(9), 5621–5623. https://doi.org/10.1128/AEM.71.9.5621-5623.2005

Assessment of carrier materials for biofilm formation and denitrification. (2008) http://kth.diva-portal.org/smash/record.jsf?pid=diva2%3A209555&dswid=1327

Banin, E., Vasil, M. L., & Greenberg, E. P. (2005). Iron and Pseudomonas aeruginosa biofilm formation. Proceedings of the National Academy of Sciences of the United States of America. https://doi.org/10.1073/pnas.0504266102

Barbooti, M. M., Mohamed, T. J., Hussain, A. A., & Abas, F. O. (2004). Optimization of pyrolysis conditions of scrap tires under inert gas atmosphere. Journal of Analytical and Applied Pyrolysis. https://doi.org/10.1016/j.jaap.2004.05.001

Beech, I. B., & Sunner, J. (2004). Biocorrosion: Towards understanding interactions between biofilms and metals. In Current Opinion in Biotechnology (Vol. 15, Issue 3, pp. 181–186). Curr Opin Biotechnol. https://doi.org/10.1016/j.copbio.2004.05.001

Bergey, D. (1994). Bergey's manual of determinative bacteriology. (Ninth edition /).

Bertaux, J., Gloger, U., Schmid, M., Hartmann, A., & Scheu, S. (2007). Routine fluorescence in situ hybridization in soil. Journal of Microbiological Methods, 69(3), 451–460. https://doi.org/10.1016/j.mimet.2007.02.012

Breisha, G. Z., & Winter, J. (2010). Bio-removal of nitrogen from wastewaters-A review. Undefined.

Brosius, J., Dull, T. J., Sleeter, D. D., & Noller, H. F. (1981). Gene organization and primary structure of a ribosomal RNA operon from Escherichia coli. Journal of Molecular Biology, 148(2), 107–127. https://doi.org/10.1016/0022-2836(81)90508-8

Buchauer, K. (1998). A comparison of two simple titration procedures to determine volatile fatty acids in influents to waste-water and sludge treatment processes. Undefined.

Calderón, K., Martín-Pascual, J., Poyatos, J. M., Rodelas, B., González-Martínez, A., & González-López,

J. (2012). Comparative analysis of the bacterial diversity in a lab-scale moving bed biofilm reactor (MBBR) applied to treat urban wastewater under different operational conditions. Bioresource Technology, 121, 119–126. https://doi.org/10.1016/j.biortech.2012.06.078

Chyan, J. M., Senoro, D. B., Lin, C. J., Chen, P. J., & Chen, I. M. (2013). A novel biofilm carrier for pollutant removal in a constructed wetland based on waste rubber tire chips. International Biodeterioration and Biodegradation. https://doi.org/10.1016/j.ibiod.2013.04.010

Daims, H., Lücker, S., & Wagner, M. (2006). daime, a novel image analysis program for microbial ecology and biofilm research. Environmental Microbiology, 8(2), 200–213. https://doi.org/10.1111/j.1462-2920.2005.00880.x

Do, K. U., Banu, J. R., Kaliappan, S., & Yeom, I. T. (2013). Influence of the thermochemical sludge pretreatment on the nitrification of A/O reactor with the removal of phosphorus by simultaneous precipitation. Biotechnology and Bioprocess Engineering, 18(2), 313–320. https://doi.org/10.1007/s12257-012-0492-5

End-of-Life Tires - World Business Council for Sustainable Development (WBCSD). (2019.). Retrieved August 12, 2020, from https://www.wbcsd.org/Sector-Projects/Tire-Industry-Project/News/End-of-Life-Tires

Environment Protection Authority Waste Guidelines Waste tyres. (2010). www.environment.gov.au/settlements/waste/tyres/index.html

ETRMA annual report 2014.. Retrieved August 12, 2020, from https://www.etrma.org/wp-content/uploads/2019/09/etrma-annual-report-2014_web_single_pages.pdf

FISH Handbook for Biological Wastewater Treatment | IWA Publishing. (2009.). Retrieved November 20, 2020, from https://www.iwapublishing.com/books/9781843392316/fish-handbook-biological-wastewater-treatment

Fridonia.. World Tires - Market Size, Market Share, Market Leaders, Demand Forecast, Sales, Company Profiles, Market Research, Industry Trends and Companies (2019)- Bridgestone, Michelin, and Goodyear. Retrieved August 12, 2020, from https://www.freedoniagroup.com/industry-study/world-tires-3357.htm

Handbook of Water and Wastewater Microbiology - 1st Edition.(2003) https://www.elsevier.com/books/handbook-of-water-and-wastewater-microbiology/mara/978-0-12-470100-7

Higgins, M. J., & Novak, J. T. (1997a). Dewatering and Settling of Activated Sludges : The Case for Using Cation Analysis Dewatering The sludges : and case settling for using of activated analysis cation. Water Environment Research, 69(2), 225–232. https://doi.org/10.2175/106143097X125380

Higgins, M. J., & Novak, J. T. (1997b). Characterization of exocellular protein and its role in bioflocculation. Journal of Environmental Engineering, 123(5), 479–485. https://doi.org/10.1061/(asce)0733-9372(1997)123:5(479)

Holst, O., Stenberg, B., & Christiansson, M. (1998). Biotechnological possibilities for waste tyre-rubber treatment. Biodegradation, 9(3–4), 301–310. https://doi.org/10.1023/a:1008337708006

In-situ characterization of microbial community in an A/O submerged membrane bioreactor with nitrogen removal - PubMed. (2004.). Retrieved November 21, 2020, from https://pubmed.ncbi.nlm.nih.gov/15566185/

Influence of Cations on Activated-Sludge Effluent Quality on JSTOR. (2001). https://www.jstor.org/stable/25045457?seq=1

internal circulation reactor: pushing the limits of anaerobic ... - eWISA. (2014.) https://www.yumpu.com/en/document/view/19613280/internal-circulation-reactor-pushing-the-limits-of-anaerobic-ewisa

Kawamura, S. (1976). Considerations on improving flocculation. Journal - American Water Works Association, 68(6), 328–336. https://doi.org/10.1002/j.1551-8833.1976.tb02421.x

Langone, M., Yan, J., Haaijer, S. C. M., Op den Camp, H. J. M., Jetten, M. S. M., & Andreottola, G.

(2014). Coexistence of nitrifying, anammox and denitrifying bacteria in a sequencing batch reactor. Frontiers in Microbiology, 5(FEB). https://doi.org/10.3389/fmicb.2014.00028

Lin, S., Wang, Y., Lin, J., Wang, X., & Gong, H. (2009). Dominant bacteria correlated with elimination of sludge in an innovative reactor. Progress in Natural Science, 19(12), 1765–1771. https://doi.org/10.1016/j.pnsc.2009.07.008

Lipponen, M. T. T., Suutari, M. H., & Martikainen, P. J. (2002). Occurrence of nitrifying bacteria and nitrification in Finnish drinking water distribution systems. Water Research, 36(17), 4319–4329. https://doi.org/10.1016/S0043-1354(02)00169-0

Liu, J., Zhou, X. H., & Shi, H. C. (2012). Inhibitory effects of pentachlorophenol on wastewater biofilms as determined by phospholipid analysis and microelectrode. Biochemical Engineering Journal, 66, 8–13. https://doi.org/10.1016/j.bej.2012.04.002

Lo, I. W., Lo, K. V., Mavinic, D. S., Shiskowski, D., & Ramey, W. (2010). Contributions of biofilm and suspended sludge to nitrogen transformation and nitrous oxide emission in hybrid sequencing batch system. Journal of Environmental Sciences, 22(7), 953–960. https://doi.org/10.1016/S1001-0742(09)60204-7

Low, E. W., Chase, H. A., Milner, M. G., & Curtis, T. P. (2000). Uncoupling of metabolism to reduce biomass production in the activated sludge process. Water Research, 34(12), 3204–3212. https://doi.org/10.1016/S0043-1354(99)00364-4

Managing End-of-Life Tires - World Business Council for Sustainable Development (WBCSD). (2019.). Retrieved August 12, 2020, from https://www.wbcsd.org/Sector-Projects/Tire-Industry-Project/Resources/Managing-End-of-Life-Tires

Manz, W., Szewzyk, U., Ericsson, P., Amann, R., Schleifer, K. H., & Stenstrom, T. A. (1993). In situ identification of bacteria in drinking water and adjoining biofilms by hybridization with 16S and 23S rRNA-directed fluorescent oligonucleotide probes. Applied and Environmental Microbiology, 59(7), 2293–2298. https://doi.org/10.1128/aem.59.7.2293-2298.1993

Manz, W., Wendt-Potthoff, K., Neu, T. R., Szewzyk, U., & Lawrence, J. R. (1999). Phylogenetic composition, spatial structure, and dynamics of lotic bacterial biofilms investigated by fluorescent in situ hybridization and confocal laser scanning microscopy. Microbial Ecology, 37(4), 225–237. https://doi.org/10.1007/s002489900148

Massonet, C., Pintens, V., Merckx, R., Anné, J., Lammertyn, E., & Van Eldere, J. (2006). Effect of iron on the expression of sirR and sitABC in biofilm-associated *Staphylococcus epidermidis*. BMC Microbiology, 6(1), 103. https://doi.org/10.1186/1471-2180-6-103

Merrylin, J., Kumar, S. A., Kaliappan, S., Yeom, I. T., & Banu, J. R. (2013). Biological pretreatment of non-flocculated sludge augments the biogas production in the anaerobic digestion of the pretreated waste activated sludge. Environmental Technology (United Kingdom), 34(13–14), 2113–2123. https://doi.org/10.1080/09593330.2013.810294

Monds, R. D., & O'Toole, G. A. (2009). The developmental model of microbial biofilms: ten years of a paradigm up for review. In Trends in Microbiology (Vol. 17, Issue 2, pp. 73–87). Trends Microbiol. https://doi.org/10.1016/j.tim.2008.11.001

Muller, C. D. (2001). High-intensity shear as a wet sludge disintegration technology and a mechanism for floc structure analysis. Virginia Tech. https://vtechworks.lib.vt.edu/handle/10919/33650

Naz, I., Khatoon, N., Ali, M. I., Saroj, D. P., Batool, S. A., Ali, N., & Ahmed, S. (2014). Appraisal of the tire derived rubber (TDR) medium for wastewater treatment under aerobic and anaerobic conditions. Journal of Chemical Technology & Biotechnology, 89(4), 587–596. https://doi.org/10.1002/jctb.4161

Nguyen, T. P., Hilal, N., Hankins, N. P., & Novak, J. T. (2008). The relationship between cation ions and polysaccharide on the floc formation of synthetic and activated sludge. Desalination, 227(1–3), 94–102. https://doi.org/10.1016/j.desal.2007.05.038

Nielsen, P. H., & Keiding, K. (1998). Disintegration of activated sludge flocs in presence of sulfide.

Water Research, 32(2), 313–320. https://vbn.aau.dk/en/publications/disintegration-of-activated-sludge-flocs-in-presence-of-sulfide

Nkosi, N., & Muzenda, E. (2014). A review and discussion of waste tyre pyrolysis and derived products. Undefined.

O'Toole, G. A., & Kolter, R. (1998). Flagellar and twitching motility are necessary for Pseudomonas aeruginosa biofilm development. Molecular Microbiology, 30(2), 295–304. https://doi.org/10.1046/j.1365-2958.1998.01062.x

Park, C., & Helm, R. F. (2008). Application of metaproteomic analysis for studying extracellular polymeric substances (EPS) in activated sludge flocs and their fate in sludge digestion. Water Science and Technology, 57(12), 2009–2015. https://doi.org/10.2166/wst.2008.620

Pavlekovic, M., Schmid, M. C., Schmider-Poignee, N., Spring, S., Pilhofer, M., Gaul, T., Fiandaca, M., Löffler, F. E., Jetten, M., Schleifer, K. H., & Lee, N. M. (2009). Optimization of three FISH procedures for in situ detection of anaerobic ammonium oxidizing bacteria in biological wastewater treatment. Journal of Microbiological Methods, 78(2), 119–126. https://doi.org/10.1016/j.mimet.2009.04.003

Peeters, B., Dewil, R., Lechat, D., & Smets, I. Y. (2011). Quantification of the exchangeable calcium in activated sludge flocs and its implication to sludge settleability. Separation and Purification Technology, 83(1), 1–8. https://doi.org/10.1016/j.seppur.2011.04.008

Purkhold, U., Pommerening-Röser, A., Juretschko, S., Schmid, M. C., Koops, H. P., & Wagner, M. (2000). Phylogeny of all recognized species of ammonia oxidizers based on comparative 16S rRNA and amoA sequence analysis: Implications for molecular diversity surveys. Applied and Environmental Microbiology, 66(12), 5368–5382. https://doi.org/10.1128/AEM.66.12.5368-5382.2000

Rajesh Banu, J., Uan, D. K., Kaliappan, S., & Yeom, I. T. (2011). Effect of sludge pretreatment on the performance of anaerobic/ anoxic/ oxic membrane bioreactor treating domestic wastewater. International Journal of Environmental Science and Technology, 8(2), 281–290. https://doi.org/10.1007/bf03326216

Rajesh Banu, J., Uan, D. K., & Yeom, I. T. (2009). Nutrient removal in an A2O-MBR reactor with sludge reduction. Bioresource Technology, 100(16), 3820–3824.https://doi.org/10.1016/j.biortech.2008.12.054

Review of Management of Used Tyres at Landfill Sites - PDF Free Download. (2006.). Retrieved November 24, 2020, from https://docplayer.net/18211503-Review-of-management-of-used-tyres-at-landfill-sites.html

Reyes, O., Sánchez, E., Rovirosa, N., Borja, R., Cruz, M., Colmenarejo, M. F., Escobedo, R., Ruiz, M., Rodríguez, X., & Correa, O. (1999). Low-strength wastewater treatment by a multistage anaerobic filter packed with waste tyre rubber. Bioresource Technology, 70(1), 55–60. https://doi.org/10.1016/S0960-8524(99)00010-3

Sabinet | Alkalinity measurement: Part 3 - A 5 pH point titration method to determine the carbonate and SCFA weak acidlbases in aqueous solution containing also known concentrations of other weak acid/bases. (1993) https://journals.co.za/content/waters/19/1/AJA03784738_1822

Sakuma, T., Jinsiriwanit, S., Hattori, T., & Deshusses, M. A. (2008). Removal of ammonia from contaminated air in a biotrickling filter - Denitrifying bioreactor combination system. Water Research, 42(17), 4507–4513. https://doi.org/10.1016/j.

Scala, D. J., Hacherl, E. L., Cowan, R., Young, L. Y., & Kosson, D. S. (2006). Characterization of Fe(III)-reducing enrichment cultures and isolation of Fe(III)-reducing bacteria from the Savannah River site, South Carolina. Research in Microbiology, 157(8), 772–783. https://doi.org/10.1016/j.resmic.2006.04.001

Schmid, M., Thill, A., Purkhold, U., Walcher, M., Bottero, J. Y., Ginestet, P., Nielsen, P. H., Wuertz, S., & Wagner, M. (2003). Characterization of activated sludge flocs by confocal laser scanning

microscopy and image analysis. Water Research, 37(9), 2043–2052. https://doi.org/10.1016/S0043-1354(02)00616-4

Serumgard, J. (2014). Internalization of Scrap Tire Management Costs: A Review of the North American Experience. Igarss 2014. https://doi.org/10.1007/s13398-014-0173-7.2

Shu, X., & Huang, B. (2014). Recycling of waste tire rubber in asphalt and portland cement concrete: An overview. Construction and Building Materials. https://doi.org/10.1016/j.conbuildmat.2013.11.027

Sienkiewicz, M., Kucinska-Lipka, J., Janik, H., & Balas, A. (2012). Progress in used tyres management in the European Union: A review. Waste Management. https://doi.org/10.1016/j.wasman.2012.05.010

Snaidr, J., Amann, R., Huber, I., Ludwig, W., & Schleifer, K. H. (1997). Phylogenetic analysis and in situ identification of bacteria in activated sludge. Applied and Environmental Microbiology. https://doi.org/10.1128/aem.63.7.2884-2896.1997

Tan, T. W., & Ng, H. Y. (2008). Influence of mixed liquor recycle ratio and dissolved oxygen on performance of pre-denitrification submerged membrane bioreactors. Water Research, 42(4–5), 1122–1132. https://doi.org/10.1016/j.watres.2007.08.028

Tang, Z., Butkus, M. A., & Xie, Y. F. (2006). Crumb rubber filtration: A potential technology for ballast water treatment. Marine Environmental Research. https://doi.org/10.1016/j.marenvres.2005.06.003

The Composition of a Tyre: Typical Components - PDF Free Download. (2006.). Retrieved November 20, 2020, from https://docplayer.net/20736072-The-composition-of-a-tyre-typical-components.html

The Effect of Cationic Salt Addition on the Settling and Dewatering Properties of an Industrial Activated Sludge on JSTOR. (1998) https://www.jstor.org/stable/25045109

The Effect of Wastewater Cations on Activated Sludge Characteristics: Effects of aluminum and iron in floc on JSTOR. (2006). https://www.jstor.org/stable/25045939?seq=1

Vukanti, R., Crissman, M., Leff, L. G., & Leff, A. A. (2009). Bacterial communities of tyre monofill sites: growth on tyre shreds and leachate. Journal of Applied Microbiology, 106(6), 1957–1966. https://doi.org/10.1111/j.1365-2672.2009.04157.x

Watanabe, M., Suzuki, Y., Sasaki, K., Nakashimada, Y., & Nishio, N. (1999). Flocculating property of extracellular polymeric substance derived from a marine photosynthetic bacterium, Rhodovulum sp. Journal of Bioscience and Bioengineering, 87(5), 625–629. https://doi.org/10.1016/S1389-1723(99)80125-X

Wijeyekoon, S., Mino, T., Satoh, H., & Matsuo, T. (2004). Effects of substrate loading rate on biofilm structure. Water Research, 38(10), 2479–2488. https://doi.org/10.1016/j.watres.2004.03.005

Wilén, B. M., Jin, B., & Lant, P. (2003). The influence of key chemical constituents in activated sludge on surface and flocculating properties. Water Research, 37(9), 2127–2139. https://doi.org/10.1016/S0043-1354(02)00629-2

Wojnowska-Baryła, I., Cydzik-Kwiatkowska, A., & Zielińska, M. (2010). The application of molecular techniques to the study of wastewater treatment systems. Methods in molecular biology. Vol 599, pp. 157–183). Methods Mol Biol. https://doi.org/10.1007/978-1-60761-439-5_11

Woznica, A., Nowak, A., Beimfohr, C., Karczewski, J., & Bernas, T. (2010). Monitoring structure and activity of nitrifying bacterial biofilm in an automatic biodetector of water toxicity. Chemosphere, 78(9), 1121–1128. https://doi.org/10.1016/j.

Xu, T., Xing, M., Yang, J., Lv, B., Duan, T., & Nie, J. (2014). Tracking the composition and dominant components of the microbial community via polymerase chain reaction-denaturing gradient gel electrophoresis and fluorescence in situ hybridization during vermiconversion for liquid-state excess sludge stabilization. Bioresource Technology, 167, 100–107. https://doi.org/10.1016/j.biortech.2014.05.109

Yang, L., Barken, K. B., Skindersoe, M. E., Christensen, A. B., Givskov, M., & Tolker-Nielsen, T. (2007). Effects of iron on DNA release and biofilm development by *Pseudomonas aeruginosa*. Microbiology, 153(5), 1318–1328. https://doi.org/10.1099/mic.0.2006/004911-0

Yang, Q., Liu, Z., & Yang, J. (2009). Simultaneous determination of chemical oxygen demand (cod) and

biological oxygen demand (bod5) in wastewater by near-infrared spectrometry. Journal of Water Resource and Protection, 01(04), 286–289. https://doi.org/10.4236/jwarp.2009.14035

Zhang, G., Dong, H., Jiang, H., Kukkadapu, R. K., Kim, J., Eberl, D., & Xu, Z. (2009). Biomineralization associated with microbial reduction of Fe3+ and oxidation of Fe^{2+} in solid minerals. American Mineralogist, 94(7), 1049–1058. https://doi.org/10.2138/am.2009.3136

Zhou, X. hong, Huang, B. cheng, Zhou, T., Liu, Y. chen, & Shi, H. chang. (2015). Aggregation behavior of engineered nanoparticles and their impact on activated sludge in wastewater treatment. Chemosphere, 119, 568–576. https://doi.org/10.1016/j.chemosphere.2014.07.037

Chapter 4

Achilli, A., Marchand, E. A., & Childress, A. E. (2011). A performance evaluation of three membrane bioreactor systems: Aerobic, anaerobic, and attached-growth. Water Science and Technology, 63(12), 2999–3005. https://doi.org/10.2166/wst.2011.559

Albalasmeh, A. A., Berhe, A. A., & Ghezzehei, T. A. (2013). A new method for rapid determination of carbohydrate and total carbon concentrations using UV spectrophotometry. Carbohydrate Polymers, 97(2), 253–261. https://doi.org/10.1016/j.carbpol.2013.04.072

Alvarez-Ordóñez, A., Mouwen, D. J. M., López, M., & Prieto, M. (2011). Fourier transform infrared spectroscopy as a tool to characterize molecular composition and stress response in foodborne pathogenic bacteria. Journal of Microbiological Methods. 84 (3), pp. 369–378. https://doi.org/10.1016/j.mimet.2011.01.009

APHA. (2012). Standard methods for the examination of water and wastewater, 22nd ed. American Public Heatlh Association. https://doi.org/10.1080/19447013008687143

Azizi, S., Valipour, A., & Sithebe, T. (2013). Evaluation of different wastewater treatment processes and development of a modified attached growth bioreactor as a decentralized approach for small communities. TheScientificWorldJournal, 2013, 156870. https://doi.org/10.1155/2013/156870

Bala Subramanian, S., Yan, S., Tyagi, R. D., & Surampalli, R. Y. (2007). Characterization of Extracellular Polymeric Substances (EPS) Extracted from both Sludge and Pure Bacterial Strains Isolated from Wastewater Sludge for Sludge Dewatering. Water Research, 12, 157–164.

Bala Subramanian, S., Yan, S., Tyagi, R. D., & Surampalli, R. Y. (2010). Extracellular polymeric substances (EPS) producing bacterial strains of municipal wastewater sludge: Isolation, molecular identification, EPS characterization and performance for sludge settling and dewatering. Water Research, 44(7), 2253–2266. https://doi.org/10.1016/j.watres.2009.12.046

Breakwell, D. P., Moyes, R. B., & Reynolds, J. (2009). Differential staining of bacteria: capsule stain. Current Protocols in Microbiology, Appendix 3(November), Appendix 3I. https://doi.org/10.1002/9780471729259.mca03is15

Brostow, W., Lobland, H., Pal, S., & Singh, R. (2009). Polymeric flocculants for wastewater and industrial effluent treatment. Journal of Materials Education, 31(October), 157–166.

Burm??lle, M., Webb, J. S., Rao, D., Hansen, L. H., S??rensen, S. J., & Kjelleberg, S. (2006). Enhanced biofilm formation and increased resistance to antimicrobial agents and bacterial invasion are caused by synergistic interactions in multispecies biofilms. Applied and Environmental Microbiology, 72(6), 3916–3923. https://doi.org/10.1128/AEM.03022-05

Cao, Y., Wei, X., Cai, P., Huang, Q., Rong, X., & Liang, W. (2011). Preferential adsorption of extracellular polymeric substances from bacteria on clay minerals and iron oxide. Colloids and Surfaces B: Biointerfaces, 83(1), 122–127. https://doi.org/10.1016/j.colsurfb.2010.11.018

Christensen, G. D., Simpson, W. A., Younger, J. J., Baddour, L. M., Barrett, F. F., Melton, D. M., & Beachey, E. H. (1985). Adherence of coagulase-negative *Staphylococci* to plastic tissue culture plates: A quantitative model for the adherence of *staphylococci* to medical devices. Journal of Clinical Microbiology, 22(6), 996–1006.

College, S. M. S. M. (2014). Assessment of biofilm formation by *Enterococcus faecalis* causing nosocomial infections and their statistical analysis. 77–79.

Comte, S., Guibaud, G., & Baudu, M. (2008). Biosorption properties of extracellular polymeric substances (EPS) towards Cd, Cu and Pb for different pH values. Journal of Hazardous Materials, 151(1), 185–193. https://doi.org/10.1016/j.jhazmat.2007.05.070

Devaraj, C. (2015). Comparision of Three Different Methods for the Detection of Biofilm in Gram Positive Cocci and Gram Negative Bacilli Isolated from Clinical Specimens. 7(June 2014), 952–955.

Donlan, R. M. (2002). Biofilms: Microbial life on surfaces. Emerging Infectious Diseases (Vol. 8, Issue 9, pp. 881–890). https://doi.org/10.3201/eid0809.020063

Faghihzadeh, F., Anaya, N. M., Schifman, L. A., & Oyanedel-Craver, V. (2016). Fourier transform infrared spectroscopy to assess molecular-level changes in microorganisms exposed to nanoparticles. Nanotechnology for Environmental Engineering, 1(1), 1. https://doi.org/10.1007/s41204-016-0001-8

Garnier, C., Görner, T., Lartiges, B. S., Abdelouhab, S., & De Donato, P. (2005). Characterization of activated sludge exopolymers from various origins: A combined size-exclusion chromatography and infrared microscopy study. Water Research, 39(13), 3044–3054. https://doi.org/10.1016/j.watres.2005.05.007

Govoreanu, R., Saveyn, H., Van der Meeren, P., & Vanrolleghem, P. a. (2004). Simultaneous determination of activated sludge floc size distribution by different techniques. Water Science and Technology : A Journal of the International Association on Water Pollution Research, 50(12), 39–46.

Guo, J., Yang, C., & Zeng, G. (2013). Treatment of swine wastewater using chemically modified zeolite and bioflocculant from activated sludge. Bioresource Technology, 143, 289–297. https://doi.org/10.1016/j.biortech.2013.06.003

Hassan, A., Usman, J., Kaleem, F., Omair, M., Khalid, A., & Iqbal, M. (2011). Evaluation of different detection methods of biofilm formation in the clinical isolates. The Brazilian Journal of Infectious Diseases : An Official Publication of the Brazilian Society of Infectious Diseases, 15(4), 305–311. https://doi.org/10.1016/S1413-8670(11)70197-0

Higgins, M. J., & Novak, J. T. (1997a). Dewatering and Settling of activated sludges : The case for using cation Analysis Dewatering The sludges : and case settling for using of activated analysis cation. Water Environment Research, 69(2), 225–232. https://doi.org/10.2175/106143097X125380

Higgins, M. J., & Novak, J. T. (1997b). Dewatering and settling of activated sludges: The case for using cation analysis. Water Environment Research. https://doi.org/10.2175/106143097x125380

Houghton, J. I., & Stephenson, T. (2002). Effect of influent organic content on digested sludge extracellular polymer content and dewaterability. Water Research, 36(14), 3620–3628. https://doi.org/10.1016/S0043-1354(02)00055-6

Jiao, Y., Cody, G. D., Harding, A. K., Wilmes, P., Schrenk, M., Wheeler, K. E., Banfield, J. F., & Thelen, M. P. (2010). Characterization of extracellular polymeric substances from acidophilic microbial biofilms. Applied and Environmental Microbiology, 76(9), 2916–2922. https://doi.org/10.1128/AEM.02289-09

Jorand, F., Boué-Bigne, F., Block, J. C., & Urbain, V. (1998). Hydrophobic/hydrophilic properties of activated sludge exopolymeric substances. Water Science and Technology, 37(4–5), 307–315. https://doi.org/10.1016/S0273-1223(98)00123-1

Klemeš, J. J., Stehlík, P., & Worrell, E. (2010). Waste treatment to improve recycling and minimise environmental impact. Resources, Conservation and Recycling, 54(5), 267–270. https://doi.org/10.1016/j.resconrec.2009.11.005

Kurane, R., Hatamochi, K., Kakuno, T., Kiyohara, M., Kawaguchi, K., Mizuno, Y., Hirano, M., & Taniguchi, Y. (1994). Purification and characterization of lipid bioflocculant produced by

Rhodococcus-erythropolis. Bioscience Biotechnology and Biochemistry, 58(11), 1977–1982. https://doi.org/10.1080/bbb.58.1977

Li, X. Y., & Yang, S. F. (2007). Influence of loosely bound extracellular polymeric substances (EPS) on the flocculation, sedimentation and dewaterability of activated sludge. Water Research, 41(5), 1022–1030. https://doi.org/10.1016/j.watres.2006.06.037

Liu, H., Chen, G., & Wang, G. (2015). Characteristics for production of hydrogen and bioflocculant by Bacillus sp. XF-56 from marine intertidal sludge. International Journal of Hydrogen Energy, 40(3), 1414–1419. https://doi.org/10.1016/j.ijhydene.2014.11.110

Liu, Y., & Fang, H. H. P. (2003). Influences of extracellular polymeric substances (EPS) on flocculation, settling, and dewatering of activated sludge. Critical Reviews in Environmental Science and Technology, 33(3), 237–273. https://doi.org/10.1080/10643380390814479

Mikkelsen, L. H., & Keiding, K. (2002). Physico-chemical characteristics of full scale sewage sludges with implications to dewatering. Water Research, 36(10), 2451–2462. https://doi.org/10.1016/S0043-1354(01)00477-8

Neu, T. R. (2000). In situ cell and glycoconjugate distribution in river snow studied by confocal laser scanning microscopy. Aquatic Microbial Ecology, 21(1), 85–95. https://doi.org/10.3354/ame021085

Nyenje, M. E., Green, E., & Ndip, R. N. (2013). Evaluation of the effect of different growth media and temperature on the suitability of biofilm formation by Enterobacter cloacae strains isolated from food samples in South Africa. Molecules, 18(8), 9582–9593. https://doi.org/10.3390/molecules18089582

O'Toole, G. A. (2003). To build a biofilm. In Journal of Bacteriology (Vol. 185, Issue 9, pp. 2687–2689). https://doi.org/10.1128/JB.185.9.2687-2689.2003

Omoike, A., & Chorover, J. (2004). Spectroscopic study of extracellular polymeric substances from Bacillus subtilis: Aqueous chemistry and adsorption effects. Biomacromolecules (Vol. 5, Issue 4, pp. 1219–1230). https://doi.org/10.1021/bm034461z

Owen, M. P., Schauwers, W., Hugh-Jones, M. E., Kiernan, J. A., Turnbull, P. C. B., & Beyer, W. (2013). A simple, reliable M'Fadyean stain for visualizing the Bacillus anthracis capsule. Journal of Microbiological Methods, 92(3), 264–269. https://doi.org/10.1016/j.mimet.2013.01.009

Pal, A., & Paul, A. K. (2008). Microbial extracellular polymeric substances: Central elements in heavy metal bioremediation. In Indian Journal of Microbiology (Vol. 48, Issue 1, pp. 49–64). https://doi.org/10.1007/s12088-008-0006-5

Patil, S. V., Patil, C. D., Salunke, B. K., Salunkhe, R. B., Bathe, G. A., & Patil, D. M. (2011). Studies on characterization of bioflocculant exopolysaccharide of *Azotobacter indicus* and its potential for wastewater treatment. Applied Biochemistry and Biotechnology, 163(4), 463–472. https://doi.org/10.1007/s12010-010-9054-5

Pihlasalo, S., Auranen, L., Hänninen, P., & Härmä, H. (2012). Method for estimation of protein isoelectric point. Analytical Chemistry, 84(19), 8253–8258. https://doi.org/10.1021/ac301569b

Rosenberg, E., DeLong, E. F., Thompson, F., Lory, S., & Stackebrandt, E. (2013). The prokaryotes: Applied bacteriology and biotechnology. The Prokaryotes: Applied Bacteriology and Biotechnology, 9783642313, 1–393. https://doi.org/10.1007/978-3-642-31331-8

Ruiz-Marin, A., Mendoza-Espinosa, L. G., & Stephenson, T. (2010). Growth and nutrient removal in free and immobilized green algae in batch and semi-continuous cultures treating real wastewater. Bioresource Technology, 101(1), 58–64. https://doi.org/10.1016/j.biortech.2009.02.076

Sheng, G., Yu, H., & Li, X. (2010). Extracellular polymeric substances (EPS) of microbial aggregates in biological wastewater treatment systems: A review. Biotechnology Advances, 28(6), 882–894. https://doi.org/10.1016/j.biotechadv.2010.08.001

Singha, T. (2012). Microbial extracellular polymeric substances: production, isolation and applications. IOSR J Pharm, 2(2), 276–281. https://doi.org/10.9790/3013-0220276281

Sombatsompop, K., Visvanathan, C., & Ben Aim, R. (2006). Evaluation of biofouling phenomenon in

suspended and attached growth membrane bioreactor systems. Desalination, 201(1–3), 138–149. https://doi.org/10.1016/j.desal.2006.02.011

Subudhi, S., Batta, N., Pathak, M., Bisht, V., Devi, A., Lal, B., & Al khulifah, B. (2014). Bioflocculant production and biosorption of zinc and lead by a novel bacterial species, Achromobacter sp. TERI-IASST N, isolated from oil refinery waste. Chemosphere, 113, 116–124. https://doi.org/10.1016/j.chemosphere.2014.04.050

Sun, P. F., Lin, H., Wang, G., Lu, L. L., & Zhao, Y. H. (2015). Preparation of a new-style composite containing a key bioflocculant produced by Pseudomonas aeruginosa ZJU1 and its flocculating effect on harmful algal blooms. Journal of Hazardous Materials, 284, 215–221. https://doi.org/10.1016/j.jhazmat.2014.11.025

Taj, Y., Essa, F., Aziz, F., & Kazmi, S. U. (2012). Study on biofilm-forming properties of clinical isolates of Staphylococcus aureus. The Journal of Infection in Developing Countries, 5(6), 403–409. https://doi.org/10.3855/jidc.1743

Tourney, J., & Ngwenya, B. T. (2014). The role of bacterial extracellular polymeric substances in geomicrobiology. In Chemical Geology (Vol. 386, pp. 115–132). https://doi.org/10.1016/j.chemgeo.2014.08.011

Tripathy, T., & De, B. R. (2006). Flocculation: A new way to treat the waste water. Journal of Physical Sciences, 10, 93–127.

Urbain, V., Block, J. C., & Manem, J. (1993). Bioflocculation in activated sludge: an analytic approach. Water Research, 27(5), 829–838. https://doi.org/10.1016/0043-1354(93)90147-A

Vijayaraghavan, G.; Sivakumar, T.; Vimal Kumar, a. (2011). Application of Plant Based Coagulants for Waste Water Treatment. International Journal of Advanced Engineering Research and Studies, 1(1), 88–92. https://doi.org/E-ISSN2249-8974

W??sche, S., Horn, H., & Hempel, D. C. (2002). Influence of growth conditions on biofilm development and mass transfer at the bulk/biofilm interface. Water Research, 36(19), 4775–4784. https://doi.org/10.1016/S0043-1354(02)00215-4

Walker, J. M. (2002). Handbook Edited by. In The Protein Protocols Handbook (Vol. 3, Issue 2). https://doi.org/10.1385/1592591698

Weiss, M., & Cargill, C. (1992). Consortia in the standards development process. Journal of the American Society for Information Science, 43(8), 559–565. https://doi.org/10.1002/(SICI)1097-4571(199209)43:8<559::AID-ASI7>3.0.CO;2-P

Wiśniewska, M., Chibowski, S., & Urban, T. (2016). Synthetic polyacrylamide as a potential flocculent to remove commercial chromium(III) oxide from aqueous suspension. International Journal of Environmental Science and Technology, 13(2), 679–690. https://doi.org/10.1007/s13762-015-0912-0

Yang, L., Liu, Y., Wu, H., Hóiby, N., Molin, S., & Song, Z. (2011). Current understanding of multi-species biofilms. International Journal of Oral Science, 3(2), 74–81. https://doi.org/10.4248/IJOS11027

Yu, H. Q. (2020). Molecular Insights into Extracellular Polymeric Substances in Activated Sludge. Environmental Science and Technology. https://doi.org/10.1021/acs.est.0c00850

Zhang, X., Bishop, P. L., & Kinkle, B. K. (1999). Comparison of extraction methods for quantifying extracellular polymers in biofilms. Water Science and Technology, 39(7), 211–218. https://doi.org/10.1016/S0273-1223(99)00170-5

Zhou, J., Zheng, G., Zhang, X., & Zhou, L. (2014). Influences of extracellular polymeric substances on the dewaterability of sewage sludge during bioleaching. PLoS ONE, 9(7). https://doi.org/10.1371/journal.pone.0102688

Zuroff, T. R., & Curtis, W. R. (2012). Developing symbiotic consortia for lignocellulosic biofuel production. Applied Microbiology and Biotechnology, 93(4), 1423–1435. https://doi.org/10.1007/s00253-011-3762-9

Chapter 5

Abbas, S. Z., Rafatullah, M., Khan, M. A., & Siddiqui, M. R. (2019a). Bioremediation and electricity generation by using open and closed sediment microbial fuel cells. Frontiers in Microbiology, 10. https://doi.org/10.3389/fmicb.2018.03348

Abbas, S. Z., Rafatullah, M., Khan, M. A., & Siddiqui, M. R. (2019b). Bioremediation and Electricity Generation by Using Open and Closed Sediment Microbial Fuel Cells. Frontiers in Microbiology, 9, 3348. https://doi.org/10.3389/fmicb.2018.03348

Abbas, S. Z. *et al.* (2019) 'Bioremediation and electricity generation by using open and closed sediment microbial fuel cells', *Frontiers in Microbiology*. Frontiers Media S.A., 10(JAN), p. 3348. doi: 10.3389/FMICB.2018.03348/BIBTEX.

Afsharian, Y. P. and Rahimnejad, M. (2022) 'Functional dynamics of microbial communities in bioelectrochemical systems: The importance of eco-electrogenic treatment of complex substrates', *Current Opinion in Electrochemistry*. Elsevier, 31, p. 100816. doi: 10.1016/J.COELEC.2021.100816.

Algar, C. K. *et al.* (2020) 'Sediment microbial fuel cells as a barrier to sulfide accumulation and their potential for sediment remediation beneath aquaculture pens', *Scientific Reports 2020 10:1*. Nature Publishing Group, 10(1), pp. 1–12. doi: 10.1038/s41598-020-70002-4.

Almatouq, A. *et al.* (2020) 'Microbial community structure of anode electrodes in microbial fuel cells and microbial electrolysis cells', *Journal of Water Process Engineering*. Elsevier, 34, p. 101140. doi: 10.1016/J.JWPE.2020.101140.

An, J., Lee, S. J., Ng, H. Y., & Chang, I. S. (2010). Determination of effects of turbulence flow in a cathode environment on electricity generation using a tidal mud-based cylindrical-type sediment microbial fuel cell. Journal of Environmental Management, 91(12), 2478–2482. https://doi.org/10.1016/j.jenvman.2010.06.022

Anam, M., Yousaf, S., Sharafat, I., Zafar, Z., Ayaz, K., & Ali, N. (2017). Comparing Natural and Artificially Designed Bacterial Consortia as Biosensing Elements for Rapid Non-Specific Detection of Organic Pollutant through Microbial Fuel Cell. Int. J. Electrochem. Sci, 12, 2836–2851. https://doi.org/10.20964/2017.04.49

Arends, J. B. A., Speeckaert, J., Blondeel, E., De Vrieze, J., Boeckx, P., Verstraete, W., Rabaey, K., & Boon, N. (2014). Greenhouse gas emissions from rice microcosms amended with a plant microbial fuel cell. Applied Microbiology and Biotechnology. https://doi.org/10.1007/s00253-013-5328-5

Baek, G., Kim, J., & Lee, C. (2019). A review of the effects of iron compounds on methanogenesis in anaerobic environments. In Renewable and Sustainable Energy Reviews (Vol. 113, p. 109282). Elsevier Ltd. https://doi.org/10.1016/j.rser.2019.109282

Banin, E., Vasil, M. L., & Greenberg, E. P. (2005). Iron and Pseudomonas aeruginosa biofilm formation. Proceedings of the National Academy of Sciences of the United States of America. https://doi.org/10.1073/pnas.0504266102

Becerril-Varela, K. *et al.* (2021) 'Generation of electrical energy in a microbial fuel cell coupling acetate oxidation to Fe3+ reduction and isolation of the involved bacteria', *World Journal of Microbiology and Biotechnology*. Springer Netherlands, 37(6), pp. 1–15. doi: 10.1007/s11274-021-03077-4.

Bergey's Manual of Systematic Bacteriology. (1990). Annals of Internal Medicine. https://doi.org/10.7326/0003-4819-112-5-391_3

Black, C. A., Evans, D. D., White, J. L., Ensminger, L. E., & F.E., C. (1965). Methods of soil analysis-Part 2: Chemical and Microbiological properties. (1ᵃ ed?). Am. Soc. Agron. Inc. Publ.Madison, USA, 2, 1191–1199.

Chatterjee, S., & Huang, K. W. (2020). Unrealistic energy and materials requirement for direct air capture in deep mitigation pathways. In Nature Communications (Vol. 11, Issue 1, pp. 1–3). Nature Research. https://doi.org/10.1038/s41467-020-17203-7

Chaturvedi, V., & Verma, P. (2016). Microbial fuel cell: a green approach for the utilization of waste for

the generation of bioelectricity. Bioresources and Bioprocessing, 3, 38. https://doi.org/10.1186/s40643-016-0116-6

Chen, J., Yang, Y., Liu, Y., Tang, M., Wang, R., Tian, Y., & Jia, C. (2019). Bacterial community shift and antibiotics resistant genes analysis in response to biodegradation of oxytetracycline in dual graphene modified bioelectrode microbial fuel cell. Bioresource Technology, 276, 236–243. https://doi.org/10.1016/j.biortech.2019.01.006

Chen, S., Patil, S. A., Brown, R. K., & Schröder, U. (2019). Strategies for optimizing the power output of microbial fuel cells: Transitioning from fundamental studies to practical implementation. In Applied Energy. https://doi.org/10.1016/j.apenergy.2018.10.015

Deng, H., Xue, H., & Zhong, W. (2017). A Novel Exoelectrogenic Bacterium Phylogenetically Related to Clostridium sporogenes Isolated from Copper Contaminated Soil. Electroanalysis, 29(5), 1294–1300. https://doi.org/10.1002/elan.201600673

Deng, Q. *et al.* (2020) 'Performance and functional microbial communities of denitrification process of a novel MFC-granular sludge coupling system', *Bioresource Technology*. Elsevier, 306, p. 123173. doi: 10.1016/J.BIORTECH.2020.123173.

Eyiuche, N. J., Asakawa, S., Yamashita, T., Ikeguchi, A., Kitamura, Y., & Yokoyama, H. (2017). Community analysis of biofilms on flame-oxidized stainless steel anodes in microbial fuel cells fed with different substrates. BMC Microbiology. https://doi.org/10.1186/s12866-017-1053-z

Felsenstein, J. (1985). Confidence Limits on Phylogenies: An Approach Using the Bootstrap. Evolution. https://doi.org/10.2307/2408678

Ferreira, M. R., & Salgueiro, C. A. (2018). Biomolecular interaction studies between cytochrome ppca from geobacter sulfurreducens and the electron acceptor ferric nitrilotriacetate (Fe-NTA). Frontiers in Microbiology, 9, 2741. https://doi.org/10.3389/fmicb.2018.02741

Flimban, S., Oh, S. E., Joo, J. H., & Hussein, K. A. (2019). Characterization and Identification of Cellulose-degrading Bacteria Isolated from a Microbial Fuel Cell Reactor. Biotechnology and Bioprocess Engineering, 24(4), 622–631. https://doi.org/10.1007/s12257-019-0089-3

González-Gamboa, N. K., Valdés-Lozano, D. S., Barahona-Pérez, L. F., Alzate-Gaviria, L., & Domínguez-Maldonado, J. A. (2017). Removal of organic matter and electricity generation of sediments from Progreso, Yucatan, Mexico, in a sediment microbial fuel cell. Environmental Science and Pollution Research, 24(6), 5868–5876. https://doi.org/10.1007/s11356-016-8286-5

Huang, D. Y., Zhou, S. G., Chen, Q., Zhao, B., Yuan, Y., & Zhuang, L. (2011). Enhanced anaerobic degradation of organic pollutants in a soil microbial fuel cell. Chemical Engineering Journal. https://doi.org/10.1016/j.cej.2011.06.024

Huang, Y. *et al.* (2021) 'Alternating current enhanced bioremediation of petroleum hydrocarbon-contaminated soils', *Environmental Science and Pollution Research 2021 28:34*. Springer, 28(34), pp. 47562–47573. doi: 10.1007/S11356-021-13942-2.

Hunter, R. C., Asfour, F., Dingemans, J., Osuna, B. L., Samad, T., Malfroot, A., Cornelis, P., & Newman, D. K. (2013). Ferrous iron is a significant component of bioavailable iron in cystic fibrosis airways. MBio. https://doi.org/10.1128/mBio.00557-13

Inohana, Y. *et al.* (2020) 'Shewanella algae relatives capable of generating electricity from acetate contribute to coastal-sediment microbial fuel cells treating complex organic matter', *Microbes and Environments*. doi: 10.1264/jsme2.ME19161.

Ishii, S., Ishii, S., Suzuki, S., Wu, A., Wu, A., Bretschger, O., Suzuki, S., Suzuki, S., Suzuki, S., Nealson, K. H., Bretschger, O., Bretschger, O., & Yamanaka, Y. (2017). Population dynamics of electrogenic microbial communities in microbial fuel cells started with three different inoculum sources. Bioelectrochemistry, 117, 74–82. https://doi.org/10.1016/j.bioelechem.2017.06.003

Islam, M. A., Ehiraj, B., Cheng, C. K., Dubey, B. N., & Khan, M. M. R. (2019). Biofilm re-vitalization using hydrodynamic shear stress for stable power generation in microbial fuel cell. Journal of Electroanalytical Chemistry, 844, 14–22. https://doi.org/10.1016/j.jelechem.2019.05.013

Janicek, A., Fan, Y., & Liu, H. (2014). Design of microbial fuel cells for practical application: A review and analysis of scale-up studies. In Biofuels. https://doi.org/10.4155/bfs.13.69

Ji, J., Jia, Y., Wu, W., Bai, L., Ge, L., & Gu, Z. (2011). A layer-by-layer self-assembled Fe2O3 nanorod-based composite multilayer film on ITO anode in microbial fuel cell. Colloids and Surfaces A: Physicochemical and Engineering Aspects. https://doi.org/10.1016/j.colsurfa.2011.08.056

Jiang, Y. Bin, Deng, H., Sun, D. M., & Zhong, W. H. (2015). Electrical signals generated by soil microorganisms in microbial fuel cells respond linearly to soil Cd^{2+} pollution. Geoderma. https://doi.org/10.1016/j.geoderma.2015.04.022

Jiang, Y. Bin, Zhong, W. H., Han, C., & Deng, H. (2016). Characterization of electricity generated by soil in microbial fuel cells and the isolation of soil source exoelectrogenic bacteria. Frontiers in Microbiology, 7(NOV), 1–10. https://doi.org/10.3389/fmicb.2016.01776

Kato, S., Hashimoto, K., & Watanabe, K. (2012). Microbial interspecies electron transfer via electric currents through conductive minerals. Proceedings of the National Academy of Sciences of the United States of America. https://doi.org/10.1073/pnas.1117592109

Kim, J. R., Min, B., & Logan, B. E. (2005). Evaluation of procedures to acclimate a microbial fuel cell for electricity production. Applied Microbiology and Biotechnology. https://doi.org/10.1007/s00253-004-1845-6

Kondaveeti, S. *et al.* (2019) 'Utilization of residual organics of Labaneh whey for renewable energy generation through bioelectrochemical processes: Strategies for enhanced substrate conversion and energy generation', *Bioresource Technology*. Elsevier, 286, p. 121409. doi: 10.1016/J.BIORTECH.2019.121409.

Kumar, S., Stecher, G., Li, M., Knyaz, C., & Tamura, K. (2018). MEGA X: Molecular evolutionary genetics analysis across computing platforms. Molecular Biology and Evolution. https://doi.org/10.1093/molbev/msy096

Liang, Q., Yamashita, T., Matsuura, N., Yamamoto-Ikemoto, R., & Yokoyama, H. (2019). Community structure analyses of anodic biofilms in a bioelectrochemical system combined with an aerobic reactor. Energies. https://doi.org/10.3390/en12193643

Li, A. *et al.* (2013) 'A pyrosequencing-based metagenomic study of methane-producing microbial community in solid-state biogas reactor', *Biotechnology for Biofuels*. doi: 10.1186/1754-6834-6-3.

Liang, Y. *et al.* (2020) 'Carbon nanomaterial-modified graphite felt as an anode enhanced the power production and polycyclic aromatic hydrocarbon removal in sediment microbial fuel cells', *Science of The Total Environment*. Elsevier, 713, p. 136483. doi: 10.1016/J.SCITOTENV.2019.136483.

Light, S. H. *et al.* (2018) 'A flavin-based extracellular electron transfer mechanism in diverse Gram-positive bacteria', *Nature*. doi: 10.1038/s41586-018-0498-z.

Liu, Q., Liu, B., Li, W., Zhao, X., Zuo, W., & Xing, D. (2017). Impact of ferrous iron on microbial community of the biofilm in microbial fuel cells. Frontiers in Microbiology, 8(JUN), 920. https://doi.org/10.3389/fmicb.2017.00920

Liu, Q., Yang, Y., Mei, X., Liu, B., Chen, C., & Xing, D. (2018). Response of the microbial community structure of biofilms to ferric iron in microbial fuel cells. Science of the Total Environment, 631–632, 695–701. https://doi.org/10.1016/j.scitotenv.2018.03.008

Logan, B. E., Hamelers, B., Rozendal, R., Schröder, U., Keller, J., Freguia, S., Aelterman, P., Verstraete, W., & Rabaey, K. (2006). Microbial fuel cells: Methodology and technology. Environmental Science and Technology, 40(17), 5181–5192. https://doi.org/10.1021/es0605016

Lovley, D. R., Holmes, D. E. and Nevin, K. P. (2004) 'Dissimilatory Fe(III) and Mn(IV) reduction', *Advances in microbial physiology*. Adv Microb Physiol, 49, pp. 219–286. doi: 10.1016/S0065-2911(04)49005-5.

Lovley, D. R., & Phillips, E. J. P. (1986). Organic matter mineralization with reduction of ferric iron in anaerobic sediments. Applied and Environmental Microbiology. https://doi.org/10.1128/aem.51.4.683-689.1986

Lovley, D. R., Stolz, J. F., Nord, G. L., & Phillips, E. J. P. (1987). Anaerobic production of magnetite by a dissimilatory iron-reducing microorganism. Nature. https://doi.org/10.1038/330252a0

Lu, Z., Chang, D., Ma, J., Huang, G., Cai, L., & Zhang, L. (2015). Behavior of metal ions in bioelectrochemical systems: A review. In Journal of Power Sources. https://doi.org/10.1016/j.jpowsour.2014.10.168

Macrae, I. C. and Edwards, J. F. (1972) 'Adsorption of colloidal iron by bacteria', *Applied Microbiology*. American Society for Microbiology (ASM), 24(5), p. 819. doi: 10.1128/aem.24.5.819-823.1972.

Mohanakrishna, G., Abu-Reesh, I. M. and Pant, D. (2020) 'Enhanced bioelectrochemical treatment of petroleum refinery wastewater with Labaneh whey as co-substrate', *Scientific Reports 2020 10:1*. Nature Publishing Group, 10(1), pp. 1–11. doi: 10.1038/s41598-020-76668-0.

Mancílio, L. B. K., Ribeiro, G. A., Lopes, E. M., Kishi, L. T., Martins-Santana, L., de Siqueira, G. M. V., Andrade, A. R., Guazzaroni, M.-E., & Reginatto, V. (2020). Unusual microbial community and impact of iron and sulfate on microbial fuel cell ecology and performance. Current Research in Biotechnology, 2, 64–73. https://doi.org/10.1016/j.crbiot.2020.04.001

Martins, M. *et al.* (2009) 'Characterization and activity studies of highly heavy metal resistant sulphate-reducing bacteria to be used in acid mine drainage decontamination', *Journal of hazardous materials*. J Hazard Mater, 166(2–3), pp. 706–713. doi: 10.1016/J.JHAZMAT.2008.11.088.

Minandri, F., Imperi, F., Frangipani, E., Bonchi, C., Visaggio, D., Facchini, M., Pasquali, P., Bragonzi, A., & Visca, P. (2016). Role of iron uptake systems in *Pseudomonas aeruginosa* virulence and airway infection. Infection and Immunity, 84(8), 2324–2335. https://doi.org/10.1128/IAI.00098-16

Miran, W., Jang, J., Nawaz, M., Shahzad, A., Jeong, S. E., Jeon, C. O., & Lee, D. S. (2017). Mixed sulfate-reducing bacteria-enriched microbial fuel cells for the treatment of wastewater containing copper. Chemosphere. https://doi.org/10.1016/j.chemosphere.2017.09.048

Nandy, A. *et al.* (2015) 'MFC with vermicompost soil: power generation with additional importance of waste management', *RSC Advances*. The Royal Society of Chemistry, 5(51), pp. 41300–41306. doi: 10.1039/C5RA00870K.

Nara, S. *et al.* (2020) 'Exploring Providencia rettgeri for application to eco-friendly paper based microbial fuel cell', *Biosensors and Bioelectronics*. doi: 10.1016/j.bios.2020.112323.

Nelson, C. E., Huang, W., Brewer, L. K., Nguyen, A. T., Kane, M. A., Wilks, A., & Oglesby-Sherrouse, A. G. (2019). Proteomic analysis of the *Pseudomonas aeruginosa* iron starvation response reveals prrf small regulatory rna-dependent iron regulation of twitching motility, amino acid metabolism, and zinc homeostasis proteins. Journal of Bacteriology, 201(12). https://doi.org/10.1128/JB.00754-18

Nevin, K. P. and Lovley, D. R. (2010) 'Mechanisms for Fe(III) oxide reduction in sedimentary environments', *http://dx.doi.org/10.1080/01490450252864253*. Informa UK Ltd, 19(2), pp. 141–159. doi: 10.1080/01490450252864253.

Obileke, K. C. *et al.* (2021) 'Microbial fuel cells, a renewable energy technology for bio-electricity generation: A mini-review', *Electrochemistry Communications*. Elsevier Inc., p. 107003. doi: 10.1016/j.elecom.2021.107003.

Park, H. S. *et al.* (2001) 'A novel electrochemically active and Fe(III)-reducing bacterium phylogenetically related to Clostridium butyricum isolated from a microbial fuel cell', *Anaerobe*. Academic Press, 7(6), pp. 297–306. doi: 10.1006/anae.2001.0399.

Pasupuleti, S. B. *et al.* (2016) 'Dual gas diffusion cathode design for microbial fuel cell (MFC): Optimizing the suitable mode of operation in terms of bioelectrochemical and bioelectro-kinetic evaluation', *Journal of Chemical Technology and Biotechnology*. John Wiley and Sons Ltd, 91(3), pp. 624–639. doi: 10.1002/JCTB.4613.

Peng, X., Yu, H., Wang, X., Zhou, Q., Zhang, S., Geng, L., Sun, J., & Cai, Z. (2012). Enhanced performance and capacitance behavior of anode by rolling Fe3O4 into activated carbon in microbial fuel cells. Bioresource Technology. https://doi.org/10.1016/j.biortech.2012.06.021

Ruiz-Urigüen, M., Shuai, W., & Jaffé, P. R. (2018). Electrode colonization by the Feammox bacterium Acidimicrobiaceae sp. strain A6. Applied and Environmental Microbiology. https://doi.org/10.1128/AEM.02029-18

Ren, L. *et al.* (2012) 'Current generation in microbial electrolysis cells with addition of amorphous ferric hydroxide, Tween 80, or DNA', *International Journal of Hydrogen Energy*. Elsevier Limited, 37(22), pp. 16943–16950. doi: 10.1016/J.IJHYDENE.2012.08.119.

Sasaki, D., Sasaki, K., Tsuge, Y., & Kondo, A. (2016). Comparative metabolic state of microflora on the surface of the anode electrode in a microbial fuel cell operated at different pH conditions. AMB Express, 6(1), 125. https://doi.org/10.1186/s13568-016-0299-4

Scott, K., J. Philips, Verbeeck, K., Rabaey, K., Arends, J. B. A., Dumitru, A., Bajracharya, S., ElMekawy, A., Srikanth, S., Pant, D., Premier, G. C., Michie, I. S., Boghani, H. C., Fradler, K. R., Kim, J. R., Gude, V. G., Cotterill, S., Heidrich, E., Curtis, T., Greenman, J. (2016). Microbial Electrochemical and Fuel Cells: Fundamentals and applications. In Woodhead Publishing Series in Energy (Vol. 88). https://doi.org/10.1016/B978-1-78242-375-1.00012-5

Shi, M. M., Jiang, Y. G., & Shi, L. (2019). Electromicrobiology and biotechnological applications of the exoelectrogens Geobacter and Shewanella spp. In Science China Technological Sciences (Vol. 62, Issue 10, pp. 1670–1678). Springer Verlag. https://doi.org/10.1007/s11431-019-9509-8

Simeon, I. M. *et al.* (2022) 'Electrochemical evaluation of different polymer binders for the production of carbon-modified stainless-steel electrodes for sustainable power generation using a soil microbial fuel cell', *Chemical Engineering Journal Advances*. Elsevier, 10, p. 100246. doi: 10.1016/J.CEJA.2022.100246.

Tamura, K., Nei, M., & Kumar, S. (2004). Prospects for inferring very large phylogenies by using the neighbor-joining method. Proceedings of the National Academy of Sciences of the United States of America. https://doi.org/10.1073/pnas.0404206101

Ter Heijne, A., Hamelers, H. V. M., De Wilde, V., Rozendal, R. A., & Buisman, C. J. N. (2006). A bipolar membrane combined with ferric iron reduction as an efficient cathode system in microbial fuel cells. Environmental Science and Technology. https://doi.org/10.1021/es0608545

The neighbor-joining method: a new method for reconstructing phylogenetic trees. (1987). Molecular Biology and Evolution. https://doi.org/10.1093/oxfordjournals.molbev.a040454

Ucar, D., Zhang, Y., & Angelidaki, I. (2017). An overview of electron acceptors in microbial fuel cells. In Frontiers in Microbiology (Vol. 8, Issue APR). Frontiers Research Foundation. https://doi.org/10.3389/fmicb.2017.00643

Wang, X., Cai, Z., Zhou, Q., Zhang, Z., & Chen, C. (2012). Bioelectrochemical stimulation of petroleum hydrocarbon degradation in saline soil using U-tube microbial fuel cells. Biotechnology and Bioengineering. https://doi.org/10.1002/bit.23351

Wei, L., Han, H., & Shen, J. (2013). Effects of temperature and ferrous sulfate concentrations on the performance of microbial fuel cell. International Journal of Hydrogen Energy. https://doi.org/10.1016/j.ijhydene.2013.01.019

Wrighton, K. C., Agbo, P., Warnecke, F., Weber, K. A., Brodie, E. L., DeSantis, T. Z., Hugenholtz, P., Andersen, G. L., & Coates, J. D. (2008). A novel ecological role of the Firmicutes identified in thermophilic microbial fuel cells. ISME Journal, 2(11), 1146–1156. https://doi.org/10.1038/ismej.2008.48

Wang, A. *et al.* (2010) 'A rapid selection strategy for an anodophilic consortium for microbial fuel cells', *Bioresource technology*. Bioresour Technol, 101(14), pp. 5733–5735. doi: 10.1016/J.BIORTECH.2010.02.056.

Wu, D., Xing, D., Lu, L., Wei, M., Liu, B., & Ren, N. (2013). Ferric iron enhances electricity generation by Shewanella oneidensis MR-1 in MFCs. Bioresource Technology, 135, 630–634. https://doi.org/10.1016/j.biortech.2012.09.106

Wu, M. S. *et al.* (2017) 'Simultaneous removal of heavy metals and biodegradation of organic matter

with sediment microbial fuel cells', *RSC Advances*. The Royal Society of Chemistry, 7(84), pp. 53433–53438. doi: 10.1039/C7RA11103G.

Xu, X., Zhao, Q., Wu, M., Ding, J., & Zhang, W. (2017). Biodegradation of organic matter and anodic microbial communities analysis in sediment microbial fuel cells with/without Fe(III) oxide addition. Bioresource Technology, 225(Iii), 402–408. https://doi.org/10.1016/j.biortech.2016.11.126

Yamashita, T., Ishida, M., Asakawa, S., Kanamori, H., Sasaki, H., Ogino, A., Katayose, Y., Hatta, T., & Yokoyama, H. (2016). Enhanced electrical power generation using flame-oxidized stainless steel anode in microbial fuel cells and the anodic community structure. Biotechnology for Biofuels. https://doi.org/10.1186/s13068-016-0480-7

Yates, M. D., Kiely, P. D., Call, D. F., Rismani-yazdi, H., Bibby, K., Peccia, J., Regan, J. M., & Logan, B. E. (2013). Convergent development of anodic bacterial communities in microbial fuel cells. 2012, 2002–2013. https://doi.org/10.1038/ismej.2012.42

Yong, Y. C., Cai, Z., Yu, Y. Y., Chen, P., Jiang, R., Cao, B., Sun, J. Z., Wang, J. Y., & Song, H. (2013). Increase of riboflavin biosynthesis underlies enhancement of extracellular electron transfer of Shewanella in alkaline microbial fuel cells. Bioresource Technology, 130, 763–768. https://doi.org/10.1016/j.biortech.2012.11.145

Zhang, F., Cheng, S., Pant, D., Bogaert, G. Van, & Logan, B. E. (2009). Power generation using an activated carbon and metal mesh cathode in a microbial fuel cell. Electrochemistry Communications. https://doi.org/10.1016/j.elecom.2009.09.024

Zhang, J., Zhang, Y., Quan, X., & Chen, S. (2013). Effects of ferric iron on the anaerobic treatment and microbial biodiversity in a coupled microbial electrolysis cell (MEC) - Anaerobic reactor. Water Research. https://doi.org/10.1016/j.watres.2013.06.056

Zhao, L., Deng, J., Hou, H., Li, J., & Yang, Y. (2019). Investigation of PAH and oil degradation along with   electricity generation in soil using an enhanced plant-microbial fuel cell. Journal of Cleaner Production, 221, 678–683. https://doi.org/10.1016/j.jclepro.2019.02.212

Chapter 6

Abrevaya, X. C., Sacco, N. J., Bonetto, M. C., Hilding-Ohlsson, A., & Cortón, E. (2015). Analytical applications of microbial fuel cells. Part I: Biochemical oxygen demand. In Biosensors and Bioelectronics. https://doi.org/10.1016/j.bios.2014.04.034

Anam, M., Yousaf, S., Sharafat, I., Zafar, Z., Ayaz, K., & Ali, N. (2017). Comparing natural and artificially designed bacterial consortia as biosensing elements for rapid non- specific detection of organic pollutant through microbial fuel cell. International Journal of Electrochemical Science, 12(4), 2836–2851. https://doi.org/10.20964/2017.04.49

Aracic, S., Manna, S., Petrovski, S., Wiltshire, J. L., Mann, G., & Franks, A. E. (2015). Innovative biological approaches for monitoring and improving water quality. Frontiers in Microbiology, 6(JUL), 826. https://doi.org/10.3389/fmicb.2015.00826

Bee Quek, S., Cheng, L., & Cord-Ruwisch, R. (2015). In-line deoxygenation for organic carbon detections in seawater using a marine microbial fuel cell-biosensor. https://doi.org/10.1016/j.biortech.2015.01.078

Bonetto, M. C., Sacco, N. J., Ohlsson, A. H., & Cortón, E. (2011). Assessing the effect of oxygen and microbial inhibitors to optimize ferricyanide-mediated BOD assay. Talanta, 85(1), 455–462. https://doi.org/10.1016/j.talanta.2011.04.007

Carpenter, S. R., Stanley, E. H., & Vander Zanden, M. J. (2011). State of the World's Freshwater Ecosystems: Physical, Chemical, and Biological Changes. Annual Review of Environment and Resources, 36(1), 75–99. https://doi.org/10.1146/annurev-environ-021810-094524

Chouler, J., & Di Lorenzo, M. (2015). Water Quality Monitoring in Developing Countries; Can Microbial Fuel Cells be the Answer? Biosensors, 5(3), 450–470. https://doi.org/10.3390/bios5030450

DU, Z., LI, Q., TONG, M., LI, S., & LI, H. (2008). Electricity Generation Using Membrane-less Microbial Fuel Cell during Wastewater Treatment. Chinese Journal of Chemical Engineering, 16(5),

772–777. https://doi.org/10.1016/S1004-9541(08)60154-8

Feng, C., Sharma, S. C. D., & Yu, C. P. (2015). Microbial fuel cells for wastewater treatment. In Biotechnologies and Biomimetics for Civil Engineering (pp. 411–437). Springer International Publishing. https://doi.org/10.1007/978-3-319-09287-4_18

He, Z., Kan, J., Wang, Y., Huang, Y., Mansfeld, F., & Nealson, K. H. (2009). Electricity production coupled to ammonium in a microbial fuel cell. Environmental Science and Technology, 43(9), 3391–3397. https://doi.org/10.1021/es803492c

Hsieh, M. C., & Chung, Y. C. (2014). Measurement of biochemical oxygen demand from different wastewater samples using a mediator-less microbial fuel cell biosensor. Environmental Technology (United Kingdom), 35(17), 2204–2211. https://doi.org/10.1080/09593330.2014.898700

Journal: Biosensors and Bioelectronics, Vol.22, Issue 12. (2007) https://www.sensorsportal.com/html/biosensors/Biosensors_22_12.htm

Liu, J., Björnsson, L., & Mattiasson, B. (2000). Immobilised activated sludge based biosensor for biochemical oxygen demand measurement. Biosensors and Bioelectronics, 14(12), 883–893. https://doi.org/10.1016/S0956-5663(99)00064-0

Liu, J., & Mattiasson, B. (2002). Microbial BOD sensors for wastewater analysis. Water Research (Vol. 36, Issue 15, pp. 3786–3802). Elsevier Ltd. https://doi.org/10.1016/S0043-1354(02)00101-X

Liu, Z., Liu, J., Zhang, S., Xing, X. H., & Su, Z. (2011). Microbial fuel cell based biosensor for in situ monitoring of anaerobic digestion process. Bioresource Technology, 102(22), 10221–10229. https://doi.org/10.1016/j.biortech.2011.08.053

Logroño, W., Guambo, A., Pérez, M., Kadier, A., & Recalde, C. (2016). A terrestrial single chamber microbial fuel cell-based biosensor for biochemical oxygen demand of synthetic rice washed wastewater. Sensors, 16(1), 101. https://doi.org/10.3390/s16010101

Malvankar, N. S., Tuominen, M. T., & Lovley, D. R. (2012). University of Massachusetts-Amherst From the SelectedWorks of Derek Lovley Lack of cytochrome involvement in long-range electron transport through conductive biofilms and nanowires of Geobacter sulfurreducens Lack of cytochrome involvement in long-range electron transport through conductive biofilms and nanowires of Geobacter sulfurreducens. https://doi.org/10.1039/c2ee22330a

Moon, H., Chang, I. S., Kang, K. H., Jang, J. K., & Kim, B. H. (2004). Improving the dynamic response of a mediator-less microbial fuel cell as a biochemical oxygen demand (BOD) sensor. Biotechnology Letters, 26(22), 1717–1721. https://doi.org/10.1007/s10529-004-3743-5

Parkash, A. (2016). Microbial Fuel Cells: A Source of Bioenergy. Journal of Microbial & Biochemical Technology, 8(3). https://doi.org/10.4172/1948-5948.1000293

Peixoto, L., Min, B., Martins, G., Brito, A. G., Kroff, P., Parpot, P., Angelidaki, I., & Nogueira, R. (2011). In situ microbial fuel cell-based biosensor for organic carbon. Bioelectrochemistry, 81(2), 99–103. https://doi.org/10.1016/j.bioelechem.2011.02.002

Rabaey, K., Boon, N., Höfte, M., & Verstraete, W. (2005). Microbial phenazine production enhances electron transfer in biofuel cells. Environmental Science and Technology, 39(9), 3401–3408. https://doi.org/10.1021/es048563o

Sazykin, I. S., Sazykina, M. A., Khmelevtsova, L. E., Mirina, E. A., Kudeevskaya, E. M., Rogulin, E. A., & Rakin, A. V. (2016). Biosensor-based comparison of the ecotoxicological contamination of the wastewaters of Southern Russia and Southern Germany. International Journal of Environmental Science and Technology, 13(3), 945–954. https://doi.org/10.1007/s13762-016-0936-0

Sharpe, M. (2003). It's a bug's life: Biosensors for environmental monitoring. Journal of Environmental Monitoring (Vol. 5, Issue 6). J Environ Monit. https://doi.org/10.1039/b314067a

Su, L., Jia, W., Hou, C., & Lei, Y. (2011). Microbial biosensors: A review. Biosensors and Bioelectronics (Vol. 26, Issue 5, pp. 1788–1799). Biosens Bioelectron. https://doi.org/10.1016/j.bios.2010.09.005

Sumaraj and M.M. Ghangrekar. (2014). Development of microbial fuel cell as biosensor for detection of organic matter of wastewater. Recent Research in Science and Technology, 6(1), 162–166.

https://www.researchgate.net/publication/269932778_Development_of_microbial_fuel_cell_as_bios
ensor_for_detection_of_organic_matter_of_wastewater

Tran, P., Nguyen, L., Nguyen, H., Nguyen, B., Nong, L., Mai, L., Tran, H., Nguyen, T., & Pham, H. (2016). Effects of inoculation sources on the enrichment and performance of anode bacterial consortia in sensor typed microbial fuel cells. AIMS Bioengineering, 3(1), 60–74. https://doi.org/10.3934/bioeng.2016.1.60

Tront, J. M., Fortner, J. D., Plötze, M., Hughes, J. B., & Puzrin, A. M. (2008). Microbial fuel cell biosensor for in situ assessment of microbial activity. Biosensors and Bioelectronics, 24(4), 586–590. https://doi.org/10.1016/j.bios.2008.06.006

Verma, N., & Singh, A. K. (2013). Development of Biological Oxygen Demand Biosensor for Monitoring the Fermentation Industry Effluent. ISRN Biotechnology, 2013, 1–6. https://doi.org/10.5402/2013/236062

Wu, L.-C., Tsai, T.-H., Liu, M.-H., Kuo, J.-L., Chang, Y.-C., & Chung, Y.-C. (2017). A Green Microbial Fuel Cell-Based Biosensor for In Situ Chromium (VI) Measurement in Electroplating Wastewater. Sensors, 17(11), 2461. https://doi.org/10.3390/s17112461

Yamashita, T., Ookawa, N., Ishida, M., Kanamori, H., Sasaki, H., Katayose, Y., & Yokoyama, H. (2016). A novel open-Type biosensor for the in-situ monitoring of biochemical oxygen demand in an aerobic environment. Scientific Reports, 6(1), 1–9. https://doi.org/10.1038/srep38552

Yousaf, S., Anam, M., & Ali, N. (2017). Evaluating the production and bio-stimulating effect of 5-methyl 1, hydroxy phenazine on microbial fuel cell performance. International Journal of Environmental Science and Technology, 14(7), 1439–1450. https://doi.org/10.1007/s13762-016-1241-7

Zheng, Q., Xiong, L., Mo, B., Lu, W., Kim, S., & Wang, Z. (2015). Temperature and Humidity Sensor Powered by an Individual Microbial Fuel Cell in a Power Management System. Sensors, 15(9), 23126–23144. https://doi.org/10.3390/s150923126

Chapter 7

Boubour, E., & Bruce Lennox, R. (2000). Stability of O-functionalized self-assembled monolayers as a function of applied potential. Langmuir. https://doi.org/10.1021/la000514b

Carmona-Martinez, A. A., Harnisch, F., Fitzgerald, L. A., Biffinger, J. C., Ringeisen, B. R., & Schröder, U. (2011). Cyclic voltammetric analysis of the electron transfer of Shewanella oneidensis MR-1 and nanofilament and cytochrome knock-out mutants. Bioelectrochemistry. https://doi.org/10.1016/j.bioelechem.2011.02.006

Cisternas, I. S., Salazar, J. C., & García-Angulo, V. A. (2018). Overview on the bacterial iron-riboflavin metabolic axis. In Frontiers in Microbiology. https://doi.org/10.3389/fimmu.2018.01478

Coman, V., Gustavsson, T., Finkelsteinas, A., Von Wachenfeldt, C., Hägerhäll, C., & Gorton, L. (2009). Electrical wiring of live, metabolically enhanced Bacillus subtilis cells with flexible osmium-redox polymers. Journal of the American Chemical Society, 131(44), 16171–16176. https://doi.org/10.1021/ja905442a

Corbett, D., Goldrick, M., Fernandes, V. E., Davidge, K., Poole, R. K., Andrew, P. W., Cavet, J., & Roberts, I. S. (2017). Listeria monocytogenes has both cytochrome bd-type and cytochrome aa 3 - type terminal oxidases, which allow growth at different oxygen levels, and both are important in infection. Infection and Immunity. https://doi.org/10.1128/IAI.00354-17

Engel, M., Bayer, H., Holtmann, D., Tippkötter, N., & Ulber, R. (2019). Flavin secretion of Clostridium acetobutylicum in a bioelectrochemical system - Is an iron limitation involved? Bioelectrochemistry. https://doi.org/10.1016/j.bioelechem.2019.05.014

Fuller, S. J., McMillan, D. G. G., Renz, M. B., Schmidt, M., Burke, I. T., & Stewart, D. I. (2014). Extracellular electron transport-mediated Fe(iii) reduction by a community of alkaliphilic bacteria that use flavins as electron shuttles. Applied and Environmental Microbiology, 80(1), 128–137. https://doi.org/10.1128/AEM.02282-13

Hederstedt, L., Gorton, L., & Pankratovab, G. (2020). Two Routes for Extracellular Electron Transfer in

Enterococcus faecalis. Journal of Bacteriology, 202(7), 1–9. https://doi.org/10.1128/JB.00725-19

Kees, E. D., Pendleton, A. R., Paquete, C. M., Arriola, M. B., Kane, A. L., Kotloski, N. J., Intile, P. J., & Gralnick, J. A. (2019). Secreted flavin cofactors for anaerobic respiration of fumarate and urocanate by Shewanella oneidensis: Cost and role. Applied and Environmental Microbiology. https://doi.org/10.1128/AEM.00852-19

Kerscher, S., Dröse, S., Zickermann, V., & Brandt, U. (2007). The Three Families of Respiratory NADH Dehydrogenases. May.

Kracke, F., Vassilev, I., & Krömer, J. O. (2015). Microbial electron transport and energy conservation - The foundation for optimizing bioelectrochemical systems. In Frontiers in Microbiology (Vol. 6, Issue JUN, p. 575). Frontiers Media S.A. https://doi.org/10.3389/fmicb.2015.00575

Light, S. H., Méheust, R., Ferrell, J. L., Cho, J., Deng, D., Agostoni, M., Iavarone, A. T., Banfield, J. F., D'Orazio, S. E. F., & Portnoy, D. A. (2019). Extracellular electron transfer powers flavinylated extracellular reductases in Gram-positive bacteria. Proceedings of the National Academy of Sciences of the United States of America. https://doi.org/10.1073/pnas.1915678116

Light, S. H., Su, L., Rivera-Lugo, R., Cornejo, J. A., Louie, A., Iavarone, A. T., Ajo-Franklin, C. M., & Portnoy, D. A. (2018). A flavin-based extracellular electron transfer mechanism in diverse Gram-positive bacteria. Nature. https://doi.org/10.1038/s41586-018-0498-z

Marsili, E., Baron, D. B., Shikhare, I. D., Coursolle, D., Gralnick, J. A., & Bond, D. R. (2008). Shewanella secretes flavins that mediate extracellular electron transfer. Proceedings of the National Academy of Sciences of the United States of America. https://doi.org/10.1073/pnas.0710525105

Monk, I. R., Gahan, C. G. M., & Hill, C. (2008). Tools for functional postgenomic analysis of Listeria monocytogenes. Applied and Environmental Microbiology. https://doi.org/10.1128/AEM.00314-08

Pankratova, G., Hederstedt, L., & Gorton, L. (2019). Extracellular electron transfer features of Gram-positive bacteria. Analytica Chimica Acta, 1076, 32–47. https://doi.org/10.1016/j.aca.2019.05.007

Pankratova, G., Leech, D., Gorton, L., & Hederstedt, L. (2018). Extracellular Electron Transfer by the Gram-Positive Bacterium Enterococcus faecalis. Biochemistry. https://doi.org/10.1021/acs.biochem.8b00600

Pankratova, G., Pankratov, D., Milton, R. D., Minteer, S. D., & Gorton, L. (2019). Extracellular Electron Transfer: Following Nature: Bioinspired Mediation Strategy for Gram-Positive Bacterial Cells (Adv. Energy Mater. 16/2019). Advanced Energy Materials. https://doi.org/10.1002/aenm.201970055

Park, H. S., Kim, B. H., Kim, H. S., Kim, H. J., Kim, G. T., Kim, M., Chang, I. S., Park, Y. K., & Chang, H. I. (2001). A novel electrochemically active and Fe(III)-reducing bacterium phylogenetically related to Clostridium butyricum isolated from a microbial fuel cell. Anaerobe, 7(6), 297–306. https://doi.org/10.1006/anae.2001.0399

Sharma, R., Deacon, S. E., Nowak, D., George, S. E., Szymonik, M. P., Tang, A. A. S., Tomlinson, D. C., Davies, A. G., McPherson, M. J., & Wälti, C. (2016). Label-free electrochemical impedance biosensor to detect human interleukin-8 in serum with sub-pg/ml sensitivity. Biosensors and Bioelectronics, 80, 607–613. https://doi.org/10.1016/j.bios.2016.02.028

Stamou, D., Gourdon, D., Liley, M., Burnham, N. A., Kulik, A., Vogel, H., & Duschl, C. (1997). Uniformly flat gold surfaces: Imaging the domain structure of organic monolayers using scanning force microscopy. Langmuir, 13(9), 2425–2427. https://doi.org/10.1021/la962123w

Whiteley, A. T., Pollock, A. J., & Portnoy, D. A. (2015). Erratum: The PAMP c-di-AMP is essential for listeria monocytogenes growth in rich but not minimal media due to a toxic increase in (p)ppGpp (Cell Host and Microbe (2015) 17 (788-798)). In Cell Host and Microbe. https://doi.org/10.1016/j.chom.2015.06.005

Zheng, T., Li, J., Ji, Y., Zhang, W., Fang, Y., Xin, F., Dong, W., Wei, P., Ma, J., & Jiang, M. (2020). Progress and prospects of bioelectrochemical systems: Electron transfer and its applications in the microbial metabolism. Frontiers in Bioengineering and Biotechnology.

https://doi.org/10.3389/fbioe.2020.00010

Chapter 9: List of Appendices

Chapter 3 (A)
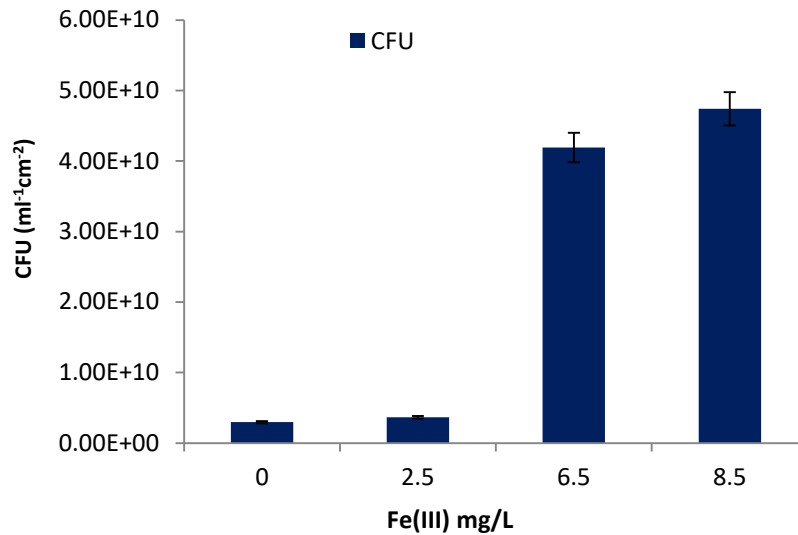
Fig. A1. Relationship between different Fe^{3+} concentrationsand total viable bacteria in biofilms in terms of CFU/ml cm^{-2} of WTR.
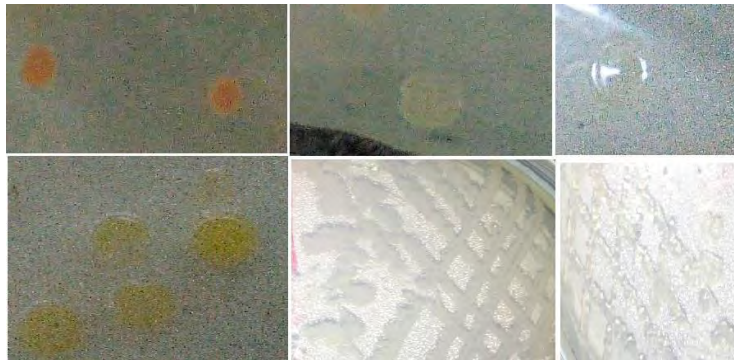
Fig. A2. Characteristic morphologies of few bacterial strains isolated from activated sludge and different biofilms under light microscope at X100. (a; orange-coloured medium sized colonies, b; large off white, c; transparent, round and large sized colony, d; large egg yolk like colonies, e; white fluffy mesh-like growth, f; shiny, string forming growth).
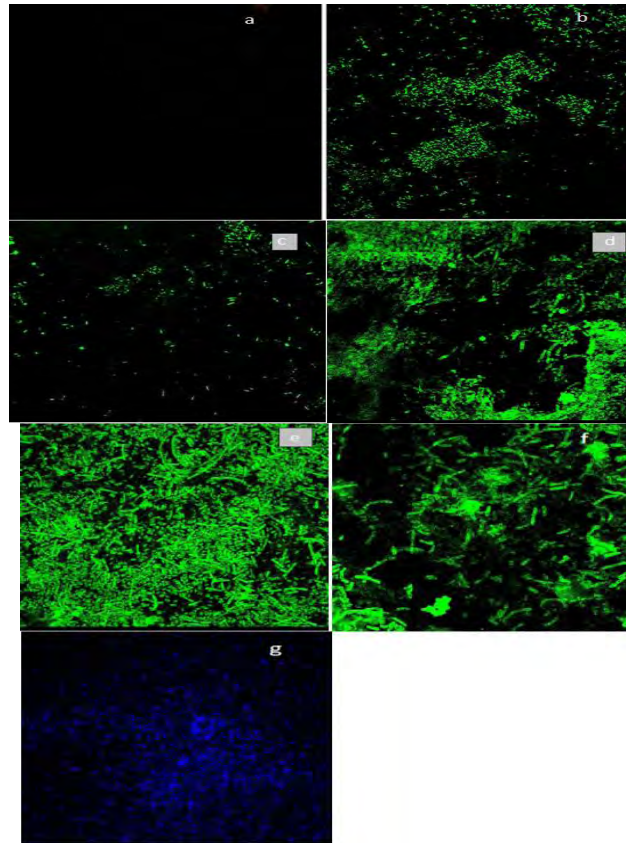
Fig.A3. CLSM projections of negative control and reference strains after hybridization with 5' end labelled 5, 6- fluorescein isothiocyanate (FLUOS) phylogenetic oligonucleotide probes. (a) negative control showing no signal with mixture of fluorescent probes, (b, c) *Pseudomonas aeruginosa* **ATCC 9027 strain exhibiting green fluorescence when hybridized with mixture of eubacterial probes (EUB338, EUB338-II, EUB338-III)at X10 and X100, respectively, (d-g) pure** *Bacillus subtilis* **strain at X100 (d; EUB mixture (EUB338, EUB338-II, EUB338-III), e; Bet42, f; EUB mixture + Bet42, g; Gam42).**
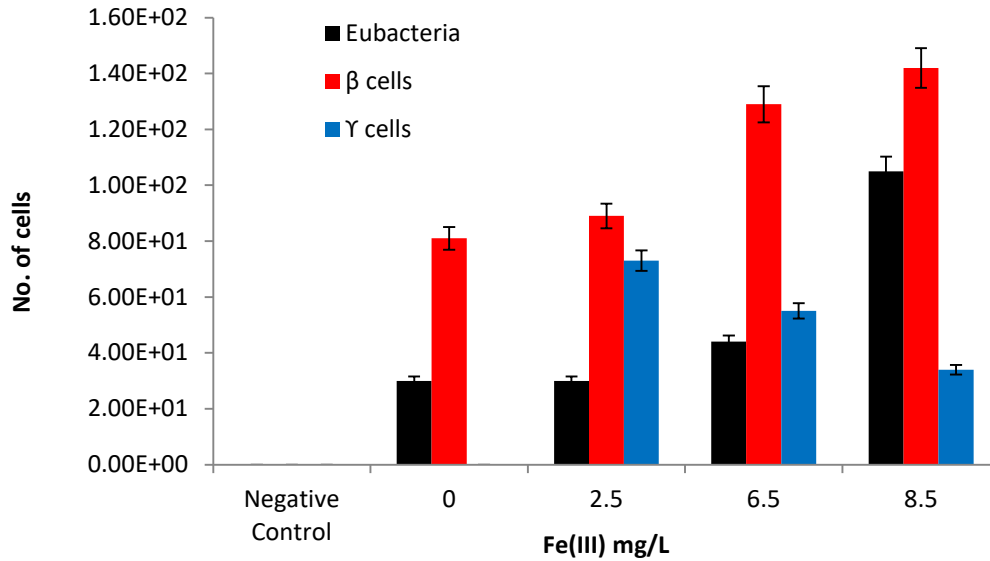
Fig.A4. Quantification of eubacteria, beta and gamma proteobacteria using *daime a*fter FISHand CLSM of biofilms after hybridization with 5' end labelled 5, 6- fluorescein isothiocyanate (FLUOS) phylogenetic oligonucleotide probes.

TableA1. Relationship between different Fe^{3+} concentrationsand total viable counts of bacteria in biofilms (CFU/ml cm^2 of WTR).

No.	Concentration of Ferric iron	CFU/ml cm^2 of WTR
1	0	2.959E+09
2	2.5	3.66E+09
3	6.5	4.19E+10
4	8.5	4.74E+10

Table A2. Percent identity and NCBI GenBank accession numbers of the organisms.

Sample No.	Organism	% Identity	NCBI GenBank Accession No.	E value
Fe^{3+}-8.5 (mg/l)-WTR	Uncultured *Nitrobacter* sp. clone K-OTU6493	94.026	|KM580410.1|	3.94E-163

Uncultured *Nitrobacter* sp. clone NCAAH	94.026	|KR537220.1|	3.94E-163
Nitrobacter sp. NBW1	94.026	|KF618620.1|	3.94E-163
Nitrobacter winogradskyi strain Nb-255	94.026	|NR_074324.1|	3.94E-163
Uncultured *Nitrobacter* sp. clone Nit4	94.026	|HM061139.1|	3.94E-163
Uncultured *Nitrobacter* sp. clone 1-G	94.026	|EU305569.1|	3.94E-163
Nitrobacter sp. 311 strain 311	94.026	|AM286397.1|	3.94E-163
Nitrobacter sp. LIP, strain LIP	94.026	|AM286385.1|	3.94E-163
Nitrobacter sp. Nato, strain Nato	94.026	|AM286376.1|	3.94E-163
Nitrobacter sp. 219, strain 219	94.026	|AM286375.1|	3.94E-163
Nitrobacter winogradskyi, strain Engel	94.026	|AM286374.1|	3.94E-163

Nitrobacter winogradskyi Nb-255	94.026	|CP000115.1|	3.94E-163
Nitrobacter sp. PBAB10	94.026	|AY508475.1|	3.94E-163
Nitrobacter winogradskyi, strain ATCC 14123	94.026	|AM114521.1|	3.94E-163
Nitrite-oxidizing bacterium MPN2	94.026	|AY135357.1|	3.94E-163
Nitrobacter winogradskyi ATCC 25381	94.026	|L35506.1|	3.94E-163
Nitrobacter sp. Termite2, strain Termite2	93.766	|AM286391.1|	1.83E-161
Nitrobacter sp. BS5/19	93.766	|AM286387.1|	1.83E-161
Nitrobacter vulgaris, strain K48	93.766	|AM286381.1|	1.83E-161
Nitrobacter sp. PBAB17	93.766	|AY508476.1|	1.83E-161
Nitrobacter sp. TH21	93.734	|AF080257.1|	2.37E-160
Nitrobacter vulgaris strain NBW3	93.506	|KF618622.1|	8.53E-160

	Uncultured bacterium clone IIEA1-rp-13Nit	96.341	|EU267432.1|	7.25E-150
Control	Uncultured Nitrobacter sp. clone K-OTU6493	93.766	|KM580410.1|	1.84E-161
	Nitrobacter sp. NBW1	93.766	|KF618620.1|	1.84E-161
	Nitrobacter winogradskyi strain Nb-255	93.766	|NR_074324.1|	1.84E-161
	Uncultured *Nitrobacter* sp. clone Nit4	93.766	|HM061139.1|	1.84E-161
	Uncultured *Nitrobacter* sp. clone 1-G	93.766	|EU305569.1|	1.84E-161
	Nitrobacter sp. 311, strain 311	93.766	|AM286397.1|	1.84E-161
	Nitrobacter sp. LIP strain LIP	93.766	|AM286385.1|	1.84E-161
	Nitrobacter sp. Nato, strain Nato	93.766	|AM286376.1|	1.84E-161
	Nitrobacter sp. 219, strain 219	93.766	|AM286375.1|	1.84E-161
	Nitrobacter winogradskyi, strain Engel	93.766	|AM286374.1|	1.84E-161

Nitrobacter winogradskyi Nb-255	93.766	|CP000115.1|	1.84E-161
Nitrobacter sp. PBAB10	93.766	|AY508475.1|	1.84E-161
Nitrobacter winogradskyi, strain ATCC 14123	93.766	|AM114521.1|	1.84E-161
Nitrite-oxidizing bacterium MPN2	93.766	|AY135357.1|	1.84E-161
Nitrobacter winogradskyi ATCC 25381	93.766	|L35506.1|	1.84E-161
Uncultured *Nitrobacter* sp. clone NCAAH 30N18	93.506	|KR537220.1|	8.55E-160
Nitrobacter sp. Termite2, strain Termite2	93.506	|AM286391.1|	8.55E-160
Nitrobacter sp. BS5/19, strain BS5/19	93.506	|AM286387.1|	8.55E-160
Nitrobacter vulgaris, strain K48	93.506	|AM286381.1|	8.55E-160
Nitrobacter sp. PBAB17, partial sequence	93.506	|AY508476.1|	8.55E-160
Nitrobacter sp. TH21, partial sequence	93.473	|AF080257.1|	1.11E-158

	Nitrobacter vulgaris strain NBW3	93.247	|KF618622.1|	3.98E-158
Fe^{3+}-6.5 (mg/l)-WTR	Uncultured *Nitrosomonas* sp. clone R2-4	96.037	|KJ023574.1|	3.37E-148
	Uncultured *Nitrosomonas* sp. clone R1-2	96.037	|KJ023568.1|	3.37E-148
	Nitrosomonas sp. HP8, isolate HP8	96.037	|HF678378.1|	3.37E-148
	Nitrosomonas europaea strain ATCC 19718	96.037	|NR_074774.1|	3.37E-148
	Nitrosomonas europaea strain ATCC 25978	96.037	|NR_117649.1|	3.37E-148
	Uncultured ammonia-oxidizing beta proteobacterium clone 2309ST0304	96.037	|JQ726143.1|	3.37E-148
	Uncultured ammonia-oxidizing beta proteobacterium clone 2309ST0311	96.037	|JQ726140.1|	3.37E-148
	Uncultured *Nitrosomonas* sp. isolate DGGE gel band E5	96.037	|JN401994.1|	3.37E-148
	Uncultured *Nitrosomonas* sp. isolate DGGE gel band E4	96.037	|JN401993.1|	3.37E-148
	Uncultured *Nitrosomonas* sp. isolate DGGE gel band B2	96.037	|JN401978.1|	3.37E-148

Uncultured ammonia-oxidizing bacterium clone PF2cln5	96.037	|JN099284.1|	3.37E-148
Uncultured bacterium clone NIT_108	96.037	|JN087936.1|	3.37E-148
Uncultured bacterium clone NIT_106	96.037	|JN087935.1|	3.37E-148
Uncultured bacterium clone NIT_105	96.037	|JN087934.1|	3.37E-148
Uncultured bacterium clone NIT_94	96.037	|JN087929.1|	3.37E-148
Uncultured bacterium clone NIT-EN-85	96.037	|HQ843751.1|	3.37E-148
Uncultured bacterium clone NIT-EN-81	96.037	|HQ843748.1|	3.37E-148
Uncultured bacterium clone NIT-EN-79	96.037	|HQ843747.1|	3.37E-148
Nitrosomonas europaea strain ATCC 25978	96.037	|NR_117368.1|	3.37E-148
Nitrosomonas europaea ATCC 19718	96.037	|AL954747.1|	3.37E-148
Uncultured *Nitrosomonas* sp. clone 61-1	96.037	|EF042983.1|	3.37E-148

Uncultured beta proteobacterium HB3	96.037	|AF210051.2|	3.37E-148
Nitrosomonas sp. WH-2	96.037	|AF338211.1|	3.37E-148
uncultured *Nitrosomonas*, isolate DGGE band MC7.1	96.037	|AJ307985.1|	3.37E-148
Nitrosomonas europaea strain C-31	96.037	|NR_040879.1|	3.37E-148
Nitrosomonas sp. ENI-11	96.037	|AB079053.1|	3.37E-148
Nitrosomonas sp. mixed culture isolate Koll-21	96.037	|AJ224941.1|	3.37E-148
Uncultured *Nitrosomonas* sp. clone 88-1	96.024	|EF042982.1|	1.21E-147
Nitrosomonas europaea	96.037	|AJ245759.1|	1.21E-147

Table A3. Quantification of Eubacteria, Beta and Gamma proteobacteria per cm^2 of biofilms developed on waste tire rubber (WTR) under various concentrations of Fe^{3+} by CLSMat X10.

Fe^{3+} (mg/l)	Total Eub cells	β cells	ϒ cells
Negative Control	0.00E+00	0.00E+00	0.00E+00

0	3.00E+01	8.10E+01	-
2.5	3.00E+01	8.90E+01	7.30E+01
6.5	4.40E+01	1.29E+02	5.50E+01
8.5	1.05E+02	1.42E+02	3.40E+01

Table A4. Dissolved oxygen (mg/l) profile within the reactors monitored periodically.

No.	Sample	1st reading	2nd reading	3rd reading	Average
		DO (mg/l)	DO (mg/l)	DO (mg/l)	DO (mg/l)
1	Activated sludge	4.57	4.57	4.56	4.57
2	Fe-0 (control)	4.06	0.74	1.20	2
3	Fe-2.5	0.4	0.16	.18	0.25
4	Fe-6.5	1.45	0.04	1.21	0.9
5	Fe-8.5	4.21	0.25	1.89	2.12

Table A5. pH profile of activated sludge in Aerobic Batch Biofilm Reactors (ABBR).

	Reading1	Reading2	Reading 3	Reading 4	Average
Fe-0 (control)	7.47	7.47	7.31	7.06	7.3275
Fe-2.5	6.44	7.26	7.6	7.47	7.1925
Fe-6.5	6.45	7.33	7.54	7.65	7.2425
Fe-8.5	6.65	7.35	7.79	7.65	7.36

Table A6. Microtiter plate assay chart representing the OD (590nm) of biofilm forming and non-biofilm forming bacteria measured by ELISA autoreader.

No.	A	B	C	D	E	F	G	H
1	(11)0.453	(25)0.208	(99)0.241	(86)0.335	(8)0.246	(20)0.168	(119)0.334	0.167
2	(4)0.282	(1)0.369	(111)0.4	(83)0.433	(95)0.468	(22)0.233	(88)0.286	0.189
3	(85)0.213	(23)0.291	(107)0.272	(27)0.56	(91)0.393	(18)0.317	(104)0.243	
4	(113)0.248	(6)0.28	(51)0.426	(118)0.296	(10)0.334	(103)0.328	0.175	
5	(116)0.379	(113)0.752	(81)0.200	(28)0.453	(12)0.255	(26)0.243	0.199	
6	(105)0.211	(33)0.256	(16)0.384	(102)0.264	(51)0.37	(21)0.65	0.277	
7	(45)0.215	(24)0.336	(14)0.698	(89)0.662	(54)0.246	(95)0.341	0.203	
8	(66)0.184	(52)0.268	(82)0.349	(94)0.302	(7)0.38	(unknown)1.199	0.217	
9	(56)0.298	(57)0.471	(5)0.200	(53)0.282	(2)0.227	(110)1.772	0.189	
10	(55)0.316	(115)0.52	(101)0.733	(87)0.262	(15)0.366	(100)0.528	0.262	
11	(92)0.499	(19)0.519	(98)0.838	(93)0.631	(17)0.288	(30)0.441	0.239	

Table A7. Gram staining of selected bacteria isolated from activated sludge and biofilms developed under varying Fe^{3+} concentration on different support materials.

		Biofilm			Activated Sludge	
	No.	Isolate	Gram Staining	No.	Isolate	Gram Staining
1		Iq7	Gram positive, long Bacilli	1	Iq1	Gram negative, Bacilli
2		Iq11	Gram positive, Bacilli	2	Iq2	Gram negative, Bacilli
3		Iq15	Gram positive, cocci (diplococcic)	3	Iq5	Gram negative Bacilli, thin and short
4		Iq20	Gram negative, chains of large Bacilli	4	Iq6	Gram negative Bacilli, chains
5		Iq26	Gram positive, Bacilli	5	Iq7	Gram negative, Bacilli
6		Iq26	Gram negative, Bacilli	6	Iq9	Gram positive, Bacilli
7		Iq54	Gram positive, Bacilli	7	Iq12	Gram positive, cocci
8		Iq87	Gram negative, short Bacilli	8	Iq13	Gram negative, short Bacilli
9		Iq88	Gram negative, Bacilli	9	q14	Gram variable
10		Iq89	Gram positive, Bacilli	10	Iq15	Gram negative, Bacilli

Chapter 3 (B)

Table A1-B. COD (mg/l) measured from different reactors under treated and control conditions with corresponding absorbance (nm).

	COD(mg/L)	Absorbance
Al 2.5 mg/L	363	0.288
Al 4.5 mg/L	371	0.232
Al 6.5 mg/L	438	0.273
CONTROL	509	0.315

Table A2-B One-way ANOVA analysis of the two physical methods carried out on sludge sample.

ANOVA

Source of Variation	*SS*	*df*	*MS*	*F*	*P-value*	*F crit*
Between Groups	6.12E+18	1	6.12E+18	0.720057	0.4104	4.60011
Within Groups	1.19E+20	14	8.5E+18			
Total	1.25E+20	15				

Table A3B. CFU/mLcm^2 at varying concentrations of Al^{3+}

Dilutions	CFU/mL/cm$_2$		
	10_4	10_6	10_7
Concentration of Al$_b$ (mg/L)			
0	$6.16 \times 10_7$	$4.20 \times 10_9$	$3.15 \times 10_{10}$
2.5	$1.19 \times 10_7$	$6.30 \times 10_8$	$2.50 \times 10_9$
4.5	$6.70 \times 10_6$	$1.50 \times 10_8$	$3.00 \times 10_8$
6.5	$4.60 \times 10_6$	$9.00 \times 10_7$	$4.00 \times 10_8$

Chapter 5

Table A1. Voltage, Current density and power density of microbial fuel cells (MFCs) with and without ferric iron using cropland soil as an inoculum.

R	voltage(mV)-soil-control	voltages(mV)-soil-Fe	current density (mAcm-2)-soil-control	current density (mAcm-2)-soil-Fe	Power density (mWcm-2)-soil-control	Power density (mWcm-2)-soil-Fe
100	154	289	1.54	0.1156	9	33.4084
1000	505	925	o.o18	0.0234	10.2	34.23
1500	645	1151	0.014	0.01813	11	35.3
2000	748	1290	0.0123	0.0148	11.2	33.3
3250	770	1385	0.04	0.00966153	7.29	23.6
4500	781	1405	0.0069	0.007564	5.4	17.5
7250	807	1415	0.004	0.007	3.5	11.04
10000	817	1427	0.003	0.003592	2.6	8.1

Chapter 6

Table A1

Days	Voltage (mV)
1	29.9
2	33.3
3	45.4
4	32.2
5	43.4
6	40.6
7	40.8
8	41.2
9	41.2
10	40.2
11	30.7
12	30.5
13	41
14	41.2

15	41.1
16	36.4
17	45.2
18	34
19	41.1
20	40.5
21	33
22	33.5
23	31.9
24	29.4
25	30.8
26	29.3
27	29.8
28	32.2
29	32.2
30	31.2

Table A2

Days	Voltage (mV)
1	32
2	21
3	49
4	36
5	63
6	56.1
7	54.7
8	110
9	59.2
10	50.8
11	60.4
12	155.8
13	145.3
14	46.3
15	44.5
16	50
17	58.9
18	29.9

19	22.7
20	24.9
21	55.2
22	78
23	64
24	27.3
25	23.4
26	20.3
27	25
28	24.5
29	23.1
30	29

Table Table A3

Days	Voltage (mV)
1	74.3
2	89.4
3	153.4
4	196
5	170
6	223.7
7	199.3
8	221
9	264.9
10	296.8
11	287.8
12	241.9
13	205
14	280
15	288
16	219
17	198
18	219.9
19	203
20	299.7
21	278
22	266.6

23	270.4
24	205
25	248
26	402
27	453
28	402
29	354
30	328

Table A4

Days	Voltage (mV)
1	80
2	76
3	58
4	37
5	130
6	97
7	230
8	412
9	446
10	432
11	350
12	311
13	318
14	197
15	225
16	186.3
17	332
18	274
19	255
20	276
21	187
22	177
23	191
24	204
25	212
26	299

27	210
28	236
29	241
30	230

Table A5

Days	Voltage (mV)		
	5	7	9
1	34.9	74.3	28
2	39.1	89.4	30.2
3	40.7	153.4	35.2
4	46.3	196	38
5	60.8	170	45
6	99.2	223.7	58.1
7	65.8	199.3	51.2
8	46.3	221	40
9	42.1	264.9	43.2
10	38.1	296.8	24.8
11	56.3	287.8	27.2
12	57.1	241.9	28.8
13	54.2	205	29.2
14	50.6	280	30.9
15	78.4	288	41.7
16	90	219	34.1
17	191	198	23.7
18	87.6	219.9	17.8
19	49.4	203	16.5
20	32	299.7	29.9
21	56	278	34.6
22	57.7	266.6	37.3
23	60	270.4	42.2
24	51.6	205	42
25	47.1	248	40
26	47.3	402	28.9
27	46.9	453	20.9
28	45	402	18.6

| 29 | 52.8 | 354 | 13.2 |
| 30 | 51 | 328 | 11.4 |

Table A6

Days	Voltage (mV)	
	HCl + PBS	NaCl + PBS
1	30	74.3
2	52	89.4
3	55	153.6
4	97	196
5	193	210
6	130	223.7
7	28	199.3
8	27	221
9	17	164.9
10	60	196.8
11	54	177.8
12	154	169.9
13	148	205
14	142	280
15	163	288
16	139.3	219
17	134.8	198
18	179.4	169.9
19	136	153
20	140	159.7
21	43.1	278
22	44.5	266.6
23	88.4	270.4
24	89.6	255
25	84.1	278
26	85	401
27	58.2	453
28	58.3	402
29	65.5	354
30	67.1	328

Table A7

Resistance (Ω)	Voltage (mV)
50	10.6
100	20.4
500	72.7
1000	113.5
3000	230
10000	453
20000	536

Table A8

Resistance (Ω)	Voltage (mV)
50	2.7
100	6
500	20.6
1000	39.8
3000	104.7
10000	189.9
20000	254
120000	326
220000	318
330000	350

Taylor & Francis
Taylor & Francis Group

Check for updates

Interactive effect of trivalent iron on activated sludge digestion and biofilm structure in attached growth reactor of waste tire rubber

Iqra Sharafat [a], Dania Khalid Saeed[a], Sumera Yasmin[b], Asma Imran[b], Zargona Zafar[a], Abdul Hameed[a] and Naeem Ali [a]

[a]Department of Microbiology, Quaid-i-Azam University Islamabad, Pakistan; [b]National Institute for Biotechnology and Genetic Engineering (NIBGE), Faisalabad, Pakistan

ABSTRACT

Waste tire rubber (WTR) has been introduced as an alternative, novel media for biofilm development in several experimental systems including attached growth bioreactors. In this context, four laboratory-scale static batch bioreactors containing WTR as a support material for biofilm development were run under anoxic condition for 90 days using waste activated sludge as an inoculum under the influence of different concentrations (2.5, 6.5, 8.5 mg/l) of trivalent ferric iron (Fe^{3+}). The data revealed that activated sludge with a Fe^{3+} concentration of 8.5 mg/l supported the maximum bacterial biomass [4.73E + 10 CFU/ml cm^2]; besides, it removed 38% more Chemical oxygen demand compared to Fe^{3+} free condition from the reactor. Biochemical testing and 16S rDNA phylogenetic analysis of WTR-derived biofilm communities further suggested the role of varying concentrations of Fe^{3+} on the density and diversity of members of Enterobacteria(ceae), ammonium (AOB) and nitrite oxidizing bacteria. Furthermore, Fluorescent *in situ* hybridization with phylogenetic oligonucleotide probes and confocal laser scanning microscopy of WTR biofilms indicated a significant increase in density of eubacteria (3.00E + 01 to.05E + 02 cells/cm^2) and beta proteobacteria (8.10E + 01 to 1.42E + 02 cells/cm^2), respectively, with an increase in Fe^{3+} concentration in the reactors, whereas, the cell density of gamma proteobacteria in biofilms decreased.

Highlights

- Waste tire is applied as a cost-effective support material for biofilm development.
- Addition of Fe^{3+} to activated sludge improved the bio-flocculation and COD removal.
- Higher Fe^{3+} concentration supported higher bacterial density and affected diversity of bacteria.

1. Introduction

The global demand for tires is estimated to rise 4.1% per year to 3.0 billion units by 2019 which corresponds to approximately 34 million tons of waste tires production annually [1]. The increasing number of waste tires poses a serious environmental threat due to their complex and resistant chemical nature in natural environment [2–4]. The extent to which these discarded tires pose an environmental and public health concerns generally increases when they are buried as evidenced by the approximately 4 billion used tires in landfills and stockpiles worldwide [5,6]. Waste tire stockpiles provide habitats for disease spreading mosquitoes, snakes, rodents [7–9] and those sites may not be utilized in future.

Majority of industrialized countries have banned scrap tires from landfills and legislations have been enacted for end of life tires management [10] in order to prevent the spread of diseases and environmental pollution. Some alternate options include pyrolysis, energy recovery, retreading, product and material recycling [11–13]. Mainly scrap tires are treated for material recovery (39%) and energy (37%) [12]. Conversion of waste tires into alternative fuels in different industrial units like cement and lime kilns, paper and thermal power stations, environmental and engineering projects needs complying with various environmental and financial constraints and is not a satisfactory solution to the waste problem [3,5,10,14]. Nevertheless, there is a need for devising more feasible means of treating waste tires with lower financial and technical requirements.

CONTACT Naeem Ali ✉ naeemali95@gmail.com, naeemali2611@gmail.com 🏢 Department of Microbiology, Quaid-i-Azam University Islamabad 45320, Pakistan

Environmentalists have focused on reducing the treatment costs of wastewater treatment and solid waste disposal. Biofilm-based attached growth reactors using support material like waste tire rubber (WTR) have been viewed as a cost-effective and highly efficient solution in order to meet the environmental conservation and disposal regulations [15,16]. Rubber has been proposed as one of the most suitable support materials for biofilm development as it holds low density and large surface area [17]. Chyan et al. [3] applied WTR as a biofilm carrier in constructed wetland for the removal of nitrogen, Chemical oxygen demand (COD) and BOD of wastewater. Tang et al. [8] suggested the potential use of rubber as a primary treatment technology that could increase the efficiency of a secondary wastewater treatment process. Similarly, Reyes et al. [18] applied used tires in anaerobic fixed bed reactor and obtained 60% reduction in BOD.

Iron (Fe) and iron salts have been reported as important environmental signaling entities in biofilm development [19,20]. Iron is essentially important for the growth of bacteria like several other nutritional elements such as carbon, nitrogen and phosphorus. For instance, it is a component of heme enzymes, for example, hydroperoxisases and cytochromes. It is an electron acceptor that chains dissimilatory ferric iron (Fe^{3+}) reduction with oxidation of organic matter during the course of anaerobic respiration [21]. During dissimilatory Fe^{3+} reduction, extra electrons released from energy production are transported to solid Fe^{3+}-bearing minerals outside of bacterial cells. As a result, the Fe^{3+} minerals are converted either to Fe^{2+} minerals or to soluble Fe^{2+} which can be leached out from the sediment system or soil. This increased iron solubility may cause the release of inorganic compounds bound to Fe^{3+} oxides such as various toxic metals and iron cyclin [22,23].

Cation ions have been shown to exert a significant impact on properties of activated sludge [24]. Monovalent to divalent ratio of cations in influent is an indicator of sludge physiognomies according to postulates of divalent cation bridging theory [25,26]. Flocculation and treatment efficiency of waste water treatment plants (WWTP) also rely on the type of the cation coming with the influent, that is, Na^+, Ca^{2+}, Mg^{2+}, Al^{3+}, Fe^{2+}, Fe^{3+} [27–30]. Divalent cations foster bio-flocculation compared to monovalent cations [31]. Fe^{2+} has more pronounced role in granules stability and is more important than Ca^{2+} and Mg^{2+} [32]. Due to their higher charge valence and outstanding affinity with multidentate negatively charged ligands in EPS, trivalent (TVI) Fe and Al contribute to extra stability of granules in sludge and are of great significance in this regard [27,32,33]. Muller [21] also reported superior flocculation

capability of Fe^{3+} compared to Fe^{2+}. Along with proper choice of coagulant as an important consideration, its proper dosage also plays a significant role [34]. Although multivalent cations such as trivalent iron salts are widely employed as coagulants in WWTP, little is known about their impacts on wastewater biomass and coagulation.

To our knowledge, this is the first direct demonstration of the impacts of trivalent ferric iron concentrations on the WTR biofilm community structures and performance of batch biofilm reactors under anoxic conditions. The specific hypothesis of the present study was that Fe^{3+} affects positively the floc formation and associated biofilm structure which then subsequently helps activated sludge process performance. The study evaluated the feasibility of applying WTR as an alternative, cost-effective and sustainable support material and investigated the interactive effects of trivalent iron (Fe^{3+}), serving as a nutrient, electron acceptor and a bioflocculant on sludge digestion performance and associated biofilms in attached growth batch reactors (AGBR) under anoxic conditions. Specific emphasis was given to ammonium oxidizing bacteria (AOB) and nitrite oxidizing bacteria (NOB). Besides, spatial organization and population dynamics of eubacteria, beta and gamma proteobacteria were determined using FISH (fluorescent *In situ* hybridization) coupled with CLSM (confocal laser scanning microscopy) and digital image analysis.

1. Methodology

1.1. Experimental set-up and operation

Experiments were conducted with four laboratory-scale rectangular AGBR, 4 L each, run under anoxic condition for a period of 90 days for the treatment of municipal sewage. The support material used in the reactors to develop biofilms was passenger car WTR strips (length; 11 cm, width; 4.065 cm, thickness; 0.13 cm, surface area; 93.48 cm^2) suspended vertically in the reactors with iron wire such that their three fourth part was covered with WAS. WTR contained crumb rubber (70%), steel (17%), fiber and scrap (13%) [35]. The reactors consisted of plastic material, with a flat bottom (length: 9 inches, width: 6.2 inches, height: 5.5 inches). Each reactor was filled with 2 L activated sludge obtained from municipal WWTP in Islamabad, Pakistan, 1L minimal salt medium, 5 g starch and 5 g technical agar (Oxoid). The characteristics of wastewater from that treatment facility, according to European standards, were as follows: hydraulic retention time: 7 days, mixed liquor suspended solids: 3000–3500 mg/l, total suspended solids (TSS) (influent): 230–235 mg/l, TSS (effluent): (35 mg/l), COD (influent): 400–440 mg/l, COD (effluent): 150 mg/l. The activated

Effects of aluminum (Al³⁺) on sludge digestion and biofilm development in attached growth batch reactors using tire-derived rubber as a media

Iqra Sharafat[a,†], Dania Khalid Saeed[a,b,†], Zargona Zafar[a], Naeem Ali[a,*]

[a]Department of Microbiology, Quaid-I-Azam University, 45320, Islamabad, Pakistan, Tel. +92 051 90643194;
emails: naeemali2611@gmail.com, naeemali95@gmail.com (N. Ali), sharafatiqra@yahoo.com (I. Sharafat),
dksaeed@mail.com (D.K. Saeed), zargonazafar@gmail.com (Z. Zafar)
[b]Department of Pathology and Laboratory Medicine, Agha Khan University, Karachi, Pakistan

ABSTRACT

Effects of varying concentrations of aluminum (Al³⁺) on sludge digestion and biofilm development on waste tire rubber were determined in attached growth batch reactors (AGBR) for 30 d under anoxic conditions. The strategy was bi-pronged where performance of the reactors was measured through activated sludge liquor digestibility and nitrogen removal viz. chemical oxygen demand (COD), NO_2^--N/NO_3^--N respectively. Overall, increase in Al³⁺ concentration (0–6.5 mg/L) resulted a decrease (7.33%) in bacterial density. Biochemical characterization of the bacterial isolates confirmed that most of them were gram negative. Moreover, fluorescence in situ hybridization (FISH) coupled with confocal laser scanning microscopy (CLSM) and spatial distribution analysis of the biofilms indicated presence of beta and gamma proteobacteria. Bacterial population densities decreased with increasing levels of Al³⁺. Additionally, sludge digestibility decreased in the reactors as high levels of COD (438 mg/L) and volatile fatty acids (VFA; 350 mg/L) were recorded at 6.5 mg/L of Al³⁺. Ammonium nitrogen (NH_4^+-N) transformation measured as NO_3^--N and NO_2^--N indicated an overall decrease in both the inorganic forms of nitrogen with highest elimination rate of NO_2^- at 4.5 mg/L Al³⁺, whereas, lowest was recorded at 2.5 mg/L Al³⁺. Generally, the study revealed a limiting effect of Al³⁺ concentration at specific levels on sludge digestibility, bacterial density, diversity and metabolism in the AGBR.

Keywords: Aluminum (Al³⁺); Biofilms; Wastewater treatment; Community composition; Tire-derived rubber; Fluorescence in situ hybridization (FISH); Confocal laser scanning microscopy (CLSM)

1. Introduction

Ubiquity of biofilms as recalcitrant three-dimensional matrices on biotic and abiotic surfaces translates into a unique conundrum. The inherent bio-catalysis of complex compounds and production of secondary metabolites by biofilms has been exploited to develop environmentally sustainable and novel technologies for waste water treatment and energy production [1,2]. Whereas, great economic losses have been incurred due to the unmitigated growth of biofilms on surfaces and membrane filters presenting a com- pounding challenge that needs to be circumvented. The pref- erence of bacteria to grow on attached rather than in the suspended phase [3] is contributed by a complex interaction between the bacteria and surface chemistry of support material [4]. The tendency of bacteria to attach to surfaces has been extensively studied with respect to microbiologically induced corrosion or biofouling of piping surfaces employed in water, waste water, oil and gas distribution networks, bioreactor membranes or other propagating surfaces [5]. In order to promote environmentally sustainable technologies, it is imperative to address the issue of low cost of treatment options by focusing on usage of cheap biofilm support materials. Billions of used tires are stockpiled annually owing to unavailability of their alternate applications. In this context, waste tire-derived rubber has been viewed as

---

* Corresponding author.

† Authors contributed equally.

an alternative to different costly materials in attached growth biofilm reactors due to its good surface area, less toxicity to microorganisms and size distribution. Previously, a number of bioreactors, such as trickling filters and hybrid sludge biofilm bed reactor using tire-derived rubber as support, have been run with considerable treatment efficiencies [6–9]. Still, detailed understanding of the factors influencing biofilm structure and growth is imperative to harness the potential of the said bioreactors.

Typically, aluminum ions and poly alum compounds have been recommended as effective coagulants for removal of chemical oxygen demand (COD) and bio- logical oxygen demand (BOD) in wastewater treatment [10]. Iron and aluminum hydroxide coatings on filtering materials such as sand have also been reported to effec- tively remove fecal coliforms from water [8] and achieved a reduction of 4 log in the bacterial count after passing waste water through sand columns coated with iron and aluminum hydroxide. Similarly, Zhu et al. [11] indicated that aluminum sulfate removed color and COD by 72% and 90%, respectively.

In vitro studies to evaluate the effect of different parameters such as oxygen, carbon dioxide, nutrients on biofilm formation rely on the use of biofilm reactors that can be either batch reactor or open systems [12–14]. The advent of scanning and transmission electron microscopy enabled an in-depth exploration and higher resolution of biofilms to be studied [15]. Bacterial density and biochemical identification have been conducted using conventional culture based methods. However, these methods have their limitations such as inability to identify non-culturable bacteria. Two major thrusts in the previous two decades have impacted our understanding of biofilms including molecular meth- ods such as fluorescence in situ hybridization (FISH) and confocal laser scanning microscopy (CLSM) [16,17]. Herten et al. [18] quantified *Staphylococcus aureus* biofilm formation on vascular graft surfaces by using conventional culture based techniques to determine colony forming units and validated their findings qualitatively using scanning elec- tron microscopy (SEM). Fish et al. [19] characterized the physical composition and microbial community composi- tion of biofilms of their full scale model water distribution system using fluorescent CLSM and digital image analysis (DIA). Similarly, Sharafat et al. [20] quantified microbial density in biofilms developed on waste tire rubber with FISH and CLSM.

Despite established role of aluminum as a coagulant, the role of these flocculating agents on biofilm develop- ment dynamics and floc stability has not been extensively studied specifically with regards to Al^{3+} [21–23]. A gap exists in our understanding of aluminum's role in terms of overall microbial diversity in biological wastewater treat- ment and water sanitation systems. Thus, this study evalu- ated the effects of varying concentrations of aluminum on biofilm development and associated bacterial densities on tire-derived rubber as a cheap support material through conventional and molecular based techniques such as FISH and CLSM. Besides, the effect of varying concentrations of aluminum on reactors performance was monitored in terms of waste water's sludge digestibility along with nitri- fication rates.

1. Materials and methods

1.1. Development of biofilms on tire-derived rubber support

1.1.1. Sampling

Activated sludge was collected from municipal waste water treatment plant located in Islamabad, Pakistan, in sterilized plastic containers. Sample was transported within an hour to laboratory in cold sampling box and stored at 4°C prior to inoculation into the reactors on the same day.

1.1.2. Set up and operation of attached growth batch bioreactors

Strips of waste tire-derived rubber (TDR) (surface area: 93.48 cm³) were cut and vertically aligned in four attached growth batch reactors (AGBR) in duplicate, with a total capacity of 4 L each and working volume of 3 L. The TDR strips incorporated in the reactors were of a passenger car and they were suspended inside the reactors with an iron wire such that three fourth was covered with waste activated sludge. The composition of the TDR included crumb rubber (70%), fibers and scrap (13%) and steel (17%) [24]. Composition of the medium used within each reac- tor was as follows: 2 L activated sludge, 1 L minimal salt media (64 g Na_2HPO_4, 15 g KH_2PO_4, 2.5 g NaCl, 5.0 g NH_4Cl, 1 M Mg_2SO_4, 20% glucose and 1 M $CaCl_2$), 5 mL trace ele- ments (10 mg $ZnSO_4.7H_2O$, 3 mg $MnSO_4$, 1 mg $CoCl_2.6H_2O$, 20 mg $NiCl_2.6H_2O$, 30 mg $Na_2Mo.2H_2O$, 30 mg H_3BO_3, 1 mg $CuCl_2.2H_2O$, 1 mg $CuSO_4$), 5 g starch and 5 g techni- cal agar (Oxoid). The characterization of the wastewater from this facility, according to European Standards was as follows: HRT: 7 d, MLSS: 3,000–3,500 mg/L, TSS: influents; 230–235 mg/L, effluents: 35 mg/L, BOD: 190–200 mg/L, COD (Influent): ≈700 mg/L, COD (effluent): 150 mg/L. The batch reactors were covered with black paper to prevent any algal growth and incubated at 30°C ± 2°C. After incubation of 2 d as an acclimatization period, three reactors were dosed with three different concentrations of $AlCl_3$ (2.5, 4.5 and 6.5 mg/L) and homogenized with stirrers, whereas, control reactor received no aluminum. The reactors were incu- bated under anoxic condition at 30°C for a period of 30 d. Mechanical stirring was carried out with sterile stainless stirrers periodically to ensure appropriate oxygen diffusion and homogeneity of the contents in the reactors.

1.2. Physico-chemical characterization of activated sludge liquor in reactors

Sludge digestion in the reactors was measured in terms of different physicochemical parameters. COD (mg/L), VFA (mg/L) and alkalinity (mEq/L) of sludge were measured initially and at final stage (after 30 d of treatment), using COD commercial kits (Merck, Germany, detection range; 25–2,500 mg/L) and three point titration method [25], respec- tively. In addition, NO_3-N and NO_2-N of the activated sludge were measured, using APHA 4500 NO_3-N and APHA 4500 NO_2–N methods (Standard Methods, 2005) [26], respectively. The pH of the samples was determined periodically using "Digital Sartorius (pp 15) pH meter". Dissolved oxygen (DO) was monitored with "Crison OXI45+ DO meter" that contained

Comparing Natural and Artificially Designed Bacterial Consortia as Biosensing Elements for Rapid Non- Specific Detection of Organic Pollutant through Microbial Fuel Cell

Maira Anam, Sameen Yousaf, Iqra Sharafat, Zargona Zafar, Kamran Ayaz, Naeem Ali[*]

Department of Microbiology, Quaid-i-Azam University, Islamabad, Pakistan
[*]E-mail: naeemali2611@gmail.com

The standard 5-days biochemical oxygen demand (BOD) method used for determination of biologically oxidizable organic material in wastewater considered to be laborious, time consuming and costly. Mediator-less microbial fuel cell (MFC) based biosensor offers an efficient alternative approach for real time monitoring of biodegradable organic matter in wastewater. Here we constructed an H- shaped MFC biosensor for comparing the efficiency of a complex natural (activated sludge) and artificially designed bacterial (*Pseudomonas aeruginosa, Staphylococcus aureus* and *Bacillus circulans*) consortia as biological sensing elements for BOD measurements. Initially, the MFC biosensor was optimized and calibrated at pH 7 and temperature 37ºC using 100 mM phosphate buffer with 100 mM NaCl solution as catholyte at 10 kΩ external resistance. Maximum power density of 14.2 mW/cm^2 was generated by MFC-I with sludge consortium and it was 5 folds higher than MFC-II with artificial consortium. Standard glucose and glutamic acid (GGA) solutions were used for establishing the calibration curves between different BOD concentrations (50-250 mg/L) and voltage (mV) outputs in MFC. The regression equations for MFC-I and MFC-II biosensors were recorded as $y_1 = 0.7834x- 11.638$ and $y_2 = 0.1667x + 0.8476$ respectively. Linear regression analysis revealed that 1 unit (mg/L) increase in organic load caused a voltage increase of 0.78 mV and 0.16 mV in the MFCs (I and II) reactors respectively. The relative performance in terms of stability (55-60 days) and reproducibility (within ±15.4%) of MFC-I BOD biosensor was almost double than MFC-II. The varying low concentrations of different electron acceptors (phosphate, nitrate and nitrite) in anodic compartments did not affect the performance of MFC biosensors.

1. INTRODUCTION

Biochemical oxygen demand (BOD) is commonly used as international index by environment protection agencies for assessment of organic matter load (pollutants) in wastewater. Many industries

regularly monitor their effluents to comply with the requirements of regulatory agencies [1]. Generally, the conventional BOD method used to analyze wastewater is not only time consuming (almost 5 days) but it also demands nitrification inhibitors (such as allyl-thiourea) and extensive training of the technicians to achieve reproducible results. Therefore, BOD_5 method is not considered suitable for dynamic intervention and real time monitoring in aquatic environments (such as ponds, lakes, rivers and ground water and wastewater). Several BOD biosensors based on bioluminescent, UV absorbance, enzymatic reactions and oxygen consumption by immobilized bacterial cells have been designed to overcome the aforementioned drawbacks. However, these methods demonstrated relatively unstable performance due to membrane fouling, volatile operation and limited utilization of substrate by reference bacteria [2]. A microbial fuel cell (MFC) based non-specific biosensor has been considered as a feasible alternative to the aforesaid methods for in-situ and ex-situ BOD monitoring of water bodies [3].

Microbial fuel cell (MFC) is an electrochemical device that converts chemical energy of wastewater into electric energy by using bacterial catalytic reaction [4]. Therefore, it is an environment friendly approach for wastewater treatment and renewable energy generation (in the form of electric current or bio-hydrogen. Recently, MFC has been viewed as a potential biosensing device for organic load measurement in aqueous environment. Redox electrochemical mediators that are phenolic toxic compounds (e.g. phenazine derivatives and flavins) have been usually employed to facilitate electrons transfer from bacterial cells to electrode [5]. Exoelectrogenic metal reducing bacteria such as *Shewanella putrefaciens, Rhodoferax ferrireducen* and *Geobacter sulfureducen* have also been reported in direct shuttling of electrons attached to anode [6]. Considering the operational suitability, lower electronic requisites, mechanical simplicity, good signal acquisition, sensitivity to change in organic load, high reproducibility and cost effectiveness, mediator-less MFC is considered more promising approach for developing an organic matter biosensor [7].

Previously, various MFC biosensors have been fabricated by immobilizing biological recognition element (bacterial cells) on physical transducer or in close proximity with transducer to convert biochemical changes into readable signals [8]. These biosensors have been successfully tested for monitoring COD, BOD, volatile fatty acid, anaerobic digestion and toxic components (cadmium, sodium acetate, chromium, and nitrate) in analyte. Pure culture biofilms of *Bacillus subtilis, Serratia marcescens* and *Photobacterium phosphoreum* have been designed for assessment of assimilable organic contamination in wastewater [9]. The use of single bacterial species in MFC biosensor has challenges of substrates selection and toxicity due to hazardous compounds that ultimately limit the electrode sensitivity. The major drawback of pure culture biosensor is inaccurate measurement of BOD concentration as only limited range of sample contaminants are metabolized [10]. Therefore, some studies have used complex bacterial community in MFC based BOD biosensors to estimate the total biodegradable organic matter of wastewater. Although the diverse nature of unknown bacterial community in sludge has been recognized as a limiting factor in terms of repeatability and stability of biosensing system [11]. Micro-aerophilic, anoxic and anaerobic bacteria produce different electric outputs utilizing organic matter through various metabolic pathways following Monod growth kinetics. Hence, it is essential to consider the effects of bacterial substrate consumption rate on MFC performance and BOD measurements of wastewater [8, 12]. The concept of MFC based biosensor has

Prof. Dr. Naeem Ali

Biofilm Dynamics and Role of Electricigens under Stressful Conditions for Wastewater Treatment, Bio-electricity Generation and Bio-monitoring by Iqra Sharafat .

From DRSM (DRSM L)

- Processed on 14-Dec-2020 11:21 PKT
- ID: 1474416282
- Word Count: 74039

Similarity Index
14%
Similarity by Source
Internet Sources:
        9%
Publications:
        10%
Student Papers:
        3%
sources:
1

1% match (Internet from 29-May-2018)

http://etheses.whiterose.ac.uk/20460/1/Joe_Thesis_2017.pdf
2

1% match (Internet from 06-Sep-2018)

http://www.esp.org/recommended/literature/biofilm/inc.files/bt-flat.txt
3

1% match (Internet from 19-Aug-2020)

http://www.electrochemsci.org/abstracts/vol12/120402836.pdf
4

< 1% match (student papers from 26-May-2014)

Submitted to Edith Cowan University on 2014-05-26

Focal Person (Turnitin)
Quaid-i-Azam University
Islamabad